ISSN 0021-9673

VOL. 668 NO. 1 MAY 6, 1994

8th International Conference on Partitioning in Aqueous Two-Phase Systems Leipzig, August 22–27, 1993

JOURNAL OF CHROMATOGRAPHY A

INCLUDING ELECTROPHORESIS AND OTHER SEPARATION METHODS

SYMPOSIUM VOLUMES

ELSEVIER

JOURNAL OF CHROMATOGRAPHY A

INCLUDING ELECTROPHORESIS AND OTHER SEPARATION METHODS

Scope. The *Journal of Chromatography A* publishes papers on all aspects of **chromatography, electrophoresis** and related methods. Contributions consist mainly of research papers dealing with chromatographic theory, instrumental developments and their applications. In the *Symposium volumes*, which are under separate editorship, proceedings of symposia on chromatography, electrophoresis and related methods are published. *Journal of Chromatography B: Biomedical Applications* —This journal, which is under separate editorship, deals with the following aspects: developments in and applications of chromatographic and electrophoretic techniques related to clinical diagnosis or alterations during medical treatment; screening and profiling of body fluids or tissues related to the analysis of active substances and to metabolic disorders; drug level monitoring and pharmacokinetic studies; clinical toxicology; forensic medicine; veterinary medicine; occupational medicine; results from basic medical research with direct consequences in clinical practice.

Submission of Papers. The preferred medium of submission is on disk with accompanying manuscript (see *Electronic manuscripts* in the Instructions to Authors, which can be obtained from the publisher, Elsevier Science B.V., P.O. Box 330, 1000 AH Amsterdam, Netherlands). Manuscripts (in English; *four* copies are required) should be submitted to: Editorial Office of *Journal of Chromatography A*, P.O. Box 681, 1000 AR Amsterdam, Netherlands, Telefax (+31-20) 5862 304, or to: The Editor of *Journal of Chromatography B: Biomedical Applications*, P.O. Box 681, 1000 AR Amsterdam, Netherlands. Review articles are invited or proposed in writing to the Editors who welcome suggestions for subjects. An outline of the proposed review should first be forwarded to the Editors for preliminary discussion prior to preparation. Submission of an article is understood to imply that the article is original and unpublished and is not being considered for publication elsewhere. For copyright regulations, see below.

Publication information. *Journal of Chromatography A* (ISSN 0021-9673): for 1994 Vols. 652–682 are scheduled for publication. *Journal of Chromatography B: Biomedical Applications* (ISSN 0378-4347): for 1994 Vols. 652–662 are scheduled for publication. Subscription prices for *Journal of Chromatography A*, *Journal of Chromatography B: Biomedical Applications* or a combined subscription are available upon request from the publisher. Subscriptions are accepted on a prepaid basis only and are entered on a calendar year basis. Issues are sent by surface mail except to the following countries where air delivery via SAL is ensured: Argentina, Australia, Brazil, Canada, China, Hong Kong, India, Israel, Japan, Malaysia, Mexico, New Zealand, Pakistan, Singapore, South Africa, South Korea, Taiwan, Thailand, USA. For all other countries airmail rates are available upon request. Claims for missing issues must be made within six months of our publication (mailing) date. Please address all your requests regarding orders and subscription queries to: Elsevier Science B.V., Journal Department, P.O. Box 211, 1000 AE Amsterdam, Netherlands. Tel.: (+31-20) 5803 642; Fax: (+31-20) 5803 598. Customers in the USA and Canada wishing information on this and other Elsevier journals, please contact Journal Information Center, Elsevier Science Inc., 655 Avenue of the Americas, New York, NY 10010, USA, Tel. (+1-212) 633 3750, Telefax (+1-212) 633 3764.

Abstracts/Contents Lists published in Analytical Abstracts, Biochemical Abstracts, Biological Abstracts, Chemical Abstracts, Chemical Titles, Chromatography Abstracts, Current Awareness in Biological Sciences (CABS), Current Contents/Life Sciences, Current Contents/Physical, Chemical & Earth Sciences, Deep-Sea Research/Part B: Oceanographic Literature Review, Excerpta Medica, Index Medicus, Mass Spectrometry Bulletin, PASCAL-CNRS, Referativnyi Zhurnal, Research Alert and Science Citation Index.

US Mailing Notice. *Journal of Chromatography A* (ISSN 0021-9673) is published weekly (total 52 issues) by Elsevier Science B.V., (Sara Burgerhartstraat 25, P.O. Box 211, 1000 AE Amsterdam, Netherlands). Annual subscription price in the USA US$ 4994.00 (US$ price valid in North, Central and South America only) including air speed delivery. Second class postage paid at Jamaica, NY 11431. **USA POSTMASTERS**: Send address changes to *Journal of Chromatography A*, Publications Expediting, Inc., 200 Meacham Avenue, Elmont, NY 11003. Airfreight and mailing in the USA by Publications Expediting.

See inside back cover for Publication Schedule, Information for Authors and information on Advertisements.

0021-9673/94/$07.00

Printed in the Netherlands

For Contents see p. VII.

JOURNAL OF CHROMATOGRAPHY A

VOL. 668 (1994)

JOURNAL OF CHROMATOGRAPHY A

INCLUDING ELECTROPHORESIS AND OTHER SEPARATION METHODS

SYMPOSIUM VOLUMES

ELSEVIER
AMSTERDAM — LONDON — NEW YORK — TOKYO

Leipzig, ca. 1830

0021-9673/94/$07.00

Printed in the Netherlands

SYMPOSIUM ISSUE

8TH INTERNATIONAL CONFERENCE ON PARTITIONING IN AQUEOUS TWO-PHASE SYSTEMS

Leipzig (Germany), August 22–27, 1993

Guest Editors

G. BIRKENMEIER
(Leipzig, Germany)

G. KOPPERSCHLÄGER
(Leipzig, Germany)

VOL. 668, NO. 1 JOURNAL OF CHROMATOGRAPHY A MAY 6, 1994

CONTENTS

8TH INTERNATIONAL CONFERENCE ON PARTITIONING IN AQUEOUS TWO-PHASE SYSTEMS, LEIPZIG, AUGUST 22–27, 1993

ELSEVIER

Journal of Chromatography A, 668 (1994) 1

JOURNAL OF CHROMATOGRAPHY A

Preface

The use of aqueous two-phase systems for the partitioning of macromolecules, organelles and cells has become of increasing interest for separation technologies in most areas of biotechnology, biochemistry and cell biology. Since 1979 biennial international conferences on "*Partitioning in Aqueous Two-Phase Systems — Application in Biochemistry, Cell Biology and Biotechnology*" have been organized. The 8th conference of this series was held in Leipzig (Germany). About 100 participants from all over the world were gathered to present and discuss recent results with respect to the following topics: partitioning of proteins, biotechnological applications, miscellaneous applications of polymers, partitioning of cells and cell particles, theory of partitioning, and novel techniques.

This special issue of the *Journal of Chromatography A* comprises a selection from 21 lectures and 30 posters presented at the conference.

We hope that the contributions will find widespread interest, not only for specialists in partitioning in aqueous two-phase systems, but also for those research groups who are not yet familiar with this interesting field of separation technology.

Leipzig, Germany Gerhard Kopperschläger
Gert Birkenmeier

SSDI 0021-9673(94)00303-Q

ELSEVIER

Journal of Chromatography A, 668 (1994) 3–11

JOURNAL OF CHROMATOGRAPHY A

Variation of protein partition coefficients with volume ratio in poly(ethylene glycol)–salt aqueous two-phase systems

J.G. Huddleston*, R. Wang, J.A. Flanagan, S. O'Brien, A. Lyddiatt

Biochemical Recovery Group, School of Chemical Engineering, Edgbaston, Birmingham, B15 2TT, UK

Abstract

Partition of total soluble protein from brewery waste in poly(ethylene glycol) (PEG)–phosphate aqueous two-phase systems reveals that the partition coefficient varies with change in volume ratio. This phenomenon has been confirmed by the examination, in more detail, of the behaviour of a pure protein (bovine serum albumin) in systems of widely different volume ratio and tie line length. The results invite interpretation in terms of salting out of protein from the lower phase. The behaviour of a number of pure proteins in hydrophobic interaction chromatography and in PEG salt aqueous two-phase partition has been compared and the results support this interpretation. This is judged to provide a useful rationalisation of three important strategies for the large-scale downstream processing of proteins, namely, precipitation, PEG salt partitioning and hydrophobic adsorption. In addition hydrophobic interaction chromatography may prove to be of benefit in "method scouting" for the development of partitioning strategies in protein purification.

1. Introduction

It is generally accepted that Nernst's distribution law applies to the partition of proteins in aqueous two-phase systems formed as a result of the phase separation of mixtures of polymers or mixtures of polymer and salt [1]. This is universally interpreted to mean that the distribution or partition coefficient takes its simplest possible form and thus may be expressed as the ratio of the concentrations of the protein in the top and bottom phases of an aqueous two-phase system at equilibrium [2]. This view is held despite the fact that proteins are complex biological polymers whose molecular surfaces are extensively hydrogen bonded with the surrounding water molecules in aqueous systems and thus potentially may lose or gain hydrogen bonds under particular conditions in such systems [3]. Such changes would lead, under a strict interpretation, to a violation of the assumptions underlying the application of the simplest form of the partition coefficient which only applies if a single molecular species is considered to be distributed between the phases [4].

Additionally it is often assumed that a linear partition isotherm is applicable to the modelling of protein partitioning in aqueous two-phase systems so that the variation in concentration of added material has little or no effect on the resulting distribution [5]. Each of these factors contribute to the assumption that the partition coefficient of a solute partitioned in an aqueous two-phase system at equilibrium distributes in a way which is independent of the relative volumes of the two phases. To some extent this may well

* Corresponding author.

0021-9673/94/$07.00
SSDI 0021-9673(93)E1264-Z

be due to the fact that the greatest wealth of data on partitioning exists for polymer–polymer systems where, for reasons which will become apparent later, such assumptions may be permissible. Poly(ethylene glycol) (PEG) salt systems on the other hand have not been studied in such detail and effects contradicting these assumptions may well have been overlooked.

In a recent paper [6], we reported an apparent variation in partition coefficient with volume ratio in the partition of total intracellular protein from brewer's yeast along with limited data, in support of this observation, for some pure proteins partitioned in PEG–phosphate aqueous two-phase systems. In this paper the variation of protein partition coefficient with volume ratio is examined in more detail for a single pure protein. The implications of this for an understanding of protein partition in PEG–salt aqueous two-phase systems are discussed in the light of some observations from the literature and from some additional experiments concerning the salting out of proteins and their distribution between a mildly hydrophobic solid phase and a mobile phase containing salt in hydrophobic interaction chromatography (HIC).

2. Methods

2.1. Preparation of aqueous two-phase systems

Poly(ethylene glycol) of molecular masses of 1450 and 1000 was obtained from Sigma (Poole, Dorset, UK). Potassium dihydrogen orthophosphate and dipotassium hydrogen orthophosphate were obtained from BDH (Atherstone, Warwickshire, UK). Phase diagrams were prepared using the cloud point method [7] and tie lines fixed using the known relationship between volume ratio and the intersection by the tie line of the overall system composition and the binodal curve [2]. In the experiments on the partition of pure proteins at differing volume ratio the systems were not made up from the overall composition as represented by points read directly from the fitted tie line. Instead a large (500 g) system was made up for each tie line having a volume ratio of 1.0 as read from the tie line. Subsystems, differing only in volume ratio were then prepared by admixture of appropriate volumes of top and bottom phase, drawn from the large initial system, to give the desired phase ratio. Subsequently, freeze-dried aliquots of pure proteins (obtained from Sigma) were added by weight to these systems to give a final concentration of approximately 1 mg/g.

PEG–phosphate systems for the volume ratio experiments were prepared using PEG 1450 and dipotassium hydrogen orthophosphate (pH 9.2). PEG 1000–phosphate systems used in correlating the hydrophobic chromatography data were prepared from appropriate amounts of the di- and monobasic potassium phosphate salt to give a final pH of 7.5. Partition in these systems was conducted at four different tie line lengths. This is procedurally necessary in order to partially characterise the partitioning behaviour of proteins for correlative purposes since their partition coefficients may vary widely with tie line length within a single biphasic system (as will become apparent later). For obvious reasons the phase ratio of these systems was fixed at unity and the tie line lengths (TTL) selected were 28.8, 35.6, 41.2, and 47.0% (w/w). Details of the preparation and partitioning of total soluble protein from wet milled brewer's yeast may be found elsewhere [6].

Assay of total protein from yeast preparations was measured by the method of Bradford [8]. Pure protein preparations were measured by spectrophotometric absorbance at 280 nm.

2.2. Hydrophobic interaction chromatography

Hydrophobic interaction experiments were performed using a chromatography system consisting of an LKB 2150 HPLC pump, an LKB 2152 controller equipped with gradient mixing valve, and a Rheodyne sample injection port fitted with a 20-μl sample injection loop. The column was a Bio-Rad PEG 300-10 of diameter 4.6 mm and length 150 mm having a poly(ethylene glycol)-capped silica matrix of 10-μm particle size as supplied by Bio-Rad RSL Bel-

gium. Output was monitored using an LKB 2158 Uvicord SD at 278 nm connected to an LKB 2210 chart recorder. All experiments were conducted at a flow-rate of 0.2 ml/min and 0.2 AUFS. Chromatograms were developed isocratically and retention times monitored for pure protein samples obtained from Sigma Chemicals. Running buffer composition was varied from run to run using gradient mixing between 2% (w/w) potassium phosphate pH 7.15 and 30% (w/w) potassium phosphate pH 7.48. Buffers were prepared from di- and monobasic potassium phosphate salts of "Hipersolv" grade obtained from BDH. The difference in pH between the high and low salt concentration buffers is due to the dilution effect on the activities of the ions in preparing low-concentration buffer from high-concentration buffer. It was considered to be more important to maintain the relative compositions of the salt solutions rather than their pH whose variation was unavoidable. Protein retention times were monitored isocratically at varied salt concentration and expressed as the distribution coefficient ln D where

$$D = \frac{V}{V_0} - 1 \tag{1}$$

V is the retention volume under given conditions of salt concentration and V_0 the retention volume using 2% (w/w) potassium phosphate pH 7.15 as the running buffer.

3. Results and discussion

3.1. Partition of total soluble protein from yeast

Previous work on the partition and recovery of a total soluble protein fraction from wet milled brewer's yeast [6] indicated an apparently large variation of the partition coefficient with change in volume ratio. In this type of recovery operation utilising partition a low molecular mass of PEG has to be used in order to raise the partition coefficient of the bulk of the intracellular protein above unity. Under these conditions the partition coefficient of total soluble protein increased from less than one to almost 20 as the volume ratio was decreased from 5 to 0.3. Unexpectedly, this resulted in the total recovery of protein remaining rather constant (ref. 6). It has been generally assumed [2] that the partition coefficient remains constant with volume ratio so that it is possible to quantitatively manipulate product yields to one or another phase by manipulation of the volume ratio. In the case of increasing yield to the top phase the following expression would apply

$$Y_t(\%) = \frac{100}{1 + \frac{V_b}{V_t} \cdot \frac{1}{K}} \tag{2}$$

where $Y_t(\%)$ is the expected yield to the top phase, V_b and V_t are the volumes of the bottom and top phases, respectively, and K is the observed partition coefficient. Under the circumstances outlined above such a relationship would not correctly predict the outcome of attempts to maximise the yield by manipulation of volume ratio.

3.2. Partition of a model protein at different volume ratios

In view of the wide ranging implications of these findings, and the theoretical considerations outlined in the introduction, the effect of volume ratio on partition was investigated for a number of pure proteins including bovine serum albumin (BSA).

Fig. 1 illustrates the PEG 1450 potassium phosphate phase diagram used to prepare the systems in these experiments. The figure also shows the tie lines determined and the points representing systems having a volume ratio of 1.0. Fig. 2 shows the results obtained for the partition of BSA in a system well removed from the critical point (system 2 of Fig. 1) at volume ratios varying between 0.2 and 5.0. Several features of this figure are worth emphasising. The concentration of protein in the lower phase is low and constant throughout. The concentration in the upper phase increases as the log

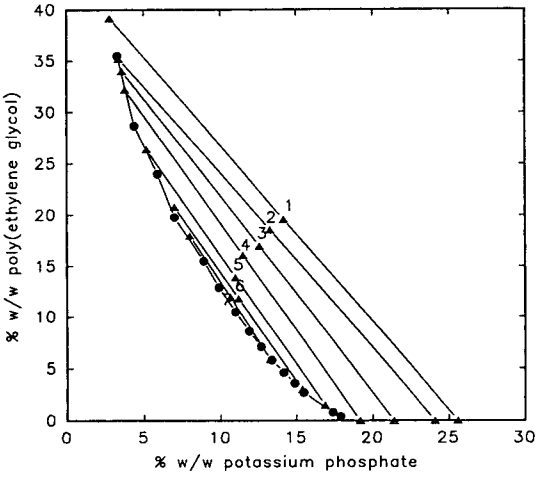

Fig. 1. Phase diagram of the PEG 1450 dipotassium hydrogen orthophosphate phase system showing experimentally determined tie lines and systems (1–7) having a volume ratio of 1.0 (△). These systems were used to construct systems of varying volume ratio but lying on the same tie line.

volume ratio decreases. In the extreme conditions of very low volume ratio, the total recovery (from both phases) is greatly reduced indicating that there is also an equilibrium with a solid-phase under these conditions. Conditions of PEG and salt concentration in the co-existing phases are sufficient to precipitate a proportion

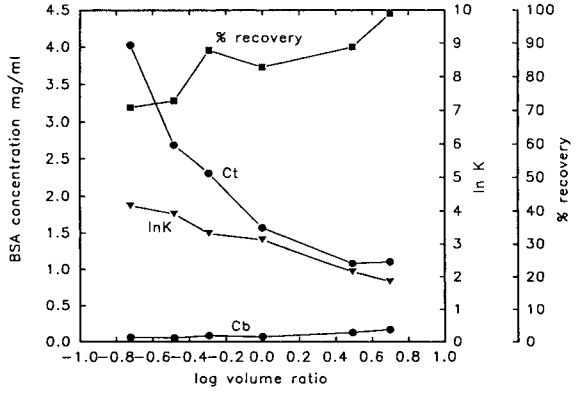

Fig. 2. Partition of BSA in a PEG 1450–potassium phosphate system well removed from the critical point and corresponding to tie line 2 of Fig. 1. [TLL = 38.4% (w/w)]. Variation of total recovery (■), protein concentration (●) top (Ct) and bottom (Cb) phases and partition coefficient (▼) are shown expressed relative to the log of the volume ratio of the system.

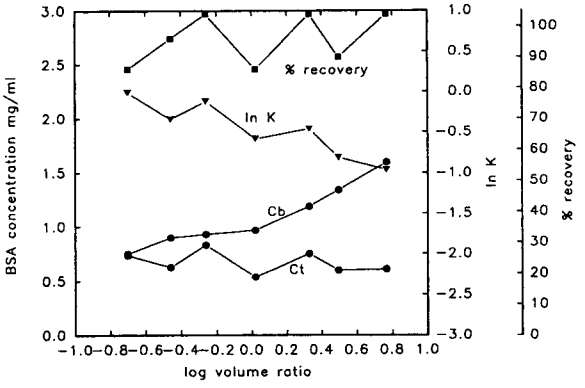

Fig. 3. Partition of BSA in a PEG 1450–potassium phosphate system relatively close to the critical point and corresponding to tie line 5 of Fig. 1. [TLL = 27.5% (w/w)]. See Fig. 2 for symbols.

of the added protein. Fig. 3 illustrates data relating to the partition of BSA in a system now chosen to be very much nearer to the critical point (system 5 of Fig. 1). Although subject to noise in its estimation, the total recovery is more constantly close to 100% than before. Note that the phase preference (phase of highest concentration) of the BSA has changed. At the lowest volume ratio the partition coefficient is approximately one but as the volume ratio increases the concentration in the top phase remains relatively constant whilst that in the bottom phase increases. As a consequence the partition coefficient falls but now only by approximately one log. In system 7 of Fig. 1, illustrated in Fig. 4,

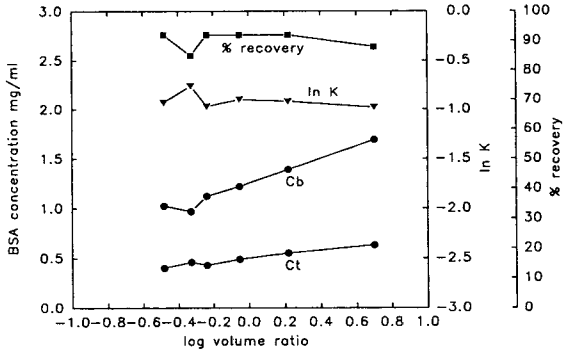

Fig. 4. Partition of BSA in a PEG 1450–potassium phosphate system close to the critical point and corresponding to tie line 7 of Fig. 1. [TLL = 13.2% (w/w)]. See Fig. 2 for symbols.

and lying closest to the critical point, overall recovery is high and the partition coefficient is constant with volume ratio. However even under these circumstances ideal partitioning behaviour is not observed. Addition of very small molar quantities of protein to systems prepared close to the critical point has profound effects on the phase diagram. The addition of protein solutes caused the observed volume ratio (V_r) to depart to a considerable extent from the expected value. For example systems prepared to give V_r 3 gave $V_r < 2$ and systems prepared to give V_r 0.2 gave $V_r > 0.3$. At the critical point very small amounts of water or any one of the phase-forming components added to the system will have profound effects on the resulting two-phase system. It is not surprising that small amounts of protein have the same effect. We conclude that there is, apparently, only a rather small region of the phase diagram in which partition of protein can be expected (in many cases) *not* to depart from simple theoretical laws. For BSA in the PEG 1450–potassium phosphate system this region can be approximated by the area bounded by the tie lines of systems 5 and 7 of Fig. 1.

Fig. 5 shows the results of the partition of BSA in the PEG 1450–potassium phosphate

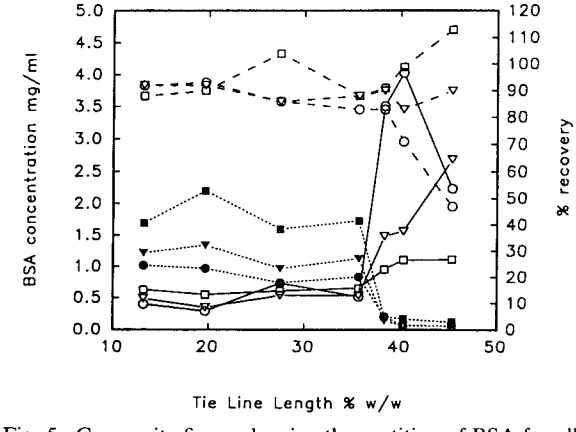

Fig. 5. Composite figure showing the partition of BSA for all tie line lengths examined in a PEG 1450–potassium phosphate system at different volume ratios. Broken lines correspond to total recovery of BSA, dotted lines to concentration of BSA in the lower phase and solid lines to concentration in the upper phase. Symbols (whether filled or solid) correspond to volume ratios of 5.0 (□), 1.0 (▽) and 0.2 (○).

phase system for all the tie lines examined. The partition coefficient is at first relatively constant for all volume ratios in this system but gradually diverges as the system tie line length increases as shown in Figs. 2–4. Corresponding data showing the concentration in top and bottom phases and total recovery of BSA in the system at volume ratios of 5.0, 1.0 and 0.2 are shown in Fig. 5. For the most part total recovery is constant and greater than 90% for these systems. Only for the lowest volume ratios (which are combined with a strong upper phase preference) is precipitation of BSA in any way marked. Most noticeable in this figure, however, is the sudden change in phase preference which occurs at a tie line length of about 38% (w/w). Below this concentration BSA strongly prefers the lower phase but above there is strong preference for the upper phase.

3.3. Classical description of partition

Many accounts of partitioning begin by reference to the Brönsted equation [9] which is often given as

$$\ln K = \frac{\lambda M(C - C_o)}{kT} \quad (3)$$

where K is the partition coefficient, λ a factor comprising the interaction of the phases with the solute, M is the molecular mass of the solute and $C - C_o$ is the difference between the composition of the system and the composition at the critical point. k is the Boltzmann constant and T the absolute temperature. Brönsted and Warming [10,11] partitioned colloidal particles of arsenical and cadmium sulphides in a two-phase system composed of ethyl alcohol, butyl alcohol and water. In order to reduce the surface tension to a level commensurate with distribution of the particles between the two bulk phases, rather than between one bulk phase and the interface, systems were confined to a region very close to the critical point [12]. This was achieved by manipulating the temperature within 0.25°C of the critical temperature for phase formation. Straight lines were used to describe the change in partition coefficient as the system composition became removed from the critical point as indi-

cated in the equation. Also implicit is the fact that at the critical point the observed arithmetic partition coefficient will be 1.

In this light the observations reported on the partition of BSA in the PEG 1450–potassium phosphate aqueous two-phase system strongly suggest that the range of applicability of the Brönsted equation may have been exceeded. However, the fact that a change of phase preference may be achieved with high yield by aiteration of the system composition, whilst contradicting the Brönsted equation, is of considerable practical significance in the design of protein purification schemes. From a practical point of view, it is worthwhile seeking alternative models which could account for these observations. Of most significance seems to be the change in phase preference occurring at around 38% (w/w) shown in Fig. 5. This is marked by a rapid decline in concentration in the lower, phosphate rich, phase and is strongly suggestive of the operation of a salting out mechanism.

3.4. The description of partition in terms of salting out

Classically the phenomenon of salting out, or more generally precipitation, can be represented by the following equation.

$$\ln S = \beta - K_s C \tag{4}$$

where S is the solubility, β is a constant which depends on the temperature and the individual protein, C is the concentration and K_s is the salting out constant which depends upon the particular protein and salt. The meaning of K_s depends on the type of precipitation involved. For example for precipitation involving addition of polymers K_s would be related to the excluded volume of the polymer [13]. In this light partition could be defined in terms of relative solubility or represented, in very general terms, as

$$K \propto \frac{S_t}{S_b} \tag{5}$$

where S_t and S_b are the solubilities in the top and bottom phases, respectively. Actually such an approach to the description of partitioning in PEG–salt aqueous two-phase systems is not new, having been proposed by Kim [14]. However, to our knowledge relatively little of this work has been published [15]. Kim ascribed solubility in the upper phase of PEG–salt systems to the excluded volume of PEG and its effect on both the concentration of the protein and of the salt to derive an expression for protein solubility. Here only solubility in the salt-rich phase is considered. Since the phase is predominantly composed of salt (see Fig. 1) the contribution of PEG in this phase may be neglected. In a derivation of "solvophobic theory" [16] by Melander and Horvath [17], precipitation due to increase in salt concentration is described by

$$\ln \frac{w}{w_0} = \beta + \Lambda m - \Omega \sigma m \tag{6}$$

where β is a term derived from Debye–Hückel theory [18] (in which proteins in aqueous solutions at low ionic strength are treated as simple ions) and describes the increase in solubility with salt concentration known as salting in. Λ is a term derived from Kirkwood's treatment of proteins as dipolar ions [18] applicable to descriptions of protein solubility in high concentrations of salt and related to the dipole moment of the protein by

$$\Lambda = \frac{D\mu}{RT} \tag{7}$$

in which D is a constant derived from Kirkwood's theory [19]. The salting out term of Eq. 6, $\Omega\sigma m$, relates the specific molal surface tension increment of the salt (σ) to its concentration (m) and to Ω which is proportional to the hydrophobic surface area of the protein and represents the energy required for the removal of water from hydrophobic regions of the protein. Salting out thus involves an ionophilic contribution due to the dipole moment and a hydrophobic contribution due to the hydrophobic surface area which can be related to the experimentally observed salting out constant by

$$K_s = \Omega\sigma - \Lambda \tag{8}$$

Both terms may be determined from a knowledge of protein structure [19,20]. However, at present this is computationally difficult and possible for only relatively few proteins, since it requires knowledge of the tertiary/quaternary structure. Furthermore, the solvophobic view of salting out has been extended [21] to cover the situation of a protein partitioning between a mobile phase and a mildly hydrophobic solid phase in HIC. In this case binding to the solid phase is described by the difference in free energy of the solute in the mobile and stationary phases.

$$\ln k = \ln k_0 - \beta' - \Lambda' m + \Omega' \sigma m \quad (9)$$

Eq. 9 describes the retention in HIC under isocratic conditions with different salt concentrations. The prime associated with various terms indicates that it is the surface area of contact between the solute and the ligand which is of importance. Thus any relationship between retention, salting out and partitioning might be expected to be tenuous because of the rather different surface areas involved.

3.5. Hydrophobic interaction chromatography of some model proteins

Fig. 6 shows the isocratic retention times of a series of proteins at increasing salt concentration. A wide range of proteins has been chosen so that some, such as α-amylase, are highly retained at relatively low concentrations of salt. At the other extreme, *e.g.* cytochrome *c* is only moderately retained even at high salt concentrations. The relationship between the difference in retention time and their partitioning behaviour in an aqueous two-phase system is shown in Fig. 7. In order to make this comparison, each protein was partitioned in a PEG 1000–phosphate system at four different tie line lengths. The concentration of phosphate in the lower phase at these tie line lengths was used to ordinate the data, and the characteristic retention of each protein in HIC, expressed as $\ln D$, was extrapolated to this concentration. This was necessary because the concentration of salt required to bring about a change in phase preference in HIC was much less than that required for partition. Although the behaviour of this sample of proteins differs in detail, there is a remarkable degree of similarity in behaviour in the two types of partition. No proteins have been found which show high partition coefficients (A2PS) associated with low distribution coefficients (HIC) and vice versa. The question why proteins partitioning in these different systems involving rather

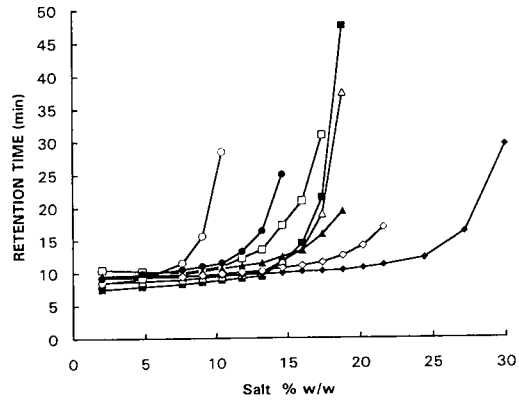

Fig. 6. Isocratic retention times on a PEG–silica HIC column of a series of proteins in response to increasing concentration of potassium phosphate pH 7.48 as detailed under methods. Symbols denote: ○: α-amylase, ●: α-chymotrypsin, □: lysozyme, ■: BSA, △: ovalbumin, ▲: ribonuclease A, ◇: myoglobin, ◆: cytochrome *c*.

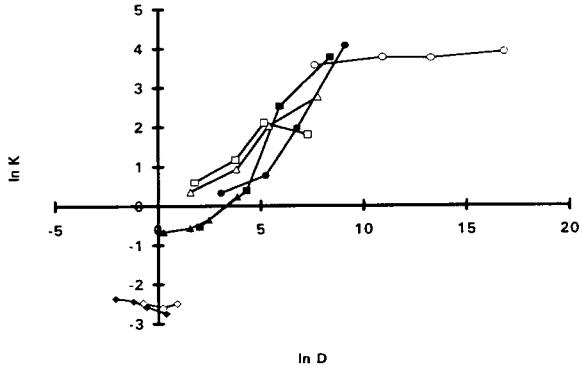

Fig. 7. Comparison of $\ln k$ obtained for selected model proteins at four tie line lengths in a PEG 1000–potassium phosphate aqueous two-phase system and their distribution coefficient $\ln D$ obtained during isocratic hydrophobic interaction chromatography on a PEG-derivatised silica HPLC column. (Symbols as for Fig. 6.)

different surface areas of contact should behave in such a similar way is intriguing and will be explored further in a subsequent publication.

Examination of the solubility behaviour of BSA in relation to increased concentration of either potassium phosphate or polyethylene glycol (Fig. 8) shows that BSA is rapidly salted out by phosphate. However this takes place at a higher concentration of phosphate than is present in the lower phase of the two-phase system of Fig. 5 when the change in phase preference of this protein occurs. By contrast, polyethylene glycol, of the same molecular mass as used in the phase system (1450), shows little tendency to precipitate albumin over a wide range of concentrations. It therefore seems reasonable to ascribe the phase change observed in partition to the salting out effect of phosphate. A greater salt concentration is required to bring about a change of phase preference in precipitation than in aqueous two-phase partition, which is in turn greater than that required to bring about a change of phase preference in chromatography involving partition to a solid phase. This might be thought to follow naturally from the surface areas and phase transitions involved in each process.

On the basis of this evidence, ascribing the

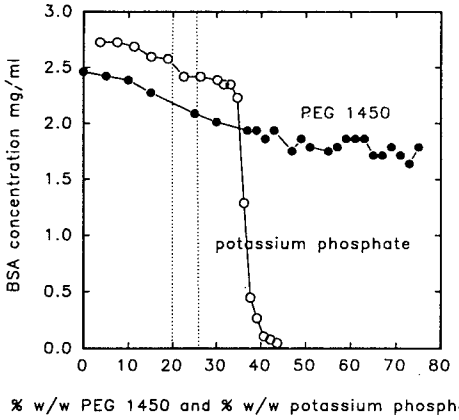

Fig. 8. Precipitation of BSA with potassium dihydrogen orthophosphate (●) and with PEG 1450 (○). Hatched lines denote the concentration of phosphate in the lower phase of the PEG 1450 aqueous two-phase system over which BSA shows a marked change in phase preference. Symbols denote concentration (mg/ml) of BSA in the supernatant.

behaviour of proteins partitioned in PEG–salt aqueous two-phase systems to the effects of salting out, leaves at least one significant problem. In the classical view of salting out, or indeed any method of solubility reduction, the final solubility is a product only of the precipitant concentration and the temperature. Indeed Florkin [22], in a series of early experiments, suggested that departures from this were evidence for an impure protein preparation. However, the concentration of albumin observed in the phases of the system reported here appears more than a little too flexible. For instance, after the solubility limits of albumin in phosphate have been approached [at 38% (w/w) TLL] the solubility in the PEG phase appears to show a dramatic increase despite increasing concentration of the top phase components. In reality what is being quite sensitively measured by the partitioning technique is the driving force toward a particular equilibrium, and recent results from a precipitation study by Shih *et al.* [23] help to shed light on this. In this study two types of solubility behaviour were observed. Type 1 behaviour, shown by lysozyme, is classical, the final protein concentration in the supernatant depends only on the salt concentration. In type 2 behaviour, shown by BSA, the final supernatant concentration is dependent not only on the concentration of the salt but also on the initial concentration of protein. The final distribution of some proteins in precipitation depends on the concentration in the supernatant and precipitate phases. Thus the apparent solubility limits of some proteins may be quite variable with operating conditions.

4. Conclusion

Our recent work on the partitioning of proteins in PEG–salt aqueous two-phase systems leads us to conclude that the salting out behaviour of proteins has a strong influence on their partitioning behaviour as outlined above. Practically this means that some current design assumptions applied to partitioning may not always be valid.

An approach to the understanding and prediction of partition in PEG–salt aqueous two-phase systems based on solubility and in particular on solvophobic theory offers some key insights into the mechanism of partition. In particular, that partition may be a sensitive measure of the interplay of molecular surface forces which are rationalised here to the dipole moment and the hydrophobic surface area of the proteins. The apparent similarities in the separation basis of hydrophobic interaction chromatography, precipitation and partition and the applicability of a common theoretical foundation based on solvophobic theory may prove to be a useful rationalisation in the development of large-scale downstream processing strategies.

It also appears that hydrophobic interaction chromatography provides an additional comparative tool for the study of partition. Considerable scope exists for developing the technique as a simple and rapid instrumental analysis of protein mixtures which could be deployed in "method scouting" for the development of partitioning strategies for protein extraction and biorecovery.

5. References

[1] P.-Å. Albertsson, *Partition of Cell Particles and Macromolecules*, Wiley-Interscience, New York, 1986.

[2] J.G. Huddleston and A. Lyddiatt, *Appl. Biochem. Biotechnol.*, 26 (1991) 249.

[3] A. Leo, C. Hansch and D. Elkins, *Chem. Rev.*, 71 (1971) 525.

[4] W. Nernst, *Z. Phys. Chem.*, 8 (1891) 110.

[5] M-R. Kula, in M. Moo-Young (Editor), *Comprehensive Biotechnology*, Vol. 2, Pergamon Press, New York, 1986, p. 451.

[6] J.A. Flanagan, J.G. Huddleston and A. Lyddiatt, *Bioseparation*, 2 (1991) 43.

[7] S. Bamberger, D.E. Brooks, K.A. Sharp, J.M. van Alstine and J.J. Webber, in H. Walter, D.E. Brooks and D. Fisher (Editors), *Partition in Aqueous Two-Phase Systems*, Academic Press, London, 1985, p. 85.

[8] M.M. Bradford, *Eur. J. Biochem.*, 48 (1976) 63.

[9] N.L. Abbott, D. Blankschtein and T.A. Hatton, *Bioseparation*, 1 (1991) 191.

[10] J.N. Brönsted, *Z. Phys. Chem. Bodenstein-Festband*, 155 (1931) 257.

[11] J.N. Brönsted and E. Warming, *Z. Phys. Chem.*, 155 (1931) 343.

[12] E.A. Boucher, *J. Chem. Soc. Faraday Trans. 1*, 85 (1989) 2963.

[13] A. Polson and B.C. Ruiz, *Vox Sang.*, 23 (1982) 107.

[14] C.W. Kim, *PhD thesis*, Massachusetts Institute of Technology, Cambridge, MA, 1986.

[15] C.W. Kim, J.T. Someren, M. Kirshen and C.K. Rha, *Phys. Chem. Liq.*, 18 (1988) 11.

[16] O. Sinanoglu and S. Abdulnur, *Fed. Proc.*, 24 (1965) S-12.

[17] W. Melander and Cs. Horvath, *Arch. Biochem. Biophys.*, 183 (1977) 200.

[18] J.T. Edsall and J. Wyman, *Biophysical Chemistry*, Vol. 1, Academic Press, New York, 1958.

[19] B. Lee and F.M. Richards., *J. Mol. Biol*, 55 (1971) 379.

[20] S. Takashima and K. Asami, *Biopolymers*, 33 (1993) 59.

[21] W.R. Melander, D. Corradini and Cs. Horvath, *J. Chromatogr.*, 317 (1984) 67.

[22] M. Florkin, *J. Biol. Chem.*, 87 (1930) 629.

[23] Y.-C. Shih, J.M. Prausnitz and H.W. Blanch, *Biotechnol. Bioeng.*, 40 (1992) 1155.

ELSEVIER

Journal of Chromatography A, 668 (1994) 13–19

JOURNAL OF CHROMATOGRAPHY A

Temperature-dependent phase inversion and its effect on partitioning in the poly(ethylene glycol)–ammonium sulfate aqueous two-phase system

Mark A. Eiteman

Department of Biological and Agricultural Engineering, Driftmier Engineering Center, University of Georgia, Athens, GA 30602, USA

Abstract

As temperature is increased, the poly(ethylene glycol) (PEG)–ammonium sulfate aqueous two-phase system exhibits a phase inversion. Specifically, the PEG-enriched phase —which at low temperature is the less dense upper phase— becomes the lower phase at elevated temperatures. The effect depends on the concentrations of PEG and ammonium sulfate in the system, with lower concentrations of either phase-forming constituent causing the inversion to occur at a lower temperature. The partitioning of several solutes is examined in this phase system at temperatures of 20–70°C. The results show that the logarithm of the partition coefficient of each solute is proportional to the PEG concentration difference between the phases (*i.e.*, upper phase concentration minus lower phase concentration), whether this difference has a positive or negative value.

1. Introduction

Albertsson [1] showed that two liquid "aqueous" phases form when threshold concentrations of two water-soluble, but mutually incompatible, components in water are exceeded. One type of aqueous two-phase system is formed when a polymer such as poly(ethylene glycol) (PEG) and a salt are dissolved together in water. The boundary between the two-phase region and the one-phase region on axes of component concentrations is referred to as the binodal, and its location for a particular pair of components depends on the system's temperature. Albertsson [2] noted that for polymer–polymer systems, the polymer which concentrates in the lower, denser phase usually does so at all component compositions. Furthermore, for PEG–salt systems, the PEG has been observed to enrich the upper, less dense phase, while the salt has been observed to enrich the lower phase. Theories of two-phase formation and partitioning in these systems have recently been reviewed [3].

A fundamental result of numerous theoretical and experimental studies concerning partitioning is that the logarithm of the partition coefficient (K) is proportional to the concentration difference of PEG between the phases by a proportionality constant, A. Mathematically,

$$\ln K = A(w_2' - w_2'') = A\,\Delta w_2 \qquad (1)$$

where w_2 indicates the concentration of component 2 (by convention, PEG) in the upper (′) and lower (″) phase. This equation describes a property of a majority of phase systems which is that the tie lines are parallel. The relationship of tie line length to partition coefficients arises from

0021-9673/94/$07.00
SSDI 0021-9673(93)E0052-V

theoretical treatments [4–6] relying on the osmotic pressure virial expansion of Edmond and Ogston [7]. This result also arises from similar derivations [8,9] using Flory–Huggins [10,11] polymer solution theory, and approaches [12–14] using the Hill constant pressure theory [15].

In PEG–salt phase systems the upper phase has been observed to be the PEG-enriched phase, in which case the PEG concentration difference, Δw_2, is positive. The conclusion drawn from these studies is straightforward: in order to increase the partition coefficient of a solute which partitions preferentially into the upper phase —and hence having a partition coefficient greater than unity— one must increase the tie line length by increasing the concentration of one or both of the phase forming components. Similarly, in order to increase the partition coefficient of a solute partitioning preferentially into the lower phase (*i.e.*, move K closer to unity), one must decrease the tie line length.

An additional method which may be used to influence the binodal and thereby affect the tie line length is to alter the temperature of the phase system. The few early studies concerning the effect of temperature on phase systems and on the partition coefficient of solutes distributed in these phase systems [16–18] did not clarify this effect. Forciniti and Hall [14] noted that the concentration difference of PEG between the phases was independent of temperature while the concentration difference of dextran was sensitive to temperature in PEG–dextran systems. In general, the tie line length decreased with increasing temperature in these systems. Recent theoretical considerations [19] suggest the change in partitioning of model proteins with temperature is a result of the combination of repulsive and attractive forces for a particular protein. In the PEG–dextran phase systems almost exclusively studied, PEG remains the predominant upper phase component for the entire temperature range.

Cohen [20] noted that at 60°C the lower phase of a PEG–ammonium sulfate system of particular concentration becomes PEG-enriched, but only very limited studies were performed. In this current study, additional investigations of this unique phase system are conducted to determine the conditions under which the observed phase inversion occurs. In addition to studying the properties of this phase system, the partitioning of several compounds is determined as a function of temperature.

2. Materials and methods

Three different PEG–ammonium sulfate aqueous two-phase systems were prepared: 7% PEG–9% salt, 6% PEG–10% salt and 7% PEG–11% salt. Reported values are in mass fractions of the compounds in the total system, that is, mass of component per mass of phase system. The particular polymer used in these solutions was PEG with a molecular mass of 8000. A 20-ml volume of each phase system containing 5–10 mg of the desired solute was refrigerated at 4°C. Systems were withdrawn when needed and placed in a bath at the desired temperature (±0.1°C). After two days of mixing and one day of equilibration, the phases were separated carefully with Pasteur pipettes and analyzed. PEG concentrations in each phase were determined by the method of Skoog [21].

The following solutes were used for partitioning studies: tryptamine, phenylalanine, tryptophol, leucine–phenylalanine (Sigma, St. Louis, MO, USA) and pentanol (Aldrich, Milwaukee, WI, USA).

A Hewlett-Packard HP-5890 gas chromatograph housing an 8 ft. × 2 mm I.D. Supelco Carbopack FT-A column (1 ft. = 30.48 cm) was used to determine the partition coefficients of pentanol. Other solutes were analyzed by liquid chromatography. The HPLC system comprised a Gilson Model 306 pumps, 231 autosampler, and an Applied Biosystems 759A UV–Vis detector. The column was a Waters Radial-Pak C_8, with eluent and detector settings appropriate to separate the pure solute of interest from impurities arising from the PEG and solute sample.

3. Results and discussion

Table 1 shows the properties of the three PEG–ammonium sulfate phase systems studied over the temperature range of 20–70°C.

The 7% PEG–9% salt solution (7/9) did not become biphasic until 30°C was exceeded. At 40°C the upper phase was PEG-enriched. Between 40 and 50°C this phase system experienced a phase inversion. The upper, PEG-enriched phase, which made up about thirty percent of the total system volume, migrated down the test tube beneath the previously lower phase. In the 50 and 60°C systems, the lower phase was PEG-enriched. The concentration of PEG in the PEG-enriched phase increased with increasing temperature, from 0.191 to 0.306.

A second PEG–ammonium sulfate phase system with slightly more salt and less PEG was also prepared and studied as a function of temperature. In this 6% PEG–10% salt system (6/10), the two-phase region was entered at temperatures less than 30°C. Like the previous system, a phase inversion occurred between 40 and 50°C. Once again the concentration of PEG in the PEG-enriched phase increased with increasing temperature, in this case from 0.165 to 0.354. For each of the three temperatures at which two-phase systems occurred for the 7/9 and 6/10 systems, the concentration of PEG in the PEG-enriched phase was greater in the 6/10 system.

The third PEG–ammonium sulfate phase system prepared contained 7% PEG and 11% salt (7/11). This system was biphasic below 20°C, and PEG remained the predominant upper phase component until 70°C. Of the three systems studied, the 7/11 phase system contained the highest concentration of PEG in the PEG-enriched phase at any given temperature. Although the highest temperature was required for the 7/9 phase system to become biphasic, this phase system exhibited a phase inversion at the lowest temperature. In all three phase systems the absolute value of the PEG concentration difference between the phases increased markedly with increasing temperature.

These results suggests two methods which may be used to cause a phase system to invert. One method would be to alter the temperature of a phase system. For example, by increasing the temperature from 40 to 50°C, the upper phase in the 6/10 system may be changed from PEG-enriched to salt-enriched. A second method to invert a phase system would be to change the concentration of one of the phase forming components. For example, a 7/9 system at 50°C (in which the lower phase is PEG-enriched) may be inverted by increasing the salt concentration to 11%. Interestingly, this same increase in salt concentration at 30°C would cause a single phase solution to become biphasic.

Since phase inversion involves the lower phase becoming PEG-enriched, the sign of Δw_2 in Eq. 1 changes from positive to negative. The question immediately arises as to whether, as Eq. 1 suggests, the logarithm of a solute's partition coefficient in these phase systems also alters sign.

Pentanol, a relatively hydrophobic uncharged model compound, was initially selected for partitioning studies. Fig. 1 shows the results of partitioning pentanol in the phase systems listed in Table 1 as a function of temperature. In general, the pentanol partitioned into the same phase in which PEG resided. At low temperatures, in phase systems which have their upper phase PEG-enriched, pentanol had a partition

Table 1
PEG concentration (mass fraction) in upper (′) and lower (″) phase of three PEG–ammonium sulfate aqueous two-phase systems as a function of temperature

T (°C)	7% PEG–9% salt		6% PEG–10% salt		7% PEG–11% salt	
	w_2'	w_2''	w_2'	w_2''	w_2'	w_2''
20	One Phase		One Phase		0.182	0.015
30	One Phase		0.165	0.028	0.228	0.015
40	0.191	0.015	0.194	0.013	0.276	0.013
50	0.0084	0.251	0.010	0.280	0.327	0.0045
60	0.0073	0.306	0.0027	0.354	0.369	0.0034
70	–	–	–	–	0.0036	0.428

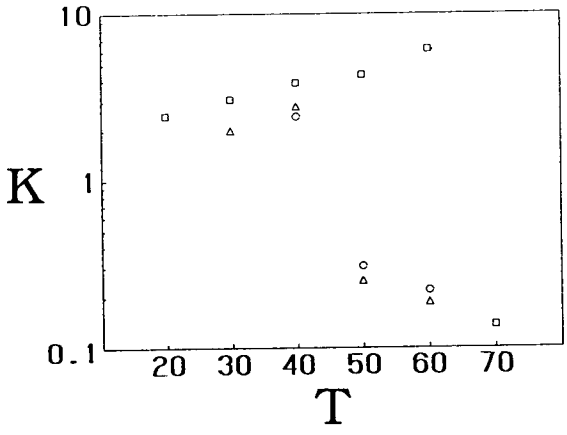

Fig. 1. Observed partition coefficients (K) of pentanol in three PEG–ammonium sulfate aqueous two-phase systems *versus* equilibration temperature. Phase systems: 7% PEG–9% salt (○), 6% PEG–10% salt (△) and 7% PEG–11% salt (□).

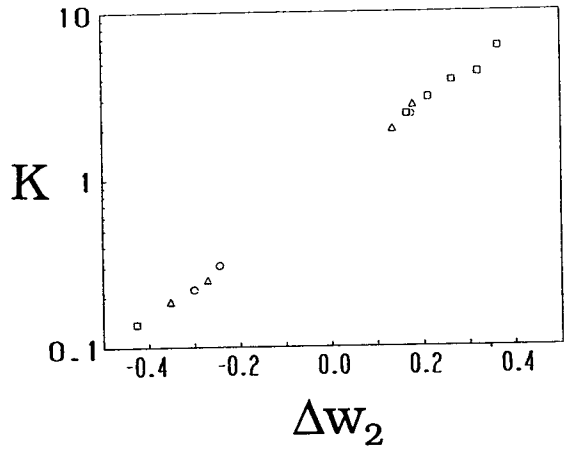

Fig. 2. Observed partition coefficients (K) of pentanol in three PEG–ammonium sulfate aqueous two-phase systems *versus* PEG concentration difference between the phases (Δw_2). Phase systems: 7% PEG–9% salt (○), 6% PEG–10% salt (△) and 7% PEG–11% salt (□).

coefficient greater than one. The partition coefficient in a particular system was observed to increase with increasing temperature until the phases inverted. After the inversion temperature, the partition coefficient became less than 1, and a continued increase in temperature resulted in a decrease in the partition coefficient.

As noted in the introduction, the logarithm of the partition coefficient theoretically may be considered proportional to the tie line length, and hence the PEG concentration difference between the phases. Fig. 2 shows the pentanol partitioning data as a function of the PEG concentration difference, as calculated from the values listed in Table 1. As this figure indicates, the logarithm of the partition coefficient was proportional to the PEG concentration difference between the phases, regardless of whether PEG was the principal upper or lower phase component.

Additional simple solutes were partitioned in these phase systems. Fig. 3 shows the partition coefficients of tryptophol as a function of temperature in the aqueous two-phase systems. Fig. 4 shows data for this solute as functions of the PEG concentration difference between the phases. The results for uncharged tryptophol were similar to those for pentanol, except that the values of the partition coefficients were about five times greater (or less after phase inversion) for tryptophol. Fig. 4 indicates that for this solute also, the logarithm of the partition coefficient was proportional to the PEG concentration difference between the phases. Only at partition coefficients far from unity did the

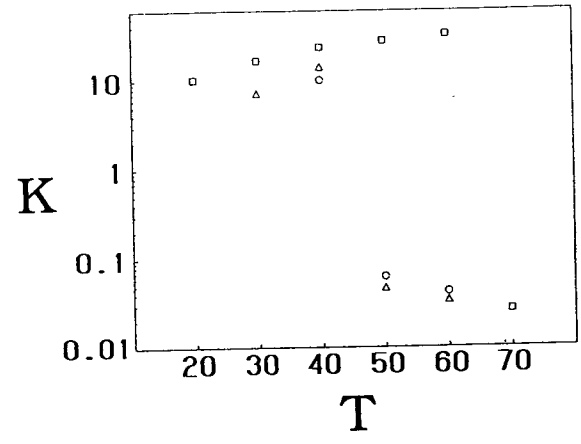

Fig. 3. Observed partition coefficients (K) of tryptophol in three PEG–ammonium sulfate aqueous two-phase systems *versus* equilibration temperature. Phase systems: 7% PEG–9% salt (○), 6% PEG–10% salt (△) and 7% PEG–11% salt (□).

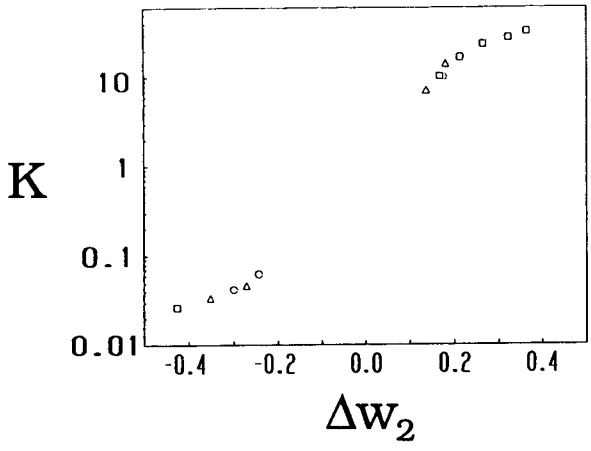

Fig. 4. Observed partition coefficients (K) of tryptophol in three PEG–ammonium sulfate aqueous two-phase systems *versus* PEG concentration difference between the phases (Δw_2). Phase systems: 7% PEG–9% salt (○), 6% PEG–10% salt (△) and 7% PEG–11% salt (□).

results begin to deviate from this theoretical proportionality, an observation explained by Cohen [20].

A less hydrophobic solute, phenylalanine, was also selected to determine the generality of the observed partitioning behavior. Fig. 5 shows the partition coefficients of this solute *versus* temperature. Since the phase systems studied were in the pH range of 5.3–5.8, phenylalanine had essentially no net charge in the aqueous two-phase systems studied. For this particular solute, the partition coefficients were less than 1 at low temperatures. At elevated temperatures, for systems in which the lower phase was PEG enriched, phenylalanine had partition coefficients greater than 1. Fig. 6 shows the partitioning data as a function of the PEG concentration difference between the phases. Once again, the logarithm of the partition coefficient was proportional to the PEG concentration difference, although for this solute the partition coefficient decreased with increasing concentration difference.

Two additional solutes (the dipeptide leucine–phenylalanine and tryptamine) were examined in these three phase systems. Fig. 7 shows the logarithm of the partition coefficient of the dipeptide versus the tie line length. The proportionality predicted by Eq. 1 was again supported. Fig. 8 shows the data for tryptamine, a positively charged analogue of tryptophol. The logarithm of this solute's partition coefficient also was observed to be proportional to the tie line length. The actual value of the partition

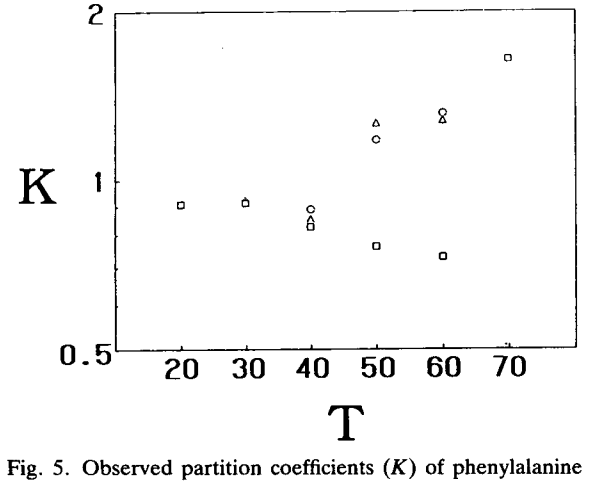

Fig. 5. Observed partition coefficients (K) of phenylalanine in three PEG–ammonium sulfate aqueous two-phase systems *versus* equilibration temperature. Phase systems: 7% PEG–9% salt (○), 6% PEG–10% salt (△) and 7% PEG–11% salt (□).

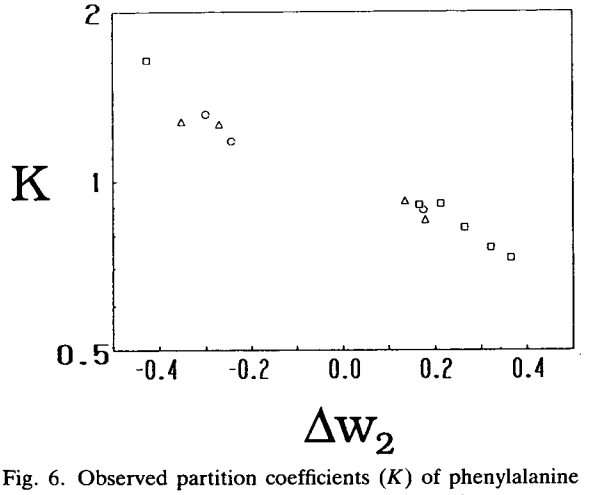

Fig. 6. Observed partition coefficients (K) of phenylalanine in three PEG–ammonium sulfate aqueous two-phase systems *versus* PEG concentration difference between the phases (Δw_2). Phase systems: 7% PEG–9% salt (○), 6% PEG–10% salt (△) and 7% PEG–11% salt (□).

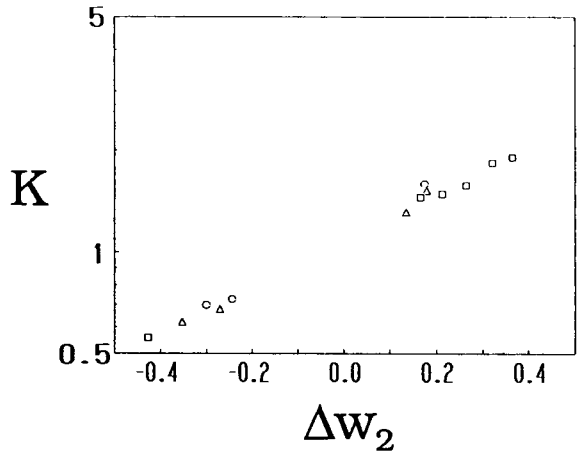

Fig. 7. Observed partition coefficients (K) of leucine–phenylalanine in three PEG–ammonium sulfate aqueous two-phase systems *versus* PEG concentration difference between the phases (Δw_2). Phase systems: 7% PEG–9% salt (○), 6% PEG–10% salt (△) and 7% PEG–11% salt (□).

coefficient in any given system was lower for tryptamine than for tryptophol.

For all five solutes studied, the data were regressed to the linear equation $\ln K = \ln K_0 + A\Delta w_2$. Table 2 shows the results of these regressions. Each of the five best-fitting lines passed very near a "y-intercept" of $K_0 = 1$, supporting

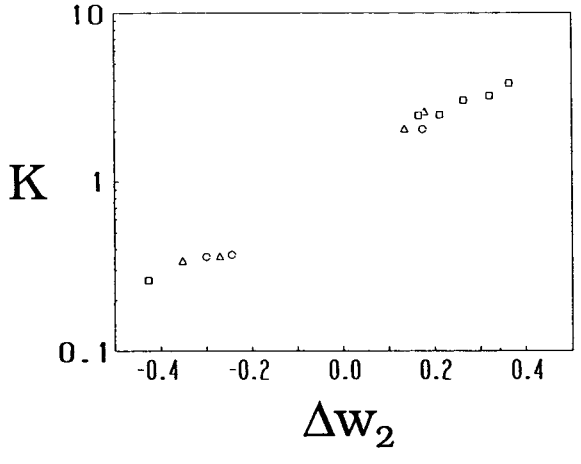

Fig. 8. Observed partition coefficients (K) of tryptamine in three PEG–ammonium sulfate aqueous two-phase systems *versus* PEG concentration difference between the phases (Δw_2). Phase systems: 7% PEG–9% salt (○), 6% PEG–10% salt (△) and 7% PEG–11% salt (□).

Table 2
Results of regressing the best-fitting line ($\ln K = \ln K_0 + A\Delta w_2$) through the observed data for each of the five solutes studied (R = correlation coefficient for $n = 13$)

Solute	A	K_0	R
Tryptophol	5.495	4.66	0.986
Pentanol	4.565	1.12	0.995
Tryptamine	3.074	1.30	0.988
Leu–Phe	1.598	1.09	0.992
Phenylalanine	−0.866	1.03	0.968

the principle that at a PEG concentration difference between the phase of zero (the plait point), any solute should distribute equally between the phases. The slope of the line, A, for each of the best-fitting lines were calculated to be different for the five solutes. Although only four uncharged solutes were examined, the calculated value of A was related to the hydrophobicity of the solutes: the greater the value of A, the greater the solute's hydrophobicity [22]. The exception of this observation was the one charged solute studied, tryptamine, which has a hydrophobicity essentially equivalent to tryptophol. In this case the calculated slope, A, was much less for tryptamine than for its uncharged analogue, tryptophol. The results support previous predictions [23] than the presence of a charge appears to shift the partition coefficients of solutes.

4. Conclusions

The PEG–ammonium sulfate aqueous two-phase system has a previously unobserved property of inverting the phases as the temperature is increased. The inversion takes place at different temperatures in phase systems of different PEG and/or salt concentration. In the three phase systems studied, the lower the component concentrations, the lower the temperature necessary for phase inversion. The logarithm of the partition coefficients of several solutes are nevertheless proportional to the PEG concentration difference between the phases. Several other PEG–salt phase systems have been studied briefly, and

presently no other phase system has been found which exhibits this phenomenon. It appears that altering temperature may serve as an additional and useful tool to shift the partitioning of compounds in aqueous two-phase systems. Clearly, additional studies are needed to determine the effect of this phase inversion on the complex partitioning of larger solutes such as proteins.

5. Acknowledgement

The author expresses thanks to Joby Miller and Daphne Golden for their experimental support and the Georgia Agricultural Experiment Stations for financial support of this research.

References

[1] P.-Å. Albertsson, *Nature*, 182 (1958) 709–711.
[2] P.-Å. Albertsson, *Partition of Cell Particles and Macromolecules*, Wiley, New York, 1986, p. 31.
[3] H. Walter, G. Johansson and D.E. Brooks, *Anal. Biochem.*, 197 (1991) 1–18.
[4] R.S. King, H.W. Blanch and J.M. Prausnitz, *AIChE J.*, 34 (1988) 1585–1594.
[5] C.A. Haynes, R.A. Neynon, R.S. King, H.W. Blanch and J.M. Prausnitz, *J. Phys. Chem.*, 93 (1989) 5612–5617.
[6] C.A. Haynes, J. Carson, H.W. Blanch and J.M. Prausnitz, *AIChE J.*, 37 (1991) 1401–1409.
[7] E. Edmond and A.G. Ogston, *Biochem. J.*, 109 (1968) 569–576.
[8] A.D. Diamond and J.T. Hsu, *Biotechnol. Bioeng.*, 34 (1989) 1000–1014.
[9] A.D. Diamond and J.T. Hsu, *J. Chromatogr.*, 513 (1990) 137–143.
[10] P.J. Flory, *J. Chem. Phys.*, 10 (1942) 51–61.
[11] M.L. Huggins, *Ann. N.Y. Acad. Sci.*, 43 (1942) 1–32.
[12] H. Cabezas, J.D. Evans and D.C. Szlag, *Fluid Phase Equil.*, 53 (1989) 453–462.
[13] H. Cabezas, M. Kabiri-Badr and D.C. Szlag, *Bioseparations*, 1 (1990) 227–233.
[14] D. Forciniti and C.K. Hall, in J.-F. Hamel, J.B. Hunter and S.K. Sikdar (Editors), *Downstream Processing and Bioseparations: Recovery and Purification of Biological Products* (*ACS Symposium Series*, No. 419), American Chemical Society, Washington, DC, 1990, pp. 53–70.
[15] T.L. Hill, *J. Am. Chem. Soc.*, 79 (1957) 4885–4890.
[16] G. Johansson, A. Hartman and P.-Å. Albertsson, *Eur. J. Biochem.*, 33 (1973) 379–386.
[17] G. Johansson and M. Andersson, *J. Chromatogr.*, 303 (1984) 39–51.
[18] F. Tjerneld, I. Persson, P.-Å. Albertsson and B. Hahn-Hägerdal, *Biotechnol. Bioeng.*, 27 (1985) 1036–1043.
[19] C.K. Hall, personal communication, 1991.
[20] L.M. Cohen, *Ph.D. Dissertation*, University of Virginia, Charlottesville, VA, 1992.
[21] B. Skoog, *Vox. Sang.*, 37 (1970) 345–349.
[22] M.A. Eiteman and J.L. Gainer, *Biotechnol. Prog.*, 6 (1990) 479–484.
[23] M.A. Eiteman and J.L. Gainer, *Chem. Eng. Commun.*, 105 (1991) 171–184.

ELSEVIER

Journal of Chromatography A, 668 (1994) 21–30

JOURNAL OF CHROMATOGRAPHY A

Predicting partition coefficients of multi-charged solutes in aqueous two-phase systems

Mark A. Eiteman

Department of Biological and Agricultural Engineering, Driftmier Engineering Center, University of Georgia Athens, GA 30602, USA

Abstract

A mathematical model incorporating the influence of a pH difference between the phases is developed to predict the partitioning of charged compounds in aqueous two-phase systems. The partition coefficients of three model compounds, terephthalic acid, benzenedimethanol and xylylenediamine, are examined in poly(ethylene glycol)–potassium phosphate aqueous two-phase systems over the pH range 5.5–9.2. The model predicts that in this particular phase system, negatively charged solutes partition higher and positively charged solutes partition lower than an otherwise identical neutral solute. The partition coefficients of the dipeptides tyrosine–tyrosine, glycine–tyrosine and leucine–phenylalanine are also examined in poly(ethylene glycol)–potassium phosphate systems, and their observed behaviour agrees with the model prediction. The addition of an alkali metal halide to a poly(ethylene glycol)–potassium phosphate system was observed to result in a decrease in the pH difference between the phases. As the model predicts for decreasing pH difference between the phases, the observed partition coefficients of negatively charged compounds decrease. The results indicate that charge and hydrophobic effects each play important roles in the partitioning of biological compounds.

1. Introduction

Aqueous solutions of two soluble but mutually incompatible components, which as poly(ethylene glycol) (PEG) and dextran, or PEG and certain salts, often form aqueous two-phase systems. Albertsson [1] showed that two liquid "aqueous" phases form when a threshold concentration of either component is exceeded with each phase tending to be enriched by one of the incompatible components. A solute such as a protein added to a two-phase system distributes between the phases, and the partition coefficient is defined as this solute's upper phase concentration divided by its lower phase concentration. Since such systems are composed primarily of water, they have received attention for the liquid–liquid extraction of biomaterials [2–6]. More recent developments have been reviewed [7].

In order to select a particular aqueous two-phase system for a given separation, models are needed to predict partition coefficients. Numerous studies have therefore focused on the general prediction of partition coefficients in aqueous two-phase systems. Partition coefficients depend on several factors including solute hydrophobicity [8,9], molecular mass [10], temperature [2], pH [11–13], solute charge [14] and the presence of additional salts [15,16].

For over 20 years, solute or particle charge has been recognized as one important factor which influences the partition coefficient. Reitherman *et al.* [17] measured an electric potential between

0021-9673/94/$07.00
SSDI 0021-9673(93)E1196-7

phases and correlated the partitioning of negatively charged human erythrocytes with this difference in potential. Johansson [18] showed that the partitioning of proteins could be correlated with salt partitioning. Johansson [19] and Albertsson [20] developed equations to express protein partition coefficients as a function of the protein's net charge and the difference in potential between the phases. However, the mechanism and magnitude of charge effects have remained poorly understood. For example, researchers refer to "charge-sensitive" and "non-charge-sensitive" phase systems and effects when describing behavior that appears to be related in some way to charge [21,22].

A related phenomenon that has been observed is the decrease in the partition coefficients of negatively charged compounds in PEG–phosphate or PEG–sulfate systems as the alkali metal halide concentration is increased [23]. No satisfactory explanation has been advanced for this observation, and it is thus not possible to predict the quantity of a halide needed for a desired reduction in the partition coefficient of a particular solute.

Eiteman and Gainer [24] showed that a measured pH difference between the phases of an aqueous two-phase system affects the partition coefficients of charged solutes. Using a mass balance for all species (charged and uncharged) in a phase system, equations were derived to predict the partition coefficient of a charged solute relative to the partition coefficient of the neutral species alone or an uncharged, but structurally analogous, solute. Specifically, the partition coefficient of a charged solute depends upon the partition coefficient of the uncharged analog, the dissociation of the solute and the pH of each phase. The objectives of this present study were to derive a general expression for the partition coefficients of charged solutes and to compare the predicted behavior with results obtained from partitioning of several solutes.

2. Mathematical model

As noted in the Introduction, the partition coefficient of a neutral solute, K_0, is defined as the concentration of that solute in the upper phase divided by that in the lower phase. This ratio of solute concentrations (c) is related to the ratio of solute mole fractions (x) by a proportionality constant:

$$K_0 = \frac{c_0'}{c_0''} = k \cdot \frac{x_0'}{x_0''} \tag{1}$$

In Eq. 1, a single prime refers to the upper phase and a double prime to the lower phase. The subscript zero emphasizes that the solute is uncharged.

In contrast, the overall (*i.e.*, measured) partition coefficient of a charged solute depends on the partitioning of all charged and uncharged species. For example, the partition coefficient of a solute which may have one positive charge depends upon the partitioning of both the positively charged species (+) and the neutral species:

$$K = k \cdot \frac{x_+' + x_0'}{x_+'' + x_0''} = K_0 \cdot \frac{\frac{x_+'}{x_0'} + 1}{\frac{x_+''}{x_0''} + 1} \tag{2}$$

The partition coefficient of the neutral species alone is again denoted by K_0. The actual measured partition coefficient, K, does not have a subscript, emphasizing that its value includes contributions from the charged and neutral species. At low pH the solute being considered will be exclusively positively charged and, as Eq. 2 indicates, its predicted partition coefficient becomes $K = kx_+'/x_+''$. Similarly, at high pH this solute's measured partition coefficient becomes equal to the partition coefficient of the uncharged species, $K = K_0$.

The solution pH and the charge of any solute are related by an equilibrium. For the positively charged compound (A^0 in the neutral form), the equilibrium is described by

$$A^+ \rightleftharpoons A^0 + H^+ \tag{3}$$

An equilibrium constant, K_{b1}, is defined by

$$K_{b1} = \frac{a_0 a_{H^+}}{a_+} \tag{4}$$

where the subscript b indicates equilibria of

positively charged compounds and the subscript 1 indicates that an uncharged species and a species having a net charge of unity are in equilibrium.

Partitioning occurs at equilibrium, and therefore Eq. 4 must be satisfied for both phases. For the upper phase, Eq. 4 may be rewritten as

$$K_{b1}\gamma'_{+}x'_{+} = \gamma'_{0}x'_{0}a'_{H^0} \tag{5}$$

where each species activity (a) is expressed as the product of its activity coefficient (γ) and mole fraction (x). For convenience, an activity ratio, Λ_+ is defined for each phase as the activity coefficient of the neutral species divided by that of the positive species. Substituting Eq. 5 for each phase into Eq. 2 and noting that $pX = -\log_{10}X$ yields

$$\frac{K}{K_0} = \frac{1 + \Lambda'_{+} \cdot 10^{(pK_{b1} - pH')}}{1 + \Lambda''_{+} \cdot 10^{(pK_{b1} - pH'')}} \tag{6}$$

This equation does not directly predict the partition coefficient of a positively charged solute, but rather predicts the ratio of the solute's partition coefficient to that of the uncharged species alone. This partition ratio depends on the pH in each phase (or $\Delta pH = pH' - pH''$), the activity ratio and the equilibrium constant. Several important practical limitations of this equation have been previously discussed [25].

Eq. 6 may be used in two different ways. It may be used directly to predict the partition coefficient of a charged solute relative to the partition coefficient of an uncharged analog [24,25]. Alternatively, one may predict the partition coefficient of the uncharged species, K_0, using an additional model and then use Eq. 6 to predict the partitioning in systems in which the solute is charged.

2.1. General expressions

In general, a multi-charged solute may have up to m positive charges and up to n negative charges, existing in solution as a distribution of charged species depending on the pH of the solution. The measured partition coefficient is the sum of the concentrations of all the species in the upper phase divided by those of all the species in the lower phase. In terms of mole fractions:

$$K = k \cdot \frac{x'_0 + \sum_{i=1}^{m} x'_{i+} + \sum_{j=1}^{n} x'_{j-}}{x''_0 + \sum_{i=1}^{m} x''_{i+} + \sum_{j=1}^{n} x''_{j-}} \tag{7}$$

At low pH, the general solute has its maximum number of positive charges and minimum number of negative charges. At this pH, the solute's net positive charge will be m, and the solute will be referred to as A^{m+}. As the pH increases, the net charge decreases until the net charge is zero at the isoelectric pH. The solute at this pH, denoted by A^0, has an equal number of positive and negative charges. Increasing pH beyond this point increases the net negative charge to the maximum of n, at which point the solute will be denoted as A^{n-}. These equilibria will be described by

$$\begin{aligned} A^{m+} &\overset{K_{bm}}{\rightleftharpoons} A^{(m-1)+} + H^+ \overset{K_{b(m-1)}}{\rightleftharpoons} A^{(m-2)+} + 2H^+ \\ &\overset{K_{b(m-2)}}{\rightleftharpoons} \cdots \overset{K_{b2}}{\rightleftharpoons} A^{1+} + (m-1)H^+ \\ &\overset{K_{b1}}{\rightleftharpoons} A^0 + mH^+ \overset{K_{c1}}{\rightleftharpoons} A^{1-} + (m+1)H^+ \\ &\overset{K_{c2}}{\rightleftharpoons} \cdots \overset{K_{c(n-1)}}{\rightleftharpoons} A^{(n-1)-} + [m + (n-1)]H^+ \\ &\overset{K_{cn}}{\rightleftharpoons} A^{n-} + (m+n)H^+ \end{aligned} \tag{8}$$

The general equilibrium constants are given by

$$K_{bi} = \frac{a_{(i-1)+}a_{H+}}{a_{i+}} \tag{9}$$

$$K_{cj} = \frac{a_{j-}a_{H+}}{a_{(j-1)-}} . \tag{10}$$

In Eq. 9, i will refer to the equilibrium between a solute of i net positive charges and $i-1$ net positive charges with $1 \leq i \leq m$. Similarly, j indicates the equilibrium between a solute of j net negative charges and $j-1$ net negative charges with $1 \leq j \leq n$. Subscripts b and c refer to equilibria of positively and negatively charged solutes, respectively.

For convenience, a general activity ratio will be defined as the activity coefficient of the

neutral species divided by the activity coefficient of a species of particular charge, q:

$$\Lambda_q = \frac{\gamma_0}{\gamma_q} \tag{11}$$

In order to derive a general expression analogous to Eq. 5, this definition of the activity ratio and the four expressions for species mole fractions (one for each phase and charge) may be substituted into Eq. 7 to obtain

$$\frac{K}{K_0} = \frac{1 + \sum_{i=1}^{m} \Lambda'_{i+} \dfrac{a'^{i}_{H+}}{\prod_{l=1}^{i} K_{bl}} + \sum_{j=1}^{n} \Lambda'_{j-} \dfrac{\prod_{l=1}^{j} K_{cl}}{a'^{j}_{H+}}}{1 + \sum_{i=1}^{m} \Lambda''_{i+} \dfrac{a''^{i}_{H+}}{\prod_{l=1}^{i} K_{bl}} + \sum_{j=1}^{n} \Lambda''_{j-} \dfrac{\prod_{l=1}^{j} K_{cl}}{a''^{j}_{H+}}} \tag{12}$$

Eq. 12 is the general charge expression which may be simplified for particular solutes of interest. For example, for the case of a solute with up to two negative charges (*e.g.*, a dicarboxylic acid such as malic acid), $i = 0$ and $j = 2$. For this particular solute, setting the activity ratios (Λ) equal to unity for simplicity and noting that $pX = -\log_{10} X$, Eq. 12 becomes

$$\frac{K}{K_0} = \frac{1 + \dfrac{K_{c1}}{a'_{H+}} + \dfrac{K_{c1}K_{c2}}{a'^{2}_{H+}}}{1 + \dfrac{K_{c1}}{a''_{H+}} + \dfrac{K_{c1}K_{c2}}{a''^{2}_{H+}}} = \frac{1 + 10^{pH' - pK_{c1}} + 10^{2pH' - pK_{c1} - pK_{c2}}}{1 + 10^{pH'' - pK_{c1}} + 10^{2pH'' - pK_{c1} - pK_{c2}}} \tag{13}$$

Since the equilibrium constants for solutes are often available or measureable, Eq. 13 requires only that the pH be measured in each phase. One important trend predicted by Eq. 12 is that in systems having a positive pH difference between the phases, the partition ratio for a negatively charged solute is greater than unity [24]. In other words, a negatively charged solute will have a greater partition coefficient than a neutral analog in such phase systems. Similarly, a positively charged solute will have a lower partition coefficient than a neutral analog. In order to calculate the actual partition coefficient of a charged solute, the partition coefficient of the uncharged species alone must be measured or calculated by a model which considers all non-charge effects.

The objectives of this study were (1) to compare qualitatively the partitioning of uncharged and multicharged analogs, (2) to predict with Eq. 12 the partition coefficients of several dipeptides over a range of pH (using an additional model to predict K_0) and (3) to determine the effect that addition of sodium chloride has on the properties of a PEG–potassium phosphate system and the predicted and observed partition coefficients of uncharged and charged solutes.

3. Experimental

A series of 1.00 *M* potassium phosphate solutions was prepared as described elsewhere [24,26]. The phase-forming polymer used in these solutions was PEG with a molecular mass of 8000, and 2.00 g of this polymer were used per 10 ml of phosphate solution. The resulting phase systems at 25.0°C had a positive pH difference between the phases, that is, the measured pH of the upper phase was greater than the pH of the lower phase, as reported previously [24].

Phase systems with sodium chloride were prepared by mixing 5 ml of 2.00 *M* potassium phosphate solution with 5 ml of NaCl solution prior to adding 2.00 g of PEG 8000. The final salt concentration in the phase systems (prior to the addition of polymer) is the value reported. The pH of each phase of these PEG–phosphate–chloride systems was measured as before [24].

The following solutes were used for partitioning studies: tryptamine, indole-3-acetic acid, tyrosine–tyrosine, glycine–tyrosine, leucine–phenylalanine (Sigma, St. Louis, MO, USA), benzene-1,4-dimethanol, terephthalic acid and 1,4-xylylenediamine (Aldrich, Milwaukee, WI, USA).

Approximately 5 mg of a single solute were added to 10 ml of two-phase solutions. The phases were adjusted to 25.0 ±0.05°C, thorough-

ly mixed for 2 days, allowed to equilibrate for 3 days, then carefully separated with Pasteur pipets immediately before analysis. The partition coefficients of other solutes at 25.0°C were determined by HPLC. The HPLC system consisted of a Gilson Model 306 pump, a Model 231 Autosampler and an Applied Biosystems Model 759A UV–Vis detector. The column was a Waters Radial-Pak C_8, with eluent and detector settings appropriate to separate and quantify the pure solute of interest from impurities arising from the PEG and solute sample.

4. Results and discussion

One objective of this research was to observe whether a multi-charged solute has a different partition coefficient than an analogous uncharged solute. Since solute hydrophobicity influences its partitioning, charged and uncharged analogs having an identical hydrophobicity were selected. Fig. 1 shows the partition coefficients of three compounds in the PEG–potassium phosphate system: terephthalic acid (which is negatively charged), benzenedimethanol (neutral), and 1,4-xylylenediamine (positively charged). The carboxylic acid, methylene-ol, and methylene-amine functional groups have approximately the same hydrophobicity [27]. The partition coefficient of the negatively charged diacid was observed to be greater than that of the neutral

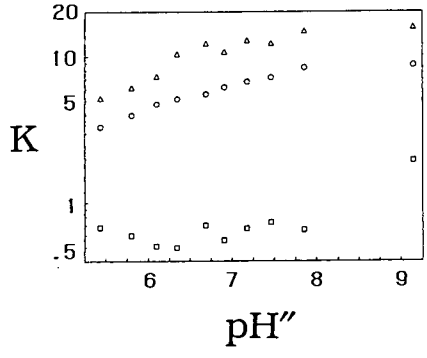

Fig. 1. Observed partition coefficients of (○) benzenedimethanol, (△) terephthalic acid and (□) 1,4-xylylenediamine in a series of PEG–potassium phosphate aqueous two-phase systems

analog, which itself was observed to be greater than those of the positively charged diamine. The results qualitatively agree with those predicted by Eq. 12 for a phase system of positive pH difference between the phases.

A second goal was to predict the partition coefficients of peptides over a range of pH. Several dipeptides were selected for this study: tyrosine–tyrosine, leucine–phenylalanine and glycine-tyrosine. Assuming that all activity ratios in Eq. 12 are equal to unity, the parameters required to predict the partition coefficients for these peptides in the PEG–potassium phosphate systems are the pH in each phase (previously measured [24]), the equilibrium constants of these solutes (shown in Table 1) and the values for the partition coefficients of the uncharged species, K_0. The value of K_0 will be estimated by an additional model.

A model to predict the partition coefficients of hypothetical uncharged amino acids and peptides in the PEG–potassium phosphate systems was advanced by Eiteman and Gainer [26]:

$$\ln K_0 = D\,\Delta w_2 \log(P/P_0) \qquad (14)$$

This simple model contains two parameters which describe a phase system. The discrimination factor, D, and the intrinsic hydrophobicity, $\log(P_0)$, have been previously determined for the PEG–potassium phosphate system [26]. Log P is the hydrophobicity (a theoretical distribution between octanol and water) of the particular solute, and Δw_2 is the PEG concentration difference between the phases and have been measured previously [26] for the PEG–potassium phosphate system. Values for the hydrophobicity of each of the three dipeptides studied are listed in Table 1.

The value of K_0 for each phase system was calculated by Eq. 14 for these three solutes. Eq. 12 was then used to predict the partition coefficient of each dipeptide in the phase systems. Figs. 2, 3 and 4 show the observed and predicted partition coefficients for tyrosine–tyrosine, leucine–phenylalanine and glycine–tyrosine, respectively. The partition coefficient of all three solutes was greatest at high pH. The model

Table 1
Hydrophobicity (log P) and equilibrium (dissociation) constants for the dipeptides used in this study

Solute	Log P	pK_{b1}	pK_{c1}	pK_{c2}	pK_{c3}
Tyr–Tyr	1.27[a]	3.52[b]	7.68[b]	9.80[b]	10.26[b]
Leu–Phe	0.06[c]	2.85	8.41[d]	–	–
Gly–Tyr	−1.12[c]	2.93[b]	8.45[b]	10.49[b]	–

[a] Ref. 9.
[b] Ref. 28.
[c] Ref. 29.
[d] Ref. 30.

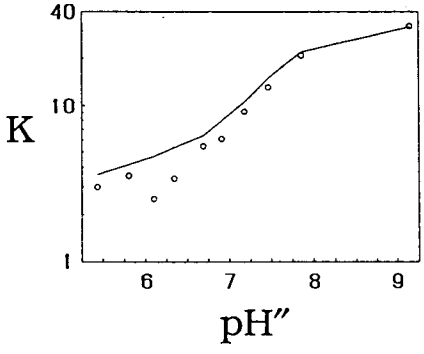

Fig. 2. Observed and predicted partition coefficients of the dipeptide tyrosine–tyrosine in a series of PEG–potassium phosphate aqueous two-phase systems. Predictions using Eq. 12 are indicated by the solid curve.

predicted this observation and the magnitudes of the partition coefficients very well. The observed partition coefficients of tyrosine–tyrosine were predicted most closely. The observed partition coefficients of leucine–phenylalanine showed an inexplicable maximum at a pH of *ca.* 8. Partition coefficients lower than unity were observed and predicted for glycine–tyrosine, although the partition coefficient at the highest pH was underpredicted.

As noted in the Introduction, the addition of alkali metal halides to phase systems has been known to influence partition coefficients of charged compounds significantly. Another objective of this study was to determine if these observed changes in partition coefficients could be explained in terms of a pH difference between the phases. The addition of what amounts to another component to a phase system may also have several unavoidable consequences. Considering Eq. 14, the addition of salt may alter the concentration difference between the

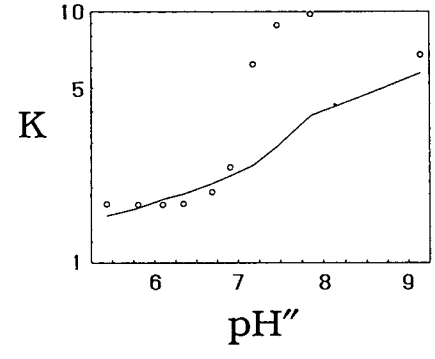

Fig. 3. Observed and predicted partition coefficients of the dipeptide leucine–phenylalanine in a series of PEG–potassium phosphate aqueous two-phase systems. Predictions using Eq. 12 are indicated by the solid curve.

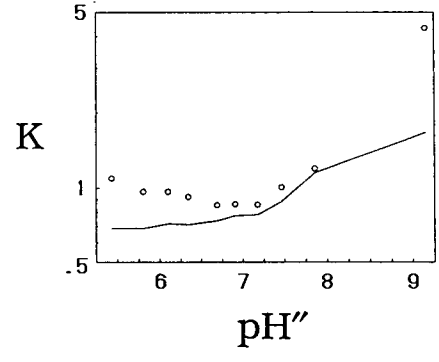

Fig. 4. Observed and predicted partition coefficients of the dipeptide glycine–tyrosine in a series of PEG–potassium phosphate aqueous two-phase systems. Predictions using Eq. 12 are indicated by the solid curve.

phases, the discrimination factor and the instrinsic hydrophobicity of the phase system. New values for each of these parameters would affect the partition coefficient calculated for uncharged compounds. Naturally, the addition of salt might also alter the pH difference between the phases, a consequence which, by itself, would alter only the partitioning of charged compounds.

To examine the effect of an alkali metal halide addition on the model parameters, a single PEG–phosphate phase system (without alkali metal halide) was selected having a lower phase pH of 8.0. Sodium chloride was added to this phase system, resulting in six PEG–phosphate–chloride phase systems with NaCl concentrations ranging from 0.0 to 2.0 *M*. In order to remove at least one variable, all systems were prepared to have identical PEG concentration differences between the phases. This continuity was accomplished by reducing the concentration of potassium phosphate (to a minimum of about 0.8 *M*) as the sodium chloride concentration was increased.

Fig. 5 shows the pH measured in each phase of the six phase systems. As the concentration of salt was increased, the pH in each phase decreased. More importantly, as the concentration of sodium chloride was increased, the pH difference between the phases decreased. At a concentration of 2.0 *M* sodium chloride, the pH difference between the phases was essentially zero. The pH difference decreased most quickly at low NaCl concentrations: between 0.0 and 0.2 *M* NaCl, the value of ΔpH decreased from 0.54 to 0.17, while between 1.0 and 2.0 *M* it decreased from only 0.05 to 0.02. Additional studies with PEG–phosphate–chloride phase systems all having a 1.00 *M* phosphate concentration showed similar pH difference behavior. Therefore, the decrease in pH difference was due to the increase in NaCl concentration, not the slight reduction in phosphate concentration required to maintain an identical PEG concentration difference between the phases.

Eq. 12 predicts that if a positive pH difference between the phases is reduced, the partition coefficient of negatively charged compounds will decrease, while the partition coefficient of positively charged compounds will increase. In order to test this prediction, two analogous compounds, indoleacetic acid and tryptamine, were partitioned in these six phase systems. These two compounds have approximately identical hydrophobicities [27], but the acid is negatively charged at pH 7.5–8.0, while the amine is positively charged in solutions in this pH range. Fig. 6 shows the results of partitioning these two compounds in the six PEG–phosphate–chloride systems.

As predicted, the partition coefficient of the negatively charged acid decreased while the partition coefficient for the positively charged amine increased. Furthermore, the rate of change in these partition coefficients decreased

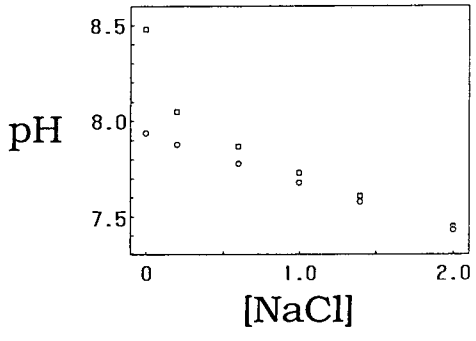

Fig. 5. Observed pH of phases (○ = lower and □ = upper phase) in a PEG–potassium phosphate–sodium chloride aqueous two-phase system (90% dibasic) as a function of sodium chloride concentration.

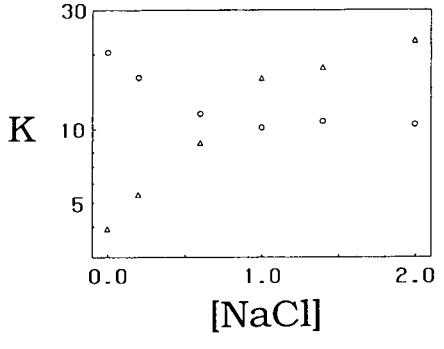

Fig. 6. Observed partition coefficients of (△) tryptamine and (○) indole-3-acetic acid in a PEG–potassium phosphate–sodium chloride aqueous two-phase system (90% dibasic) as a function of sodium chloride concentration.

at higher salt concentrations, where the rate of decrease in the pH difference between the phases was reduced. The difference between the partition coefficients of these two compounds at the highest NaCl concentration, where the charge effects should be negligible since $\Delta pH \approx 0$, might be due to a slight difference in the hydrophobicities of the two compounds or to other interactions between the solutes and components.

The partitioning of the three dipeptides was next reconsidered in these PEG–phosphate–chloride phase systems. Again, Eq. 14 was used to predict the theoretical partition coefficients of the uncharged dipeptide species. In this case, the values for the two parameters, the discrimination factor and the intrinsic hydrophobicity, were assumed to remain constant in phase systems of varying sodium chloride concentration. This simplification means that the value of K_0 calculated by Eq. 14 is the same for all sodium chloride concentrations. As before, with the value of K_0, the pH measured in each phase and the equilibrium constants, Eq. 12 may be used to predict the partition coefficients of these dipeptides as sodium chloride is added.

Figs. 7, 8 and 9 show the measured and predicted partition coefficients for tyrosine–tyrosine, leucine–phenylalanine and glycine–tyrosine, respectively, in PEG–potassium phosphate systems of increasing sodium chloride concentration. The measured partition coefficients for tyrosine–tyrosine were observed to decrease from about 22 to 14 as the concentration of sodium chloride in the phase system was increased. The model successfully predicted that the partition coefficients of this dipeptide will decrease initially with increasing sodium chloride concentration, but generally underestimated the partition coefficients. The predicted partition coefficients agreed with the observation that the partition coefficients change more slowly as more salt was added.

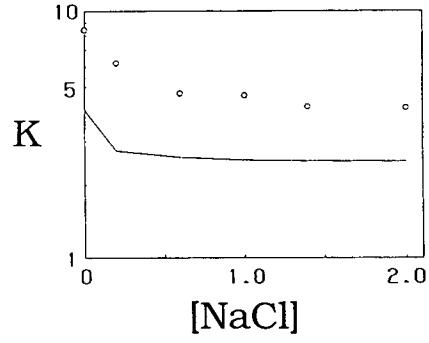

Fig. 8. Observed and predicted partition coefficients of leucine–phenylalanine in a PEG–potassium phosphate–sodium chloride aqueous two-phase system (90% dibasic) as a function of sodium chloride concentration.

The measured partition coefficients for leucine–phenylalanine shown in Fig. 8 similarly decreased with increasing sodium chloride concentration, in this case from about 8.5 to 4. The model prediction again underestimated the partition coefficients, but the trend agreed with the

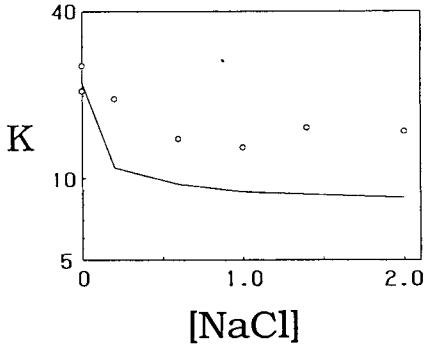

Fig. 7. Observed and prediction partition coefficients of tyrosine–tyrosine in a PEG–potassium phosphate–sodium chloride aqueous two-phase system (90% dibasic) as a function of sodium chloride concentration.

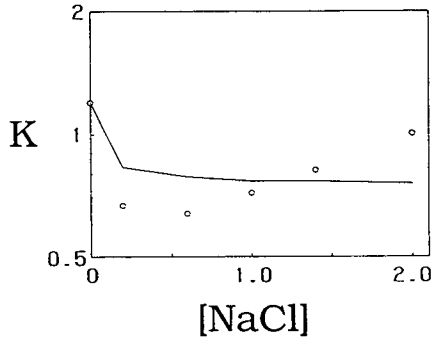

Fig. 9. Observed and predicted partition coefficients of glycine–tyrosine in a PEG–potassium phosphate–sodium chloride aqueous two-phase system (90% dibasic) as a function of sodium chloride concentration.

observation. In this case, the partition coefficient predicted at zero salt concentration was also significantly underestimated (as noted in Fig. 3). The predicted and observed partition coefficients again decreased more slowly as more salt was added.

The measured partition coefficients for glycine–tyrosine (Fig. 9) decreased with increasing sodium chloride up to a concentration of about 0.6 *M*, then increased slowly with a further increase in salt concentration. At this point, glycine–tyrosine also shifted from partitioning predominantly into the upper phase to partitioning predominantly into the lower phase. The model correctly predicted the decrease in partition coefficient from above to below unity, but did not predict the subsequent increase in partition coefficient as the sodium chloride concentration was further increased.

Discrepancies between the observed and predicted partition coefficients could be explained as resulting from the assumption that the discrimination factor and intrinsic hydrophobicity remained constant as sodium chloride was added, or from the assumption that the activity ratios were equal to unity. The observed increase in partition coefficient for glycine–tyrosine suggests another mechanism. One should note that the two equations used in the prediction of partition coefficients of the dipeptides, Eqs. 12 and 14, contain no adjustable parameters. Eq. 12 contains exclusively measurable quantities: the pH and the equilibrium constants. Eq. 14 contains quantities that are determined independently (log P, log P_0, D) and one which is directly measured (Δw_2).

5. Conclusions

Solutes of different charge do not necessarily partition preferentially into different phases. Rather, changing the charge of a solute shifts the partition coefficient of the compound. The size of this shift depends on the pH difference between the phases and the dissociation constants for the two charged compounds. As Eq. 12 predicts for a system having a positive pH difference between the phases, a negatively charged solute has a greater partition coefficient than an otherwise identical neutral solute, which in turn is greater than that for a positively charged solute. The partition coefficients of solutes may be predicted by considering models which account for both a charge effect (as discussed here) and a hydrophobic effect (as discussed elsewhere).

Addition of an alkali metal halide to the PEG–phosphate phase system decreased the positive pH difference between the phases and, as the model predicted, decreased the partition coefficients of negatively charged compounds and increased the partition coefficients of positively charged compounds. Observed partition coefficients of glycine–tyrosine did not follow this prediction at high pH. The partition coefficient of this solute also was predicted and observed to shift from a value greater than unity to a value lower than unity as this salt was added. These results suggest that the proper selection of pH, phase system and salt concentration could greatly enhance the separation of solutes.

6. Acknowledgements

The author expresses his thanks to Joby Miller and Daphne Golden for technical support and to the Georgia Agricultural Experiment Stations for financial support of this research.

7. References

[1] P.-Å. Albertsson, *Nature*, 182 (1958) 709.
[2] P.-Å. Albertsson, in *Partition of Cell Particles and Macromolecules*, Wiley, New York, 1986, pp. 28, 212–226.
[3] A. Veide, A.-L. Smeds and S.-O. Enfors, *Biotechnol. Bioeng.*, 25 (1983) 1789–1800.
[4] H. Walter, D.E. Brooks and D. Fisher (Editors), *Partitioning in Aqueous Two-Phase Systems*, Academic Press, New York, 1985, pp. 161–589.
[5] H. Hustedt, K.H. Kroner, U. Menge and M.-R. Kula, *Trends Biotechnol.*, 3 (1985) 1–6.
[6] B. Mattiasson and R. Kaul, *ACS Symp. Ser.*, 314 (1986) 78–92.

[7] H. Walter, G. Johansson and D.E. Brooks, *Anal. Biochem.*, 197 (1991) 1–18.
[8] V.P. Shanbhag and C.-G. Axelsson, *Eur. J. Biochem.*, 60 (1975) 17–22.
[9] M.A. Eiteman and J.L. Gainer, *Biotechnol. Prog.*, 6 (1990) 479–484.
[10] P.-Å. Albertsson, A. Cajarville, D.E. Brooks and F. Tjerneld, *Biochim. Biophys. Acta*, 926 (1987) 87–93.
[11] P.-Å. Albertsson, S. Sasakawa and H. Walter, *Nature*, 228 (1970) 1329–1330.
[12] H. Walter, S. Sasakawa and P.-Å. Albertsson, *Biochemistry*, 11 (1972) 3880–3883.
[13] C.L. DeLigny and W.J. Gelsema, *Sep. Sci. Technol.*, 17 (1982) 375–380.
[14] R.S. King, H.W. Blanch and J.M. Prausnitz, *AIChE J.*, 34 (1988) 1585–1594.
[15] S. Bamberger, G.V.F. Seaman, J.A. Brown and D.E. Brooks, *J. Colloid Interface Sci.*, 99 (1984) 187–193.
[16] B.Yu. Zaslavsky, L.M. Miheeva, G.Z. Gasanova and A.U. Mahmudov, *J. Chromatogr.*, 392 (1987) 95–100.
[17] R. Reitherman, S.D. Flanagan and S.H. Barondes, *Biochim. Biophys. Acta*, 297 (1973) 193–202.
[18] G. Johansson, *Acta Chem. Scand., Ser. B*, 28 (1974) 873–882.
[19] G. Johansson, *Mol. Cell. Biochem.*, 4 (1974) 169–180.
[20] P.-Å. Albertsson, *J. Chromatogr.*, 159 (1978) 111–122.
[21] C. LaMarca, A.M. Lenhoff and P. Dhurjati, *Biotechnol. Bioeng.*, 36 (1990) 484–492.
[22] C.-K. Lee and S.I. Sandler, *Biotechnol. Bioeng.*, 35 (1990) 408–416.
[23] O. Cascone, B.A. Andrews and J.A. Asenjo, *Enzyme Microb. Technol.*, 13 (1991) 629.
[24] M.A. Eiteman and J.L. Gainer, *Chem. Eng. Commun.*, 105 (1991) 171–184.
[25] M.A. Eiteman, *Sep. Sci. Technol.*, in press.
[26] M.A. Eiteman and J.L. Gainer, *J. Chromatogr.*, 586 (1991) 341–346.
[27] R.F. Rekker and H.M. de Kort, *Eur. J. Med. Chem. Chim. Ther.*, 14 (1979) 479–488.
[28] D.D. Perrin, in *Dissociation Constants of Organic Bases in Aqueous Solution*, Butterworths, London, 1965, p. 403.
[29] M.A. Eiteman and J.L. Gainer, *Biochim. Biophys. Acta*, 1073 (1991) 451–455.
[30] T. Hirokawa, T. Gojo and K. Yoshiyuki, *J. Chromatogr.*, 390 (1987) 201–223.

ELSEVIER

Journal of Chromatography A, 668 (1994) 31–45

JOURNAL OF CHROMATOGRAPHY A

Application of a statistical geometrical theory to aqueous two-phase systems

Yue Guan[a,b], Timothy E. Treffry[a], Terence H. Lilley[*,b]

[a]*Department of Molecular Biology and Biotechnology, and Krebs Institute for Biomolecular Research, The University, Sheffield S10 2UH, UK*

[b]*Biothermodynamics Laboratory, Department of Chemistry, and Krebs Institute for Biomolecular Research, The University, Sheffield S3 7HF, UK*

Abstract

In a recent publication, we presented a novel theory based on a statistical geometric concepts which gave a simple analytical expression for the coexistence curves (binodals) of aqueous two-phase systems. In the present paper, this theory (which we term the binodal model) has been applied, with considerable success, to polymer + polymer and polymer + salt aqueous two-phase systems. For polyethylene glycol (PEG) + Dextran (Dex) aqueous two-phase systems, the binodal model gives satisfactory agreement with experiment when the molar mass ratio of Dex to PEG $\geq ca.$ 4. For PEG + salt aqueous two-phase systems, where the molar mass ratio of PEG to salt is almost invariably large, the binodal model works well. The model also explains the influence of both temperature and polymer molar mass on binodals and confirms the experimental observation found for some systems that under some circumstances the lower-molar-mass polymer can induce phase separation at lower concentrations than the polymer with the higher molar mass.

1. Introduction

Aqueous two-phase systems provide benign and non-destructive environments for biosepa-ration processes. Systems such as these are attractive in that they provide a means of separation which is, easy to manipulate, reliable in scaling-up, simple and effective in operation. A major objective of our recent work on aqueous two-phase systems is toward the establishment of soundly based, predictive methods for the determination of the system variables which give very efficient separation and purification of biomacromolecules under commercial conditions.

The prediction of the behaviour of aqueous systems is a notoriously difficult problem. Some approaches which have been used to solve problems associated with the formation of aqueous two-phase systems and/or protein partitioning behaviour in these systems are polymer lattice theories [1,2], the UNIQUAC and UNIFAC models [3–5], osmotic virial expansions [6], polymer scaling analyses [7] and the generalised means-spherical approximation [8].

Most of the protein partitioning models currently available are applicable only to very low protein concentrations, but any process using aqueous two-phase systems which could be applicable in an industrial situation would need to use high biomass loadings. We have recently demonstrated the feasibility of using aqueous two-phase partitioning to extract, from systems

* Corresponding author.

0021-9673/94/$07.00
SSDI 0021-9673(94)00002-Q

containing biomass loadings of up to 15% (w/v), the commercially important intracellular enzyme, penicillin acylase [9,10]. As well as introducing the problem of an extra insoluble phase when, for example, the protein concentration (or the total biomaterial concentration) is high enough for protein–protein molecular interactions to contribute significantly to the thermodynamic properties of these systems, perturbations of phase behaviour must also occur. Given, however, the hydrophilic nature of the protein surface, rather than having a system with two phase-forming components, in effect, such a system would now consist of three phase-forming components.

An aqueous two-phase system for protein separation contains at least four components, but molecular information on interactions between components can be obtained by studying some three-component systems, one of which is the aqueous two-phase system without the addition of biomacromolecules to be separated. Information of this nature is useful and applicable to systems containing both low and high concentrations of biomacromolecules. At very low protein concentrations, the contribution of protein to the formation of a two-phase system need not be considered since the molecular environment of the phase-forming components before and after the addition of protein is essentially unchanged. In contrast, at high total protein concentration, as mentioned above, the protein can also act as a phase-forming polymer and so initiate a redistribution of the primary phase-forming components with consequent perturbation of the phase diagram and it is the modified system which now controls the partitioning of the protein of interest.

In phase diagrams the axes give the concentrations of the phase-forming components and a curve, the binodal, separates the two-phase region, which is distal to the origin, from the single-phase region lying between the axes and the binodal. In a three-component system (solvent + two solutes), for any particular pair of solute concentrations leading to two phases in equilibrium, the concentrations of the solute components in each phase lie at two points on the binodal. A line connecting these points (the tie-line) must (because of material balance considerations) pass through a point on the phase diagram which represents the imaginary concentration of the phase-forming components in the bulk system: this point must divide the tie-line in the same proportion as the ratio of the masses of the phases. A necessary first step in quantifying the partitioning of a protein is the complete description of the phase diagram. At low protein concentrations, one of the "driving forces" for protein partitioning can be ascribed to the concentration of either of the phase-forming components. There are several ways to express this "driving force" such as the tie-line length [6] and the concentration difference of a phase-forming component between the two phases [11]. Our philosophy in dealing with problems on such systems has been that any adequate approach should be (i) consistent with thermodynamics, and (ii) applicable to both phase-forming components ("1" and "2") + water ternary systems and to phase-forming components ("1" and "2") + water + biomolecule quaternary systems. As mentioned above, although the Flory–Huggins theory, osmotic virial expansions, UNIQUAC and integral-equation approaches have been applied to these problems with some success, all have shortcoming when the complete calculation of phase diagrams is sought, or if protein distribution is to be predicted. However, notwithstanding the deficiencies of these approaches some useful and quite general empirical relationships of phase diagrams of aqueous two-phase systems have been suggested recently.

If we consider the application of the empirical Setchenow equation [12] (which can be related to osmotic virial expansions under restricted conditions [13]) to aqueous two-phase systems, we may write

$$\ln \frac{w_i^{\mathrm{T}}}{w_i^{\mathrm{B}}} = \beta_i + k_j^i (w_j^{\mathrm{B}} - w_j^{\mathrm{T}}) \qquad (1)$$

where k_j^i is the Setchenow salting-out coefficient of the ith component by the jth component, β_i is a constant accounting for the activity coefficient of the ith component in the coexisting phases,

$w_i^T(w_j^T)$ and $w_i^B(w_j^B)$ are the mass concentrations of species i (j) in the top and bottom phases, respectively. The correlation by Vainerman *et al.* [14] indicates that for aqueous two-phase systems the coefficient β_i is close to zero compared to the term $(w_i^B - w_i^T)$ and so we obtain the following expressions linking the compositions of the phase-forming components:

$$\ln \frac{w_1^T}{w_1^B} = \alpha_1(w_2^T - w_2^B) \quad (2a)$$

or

$$\ln \frac{w_2^T}{w_2^B} = \alpha_2(w_1^T - w_1^B) \quad (2b)$$

A somewhat unexpected feature is that the experimental information which is available indicates that Eqs. 2a and 2b are applicable to both polymer + polymer and polymer + salt aqueous two-phase systems [14]. Independently, Diamond and Hsu [15] obtained Eqs. 2a and 2b from the Flory–Huggins theory [16] and further compared them with a number of experimental results. However, the derivation used and the assumptions on which this is based are such that, at best, it could only apply to polymer + polymer aqueous two-phase systems and it is difficult to justify its use to systems containing salts. Using a different approach we have recently demonstrated [17] that one can also arrive at Eqs. 2a and 2b using what we call empirical "effective" osmotic virial coefficients for polymer + polymer aqueous two-phase systems but this approach has similar theoretical limitations regarding its application to systems containing electrolytes.

Even assuming the correctness of Eqs. 2a and 2b, they are insufficient to describe the phase diagram or even the binodal, and to get this some further relations are needed.

A novel approach [18], which we term the "binodal model," to the description of phase diagrams has been made very recently using the concepts of statistical geometry and, as a consequence, it has been shown that most of the binodals used in polymer + polymer aqueous two-phase systems can be described by

$$\ln\left(\langle V\rangle_{210}\frac{\rho N_A w_2}{\langle M\rangle_2}\right) + \langle V\rangle_{210}\frac{\rho N_A w_1}{\langle M\rangle_1} = 0 \quad (3)$$

where $\langle V\rangle_{210}$ is the effective excluded volume (EEV) of species 2 in the species 1 aqueous solution, ρ is the solution density, N_A is Avagadro's constant $\langle M\rangle_1$ and $\langle M\rangle_2$ are mean molar masses for species 1 and 2, and usually the root-mean-square average molar masses for polydisperse components are taken. One advantage of Eq. 3 over Eqs. 2a and 2b is that it describes the entire binodal using only one parameter which has a clearly defined physical meaning. An important feature of Eq. 3 is that Eqs. 2a and 2b can be derived from it, but the converse does not apply.

It is worth mentioning that although most of the existing theories or semiempirical treatments contain a logarithmic first term, they generally cannot be truncated to the form of the binodal model [17].

In the present paper we outline the theoretical bases of our binodal model and demonstrate situations where this model can be applied. Another objective of the present work is to collect most of the available phase diagram data for both polymer + polymer and polymer + salt aqueous two-phase systems to (i) determine the experimental validity of the binodal model and (ii) its range of suitability for different types of systems, and (iii) calculate and collect "effective excluded volume" parameters for different systems to guide subsequent engineering design of aqueous two-phase systems for bioseparation.

2. Theoretical aspects

A detailed description of the approach we have used to derive the binodal model has been given elsewhere [18] and in this section we simply outline a summary of the assumptions necessary to formulate this theory. We also, however, include some of the more mathematical details which were not stressed in the earlier paper.

Our analyses of the phase separation problem for polymer + polymer aqueous two-phase systems are based on the following assumptions:

(i) Molecules of the same species are distributed at random in a homogeneous phase.

(ii) On the coexistence curve, the structure of the solution is geometrically saturated [18] in terms of the sizes and shapes of all of the molecules in the system.

(iii) The existence of molecular interactions does not change the nature of this random molecular distribution and, on the coexistence curve, their effects are exhibited simply as an adjustment of the average distances between the unlike molecular centres.

Assumption i can include situations where specific association effects at the molecular level are very strong if the aggregated species are taken to be the primary components. For example, for a semi-ordered liquid phase such as a micellar solution [19], one must regard the associated "polymers" as the solutes and it is these to which the random distribution assumption is applied. In making assumption ii, we have indicated that the solution structures before and after (or from) phase separations are different. Before phase separation (*i.e.* in the one-phase region), solute molecules are separated so that additional solute molecules can still be inserted into the free space which is present. At the point of phase separation, the solute molecules are now so closely packed that the solution is not able to accept any additional solute molecules and when the total solute concentration is increased, what happens is the formation of two geometrically saturated yet structurally quite different solutions. The further the system is from the critical point (the plait point), the more different are the structures of these two saturated solutions. Assumption iii recognises an important phenomenon which has been verified by computer simulations [20], *viz.* that molecular interactions are not always necessary for the occurrence of phase separation.

For an aqueous solution containing two very soluble solutes (or indeed any other binary solute solution in a "good" solvent), when the steric hindrance of the water molecules to the solutes is small compared with that between the two solute species (under these circumstances we say the two solute components are "geometrically incompatible"), we can regard the system as a pseudo-binary system. To model such a system we consider the size distribution of convex "holes" in a network of species i which could possibly accommodate molecules of type j. If we let ν_i and ν_j be the corresponding molecular number densities, φ_i the probability density function of finding holes with a volume at least V in the molecular centre network formed by species i, then it has been shown [18] that

$$\varphi_i(V)\,\mathrm{d}V = \lambda_{i(01)}(V)\,\mathrm{d}V \int_0^\infty \varphi(x)\,\mathrm{d}x \tag{4}$$

where $\lambda_{i(01)}(V)$ is a function which only depends on the hole size in the molecular centre network of species i, $\lambda_{i(01)}(V)\,\mathrm{d}V$ is the conditional probability that the infinitesimal shell of volume $\mathrm{d}V$ contains one molecular centre of species i when there is no molecular centre of species i in the volume V (see Fig. 1). According to this definition, when $\nu_i \neq 0$, $\lambda_{i(01)}(V)\,\mathrm{d}V$ must always adopt positive values and must not be a decreasing monotonic function, *i.e.*

$$\lambda_{i(01)}(V_2)\,\mathrm{d}V_2 \geqslant \lambda_{i(01)}(V_1)\,\mathrm{d}V > 0 \quad (V_2 > V_1) \tag{5}$$

Using Eq. 5, we obtain

$$\int_0^\infty \lambda_{i(01)}(V)\,\mathrm{d}V = \infty\,, \tag{6}$$

which will be used later. Solving Eq. 4 gives

$$\varphi_i(V) = \frac{\varphi_i(0)}{\lambda_{i(01)}(0)} \cdot \lambda_{i(01)}(V) \exp\left[-\int_0^V \lambda_{i(01)}(x)\,\mathrm{d}x\right] \tag{7}$$

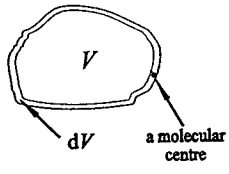

Fig. 1. Diagram illustrating a convex cavity of volume V in a network of species "i" where only single molecular centre of component i occupies the infinitesimal shell of volume $\mathrm{d}V$ around this cavity.

Substituting Eq. 7 into the following restriction to $\varphi_i(V)$:

$$\int_0^\infty \varphi_i(V)\,dV = 1 \tag{8}$$

Noting the following relation:

$$d\exp\left[-\int_0^V \lambda_{i(01)}(x)\,dx\right] = -\lambda_{i(01)}(V)\,dV \exp\left[-\int_0^V \lambda_{i(01)}(x)\,dx\right] \tag{9}$$

and Eq. 6, we get: $\varphi_i(0)/\lambda_{i(01)}(0) = 1$ and so Eq. 7 becomes

$$\varphi_i(V) = \lambda_{i(01)}(V)\exp\left[-\int_0^V \lambda_{i(01)}(x)\,dx\right] \tag{10}$$

Using Eq. 10, the probability of finding interstitial spacings V adjacent to molecules of species i is given by

$$P(\underline{V} \geq V) = \int_V^\infty \varphi_i(V)\,dV = \exp\left[-\int_0^V \lambda_{i(01)}(x)\,dx\right] \tag{11}$$

where $P(\underline{V} \geq V)$ is the probability of finding a cavity of volume at least V. The function $\lambda_{i(01)}(V)$ may be determined by the following further restriction to $\varphi_i(V)$:

$$\int_0^\infty V\varphi_i(V)\,dV = \frac{1}{\nu_i} \tag{12}$$

Substituting Eq. 10 into Eq. 12 gives

$$\int_0^\infty \exp\left[-\int_0^V \lambda_{i(01)}(x)\,dx\right] dV = \frac{1}{\nu_i} \tag{13}$$

If, since in our model the molecular distribution is random, we consider, for guidance, the random spheres model where molecules are mutually penetrable [21], we expect:

$$\lambda_{i(01)}(V) = \text{constant} \tag{14}$$

and by insertion of Eq. 14 into Eq. 13, we determine $\lambda_{i(01)} = 1/\nu_i$ and so Eq. 11 becomes

$$P(\underline{V} \geq V) = \exp(-V\nu_i) \tag{15}$$

However, molecular repulsions become ever more significant and the deviations from completely random behaviour become greater as the distance between molecular centres becomes smaller. If for mathematical simplicity and for purposes of illustration a linear repulsion is assumed, *i.e.*

$$\lambda_{i(01)} = \gamma V \tag{16}$$

where γ is a constant, then insertion of Eq. 16 into Eq. 13 leads to $\lambda_{i(01)}(V) = \pi\nu_i^2 V/2$. Correspondingly, Eq. 11 becomes

$$P(\underline{V} \geq V) = \exp\left(-\frac{\pi}{4}\cdot\nu_i^2 V^2\right) \tag{17}$$

We conclude from this that Eq. 15 is a reasonable approximation to the real systems when the minimum hole size is relatively large and Eq. 17 is a plausible approximation when this hole size is relatively small. For the particular systems which we are considering here, since the size of the cavity is at least that of the effective excluded volume (which is greater than the molecular size of either species), Eq. 15 should be a good approximation.

Combination of Eq. 15 with assumption ii, for the pseudo-binary system i–j–0 [18] allows us to write:

$$e^{-V_{ji0}\nu_i} = V_{ji0}\nu_j + f_{ji0} \tag{18}$$

where V_{ji0} is the effective excluded volume of species j in the species i aqueous solution, and is the minimum volume in the molecular centre network of species i which holds an individual j molecule, and f_{ji0} represents the volume fraction of unfilled effective available volume after tight packing of species j in the network of species i aqueous solution.

We now define a new parameter, R, the ratio of molecular masses of the two phase-forming components, as

$$R = \frac{\langle M\rangle_j}{\langle M\rangle_i} \tag{19}$$

Usually, for most systems of interest [*e.g.*, the phase-forming components are polyethylene glycol (PEG) + Dextran (Dex) or PEG + salt], the value of R is greater than unity. It should be noted that as R becomes large f_{ji0} approaches

zero, and consequently, the coexistence curves of most aqueous two-phase systems may be simply expressed as:

$$\exp(-V_{ji0}\nu_i) = V_{ji0}\nu_j \tag{20}$$

3. The use of Eq. 20

There are usually two types of aqueous two-phase systems currently adopted for bioseparations of biomacromolecules, *viz.* polymer + polymer and polymer + salt systems. For polymer + polymer systems, the difference of the densities of the two equilibrated phases is so small that one can neglect this difference in modelling the phase diagram. For polymer + salt systems, however, this difference should be considered even when allowing for the experimental inaccuracy in determining the phase diagram. Because of this, there are two resultant expressions in the application of Eq. 20 to aqueous two-phase systems.

3.1. Polymer + polymer aqueous two-phase systems

Using the root-mean-square molar mass ($\langle M_{rms}\rangle$) for a polydisperse species and since the densities along the binodal are almost the same (the density difference between the two phases of PEG + Dex systems is less than 10^{-5} kg m^{-3} [22]), we can therefore create a new parameter the average scaled EEV ($\langle V^*\rangle_{ji0} = N_A\langle \rho V_{ji0}\rangle$) and using this, the following expression results from Eq. 20:

$$\ln\left(\langle V^*\rangle_{210}\frac{w_2}{\langle M_{rms}\rangle_2}\right) + \langle V^*\rangle_{210}\frac{w_1}{\langle M_{rms}\rangle_1} = 0 \tag{21}$$

For PEG + Dex aqueous two-phase systems, species 1 and 2 refers to PEG and Dex, respectively.

3.2. Polymer + salt aqueous two-phase systems

The coexistence of electrolytes and the non-ionic polymers necessarily makes the molecular interactions in solutions more complex and the assumption of a completely random distribution must be doubtful since one would expect some degree of correlation between the ions of the electrolyte [23]. However, the exponential law of Eq. 15 is still expected to be a useful approximation for polymer molecules. We do not know why the approach adopted works as well as it does for systems containing electrolytes and for this reason we prefer to consider the following expression to be semi-empirical:

$$\ln\left(\langle V^{**}\rangle_{210}\frac{\rho w_2}{\langle M_{rms}\rangle_2}\right) + \langle V^{**}\rangle_{210}\frac{\rho w_1}{\langle M_{rms}\rangle_1} = 0 \tag{22}$$

In this, $\langle V^{**}\rangle_{ji0} = \rho N_A\langle V_{ji0}\rangle$ is taken as the average scaled EEV. For PEG + salt aqueous two-phase systems, species 1 and 2 denotes salt and PEG respectively.

Uses of Eqs. 21 and 22 are examined and discussed briefly below.

4. Results and discussion

One of the major objectives of the present work is to compare our theoretical expressions with experimental phase diagram.

It is true that polymers are complex molecules and their solution behaviour has been represented in different ways depending on the concentration regime considered. For aqueous two-phase systems, the concentrations of the polymers are in the "semi-dilute" region or perhaps approaching a crossover domain [24]. Although these different physical situations are not detailed in our model, the links of the binodal model to these have been indicated [18]. We have found Fig. 6 of ref. 18) that the change of the EEV with Dextran molar mass in PEG + Dex aqueous two-phase systems is marked at lower Dextran molar masses, but increasingly less marked at higher molar masses. This observation is in accordance with the physical model on which a recent theoretical analysis [7] is based. We would expect from the assumptions

made in the formulation of the theory, that for systems containing high-molar-mass polymers in the concentration region considered, the polymer molecules will form an entangled network rather than exist as identifiable polymer coils. The consequence of this is that the solution properties should be little influenced by the polymer molar mass at high molar masses but we would expect some influence at low molar masses. Within the limitations imposed by the model formulation it is therefore able to reflect different scale lengths. It is appreciated that the model used is oversimplified and cannot represent in detail all aspects of the molecular idiosyncrasies of all polymers. Comparisons with experimental information indicate that the theory is robust, but, undoubtedly, the EEV acts to some extent as a "catch-all" and must reflect, to some extent, "chemical" as distinct from geometric properties of the polymers.

For PEG + Dex aqueous two-phase systems, the phase diagram data obtained by Forciniti *et al.* [25], Diamond and Hsu [26], and Albertsson [27] have been correlated using Eq. 21 and the results obtained are given in Tables 1–3. It is clear from the information presented that the data from all of these sources, when the molecular mass ratio, R, is greater than *ca.* 4, is satisfactorily represented by Eq. 21. However, when R is less than this value, significant deviations of experimental results sometimes are evident. We can therefore conclude that for PEG + Dex aqueous two-phase systems, when $R > ca.$ 4 the binodal model works well.

A feature of the results given in Tables 1–3 is that the calculated EEVs from different sources but for seemingly identical PEG + Dex pairs, at similar temperatures (*e.g.*, 293 and 298 K), are sometimes very different. Some of the variation may be due to differing experimental conditions in different laboratories but the major contributions to the variations most probably arise from variations in the molar masses and polydispersity of the phase-forming polymers used. These variations however have a much less pronounced effect with PEG than with Dex. The variability

Table 1
Calculated effective excluded volumes ($\langle V^* \rangle_{\text{Dex-PEG-H}_2\text{O}}$) in PEG + Dextran aqueous two-phase systems at 298 K, obtained by fitting the experimental data [25] to Eq. 21

PEG + Dex aqueous systems[a]	$10^2 \times \langle V^*_{\text{Dex-PEG-H}_2\text{O}} \rangle$ (kg mol^{-1})	r	n	R
PEG 20 000 + Dex 17[b]	2.354	0.865	8	0.8
PEG 10 000 + Dex 17[b]	1.344	0.902	8	1.5
PEG 20 000 + Dex 19[b]	4.397	0.922	8	1.6
PEG 6000 + Dex 17	0.806	0.948	7	2.9
PEG 10 000 + Dex 19[b]	2.630	0.962	8	3.0
PEG 20 000 + Dex 37	7.191	0.958	8	3.3
PEG 4000 + Dex 17	0.614	0.968	8	4.1
PEG 6000 + Dex 19	1.393	0.988	8	5.9
PEG 10 000 + Dex 37	4.316	0.989	8	6.2
PEG 20 000 + Dex 48	9.426	0.987	8	6.87
PEG 4000 + Dex 19	1.025	0.995	8	8.1
PEG 6000 + Dex 37	2.308	0.986	8	12.2
PEG 10 000 + Dex 48	4.934	0.961	8	12.7
PEG 4000 + Dex 37	1.499	0.997	8	17.0
PEG 6000 + Dex 48	2.621	0.970	8	25.1
PEG 4000 + Dex 48	1.781	0.977	8	34.8

[a] Root-mean-square molar masses were used as the average molar masses and, for PEG 4000, PEG 6000, PEG 10 000, PEG 20 000, Dex 17, Dex 19, Dex 37 and Dex 48, they were 3951, 5476, 10 809, 20 038, 15 996, 32 017, 66 983 and 13 657, respectively.
[b] Phase diagrams for these systems are not given.

Table 2
Calculated effective excluded volumes ($\langle V^* \rangle_{Dex-PEG-H_2O}$) in PEG + Dextran aqueous two-phase systems at 277 K, obtained by fitting the experimental data [26] to Eq. 21

PEG + Dex aqueous systems[a]	$10^2 \times \langle V^*_{Dex-PEG-H_2O} \rangle$ (kg mol^{-1})	r	n	R
PEG 20 000 + Dex T40[b]	3.784	0.923	8	1.6
PEG 20 000 + Dex T70[b]	5.447	0.952	14	2.6
PEG 8000 + Dex T40	1.832	0.977	10	3.9
PEG 8000 + Dex T70	2.624	0.996	10	6.6
PEG 3400 + Dex T40	0.830	0.995	8	9.2
PEG 3400 + Dex T70	1.078	0.993	8	15.5
PEG 20 000 + Dex T500	14.696	0.983	8	17.2
PEG 8000 + Dex T500	6.129	0.978	8	43.1
PEG 3400 + Dex T500	2.279	0.991	8	101.3

[a] The average molar masses of PEG 3400, PEG 8000 and PEG 20 000 were 3400, 8000 and 20 000, respectively. The root-mean-square average molar masses used for Dex T40, T70 and T500 were 31 319, 52 654 and 344 586, respectively.
[b] Phase diagrams for these systems are not given.

of molar mass and polydispersity from different manufacturers and different batches is the main obstacle to achieving a general design approach to polymer + polymer aqueous two-phase systems using parameters such as the EEV. It has ben suggested [17] that at the outset of experiments in which an aqueous two-phase system is to be used, the EEV should be measured using, for example, the experimentally simple "turbidity" approach [27] to characterise the particular system studied. The suitability of this experimental approach for both types of aqueous two-phase systems has been demonstrated [28]. It is possible that a series of batches of the polymers

Table 3
Calculated effective excluded volumes ($\langle V^* \rangle_{Dex-PEG-H_2O}$) in PEG + Dextran aqueous two-phase systems, obtained by fitting the experimental data [27] to Eq. 21

PEG + Dex aqueous systems[a]	$10^2 \times \langle V^*_{Dex-PEG-H_2O} \rangle$ (kg mol^{-1})	r	n	R
PEG 20 000 + Dex D17 at 293 K[b]	2.722	0.894	12	1.3
PEG 6000 + Dex D17 at 273 K	1.564	0.954	8	2.9
PEG 6000 + Dex D17 at 293 K	1.527	0.959	14	2.9
PEG 6000 + Dex D24 at 293 K	2.069	0.993	10	5.1
PEG 4000 + Dex D17 at 293 K	0.742	0.975	8	5.8
PEG 6000 + Dex D37 at 273 K	3.976	0.991	10	10.4
PEG 6000 + Dex D37 at 293 K	3.552	0.995	8	10.4
PEG 6000 + Dex D48 at 273 K[b]	5.811	0.995	10	36.0
PEG 6000 + Dex D48 at 277 K	6.650	0.992	10	36.0
PEG 6000 + Dex D48 at 293 K	4.967	0.987	14	36.0
PEG 6000 + Dex D68 at 273 K	7.337	0.993	8	37.3
PEG 6000 + Dex D68 at 293 K	6.033	0.986	10	37.3
PEG 4000 + Dex D48 at 273 K	2.534	0.996	10	45.0
PEG 4000 + Dex D48 at 293 K	1.932	0.989	10	47.7

[a] Average molar masses for PEG 4000, PEG 6000 and PEG 20 000 were 4000, 8000 and 17 500, respectively. Those for Dex D17, D24, D37, D48 and D68 were 23 000, 40 500, 83 000, 180 000 and 280 000, respectively.
[b] Phase diagram for this system is not given.

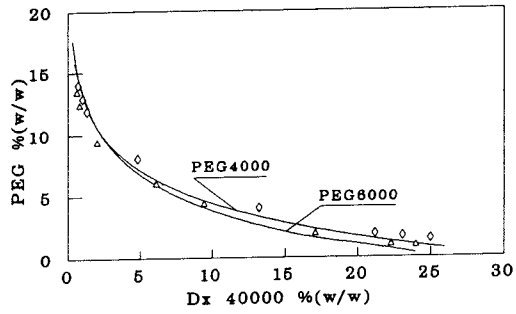

Fig. 2. Comparison of experimental binodals [25] for PEG 4000–Dextran (Dx) 40 000–water (◇) and PEG 6000–Dextran 40 000–water (△) systems at 298 K with those calculated (–) from Eq. 21.

obtained from a given manufacturer, might well be consistent in their properties. This would be fortunate but should always be checked.

Calculated and experimental binodals of a number of PEG + Dex aqueous two-phase systems are shown in Figs. 2–10. Without exception, for all of the experimental data considered (including systems containing salt, see later), we find that for different pairs of phase-forming components of similar chemical nature, the greater the polymer molar mass, the greater is the EEV: this is consistent with the physical meaning of the EEV.

From the results shown in Figs. 2–10 we find another important feature of the binodal model is that it reflects influences of both polymer molar mass and temperature on shifts in the

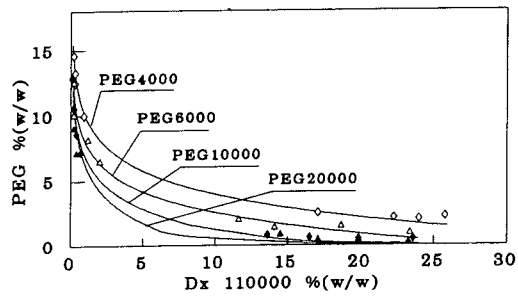

Fig. 3. Comparison of experimental binodals [25] for PEG 4000–Dextran (Dx) 110 000–water (◇), PEG 6000–Dextran 110 000–water (△), PEG 10 000–Dextran 110 000–water (◆) and PEG 20 000–Dextran 110 000–water (▲) systems at 298 K with those calculated (–) from Eq. 21.

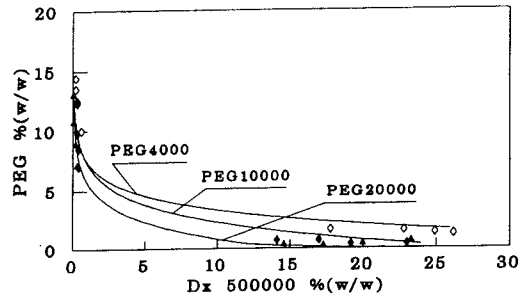

Fig. 4. Comparison of experimental binodals [25] for PEG 4000–Dextran (Dx) 500 000–water (◇), PEG 10 000–Dextran 500 000–water (◆) and PEG 20 000–Dextran 500 000–water (▲) systems at 298 K with those calculated (–) from Eq. 21.

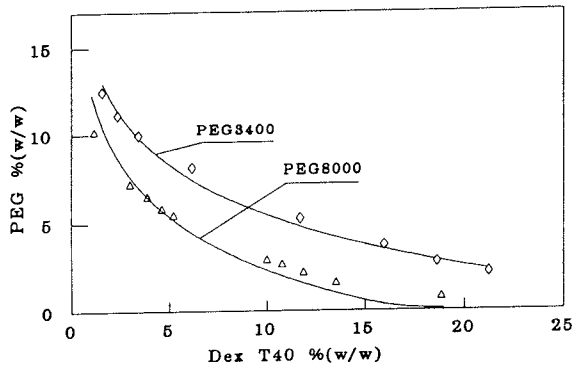

Fig. 5. Comparison of experimental binodals [26] for PEG 3400–Dextran T40–water (◇) and PEG 8000–Dextran T40–water (△) systems at 295 K with those calculated (–) from Eq. 21.

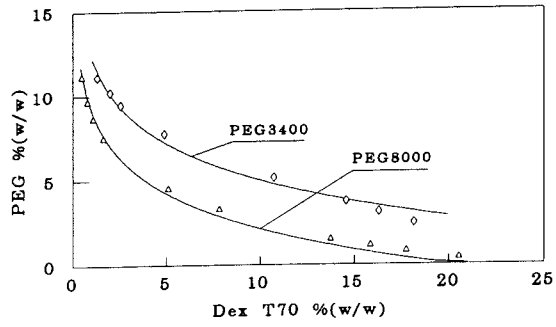

Fig. 6. Comparison of experimental binodals [26] for PEG 3400–Dextran T70–water (◇) and PEG 8000–Dextran T70–water (△) systems at 295 K with those calculated (–) from Eq. 21.

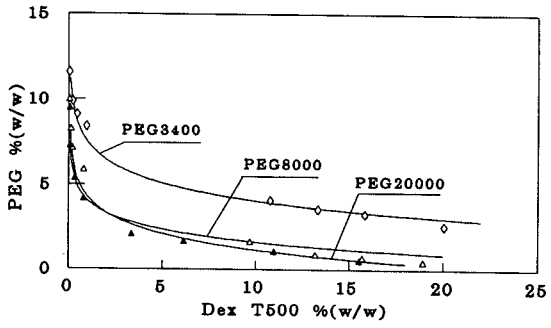

Fig. 7. Comparison of experimental binodals [26] for PEG 3400–Dextran T500–water (◇), PEG 8000–Dextran T500–water (△) and PEG 20 000–Dextran T500–water (▲) systems at 295 K with those calculated (–) from Eq. 21.

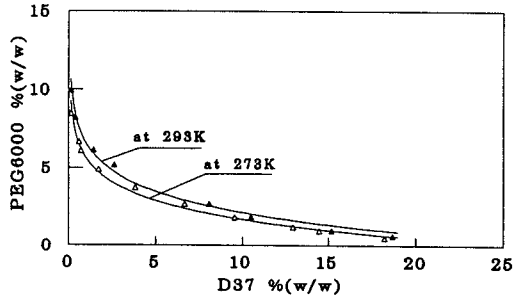

Fig. 8. Comparison of experimental binodals [27] for PEG 6000–Dextran D37–water systems at 293 K (▲) and at 273 K (△) with those calculated (–) from Eq. 21.

binodal. Two empirical concepts, which have been established for many years and are based primarily on experimental observations, are (i)

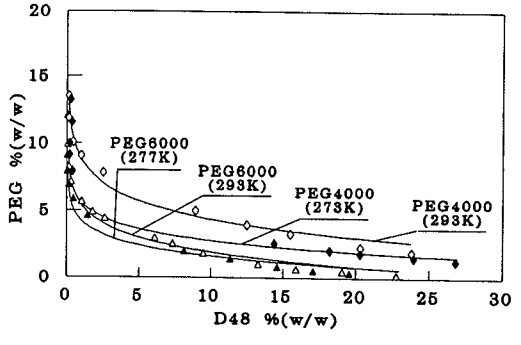

Fig. 9. Comparison of experimental binodals [27] with PEG 4000–Dextran D48–water systems at 293 K (◇) and at 283 K (◆) and PEG 6000–Dextran D48–water systems at 293 K (△) and at 277 K (▲) with those calculated (–) from Eq. 21.

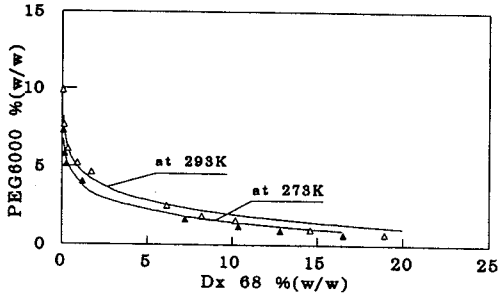

Fig. 10. Comparison of experimental binodals [27] for PEG 6000–Dextran (Dx) 68–water systems at 293 K (△) and 273 K (▲) with those calculated (–) from Eq. 21.

the higher the temperature the higher the concentration of polymers needed for phase separation and (ii) the higher the molar mass the lower the concentration of polymers needed for phase separation (see, *e.g.*, refs. 27, 29 and 30).

The first of these two concepts is completely in accordance with the predictions of the binodal model in that for a given polymer + polymer system, if the temperature is increased, then the EEV necessarily will decrease, resulting in a consequent perturbation of the coexistence curve away from the axes. In other words, for a fixed pair of polymers at higher temperatures, higher concentrations of the phase-forming polymers are always required for phase separation. It should perhaps be mentioned that, because of experimental problems at the extremes of coexistence curves, it is often difficult to delineate the exact relative positions of the curves (see, *e.g.*, Figs. 8 and 10).

The second of the empirical observations is consistent with the binodal model but is not a necessary condition of it. If the concentrations of the phase-forming solutes are expressed as molecular number densities then one can categorically state for two binary solute systems in which the molar mass of one of the solutes is fixed but the molar mass of the other solute varies, that the system with the lower-molar-mass solute will have its coexistence curve more distance from the axes than the higher-molar-mass solute containing system. However, usually phase compositions are expressed using mass fraction (or a similar scale) and depending upon the molar

masses it is possible for overlap of coexistence curves to occur when such scales are used. The EEV is related to the molecular size of both phase-forming components. When the molar mass ratio of the phase-forming components is large, a change in molar mass of the larger sized species will significantly alter the EEV whereas a change of the smaller sized species will have a lesser effect on the coexistence curve. As observed in Figs. 2, 3, 4, 7 and 9, for PEG + Dex aqueous two-phase systems when the molar mass of the larger sized species (Dex) is constant, the experimental evidence for binodal overlap with PEG of varying molar masses is unclear. In contrast, as shown in Figs. 11 and 12, when the molar mass of PEG is kept constant but that of Dex varies, binodal overlap obviously occurs.

As was mentioned above, changing the temperature leads to a change in the EEV and several examples illustrating this in polymer + polymer aqueous two-phase systems are given in Table 3. It is also possible to perturb the EEV, without changing the molar masses of the phase-forming polymers, by for example, the addition of a small amount of low-molar-mass additives, such as a salt or urea [30,31]. Changes in the EEV can also occur, with consequent changes in the phase diagrams, by derivatisation of the polymer(s).

A considerable amount of high-quality and

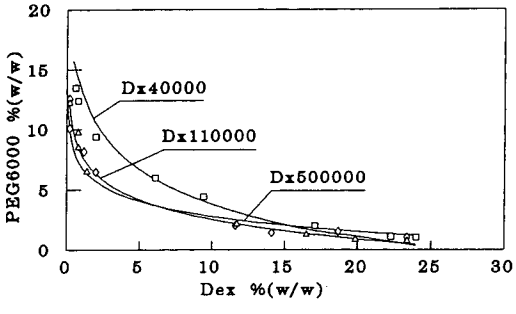

Fig. 11. Comparison of experimental binodals [25] for PEG 6000–Dex–water systems at 298 K, where the molecular mass of the PEG is fixed and those of Dex vary, with those calculated (–) from Eq. 21. Experimental results: □ = PEG 6000 + Dextran (Dx) 40 000 system; ◇ = PEG 6000 + 110 000 system; △ = PEG 6000 + Dextran 500 000 system.

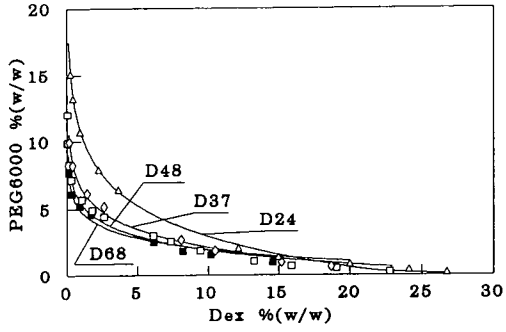

Fig. 12. Comparison of experimental binodals [27] for PEG 6000–Dex–water systems at 293 K, where the molecular mass of the PEG is fixed and those of Dex vary, with those calculated (–) from Eq. 21. Experimental results: ■ = PEG 6000 + Dextran D68 system; □ = PEG 6000 + Dextran D48 system; ◇ = PEG 6000 + Dextran D37 system; △ = PEG 6000 + Dextran D24 system.

comprehensive data on PEG + salt systems has recently been reported [32] and we have treated these using the binodal model. The results obtained are presented in Table 4 and shown in Figs. 13–17. It is apparent that the binodal model (Eq. 22), usually gives a satisfactory description of the experimentally determined binodals of polymer + salt aqueous two-phase systems. The molar mass ratio restriction on the binodal model seldom applies and generally since the molar mass ratio for this type of two-phase system is almost invariably rather high, polymer molecules would tend to be close packed in aqueous salt solutions [18]. One of the clear conclusions which is evident from Table 4 is that for each of the salt-containing systems investigated, as the molar mass of the PEG increases, so too does the EEV. This is in accordance with the binodal model. It seems quite apparent from the information shown in Figs. 14–17 that for PEG + salt systems binodal overlaps do occur. This is the feature which was commented on above when polymer + polymer systems were considered and now, largely because of the great molar mass disparity between the polymer and the salt and the variation in the larger sized species PEG, the non-monotonic shift of coexistence curves with polymer molar mass is very evident. In contrast to the polymer + polymer systems, where in the usual

Table 4
Calculated effective excluded volumes ($\langle V^{**} \rangle_{PEG-salt-H_2O}$) in PEG + salt aqueous two-phase systems at 298 K, obtained by fitting the experimental data [32] to Eq. 22

PEG + salt aqueous systems[a]	$10^7 \times \langle V^{**}_{PEG-salt-H_2O} \rangle$ ($m^3\ mol^{-1}$)	r	n	R
PEG 1000 + $MgSO_4$	1.777	0.994	8	9.1
PEG 3350 + $MgSO_4$	3.925	0.980	8	27.4
PEG 8000 + $MgSO_4$	5.500	a	10	73.5
PEG 1000 + K_3PO_4 at pH 8.0[b]	1.869	0.997	8	6.5
PEG 8000 + K_3PO_4 at pH 8.0[b]	7.400	0.975	12	52.4
PEG 1000 + Na_2CO_3	1.905	0.996	10	10.4
PEG 3350 + Na_2CO_3	2.480	0.998	6	31.1
PEG 8000 + Na_2CO_3	8.770	0.990	8	83.5
PEG 1000 + $(NH_4)_2SO_4$	1.387	0.995	8	8.3
PEG 8000 + $(NH_4)_2SO_4$	5.733	0.993	8	67.0
PEG 1000 + Na_2SO_4	1.994	0.997	10	7.7
PEG 3350 + Na_2SO_4	3.804	0.981	8	23.2
PEG 8000 + Na_2SO_4	5.557	0.995	10	62.3

[a] The root-mean-square-average molar masses were used for the average molar masses of PEG and for PEG 1000, PEG 3350 and PEG 8000 they were 1100, 3299 and 8848, respectively [32].

[b] For systems containing K_2HPO_4 and KH_2PO_4 the fractions of phosphate species ($x_{K_2HPO_4}$, $x_{KH_2PO_4}$) were determined using the Henderson–Hasselbach equation in association with the well documented pK_a of $H_2PO_4^-$. The mean molar mass of the phosphate was obtained by $\langle M \rangle_{phosphate} = M_{K_2HPO_4} x_{K_2HPO_4} + M_{KH_2PO_4} (1 - x_{K_2HPO_4})$, where $M_{K_2HPO_4}$ and $M_{KH_2PO_4}$ are the molar masses of K_2HPO_4 and KH_2PO_4, respectively.

composition ranges, as the molar mass of one of the polymer is increased the coexistence curve moves towards the axes, for polymer + salt systems as the molar mass of the polymer is increased either enhanced or diminished phase separation can occur. At the cross-over point

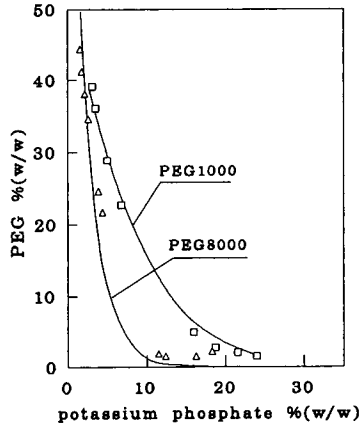

Fig. 13. Comparison of experimental binodals [32] for PEG 1000–potassium phosphate–water (□) and PEG 8000–potassium phosphate–water (△) systems at pH 8.0 and 298 K with those calculated (–) from Eq. 22.

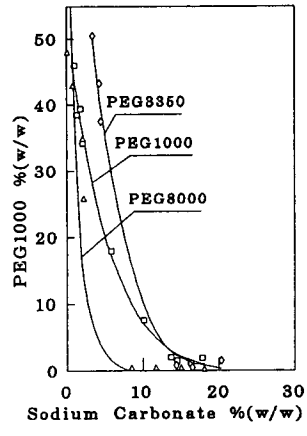

Fig. 14. Comparison of experimental binodals [32] for PEG 1000–Na_2CO_3–water (□), PEG 3350–Na_2CO_3–water (◇) and PEG 8000–Na_3Co_3–water (△) at 298 K with those calculated (–) from Eq. 22.

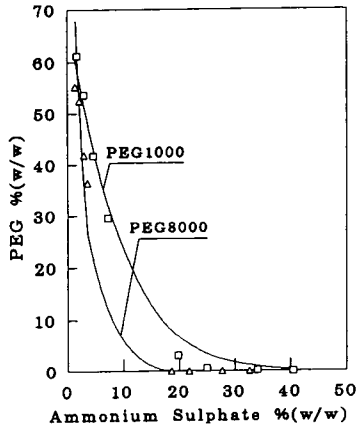

Fig. 15. Comparison of experimental binodals [32] for PEG 1000–$(NH_4)_2SO_4$–water (□) and PEG 8000–$(NH_4)_2SO_4$–water (△) systems at 298 K with those calculated (–) from Eq. 22.

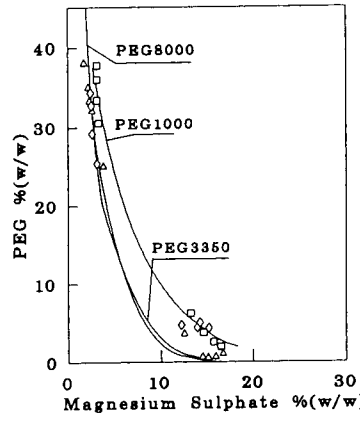

Fig. 17. Comparison of experimental binodals [32] for PEG 1000–Na_2SO_4–water (□), PEG 3350–Na_2SO_4–water (◇) and PEG 8000–Na_2SO_4–water (△) systems at 298 K with those calculated (–) from Eq. 22.

obviously no change in phase separation occurs with change in molar mass.

In the treatment of polymer + salt aqueous two-phase systems, the disadvantage of using Eq. 22 to predict the binodal is that a means of estimating the change of solution density along the binodal is needed. In order to obtain a simple expression for the polymer + salt aqueous two-phase systems, a tentative empirical approach for the present situation may be the use of Eq. 21. Tables 5 and 6 list the correlation of some PEG + phosphate binodals determined by Lei *et al.* [33] and Albertsson [27], and in these $N_A\langle\rho V_{\text{polymer-salt}}\rangle$ is used to represent the apparent EEV. It can be seen that although the correlation coefficients are somewhat reduced for the data reported by Albertsson [27], the approach is quite satisfactory for the binodals determined by Lei *et al.* [33]. From Table 5 it is apparent that for molar mass ratios greater than approximately 4 Eq. 21 gives satisfactory representations of the experimental binodals of PEG + phosphate systems. It would seem therefore that the application of Eq. 21 to polymer + salt aqueous two-phase systems should be satisfactory if this condition is met.

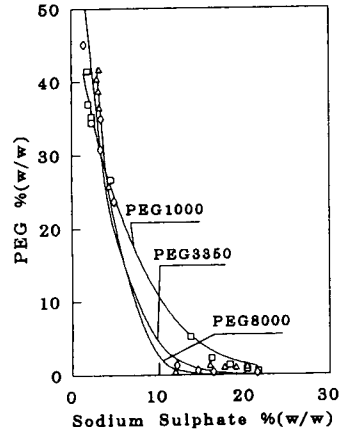

Fig. 16. Comparison of experimental binodals [32] for PEG 1000–$MgSO_4$–water (□), PEG 3350–$MgSO_4$–water (◇) and PEG 8000–$MgSO_4$–water (△) systems at 298 K with those calculated (–) from Eq. 22.

It was mentioned earlier that the application of binodal model to polymer + salt aqueous two-phase systems is semi-empirical, and there are some obvious theoretical difficulties. As an example as shown in Table 6, the influence of temperature on the EEV is different to that observed in polymer + polymer aqueous two-phase system in that for polymer + salt aqueous two-phase systems increase in temperature increases the EEV. It is our intention to study the

Table 5
Calculated effective excluded volumes ($\langle V^* \rangle_{PEG-salt-H_2O}$) in PEG + salt aqueous two-phase systems at 277 K, obtained by fitting the experimental data [33] to Eq. 21

PEG + salt aqueous systems[a]	$10^7 \times \langle V^*_{PEG-salt-H_2O} \rangle$ (kg mol^{-1})	r	n	R
PEG 400 + potassium phosphate at pH 7	0.880	0.979	8	2.7
PEG 600 + potassium phosphate at pH 7	1.240	0.990	8	4.0
PEG 1000 + potassium phosphate at pH 7	1.795	0.998	8	6.6
PEG 1500 + potassium phosphate at pH 7	2.415	0.999	8	10.0
PEG 3400 + potassium phosphate at pH 6	3.215	0.997	8	24.6
PEG 3400 + potassium phosphate at pH 7	3.865	0.994	8	22.6
PEG 3400 + potassium phosphate at pH 8	4.558	0.999	8	20.1
PEG 3400 + potassium phosphate at pH 9.2	4.616	0.999	8	19.6
PEG 8000 + potassium phosphate at pH 7	6.148	0.990	8	53.1
PEG 20 000 + potassium phosphate at pH 7	8.375	0.997	8	132.6

[a] The nominal masses were used for the PEGs. The average molar masses of phosphates were obtained as given in the footnote to Table 4.

behaviour of salt-containing systems in more detail, both from experimental and theoretical viewpoints.

5. Conclusions

Eqs. 21 and 22, which are based on a statistical geometrical theory, can represent both polymer + polymer or polymer + salt aqueous two-phase systems. The establishment of the binodal model represents a major step in the quantitative description of aqueous two-phase systems and biomacromolecular partitioning in these systems. In practice, given the marked influence of polymer polydispersity on the binodals of polymer + polymer aqueous two-phase systems and the variation of this between manufacturers and between batches, the preliminary determination of the parameter, the EEV, is recommended. For polymer + salt aqueous two-phase systems, the value of the EEV varies little

Table 6
Calculated effective excluded volumes ($\langle V^* \rangle_{PEG-salt-H_2O}$) in PEG + phosphate aqueous two-phase systems, obtained by fitting the experimental data [27] to Eq. 21

PEG + salt aqueous systems[a]	$10^6 \times \langle V^*_{PEG-salt-H_2O} \rangle$ (kg mol^{-1})	r	n	R
PEG 1540 + potassium phosphate at 293 K	2.388	0.994	8	9.7
PEG 4000 + potassium phosphate at 273 K	3.736	0.979	8	23.8
PEG 4000 + potassium phosphate at 293 K	4.021	0.972	12	23.8
PEG 6000 + potassium phosphate at 273 K	5.363	0.972	8	50.5
PEG 6000 + potassium phosphate at 293 K	5.656	0.979	8	50.5
PEG 20 000 + potassium phosphate at 293 K	6.809	0.988	6	110.4

[a] The average molar masses for PEG 1540, PG 4000, PEG 6000 and PEG 20 000 were 1540, 3774, 8000 and 17 500, respectively. The average molar masses of the phosphate used here were obtained as given in the footnote to Table 4.

for PEGs with molecular masses less than 10 000 for a given salt and at a given pH, and so such preliminary experimentation is unnecessary.

6. Acknowledgement

This work was supported by the Science and Engineering Research Council under Grant No. GR/G19824.

7. References

[1] D.E. Brooks, K.A. Sharp and D. Fisher, in H. Walter, D.E. Brooks and D. Fisher (Editors), *Partitioning in Aqueous Two-Phase Systems*, Academic Press, Orlando, FL, 1985, Ch. 2, p. 11.
[2] J.N. Baskir, T.A. Hatton and U.W. Suter, *Macromolecules*, 20 (1987) 1300.
[3] C.H. Kang and S.I. Sandler, *Fluid Phase Equilib.*, 38 (1987) 245.
[4] C.H. Kang and S.I. Sandler, *Biotechnol. Bioeng.*, 32 (1988) 1158.
[5] Y.-L. Gao, Q.-H. Peng, Z.-C. Li and Y.-G. Li, *Fluid Phase Equilib.*, 63 (1991) 173.
[6] R.S. King, H.W. Blanch and J.M. Prausnitz, *AIChE J.*, 34 (1988) 1585.
[7] N.L. Abbott, D. Blankschtein and T.A. Hatton, *Macromolecules*, 24 (1991) 4334.
[8] C.A. Haynes, F.J. Benitez, H.W. Blanch and J.M. Prausnitz, *AIChE J.*, 39 (1993) 1539.
[9] Y. Guan, X.-Y. Wu, T.E. Treffry and T.H. Lilley, *Biotechnol. Bioeng.*, 40 (1992) 517.
[10] Y. Guan, T.E. Treffry and T.H. Lilley, *Bioseparation*, 4 (1993) in press.
[11] A.D. Diamond and J.T. Hsu, *AIChE J.*, 36 (1990) 1017.
[12] M. Setchenow, *Ann. Chim. Phys.*, 25 (1892) 226.
[13] H.L. Friedman, *J. Solution Chem.*, 1 (1972) 387.
[14] E.S. Vainerman, V.Yu. Ryashentsev and S.V. Rogozhin, *Solvent Extr. Ion Exch.*, 8 (1990) 361.
[15] A.D. Diamond and J.T. Hsu, in M.M. Ataai and S.K. Sikdar (Editors), *New Developments in Bioseparation (AIChE Symposium Series*, No. 290), American Institute of Chemical Engineers, New York, 1992, ch. 13.
[16] P.J. Flory, *Principles of Polymer Chemistry*, Cornell University Press, Ithaca, NY, 1953.
[17] Y. Guan, T.H. Lilley and T.E. Treffry, *J. Chem. Soc., Faraday Trans.*, 89 (1993) 4283.
[18] Y. Guan, T.H. Lilley and T.E. Treffry, *Macromolecules*, 26 (1993) 3971.
[19] Y. Hu and J.M. Prausnitz, *AIChE J.*, 35 (1988) 814.
[20] B.J. Alder, W.G. Hoover and D.A. Young, *J. Chem. Phys.*, 49 (1968) 3688.
[21] H.L. Weissberg, *J. Appl. Phys.*, 34 (1963) 2636.
[22] D. Forciniti, C.K. Hall and M.-R. Kula, *J. Biotechnol.*, 16 (1990) 279.
[23] R.H. Fowler and E.A. Guggenheim, *Statistical Thermodynamics*, Cambridge University Press, Cambridge, 1965.
[24] J. des Cloizeaux and G. Jannink, *Polymers in Solution: Their Modelling and Structure*, Clarendon Press, Oxford, 1990.
[25] D. Forciniti, C.K. Hall and M.-R. Kula, *Biotechnol. Bioeng.*, 38 (1991) 986.
[26] A.D. Diamond and J.T. Hsu, *Biotechnol. Techniq.*, 3 (1989) 119.
[27] P.-Å. Albertsson, *Partition of Cell Particles and Macromolecules*, Wiley, New York, 3rd ed., 1986.
[28] B.K. Kim, Y.-B. Ban and J.-D. Kim, *Korean J. Chem. Eng.*, 9 (1992) 219.
[29] Å. Sjöberg and G. Karlström, *Macromolecules*, 22 (1989) 1325.
[30] B.Yu. Zaslavsky, T.O. Bagirov, A.A. Borovskaya, N.D. Gulaeva, L.H. Miheeva, A.U. Mahmudov and M.N. Rodnikova, *Polymer*, 30 (1989) 2104.
[31] T.E. Treffry, T.H. Lilley and P.J. Cheek, in D. Fisher and I.A. Sutherland (Editors), *Separations Using Aqueous Phase Systems*, Plenum Press, London, 1989, p. 233.
[32] S.M. Snyder, K.D. Cole and D.C. Szlag, *J. Chem. Eng. Data*, 37 (1992) 268.
[33] X. Lei, A.D. Diamond and J.T. Hsu, *J. Chem. Eng. Data*, 35 (1990) 420.

ELSEVIER

Journal of Chromatography A, 668 (1994) 47–54

JOURNAL OF CHROMATOGRAPHY A

Model for predicting the partition behaviour of proteins in aqueous two-phase systems

J.A. Asenjo *, A.S. Schmidt, F. Hachem, B.A. Andrews

Biochemical Engineering Laboratory, University of Reading, Reading RG6 2AP, UK

Abstract

The effect of protein hydrophobicity, charge, molecular mass and concentration has been studied in poly(ethylene glycol) (PEG)–phosphate and PEG–dextran aqueous two-phase systems in the presence and absence of NaCl for several model proteins. The surface hydrophobicity of the protein measured by precipitation correlated well with the partition coefficient in PEG–salt systems at high levels of NaCl. The charge of proteins also has an important effect on partition; this is expected to be more pronounced at lower NaCl concentrations. For molecular mass a tendency was found in PEG–dextran systems at low NaCl concentrations. No clear tendency was observed in the PEG–salt systems. The solubility of the protein in the phases also affects its partition behaviour. This behaviour was fitted to a saturation type equation for α-amylase in each of the phases of a PEG–phosphate system

1. Introduction

Aqueous two-phase systems (ATPSs) have important potential in downstream processing as a large-scale continuous operation for the separation of proteins and removal of contaminants from fermentations as they can process streams continuously and rapidly produce an initial separation including separation of whole cells or cell debris as in the case of intracellular proteins. However, the wider implementation in many applications has been restrained in part by the limited predictability of the partition behaviour of proteins in ATPSs. Factors and mechanisms that cause the uneven distribution of biomolecules are poorly understood. Fundamental theories of protein partition derived from classical polymer solution thermodynamics are being developed [1–4]. Although the present models provide important information, no comprehensive theory currently exists to guide the design of systems for separation of specific mixtures of proteins. The value of the partition coefficient, K (defined as the ratio of the protein concentration in the lighter phase to that in the heavier phase) relies on the physico-chemical properties of the target protein and contaminants (*e.g.* hydrophobicity, charge, molecular mass) and their interactions with those of the chosen system (*e.g.* composition, ionic strength, addition of specific salt ions, pH). Depending on the manipulation of these system parameters the target protein and contaminants can be partitioned selectively.

This paper describes preliminary work on a model to correlate the physico-chemical properties of a protein to its partition coefficient in ATPSs using a modified group contribution approach:

* Corresponding author.

0021-9673/94/$07.00
SSDI 0021-9673(94)00102-F

$$K = K_{hphob} \cdot K_{el} \cdot K_{size} \cdot K_{sol} \cdot K_{aff} \quad (1)$$

where K_{hphob}, K_{el}, K_{size}, K_{sol} and K_{aff} denote the contribution to the overall partition coefficient by hydrophobicity, electrostatic forces, size, solubility and affinity, respectively. Changes in conformation will usually affect K_{el}, K_{hphob}, K_{sol} or even K_{aff}. Not all the properties are equally important, this depends on the type of system used. The initial results of our investigation into the effects of hydrophobicity, charge, molecular mass and solubility are described.

2. Materials and methods

2.1. Materials

Poly(ethylene glycol) (PEG) with molecular masses of 4000 and 8000 was obtained from Fluka. Dextran T500 was purchased from Pharmacia, Sweden. All other chemicals were analytical grade. Thaumatin was a gift from Four-F Nutrition, Northallerton, UK. Subtilisin and α-amylase (both from *Bacillus subtilis*) were obtained from Boehringer Mannheim, Germany. Other proteins were purchased from Sigma. α-Chymotrypsinogen A was from bovine pancreas, α-lactalbumin and β-lactoglobulin from bovine milk, invertase from Bakers yeast and lysozyme from chicken egg white. Molecular mass and p*I* values of the proteins used in this study are shown in Table 1.

2.2. Preparation of phase systems

Phase systems were prepared from stock solutions of PEG (50%, w/w), phosphate (40%, w/w) and NaCl (25%, w/w). The phosphate stock solution consisted of a mixture of K_2HPO_4 and NaH_2PO_4 at the appropriate pH. Stock solutions were stored at 4°C. Before use the temperature of all solutions was equilibrated by standing at room temperature. All partition experiments were done at 20°C. Total protein was added to the systems at a final concentration of 1 g/l unless otherwise stated. Samples of top and bottom phase were assayed for protein concentration.

2.3. Protein assays

Total protein was measured by the modified Lowry assay [5] using bicinchoninic acid (BCA) at 37°C or by the modified Bradford dye-binding assay [6]. The BCA assay kit was supplied by Pierce Europe, Netherlands, standard curves were prepared for each protein. Blank systems without protein were used as reference and no interference from phase components was observed.

α-Amylase concentration was assayed as activity as described previously [7].

Table 1
Molecular mass and p*I* of the model proteins

Proteins	Abbreviation	M_r	p*I*
α-Amylase	Amy	50 000	5.0
Bovine serum albumin	BSA	67 000	4.7
α-Chymotrypsinogen A	Chy	23 600	8.9
Conalbumin	Con	77 000	5.9
Invertase	Inv	270 000	3.4
α-Lactalbumin	Lac	17 400	5.1
β-Lactoglobulin A	Lag	37 100	5.1
Lysozyme	Lys	14 300	10.3
Subtilisin	Sub	27 500	8.4
Thaumatin	Tha	28 000	10.8

2.4. Reversed-phase chromatography

A Nucleosil 300-7 C_{18} column (25 cm × 4.6 mm I.D.) was used with a Perkin-Elmer Binary LC pump and a Rheodyne Model 7125 valve. Gradient elution at a flow-rate of 1 ml/min was used. Further experimental details have been previously described [8].

2.5. Hydrophobic interaction chromatography (HIC)

A fast protein liquid chromatography (FPLC) system (Pharmacia) was used with an HR 5/5 (1 ml) column with fast flow Phenyl-Sepharose (Pharmacia). Further details can be found in ref. 8.

2.6. Precipitation of proteins

Proteins were dissolved in sodium phosphate buffer (0.05 M, pH 7) at a concentration of 2 g/l. To a measured volume of each solution solid ammonium sulphate was added slowly with continuous stirring. The solutions were left to equilibrate for 15 min at 24°C. After centrifugation (25 000 g, 20 min) a sample was taken from the supernatant and assayed for protein concentration. More ammonium sulphate was added to the rest of the supernatant making the saturation higher; after each addition the supernatant was assayed for protein concentration. This was repeated until no protein could be precipitated. A blank was prepared and treated in the same way to account for the interference of ammonium sulphate in the protein assays.

3. Results and discussion

The systems chosen for this study, PEG 4000–phosphate, PEG 8000–phosphate and PEG 4000–dextran, were selected on their ability to illustrate differences in physico-chemical properties of proteins. Initially PEG 8000–phosphate systems at several NaCl concentrations were used to correlate the surface hydrophobicity of proteins measured by different techniques, RP-HPLC, HIC and ammonium sulphate precipitation. Five levels of NaCl were added to the systems [0, 0.3, 4.8, 9.6 and 17.6% (w/w)] as very different partition behaviours have been observed at these concentrations [7,9]. The difference in partition behaviour observed at high NaCl concentrations in PEG–phosphate systems [7,9] has been attributed to hydrophobicity. Proteins were chosen with clear differences in hydrophobicity, molecular mass (14 300–270 000) and surface charge (pI 3.4–10.8).

3.1. Hydrophobicity

In order to develop possible correlations for prediction of partitioning behaviour of proteins five model proteins (α-lactalbumin, β-lactoglobulin A, bovine serum albumin, conalbumin and lysozyme) with different physico-chemical properties were initially chosen. Evaluation of the relationship between hydrophobicity and behaviour of the proteins in different aqueous two-phase systems was investigated in detail by measuring surface hydrophobicity by HIC and precipitation/solubility in addition to reversed-phase chromatography (RP-HPLC) which although separating proteins and peptides based on their hydrophobicity can denature larger proteins. Molecular masses and pI values of these proteins are shown in Table 1.

For the five proteins a poor correlation was found between the hydrophobicity measurements evaluated as retention time in an RP-HPLC column and HIC and log K in all aqueous two-phase systems investigated which included PEG–dextran and PEG–phosphate with and without the addition of NaCl [8]. Some of the better correlations found (in PEG–phosphate systems with NaCl) are shown in Figs. 1 and 2 for RP-HPLC and HIC; however, this correlation was still rather poor. The hydrophobicity, log P, measured by RP-HPLC is expressed as the log of the volumetric fraction of acetonitrile (P) at which the proteins elute from a C_{18} column. The hydrophobicity measured by HIC is expressed as the log of (1/molar fraction of ammonium sulphate) at which the proteins elute from a Phenyl-Sepharose column using a linear

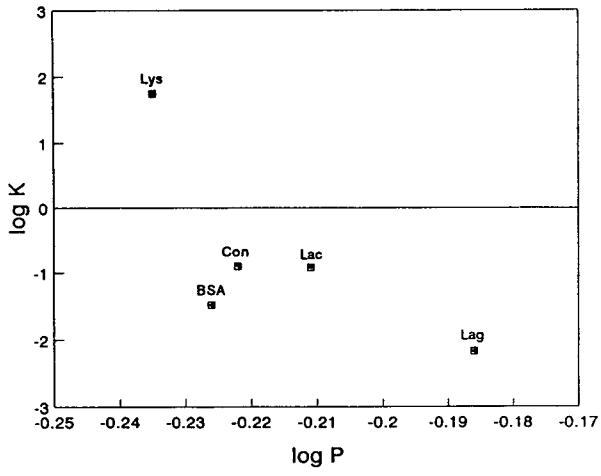

Fig. 1. The relationship between the partition coefficient (log K) of several model proteins in PEG 8000 (8%, w/w)–phosphate (12%, w/w) system with 9.6% (w/w) NaCl at pH 7 and the hydrophobicity of the proteins (log P) measured by RP-HPLC on a C_{18} column as the volumetric fraction of acetonitrile at which they eluted. Abbreviations as in Table 1.

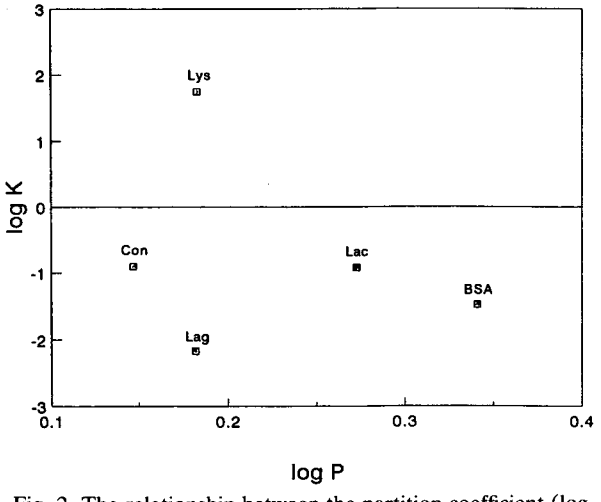

Fig. 2. The relationship between the partition coefficient (log K) of several model proteins in PEG 8000 (8%, w/w)–phosphate (12%, w/w) system with 9.6% (w/w) NaCl at pH 7 and the hydrophobicity of the proteins (log P) measured by HIC–FPLC on a Phenyl-Sepharose columns. The hydrophobicity is expressed as the log of (1/molar fraction of ammonium sulphate) at which the proteins eluted from the column using a linear gradient from 1.5 to 0.0 M ammonium sulphate. Abbreviations as in Table 1.

gradient from 1.5 to 0.0 M ammonium sulphate in 0.05 M sodium phosphate buffer (pH 7).

An alternative method to evaluate a proteins hydrophobicity in solution is by measuring the point at which precipitation begins in a typical ammonium sulphate precipitation curve [10,11]. In a typical protein precipitation graph, as shown in Fig. 3 for β-lactoglobulin, the solubility of the protein (and thus its hydrophilicity) can be expressed by point m* which is the point at which the protein starts to precipitate. Thus the hydrophobicity, P, can be represented as $1/m^*$. Fig. 4 shows the relationship between log K and the hydrophobicity of the five model proteins measured by ammonium sulphate precipitation ($1/m^*$). It is clear from Figs. 1, 2 and 4 that the inverse of the solubility (point $1/m^*$) gave a good correlation of log K with log P (log P = log $1/m^*$) whereas the hydrophobicity evaluated by RP-HPLC and HIC did not. The reason for this seems to be that solubility represents a measurement of a protein's "average" surface hydrophilicity (or hydrophobicity) in "bulk solution" similar to that measured in certain ATPSs whereas in HIC the hydrophobicity/hydrophilicity distribution on the protein's surface (*e.g.* hydrophobic patches) probably plays a greater role in the interaction of the protein with the

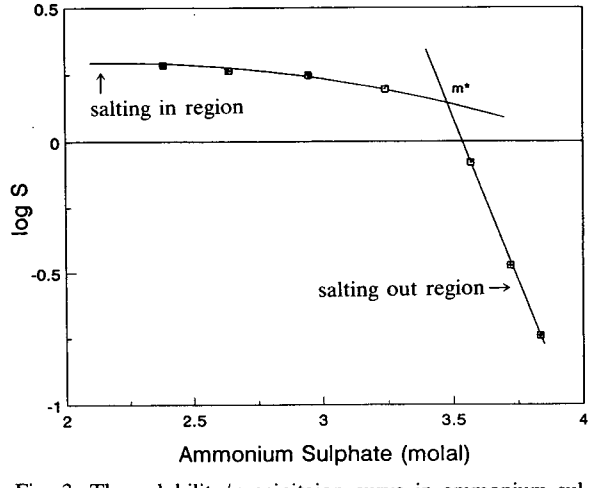

Fig. 3. The solubility/precipitaion curve in ammonium sulphate of β-lactoglobulin A at 25°C. The intercept of the two fitted lines x value represent the solubility, m*.

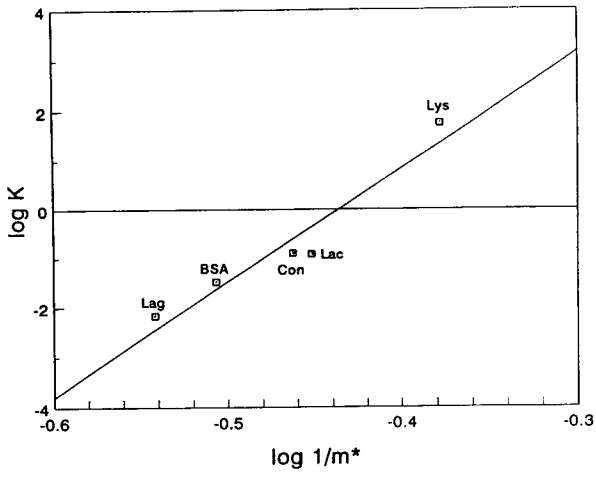

Fig. 4. The relationship between the partition coefficient (log K) of several model proteins in PEG 8000 (8%, w/w)–phosphate (12%, w/w) system with 9.6% (w/w) NaCl at pH 7 and the hydrophobicity of the proteins (log P) measured by ammonium sulphate precipitation [log P = log (1/m*)] (r = 0.957). Abbreviations as in Table 1.

hydrophobic matrix. In the case of RP-HPLC this is probably even more evident as the solvent used may partially denature larger proteins exposing some of the internal amino acids and thus affecting the hydrophobic/hydrophilic behaviour.

A model for the prediction of partitioning of proteins in certain ATPSs that mainly exploit hydrophobicity has thus been proposed [4,8]:

$$\log K = D\Delta W \log(P/P_0) \quad (2)$$

or

$$\log K = D\Delta W \log P - D\Delta W \log P_0 \quad (3)$$

in this equation $D\Delta W$ describes its resolution power in which ΔW represents the difference in concentration of one component between the top and bottom phases (*e.g.* PEG; this takes into account the effect of the tie-line length). D has been called the discrimination factor. This equation is similar to that proposed for smaller molecules and peptides [4]. According to this model, PEG–phosphate systems with added NaCl mainly exploit the surface hydrophobicity for partitioning of different proteins. Table 2

Table 2
The calculated values of $D\Delta W$ and the intrinsic hydrophobicity (log P_0) of PEG 8000 (8%, w/w)–phosphate (12%, w/w) systems with varying concentration of NaCl at pH 7

NaCl (%, w/w)	$D\Delta W$	log P_0
0	5.4	−0.23
0.48	8.3	−0.29
4.8	14.9	−0.38
9.6	22.4	−0.45
17.6	22.8	−0.45

shows the calculated values of $D\Delta W$ and the intrinsic hydrophobicity, log P_0, of the ATPSs used at 20°C. Clearly the systems with higher concentrations of NaCl give a higher resolution to exploit the proteins hydrophobicity in partitioning which is given by the value of the slope, $D\Delta W$, in Fig. 4.

This behaviour is presently being investigated for a larger number of proteins (listed in Table 1). Fig. 5 shows the partition behaviour (log K) and hydrophobicity (1/m* = P) of these proteins as measured by solubility (m*) during ammonium sulphate precipitation in a PEG 4000–phosphate system with 8.8% NaCl.

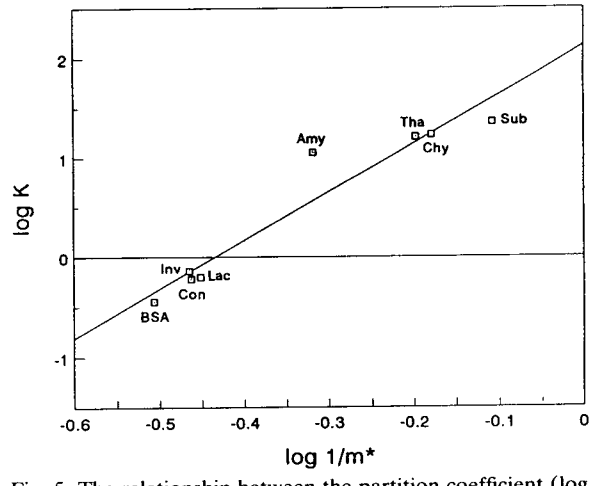

Fig. 5. The relationship between the partition coefficient (log K) of several model proteins in PEG 4000 (13%, w/w)–phosphate (10.7%, w/w) system with 8.8% (w/w) NaCl at pH 7 and the hydrophobicity of the proteins (log P) measured by ammonium sulphate precipitation [log P = log (1/m*)] (r = 0.965). Abbreviations as in Table 1.

3.2. Charge

Electrical potential differences between the phases of an aqueous two-phase system will affect the partition coefficient of proteins according to their charge. This has been demonstrated in PEG–dextran systems with addition of small concentrations of salts whose charged ions will partition between the phases (*e.g.* 0.1 *M* NaCl or 0.05 *M* Na_2SO_4) and also by manipulating the pH of the system [12,13]. In PEG–salt systems a change in the pH can affect the value of *K*. Fig. 6 shows the increase in partition coefficient with pH of α-amylase in a PEG–phosphate system. As the bottom phase has a very high concentration of salt, it appears that it is the pH of the top phase that will determine partitioning due to electrostatic effects. Theory has been recently developed to describe this effect as a function of the pH difference between the phases [14]. α-Amylase has a p*I* of 5. As pH was increased the protein becomes more negatively charged following its titration curve. In Fig. 6 there was a small increase in tie-line length as pH was increased but the effect shown is mainly due to pH change. This clearly suggests that the top phase has a higher density of positive charges. This behaviour is presently being investigated following titration curve analysis in several ATPSs for most of the proteins shown in Table 1.

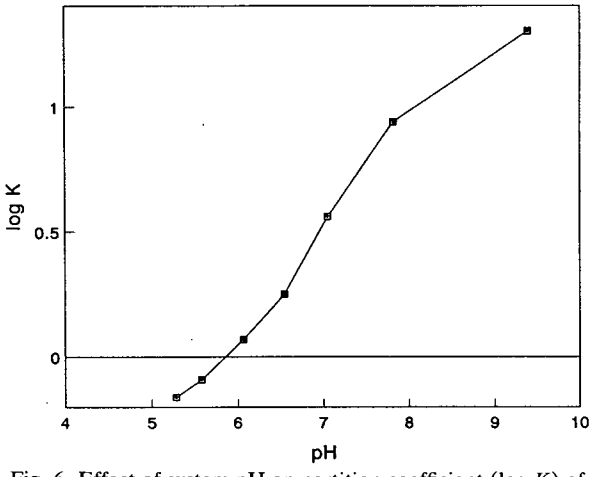

Fig. 6. Effect of system pH on partition coefficient (log *K*) of α-amylase in PEG 4000 (10%, w/w)–phosphate (11.5%, w/w) systems.

3.3. Molecular mass

The effect of protein molecular mass on its partition coefficient has been described in PEG–dextran systems with a low concentration of added NaCl [1,15]. This work is now being extended to include different ATPSs and proteins with a wider range of molecular masses. A correlation has been obtained at low concentrations of NaCl [1].

$$\log K_{size} = \beta + \alpha M_r \quad (4)$$

where α and β are constants depending on system properties.

Fig. 7A and B show the correlation of molecular mass with partition coefficient for proteins in PEG–dextran and PEG–phosphate systems, respectively. In the PEG–salt system there was no apparent correlation of molecular mass and log *K*. However, the correlation is far better in the PEG–dextran system as has been previously observed [1,15].

3.4. Protein concentration

As the concentration of protein in an ATPS is increased, a solubility limit in each of the phases is reached often leading to saturation in that phase [7]. True partitioning is only observed at low protein concentration (*e.g.* <2 g/l) depending on the protein [9]. This behaviour results in changes in the value of *K* at higher concentrations. Precipitation of the protein at the interphase is also usually observed. This phenomenon is demonstrated in Fig. 8 which shows the concentration of α-amylase in each of the phases as well as the partition coefficient as a function of overall concentration in the system. It can be seen that the α-amylase reaches saturation in the heavy, phosphate-rich bottom phase at a relatively low protein concentration (*ca.* 2 g/l), far lower than in the top, PEG phase (*ca.* 4–5 g/l). This results in a change in the "appar-

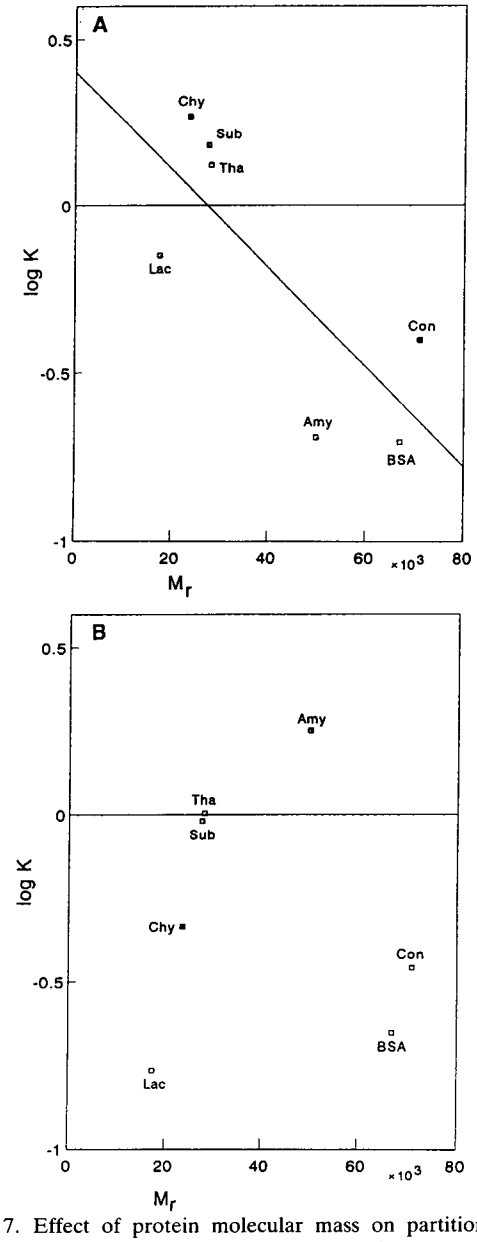

Fig. 7. Effect of protein molecular mass on partition behaviour of proteins in ATPS with 0.6% (w/w) NaCl at pH 7. (A) PEG 4000–dextran ($r = 0.8$); (B) PEG 4000–phosphate.

ent" partition coefficient (higher at higher protein concentration).

The concentration of protein in each phase has been satisfactorily modelled with a "saturation" type curve for α-amylase (Fig. 8).

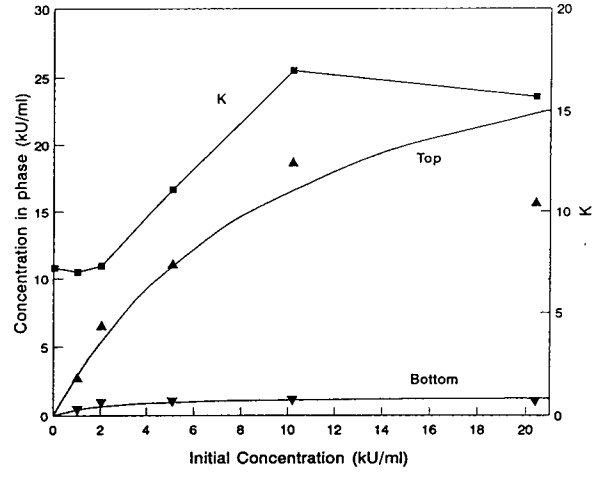

Fig. 8. Effect of overall (initial) system concentration of α-Amylase (1800 U/mg) on the saturation in the two phases (top and bottom) and partition coefficient, K (□) in PEG 4000 (10%, w/w)–phosphate (11.5%, w/w) system with 3% (w/w) NaCl at pH 7. 1 kU = 1000 U.

$$C_{phase} = C_M C_i / (C_0 + C_i) \quad (5)$$

where C_{phase} and C_i denote the concentration in the phase (U/l) and the overall protein concentration (U/l) respectively. C_M and C_0 are constants. The partition behaviour of α-amylase can thus be expressed as $K = C_{top\ phase} / C_{bottom\ phase}$ using Eq. 5 for the concentration in each of the phases.

4. Conclusions

The effect of protein hydrophobicity, charge, molecular mass and concentration has been studied in PEG–phosphate and PEG–sulphate ATPSs in the presence and absence of NaCl for several model proteins. The proteins' hydrophobicity evaluated both by RP-HPLC and HIC did not give a good correlation with partition coefficients in several ATPSs. The surface hydrophobicity of the protein measured by solubility correlated well with the partition coefficient in PEG–salt systems, particularly at high levels of NaCl (5–18%). The charge of proteins also has an important effect on partition; this is expected

to be more pronounced at lower NaCl concentrations. As pH was increased (5.5–9.5) the partition coefficient of α-amylase also increased suggesting a higher concentration of positive charges in the top phase. For molecular mass a tendency was found in PEG–dextran systems at low NaCl concentrations. No clear tendency was observed in the PEG–salt systems. The solubility of the protein in the phases affects its partition behaviour. It was found that α-amylase reaches saturation in the heavy, phosphate-rich phase at relatively low protein concentration, far lower than in the top, PEG-rich phase, results in an increase in the "apparent" partition coefficient. This behaviour was fitted to a saturation type equation for α-amylase in each of the phases of a PEG–phosphate system.

5. Acknowledgements

This work was partially supported by a grant from the European Community to whom thanks are due. Financial assistance from the Hariri Foundation (F.H.) and the European Science Foundation (A.S.S.) is also gratefully acknowledged.

6. References

[1] J.N. Baskir, T.A. Hatton and U.W. Suter, *Biotechnol. Bioeng.*, 34 (1989) 541.
[2] A.D. Diamond and J.T. Hsu, *Biotechnol. Bioeng.*, 34 (1989) 1000.
[3] N.L. Abbott, D. Blankschtein and T.A. Hatton, *Bioseparation*, 1 (1990) 191.
[4] M.A. Eiteman and J.L. Gainer, *Bioseparation*, 2 (1991) 31.
[5] P.K. Smith, R.I. Krohn, G.T. Hermanson, A.K. Mallia, F.H. Gartner, M.D. Provenzano, E.K. Fujimoto, N.M., Goeke, B.J., Olson and D.C. Klenk, *Biochemistry*, 150 (1985) 76.
[6] J.J. Sedmak and S.E. Grossberg, *Anal. Biochem.*, 79 (1977) 544.
[7] A.S. Schmidt, A.M. Ventom and J.A. Asenjo, J.A., *Enzyme Microb. Technol.*, 16 (1994) 131.
[8] F.M. Hachem, *Ph.D. Thesis*, University of Reading, Reading, 1992.
[9] O. Cascone, B.A. Andrews and J.A. Asenjo, *Enzyme Microb. Technol.*, 13 (1991) 629.
[10] W. Melander and Cs. Horváth, *Arch. Biochem. Biophys.*, 183 (1977) 200.
[11] T.M. Przybycien and J.E. Bailey, *Enzyme Microb. Technol.*, 11 (1989) 264.
[12] G. Johansson, *J. Chromatogr.*, 322 (1985) 425.
[13] J.A. Asenjo, T. Franco, A.T. Andrews and B.A. Andrews, in M. White, S. Reuveny and A. Shafferman (Editors), *Biologicals from Recombinant Microorganisms and Animal Cells: Production and Recovery*, VCH, Weinheim, 1991, p. 439.
[14] M.A. Eiteman, *J. Chromatogr.*, 668 (1994) in press.
[15] Sasakawa, S. and H. Walter, *Biochemistry*, 11 (1972) 2760.

ELSEVIER

Journal of Chromatography A, 668 (1994) 55–60

JOURNAL OF CHROMATOGRAPHY A

Effect of pH, ion type and ionic strength on partitioning of proteins in reverse micelle systems

B.A. Andrews*, K. Haywood

Biochemical Engineering Laboratory, University of Reading, Reading RG6 2AP, UK

Abstract

Two proteins with different physico-chemical properties have been partitioned in reversed micelle systems: thaumatin and ribonuclease A. The organic phase was formed by sulphosuccinic acid bis(2-ethylhexyl) ester, sodium salt, in isooctane and the aqueous phase contained either KCl, KBr, $MgCl_2$ or NaCl. Aqueous phase pH was varied between 2 and 13 and ionic strength between 0.1 and 2.8. Small changes in pH (around the p*I*) were found to influence the solubilization of ribonuclease A but for thaumatin the pH change necessary to affect partition was much greater as a consequence of the difference in net charge (titration curves) of these protein molecules as pH changes. The type of ions present in the system was also a determining factor for partition, the larger ions (K^+) produced more electrostatic screening and hence less protein solubilization than the smaller ions (Na^+). With changes in ionic strength surface hydrophobicity was an important factor affecting solubilization of thaumatin.

1. Introduction

The extraction and purification of proteins using reversed micelle systems has been the subject of extensive study in recent years [1–6]. Reversed micelle systems have great potential for the liquid–liquid extraction of biomolecules under moderate conditions. Protein partitioning is dependent upon many factors which are directly related to the interaction between properties inherent to the system itself and those pertaining to the protein under investigation. Fundamental studies of the factors determining selective separation of biomolecules are necessary to establish correlations between the physico-chemical properties of the proteins and the reversed micelle system. These factors include pH, ionic strength and type of ions present in the system, type of surfactant and organic solvent used and physico-chemical properties of the proteins such as isoelectric point, hydrophobicity, size, charge density and charge distribution.

Reversed micelle systems formed from sulphosuccinic acid bis(2-ethylhexyl) ester, sodium salt (AOT), isooctane and water were used in this work. AOT is an anionic surfactant which will form micelles in non-polar solvents without the need for a cosurfactant. In reversed micelle systems the polar head groups of the surfactant molecules are directed towards the interior of the micelle and form a polar core which can solubilize water; the lipophilic chains are exposed to the solvent. Inside the micelles is a pool of water and it has been demonstrated that water in this pool behaves differently from normal water especially at low concentrations ($w_0 =$

* Corresponding author.

0021-9673/94/$07.00
SSDI 0021-9673(94)00090-V

$[H_2O]/[AOT] < 10$). The solubilities of ions and proteins in the water pool can be greater than normal. Water content of a micellar system and phase ratio both have a strong effect on protein solubilization and subsequent function.

In AOT–isooctane systems the micelles are spherical, nanometre sized particles (with diameters ranging from 10 to 200 Å) which are thermodynamically stable. The molar water-to-surfactant ratio (w_0) is used to characterize micelle size.

Increasing ionic strength can affect micelle size, since charged surfactant headgroups repel each other and larger micelles are formed at lower ionic strengths. Also at higher ionic strengths there is a shielding effect between the charged surfactant head groups and the protein, making solubilization in the micelles more electrostatically unfavourable.

The aqueous phase pH in which the protein is dissolved directly affects the charge on the protein: at pH values below its isoelectric point (p*I*) a protein will have a net positive charge and at pH above the p*I* it will have a net negative charge. The net charge of a protein and the distribution of those charges on the protein molecules will affect the interaction with the surfactant headgroups and hence the transfer of the protein to the reversed micelles. The aim of this paper is to investigate the effects of pH, salt type and ionic strength on the partitioning of proteins in AOT–isooctane reversed micelle systems.

2. Materials and methods

2.1. Proteins

Ribonuclease A (type III-A from bovine pancreas) was purchased from Sigma, thaumatin (100% pure Talin, human-food grade) was obtained from Four-F Nutrition, Northallerton, UK.

2.2. Chemicals

AOT was obtained from Sigma and spectrophotometric-grade isooctane (2,2,4-trimethylpentane) from Aldrich. Both were used as supplied. All other chemicals used were of analytical-reagent grade.

2.3. Partition experiments

Protein transfer experiments were done in 25-ml stoppered flasks at room temperature (*ca.* 21°C). The organic phase was composed of 50 m*M* AOT in isooctane. The aqueous phase consisted of NaCl or KCl at different concentrations and pH values. The pH was adjusted by the addition of concentrated acid or base, buffers were not used because over such a wide range of pH values several different buffers would have been necessary involving the addition of a mixture of ions to the system. The pH given is the aqueous phase pH measured after phase equilibrium. Protein was dissolved in the aqueous phase at a concentration of 0.25 mg/ml. Equal volumes of organic and aqueous solutions were mixed and stirred for 5 min which was found to be ample time for equilibration. Phase separation was aided by centrifugation at 2000 rpm (*ca.* 450 *g*) for 5 min. Samples from both phases were then assayed for protein and water content.

2.4. Assays

Protein in both phases was assayed by absorbance at 280 and 310 nm in a Pharmacia Ultrospec III spectrophotometer, standard curves were prepared for each phase with each protein. Water was measured in some organic phases by Karl Fischer titration using a Mettler DL37 KF coulometer.

3. Results and discussion

The molecular masses of thaumatin and ribonuclease A are 22 200 and 13 500, respectively, and their p*I* values are *ca.* 11.5 and 7.8. These two proteins have fairly low molecular masses and should be accommodated into the reversed micelles without an appreciable increase in micelle size and their p*I* values are quite different so the effect of protein charge over a large pH range can be studied. The

surface hydrophobicities of these proteins have been measured, thaumatin has a very high surface hydrophobicity [7], and ribonuclease A is a hydrophilic protein.

3.1. Effect of pH

Fig. 1 shows the effect of the pH of the aqueous phase on the solubilization of thaumatin in reversed micelle systems composed of AOT, isooctane and 0.1 *M* KCl or KBr. All experiments were carried out with initial protein concentration of 0.25 mg/ml. The protein shows similar behaviour with both salts. At pH values 2 or 3 units below its p*I* most thaumatin (*ca.* 100%) partitions to the reversed micelles, at pH values around the p*I* there is a drop in the amount solubilized and at pH values above the p*I* little protein is in the reversed micelle phase. There are slight differences in the two curves; with KCl the pH values at which a drop in solubilization occurs are higher than those for KBr.

At pH values above their p*I* proteins have a net negative charge and so do not interact with, but are repelled by, the negatively charged head groups of the surfactant in the reversed micelles. Conversely, at pH values below their p*I* proteins have a net positive charge and are able to interact with the surfactant and become solubilized in the reversed micelles as in Fig. 1.

The change from net negative charge to net positive charge that occurs at pH values close to the p*I* of the protein depends on the titration curve and charge distribution of the protein. For example, the titration curve for thaumatin is very flat between pH 5 and 9.5 indicating that there is little change in the net charge of the protein molecules in this pH range [7] and hence in Fig. 1 the curve for thaumatin is not as steep as those for other proteins such as ribonuclease A (Fig. 2) where the net charge is much more sensitive to changes in pH.

Fig. 2 shows the solubilization of ribonuclease A in reversed micelles with three different salts; KCl, KBr and $MgCl_2$ over a range of pH values. With all three salts there is an apparent drop in % solubilization at the lowest pH values. This has been attributed to denaturation of the protein or hydrolysis of the AOT at low pH but is now thought to be due to aggregation of AOT and protein at the interface. We have measured the absorbance spectrum of AOT between 190 and 950 nm over a range of pH values from 2 to 12. An absorbance peak occurred at 232 nm in all the samples and no significant differences in the absorbance spectra were seen indicating that hydrolysis of AOT is not occurring in this range of pH values. Lye [8] has found AOT–protein precipitates when working with proteins in

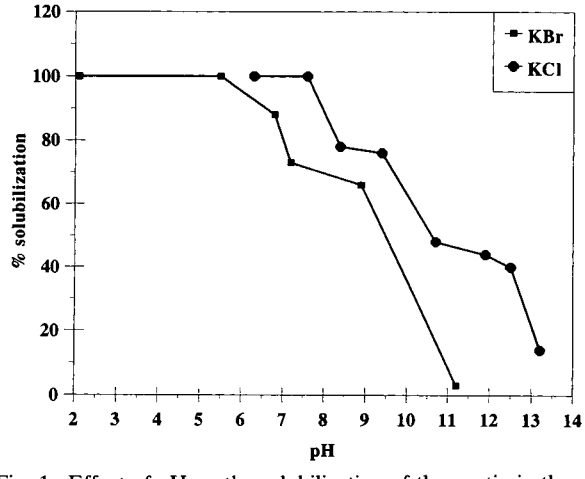

Fig. 1. Effect of pH on the solubilization of thaumatin in the reversed micelle phase; 50 m*M* AOT in isooctane, 0.1 *M* KBr or KCl as aqueous phase, 0.25 mg/ml protein.

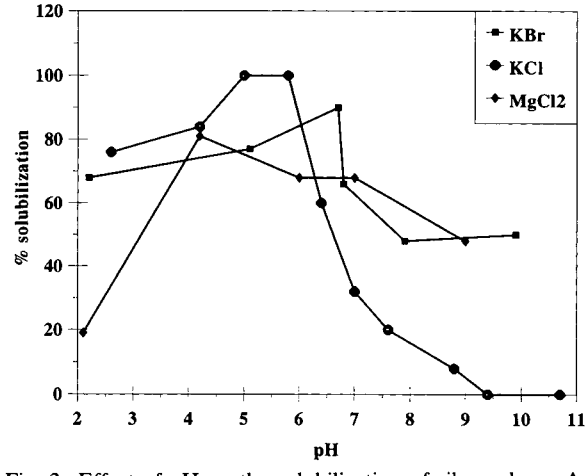

Fig. 2. Effect of pH on the solubilization of ribonuclease A in the reversed micelle phase. Conditions as for Fig. 1.

AOT–isooctane systems. Göklen and Hatton [9] also observed lower solubilities for some proteins at low pH and attributed this to possible protein denaturation. Matzke *et al.* [4] obtained similar results for chymotrypsin using AOT as surfactant; they tested for denaturation using circular dichroism and fluorescence absorption and found no evidence of gross conformational changes in protein structure or changes in the spectra over the pH range 2 to 12. Using organic-phase atomic absorption Matzke *et al.* [4] determined the amount of AOT in the organic phase. As AOT is the major source of sodium in the organic phase, any significant changes could be attributed to a change in the amount of AOT in the organic phase. It was found that at pH 4 the sodium ion concentration is much lower for the chymotrypsin-containing sample than for the protein-free sample. In the intermediate pH range (6–10) the concentrations are similar and at pH 11 the protein-containing sample again has a lower sodium ion concentration. These results suggest that less AOT is present in the organic phase at low and high pH for the samples containing protein, which indicates that AOT may be aggregating at the interface.

Fig. 2 shows that with $MgCl_2$ at low pH values (below 4) the decrease in transfer of ribonuclease is larger than with the other salts indicating that the ions present in the system may also influence the degree of AOT–protein precipitation.

3.2. Effect of ionic strength and salt type

To study the influence of aqueous phase ionic strength (I) on protein transfer to the organic phase each protein was partitioned in reversed micelle systems with KCl, KBr and NaCl of ionic strengths varying from 0.1 to 1.0.

Fig. 3 shows the effect of ionic strength of KCl, KBr and NaCl on thaumatin solubilization into the reversed micelle phase (50 mM AOT in isooctane). In Fig. 3 the curves show a very sharp drop in solubilization at ionic strengths between 0.2 and 0.4 with KCl, between 0.1 and 0.3 with KBr and between 0.4 and 0.7 with NaCl. As the ionic strength increases the ions

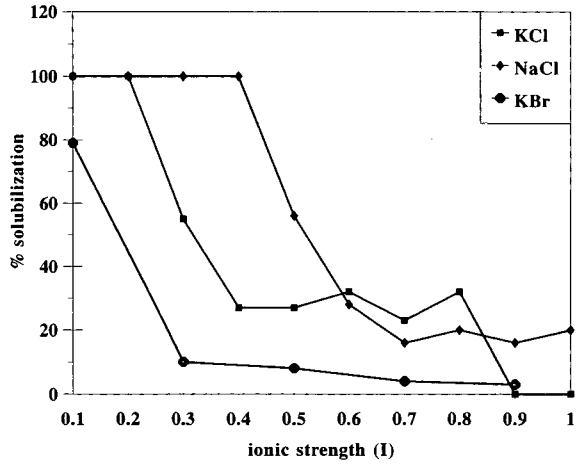

Fig. 3. Effect of ionic strength of aqueous phase on the solubilization of thaumatin into the reversed micelle phase; 50 mM AOT in isooctane, KCl, KBr and NaCl as aqueous phase, pH 7.

form an electrostatic shield around the micelles so the protein molecules cannot interact with them and hence the percentage of protein in the organic phase decreases. At higher ionic strengths the screening effect decreases charged surfactant headgroup repulsions resulting in a decrease in water solubilization and a lower w_0. For example, in a system with NaCl and thaumatin the w_0 value decreases from 48 with 0.1 M salt to 18 with 1.0 M NaCl. Hence the resulting micelles are smaller than at low ionic strengths and this can lead to the protein being excluded on the basis of size as ionic strength is increased.

The differences in the solubilization curves with the three different salts may be a consequence of the relative sizes of the K^+ and Na^+ ions. The atomic radii of these ions are 1.33 and 0.97 Å, respectively. In general the smaller ions (Na^+) produce less screening and hence allow more protein to interact with and transfer to the micelles. This is seen in the figures as a shift to higher ionic strengths of NaCl at which the percentage solubilization decreases. KBr gave very similar results to KCl indicating, as expected, that with AOT as surfactant (with negatively charged head groups) the cations have more influence than the anions.

Thaumatin has a very high surface hydrophobicity and this can influence the interactions between the protein and the surfactant molecules under certain conditions and hence determine partitioning behaviour. We have studied the behaviour of thaumatin at pH values near to and above its p*I* [10] with KCl and NaCl. With NaCl at high pH values (12) all of the protein is solubilized in the organic phase at ionic strengths between 0.3 and 0.8, this has been attributed to the high surface hydrophobicity of the thaumatin molecules which enables them to interact with the non-polar chains of the AOT. When comparing the behaviour of thaumatin in the systems with Na^+ and K^+ it appears that the order by which the ions promote hydrophobic interactions follows the Hofmeister or lyotropic series ($Mg^{2+} > Li^+ > Na^+ > K^+ > NH_4^+$).

Fig. 4 shows the partitioning of ribonuclease A in reversed micelles with an aqueous phase consisting of KCl, KBr, NaCl and $MgCl_2$ with ionic strengths from 0.1 to 2.7. $MgCl_2$ allowed protein transfer in the range of ionic strengths from 0.3 to 2.7, significantly higher than both KCl and NaCl. The Mg^{2+} ion has an atomic radius of 0.66 Å and is thus smaller than both K^+ and Na^+, this result supports the idea that smaller ions produce less screening of the micelles and thus allow more protein transfer.

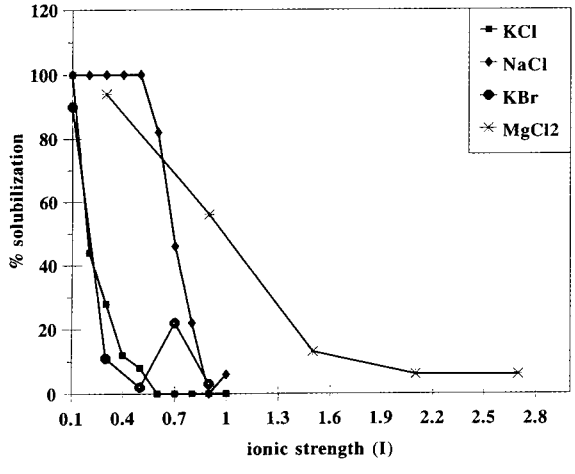

Fig. 4. Effect of ionic strength of aqueous phase on the solubilization of ribonuclease A into the reversed micelle phase. KCl, KBr, NaCl and $MgCl_2$ as aqueous phase, pH 5.

Marcozzi *et al.* [3] have studied the factors affecting the forward and backward transfer of α-chymotrypsin in AOT–isooctane systems. They used four salts, KCl, NaCl, LiCl and $CaCl_2$ and found that protein transfer occurred at lowest ionic strengths with KCl followed by $CaCl_2$, NaCl and LiCl. The atomic radii of K^+, Ca^{2+}, Na^+ and Li^+ are 1.33, 0.99, 0.97 and 0.68 Å, respectively, indicating that the size of the ions may also be important in this system.

4. Conclusions

Thaumatin and ribonuclease A have been partitioned in reversed micelle systems and the effects of pH, ionic strength and ion type have been investigated.

With changes in pH the protein solubilization depends on the p*I* and net charge (titration curve) of the protein. The type of ions in the system affect protein solubilization by causing electrostatic screening of the surfactant headgroups and thus hindering interactions between the protein and the surfactant. Larger ions such as K^+ cause more screening and hence less solubilization than smaller ions such as Na^+.

Increasing ionic strength decreases protein partition to the reversed micelle phase with proteins that do not have high surface hydrophobicities (*e.g.* ribonuclease A). In the case of hydrophobic proteins (*e.g.* thaumatin) the interaction of the protein with the surfactant and/or organic solvent is so strong that no effect of ionic strength is seen at some values of pH.

5. Acknowledgement

This work was supported by a grant from the Agricultural and Food Research Council (AFRC) to whom thanks are due.

6. References

[1] K.L. Kadam, *Enzyme Microb. Technol.*, 8 (1986) 266–273.

[2] P.L. Luisi, *Angew. Chem.*, 24 (1985) 439–528.
[3] G. Marcozzi, N. Correa, P.L. Luisi and M. Caselli, *Biotechnol. Bioeng.*, 38 (1991) 1239–1246.
[4] S.F. Matzke, A.L. Creagh, C.A. Haynes, J.M. Prausnitz and H.W. Blanch, *Biotechnol. Bioeng.*, 40 (1992) 91–102.
[5] R.S. Rahaman and T.A. Hatton, *J. Phys. Chem.*, 95 (1991) 1799–1811.
[6] R.B.G. Wolbert, R. Hilhorst, G. Voskuilen, H. Nachtegaal, M. Dekker, K. van 't Riet and B.H. Bijsterbosch, *Eur. J. Biochem.*, 184 (1989) 627–633.
[7] T. Franco, *Ph.D. Thesis*, University of Reading, Reading, 1993.
[8] G.J. Lye, *Ph.D. Thesis*, University of Reading, Reading, 1993.
[9] K.E. Göklen and T.A. Hatton, *Sep. Sci. Technol.*, 22 (1987) 831–841.
[10] B.A. Andrews, D.L. Pyle and J.A. Asenjo, *Biotechnol. Bioeng.*, in press.

ELSEVIER

Journal of Chromatography A, 668 (1994) 61–64

JOURNAL OF CHROMATOGRAPHY A

Improvement in the polyethylene glycol–Cibacron Blue purification method

L.P. Fonseca, J.C.G. Caldeira, J.M.S. Cabral*

Laboratório de Engenharia Bioquímica, Instituto Superior Técnico, 1000 Lisbon, Portugal

Abstract

A new approach was developed for the purification of polyethylene glycol (PEG)–Cibacron synthesized from PEG 8000 and Cibacron 3G-A, using an NH_2-silica anion exchanger for separation of the unreacted PEG 8000 from the other compounds of the reaction mixture. The adsorption of PEG–Cibacron and Cibacron under acidic conditions (pH 4.7) was 22.4 mg (Cb and PEG–Cb) per gram of silica and 100% elution was achieved with 1% (v/v) ethanolamine solution at pH 9. The silica exchanger can be reused several times without loss of performance. An extraction step with chloroform was used to separate the PEG–dye from the non-bonded Cibacron, which completely partitioned into the aqueous phase. After drying, a dark-blue solid polymer with a yield of 7.6% in relation to the initial mass of PEG was obtained, which is an increase of 50% in relation to earlier work.

1. Introduction

Two-phase aqueous systems have been studied and used in separations of microbial cells and cellular debris [1], in the purification of proteins and enzymes [2] and in bioconversion systems [3]. Affinity partitioning with the objective of increasing the specific purification of biological products (*e.g.*, enzymes and proteins) has also been used, based on two-phase aqueous systems [4]. Synthetic dyes are common and advantageous affinity ligands, Cibacron Blue (Cb) bound to polyethylene glycol (PEG) being one of the most studied ligands [5] for extraction with aqueous two-phase systems.

Different reactions and mainly three purification methods [6–8] (Table 1) have been used to obtain pure PEG–Cb. The aim of this work was to contribute to the improvement of the purification of PEG–Cb by eliminating the first step (Table 1) and to replace DEAE-cellulose with another anion exchanger, namely a silica carrier modified by silanization [9] with a primary amine group.

2. Experimental

2.1. Materials

Cibacron Blue 3GA and polyethylene glycol (PEG) of average molecular mass 8000 were obtained form Sigma (St. Louis, MO, USA). Silica gel (XWP 500 MP) with a pore diameter of 50 nm and a particle size between 0.5 and 1.0 mm was purchased from Grace (Worms, Ger-

* Corresponding author.

0021-9673/94/$07.00
SSDI 0021-9673(93)E1186-4

Table 1
PEG–CB purification methods

Ref.	1st step	2nd step	3rd step	PEG 8000 yield (%)
Kopperschlager and Johansson [7]	Drying	Chloroform extraction	Methanol recrystallization	4.2
Johansson *et al.* [8]	Chloroform extraction	DEAE ion exchange	Chloroform extraction	5.0
Johansson and Joelsson [6]	Dilution or dialysis	DEAE ion exchange	Chloroform extraction	5.0

many). 3-(Triethoxysilyl)propylamine (99%) and ethanolamine (98%) were obtained from Merck (Hohenbrunn, Germany). Sephadex G-75 was supplied by Pharmacia (Uppsala, Sweden). Other reagents were of analytical-reagent grade.

2.2. Analytical methods

Cb, PEG–CB, ethanolamine and PEG determinations. The absorbance of the Cb and PEG–Cb complex was measured at 612 nm [6]. Ethanolamine was measured by spectrophotometry at 310 nm. The concentration of PEG was determined using the method of Skoog [10] by reading the absorbance at $\lambda_{max} = 546$ nm.

Amine groups in silica. Silica amine groups were determined by the 2,4,6-trinitrobenzenesulphonic acid (TNBS) method [11] after alkaline solubilization.

Preparation of PEG–Cb. The covalent binding of Cb to PEG was based on the method described by Johansson and Joelsson [6]. A solution of PEG and Cb was prepared by mixing 20 g of PEG, 0.66 g of Cb and 20 ml of water. The reaction was started with 16 ml of a solution of 14% (w/v) NaOH and 6% (w/v) $NaSO_4$. After 7 h of agitation at room temperature the reaction was stopped by lowering the pH with pure acetic acid (99.8%).

3. Results and discussion

3.1. Adsorption conditions

The acidic reaction mixture obtained from PEG–Cb preparation produced a PEG–salt-type aqueous two-phase system after settling. The purest top phase was used in further processing; however, this phase was diluted fivefold to decrease its viscosity.

Adsorption of top-phase Cb and PEG–Cb on a silica anion exchanger was tested at different pH values and amine levels. The adsorption capacity was highest at the lowest pH in the range 4–7 (Fig. 1) without adsorption of PEG.

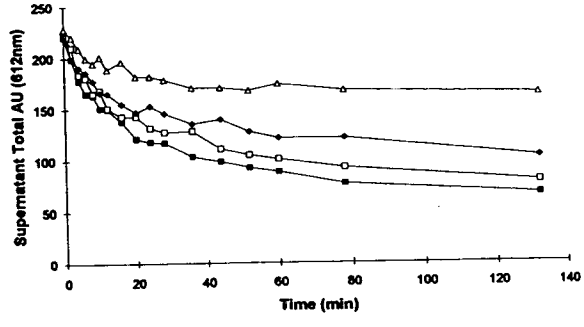

Fig. 1. Cibacron and PEG–Cb batch adsorption at 23°C on modified silica (1 g with 12.5 mg NH_2) at different pH values: (△) pH 7; (◆) pH 6; 9□) pH 5; (■) pH 4.

Adsorption was done at pH 4.7 owing to the buffer capacity of acetic acid at this pH [12].

The capacity of the modified silica was improved by increasing the amine group loading (Fig. 2). There was no adsorption on the unmodified silica and with the aqueous silanization method [9] the best binding was 22.4 mg (Cb and PEG–Cb) per gram of silica for an average amine level of 13.6 mg NH_2 per gram of silica.

3.2. Elution conditions

The method described in the literature [6,8] uses 2 *M* KCl to destabilize the ionic interaction between DEAE-cellulose and PEG–Cb. It could be verified that using silica modified with a primary amine group, which is a milder ion exchanger than the DEAE group, it was possible to elute Cb and PEG–Cb with an alkaline buffer (pH 9) (Fig. 3) by neutralizing the electric charge of amine groups on the silica surface. Ethanolamine solution (1%, v/v) was chosen as the eluent as it efficiently regenerates the modified silica and presents a buffer capacity at high pH.

3.3. Extraction

PEG–Cb was extracted from the silica eluate in a two-phase system (aqueous chloroform) with a volumetric phase ratio of 10:1. Ethanolamine

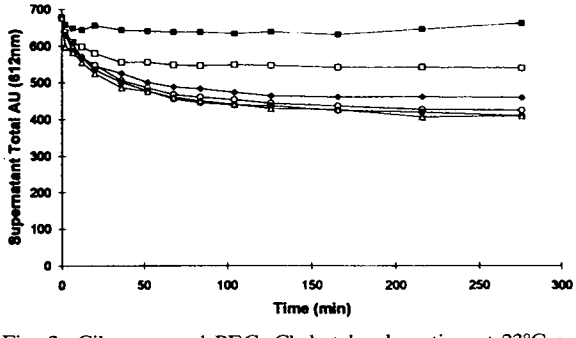

Fig. 2. Cibacron and PEG–Cb batch adsorption at 23°C on modified silica with different amine levels (1 g with different amounts of NH_2) at pH 4.7. NH_2: (■) 0.0; (□) 5.3; (◆) 11.3; (○) 12.5; (●) 13.0; (△) 14.2 mg.

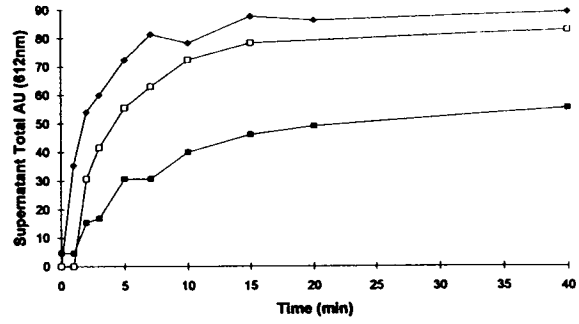

Fig. 3. Cibacron and PEG–Cb batch elution from modified silica (1 g with 5.3 mg NH_2) with 2.3% ethanolamine at different pH values. (■) pH 8; (□) pH 8.5; (◆) pH 9.

(partition coefficient 16.4) and Cibacron partition favourably to the aqueous phase, but total phase separation was only possible if 0.4 *M* KCl was present in the aqueous phase.

PEG–Cb was obtained as solid product after drying the chloroform phase with anydrous sodium sulphate and vacuum evaporation at 40°C.

3.4. PEG–Cb purity and yield

A purification strategy, shown in Fig. 4, was tested to obtain the PEG–Cb complex. Several cycles of column adsorption and elution were

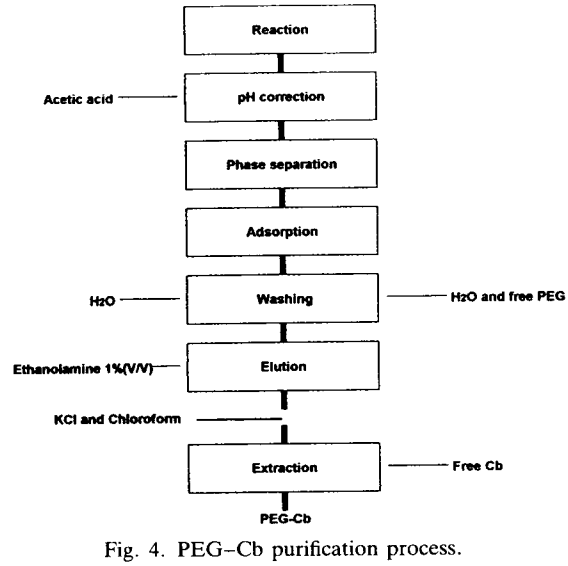

Fig. 4. PEG–Cb purification process.

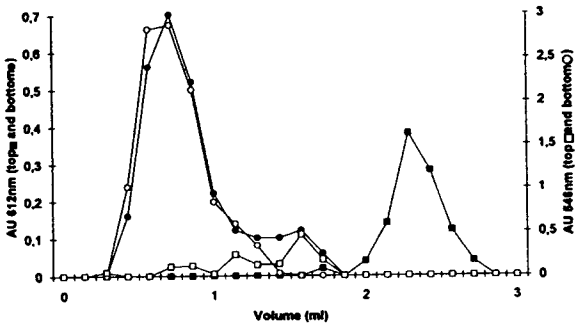

Fig. 5. Chloroform extraction of PEG–Cb demonstrated by gel filtration chromatography. PEG–Cb is present in the bottom phase (signal at 546 nm, ○; and 612 nm, ●), and in a parallel run Cb is only present in the top phase (signal at 612 nm, ■; and no signal at 546 nm, □).

used to purify a total reaction batch (20 g of PEG reacted with 0.66 g of Cibacron Blue 3G-A). The NH_2-silica exchanger could be totally recycled using 1% (v/v) ethanolamine solution at pH 9. These adsorption–elution cycles were extended to more than ten runs without any apparent loss of adsorption and elution capacity.

The efficiency of the chloroform extraction step in separating PEG–Cb and Cb was tested by gel filtration chromatography using a Sephadex G-75 column (8 cm × 0.4 cm I.D.). From fig. 5, it can be seen that PEG–Cb was collected in the first fractions and Cb in the last fractions. It can also be concluded that Cb is present only in the top phase and PEG–Cb in the bottom phase.

The final yield was 0.076 g of PEG–Cb per gram of initial PEG, based on dry mass measurements, whereas the value of monosubstituted PEG 8000 (0.117 mmol Cb per gram of polymer) found experimentally is similar to the theoretical value (0.125 mmol Cb per gram of polymer). These results compare favourably with those in the literature (Table 1).

4. Conclusions

A two-step procedure was achieved for PEG–Cb purification. The PEG–Cb was adsorbed on an NH_2-silica anion exchanger and was easily and completely eluted with 1% (v/v) ethanolamine solution, leading to a higher (50%) purification yield in comparison with previous procedures. The anion exchanger can be reused several times (>10) without a decrease in capacity.

5. References

[1] M.-R. Kula, K.H. Kroner and H. Hustedt, *Adv. Biochem. Eng.*, 24 (1982) 73.
[2] P.-A. Albertsson, *Partition of Cell Particles and Macromolecules*, Wiley, New York, 1975.
[3] E. Andersson and B. Hahn-Hagerdal, *Enzyme Microb. Technol.*, 12 (1990) 242.
[4] M. Joelsson and G. Johansson, *Enzyme Microb. Technol.*, 9 (1987) 233.
[5] J. Huddlston, A Veide, K. Kohler, J. Flanegan, S.-O. Enfors and A. Lyddiatt, *Trends Biotechnol.*, 9 (1991) 381.
[6] G. Johansson and M. Joelsson, *Biotechnol. Bioeng.*, 27 (1985) 621.
[7] G. Kopperschlager and G. Johansson, *Anal. Biochem.*, 124 (1982) 117.
[8] G. Johansson, G. Kopperschlager and P.-A. Albertsson, *Eur. J. Biochem.*, 131 (1983) 589.
[9] H.H. Weetall, *Methods Enzymol.*, 44 (1976) 134.
[10] B. Skoog, *Vox Sang*, 37 (1979) 345.
[11] P.D.G. Dean, W.S. Johnson and F.A. Middle, *Affinity Chromatography*, IRL Press, Oxford, 1985, p. 76.
[12] R.A. Cooper, in R.M.C. Dawson, D.C. Elliott and K.M. Jones (Editors), in *Data for Biochemical Research*, Oxford University Press, London, 1969, p. 66.

ELSEVIER

Journal of Chromatography A, 668 (1994) 65–73

JOURNAL OF CHROMATOGRAPHY A

Supports for liquid–liquid partition chromatography in aqueous two-phase systems: a comparison of LiChrospher and LiParGel

Christer Wingren*, Boel Persson, Ulla-Britt Hansson

Department of Biochemistry, University of Lund, P.O. Box 124, S-221 00 Lund, Sweden

Abstract

Polyacrylated particles of silica (LiChrospher Diol 4000) or hydrophilic polyvinyl polymers (LiParGel 650) were used as supports for liquid–liquid partition chromatography in an aqueous polyethylene glycol–dextran two-phase system. High packing pressures gave high and reproducible values of the stationary mobile phase volume ratio ($V_S/V_M = 1.5$) on both supports. The volume of one theoretical plate was only 6 μl on LiChrospher and 20 μl on LiParGel. The performance of a 3-ml LiChrospher column was comparable to that of 15-ml LiParGel columns. In addition, the resolution of immunoglobulins was higher on LiChrospher. The influence of the supports on the retention of proteins is discussed.

1. Introduction

Partitioning in aqueous two-phase systems has been used to separate and isolate cells, organelles and macromolecules. As the distribution of a molecule in these systems depends on its conformation and general surface properties [1–4], the method may also be used to obtain information about conformational changes occuring on interaction between molecules [1,5]. By optimizing the composition of the phases, separation may be achieved in only a few steps. However, finding such optimum systems may pose difficulties in order to obtain adequate separation, and various forms of automated counter-current extraction have therefore been developed [6–8]. The time required for the analyses may be further shortened by employing column chromatography. A column chromatographic approach would also increase the plate number and, hence, the sensitivity of the method.

Finding materials suitable as supports for liquid–liquid partition chromatography in aqueous two-phase systems (LLPC) was a problem, however. Several attempts have been made to adsorb the dextran-rich bottom phase of the most thoroughly studied two-phase system, formed by polyethylene glycol (PEG) and dextran, on supports made of, for example, agarose beads [9], polyethers immobilized on Sepharose [10], silicates [11,12] or cellulose [13,14]. Eventually, the problem was solved by combining the affinity of polyacrylamide for the dextran-rich phase with the mechanical strength of hydrophilic vinyl (LiParGel) or silica (LiChrospher Diol) polymers [15]. LLPC on LiParGel has been shown to be a powerful tool for the

* Corresponding author.

0021-9673/94/$07.00
SSDI 0021-9673(93)E0075-6

separation and qualitative structural analysis of proteins and nucleic acids [15–18]. Despite their low solubility in the presence of the phase-forming polymers, immunoglobulins and antigen–antibody complexes can also be analysed by LLPC [19–21].

In an attempt to improve the performance of the LLPC columns, we examined the possibility of using dextran-grafted agarose beads as a support [19]. This matrix, Superdex 200, was found to give a larger plate number and a better resolution than LiParGel 650. However, immunoglobulins and other large molecules were strongly retarded, making LLPC on Superdex 200 unsuitable for the analysis of large molecules.

As mentioned above, LiChrospher Diol 4000 consists of silica particles which are polyacrylated [15]. As the LiChrospher particles are smaller than the LiParGel particles, larger theoretical plate numbers may be obtained [15]. In addition, the influence of LiChrospher on the retention of proteins is less pronounced than that of LiParGel [18].

In this work, we compared the properties of LiChrospher Diol 4000 with those of LiParGel 650 with respect to their ability to adsorb the dextran-rich bottom phase of an aqueous PEG–dextran two-phase system. The influence of the supports on the retention of proteins was also studied.

2. Experimental

2.1. Materials

Dextran T 500 (M_r = 500 000) was obtained from Pharmacia–LKB Biotechnology (Uppsala, Sweden) and PEG 8000 (M_r = 6000–7500) from Union Carbide (New York, USA). LiParGel 650 and LiChrospher Diol 4000 were a gift from Merck (Darmstadt, Germany). Protein G-Sepharose 4 Fast Flow, Ampholine PAGplate (3.5–9.5) and Ultropac TSK G3000SW columns (600 × 7.5 mm I.D.) were supplied by Pharmacia–LKB Biotechnology. Horseradish peroxidase was obtained from Merck, human albumin and bovine thyroglobulin from Pharmacia–LKB Biotechnology, human immunoglobulin G (IgG) from Sandox (Basle, Switzerland), Ig fractions of rabbit anti-human albumin and anti-human IgG from Dakopatts (Glostrup, Denmark), human apo-transferrin and whale skeletal myoglobin from Sigma (St. Louis, MO, USA) and bovine serum albumin (BSA) from Wilfried Smith (Edgware, UK). Sera from four patients with multiple myeloma were a gift from Dr. F. Lindström (Department of Medicine, Linköping, Sweden).

2.2. Isolation of myeloma IgG1

IgG was isolated from myeloma sera by affinity chromatography on Protein G-Sepharose in 20 m*M* sodium phosphate (pH 7.0). Bound immunoglobulins were eluted with 0.1 *M* glycine–HCl (pH 2.7). The purity of the preparations (95%) was checked with agarose gel electrophoresis [0.8% agarose in 75 m*M* barbital buffer–2m*M* calcium lacate (pH 8.6)], double immunodiffusion and high-performance size-exclusion chromatography HPSEC on the Ultropac TSK G3000SW column in 10 m*M* sodium phosphate–0.14 *M* NaCl (pH 7.4).

2.3. Characterization of the proteins

Molecular masses were determined by sodium dodecyl sulphate–polyacrylamide gel electrophoresis (SDS-PAGE) on a 5% or 7.5% polyacrylamide gel [22] and by HPSEC on an Ultropac TSK G3000SW column in 10 m*M* sodium phosphate–0.14 *M* NaCl (pH 7.4). Isolectric points were determined by isoelectric focusing on an Ampholine PAGplate (limits 3.5–9.5).

2.4. Two-phase system

All experiments were performed in a 4.4% (w/w) PEG 8000–6.2% (w/w) dextran T 500 two-phase system containing 50 m*M* sodium phosphate–0.1 *M* NaCl–0.1 M glycine (pH 7.0). The two-phase system was prepared by thoroughly mixing PEG, dextran and water. In experiments where LiParGel 650 was used as a support, sodium chloride, glycine and sodium

phosphate were added to the phase system and the pH was adjusted with HCl. The system was then equilibrated at 20°C for 72 h and the clear phases were separated. In experiments where LiChrospher Diol 4000 was used as a support, the two-phase system was equilibrated at 20°C for 72 h and the clear phases were separated. Salts were added to the top phase whereas the bottom phase was adsorbed on LiChrospher without any additional salts or buffer substances.

2.5. Determination of partition coefficients in batch

A 4-g amount of the two-phase system was thoroughly mixed with 0.5–4 mg of protein and the phases were allowed to separate at 20°C overnight. No precipitates were observed. The partition coefficient, K_{batch}, which describes the ideal partitioning of the protein in the phase system, was defined in accordance with the notation commonly used in aqueous two-phase partitioning, *i.e.*,

$$K_{batch} = C_{top\ phase}/C_{bottom\ phase} \quad (1)$$

where $C_{top\ phase}$ and $C_{bottom\ phase}$ are the concentrations of the protein in the top phase and bottom phase, respectively, determined spectrophotometrically at 280 nm.

2.6. Preparation of the LLPC columns

The matrix, LiParGel 650 or LiChrospher Diol 4000, was equilibrated with the dextran-rich bottom phase (stationary phase) overnight. The coated matrix was rinsed with the PEG-rich top phase (mobile phase) to remove any excess of stationary phase, suspended in mobile phase and poured into a thermostated (20°C) column with a filling reservoir. LiParGel was packed in steel columns (200 × 4.5 mm I.D. or 300 × 8.0 mm I.D.) under gravitational sedimentation for 5–30 h. The columns were further packed at a flow-rate of ≤0.2 ml/min (≤0.7 MPa), giving a volume ratio of the stationary phase to the mobile phase (V_S/V_M) of ≤1.0, or at ≤1.0 ml/min (≤25 MPa), giving a V_S/V_M of 1.5. Amounts of 20–150 μg of protein were applied to the columns in 0.1 ml of mobile phase at a flow-rate of 0.01–0.30 ml/min. LiChrospher (200 × 4.5 mm I.D. steel columns) was packed at a flow-rate of ≤0.025 ml/min (≤2.6 MPa), giving a V_S/V_M of ≤1.5 Large LiChrospher columns (300 × 8.0 mm I.D.) were not used as the dense packing considerably reduced the flow-rate. The columns were equilibrated with at least three volumes of mobile phase until the eluates were clear. Amounts of 100–200 μg of protein were applied to the columns in 0.1 ml of mobile phase at a flow-rate of 0.025 ml/min. The eluates were continuously monitored at 280 nm.

2.7. Calculations

The parameters of the LLPC columns were determined as described previously [17]. Two reference proteins, peroxidase and myoglobin (0.02–0.2 mg), were applied to the columns. Ideal partitioning was assumed for the references, *i.e.*, K_C was taken as $1/K_{batch}$ (Eq. 1). K_C is the ratio of the concentration of a molecule in the stationary phase to that in the mobile phase:

$$K_C = C_{stationary\ phase}/C_{mobile\ phase} \quad (2)$$

The volumes of the stationary and mobile phases, V_S and V_M, were calculated form the retention volumes of the references, V_R, using the relationship

$$V_R = V_M + K_C V_S \quad (3)$$

The plate number, N, was calculated from the peak width at half-height (w_h) of the myoglobin peak according to

$$N = 5.54\,(V_R/w_h)^2 \quad (4)$$

The resolution of the peroxidase and myoglobin peaks, R_s, was calculated as

$$R_s = (\sqrt{N}/4)[k/(1+k)](\alpha - 1) \quad (5)$$

where k is the capacity factor [$k = (V_S/V_M)K_C$] and α is the ratio of the partition coefficients of the references ($\alpha = K_{batch,\ peroxidase}/K_{batch,\ myoglobin}$).

3. Results

The influence of packing pressure on the prestanda of LiParGel 650 columns was examined. The parameters of columns packed at low pressure (in accordance with the packing procedure commonly used) or at higher pressure (see Experimental) are compared in Table 1. While the content of the stationary phase (V_S) was not affected by the higher packing pressure, the amount of mobile phase (V_M) decreased, indicating that the elevated pressure did not affect the volume of the LiParGel particles. The denser packing increased not only the ratio of V_S to V_M but also the plate number and the resolution of the reference proteins. The column performance in terms of plate numbers increased with decreasing flow-rate in the range 0.01–0.30 ml/min. It should be noted that the flow-rates used in this study were those required to elute the reference proteins within 2 h (Table 1).

In an attempt to reduce the consumption of material, small, densely packed LiParGel columns were prepared. The parameters of the 3.2-ml columns were compared with those of the 15.1 ml columns (Table 1). It is interesting that V_S and V_M per unit column volume and the volume of one theoretical plate (about 20 μl) were independent of the column volume. Running two small, densely packed columns in tandem did not improve the performance as the flow-rates had to be doubled. Thus, by employing a higher packing pressure, reproducible column packings were obtained and smaller columns with adequate performance could be used.

The influence of the properties of the support on the chromatographic performance was also examined. A polyacrylate support with a smaller particle size than LiParGel, LiChrospher Diol 4000, was used as a support in small, densely packed LLPC columns (Table 1). Although the volume of the LiChrospher matrix was smaller than that of LiParGel (10% of the column volume compared with 30% for LiParGel), the volume of stationary phase adsorbed on LiChrospher was larger per unit column volume. Further, the plate numbers were larger for the LiChrospher columns (the volume of one theoretical plate was only 6 μl), which would imply that the surface area of the stationary phase that is available for partitioning is larger on the LiChrospher particles. The resolution between the references was also higher on the LiChrospher columns than on LiParGel. Hence, using LiCrospher as a support improved the chromatographic performance of LLPC columns.

The variation in column parameters with repeated use is exemplified by the ratio of V_S to V_M in Fig. 1. V_S/V_M was found to be constant on LiParGel columns. The columns could even be stored at 20°C for several weeks without any change in the performance. In contrast, V_S/V_M

Table 1
Influence of packing pressure, size of the column and choice of support (LiParGel 650 and LiChrospher Diol 4000) on the parameters of the LLPC columns used

Matrix	Pressure (MPa)	I.D. (cm)	L (cm)	V_S/V_M	V_S/V_C	V_M/V_C	N	R_s	Flow-rate[a] (ml/min)
LiParGel	0.7	0.80	30	1.0 ± 0.1	0.36 ± 0.01	0.38 ± 0.01	595 ± 50	2.63 ± 0.07	0.12
LiParGel	25	0.80	30	1.5 ± 0.1	0.41 ± 0.01	0.27 ± 0.01	725 ± 50	3.64 ± 0.07	0.12
LiParGel	25	0.45	20	1.5 ± 0.1	0.41 ± 0.01	0.27 ± 0.01	200 ± 10	1.92 ± 0.05	0.025
LiParGel	25	0.45	2 × 20	1.5 ± 0.1	0.41 ± 0.01	0.28 ± 0.01	250 ± 25	2.10 ± 0.07	0.05
LiChosper	2.6	0.45	20	1.5	0.53	0.35	500	3.00	0.025
LiChrosper	2.6	0.45	20	1.0	0.45	0.44	200	1.64	0.025

I.D. = Column internal diameter; L = column length; V_S = volume of the stationary phase; V_M = volume of the mobile phase; V_C = column volume; N = plate number for myoglobin; R_s = resolution of peroxidase and myoglobin.
[a] Flow-rate required to elute the reference proteins within 2 h.

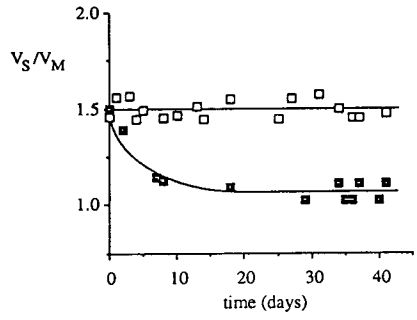

Fig. 1. Variations in the column parameters, exemplified by the volume ratio of the stationary phase (V_S) to the mobile phase (V_M), for (□) LiParGel 650 and (■) LiChrospher Diol 4000 columns run 8 h per day, 1–5 days per week, during a period of 6 weeks.

on LiChrospher columns varied until a value around 1.0 was achieved. The performance was considerably reduced with decreasing V_S/V_M, but still comparable to that of LiParGel (Table 1). After several weeks' of storage at 20°C, the plate numbers had returned to the original value whereas the ratio of V_S to V_M was still about 1.0.

Fig. 2 shows the chromatogram for rabbit IgG (anti-albumin), human IgG and albumin obtained by LLPC on LiParGel and LiChrospher. In order to facilitate the comparison of results obtained on columns with different parameters, retention volumes were expressed as K_C according to Eq. 3. The relative standard deviation of

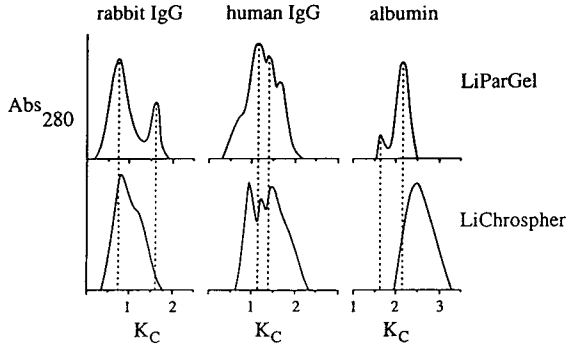

Fig. 2. Chromatograms for rabbit IgG (anti-albumin), human IgG and albumin obtained on LiParGel 650 (polyvinyl–polyacrylamide) ($V_S/V_M = 1.5 \pm 0.1$; $N = 725 \pm 50$; $R_s = 3.64 \pm 0.07$) and LiChrospher Diol (silica–polyacrylamide) 4000 ($V_S/V_M = 1.1 \pm 0.1$; $N = 470 \pm 100$; $R_s = 2.6 \pm 0.3$).

K_C for a given component was <5% on LiParGel columns and <15% on LiChrospher columns. Rabbit IgG was eluted as two peaks on LiParGel whereas LLPC on LiChrospher gave two poorly resolved components. Human IgG was fractionated into three components on both matrices. Human albumin was eluted as two peaks on LiParGel but as a single, broad component on LiChrospher. The differences between the elution patterns obtained for a given protein on the two matrices indicated a profound influence of the properties of the supports on the partitioning of proteins.

In order to evaluate the influence of the supports on the retention of proteins in LLPC columns, seven proteins with different physicochemical properties was analysed. The experimentally obtained retention volumes were compared with those calculated according to Eq. 3, using $1/K_{batch}$, where K_{batch} is determined in the absence of any matrix, as K_C (Fig. 3). The calculated volumes are assumed to describe ideal partitioning. It should be noted that for proteins that were fractioned into more than one component, all calculations refer to the average

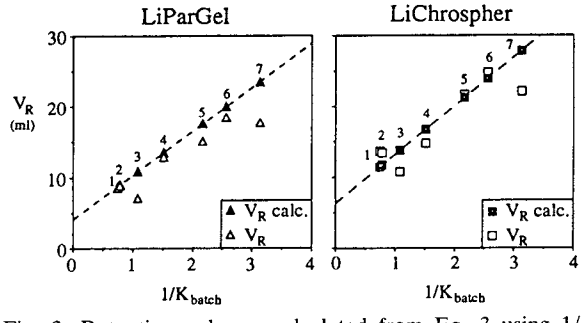

Fig. 3. Retention volumes calculated from Eq. 3 using $1/K_{batch}$ as K_C ($V_{R,calc}$) as a function of $1/K_{batch}$, plotted together with the experimentally obtained retention volumes (V_R), for LiParGel 650 ($V_S/V_M = 1.5 \pm 0.1$; $N = 725 \pm 50$; $R_s = 3.64 \pm 0.07$) and LiChrospher Diol 4000 ($V_S/V_M = 1.1 \pm 0.1$; $N = 425 \pm 100$; $R_s = 2.4 \pm 0.2$). All retention volumes given refer to a column volume of 15.1 ml. Molecular masses (M_r) were determined by SDS-PAGE and isoelectric points (pI) were determined by isoelectric focusing. 1 = Rabbit anti-IgG (M_r 160 000, pI 5.8); 2 = rabbit anti-albumin (M_r 160 000, pI 5.8); 3 = thyro-globulin (M_r 670 000, pI 4.5); 4 = human IgG (M_r 160 000, pI 6.8); 5 = transferrin (-Fe) (M_r 80 000, pI 6.2); 6 = BSA (M_r 65 000, pI 4.9); 7 = albumin (M_r 70 000, pI 4.9).

retention volume for the entire population. Whereas ideal partitioning was observed for bovine serum albumin (BSA), human serum albumin (albumin) was eluted earlier than expected on both matrices. As the molecular mass and the isoelectric point are similar for these proteins, this difference in retention would indicate that the conformation of the molecules is of importance to their ability to gain access to the stationary phase. Thyroglobulin, which has an isoelectric point similar to that of BSA and albumin but is considerably larger, was eluted earlier than expected on both matrices, indicating that molecules might be partially excluded owing to their size. The partitioning of polyclonal antibodies did not seem to be disturbed by either LiParGel or LiChrospher to any great extent, although the elution patterns on LiParGel differed from those on LiChrospher (*cf.*, Figs. 2 and 3).

In order to investigate further the influence of the matrices on LLPC of immunoglobulins, four monoclonal IgG1 antibodies (mIgG) were analysed. The chromatograms are shown in Fig. 4. The proteins were eluted mainly as single peaks with different partition coefficients. Although the resolution between the references was lower on LiChrospher than on LiParGel (2.7 compared with 3.6), the separation of the monoclonal antibodies was better on LiChrospher than on LiParGel. As the K_C values obtained on LiChrospher differed from those obtained on LiParGel, the two matrices appeared to affect the retention of immunoglobulins in different

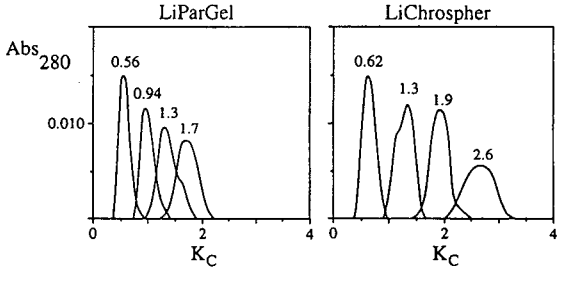

Fig. 4. Chromatograms for four monoclonal IgG1 antibodies obtained on LiParGel 650 ($V_S/V_M = 1.5 \pm 0.1$; $N = 725 \pm 50$; $R_s = 3.64 \pm 0.07$) and LiChrospher Diol 4000 ($V_S/V_M = 1.1 \pm 0.1$; $N = 530 \pm 100$; $R_s = 2.7 \pm 0.4$).

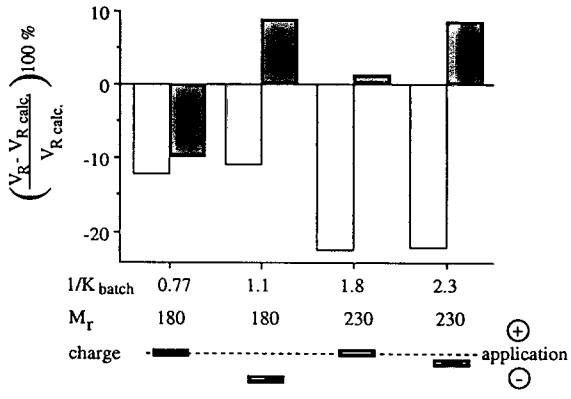

Fig. 5. Differences between the retention volumes calculated as described in Fig. 3 ($V_{R,calc}$) and those obtained experimentally (V_R) for four monoclonal myeloma IgG1 on (□) LiParGel 650 ($V_S/V_M = 1.5 \pm 0.1$; $N = 725 \pm 50$; $R_s = 3.64 \pm 0.07$) and (■) LiChrospher Diol 4000 ($V_S/V_M = 1.1 \pm 0.1$; $N = 530 \pm 100$; $R_s = 2.7 \pm 0.4$). Molecular masses (M_r) were determined by HPSEC and electrophoretic mobilities were determined by agarose gel electrophoresis at pH 8.6.

ways (Fig. 5). In addition, all monoclonal antibodies were eluted earlier than expected on LiParGel whereas antibodies favouring the stationary phase tended to elute later than expected on LiChrospher. The non-ideal behaviour could not be ascribed solely to either the size or the net charge of the otherwise homogeneous mIgGs (Fig. 5). Further, plate numbers calculated from the mIgG peaks were found to be independent of K_C (Table 2). Hence, the non-ideal retention of proteins in LLPC columns may not be ascribed to variations in column-bed packing structure or to poor diffusion in the stationary phase.

Table 2
Plate numbers calculated for four monoclonal IgG1 antibodies on LiParGel 650 and LiChrospher Diol 4000

$1/K_{batch}$	Plate number	
	LiParGel	LiChrospher
0.77	145	250
1.1	155	270
1.8	145	310
2.3	155	295

4. Discussion

LiParGel 650 and LiChrospher Diol 4000 have previously been used as supports for LLPC in aqueous PEG–dextran two-phase systems [15,18,23,24]. In this paper we have shown that LiParGel and LiChrospher columns could be packed at considerably higher pressures than recommended (25 and 0.7 MPa compared with 2.6 and 0.15 MPa [15,16], respectively) without damaging the supports.

The amount of stationary phase in the LLPC columns was larger than that reported by others ($\leqslant$30% of the column volume on LiParGel [16] and $\leqslant$20% on LiChrospher [15]; *cf.*, Table 1), indicating a strong adsorption of the dextran-rich bottom phase to both LiParGel and LiChrospher. The coating of LiParGel and LiChrospher is considered to be due to incompatibility of the polyacrylamide chains of the supports with PEG in the mobile phase rather than to attraction of the dextran-rich phase to the matrix [16]. Both supports have been shown to carry negative charges [18], which may be neutralized by high concentrations of salts (see below). In addition, a high ionic strength would increase the relative hydrophobicity of the PEG-rich top phase and decrease the repulsion of the dextran-rich bottom phase from the support, in this way facilitating adsorption.

A normal procedure to improve resolution is to increase the separation selectivity, determined as α in Eq. 5. This may be achieved by altering the composition of the two-phase system, *e.g.*, by reducing the size of the dextran molecules [1]. However, the concentration of PEG in the top phase would then increase, reducing the solubility of many proteins. We have previously shown that also immunoglobulins, which are easily precipitated by PEG, are soluble in appropriate concentrations (1 mg/ml) at a biological pH in two-phase systems containing dextran 500 but not dextran 40 [21]. Hence, we had to find other approaches to increase the resolution in our two-phase system.

Another common procedure to improve the resolution is to increase the capacity factor, k, in Eq. 5. This is accomplished by increasing the volume ratio of the stationary phase (V_S) to mobile phase (V_M). As the mechanical strength of both supports allows high packing pressures [16], we were able to achieve a ratio of V_S to V_M of 1.5 by packing the columns densely. This values ensures a high resolution for a wide range of K_C values. We were also able to achieve large theoretical plate numbers, in this way improving the resolution considerably (Table 1). A comparison with LLPC performance obtained by others may be misleading owing to differences in phase composition, temperature and flow-rates. However, it might still be of interest that our improved packing procedure reduces the volume of one theoretical plate from 45 to 20 μl for LiParGel and from 11 to 6 μl for LiChrospher [16]. In this context it should also be noted that the flow-rates used here were those required to elute the reference proteins within 2 h. Lower flow-rates would improve the column performance even further.

The partitioning properties of a biomolecule in a given aqueous two-phase system reflects a combination of its conformation and general surface properties, *e.g.*, net charge, hydrophobicity, shape and size. The distribution of the molecule between the phases depends mainly on the balance between its interactions with the phase-forming polymers, as interactions with the solvent, water, may be neglected [25]. The presence of salts partitioning towards one of the phases creates an electrical potential between the phases which may obstruct the free movement of proteins across the interphase. Considering our system, the concentrations of phosphate and sodium chloride are not likely to affect the distribution of proteins [2,26]. As glycine is distributed evenly between the phases [20], each protein should be able to partition freely towards the most energetically favourable phase. Thus, the partition coefficients determined in batch experiments are likely to describe the ideal partitioning properties of the molecules.

However, in LLPC, partitioning may be disturbed by the presence of the support. Although non-ideal retention of several proteins was indeed observed (Fig. 3), deviations from ideal partitioning could not be related to their charge.

LLPC of four monoclonal antibodies with different partition coefficients and physico-chemical properties strengthened this indication (Fig. 5). Our results confirm that the presence of negatively charged groups on the supports may be neglected at the ionic strength used in our two-phase system [16].

As the stationary phase is considered to be adsorbed inside the pores of the particles of both matrices [15,24], size-exclusion phenomena might be a problem in LLPC columns. However, the retention of IgM and antigen–antibody complexes ($M_r \leq 1\,000\,000$) on LiParGel agrees well with their partitioning properties determined in batch [20,21]. Ideal partitioning has been observed for large proteins ($M_r < 500\,000$) on LiChrospher 1000 [24] with a pore size that is four times smaller than that of LiChrospher 4000 [15]. Thus, the non-ideal behaviour of thyroglobulin (M_r 670 000) that was observed on both matrices may not be ascribed to exclusion phenomena.

Whereas polyclonal immunoglobulins were eluted in accordance with their partitioning properties (Fig. 3), four monoclonal IgG1 antibodies were found to deviate from ideal retention (Fig. 5). This apparent contradiction may be explained by the heterogeneity of polyclonal immunoglobulins of which a monoclonal preparation may be considered to represent a homogeneous subfraction. In polyclonal populations, positive and negative deviations from ideal partitioning by such subfractions may cancel each other out. This should be taken into account when ideal partitioning of heterogenous proteins in LLPC is discussed.

As the size of antibodies of a particular subclass is similar [27], the differences in M_r estimated by size-exclusion chromatography would indicate a difference in conformation. The degree of deviation from ideal partitioning in LLPC columns may then be determined by the conformation of the molecule together with the properties of the support with respect to pore size and polyacrylamide coating.

Although the influence of the LLPC supports on immunoglobulins and other proteins is obvious, the general applicability of the matrices is not invalidated as the interactions may be exploited as an additional parameter for separation.

5. Acknowledgements

We thank Professor Per-Åke Albertsson for introducing us to the field of aqueous two-phase partitioning and Professor Werner Müller for generous gifts of LiParGel and LiChrospher. This work was supported by grants from the Swedish National Board for Technical Development (STUF) and from the Alfred Österlund foundation.

6. References

[1] P.-Å. Albertsson, *Partition of Cell Particles and Macromolecules*, Wiley, New York, 3rd ed., 1986.
[2] G. Johansson, in H. Walter, D.E. Brooks and D. Fisher (Editors), *Partitioning in Aqueous Two-Phase Systems*, Academic Press, Orlando, FL, 1985, pp. 161–226.
[3] P.-Å. Albertsson, *J. Chromatogr.*, 159 (1978) 111.
[4] H. Walter, G. Johansson, and D.E. Brooks, *Anal. Biochem.*, 197 (1991) 1.
[5] L. Backman, in H. Walter, D.E. Brooks and D. Fisher (Editors), *Partitioning in Aqueous Two-Phase Systems*, Academic Press, Orlando, FL, 1985, pp. 267–314.
[6] B. Andersson and and H.-E. Åkerlund, *Biochim. Biophys. Acta*, 503 (1978) 462.
[7] P.-Å. Albertsson, B. Andersson, C. Larsson, and H.-E. Åkerlund, *Methods Biochem. Anal.* 28 (1982) 115.
[8] H.-E. Åkerlund, *J. Biochem. Biophys. Methods*, 9 (1984) 133.
[9] H.S. Anker, *Biochim. Biophys. Acta*, 229 (1971) 290.
[10] P. Hubert, R. Mathis, and E. Dellacherie, *J. Chromatogr.*, 539 (1991) 297.
[11] C.J.O.R. Morris, *Protides Biol. Fluids, Proc. Colloq.*, 10 (1963) 325.
[12] W. Müller in H. Walter, D.E. Brooks and D. Fisher (Editors), *Partitioning in Aqueous Two-Phase Systems*, Academic Press, Orlando, FL, 1985, pp. 227–263.
[13] W. Müller, H.-J. Schuetz, C. Guerrier-Takada, P.E. Cole and R. Potts, *Nucleic Acids Res.*, 7 (1979) 2483.
[14] W. Müller and G. Kütemeier, *Eur. J. Biochem.*, 128 (1982) 231.
[15] W. Müller, *Eur. J. Biochem.*, 155 (1986) 213.
[16] W. Müller, in W. Müller (Editor), *Liquid–Liquid Partition Chromatography of Biopolymers*, GIT, Darmstadt, 1988, pp. 5–20.
[17] W. Müller, *Bioseparation*, 1 (1990) 265.

[18] A. Walsdorf and M.R. Kula, *J. Chromatogr.*, 542 (1991) 55.
[19] C. Wingren, U.-B. Hansson and K. Andersson, *J. Chromatogr.*, 603 (1992) 73.
[20] K. Andersson, C. Wingren and U.-B. Hansson, *Scand. J. Immunol.*, 38 (1993) 95.
[21] U.-B. Hansson, K. Andersson, Y. Liu and P.-Å. Albertsson, *Anal. Biochem.*, 183 (1989) 305.
[22] U.K. Laemmli, *Nature*, 227 (1970) 680.
[23] W. Müller, A. Heubner and J. Kaniecki, in W. Müller (Editor), *Liquid–Liquid Partition Chromatography of Biopolymers*, GIT, Darmstadt, 1988, pp. 21–38.
[24] M.R. Kula, L. Elling and A. Wallsdorf, *J. Chromatogr.*, 548 (1991) 3.
[25] D.E. Brooks and K.A. Sharp, in H. Walter, D.E. Brooks and D. Fisher (Editors), *Partitioning in Aqueous Two-Phase Systems*, Academic Press, Orlando, FL, 1985, pp. 11–84.
[26] S. Bannberger, D.E. Brooks, K.A. Sharp, J.M. van Alstine and T.J. Webber, in H. Walter, D.E. Brooks and D. Fisher (Editors), *Partitioning in Aqueous Two-Phase Systems*, Academic Press, Orlando, FL, 1985, pp. 85–130.
[27] R. Jefferis, in F. Shakib (Editor), *The Human IgG Subclasses: Molecular Analysis of Structure, Function and Regulation*, Pergamon Press, Oxford, 1990, pp. 15–30.

ELSEVIER

Journal of Chromatography A, 668 (1994) 75–83

JOURNAL OF CHROMATOGRAPHY A

Review

Triton X-114 phase partitioning in plant protein purification

A. Sánchez-Ferrer, M. Pérez-Gilabert, E. Núñez, R. Bru, F. García-Carmona*

Departamento de Bioquímica y Biología Molecular (A), Facultad de Biología, Universidad de Murcia, E-30071 Murcia, Spain

Abstract

A brief overview is given of how Triton X-114 can be used not only to solubilize plant membranes but also as an excellent reagent in a bulk fractionation method to purify enzymes compared with the classical drastic methods using acetone powder or ammonium sulphate fractionation. Triton X-114 removes the tenacious phenols and chlorophylls on centrifugation. There is no need to use insoluble synthetic resins or organic solvents as Triton X-114 is so mild that the enzymes can be extracted in their natural form without activating them. The methods developed with Triton X-114 are easily reproducible and sufficiently cheap to be used in large-scale purification procedures. The classical topological use of Triton X-114 in plant membranes is also discussed.

Contents

1. Introduction

Protein purification from a complex biological crude extract containing thousands of different proteins and biomolecules is often a difficult multi-step process [1]. The time needed and the steps involved in developing a protein purification procedure depend on the protein, the starting material and the final use for which it is intended and the starting material. In plants, the isolation of enzymes is complicated by the existence of an important secondary metabolism [2], which produces highly reactive phenols and tannins that are *in vivo* confined to vacuoles.

During purification, these reactive compounds interact with proteins to produce both covalent and non-covalent complexes. To overcome this problem, three different methods have been used traditionally: the use of reducing agents (ascorbic acid, metabisulphite, etc.) to avoid the oxygen-driven oxidation of phenols to quinones, insoluble hydrophobic phenol-binding resins

* Corresponding author.

0021-9673/94/$07.00
SSDI 0021-9673(93)E1303-H

(*e.g.*, polyvinylpyrrolidone, Amberlite XAD-2) [3] and organic solvents (acetone, ethanol, etc.). However, in many instances their use is ineffective or can lead to partial enzyme inhibition or denaturation and/or the uncontrolled activation of the native inactive forms (latent enzymes).

An additional problem in aerial tissues is the release of chlorophylls, which occurs with the breakdown of chloroplasts during homogenization or during the digestion of their organelle membranes by detergents [4]. The resulting green extracts can be clarified by ammonium sulphate fractionation or the use of acetone powder, although these agents may alter the conformational structure of the protein and lead to a loss of certain activities in multifunctional enzymes.

Recent developments in the purification of plant proteins have been reviewed [5]. The topics discussed include immunoaffinity chromatography, subunit affinity chromatography, immobilized metal affinity chromatography (IMAC) and the use of detergents in protein isolation [6,7].

This paper presents a brief overview of the special characteristics of polyoxyethylene-type non-ionic detergents, especially Triton X-114 (TX-114), which can be used in the solubilization and purification of plant enzymes owing to their ability to produce aqueous two-phase systems in the biocompatible temperature range (4–30°C). TX-114 is particularly useful for purifying polyphenol oxidase (PPO) from both aerial and non-aerial plant tissues. This enzyme is a good example of a plant protein that is difficult to purify as it presents all the above-mentioned purification problems.

2. Physico-chemical characteristics of polyoxyethylene-type non-ionic detergents

Organic compounds that are insoluble or barely soluble in water can often be brought into aqueous solution by the addition of suitable surfactants. This phenomenon, called solubilization, has been the subject of much research involving ionic surfactants, although many fewer data are available concerning the use of non-ionic surfactants [8]. Surfactant molecules form micelles in aqueous solution when the concentration exceeds a certain value, and this concentration is generally called the critical micelle concentration (cmc). Little or no uptake of solute occurs until the cmc is reached, which suggests that the solute molecules are taken up in some way by the micelles. In our case, the solute is the protein that is to be solubilized from a particular membrane.

Among non-ionic surfactants, the polyoxyethylene type represents a large group whose formulae are shown in Table 1. The structure is normally abbreviated to C_nE_m, where C_n represents the length of the alkyl group and E_m the number of oxyethylene units. These detergents

Table 1
Structures and properties of some polyoxyethylene-type non-ionic detergents [19]

Formula	Abbreviation	Trivial name	cmc (m*M*)	*N*[a]	HLB[a]	CP[a] (1%, w/v)
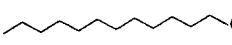	$C_{12}E_8$		0.087	120	13.7	75
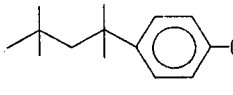	t-$C_8\phi E_9$	Triton X-100	0.30	140	13.5	65
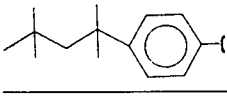	t-$C_8\phi E_7$	Triton X-114	0.17	140	12.4	22

[a] *N* = aggregation number; HLB = hydrophilic–lipophilic balance; CP = cloud point (°C).

are solubilized in water by the hydration of the ether oxygens of the polyoxyethylene groups [9]. An increase in temperature leads to a decrease in the number of hydrogen bonds, which raises the micellar mass and decreases the cmc [10]. If the temperature continues to increase, the micelle becomes so large and the number of intermicellar interactions increase to such an extent that a sudden onset of turbidity is perceptible even to the naked eye [11,12]. This temperature is called the cloud point. A further rise in temperature causes the solution to begin to separate into two phases, one detergent-rich and the other detergent-depleted with no or few micelles present.

The cloud point depends on the length of the hydrophilic (oxyethylene units) and hydrophobic (alkyl) chains. In the Triton series, the cloud point ranges from 22°C for TX-114 (7 units) to 67°C for Triton X-100 (TX-100) (9 units) [13]. Surfactant concentration is also important [14] because, for example, a 3% (w/v) concentration is necessary for C_6E_3 to partition at 37°C. However, surfactant concentration has less influence than the concentration of the additives, which are usually inorganic salts and hydrocarbons.

Normally, salts lower the cloud point owing to their salting-out effect. This effect is substantial with TX-100, especially when sulphate salts are added to the solution (Fig. 1) [14]. The salting-out effect with TX-114 is of biological importance as only low salt concentrations are needed to lower the cloud point to below 22°C [15]. However, high salt concentrations should be avoided in order to prevent enzyme inhibition by salts, mainly Cl^-, and to permit the use of ion-exchange chromatography in subsequent purification steps [16].

Saturated hydrocarbons do not lower the cloud point temperature to any great extent and can sometimes even raise it, whereas aliphatic alcohols, fatty acids and phenols lower the cloud point substantially [8].

Among the alcohols, glycerol has been used in conjunction with TX-114 in the isolation of the plant cytochromes P-450 and b_5, as its addition lowers the cloud point to 4°C [16]. Glycerol reduces TX-114 micelle solvation by decreasing

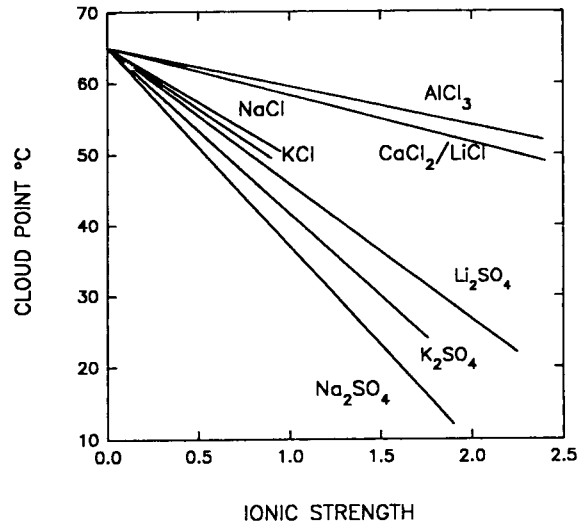

Fig. 1. Effect of added electrolytes on the cloud point of 2% TX-100 solutions [14].

the number of hydrogen bonds formed by the detergent's polyoxyethylene groups with water.

Other detergents that are sometimes added to digest biological membranes strongly influence the cloud point of polyoxyethylene-type detergents, the resulting cloud point being between those of the two individual surfactants. In fact, the cloud point of TX-114 can be decreased by adding Triton X-45 ($m = 5$), which has a lower cloud point. The combination of these two detergents (9:1) has been used to isolate phosphatidylinositol kinase at 9°C [17]. As is to be expected, the opposite occurs (*i.e.*, the cloud point is raised) when more hydrophilic detergents (deoxycholate, TX-100 and *n*-octyl glucoside) are used because of the increased solubilization of TX-114 [18].

Finally, phospholipids released from plant membranes also lower the cloud point to an extent that depends on the lipidic nature of the membrane. With plant microsome membranes, the temperature is lowered by 5°C [16].

3. Biomolecule phase separation in PEG non-ionic detergents

Non-ionic polyoxyethylene detergents have been used in various protein membrane studies.

TX-100 is probably the most widely used and best characterized of commercially available polydisperse compounds. It possesses an alkylaryl hydrophobic and a hydrophilic moiety composed of a polyoxyethylene chain with an average of 9–10 oxyethylene units. Its usefulness stems from its high solubility, low cost, mildness in solubilizing membrane proteins, low cmc and relatively large micelle size [19].

TX-114 shares the same properties as TX-100 but is insoluble in buffers at room temperature because of its low cloud point. This explains why TX-114 was not used as a biological detergent until Bordier [18] used it in 1981 to separate membrane proteins according to their different partitioning behaviour after phase separation. Bordier demonstrated that proteins which had been dissolved in TX-114 solution at 4°C (below the cloud point) partition between the lower (detergent-rich) and the upper (detergent-depleted) phase when the solution is warmed above the cloud point. The distribution appeared to depend on the protein's relative hydrophobicity: hydrophobic integral membrane proteins partitioned into the lower phase, whereas hydrophilic globular proteins partitioned into the upper phase. Thermal phase partitioning has since been employed as an analytical procedure is cellular and molecular biology [20]. Their distribution during phase separation has been used to indicate the cellular location of various proteins in membranes and cytoplasm. However, such a correlation is not always accurate, especially with integral membrane proteins with very large hydrophilic regions (glycoproteins), such as *Torpedo* nicotinic acetylcholine receptor (AchR) and the α subunit of the Na^+,K^+-ATPase of kidney microsome membranes, both of which partition into the aqueous phase [21].

4. Purification of plant enzymes by temperature-induced phase partitioning in Triton X-114

TX-114 was first used in plants by Bricker and Sherman [22] to assist in the investigation of the topological orientation of maize chloroplast thylakoid membranes. These membranes were first enzymatically labelled with ^{125}I or treated with trypsin and then phase fractionated with TX-114. The integral polypeptides which resolved in the detergent-rich phase were CP1 apoprotein, the PSII reaction centre polypeptides I and II, cytochrome *f* and b_6 and the major LHC apoprotein. Among peripheral polypeptides retained in the aqueous phase, the α and β subunits of CF1 were predominant.

These topological studies were extended to the other plant membranes and species. For example, the hydrophobicity of protochlorophyllide oxidoreductase from wheat etioplast membrane fractions was clearly demonstrated to be higher than that of ATP synthase polypeptides and ribulose bisphosphate carboxylase oxygenase and so this oxidoreductase was classified as an integral membrane protein with a hydrophilic domain that binds its water-soluble cofactor, NADPH [23].

Plasma membrane vesicles were also studied using TX-114. In spinach leaf, 80% of the protein was recovered in the hydrophobic phase of TX-114 and the remaining 20% in the aqueous phase [24]. Peripheral proteins were largely located in the inner, cytoplasmic surface of the plasma membrane.

Bulk protein fractionation in TX-114 was first used by our group in the purification of grape PPO [25] to avoid the difficulties normally associated with the purification of the phenol-oxidizing enzyme, as its self-generated *o*-quinones can sometimes modify or inactivate the enzyme. In addition, grape berry polyphenol oxidase (GB-PPO) was discovered to be a thylakoid-bound enzyme, as only detergents were able to extract from 1 to 100% of activity depending on the characteristics of the detergent used, the non-ionic detergents (TX-100, TX-114) being the most effective [25]. Ionic strength and typsin alone extracted only 2% and 10%, respectively.

Among non-ionic detergents, TX-114 solubilized the protein and chlorophylls with the same efficiency as TX-100. However, unlike TX-100, TX-114 failed to maintain all of the proteins and chlorophylls in solution at 4°C. This was used to

advantage, because after a few minutes a dark precipitate was formed due to the aggregation of large mixed micelles of TX-114, which contained membrane proteins, phospholipids, phenols and chlorophylls. After high-speed centrifugation, the supernatant was slightly green, clearly indicating that chlorophylls and phenols had been eliminated from the original extract.

This removal of non-protein material by TX-114 at 4°C had never before been described. The total removal of unwanted compounds was achieved by subjecting the clear green supernatant to a classical temperature-induced phase partitioning [18], adding an additional 4% of TX-114 to the mixture and warming it at 37°C for 15 min [25]. After this phase partitioning, GB-PPO remained in the aqueous phase and, for the first time, as an inactive (latent) form similar to that previously described for other leaf thylakoid-bound PPO (spinach, broad bean).

Table 2 shows the results obtained when the TX-114 method was compared with the well established method for purifying GB-PPO involving ammonium sulphate fractionation [25]. The degree of purification was the same in both methods, although the recovery was greater in the TX-114 method. The enzyme purified by TX-114 was latent, and was activated 64-fold with trypsin compared with the two times it could be activated with the ammonium sulphate fractionation method. As much as 75–80% of phenols and chlorophylls were removed by TX-114 by ultracentrifugation without the need for any synthetic resin such as Amberlite XAD-2 or organic solvents. Complete removal was attained in the next step by temperature-induced phase partitioning in 4% TX-114.

The TX-114 method also preserved the two activities of PPO, the cresolase activity that oxidizes monophenols to *o*-diphenols and the catecholase activity that oxidizes diphenols to their corresponding quinones (Fig. 2) [26]. The first activity is very low compared with the catecholase activity and it is necessary to activate the latent enzyme to obtain any measurable activity. It should be noted that this activity presents a lag period, which is a consequence of the dynamic equilibrium between the enzymatic and chemical steps involved in the complex kinetic mechanism of this enzyme [27–30].

In addition, TX-114 avoids one of the problems normally encountered when plant PPO extracts are subjected to sodium dodecyl sulphate–polyacrylamide gel electrophoresis (SDS-PAGE), namely the multiplicity of activity bands arising from the formation of artefactual bands caused by the covalent interaction of *o*-quinones and phenols with the enzyme [31].

Another characteristic of GB-PPO purification was its unexpected behaviour, as it was retained in the aqueous phase after phase partitioning. This is explained by the presence of a short hydrophobic tail, which anchors it to the membrane but which is not long enough to bind a sufficient number of detergent molecules to be precipitated with the larger micelles of TX-114 during temperature-induced phase partitioning [25]. This hypothesis is based on the different activations found in the latent enzyme with trypsin, detergents and lectins.

The TX-114 method was also used to purify previously described latent leaf thylakoid-bound PPO. With spinach [32] and broad bean leaves [33], 1.5% TX-114 partially removed the undesirable phenol and chlorophyll components on centrifugation at 4°C, when osmotically shocked chloroplast membranes were digested by the detergent. The remaining chlorophylls and phenols were removed after phase partitioning at 37°C in 8% TX-114.

Latent PPO remained in the aqueous phase in both instances with fivefold purification and recoveries of 86% and 43% for spinach and broad bean PPO, respectively [32,33]. The activation found in both latent enzymes was 5–10 times higher than that obtained in previously published methods (acetone powder and ammonium sulphate fractionation) [34], clearly demonstrating the mild purification in the TX-114 method compared with the classical methods.

The final example of leaf thylakoid-bound enzyme purified by the TX-114 method is potato leaf PPO, which had never been purified previously. The method used differed from the above TX-114 methods in that the second phase partitioning step must be repeated as the level of

Table 2
Partial purification of GB-PPO using both ammonium sulphate and TX-114 methods [35]

Method	Material	Total protein (mg)	Total activity (units)[a]		Specific activity (units/mg)	Purification (-fold)	Recovery (%)	Activation (%)	Chl (μg/ml)	Phenolic compounds (mg/ml)
			−Trypsin	+Trypsin						
Ammonium sulphate	Crude extract	15	500	500	33	1	100	100	11	42.5
	TX-100 extract	7.8	30	370	47	1.5	74	1233	16	14.5
	Supernatant of TX-100 extract	5.7	5.7	324	57	1.7	65	5684	13	12.1
	45–95% ammonium sulphate	0.6	50	101	168	5.1	20	200	ND[b]	0.5
TX-114	Crude extract	15	500	500	33	1	100	100	11	42.2
	TX-114 extract	7.8	10	270	47	1.4	74	3700	19	14.5
	Supernatant of TX-114 extract	4.3	5.5	322	75	2.3	65	5854	4	3.5
	Supernatant 4% of TX-114	1.9	5.0	320	168	5.1	64	6400	ND[b]	0.6

[a] Assayed with 4-methylcatechol as substrate..
[b] Not detected.

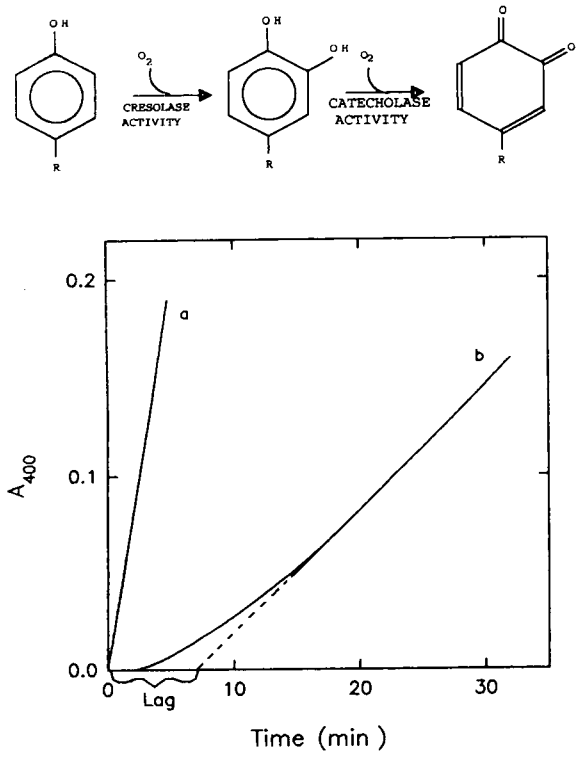

Fig. 2. Enzyme activities of trypsin-activated latent GB-PPO. (a) Catecholase activity (1 μg/ml of enzyme) using 24 m*M* 4-methylcatechol as diphenolic substrate; (b) cresolase activity (100 μg/ml of enzyme) using 2.1 m*M* *p*-cresol as monophenol.

phenols was higher than in the other leaves studied. This additional step is necessary because, at high phenol concentrations, the phenol-binding sites in the TX-114 micelles are saturated [35].

Recently, TX-114 was extended to non-aerial tissues, such as potato tubers [36]. The purification of potato tuber PPO is completely different from that of the leaves as the level of phenols, mostly as chlorogenic acid, is so high that the extract becomes black only a few seconds after homogenization. To avoid this, ascorbic acid, metabisulphite and insoluble phenol scavengers were used at high concentrations in previously published methods [37–39]. However, all of these are inhibitors of potato PPO and so the new strategy was to keep phenols away from the enzyme by adding 6% TX-114 to the homogenization buffer without any other phenol scavenger and to insolubilize the starch by keeping the homogenate at 4°C for 90 min. The extract remained light yellow during this time owing to the presence of TX-114. After centrifugation, the starch was removed and the supernatant subjected to phase partitioning by increasing the TX-114 concentration by a further 4% and warming it for 15 min.

An attempt was made to activate the PPO thus obtained in the aqueous phase with trypsin or detergents, but no activation was found [36]. As potato tuber PPO was present in its active form, ammonium sulphate fractionation could be used to purify it further. The degree of purification finally achieved was fivefold, similar to that obtained with the previously described methods [37,38], although the recovery was lower, owing to the transfer of particulate PPO to the detergent-rich phase. This particulate enzyme has been evaluated and represents over half of the enzyme activity [40].

Phenols were almost totally removed, only 3% remaining. This prevented the enzyme solution from browning and enabled enzyme stability to be preserved for months at −20°C. This removal of phenols also avoids the multiplicity of enzyme bands found with SDS-PAGE for potato PPO (up to eighteen bands) when it is purified with ammonium sulphate alone, without TX-114 [41].

Finally, the purification of cinnamic acid 4-hydrolase, a plant cytochrome P_{450}, is worth mentioning as it is the first example of a plant enzyme, which remains in the detergent rich phase, being purified to electrophoretic homogeneity using chromatography with DEAE-Trisacryl and hydroxyapatite [42]. This was achieved by adding 0.5% (w/v) of Emulgen 911 (Kao, Atlas, Tokyo, Japan) and 0.5% (w/v) of TX-114 to the eluting buffers. The presence of Emulgen 911 during the chromatographic steps was essential to avoid aggregation of TX-114 micelles.

5. Conclusion

The use of TX-114 not only for solubilization but also as a phase partitioning reagent is a

useful tool in plant biochemistry as it overcomes the main problems associated with plant protein purification. It removes phenols and chlorophylls by simple centrifugation; it is mild, and so does not alter the structure of inactive native enzymes (latent enzymes); it is rapid, reducing purification times from days to hours [25]; it is cheap and reproducible, and can easily be used in practical classes [43,44] or in large-scale purification processes. However, method has to be optimized according to the starting material and the enzyme to be purified.

Future challenges in purifying plant enzymes with detergents appear to be strongly linked to interdisciplinary collaboration between biochemistry and synthetic organic chemistry [5] to develop new detergents with a wide range of cloud points and which are transparent in the UV region and easily removed by dialysis.

6. Acknowledgements

This work was partially supported by CICYT (Proyecto BIO91-0790) and Comunidad Autónoma de Murcia ("Ayudas a Graduados para Ampliación de Estudios", 1992).

7. References

[1] A. Kornberg, *Methods Enzymol.*, 182 (1990) 1.
[2] W.D. Loomis, *Methods Enzymol.*, 31 (1974) 528.
[3] W.D. Loomis, J.D. Lile, R.P. Sandstrom and A.J. Burbott, *Phytochemistry*, 18 (1979) 1049.
[4] P.F.T. Vaughan, R. Eason, J.Y. Paton and G.A. Ritchie, *Phytochemistry*, 14 (1975) 2383.
[5] R.J. Weselake and J.C. Jain, *Physiol. Plant.*, 84 (1992) 301.
[6] A. Helenius and K. Simons, *Biochim. Biophys. Acta*, 415 (1975) 29.
[7] T.C. Thomas and M.G. McNamee, *Methods Enzymol.*, 182 (1990) 499.
[8] T. Nakagawa, in M.J. Schick (Editor), *Noniomic Surfactants*, Marcel Dekker, New York, 1967, Ch. 17, p. 558.
[9] L.N. Ferguson, *J. Am. Chem. Soc.*, 77 (1955) 5288.
[10] M.J. Schick, *J. Phys. Chem.*, 67 (1963) 1796.
[11] R. Kjellander, *J. Chem. Soc., Faraday Trans. 2*, 78 (1982) 2025.
[12] V. Degiorgio, in V. Degiorgio (Editor), *Physics of Amphiphiles: Micelles, Vesicles and Microemulsions*, North-Holland, Amsterdam, 1985, p. 303.
[13] R.C. Mansfield and J.E. Locke, *J. Am. Oil Chem. Soc.*, 41 (1964) 267.
[14] W.N. Maclay, *J. Colloid Sci.*, 11 (1956) 272.
[15] A. Doren and J. Goldfarb, *Colloid Interface Sci.*, 32 (1970) 67.
[16] D. Werck-Reichhart, I. Benveniste, H. Teutsch, F. Durst and B. Gabriac, *Anal. Biochem.*, 197 (1991) 125.
[17] B.R. Ganong and J.P. Delmore, *Anal. Biochem.*, 193 (1991) 35.
[18] C. Bordier, *J. Biol. Chem.*, 256 (1981) 1604.
[19] J.M. Neugebauer, *Methods Enzymol.*, 182 (1990) 239.
[20] J.G. Pryde, *Trends Biochem. Sci.*, 11 (1986) 160.
[21] P.A. Maher and S.J. Singer, *Proc. Natl. Acad. Sci. U.S.A.*, 82 (1985) 958.
[22] T.M. Bricker and L.A. Sherman, *FEBS Lett.*, 149 (1982) 197.
[23] E. Selstam and A. Widell-Wigge, *Physiol. Plant.*, 77 (1989) 401.
[24] N.M. Hooper and A. Bashir, *Biochem. J.*, 280 (1991) 745.
[25] A. Sánchez-Ferrer, R. Bru and F. García-Carmona, *Plant Physiol.*, 91 (1989) 1481.
[26] A. Sánchez-Ferrer, R. Bru, J. Cabanes and F. García-Carmona, *Phytochemistry*, 27 (1988) 319.
[27] J. Cabanes, F. García-Cánovas, J.A. Lozano and F. García-Carmona, *Biochim. Biophys. Acta*, 923 (1987) 187.
[28] F. García-Carmona, J. Cabanes and F. García-Cánovas, *Biochim. Biophys. Acta*, 914 (1987) 198.
[29] F. García-Carmona, E. Valero and J. Cabanes, *Phytochemistry*, 27 (1988) 1961.
[30] A. Sánchez-Ferrer, F. Laveda and F. García-Carmona, *J. Agric. Food Sci.*, 41 (1993) 1225.
[31] A.M. Mayer and E. Harel, *Phytochemistry*, 18 (1979) 193.
[32] A. Sánchez-Ferrer, J. Villalba and F. García-Carmona, *Phytochemistry*, 28 (1989) 1321.
[33] A. Sánchez-Ferrer, R. Bru and F. García-Carmona, *Anal. Biochem.*, 184 (1990) 279.
[34] R.S. King and W.H. Flurkey, *J. Sci. Food Agric.*, 41 (1987) 231.
[35] A. Sánchez-Ferrer, F. Laveda and F. García-Carmona, *J. Agric. Food Sci.*, 41 (1993) 1583.
[36] A. Sánchez-Ferrer, F. Laveda and F. García-Carmona, *J. Agric. Food Sci.*, 41 (1993) 231.
[37] S.S. Patil and M. Zucker, *J. Biol. Chem.*, 210 (1965) 3938.
[38] J.P. Batistuti and E.J. Lourenço, *Food Chem.*, 18 (1985) 251.
[39] P. Reddanna, J. Whelan, K.R. Maddipati and C.C. Reddy, *Methods Enzymol.*, 187 (1990) 269.

[40] H. Ruis, *Phytochemistry*, 11 (1972) 53.
[41] G. Matheis, *Chem. Mikrobiol. Technol. Lebensm.*, 11 (1987) 5.
[42] B. Gabriac, D. Werck-Reichhart, H. Teutsch and F. Durst, *Arch. Biochem. Biophys.*, 288 (1991) 302.
[43] A. Sánchez-Ferrer and F. García-Carmona, *Biochem. Educ.*, 20 (1992) 178.
[44] A. Sánchez-Ferrer and F. García-Carmona, *Biochem. Educ.*, 20 (1992) 235.

ELSEVIER

Journal of Chromatography A, 668 (1994) 85–94

JOURNAL OF CHROMATOGRAPHY A

Continuous separation of whey proteins with aqueous two-phase systems in a Graesser contactor

J. Dos Reis Coimbra, J. Thömmes, M.-R. Kula *

Institute of Enzyme Technology, Heinrich-Heine University Düsseldorf, P.O. Box 2050, 52404 Jülich, Germany

Abstract

The isolation and purification of α-lactalbumin and β-lactoglobulin from whey can be conducted continuously in a Graesser contactor using an aqueous two-phase system based on polyethylene glycol and potassium phosphate. Processing of more than 600 g of whey proteins per day was performed in the apparatus described. β-Lactoglobulin partitioned almost quantitatively into the salt-rich bottom phase, and α-lactalbumin was enriched in the top-phase of the system applied. The residence time distribution and the fractional hold-up as a hydrodynamic parameter were determined as the basis for a qualitative prediction of the extraction efficiency of the process described.

1. Introduction

The application of aqueous two-phase systems to the large-scale purification of proteins implies the consideration of continuous counter-current operation in the design of such a process [1]. This mode of operation may reduce fixed and variable costs, increase space–time yield, maintain high yields of labile proteins and allow process automatization and the continuous recycling of process chemicals [2,3]. Single or multi-stage equipment of conventional liquid–liquid extraction can be applied for extraction using aqueous two-phase systems (ATPS). Mixer–settler designs have been successfully operated continuously, offering one theoretical stage for protein purification [4]. Multi-stage installations were described by use of spray, York–Scheibel, packed bed or pulsed sieve plate columns [1,5,6].

Another tool for liquid–liquid extraction is the Graesser raining bucket contactor (see Fig. 1). Being patented in 1962 [7] it offered a very promising technology for the treatment of phase systems with low interfacial tension, low density difference and a high tendency of emulsification. The contactor has been used previously in many

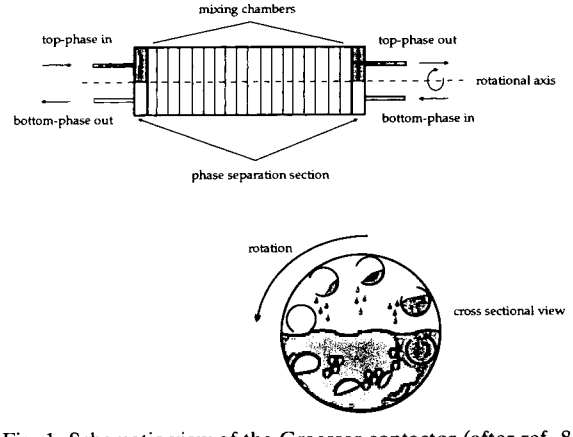

Fig. 1. Schematic view of the Graesser contactor (after ref. 8, compare also ref. 10 and 11).

* Corresponding author.

0021-9673/94/$07.00
SSDI 0021-9673(94)00004-S

industrial processes, *e.g.* pyrethrum refining, purification of herbicides or dearomatization of naphtas [8].

The Graesser contactor consists of a cylindrical glass vessel and is operated horizontally, two immiscible phases being introduced in counter-current mode from both ends of the cylinder. On the horizontal axis a single rotor performs mixing by a series of cylindrical buckets, mounted around the axis and partly open in the direction of mixing, that are separated by circular baffles. Counter-current flow occurs by the annular gap between the baffles and the contactor walls. Under operation the interface level of the immiscible liquids is controlled at the centre line of the vessel. Gentle mixing is provided by the movement of the buckets, transporting portions of each phase to the other phase, releasing them at the top or bottom of its circular movement and causing the liquid to cascade through the opposing phase back to the interface. Phase separation occurs in the end zones on the right and left of the cylindrical vessel. Fig. 1 schematically shows the operating principle of the Graesser contactor. For details of construction and operational principles see also ref. [8].

This special design leads to some specific hydrodynamic characteristics of the Graesser contactor, which makes it especially suitable for aqueous two-phase systems:

(i) The gentle mixing avoids emulsification, as the mean drop size is kept large compared to other continuously operated extractors.

(ii) The drop rise and fall velocities are high, thus a fast interface renewal is achieved leading to good mass transfer characteristics of the extraction system.

(iii) Maintaining the interface level at the equatorial centre of the glass vessel and keeping the two phases thoroughly separated by the horizontal mode of operation, helps processing systems with low density difference.

(iv) The separation of the vessel into different compartments reduces axial mixing, a problem in vertically operated column extractors [1].

(v) Good mass transfer in spite of very gentle mixing makes this extractor suitable for sensible products, *e.g.* proteins.

In conclusion, the Graesser raining bucket contactor seems to fit the demands very well of continuously operated purification of proteins using ATPS. This was predicted already by Hustedt *et al.* [9], who used a Graesser contactor for continuous operation with ATPS, simulating protein purification by separation of two dyes.

Fundamental research of the special features of the Graesser contactor has not been performed as intensively as with other extraction systems. Sheikh *et al.* [10] and Wang *et al.* [11] studied axial mixing as well as back mixing in a bench-scale Graesser contactor (75 cm length, 15 cm diameter) with a kerosene–butylamine–water system. They found, that axial mixing behaviour was considerably influenced by the phase properties. The authors proposed slow agitation rates and a high ratio of solvent feed flow for successful extraction in this type of contactor. Al-Hemiri and Kareem [12] described the drop size distribution in a Graesser contactor. By photographic techniques they determined a decreasing mean drop size along the horizontal axis reaching a constant drop size distribution towards the outlet of the contactor using several water–organic solvent systems. To our knowledge, these are the only reports on the basic principles of the Graesser contactor.

Studies on the applications of the Graesser contactor to protein purification using ATPS calls for a real "bulk product" as a model. First, to keep the process close to reality, and secondly to minimise the cost of raw material as much as possible, as the high capacity of even bench-scale contactors demands large amounts of process chemicals and proteins to obtain steady-state data in a continuous mode of operation. A group of proteins, that has steadily gained interest, are the whey proteins. The world production in the 80's was nearly 90 million tons of whey per year [13], a considerable amount of which is presently discarded, while the rest is used in lactose production or in animal feed. The average protein content in bovine whey is 6–9 g/l, so there is a large potential of unused protein in whey. Formulations for infant nutrition are designed on the basis of whey proteins. A fact, that should be considered when using whey directly for infant

formulae is the elevated content of β-lactoglobulin (β-Lg) in bovine milk compared to mammalian milk [14]. β-Lg is known as the major allergenic milk protein [15], therefore in processing whey proteins for infant nutrition the reduction of the β-Lg content, while retaining the concentrations of the other milk proteins, is important. Up to now several procedures for the isolation of β-Lg from the rest of the whey proteins have been described, with the major aim to separate α-lactalbumin (α-La) from β-Lg. Kaneko *et al.* [14] described the importance of retaining immunologic properties of whey, *e.g.* keeping the immunoglobulin and lactoferrin concentration in the formulations close to the original values. The methods proposed are precipitation of β-Lg with $FeCl_3$ [14], precipitation of β-Lg with polyphosphate [16], ion-exchange chromatography [13], sub-unit exchange chromatography [17], salting out [18] and thermal methods [19]. Recently, a polyethylene glycol (PEG) –phosphate aqueous two-phase system was described, which separated the two important whey proteins by the partitioning of β-Lg predominantly into the salt-rich bottom-phase and by the enrichment of α-La in the top phase [20].

Based on these literature results, we studied the separation of α-La and β-Lg from bovine whey as an example of a bulk product, that can be processed in a Graesser contactor using ATPS. On the one hand whey is an easy accessible and cheap source of proteins, and on the other hand there is a need for large-scale processes in whey protein purification that do not require intense pretreatment of the protein source. Whey contains considerable amounts of salts, so many purification methods cannot be applied directly. ATPS are salt-tolerant and should be well suited for direct processing of whey proteins.

The first purpose of our examinations was to evaluate the basic hydrodynamic features of the Graesser contactor with ATPS. As Wang *et al.* [11] found the contactor hydrodynamics to be dependent on the phase composition, their results with the kerosene–dibutylamine–water system cannot be transferred to ATPS; therefore experimental effort was necessary in this respect. Based on the results of Chen [20], a phase system was chosen, that allowed separation of α-La and β-Lg from whey in batch experiments, and this system was utilized for the continuous experiments with the Graesser contactor. The results of these experiments were compared to the qualitative predictions made from the hydrodynamic characterization of the contactor.

2. Experimental

2.1. Materials

Pure α-Lactalbumin and β-Lactoglobulin were obtained from Sigma (Deisenhofen, Germany), PEG 400, 600, 1550, 4000 and 12 000 from Hüls AG (Marl, Germany), potassium phosphate from B.K. Landenburg (Landenburg, Germany), cibacron blue from Sigma and cheese whey powder (whey protein index, Nx6.38, 26%) was a generous gift from Meggle Milchindustrie GmbH (Wasserburg, Germany).

2.2. Partition experiments

Aqueous two-phase systems of PEG–salt (potassium phosphate) were prepared from stock solutions of PEG (50%, w/w) and salt (pH 7.0, 30% w/w) for the experiments with pure α-La and β-Lg. The required mass of the phase system was obtained by weighing of the solutions in centrifuge tubes on a 10-g scale. Amounts of 5 mg of protein were added followed by adjustment with water until the total mass was 10 g. The systems were mixed by inversion (5 min) and separated by centrifugation for 5 min at 4000 *g*. Aliquots of the top and bottom phase were withdrawn for protein determination.

The influence of the salt content and different PEG molecular masses on the phase volume relation was observed. By this criterion the use of PEG 400, 600, 4000, 12 000 were considered unfavourable.

For the large-scale experiments with whey different quantities of PEG (1550), potassium phosphate (predetermined amounts of mono- and dihydrogenphosphate were adjusted to give

Table 1
Buffer systems investigated

	Buffer A (pH = 7)	Buffer B
1	0.02 *M* Piperazine	1 *M* NaCl in A
2	0.02 *M* Bis-Tris	1 *M* NaCl in A
3	0.02 *M* Bis-Tris	1 *M* NaAc in A
4	0.01 *M* Potassium phosphate	1 *M* NaCl in A

pH 7.0) and water were weighed. The compounds were gently stirred for about 2 h and the system was allowed to settle overnight in a 300-l recipient. Whey was dissolved in the bottom phase obtained at a concentration of 15% w/w and filtered (press filter Seitz Enziger Noll, filter sheet 4946 Seitz-Filterwerke, Germany) to remove undissolved material. The permeate was used as the salt-rich phase for the experiments in the Graesser contactor. All experiments were carried out at room temperature.

2.3. Determination of α-La and β-Lg concentration

A chromatographic method was developed for the simultaneous determination of both proteins. A calibration curve was constructed with an aqueous solution of α-La–β-Lg (1:2.5 average whey concentration) in a Pharmacia fast protein liquid chromatography (FPLC) system. The FPLC system was equipped with a Mono Q HR 5/5 anion-exchange column [21] and operated at 1.5–2 MPa pressure and 1.0 ml/min flow-rate. The sample size at ambient temperature was 1 ml and the absorbance of the eluate was measured at 280 nm.

Before injection the samples were desalted by gel filtration (PD-10 Sephadex column-Pharmacia) and filtered (0.2 μm).

The buffer systems given in Table 1 were investigated. System No. 4 allowed the best separation with the following stepwise gradient shown in Table 2.

Table 2
Stepwise gradient used in this study

	Time (min)	Buffer B (%)
Gradient	0–20	10
Step	20–25	10
Step	25–40	30
Gradient	40–50	100

The Mono Q column should be cleaned after each run with 2 *M* NaCl, 1 *M* NaOH, 1 *M* HCl and 2 *M* NaCl and equilibrated with 100% buffer B. This procedure is necessary to obtain reproducible results.

2.4. Experiments in the Graesser contactor

The 100 cm × 10 cm I.D. Graesser contactor employed was manufactured by QVF Glastechnik. (Wiesbaden, Germany). The extractor consists of a glass cylinder with an internal rotor containing 36 compartments. Each of them is formatted for 6 buckets. A 0.25-kW motor is used to drive the rotor, the speed is set via a variable gear box. The connection between rotor and motor is propitiated by gears and linked chains. The direction of rotor movement had been reversed to obtain more stable operational conditions [22]. The interface level is kept at the centre of the contactor by a hydrostatic control.

In all the experiments the salt-rich phase (permeate of filtration) was the heavy (bottom) and the PEG-rich phase was the light (top) phase. The upper and lower phases were pumped (peristaltic pump, Verder, Düsseldorf, Germany) into the extractor above and below the rotor axis at opposite ends of the contactor.

2.5. Operational conditions

Rotor speeds of 3, 5, 7 and 9 rpm and top–bottom phase flow-rate ratios of 2:1, 1.2:1, 0.8:1 and 0.5:1 were investigated during the residence time and hold-up experiments. For the mass transfer experiments these values were 2 and 5 rpm and 2:1 and 1.5:1. Correspondent phase flow-rates were 36, 66 and 88 ml/min for the PEG-rich phase and 44 and 70 ml/min for the salt-rich phase.

2.6. Residence time distribution experiments

The PEG phase residence time distribution was determined by the pulse injection method. A pulse of cibacron blue was used as the dye (15

mg/ml, 1 ml, injection time 2 s) and was injected into the system at the PEG phase inlet. The tracer concentration was determined at the PEG phase outlet by measuring the absorption at 595 nm (spectrophotometer LKB Biochrom 4049).

The applicability of the dispersion model for this real situation was examined. The basic differential equation which represents this model in its dimensionless form [23]

$$\frac{dc}{d\theta} = \left(\frac{E_A}{UL}\right) \cdot \frac{d_2 c}{dz^2} - \frac{dc}{dz} \quad (1)$$

where c is the dimensionless dye concentration, θ is the dimensionless time, z is the dimensionless space coordinate, (E_A/UL) is the dimensionless inverse of the Bodenstein number (Bo). E_A is the coefficient of axial mixing, U is the linear phase flow velocity and L is the extractor length.

The response function obtained when the system is considered as an open vessel is

$$E_\theta = \frac{1}{2 \cdot \sqrt{\pi\theta\left(\frac{E_A}{UL}\right)}} \cdot \exp\left[-\frac{(1-\theta)^2}{4\theta\left(\frac{E_A}{UL}\right)}\right] \quad (2)$$

with mean

$$\theta_c = 1 + 2 \cdot \left(\frac{E_A}{UL}\right) \quad (3)$$

and variance

$$\sigma_\theta^2 = 2 \cdot \frac{E_A}{UL} + 8 \cdot \left(\frac{E_A}{UL}\right)^2 \quad (4)$$

2.7. Hold-up experiments

After steady state was reached for defined operation conditions the fractional hold-up of the PEG-rich phase was measured. This was performed by the simultaneous stop of the inlet and outlet streams and the rotor, followed by rapid removal of the extractor contents and volume determination of the two phases. This method leads to an average hold-up measurement that is calculated by

$$H_d = \frac{V_t}{V} \quad (5)$$

where H_d is the fractional hold-up of the top-phase, V_t and V are the volume of the top phase and total volume.

The top-phase hold-up at the top and bottom of the contactor was calculated after samples of 10 ml of the top and bottom phase had been withdrawn from the sample port at the middle of the extractor.

2.8. Mass transfer experiments

The direction of mass transfer was from bottom- to top-phase. The samples were collected at the outlets of the heavy and light phases. Up to 6 mean residence times of unchanged experimental conditions in continuous mode of operation were maintained to reach steady-state data. The concentration of the proteins was determined by FPLC as described above.

3. Results and discussion

3.1. Hydrodynamic characterization

Our experiments describing contactor hydrodynamics were based on measurements of the residence time distribution (RTD) of the Graesser contactor under defined conditions after application of a dye pulse. The time course of the outlet dye concentration was plotted *vs.* time to evaluate the first momentum of the RTD, that stands for the mean residence time. As the experimental setup was considered as an open system, the normalized first momentum had to be used for the determination of the mean residence time [23]. The result was then used to plot the value of the $C(\theta)$ function *vs.* the dimensionless time θ, to achieve independence of the RTD from flow-rate. The diffusion model of the RTD was then applied by non-linear regression and the result was compared to the experimental data. As described above, the diffusion model yields the Bodenstein number, a dimensionless number expressing the relation of convective and diffusional flows, containing the coefficient of axial mixing E_A. This coefficient was determined for each RTD and then used as a measure of axial mixing under different conditions. Fig. 2 shows an RTD after a dye pulse, the experimental values (points) show a reasonable correlation to the model calculations (line)

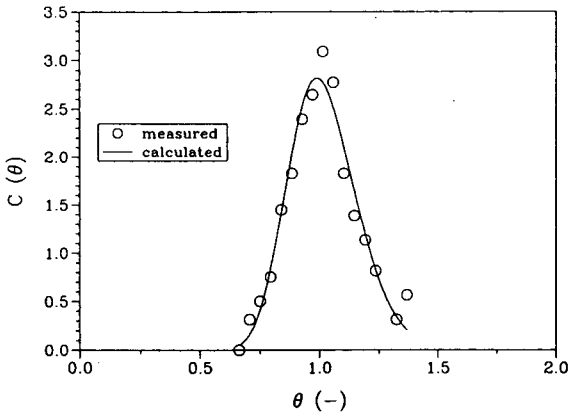

Fig. 2. Residence time distribution after dye-pulse. Experimental conditions: 14% PEG 1550–18% potassium phosphate pH 7; dye pulse: 1 ml of 2 mg/ml aqueous solution of Cibachron Blue.

thus validating the use of RTD measurements to represent axial mixing in our case.

Another important hydrodynamic parameter is the fractional hold-up of the phases. For the dispersed phase this parameter describes the amount of solvent actually available to remove the desired product from the feed at a certain point of the equipment. In this specific case, hold-up signifies the percentage of PEG-rich phase capable of extracting α-La from the salt-rich phase containing the protein mixture. Thus measurements of hold-up are valuable for the estimation of the mass transfer capabilities of an extraction unit under defined conditions.

A very important result of RTD measurements was the fact, that the flow of the salt-rich phase did not influence the residence time in the PEG-rich phase. This was evaluated by applying a dye pulse into the PEG-rich phase at different flows of the salt-rich phase and a fixed flow of the PEG-rich phase. The dye solely partitioned into the PEG-rich phase. All the experiments performed under these conditions yielded the same mean residence time, underlining the main feature of the Graesser contactor — the existence of two independently flowing phases, that are dispersed into each other by gentle mixing.

Another experiment to visualize this fact was performed by examining the PEG-rich phase hold-up at two different vertical positions in the contactor: The contactor was loaded with the two-phase system (14 % PEG 1550–18% phosphate, w/w) and operated at different rotor speeds. The port in the middle of the contactor was used to take samples from the upper and the lower half of the horizontal glass cylinder. Measurements of the PEG-rich phase hold-up of the respective samples demonstrated that the upper half of the contactor was predominantly (96–98%) filled with PEG-rich phase, the section below the interface line was filled with salt-rich phase (PEG-rich phase hold-up 2–3%). Fig. 3 shows the independence of the PEG-rich phase hold-up above and below the interface line from rotor speed.

To characterize axial mixing in the PEG-rich phase, the dependency of E_A from rotor speed was examined. Fig. 4 shows the independence of axial mixing from rotor speed, at least at the low speeds applied in our experiments. The low rotor speeds were chosen, to minimize shear forces, that may prove harmful for labile proteins.

Axial mixing may also be influenced by the linear velocity of the two phases as well as by the ratio of the two respective linear flow velocities. To examine this dependency the coefficient of axial mixing E_A was measured as a function of PEG- and salt-rich phase linear velocity. To determine the influence of phase velocity on axial mixing, the experiments were performed at

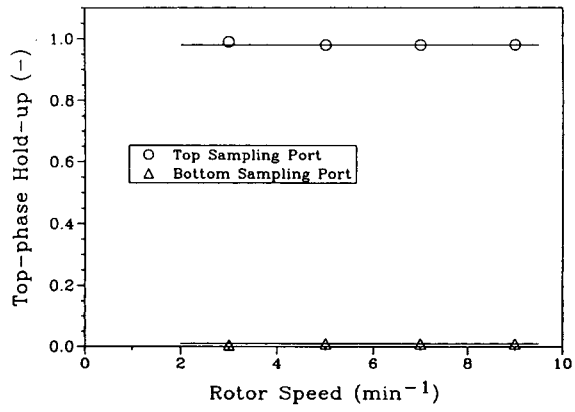

Fig. 3. Fractional hold-up at top and bottom of the extraction unit. Experimental conditions: 14% PEG 1550–18% potassium phosphate pH 7.

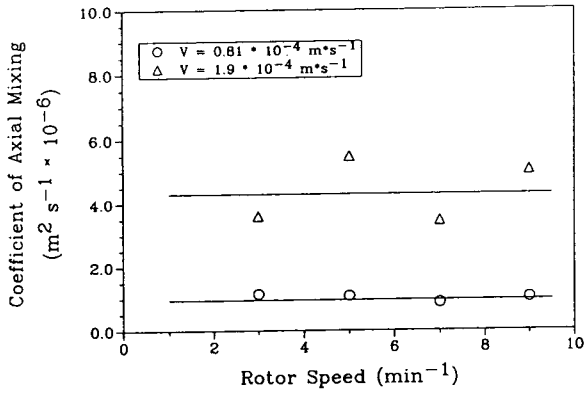

Fig. 4. Axial mixing *versus* rotor speed; parameter: linear phase velocity. Experimental conditions: 14% PEG 1550–18% potassium phosphate pH 7.

different top-phase linear velocities. As can be seen from Fig. 4, higher linear velocities of the top-phase lead to an increased degree of axial mixing expressed by higher E_A values, which seems to be independent from rotor speed at constant phase velocity. In Fig. 5 it is demonstrated that the ratio of the linear phase velocities does not influence the degree of axial mixing in the Graesser contactor. Again the independence of E_A from rotor speed is evident. Since in our case the salt-rich phase can be regarded as the feed and the PEG-rich phase as the solvent stream, this means that increasing the process capacity by a higher solvent-to-feed flow-ratio does not affect the quality of counter-current extraction.

The performance of a continuously operated extraction unit is strongly dependent on the amount of solvent, that is present in the extractor to remove the solute from the feed. At high amounts of solvent compared to feed the solute concentration gradients are favourable for mass transfer from feed to solvent. In our case top-phase hold-up stands for the amount of PEG-rich phase (solvent) available to extract proteins (solute) from the whey-containing phosphate-rich phase (feed). Thus the influence of rotor speed and ratio of phase velocities on top-phase hold-up was examined. Fig. 6 shows the independence of the top-phase hold-up from rotor speed as well as from the ratio of phase velocities. Thus the capacity and performance of the extractor is not reduced by low rotor speeds, that provide favourable mixing conditions for labile products. Additionally, a high ratio of solvent-to-feed flow can be applied without affecting extractor performance.

Summarizing the results of the hydrodynamic measurements the special characteristics of the Graesser Raining Bucket contactor can be applied for operation with aqueous two-phase systems. There are two independently flowing phases with an interface line that can be controlled in the equatorial position of the contac-

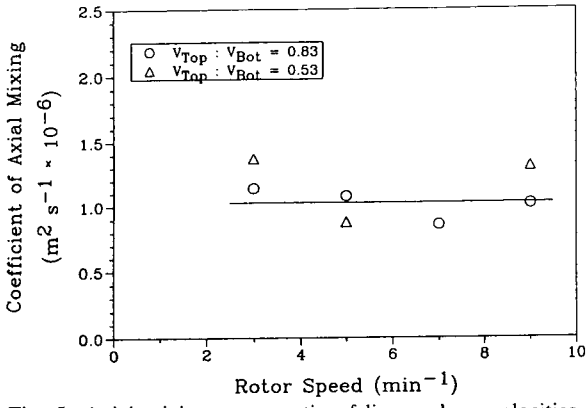

Fig. 5. Axial mixing *versus* ratio of linear phase velocities. Experimental conditions: 14% PEG 1550–18% potassium phosphate pH 7.

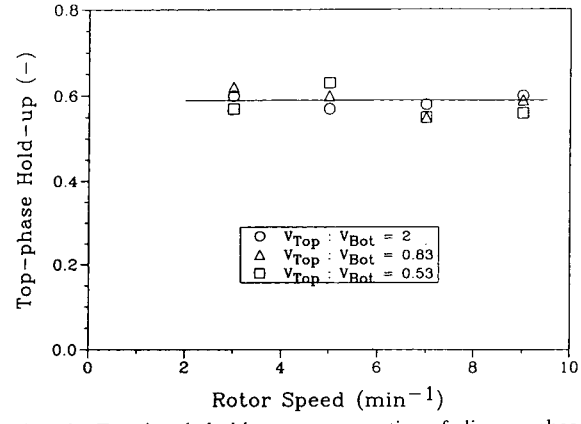

Fig. 6. Fractional hold-up *versus* ratio of linear phase velocities. Experimental conditions: 14% PEG 1550–18% potassium phosphate pH 7.

tor, both phases being dispersed into each other. An independence of the axial mixing from rotor speed and from the ratio of linear phase velocities can be stated. Additionally, both rotor speed and ratio of phase velocities do not affect top-phase hold-up, thus leading to constant extraction efficiency within the range of experiments performed here. Linear phase velocity strongly affects axial mixing, so there is a limiting phase velocity, above which the quality of counter-current extraction is severely diminished.

Comparing our results to the experiments described with kerosene–water systems [10,11] reveals several differences when operating the Graesser contactor with ATPS compared to the organic solvent–water systems. In the studies with the latter system a decrease in axial mixing in the organic phase was detected with increasing rotor speed, while the opposite behaviour was observed for the aqueous phase. The influence of linear phase velocity on back mixing was similar to our results. Contrary to the results presented here, the authors found increasing aqueous phase hold-up at increasing linear flow-rates, but also described the hold-up to be independent from rotor speed. These discrepancies can be attributed to the different properties of the phase system used in this work: ATPS are systems with especially low interfacial tension and increased viscosity, thus some deviations in their hydrodynamic behaviour compared to classical water–organic solvent systems are to be expected. Nevertheless, the special hydrodynamic features of the Graesser contactor also apply for operation with ATPS, thus allowing the use of phase systems with low density difference and interfacial tension.

3.2. Continuous separation of whey proteins

The promising results of the initial experiments to test the hydrodynamic behaviour of the Graesser contactor with ATPS prompted us to test the performance of continuous experiments with real solutions. As mentioned in the Introduction, our model system was the separation of α-La and β-Lg from whey with a PEG 1550–potassium phosphate system. Based on the work of Chen [20] we performed some preliminary experiments in order to find a useful phase system for the continuous experiment. From the partition coefficient and phase ratios obtained by several batch experiments (data not shown) we decided to use 14% PEG 1550–18% potassium phosphate at pH 7. Since the whey was delivered as spray dried powder, we used a 15% solution of whey powder in the salt-rich phase as feed. The experimental conditions for the continuous experiment were chosen according to the results of the hydrodynamic study. The continuous extraction was conducted at two different rotor speeds to confirm the independence of axial mixing and hold-up from rotor speed, as was already observed during the hydrodynamic measurements. In the second set of experiments two different ratios of phase velocities were used to show an increase of extraction efficiency by increasing the ratio of solvent-to-feed flow. Thus a ratio of PEG-rich phase linear velocity (solvent flow) to salt-rich phase linear velocity (feed-flow) of 2 and 1.5 were used.

The continuous experiments were performed for at least 6 residence times before a parameter was changed. To determine the quality of extraction, the phases were analyzed for content of α-La and β-Lg by FPLC as described above. The results of the variation of rotor speed is shown in Table 3 for the first set of experiments ($\tau = 1$ h, $V_{TOP} = 88$ ml/min, $V_{BOT} = 44$ ml/min). β-Lg completely partitioned into the salt-rich phase, while α-La had similar concentration in PEG-rich and salt-rich phase. Fig. 7 shows chromatograms of the feed solution and of the two phases at steady state in a continuous experiment. As the ratio of top-phase to bottom-phase linear velocity was 2:1, the extraction yield of α-La from the continuous process was 63%. Total protein recovery was 99% for β-Lg and 97% for α-La. As indicated from the hydrodynamic measurements the extraction yield was independent from rotor speed. Reducing the top-phase flow from 88 ml/min to 66 ml/min at constant flow of bottom-phase reduced the ratio of linear velocities from 2 to 1.5. As shown in Table 3 the PEG-rich phase concentration of α-La remained unchanged while α-La concen-

Table 3
Results of the continuous extraction of whey proteins

	α-Top-phase	α-Bottom phase	β-Top phase	β-Bottom phase
Rotor speed[a]				
2 rpm	0.42 mg/ml	0.45 mg/ml	n.d.	7.4 mg/ml
5 rpm	0.43 mg/ml	0.3 mg/ml	n.d.	7.2 mg/ml
Ratio of linear phase velocities[b]				
2:1	0.43 mg/ml	0.45 mg/ml	n.d.	7.4 mg/ml
1.5:1	0.41 mg/ml	0.61 mg/ml	n.d.	7.9 mg/ml

[a] Effect of rotor speed (starting conditions 1.4 Mg/ml α-La, 7.4 Mg/ml β-Lg).
[b] Effect of ratio of linear phase velocity (starting conditions 1.4 mg/ml α-La, 7.4 mg/ml β-LG).

tration increased in the salt-rich phase. Calculating the yield of α-La shows a reduction to 44%. However, the partitioning of β-Lg into the salt-rich bottom-phase still was complete. The total amount of protein processed in our experiments was 660 g of protein per day, the amount of α-La purified from whey was 70 g per day.

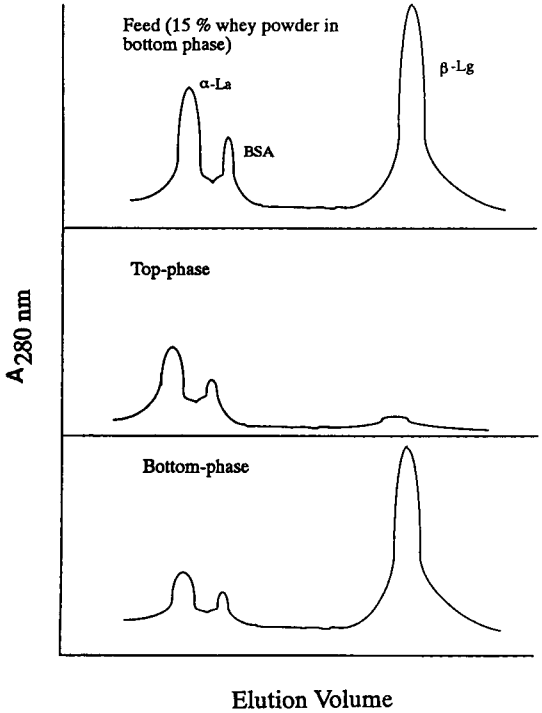

Fig. 7. Schematic presentation of the FPLC chromatograms of feed, top- and bottom-phase from the continuous experiment at steady state.

Comparing these results to the suggestions of Wang *et al.* [11] with respect to optimum extraction conditions in a Graesser contactor shows good agreement: low rotor speeds at high ratio of solvent-to-feed flow also yielded the best results in our experiments. The low rotor speeds prevent protein inactivation by shear forces and moreover simplify the handling of the extraction unit: phase separation in the end zones of the contactor is better at reduced rotor speed. A high ratio of solvent-to-feed flow increases the interface area per unit time that is available for mass transfer and thus favours efficient extraction.

4. Conclusions

The Graesser raining bucket contactor proved to be an extraction unit well suited for work with aqueous two-phase systems. The general hydrodynamic features as described in the literature —independent phases, that are separated at the equatorial line of the extraction vessel and are dispersed into each other— were also found in basic experiments. Examination of the influence of rotor speed, phase velocity and phase ratio resulted in a high extraction efficiency at conditions favourable for protein processing. The flow-rates that could be applied in continuous operation indicated a large capacity of the bench-scale contactor used in our experiments.

Transferring these results to the separation of α-La and β-Lg from whey confirmed the expectations from the initial measurements with PEG–salt systems: the Graesser contactor is capable of continuously separating α-La and β-Lg with satisfactory yields at a rotor speed of 2 rpm. The residence time of 1 h leads to short process times, allowing processing of 660 g of total whey protein per day under the conditions applied here (15% solution of whey powder in salt-rich phase). The PEG-rich phase was free of β-Lg, thus the primary goal of the process, the reduction of the content of the major allergen in infant nutrient formulations was achieved. The space time yield with respect to α-La production is 8.8 g/l per day. Increasing the ratio of linear phase velocities in favour of the PEG-rich phase velocity should lead to even higher space–time yields. Another possibility of increasing the process productivity might be the increase of protein load of the phase system above 15% of whey powder.

Interesting points, that remain to be examined are the distribution of other whey proteins, as for example serum albumin, lactoferrin and immunoglobulins. These proteins are important for retaining the immunologic properties of the artificial infant milk formulations from bovine whey [14]. Research with respect to these questions has been initiated. Another point of interest is the degree of back mixing under the hydrodynamic conditions applied. Sheik *et al.* [10] performed experiments with a kerosene–water system to evaluate back mixing in the Graesser contactor. The question of back mixing with ATPS in the contactor described here is presently under investigation.

Vernau and Kula [24] established a PEG–sodium citrate two-phase system to replace phosphate as the water-structuring salt for ecological and economic reasons. Preliminary experiments have been performed that try to transfer this technique to the separation of whey proteins. Based on the results of Vernau and Kula [24] the replacement of phosphate by citrate seems possible although thorough investigations must follow.

5. Acknowledgements

The authors gratefully acknowledge the technical assistance by Mrs. Monika Gehsing, as well as financial support of the DAAD (Deutscher Akademischer Austauschdienst, Germany) and the CNPq (Conselho Nacional de Desenvolvimento Cientifico e Tecnologico, Brazil). We also thank Meggle Milchindustie GmbH for the gift of whey powder.

6. References

[1] J.B. Joshi, S.B. Sawant, K.S.M.S. Raghava Rao, T.A. Patil, K.M. Rostami and S.K. Sikdar, *Bioseparation*, 1 (1990) 311.
[2] H. Hustedt and N. Papamichael, *Enzyme Eng.*, 9 (1988) 135.
[3] Greve, A. and Kula, M.-R., *Bioprocess Eng.*, 6 (1990) 173.
[4] N. Papamichael, B. Börner and H. Hustedt, *J. Chem. Technol. Biotechnol.*, 54 (1992) 47.
[5] S. V. Save, V.G. Pangarkar and S.V. Kumar, *Bioechnol. Bioeng.*, 41 (1993) 72.
[6] T.A. Patil, K. Rostami Jafarabad, S.B. Sawant and J.B. Joshi, *Can. J. Chem. Eng.*, 69 (1991) 548.
[7] J. Coleby, *U.S. Pat.*, 3 017 253 (1962).
[8] J. Coleby, in L.O. Baird and C. Hanson (Editors), *Handbook of Solvent Extraction*, Wiley, New York, 1983, Ch. 13.6 p. 449.
[9] H. Hustedt, K.-H. Kroner, U. Menge and M.-R. Kula, *Enzyme Eng.*, 5 (1980) 45.
[10] A.R. Sheikh, J. Ingham and C. Hanson, *Trans Inst. Chem. Eng.*, 50 (1972) 199.
[11] P.S.M. Wang, J. Ingham and C. Hanson, *Trans Inst. Chem. Eng.*, 55 (1977) 196.
[12] A.A. Al-Hemiri and A. Kareem, *Can. J. Chem. Eng.*, 68 (1990) 569.
[13] P.J. Skudder, *J.Dairy Res.*, 52 (1985) 167.
[14] T. Kaneko, B.T. Wu and S. Nakai, *J. Food Sci.*, 50 (1985) 1531.
[15] E. Lebenthal, *Pediatr. Clin. N. Am.*, 22 (1975) 827.
[16] S.A. Al-Mashiki and S. Nakai, *J. Food Sci.*, 52 (1987) 1237.
[17] E. Chiancone and M. Gattoni, *J. Chromatogr.*, 539 (1991) 255.
[18] P. Maillart and B. Ribadeau-Dumas, *J. Food Sci.*, 53 (1988) 743.
[19] R.J. Pearce, *Aust. J. Dairy Technol.*, Dec. 1983 144.
[20] J.-P. Chen, *J. Ferm. Bioeng.*, 73 (1992) 140.
[21] B. Manji, A. Hill, Y. Kakuda and D.M. Irvine, *J. Dairy Sci.*, 68 (1985) 3176.
[22] K.H. Kroner, H. Hustedt and M.-R. Kula, 1980, unpublished results.
[23] O. Levenspiel, *Chemical Reaction Engineering*, Wiley, New York, 1992.
[24] J. Vernau and M.-R. Kula, *Biotechnol. Appl. Biochem.*, 12 (1990) 397.

ELSEVIER

Journal of Chromatography A, 668 (1994) 95–100

JOURNAL OF CHROMATOGRAPHY A

Protein refolding using aqueous two-phase systems

Daniel Forciniti

Chemical Engineering Department, University of Missouri-Rolla, Rolla, MO 65401, USA

Abstract

We present a novel refolding technique in which aqueous two-phase systems are used to both dissociate protein aggregates (inclusion bodies) and to refold the protein in only one operation. Three denaturant salts (sodium thiocyanate, calcium chloride, and lithium bromide) were used as phase-forming salts with poly(ethylene glycol) (PEG). We have tested the technique by dissolving carbonic anhydrase II aggregates and refolding the denatured protein in PEG–NaCl–NaSCN systems.

1. Introduction

The expression of eukariotic proteins in a foreign host is frequently accompanied by the formation of aggregates or inclusion bodies of inactive proteins which accumulate within the cell [1–3]. Although inclusion bodies have been found mainly in *Escherichia coli* they have also been found in other bacteria [4–9], and even in insect cells [10].

Inclusion bodies are roughly spherical amorphous aggregates of protein. It is generally accepted that these protein aggregates are held together by hydrophobic, ionic, and covalent (disulfide bonds) forces. Studies performed on the temperature dependence of protein association suggest that hydrophobic forces play a dominant role in maintaining the proteins in the aggregates. This last observation also suggests that chaotropic salts can be used to dissolve the aggregates. Indeed, inclusion bodies are solubilized by chaotropic agents such as urea, guanidine hydrochloride (GuClH), detergents, and salts. Urea and GuClH are the most effective and commonly used solubilizing agents. Chaotropic salts at a concentration of 1 *M* are also effective in solubilizing protein aggregates [11]. If the aggregate is held together by covalent bonds such as disulfide bonds, it may be necessary to add β-mercaptoethanol [12]. However, the addition of thiol reagents is not necessary even though intermolecular and intramolecular disulfide bonds exist in the inclusion bodies if the solubilization of the aggregates is carried out at high temperatures [13].

The formation of inclusion bodies provides a convenient and clean alternative for protein purification. Under ordinary circumstances only a small amount of impurities contaminates the inclusion bodies formed by the eukariotic protein. Thus by separating the inclusion bodies from the cell debris by centrifugation [1] or ultrafiltration [14], it is possible to obtain a highly pure protein in a single purification step. After the inclusion bodies have been isolated, they are suspended in a buffer and exposed to denaturing conditions to solubilize the protein. The denaturing agent is then diluted (either by dialysis or by adding an appropriate buffer) to refold the protein. Unfortunately, during the refolding process the proteins re-aggregate. Thus only a fraction of the active protein is recovered [15].

0021-9673/94/$07.00
SSDI 0021-9673(93)E0053-W

Several routes have been explored to prevent the re-aggregation of the proteins and thus improve the recovery of the active protein. Hagen *et al.* have used reverse micelles to decrease the local density of proteins in order to minimize protein association [16,17]. Although this approach is attractive, some hydrophobic proteins do not fold correctly because they interact with the hydrophobic moieties of the micelles [17]. Finally, Cleland and Wang [18] have found that by adding a cosolvent like poly(ethylene glycol), PEG, to the refolding mixture the formation of aggregates is minimized and the recovery of the active protein is enhanced. Cleland and Wang have successfully used PEG (3 to 30 g/l) for the recovery of carbonic anhydrase II. This approach is especially appealing because it seems independent of the kind of protein. However, this protocol produces a highly dilute protein solution contaminated by large amounts of denaturant. Clearly improvements to this technique are highly desirable to make it more commercially attractive.

In this paper we report preliminary results of a novel refolding technique in which aqueous two-phase systems are used to both dissociate the inclusion bodies and refold the protein in one operation. The aqueous two-phase system is a PEG–salt system chosen so that the proteins are conformationally stable in the PEG phase and are conformationally unstable in the salt phase. Therefore, the inclusion bodies dissociate in one phase and the denatured protein refolds in the other phase. The dissociation–refolding process continues until equilibrium is reached.

2. Experimental

2.1. Materials

PEG 6000 and carbonic anhydrase II (Lot # 30H9490) were obtained from Sigma (St. Louis, MO, USA). All the other chemicals were of analytical-reagent grade.

2.2. Preparation of the phase systems

Four-gram phase systems were prepared by mixing the polymer with nanopure water and salts in the appropriate amount and stirring for several minutes [19]. The pH was adjusted by adding either phosphate or Tris buffers at a concentration of 50 m*M*. Duplicates were prepared for each phase system. Most of the systems considered in this work are in the one-phase region at room temperature. Therefore, the systems are driven into the two-phase region by increasing the temperature. Three alternative techniques were used to determine the phase diagrams: protocols 1, 2 and 3.

Protocol 1

The phase systems were prepared as indicated above. They were placed in a controlled-temperature water bath and the temperature of the water bath increased in intervals of 2 or 3°C. The systems remained in the water bath at each temperature for about 30 min to allow stabilization. The temperature at which the systems become cloudy was recorded as the cloud point temperature. The cloud point temperature indicates the onset of the liquid–liquid phase transition.

Protocol 2

The phase systems were prepared as indicated above. They were placed into a stirred cell of a temperature-controlled spectrometer and the absorbance at 450 nm was measured as a function of temperature. First, we increased the temperature until a sharp increase in the absorbance was observed indicating that the system had become cloudy. The temperature at which the systems became cloudy was recorded as the cloud point temperature (forward experiments). Second, we decreased the temperature until the absorbance observed at room temperature was recovered. The temperature at which the system became transparent was recorded as the cloud point temperature (backward experiments). The cloud point temperature obtained by the backward and forward experiments agreed within 1°C.

Protocol 3

The phase diagrams were determined as indicated by Albertsson [20]. A salt or PEG solution of known concentration was titrated with PEG or salt, respectively, until the solution turned turbid. The composition of the mixture was followed by weight.

2.3. Partition experiments

For the partition experiments 0.5 or 1 ml of a 2.5 mg/ml protein stock solution was added to the phase systems replacing an equal amount of buffer. The systems were stirred for several minutes and placed into a water bath to induce the phase transition. After complete phase separation (between 5 to 12 h), samples from top and bottom phase were taken carefully with a micropipette. After dilution, the absorbance at 280 nm was measured using quartz cuvettes in a double-beam Hitachi spectrophotometer (Model U-2000). The calculated extinction coefficient for the native protein was 1.90 mg/ml, while the extinction coefficient for the denatured protein was 1.65 mg/ml. The enzymatic activity was measured by recording the increase of absorbance at 348 nm due to the hydrolysis of *p*-nitrophenylacetate [15]. The activity of the enzyme was determined as the slope of the absorbance at 348 nm *versus* time plot. Since *p*-nitrophenylacetate hydrolyses even in the absence of the protein a blank was discounted to account for the changes in the reactant. The enzymatic activity of the fresh enzyme was 1.9 units/mg of protein at 20°C.

2.4. Protein denaturation

Carbonic anhydrase II was denatured by incubating 25 mg of the enzyme for 24 h in 1 ml of 5 *M* guanidine hydrochloride. A volume of 0.1 ml of this solution diluted to 10 ml with 5 *M* guanidine hydrochloride was used as our denatured protein. This solution was diluted with 25 ml of Tris buffer pH 7.5 to a final concentration of 0.174 *M* guanidine hydrochloride to induce the formation of aggregates [18]. These aggregates were centrifuged at 3000 *g* for 20 min and the precipitate was used in the partition experiments. These protein aggregates resemble inclusion bodies.

3. Results and discussion

3.1. Phase system selection

Our first objective was to find a PEG–salt system such that the phase-forming salt was able to dissolve the aggregates. Non-chaotropic salts such as phosphate, sulphate or citrate which form two liquid phases with PEG at room temperature cannot dissolve the inclusion bodies. Therefore, only chaotropic salts needed to be considered. However, we found very difficult to obtain two phases by mixing chaotropic salts with PEG even at high temperatures. Fortunately, we also found that by replacing a fraction of the chaotropic salt with NaCl the phase transition temperature decreased to acceptable limits. To induce phase separation at high temperatures may be beneficial for this project because the dissociation of the aggregates is generally facilitated at high temperatures. The refolding process in the PEG-rich phase will not be adversely affected at high temperatures because PEG increases the protein melting temperature (the temperature at which the protein unfolds).

LiBr, $CaCl_2$, and NaSCN were tested as phase-forming salts with PEG at several temperatures. Our studies show that the addition of small amounts of NaCl to NaSCN–PEG, $CaCl_2$–PEG and LiBr–PEG systems generally facilitates the phase separation. Fig. 1 shows the transition temperature *versus* the amount of NaCl replaced by NaSCN, LiBr or $CaCl_2$ for a total salt concentration of 15% (w/w) and a polymer concentration of 20% (w/w) (in this Figure and in all subsequent ones the lines are given solely to guide the reader's eye). LiBr and $CaCl_2$ form two liquid phases with PEG at rather high temperatures. The cloud point temperature for PEG–NaCl–LiBr and PEG–NaCl–Ca_2Cl sys-

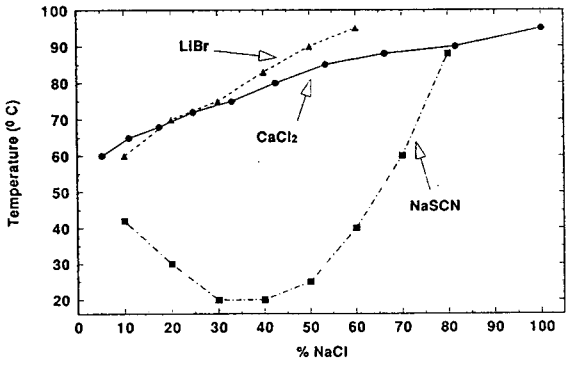

Fig. 1. Cloud point temperature *versus* % of NaCl replaced by LiBr, CaCl or NaSCN. Total salt concentration 15% (w/w). Total PEG concentration 20% (w/w).

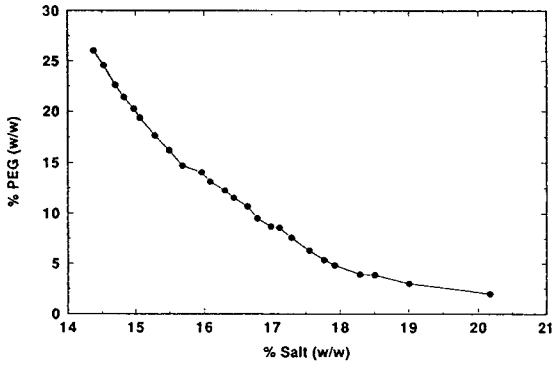

Fig. 2. Phase diagram for PEG–NaCl–NaSCN system at 20°C. The salt composition is 60% NaSCN and 40% NaCl.

tems increases with increasing substitution of NaCl by the chaotropic salt. NaSCN, on the contrary, forms two liquid phases at reasonable temperatures even if a large amount of NaCl is replaced by NaSCN. In addition, the mutual solubility of PEG–NaCl–NaSCN systems exhibits a minimum at about 25°C. Further experiments are needed to explain this phenomenon. In conclusion, NaSCN is the most promising salt from those tested by us since it is a very strong denaturant and forms two-liquid phases with PEG over a wide range of temperatures. Therefore all the following experiments were performed in PEG–NaCl–NaSCN systems.

In an attempt to understand the PEG–NaCl–NaSCN systems we determined phase diagrams and we studied the effect that the total concentration of PEG and the pH have on the cloud point temperature of these systems. Fig. 2 shows a phase diagram for NaSCN–NaCl–PEG at 20°C; 60% of the total salt is NaCl and 40% is NaSCN; the total salt concentration is 15% (w/w). This figure shows that the amount of salt in each phase is rather high. A high concentration of salt in the bottom phase is desirable because it will favor the dissolution of the aggregates. On the other hand, a high concentration of salt in the top phase is undesirable because it will inhibit the refolding of the protein. The total amount of salt and the proportion of NaSCN in the mixture have to be optimized in the partition experiments to allow the dissolution of the inclusion bodies in either the homogeneous systems or in the salt-rich phase and to facilitate the refolding of the protein in the PEG-rich phase. Fig. 3 shows the cloud point temperatures at two different PEG concentrations, 15 and 20% at a total salt concentration of 25%; 10% NaCl and 90% NaSCN. This figure shows that an increase in the PEG concentration favors the phase separation. Finally, in Fig. 4 we show the effect that pH has on the two-phase system. This figure is for a total salt concentration of 25%, with a salt composition of 10% NaCl, and 90% NaSCN at pH values 7.5 and 5.6. Clearly, a decrease in the pH favors the phase separation.

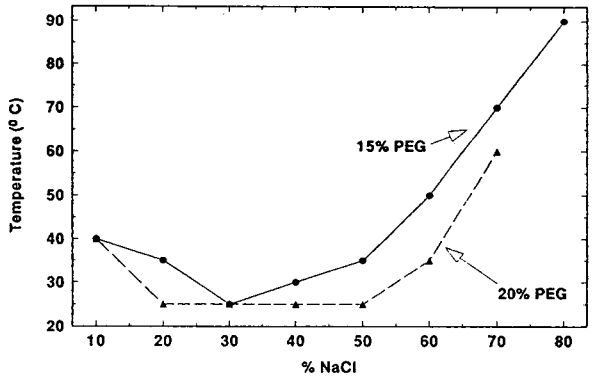

Fig. 3. Cloud point temperature *versus* % of NaCl replaced by NaSCN at two PEG concentrations. Total salt concentration 15% (w/w).

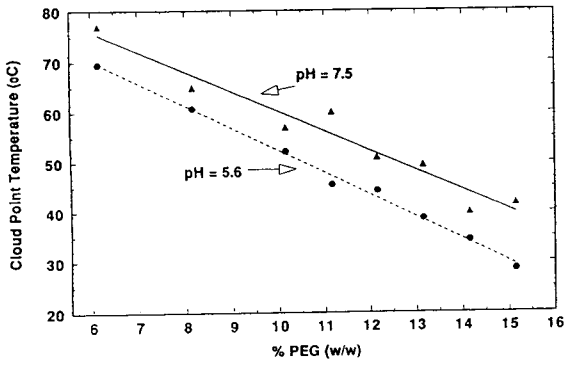

Fig. 4. Cloud point temperature *versus* PEG concentration in % (w/w) at two different pH values. Total salt concentration 25% (w/w). Salt composition is 10% NaCl and 90% NaSCN.

3.2. Protein partition experiments

Partition experiments were performed with the native protein and with the protein aggregates. Three phase systems containing 20% PEG and 15% salt with variable amounts of NaSCN were selected for our partition experiments. All experiments were performed at 40°C and the systems were buffered with Tris (pH = 7.0). Table 1 summarizes our results for the native protein. System A contains 50% NaSCN and 50% NaCl, System B contains 40% NaSCN and 60% NaCl, and system C contains 30% NaSCN and 70% NaCl. System A is at the onset of phase separation at room temperature while systems B and C are in the one-phase region at room temperature. The protein partition coefficient, $K = C_{top}/C_{bottom}$, was very high in all cases. The protein mass balance, however, did not close indicating some absorption of the protein at the interface. The interface of the system containing a high concentration of NaSCN becomes turbid and very broad when 1 ml of the stock protein solution is added but remains clear when 0.5 ml of the stock protein solution is added. This indicates that the composition of the phases depends on the amount of protein present in the system. Our findings suggest that the usual assumption that the phase systems are not altered by the addition of low protein concentrations is not valid for these systems.

Table 1
Partition coefficient and activity of carbonic anhydrase II in PEG–NaCl–NaSCN systems

System	Partition coefficient	Activity (units/mg)	
		Top	Bottom
A	1.94	0.016	0.0
B	1.26	1.39	0.0
C	3.58	0.239	0.0

Systems composition: 20% PEG and 15% salt; $t = 40$°C; pH 7.0. System A contains 50% NaSCN and 50% NaCl, system B contains 40% NaSCN and 60% NaCl and system C contains 30% NaSCN and 70% NaCl. Total protein concentration: 0.625 g/l.

The enzymatic activity was monitored before and after demixing of the phase systems. Our results are reported in the last columns of Table 1. We did not observe any enzymatic activity in the systems before demixing, in the salt-rich phases (bottom phases), and in the PEG-rich phase (top phase) of the system containing large amounts of NaSCN (System A). We did observe activity in the top phase of the systems containing relatively small amounts of NaSCN. These observations suggest that we can optimize the protocol by varying the relative amounts of non-chaotropic to chaotropic salts. In independent experiments we found that the activity of carbonic anhydrase II was completely lost in NaSCN concentrations as low as 5% (w/w). However, the activity was recovered by diluting the denaturating mixture with Tris buffer.

Finally, we used the PEG–NaCl–NaSCN systems described above (Systems A,B, and C) to dissolve the carbonic anhydrase aggregates and to refold the protein. First, we suspended the aggregates in different amounts of Tris buffer. The aggregates did not dissolve and no enzymatic activity was observed. The aggregates were then placed into the selected phase systems. The aggregates dissolved almost instantaneously when the systems were still in the one phase region and no enzymatic activity was detected. The systems were placed in a water

bath at 40°C to induce the phase separation. Samples from top and bottom phase were analyzed for protein content and enzymatic activity. No enzymatic activity was found in either phase of systems A and B. In the system containing 30% NaSCN no activity was recovered in the bottom phase but 0.386 units/mg were recovered in the top phase. We did not find any protein in the bottom phase, indicating that the protein accumulates at the interface.

4. Conclusions

It is evident that to efficiently produce a recombinant protein the active protein has to be recovered from the aggregates. A refolding process should provide: (a) high recovery of the biologically active protein; (b) easy separation of the product from misfolded polypeptides; and (c) highly concentrated protein (volume reduction) at the end of the refolding process. In addition, the refolding process should be easy to scale up and it should proceed at an acceptable rate. We believe that the combined dissociation–refolding technique that we are developing will fulfil these requirements.

Our results show that a new kind of two-phase system developed by us may be used for the recovery of active proteins from inclusion bodies. Still the protocol has to be optimized to increase the recovery of the active protein. Work is in progress in this direction. The use of a harmful salt like NaSCN may raise some concerns. However, the salt normally used in solubilizing inclusion bodies, guanidine hydrochloride, is as toxic as NaSCN. The ultimate challenge of our protocol will be to test it with inclusion bodies from eukariotic proteins engineered in *E. coli*.

5. References

[1] F.A.O. Marston, *Biochem. J.*, 240 (1986) 1.
[2] J.F. Kane and D.L. Hartley, *Trends Biotechnol.*, 6 (1988) 95.
[3] A. Mitraki and J. King, *Bio/Technology*, 7 (1989) 690.
[4] R. Leemans, E. Remaut and W. Fiers, *J. Bacteriol.*, 169 (1987) 1899.
[5] C.H. Schein, K. Kashiwagi, A. Fujisawa and C. Weissman, *Bio/Technology*, 4 (1986) 719.
[6] L.S. Cousens, J.R. Shuster, C. Gallegos, L. Ku, M.M. Stempien, M.S. Urdea, R. Sanchez-Pescador, A. Taylor and P. Tekamp-Olson, *Gene*, 61 (1987) 265.
[7] T. Hayakawa, A. Toibana, R. Marumoto, K. Nakahama, M. Kikuchi, K. Fujimoto and M. Ikehara, *Gene*, 56 (1987) 53.
[8] A.V. Quirk, M.J. Geisow, J.R. Woodrow, S.J. Burton, P.C. Wood, A.D. Sutton, R.A. Johnson and N. Dodsworth, *Biotechnol. Appl. Biochem.*, 11 (1989) 273.
[9] I. van der Klei, M. Veenhuis, I. van der Ley and W. Harder, *FEMS Microbiol. Lett.*, 57 (1989) 133.
[10] V.A. Luckow and M.D. Summers, *Bio/Technology*, 6 (1998) 47.
[11] W.K. Lim, H.E. Smith-Somerville and J.K. Hardman, *Appl. Environ. Microbiol.*, 55 (1989) 1106.
[12] C.J. Epstein and R.F. Goldberger, *J. Biol. Chem.*, 238 (1963) 1380.
[13] F.A.O. Marston, P.A. Lowe, M.T. Doel, J.M. Schoemaker, S. White and S. Angal, *Bio/Technology*, 2 (1984) 800.
[14] S.M. Forman, E.R. DeBernardez, R.S. Feldberg and R.W. Swartz, *J. Membrane Sci.*, 48 (1990) 263.
[15] A. Ikai, S. Tanaka and H. Noda, *Arch. Biochem. Biophys.*, 190 (1978) 39.
[16] A.J. Hagen, T.A. Hatton and D.I.C. Wang, *Biotechnol. Bioeng.*, 35 (1990) 955.
[17] A.J. Hagen, T.A. Hatton and D.I.C. Wang, *Biotechnol. Bioeng.*, 35 (1990) 966.
[18] J.L. Cleland and D.I.C. Wang, *Biochemistry*, 29 (1990) 11072.
[19] D. Forciniti, C.K. Hall and M.-R. Kula, *Fluid Phase Equilibr.*, 61 (1991) 243.
[20] P.A. Albertsson, *Partitioning of Macromolecules*, John Wiley and Sons, New York, N.Y., 1986.

ELSEVIER

Journal of Chromatography A, 668 (1994) 101–106

JOURNAL OF CHROMATOGRAPHY A

Use of hydrophobic affinity partitioning as a method for studying various conformational states of the human α-macroglobulins

Poul Erik Hyldgaard Jensen[a], Torgny Stigbrand[a], Vithaldas P. Shanbhag*[,b]

[a] *Department of Medical Biochemistry and Biophysics, University of Umeå, S-901 87 Umeå, Sweden*

[b] *Department of Biochemistry, University of Umeå, S-901 87 Umeå, Sweden*

Abstract

The serum proteins α_2-macroglobulin and pregnancy zone protein undergo major conformational changes when complexed with proteinases. It is shown that the changes in $\Delta\log K_{max}$ determined by hydrophobic affinity partitioning is a measure of the extent of changes in the conformation of these α-macroglobulins. We introduce a new term for the changes of surface hydrophobicity in a protein as $\Delta\log K_{acc}$. This defines the difference of $\Delta\log K_{max}$ between a modified and an unmodified conformational state of a specific protein and can be useful as a parameter to describe the apparent conformational changes in the protein.

1. Introduction

Many proteins exhibit their functions at certain conformational states, which can be reversibly or non-reversibly changed by various factors. Some proteins change conformation by binding ligands or ions and some by proteolytic cleavage. The changes in conformational states are caused by changes in the protein structure, which involve changes in the exposure of protein regions to the surroundings. Some of these regions can be hydrophilic or hydrophobic and these characteristics play dominating roles in the function and stability of the protein. Changes in exposure of hydrophobic regions to the surroundings have been detected in many proteins upon regulation of functions. Strong hydrophobic regions are often exposed for direct functional reasons, which, in the case of serum proteins, may involve binding and transport of specific ligands. In general hydrophobic regions are concealed and hydrophilic regions exposed in proteins [1]. Hydrophobic affinity partitioning has been documented to be a sensitive method for studying changes in hydrophobicity of the surface of proteins [2]. It has been demonstrated that calmodulin and α-lactalbumin undergo a considerable change in surface hydrophobicity upon Ca^{2+} binding [3–5]. These changes in hydrophobicity have been correlated with changes in conformation of these proteins [4,5].

Human α_2-macroglobulin (α_2M) and the related pregnancy zone protein (PZP) are two serum proteins which undergo large conformational changes during inhibition of proteinases. The two proteins have many characteristics in common and have 71% identically positioned amino acids [6]. The conformational changes in α_2M have been studied extensively by various methods such as polyacrylamide gel electropho-

* Corresponding author.

0021-9673/93/$06.00
SSDI 0021-9673(93)E1154-R

resis (PAGE) [7,8], hydrodynamic methods, absorption, fluorescence and circular dichroism spectra [9] and by electron microscopy [10]. α_2M is a homotetrameric protein with a molecular mass of 720 000; 1 mol is capable of inhibiting 2 mol of a proteinase [11]. Native PZP is a homodimeric protein with a molecular mass of 360 000, but can generate a 720 000 species after inhibition of a proteinase [12–14]. The conformational changes in the two proteins are complex, but the importance of three specific regions for the conformational changes is known, which are the bait region, the γ-glutamyl-β-cysteinyl thiol ester and the receptor recognition site [15]. The bait region is a region sensitive to proteolytic cleavage by a large number of proteinases. Cleavage of α_2M or PZP in this region leads to conformational changes by which thiol esters become susceptible to nucleophilic attacks. The γ-glutamyl residues of the thiol esters can generate covalent bonds with lysine residues of the proteinase and the sulfhydryl groups are liberated. The conformational changes due to cleavage of the bait region(s) and thiol ester(s) lead to "trapping" of proteinases by compaction of α_2M whereby the proteinases become sterically inhibited. In PZP the conformational changes also lead to steric hindrance of the proteinase by tetramerization of two PZP molecules, but no "trapping" occurs as in α_2M [13,14]. In both α_2M and PZP previously concealed receptor recognition sites are exposed by the conformational changes [16], whereby the inhibitor–proteinase complexes can be specifically removed from the circulation.

Previous studies have indicated that changes in hydrophobicity occur on the surface of α_2M, *i.e.* two conformationally different forms can be separated by high-performance hydrophobic chromatography [17]. Further Birkenmeier *et al.* [18] have documented differences in hydrophobic properties for α_2M and PZP by affinity phase partitioning. We have studied α_2M and PZP by hydrophobic affinity partitioning to obtain further information on the differences in conformation of these two unique proteinase inhibitors. This technique is especially advantageous in the study of different states of the same protein since most of the factors that can influence the partitioning, such as size, charge and polarity, are eliminated and only hydrophobic interactions are determined.

2. Experimental

2.1. Chemicals and enzymes

α-Chymotrypsin (EC 3.4.21.1), phenylmethylsulphonyl fluoride, sodium thiocyanate, methyl methanethiosulphonate and methylamine were purchased from Sigma (MO, USA). Poly(ethylene glycol) (PEG) 8000 was from Union Carbide (NY, USA, and Dextran T70 was from Pharmacia (Uppsala, Sweden). PEG-palmitate was synthesized as described [19] and had a degree of substitution of 0.82 mol of palmitate per mol PEG. All other chemicals were of analytical-reagent grade.

2.2. Proteins

α_2M was purified from fresh human plasma as described by Imber and Pizzo [20], and PZP was purified as described by Sand *et al.* [12]. The proteins were iodinated by the use of Iodobeads (Pierce, IL, USA) with $Na^{125}I$ from Amersham, UK. The specific activity (300–600 cpm/ng) was determined in a Unigamma γ-counter (LKB, Stockholm, Sweden). All derivatives of α_2M and PZP treated with methylamine and chymotrypsin were prepared according to Jensen and Stigbrand [14]. Modification of thiol groups was performed by incubation of α_2M with methylamine at a concentration of 0.4 *M* in the presence of methyl methanethiosulphonate at a concentration of 100 μM for 1 h at room temperature. Dimeric α_2M was prepared by incubation of α_2M with 1.2 *M* NaSCN in 0.1 *M* sodium phosphate, pH 8.0 for 4 h at room temperature. Excesses of reagents were removed by gel filtration on a NAP-5 column (Pharmacia) equilibrated with 0.1 *M* sodium phosphate buffer, pH 8.0, before analysis.

2.3. Hydrophobic affinity partitioning

Aqueous two-phase systems contained 7% Dextran T70, 4.5% PEG 8000, including PEG-palmitate, 20 m*M* potassium phosphate and 75 m*M* sodium chloride, pH 7.4. The systems were quickly mixed with protein (1–2.5 μg) at room temperature by approx. 60 inversions and phase separation was speeded up by centrifugation at 2000 *g* for 5 min. The concentration of PEG-palmitate expressed as percent of total PEG in the system was varied from 0.02 to 0.72%. K_0 and K_{max} are partition coefficients of the protein in the absence and presence of 0.7% PEG-palmitate, respectively. $\Delta\log K$ is defined as $\log K_{aff} - \log K_0$, where K_{aff} is the partition coefficients of the protein in the presence of PEG-palmitate in the system [2]. The values are averages from two experiments.

3. Results and discussion

Since human α_2M is a tetrameric protein consisting of two non-covalently associated dimeric molecules and PZP is dimeric in the native state, it is of interest to study the conformational changes occurring in these two homologous proteins in connection with inhibition of proteinases, since both can generate covalent tetrameric complexes with proteinases. The study of dimeric α_2M is included for comparison of differences in oligomerization.

The K_0 values for the native molecules as well as for the derivatives of α_2M and PZP are low. This reflects low affinity of these proteins and their derivatives for the upper PEG phase. However, the values demonstrate that there are differences in the overall conformation of PZP, tetrameric and dimeric α_2M, but the differences are too small to justify any specific conclusions.

The curves of $\Delta\log K$ values in Fig. 1 demonstrate that these proteins have high affinity for PEG-palmitate. The maximum affinity, $\Delta\log K_{max}$ of dimeric α_2M is more than twice that of native α_2M. This may indicate that the stabilization of the tetrameric form of native α_2M involves hydrophobic interactions and/or that the

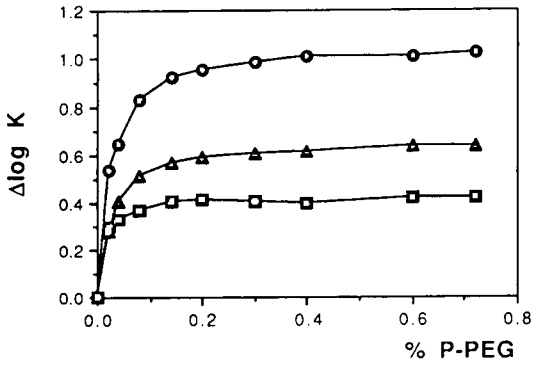

Fig. 1. $\Delta\log K$ plotted as a function of PEG-palmitate (P-PEG) for (▲) native PZP, (□) native α_2M and (○) dimeric α_2M. The partitioning coefficient, *K*, defined as the ratio of concentrations in the upper and the lower phases was taken as the ratio of radioactivities in equal aliquots of the upper and lower phases of the system. $\Delta\log K$ is defined in the Experimental section.

dimeric α_2M has changed conformation during the dissociation. Studies by use of dodecyl sulphate, urea or low pH to dissociate α_2M into dimeric forms have demonstrated drastic changes in conformation of the protein [21–23]. It has been proposed that hydrophobicity is involved in the non-covalent interactions between the dimers in α_2M [24]. The native dimeric PZP has a higher $\Delta\log K_{max}$ value than that of tetrameric α_2M, which may suggest that hydrophobic forces holding α_2M in a tetrameric form are at least partly exposed in the dimeric PZP, but if present, they may not be strong enough to retain PZP in a tetrameric form.

Treatment with methylamine cleaves the thiol esters by amidation of the γ-glutamyl residues leaving the bait regions intact.

By treatment of tetrameric α_2M with methylamine the $\Delta\log K_{max}$ value is drastically increased as compared to that of native tetrameric α_2M (Table 1). The increase suggests major conformational changes. These results agree with previous conclusions that methylamine treatment of α_2M generates large conformational changes [25]. In the case of dimeric α_2M and PZP, no significant changes occur upon cleavage of the thiol esters by methylamine, indicating that no major conformational changes occur when the thiol esters alone are cleaved in the dimeric

Table 1
K_0, K_{max} and $\Delta\log K_{max}$ values for α_2M, dimeric α_2M and PZP (a); after treatment with methylamine (b); α_2M simultaneously treated with methylamine and methyl methanethiosulphonate (c)

	Protein	K_0	K_{max}	$\Delta\log K_{max}$
a	Tetrameric α_2M	0.14	0.36	0.41[a]
	Dimeric α_2M	0.23	2.35	1.01
	PZP	0.20	0.87	0.64[a]
b	Tetrameric α_2M	0.18	2.99	1.22[a]
	Dimeric α_2M	0.29	2.90	1.00
	PZP	0.20	0.94	0.67[a]
c	Tetrameric α_2M	0.08	0.21	0.41

[a] Results obtain from Jensen *et al.* [29].

forms as has been previously suggested for PZP [13,14].

Simultaneous treatment with methylamine and the thiol modifying reagent methyl methanethiosulphonate (MMTS), which binds to the liberated thiol groups of the thiol esters, generates a derivative of α_2M with similar conformation as native α_2M, *i.e.* with an open "trap" and a slow electrophoretic form (data not shown). This derivative of α_2M gives a $\Delta\log K_{max}$ value similar to that of native α_2M in support of the similarity with native α_2M (Table 1). A derivative generated by treatment with methylamine and dinitrophenyl thiocyanate, which has been shown to be similar in conformation to native α_2M [14,26–28] also had a similar $\Delta\log K_{max}$ [29].

Chymotrypsin treatment of the α_2M derivative modified by methylamine and methyl methanethiosulphonate restores the surface hydrophobicity close to that of methylamine-treated tetrameric α_2M (Table 2). This result suggests that the cleavage of the bait regions in the derivative generates a conformational state of the derivative, which is close to that of the methylamine-treated state. PAGE has demonstrated this form to be the electrophoretic "fast" form similar to the methylamine as well as the proteinase-treated forms of tetrameric α_2M (data not shown).

Table 2
K_0, K_{max} and $\Delta\log K_{max}$ values of dimeric α_2M and PZP after treatment with methylamine and then chymotrypsin, and tetrameric α_2M treated with methylamine and methyl methanethiosulphonate before treatment with chymotrypsin

Protein	K_0	K_{max}	$\Delta\log K_{max}$
Tetrameric α_2M	0.18	2.32	1.11
Dimeric α_2M	0.35	2.37	0.83
PZP	0.52	1.31	0.40

The derivatives were generated as described in Experimental.

As seen in Table 2 both PZP and the dimeric α_2M treated with methylamine and then with chymotrypsin generate changes in $\Delta\log K_{max}$ values as compared to those treated with methylamine alone. For the PZP derivative the $\Delta\log K_{max}$ is the same as that of proteinase-treated PZP (Table 3). PAGE of the derivatives has demonstrated that the bait regions become cleaved in methylamine-treated dimeric α_2M even though this does not occur in methylamine-treated tetrameric α_2M (not shown), which supports the interpretation of the surface hydrophobicity changes by methylamine. The change in exposed hydrophobicity only occurs when the bait region is cleaved in PZP and cleavage of the thiol ester has no effect in accordance with ref. 14 as studied by use of monoclonal antibodies, PAGE and *in vivo* clearance studies.

The $\Delta\log K_{max}$ values for the derivatives treated with chymotrypsin are different (Table 3). For the tetrameric α_2M the value is approxi-

Table 3
K_0, K_{max} and $\Delta\log K_{max}$ values of PZP and dimeric and tetrameric α_2M after treatment with chymotrypsin at different molar ratios

Protein	K_0	K_{max}	$\Delta\log K_{max}$
Tetrameric α_2M (1:1)	0.23	1.32	0.76[a]
Tetrameric α_2M (1:4)	0.29	2.20	0.88[a]
Dimeric α_2M (1:1)	0.29	2.36	0.91
Dimeric α_2M (1:2)	0.34	2.15	0.80
PZP (1:1)	0.36	1.04	0.46[a]
PZP (1:2)	0.47	1.18	0.40[a]

The derivatives were generated as described in Experimental.
[a] Results obtained from Jensen *et al.* [29].

mately twice that for the value of the native molecule, which demonstrates large changes in the hydrophobic surface of α_2M. This can be correlated with the major conformational changes occurring in α_2M after bait region cleavage and inhibition of the proteinase, which have been documented using several methods [25]. The conformational state is similar to that of α_2M treated with methylamine as judged by various methods [8,9,30,31]. The surface hydrophobicity increases with an increase in molar ratio of proteinase to α_2M that is when more bait regions are cleaved. These results suggest that the extent of "trapping" in α_2M is correlated with the value of $\Delta\log K_{max}$. The $\Delta\log K_{max}$ values of the proteinase-treated dimeric form of α_2M indicate differences between the dimeric and tetrameric forms of α_2M. The value for the dimeric α_2M decrease at a molar ratio of 1:1 proteinase to dimeric α_2M and decrease further at a molar ratio of 2:1. For PZP, which, in contrast to dimeric α_2M, can tetramerize on proteinase binding, but also exists as a proteinase-complexed dimeric form, the $\Delta\log K_{max}$ values also decrease at a molar ratio of 1:1 proteinase to PZP and decrease further at a molar ratio of 2:1. It is of interest that the hydrophobic affinity of the dimeric α_2M decreases as it does for PZP.

In native α_2M the changes in surface hydrophobicity are sensitive to bait region cleavage as well as thiol ester modification, while the dimeric forms of PZP and α_2M seem only to be sensitive to changes upon proteinase treatment. The generation of dimeric α_2M might introduce a high degree of disorganisation, and cause the large differences in surface hydrophobicity observed between native α_2M and dimeric α_2M. This is supported by the fact that dissociation to dimeric α_2M caused by various agents (dodecyl sulphate, urea, thiocyanate, low pH) is irreversible [21–23].

For lucidity, we introduce a new term $\Delta\log K_{acc}$ to define the difference in $\Delta\log K_{max}$ between the modified and the unmodified forms of the same protein. This means that $\Delta\log K_{acc}$ can be written as:

$$\Delta\log K_{acc} = \Delta\log K_{max\ (modified)} - \Delta\log K_{max\ (unmodified)}$$

The index "acc" is the abbreviation of "apparent conformational change". Thus, $\Delta\log K_{acc}$ is correlated with conformational changes which result in changes in surface hydrophobicity. The values of this parameter are recorded in Table 4.

This table clearly demonstrates the difference between the tetrameric and dimeric forms, *i.e.* the dimeric forms present negative values (decreased surface hydrophobicity) while the tetrameric α_2M present positive values (increased surface hydrophobicity). The table further reveals the similarity in changes between dimeric α_2M and PZP in contrast to the changes in tetrameric α_2M, which may suggest that the differences in oligomerization between α_2M and PZP may to a high degree influence the differences observed in conformational states.

Table 4
$\Delta\log K_{acc}$ values of the apparent conformational changes in PZP, α_2M and dimeric α_2M

Δ log K_{acc}	α_2M	Dimeric α_2M	PZP
Methylamine	0.81	−0.02	0.03
Chymotrypsin (1:1)	0.35	−0.11	−0.18
Chymotrypsin (1:2)		−0.22	−0.24
Chymotrypsin (1:4)	0.47		
Methylamine, chymotrypsin (1:1)		−0.18	−0.24
Methylamine, MMTS	0.00		
Methylamine, MMTS, chymotrypsin (1:1)	0.70		

The numbers following chymotrypsin denotes the molar ratio of derivative to proteinase.

4. Conclusions

This study demonstrates that hydrophobic partitioning with PEG-bound palmitate is a sensitive method for monitoring changes in surface hydrophobicity of α-macroglobulins. All results obtained on tetrameric α_2M and PZP by the affinity partitioning can be correlated to conformational changes, since they are in line with results of conformational studies by several other methods. The method in addition reveals differences in the changes of structures, which have not been detected by other methods.

5. Acknowledgements

Mrs. Eva-Maj Hägglöf is thanked for skillful technical assistance and Luis F. Arbelaez for kindly providing PZP. This investigation was supported by grants from the Swedish Medical Research (MFR) and the Swedish Natural Sciences Research Council (NFR).

6. References

[1] J. Kyte and R.F. Doolittle, *J. Mol. Biol.*, 157 (1982) 105.
[2] V.P. Shanbhag, *Methods Enzymol.*, 228 (1993) in press.
[3] V.P. Shanbhag and L. Backman, in D. Fisher and I.A. Sutherland (Editors), *Separations using Aqueous Phase Systems*, Plenum Press, New York, London, 1989, Ch. 1, p. 25.
[4] Å. Berglund, V.P. Shanbhag and L. Backman, *Biochem. (Life Sci. Adv.)*, 7 (1988) 309.
[5] V.P. Shanbhag, G. Johansson and A. Ortin, *Biochem. Int.*, 24 (1991) 439.
[6] K. Devriendt, H. Van den Berghe, J.-J. Cassiman and P. Marynen, *Biochim. Biophys. Acta*, 1088 (1991) 95.
[7] A.J. Barrett, M.A. Brown and C.A. Sayers, *Biochem. J.*, 181 (1979) 401.
[8] F. Van Leuven, J.-J. Cassiman and H. Van Den Berghe, *J. Biol. Chem.*, 256 (1981) 9016.
[9] I. Björk and W.W. Fish, *Biochem. J.*, 207 (1982) 347.
[10] E. Delain, F. Pochon, M. Barray and F. Van Leuven, *Electron Microsc. Rev.*, 5 (1992) 231.
[11] U. Christensen and L. Sottrup-Jensen, *Biochemistry*, 23 (1984) 6619.
[12] O. Sand, J. Folkersen, J.G. Westergaard and L. Sottrup-Jensen, *J. Biol. Chem.*, 260 (1985) 15 723.
[13] U. Christensen, M. Simonsen, N. Harrit and L. Sottrup-Jensen, *Biochemistry*, 28 (1989) 9324.
[14] P.E.H. Jensen and T. Stigbrand, *Eur. J. Biochem.*, 210 (1992) 1071.
[15] L. Sottrup-Jensen, *J. Biol. Chem.*, 264 (1989) 11539.
[16] F. Van Leuven, J.-J. Cassiman and H. Van den Berghe, *J. Biol. Chem.*, 261 (1986) 16622.
[17] F. Van Leuven, J.-J. Cassiman and H. Van den Berghe, *Sci. Tools*, 32 (1985) 41.
[18] G. Birkenmeier, L. Carlsson-Bostedt, V. Shanbhag, T. Kriegel, G. Kopperschläger, L. Sottrup-Jensen and T. Stigbrand, *Eur. J. Biochem.*, 183 (1989) 239.
[19] V.P. Shanbhag and G. Johansson, *Biochem. Biophys. Res. Commun.*, 61 (1974) 1141.
[20] M.J. Imber and S.V. Pizzo, *J. Biol. Chem.*, 256 (1981) 8134.
[21] B. Sjöberg, S. Pap and J. Kjems, *Eur. J. Biochem.*, 162 (1987) 259.
[22] B. Sjöberg, S. Pap, S.-E. Järnberg and K. Mortensen, *Biochem. J.*, 278 (1991) 325.
[23] S. Pap, B. Sjöberg and K. Mortensen, *Eur. J. Biochem.*, 191 (1990) 41.
[24] B. Sjöberg, S. Pap and K. Mortensen, *J. Mol. Biol.*, 225 (1992) 551.
[25] L. Sottrup-Jensen, in F.W. Putnam (Editor), *The Plasma Proteins*, Academic Press, Orlando, FL, 2nd ed., 1987, Vol. 5, p. 191.
[26] F. Van Leuven, P. Marynen, J.-J. Cassiman and H. Van den Berghe, *Biochem. J.*, 203 (1982) 405.
[27] I. Björk, *Biochem. J.*, 231 (1985) 451.
[28] L.W. Cunningham, B.C. Crews and P. Gettins, *Biochemistry*, 29 (1990) 1638.
[29] P.E.H. Jensen, E.-M. Hägglöf, L.F. Arbelaez, T. Stigbrand and V.P. Shanbhag, *Biochim. Biophys. Acta*, 1164 (1993) 152.
[30] C.S. Dott, A. Howard and B.M. Ansell, *Clin. Chim. Acta*, 146 (1985) 157.
[31] H.S. Cummings, S.V. Pizzo, D.K. Strickland and F.J. Castellino, *Biophys. J.*, 45 (1984) 721.

ELSEVIER

Journal of Chromatography A, 668 (1994) 107–116

JOURNAL OF CHROMATOGRAPHY A

Partitioning of chemically modified low-density lipoprotein in aqueous polymer two-phase systems

D. Wiegel*, O. Richter, K. Arnold

University of Leipzig, School of Medicine, Institute of Medical Physics and Biophysics, Liebigstrasse 27, 04103 Leipzig, Germany

Abstract

Aqueous polyethylene glycol (PEG)–dextran two-phase systems containing 10 m*M* Tris · HCl (pH 7.4) were used for the partitioning of chemically modified low-density lipoprotein (LDL). Anionic modification connected with an increase in the negative surface charge of lipoproteins favours the accumulation of modified LDL in the top phase. The partition coefficient increases depending on the extent of modification. Cationic modification yields lower values for the partition coefficient. Positively charged LDL favours a bottom-phase accumulation. With weakly charged and nearly neutral particles, the Van der Waals interaction between polymer and particle preponderates over electrostatic interactions, leading to a favoured accumulation of LDL in the PEG-rich top phase. Results of measurements of the relative electrophoretic mobility and the determination of free amino groups are in agreement with the calculated values of the partition coefficient. Because the partitioning of LDL is accompanied by aggregation at the interface, experimental techniques have to be carefully standardized. Subtle differences in the surface properties of modified LDL can be detected.

1. Introduction

Lipoproteins perform the transport function for lipids and cholesterol in the blood. A core of hydrophobic molecules (triglycerides, cholesteryl esters) is surrounded by an amphiphilic envelope of phospholipids and a mixture of specific apoproteins. All components are organized by the action of non-covalent forces to form particles of qualitatively and quantitatively different composition. The dispersive potential of such complex structures is very high [1].

In addition to the heterogeneity at the site of synthesis, lipoproteins undergo a considerable degree of metabolic alteration, including size and structure in the blood and liver and in the extrahepatic vascular system. Despite the normal heterogeneous native lipoprotein classes *in vivo*, modified particles are discussed as the main source for pathological processes in cells and tissues.

Native lipoproteins are negatively charged particles. Lipoprotein LP(X) migrating towards the cathode in an electric field has been found as an abnormal plasma constituent of patients with obstructive jaundice [2].

Chemical modification of low-density lipoprotein (LDL) connected with a strong increase in the negative surface charge of LDL has been proposed as the reason for the induction of foam cell formation [3]. Peroxidation processes [4,5], malondialdehyde reactions [6], glycosylation [7] and oxidation by endothelial cells, smooth muscle cells [8–11] and macrophages [12] have been

* Corresponding author.

0021-9673/94/$07.00
SSDI 0021-9673(93)E1191-2

suggested as sources of pathologically altered LDL *in vivo*. Reactions catalysed by myeloperoxidase probably result in the formation of hypochlorite-modified LDL [13,14]. Acetylated LDL is often used in experiments to study the receptor–lipoprotein interaction [15,16]. Modification via acetylation, malonylation and oxidation is connected with changes in the apoprotein structure and surface charge of LDL, rendering the lipoprotein highly anionic [17].

In contrast to native LDL, this modified anionic LDL cannot interact with the classical LDL receptor of tissues. Modified anionic LDL is recognized only by the scavenger receptor of macrophages [18]. The unregulated lipoprotein uptake via scavenger cell receptor-mediated endocytosis leads to lipid loading of cells and generation of atheriosclerotic plaques.

Chemically cationized LDL enters the cell membrane without receptor-mediated endocytosis. Similarly to native LDL, this modified lipoprotein effectively regulates the cholesterol metabolism in cells [19]. Chemical modification of LDL involves changes in surface charge [20] and/or conformation [21] of the particles.

On the other hand, a certain spatial organization of negative charges in modified lipoproteins or charged macromolecules is suspected to be important for the receptor–particle interaction [15]. The involvement of more than one receptor for the recognition of modified LDL species has been discussed [22–24].

Physico-chemical and physiological properties of modified HDL were studied by Salmon *et al.* [25].

A suitable method for identifying modifications on the lipoprotein surface would be a useful tool for investigating such processes *in vitro* and *in vivo*.

In previous papers, the application of two-phase systems for the characterization of the surface properties of lipoproteins was demonstrated [26,27]. The partitioning of particles and molecules in aqueous polymer two-phase systems depends mainly on the size, charge and hydrophobicity of the particle surface [28], *i.e.*, the partitioning of particles is a surface-dependent phenomenon. Because the interaction between lipoproteins and cells strongly depends on exposed groups on the surfaces, two-phase systems could be expected to provide a method for detecting surface changes of lipoproteins relevant to the lipoprotein–receptor interaction.

In this work, the partitioning of chemically modified LDL was studied. Both anionic and cationic modified LDL were studied as a function of the degree of modification, using the fluorescamine method to detect the number of functional groups, electrophoretic measurements to describe the relative changes in surface charges and two-phase partitioning to obtain the partition coefficient and mass distribution between the two bulk phases and the interface.

2. Experimental

2.1. Materials

LDL preparation

LDL was obtained from freshly taken plasma from healthy volunteers by sequential ultracentrifugation according to Havel *et al.* [29]. After separation of VLDL the remaining plasma was adjusted with NaBr to a density of 1.072 kg/l, covered with a density solution of 1.064 kg/l and centrifuged for 24 h at 40 000 rpm (UP 65 M centrifuge, 8 × 11 rotor). LDL was recentrifuged and dialysed twice at 4°C for 25 h against 10 mmol/l phosphate buffer (pH 7.4) containing 0.137 mol/l NaCl, 0.005 mol/l KCl and $1 \cdot 10^{-4}$ mol/l Na_2EDTA. The protein concentration of LDL was determined using the Lowry procedure [30]. All samples were checked for purity by horizontal agarose gel electrophoresis or non-denaturing polyacrylamide gel electrophoresis (PAGE), placing the gels on a cooling plate (16°C) according to the instructions given in the users' information for the Multiphor II Electrophoresis System from Pharmacia–LKB, Biotechnology.

For the electrophoretic control of purity, gels of size 125 × 260 mm and thickness 2 mm were used. Up to sixteen samples can be applied simultaneously and checked under equal running

conditions. Samples were applied in 0.5-mm deep gel slots of size 7×1 mm. Gels with gel concentrations of 3.5% and 5.0% in PAGE and 1.2% in agarose gel electrophoresis were prepared on the hydrophilic side of a gel support by using suitable moulds. Substances for PAGE were obtained from Bio-Rad Labs. and agarose was purchased from Serva.

Lipoproteins were revealed by staining with Coomassie Brilliant Blue (Fluka) for the recognition of the apo-proteins and Sudan Black (Chemapol, Prague, Czech Republic) or Fat Red 7B (Serva) for the determination of the lipid components.

LDL diluted to 1, 2, and 4 mg/ml protein with dialysis buffer was stored at 4°C and used within 2 days after dialysis.

LDL modification

All LDL samples were thoroughly dialysed against isotonic phosphate-buffered saline (PBS) buffer solution (pH 7.4).

Acetylation

Acetylation was performed in a modified procedure according to the method of Fraenkel-Conrat [31] by mixing the LDL samples with a saturated solution of sodium acetate (1:2, v/v) at 0 and 22°C. Acetic anhydride was added slowly in small portions during continuous stirring of the mixture in the range $0–100 \cdot 10^{-3}$ mmol acetic anhydride/mg LDL.

After an incubation period of 30 min, each sample was dialysed for 24 h at 4°C against isotonic PBS buffer solution (pH 7.4).

Hypochlorite modification

Sample volumes of 1 ml containing 2 mg of lipoprotein were incubated at 22°C with 20 m*M* NaOCl solution. The amount of NaOCl in the samples was varied in the range $0–100 \cdot 10^{-5}$ mmol NaOCl/mg LDL [27]. After an incubation time of 5 min the non-dialysed samples were used for partitioning and determination of unreacted groups and for the measurement of the electrophoretic mobility.

Cationization of LDL

LDL was cationized at room temperature in a modified version of the original method [19,32]. Briefly, sample volumes of 20 ml with protein concentrations of 2 mg/ml were added to 20 ml of a 2 *M* solution of N,N-dimethyl-1,3-propanediamine (DMPA) (Fluka) previously adjusted to pH 6.5 with HCl. The amount of DMPA in the mixture was 10^{-3} mol/mg LDL.

Solid 1-ethyl-3(3-dimethylaminopropyl)carbodiimide · HCl (Sigma) was added to the mixture to a final concentration of 0.3 *M* with stirring.

During the reaction the pH was maintained at 6.5 by continuous addition of HCl. Depending on the rection time, samples were drawn from the reaction pool and immediately transferred into dialysis tubes. Dialysis at 4°C for 24 h against PBS buffer solution (pH 7.4) stops the reaction and removes unreacted DMPA and carbodiimide. The sample immediately drawn from the pool after all the reagents had been mixed (time point $t = 0$) serves as a reference (unmodified LDL).

All modification experiments were repeated three times. After dialysis all modified and unmodified LDL samples represented optically clear solutions. Lowry estimation of the apoprotein concentration and electrophoresis was repeated for each sample and control to exclude degradation events and to check the purity of the samples.

2.2. Methods

Two-phase partitioning

Two-phase systems were prepared by mixing stock solutions of dextran T 500 (20%, w/w; Pharmacia) and polyethylene glycol (PEG) 6000 (40%, w/w; Ferak) with 10 m*M* Tris · HCl buffer (NaCl-free) (pH 7.4) and water. We used 10-g systems containing 0.71 g of dextran, 0.5 g of polyethylene glycol, 2.50 g of buffer solution and 6.09 g of distilled water. These systems, carefully prepared by shaking the mixture in 10-ml graduated tubes at room temperature, were filled up with 0.2 g of lipoprotein solution or the same amount of lipoprotein-free buffer in the case of controls.

Lipoproteins or control samples were distributed in the polymer mixture by 40 inversions of the glass tubes. The turbid mixtures were allowed to stand overnight. It is not favourable to enforce the phase separation by centrifugation, because the particles themselves begin to settle, leading to irreproducible results. After phase separation and equilibration, the two immiscible polymer phases are characterized by a sharp interface.

The total volume V and the particular volumes $V(b)$ and $V(t)$ of the bottom and the top phase, respectively, were measured in control samples after phase separation and equilibration of the mixture.

After mixing the lipoprotein with the polymer solutions by shaking the tubes, a volume of 2 ml from the centre of the turbid mixture was removed for the determination of the total concentration by using a syringe. When the phase separation was finished, a further 2 ml were removed from the centre of each separation phase to determine the top and bottom phase concentrations.

Before drawing the sample from the bottom phase, the remainder of the top phase has to be removed completely to exclude the contamination of the bottom phase with top-phase material. Owing to the high viscosity of the polymeric phases, it is difficult to take accurate volumetric aliquots using a pipette. Therefore, we used only weighed aliquots of the top and bottom phases.

To determine the concentration of the partitioned lipoprotein between the top and bottom phases, the UV absorption of the protein component in the lipoprotein was measured. The samples were diluted 1:2 (w/w) with buffer solution before measuring the absorption at 280 nm. As the polymer solutions absorb UV radiation, blanks are always prepared of a system without lipoprotein.

Samples and controls for all modified and unmodified lipoproteins were prepared in triplicate.

The linearity between absorption and lipoprotein concentration for the top, bottom and mixed phases was checked by calibration. The slopes of the lines for all three phases were the same. Therefore, the measured values for the extinction are proportional to the phase concentrations.

The partition coefficient was calculated as the ratio of the top and bottom phase concentrations [33].

Lipoprotein aggregation leads to accumulation of aggregated LDL at the interface. This material has to be removed before bottom-phase material can be taken for concentration determination.

Electrophoresis of modified samples

We used agarose gel electrophoresis and PAGE to characterize the degree of modification. The procedure was the same as used to check native unmodified LDL for purity. The relative electrophoretic mobility (REM) was calculated as the ratio of the mobilities for modified and unmodified LDL.

Fluorescamine assay

The relative number of free amino groups in LDL samples was determined using fluorescamine (Serva) as described [34].

The non-fluorescent fluorescamine reacts with amino groups on the surface, yielding a highly fluorescent product. The unreacted fluorescamine hydrolyses into non-fluorescent compounds. For the fluorescence measurements 50 μl of the LDL suspension (protein concentration 2 mg/ml in experiments with hypochlorite; 2–4 mg/ml in the case of acetic anhydride modification) were mixed with 170 μl of 0.01 mol/l Na_2HPO_4 solution. To this solution 5 μl of a 2 mmol/l solution of fluorescamine in acetone were added. After 2 min the fluorescence was measured at 470 nm. The exitation wavelength was set at 396 nm.

2.3. Instrumentation

Measurements of the fluorescence were carried out using a Perkin-Elmer LS 50 spectrofluorimeter. Both slits were installed at 5 mm. The READ regime of the Fluorescence Data Manager Software (Perkin-Elmer) was used.

Measurements of the UV absorption at 280 nm

were performed with a U-2000 spectrophotometer (Hitachi).

All measurements were repeated four times with stirring the samples.

If not indicated otherwise, all reagents were of analytical-reagent grade from Laborchemie (Apolda, Germany).

3. Results and discussion

Cationization of LDL with the nucleophilic N,N-dimethyl-1,3-propanediamine via carbodiimide activation of the apo-protein carboxyl groups converts a negatively charged free carboxyl group of the apo-protein into a positively charged tertiary amine derivative. In other words, the modification of protein carboxyls effects a change of two unit charges per modified carboxyl group [32].

Owing to the complexity of the reaction, it is difficult to maintain identical reaction conditions for each sample in a series of different samples. Therefore, instead of the usually used variation of the pH or the reaction temperature and the concentration of the modifying agent to modify the extent of modification, we preferred to vary the reaction time as a possibility of changing the degree of modification.

Fig. 1 shows the electrophoretic mobilities of LDL samples with increasing degree of cationization. Native LDL (1) with a negative surface charge corresponding to its negative

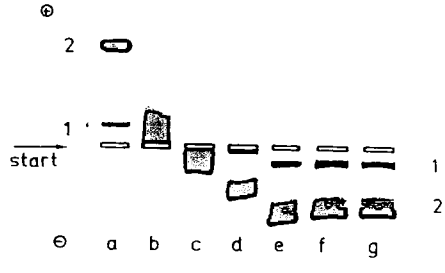

Fig. 1. Influence of reaction time on the degree of cationization (results of PAGE). 1 = LDL; 2 = albumin; reaction time: (a) 0; (b) 1; (c) 15; (d) 30; (e) 120; (f) 360 min; (g) sample after standing overnight.

mobility is changed into a form of LDL with reduced and neutral surface charge. The increase in reaction time effects an increase in positive surface charge. The LDL migrates towards the cathode in the electric field. The electrophoretic bands estimated by Coomassie Brilliant Blue staining of the polyacrylamide gel are identical with those detectable by Sudan Black staining, showing that a separation of the apo-protein from the lipoprotein does not occur during the modification process (data not shown). In contrast to LDL, the albumin shows higher negative and positive mobility.

The electrophoretically checked LDL samples with different degrees of cationization were used to study the LDL partitioning between the top and bottom phases of a PEG–dextran two-phase system. After phase separation for all the samples studied optically clear bulk phases were obtained. Only the bottom phase was slightly turbid for unmodified LDL (reaction time $t = 0$), but the phase became completely clear after dilution 1:2 with buffer solution. In all instances aggregated LDL was accumulated at the interface.

The partition coefficient K and the changes in the relative electrophoretic mobility (REM) as a function of the degree of modification are shown in Table 1. The greatest changes in electrophoretic mobility take place in the first few minutes after the reaction has started. In the course of a very short time the REM decreases from the value -1 to zero (neutral state of LDL) but only after several hours is the value $+1$ reached (cationized form of LDL).

Two-phase systems for controls and samples were prepared in triplicate. The calculated partition coefficients in Table 1 are mean values representing the ratio of LDL concentrations in the top and bottom phases.

The initial phase of LDL cationization seems to be connected with drastic changes in the surface properties of lipoprotein particles. The partition coefficient increases from $K = 0.202$ to a maximum of $K = 1.205$ with decreasing negative surface charge of the LDL particles. The results obtained show that subtle differences in the surface properties of modified LDL can be

Table 1
Partition coefficient (K) and relative electrophoretic mobility (REM) of LDL with increasing degree of cationization

Reaction time (min)	REM	K	Remarks
		0.22 ± 0.05 ($n = 9$)	Native LDL
0	−1.00	0.202	Unmodified LDL
1	−0.05	1.205	Electrically neutral LDL
15	+0.16	0.917	LDL with increasing degree of cationization
30	+0.15	0.306	
120	+0.66	0.268	
360	+0.89	0.277	

Experiments carried out in triplicate. The mean error is of the order of 20%.

detected by phase partitioning with high sensitivity.

With weakly charged and nearly neutral particles the Van der Waals interaction between polymer and particle preponderates over electrostatic interactions. LDL in its neutral state accumulates in the more PEG-rich top phase, leading to high values of K.

Increasing surface charge as the result of a greater degree of modification increases the hydrophilic character of the lipoprotein. Both the increase in the positive surface charge and the higher hydrophilicity of the cationized LDL now favour accumulation in the dextran-rich hydrophilic bottom phase. The calculated values for the partition coefficient decrease as the degree of cationic modification increases. According to our earlier findings [27] using the same composition of the two-phase system as described above, the results obtained with cationized LDL are in agreement with the existence of an electrically positive potential difference between the top and bottom phases.

Anionic modification of LDL connected with an increase in the negative surface potential of the modified particles is based on the reaction of the ε-amino groups in lysine and the sulphydryl groups of the apo-B protein with the modifying agent. The derivatization of an amino group causes the transformation of a positively charged group into a neutral group. In contrast to cationization, the anionic modification results in a change of only one unit charge per modified group.

We used the acetylation and hypochlorite modification as reactions to increase the anionic character of LDL. The former leads to acetyl derivatives and the latter to chloramines. In both instances the degree of modification was varied by the ratio of the amount of modifying agent per mg of LDL.

The modified LDL samples checked for purity by agarose gel electrophoresis and PAGE were characterized by single bands.

Fig. 2 shows the relative electrophoretic mobility of modified anionic LDL as a function of the concentration of added modifying reagent.

In Fig. 2a, results of acetylation carried out at 0 and 22°C are shown. As expected, the mild reaction conditions at 0°C effect only a slow increase in the relative electrophoretic mobility, in contrast to the high slope of the corresponding curves observed for samples prepared under conditions of a strong interaction between the reagent and lipoprotein.

Fig. 2b shows the corresponding changes observed with hypochlorite modification of LDL. The curves represent results obtained from two independent LDL preparations. In both instances the modification was carried out under identical conditions. Both curves are in qualitative agreement. The difference in the slopes reflects a different sensitivity of the two LDL preparations to hypochlorite and appears to be connected with donor specificity.

In Fig. 3 the content of functional groups is shown as a function of the concentration of added modifying reagent. In agreement with the

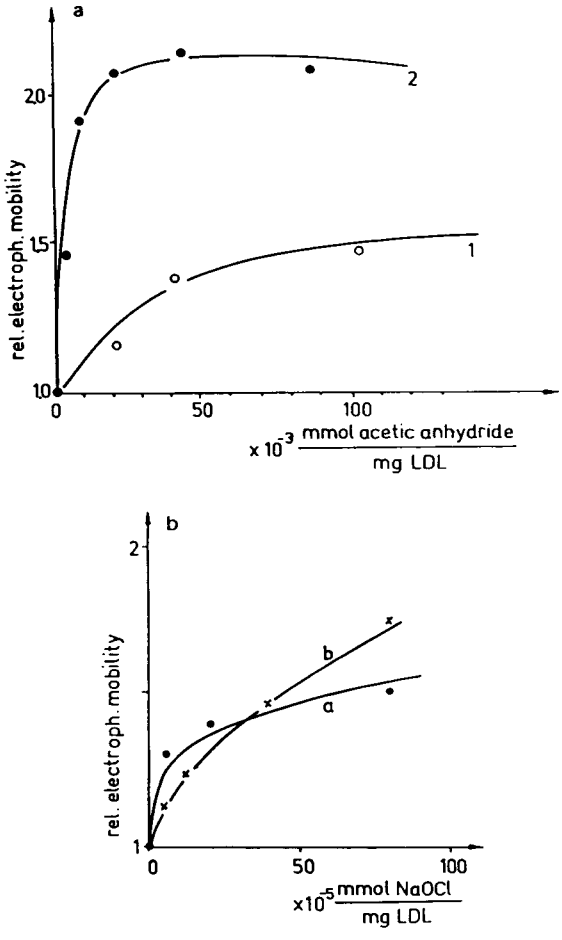

Fig. 2. Relative electrophoretic mobility for modified anionic LDL (results of agarose electrophoresis) (a) Acetylated LDL. Acetylation carried out at (1) 0 and (2) 22°C. (b) Results for NaOCl-modified LDL. Modification carried out under identical conditions for two separate LDL preparations (curves a and b).

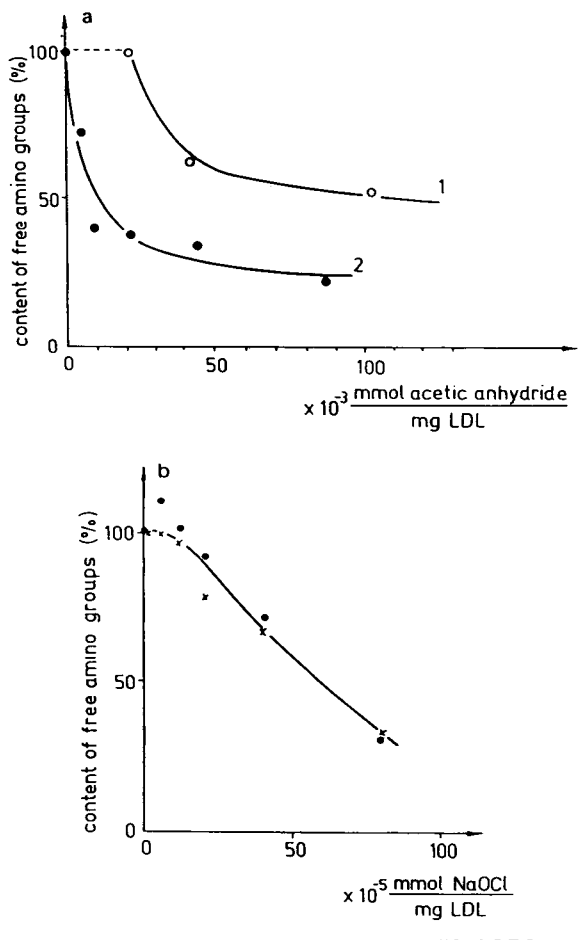

Fig. 3. Content of functional groups in modified LDL as a function of the concentration of added modifying reagent. (a) Acetylation carried out at (1) 0 and (2) 22°C. (b) NaOCl modification of two separate LDL preparations.

results given by measurements of the electrophoretic mobility (Fig. 2a), it can be seen that the level of unreacted groups remains higher with mild modification of LDL than with stronger modification (Fig. 3a). Only for ratios higher than $20 \cdot 10^{-3}$ mmol of acetic anhydride per mg of LDL could a decrease in the content of functional groups be detected, if the modification took place at 0°C.

Chloramine derivatives of the NH_2 groups produced by hypochlorite modification cause a nearly linear decrease in the content of free groups (Fig. 3b).

In Fig. 4 the calculated partition coefficient is shown as a function of the degree of modification.

The degree of modification was obtained from measurements of the amount of free functional amino groups using the fluram method. The absolute number of free groups determines the reactivity of the LDL particle. This number for the unmodified state is always set at 100% (degree of modification = 0). We assume that this number and the attainable maximum degree of

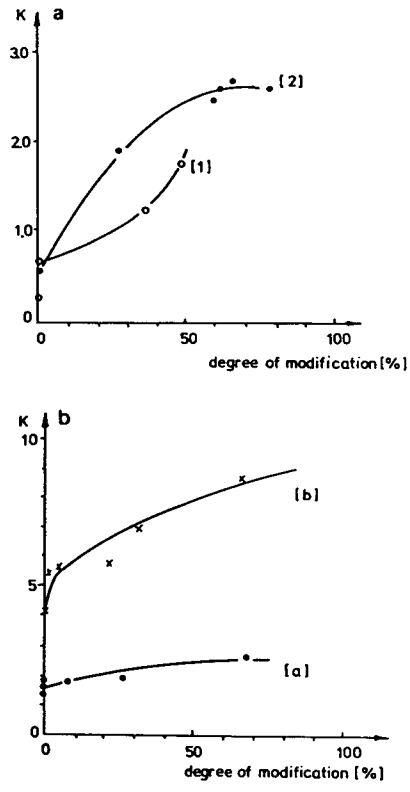

Fig. 4. Partition coefficient as a function of the degree of modification for modified anionic LDL. The degree of modification was determined from the data in Fig. 3a and b. Composition of the two-phase system: 7.1% dextran T 500–5% PEG 6000–10 m*M* Tris·HCl (pH 7.4). (a) Partition coefficient of acetylated LDL with acetylation carried out at (1) 0 and (2) 22°C. (b) Partition coefficient of NaOCl-modified LDL for two separate LDL preparations (curves a and b).

modification depend on the molecular structure of the particle surface, *i.e.*, on its steric conformation. It represents a specific property of the particle. Therefore, a special degree of modification may have different quantitative effects on the electrophoretic mobility and the partitioning of LDL particles.

The curves are characterized by a strong increase in K at low degrees of modification. The K values for acetylated LDL at 22°C are considerably higher than the values calculated for material modified at 0°C (Fig. 4a). For hypochlorite-modified LDL, differences between the LDL samples of two different donors are detectable (Fig. 4b).

Changes in partitioning and electrophoretic mobility of hypochlorite-modified LDL are clearly visible at low NaOCl concentrations, where the relative number of amino groups remains nearly constant. In this range surface properties of LDL other than those based on direct interaction between hypochlorite and amino groups could contribute to changes in surface charge [26]. The possibility of lipid oxidation by hypochlorite has to be taken into account, but experimental results given by different workers are conflicting [35,36]. An influence of OCl^- ions on the electric potential of the top phase similar to that of Cl^- ions can be excluded, because the lifetime of the OCl^- ion is very short [37]. Within a few seconds the HOCl–OCl^- system reacts completely under conditions of an excess of target groups.

A general result in the experiments dealing with anionic modification of LDL is the increased top-phase accumulation of LDL with increasing negative surface charge of the particles. These results are in agreement with the observed decrease in partitioning for cationic-modified LDL with increasing degree of modification.

Especially small changes in surface charge representing low degrees of modification are detectable with high sensitivity. Small changes in surface charge effect a strong increase in the K value.

As expected, samples with a high negative electrophoretic mobility are characterized by high values of the partition coefficient.

In all experiments, measurements on controls and samples were performed in triplicate. The partition coefficient is always given as a mean value. The error connected with the calculation of the partition coefficient or with the determination of the relative mass distribution between the two bulk phases and the interface is a maximum of 20% using the experimental techniques described above.

When LDL was modified in a special manner, the same LDL preparation was used to obtain spectrofluorimetric, electrophoretic and spectro-

photometric data. The results in Figs. 2–4 are representative examples.

To be certain that all experiments were performed with LDL in its native state, for the acetylation at 4 and 22°C and for the NaOCl modification freshly prepared LDL from different donors was always used. A statistical study of the physiological variation of measured values was not the aim of this investigation.

The obtained changes in electrophoretic mobility and the content of free functional groups for modified LDL as a function of the degree of modification are in agreement with the calculated values of the partition coefficient.

4. Conclusions

The two-phase method is a suitable technique for detecting alterations in the surface properties of lipoproteins. Nevertheless, the partitioning of particles is always accompanied by an accumulation of aggregated particles at the interface [38]. This property of particles often leads to errors connected with the application of this method. Moreover, after a well defined macroscopic interface has formed, clearing of the top phase can be observed [39].

One can retain the native state of LDL samples for only a limited time. An increased storage time of the LDL samples leads to a strong accumulation of aggregated LDL in the interface during phase partitioning. The larger the particle size as a result of aggregation and denaturation, the stronger is the interphase accumulation.

When using this method to characterize lipoproteins, it is necessary carefully to standardize the experimental techniques.

5. References

[1] G.L. Mills, P.A. Lane and P.K. Weech, *Laboratory Techniques in Biochemistry and Molecular Biology—a Guidebook to Lipoprotein Technique*, Elsevier, Amsterdam, 1989.

[2] D. Seidel, P. Alaupovic and R.H. Furman, *J. Clin. Invest.*, 48 (1969) 1211.

[3] H.C. McGill, *Lab. Invest.*, 18 (1968) 560.

[4] H. Esterbauer, G. Jürgens, O. Quehenberger and E. Koller, *J. Lipid Res.*, 8 (1987) 495.

[5] J.W. Heinecka, *Free Rad. Biol. Med.*, 3 (1987) 65.

[6] M.E. Haberland, A.M. Fogelman, P.A. Edwards, *Proc. Natl. Acad. Sci. U.S.A.*, 79 (1982) 1712.

[7] J. Turk, *Period. Biol.*, 89 (1987) 155.

[8] U.P. Steinbrecher, S. Parthasarathy, D.S. Leake, J.L. Witztum and D. Steinberg, *Arteriosklerosis*, 4 (1984) 357.

[9] J.W. Heinecke, H. Rosen and A. Chait, *J. Clin. Invest.*, 74 (1984) 1890.

[10] J.F. Nagelkerke, L. Havekes, V.W.M. van Hinsbergh and T.J.C. van Berbel, *Arteriosklerosis*, 4 (1984) 256.

[11] U.P. Steinbrecher. *Biochim. Biophys. Acta*, 959 (1988) 20.

[12] M.K. Cathcart, D.W. Morel and G.M. Chisolm, *J. Leukotr. Biol.*, 38 (1985) 341.

[13] J.M. Albrich, C.A. McCarthy and J.K. Hurst, *Proc. Natl. Acad. Sci. U.S.A.*, 78 (1981) 210.

[14] L.R. de Chatelet, L.D. Long, P.S. Shirley, D.A. Bass, M.J. Thomasa, F.W. Henderson and M.S. Cohen, *J. Immunol.*, 129 (1982) 1589.

[15] M.S. Brown and J.L. Goldstein, *Anna. Rev. Biochem.*, 52 (1983) 223.

[16] J.M. Shaw, W.S. Futch and L.B. Schook, *Proc. Natl. Acad. Sci. U.S.A.*, 85 (1988) 6112.

[17] H.F. Hoff, J. O'Neil, G.M. Chisolm, T.B. Cole, O. Quehenberger, H. Esterbauer and G. Jürgens, *Arteriosclerosis*, 9 (1989) 538.

[18] J.L. Goldstein, Y. K. Ho, S.K. Basu and M.S. Brown, *Proc. Natl. Acad. Sci. U.S.A.*, 76 (1979) 333.

[19] S.K. Basu, J.L. Goldstein, R.G.W. Anderson and M.S. Brown, *Proc. Natl. Acad. Sci. U.S.A.*, 73 (1976) 3178.

[20] S. Salmon, C. Moziere, L. Theron, J. Bender, M. Ayrault-Jarrier, S. Goldstein and J. Polonowski, *Biochim. Biophys. Acta*, 920 (1987) 215.

[21] Y.L. Marcel, M. Hogne, P.K. Weech and R.W. Milne, *J. Biol. Chem.*, 259 (1984) 6952.

[22] S. Horiuchi, M. Murakami, K. Takata and Y. Morino, *J. Biol. Chem.*, 261 (1986) 4962.

[23] M. Murakami and S. Honriuchi, *Biochim. Biophys. Res. Commun.*, 137 (1986) 29.

[24] C.P. Sparrow, S. Parthasarathy and S. Steinberg, *J. Biol. Chem.*, 264 (1989) 2599.

[25] S. Salmon, C. Maziere, M. Auclair, L. Theron, R. Santus and J.-C. Mazierie, *Biochim. Biophys. Acta*, 1125 (1992) 230.

[26] J. Arnold, D. Wiegel, S. Hammerschmidt, K. Arnold and M. Krumbiegel, *Biomed. Biochim. Acta.*, 50 (1991) 967.

[27] D. Wiegel, O. Richter, J. Arnhold and K. Arnold, *Biomed. Biochim. Acta*, 50 (1991) 207.

[28] D. Fisher and I.A. Sutherland (Editors), *Separations Using Aqueous Phase Systems*, Plenum Press, New York, 1989.

[29] R.J. Havel, H.D. Eder and J.H. Brangton, *J. Clin. Invest.*, 34 (1955) 1345.

[30] O.H. Lowry, N.J. Rosebrough and R.J. Randall, *J. Biol. Chem.*, 193 (1951) 265.
[31] H. Fraenkel-Conrat, *Methods Enzymol.*, 4 (1957) 247.
[32] D. Danon, L. Goldstein, Y. Marikovsky and E. Skutelsky, *J. Ultrastruct. Res.*, 38 (1972) 500.
[33] P.A. Albertson, *Partition of Cell Particles and Macromolecules*, Wiley-Interscience, New York, 1971.
[34] P. Böhlau, S. Stein, W. Dairman and S. Udenfriend, *Arch. Biochem. Biophys.*, 155 (1973) 213.
[35] T. Stelmaszynska, E. Kukovetz, G. Egger and R.J. Schaur, *Int. J. Biochem.*, 24 (1992) 121.
[36] C.C. Winterbourn, J.J.M. van den Berg, E. Roitman and F.A. Kuypers, *Arch. Biochem. Biophys.*, 296 (1992) 547.
[37] J.C. Morris, *J. Phys. Chem.*, 70 (1966) 3798.
[38] H. Walter, D.E. Brooks and D. Fisher (Editors), *Partitioning in Aqueous Two-Phase Systems*, Academic Press, New York, 1985.
[39] C. Tilcock, P. Cullis, T. Dempsey, B.N. Yonnes and D. Fisher, *Biochim. Biophys. Acta*, 979 (1989) 208.

ELSEVIER

Journal of Chromatography A, 668 (1994) 117–120

JOURNAL OF CHROMATOGRAPHY A

Liquid–liquid extraction of a recombinant protein, cytochrome b_5, with aqueous two-phase systems of polyethylene glycol and potassium phosphate salts

Maria João Sarmento, Mário J. Pires, Joaquim M.S. Cabral, Maria Raquel Aires-Barros*

Laboratório de Engenharia Bioquímica, Instituto Superior Técnico, 1000 Lisbon, Portugal

Abstract

The partitioning of cytochrome b_5 in aqueous two-phase systems of polyethylene glycol (PEG) and potassium phosphate salts was investigated. Cytochrome b_5 partitioning is enhanced with decreasing polymer molecular mass and with increasing tieline length and pH. The effect of cytochrome b_5 mutation, by substitution of the glutamic acid at positions 56 and 92 of the polypeptide chain by a lysine, on protein partitioning was also studied. Partitioning of cytochrome b_5 mutants shows the same dependence on tieline length and pH, following the order cytochrome b_5 > mutant 56 > mutant 92.

1. Introduction

The downstream processing of biological materials requires separation and purification techniques leading to a high degree of purification and high recoveries and to low operating costs. One of the bioseparation processes that fulfils these criteria is liquid–liquid extraction using aqueous two-phase systems.

This technique can be used in the early steps of the purification process (*e.g.*, separating proteins from cell debris), replacing difficult solid–liquid separations, and also for further purification [1]; the scale-up is relatively simple because it utilizes equipment common in the chemical industry. Aqueous two-phase systems contain a high proportion of water in both phases, providing an excellent environment for cells, cell organelles or biologically active proteins [2].

In order to find suitable conditions for the extraction of proteins with aqueous two-phase systems, it is necessary to know the partitioning behaviour of the desired proteins. Protein partitioning depends on the physico-chemical parameters of the systems, namely the type and molecular mass of polymers, tieline length (a function of the concentration of the system components), type and concentration of component or added salts, pH, temperature and addition of biospecific affinity ligands [2].

This paper reports the partitioning of cytochrome b_5 in polyethylene glycol (PEG)–potassium phosphate salt two-phase systems. The effects of polymer molecular mass, tieline length and pH on cytochrome b_5 partitioning were investigated. The influence of cytochrome b_5 mutation, by substitution of the glutamic acid at positions 56 or 92 of the polypeptide chain by a lysine, on protein partitioning was also studied, in order to evaluate the effect of genetic manipu-

* Corresponding author.

0021-9673/94/$07.00
SSDI 0021-9673(93)E1195-6

lation techniques on the downstream processing of proteins.

2. Experimental

2.1. Chemicals

PEG 400, 1000, 3350 and 8000 were supplied by Sigma and anhydrous potassium dihydrogenphosphate (KH_2PO_4) and dipotassium hydrogenphosphate (K_2HPO_4), both of analytical-reagent grade, by Merck.

2.2. Cytochrome b_5

The cytochrome b_5 used consists of the hydrophilic domain of cytochrome b_5 from mouse [3] that was cloned in a pUC 13 vector and expressed in *Escherichia coli* (TB1) [4]. This protein has a molecular mass of 13 600 and an isoelectric point (p*I*) of 4.4 [5].

This protein was mutated by site-specific mutagenesis in the glutamic acid at positions 56 or 92 of the polypeptide chain that was substituted by a lysine [5]. The p*I* of the mutants is 4.7 [5].

Cytochromes b_5 were produced by fermentation and purified using sequential chromatographic steps [5].

2.3. Preparation of aqueous two-phase systems

Aqueous two-phase systems of total mass 6 g were prepared by weighing appropriate amounts of concentrated solutions of PEG, KH_2PO_4 and K_2HPO_4 solutions, which were added until the required pH value was obtained, and water into 10-ml graduated centrifuge tubes. The contents of the tubes was intensively mixed on a vortex agitator and then 100 μl of purified cytochrome b_5 solution (2.8 mg ml^{-1}) were added. After vortex mixing, the phases were separated by centrifugation (10 min at 128 *g*).

The concentrations of cytochrome b_5 and cytochrome b_5 mutants in each phase were determined by measuring the absorbance at 411 nm (molar absorptivity $\varepsilon = 130$ l $mmol^{-1}$ cm^{-1} [4]) using a Hitachi UV–Vis spectrophotometer.

Table 1
PEG–salt systems used in cytochrome b_5 partitioning studies

Polymer	PEG–potassium phosphates (%, w/w)		
	Tieline 1	Tieline 2	Tieline 3
PEG 400	16.7/14.8	17.7/15.7	19.7/17.7
PEG 1000	16.2/14.3	17.7/15.7	19.7/17.7
PEG 3350	14/11.8	17.7/15.7	19.7/17.7
PEG 8000	14/11.8	–	–

The pH in each phase was measured with a Metrohm pH meter.

The PEG–salt systems prepared are shown in Table 1.

3. Results and discussion

The effect of polymer molecular mass, tieline length and pH on cytochrome b_5 partitioning in PEG–potassium phosphate systems is shown in Fig. 1. The partition coefficient, K_p, was defined as the ratio between cytochrome b_5 concentration in the upper and lower phases and the yield, Y, as the ratio between cytochrome b_5 mass in the top phase and in the total system. Each K_p and Y value represents the average of at least two measurements.

Cytochrome b_5 partition coefficients and yields increase with decrease in polymer molecular mass. For aqueous two-phase systems of PEG 400 cytochrome b_5 is mainly in the PEG-rich phase under all the experimental conditions studied ($K_p > 2.7$ and $Y > 86\%$); for PEG 1000, depending on tieline length and pH, cytochrome b_5 may partition preferentially to the salt-rich phase or to the PEG-rich phase; for PEG 3350 cytochrome b_5 is mainly in the salt-rich phase except for the longest tieline at high pH ($K_p = 1.8$ and $Y = 61\%$); for PEG 8000, with only one tieline tested, cytochrome b_5 accumulates in the salt-rich phase at all pH values ($K_p < 8 \cdot 10^{-3}$ and $Y < 0.6\%$).

The effect of polymer molecular mass can be attributed to the increasing number of hydrophilic end groups on shorter PEG chains, which reduces the overall hydrophobicity [6], and to

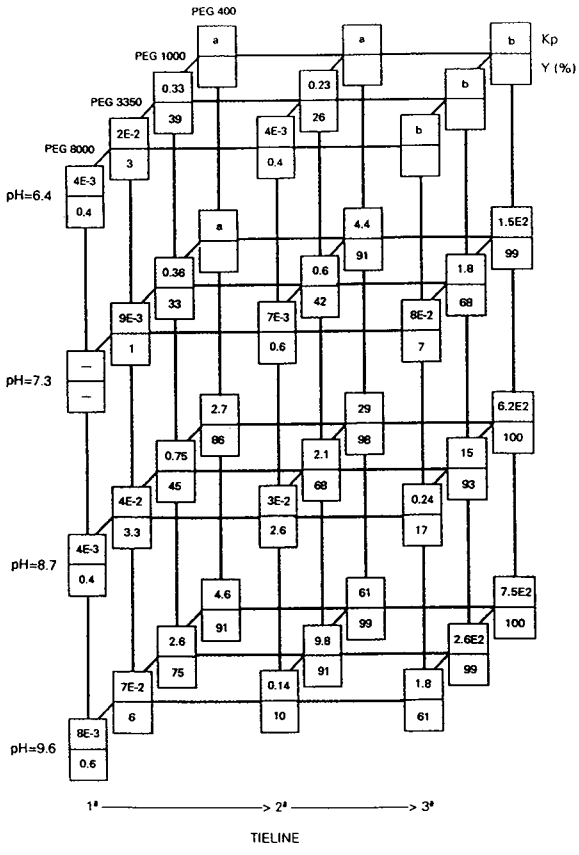

Fig. 1. Effect of polymer molecular mass, tieline length and pH on cytochrome b_5 partition coefficient, K_p, and yield, Y, in PEG–potassium phosphate systems at 23°C. (a) No formation of two phases; (b) KH_2PO_4 did not dissolve.

the excluded volume effects that increase with increasing polymer molecular mass [7].

The enhancement of cytochrome b_5 partitioning with increase in tieline length (Fig. 1) may be attributed to changes in the relative composition of the phases [8]. An increase in tieline length promotes an increase in phosphate concentration in the lower phase whereas in the upper phase it remains relatively constant and equal to its solubility limit in PEG. This results in the salting-out of proteins from the phosphate-rich phase to the PEG-rich phase mediated by the excluded volume effects of PEG. In the limit proteins will precipitate.

Cytochrome b_5 partitioning also increases with increase in pH (Fig. 1). This is probably due to an increase of the $[HPO_4^{2-}]/[H_2PO_4^-]$ ratio, which promotes the shift of the phase diagram to lower polymer and salt concentrations. It is well known that small multivalent anions such as HPO_4^{2-}, used in conjunction with PEG, are more effective in inducing phase formation than monovalent anions [9] owing to the conflicting interaction between ether oxygens of PEG and small ions of high charge density [10]. The approach of salts, with these multivalent anions, to the polymer surface is constrained and a region of salt-depleted structured water is created at the polymer surface which might permit protein polyanion–PEG interactions [10]. The increase in the protein charge with increase in pH seems to be less important because cytochrome b_5 already has a high negative charge at the studied pH values.

Cytochrome b_5 partitioning in systems of PEG 1000 is strongly affected by the tieline length and pH. By changing the pH and/or the tieline length of the two-phase systems it is possible to manipulate cytochrome b_5 partitioning to the phosphate-rich phase or to the PEG-rich phase. This versatility of PEG 1000 systems for cytochrome b_5 partitioning makes them very attractive for separation and purification of cytochrome b_5 from an impure extract.

PEG 1000 was chosen for further partitioning studies with cytochrome b_5 mutants. Fig. 2 shows the effect of tieline length and pH on the partition coefficients and yields of cytochrome b_5 and cytochrome b_5 mutants in PEG 1000–potassium phosphate systems. Partitioning of the modified proteins (mutants 56 and 92) also increases with increasing tieline length and pH. The partition coefficients and yields obtained follow the order cytochrome b_5 > mutant 56 > mutant 92.

The isoelectric point of cytochrome b_5 mutants (pI 4.7) is greater than the isoelectric point of cytochrome b_5 (pI 4.4), hence a decrease in modified protein partitioning would be expected due to the increase in their net positive charge. The differences in the partitioning behaviour of mutants 56 and 92 were attributed to the position of the mutated amino acids in the polypeptide chain. For mutant 92 the mutated amino acid is

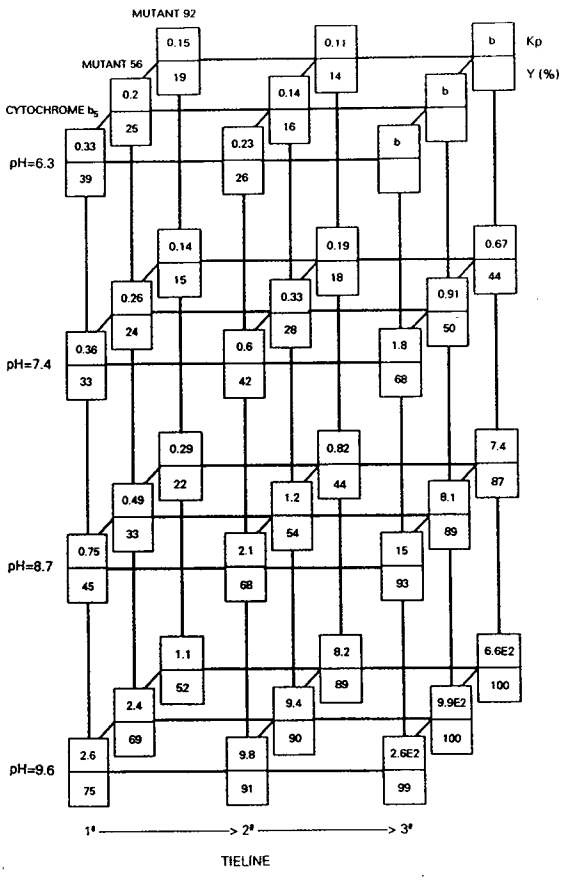

Fig. 2. Effect of tieline length and pH on the partition coefficients, K_p, and yields, Y, of cytochrome b_5 and cytochrome b_5 mutants (56 and 92) in PEG 1000–potassium phosphate systems at 23°C. (b) KH_2PO_4 did not dissolve.

situated at the C-terminus and is more accessible to interaction with both phases of the two-phasic system.

4. Conclusions

Cytochrome b_5 partitioning in PEG–potassium phosphate two-phase systems is enhanced with decreasing polymer molecular mass and increasing tieline length and pH. Partitioning of cytochrome b_5 mutants using PEG 1000 systems show the same dependence on tieline length and pH, following the order cytochrome b_5 > mutant 56 > mutant 92. Owing to their versatility, PEG 1000–potassium phosphate systems seem to be suitable for application in more impure media.

The results of this work suggest that it is possible to change the partitioning behaviour of proteins by engineering the protein surface, for example by making it more positive or negative.

5. Acknowledgement

Maria João Sarmento acknowledges an M.Sc. Fellowship from Programa Ciência Junta Nacional de Investigação Científica e Tecnológica, Portugal.

6. References

[1] M.-R. Kula, K.H. Kroner and H. Hustedt, *Adv. Biochem. Eng.*, 24 (1982) 73.
[2] P.A. Albertsson, *Partition of Cell Particles and Macromolecules*, Wiley, New York, 1986.
[3] F.S. Mathews and E.W. Czerwinski, in A.N. Martonosi (Editor), *The Enzymes of Biological Membranes*, Vol. 4, Plenum Press, New York, 1989, p. 235.
[4] S.B. von Bodman, M.A. Schuller, D.R. Jollie and S.G. Sligar, *Proc. Natl. Acad. Sci. U.S.A.*, 83 (1986) 9443.
[5] M.J. Pires, *Ph.D. Thesis*, Technical University of Lisbon, Instituto Superior Técnico, Lisbon, 1993.
[6] M.-R. Kula, in C.L. Cooney and A.E. Humphrey (Editors), *Comprehensive Biotechnology*, Vol. 2, Pergamon Press, New York, 1985, p. 451.
[7] C.W. Kim, *Ph.D. Thesis*, Massachusetts Institute of Technology, Cambridge, MA, 1986.
[8] J.G. Huddleston, K.W. Ottomar, D.M. Ngonyani and A. Lyddiatt, *Enzyme Microb. Technol.*, 13 (1991) 24.
[9] K.P. Ananthapadmanabhan and E.D. Goddard, *J. Colloid Interface Sci.*, 113 (1986) 294.
[10] J. Huddleston, A. Veide, K. Köhler, J. Flanagan, S-O. Enfors and A. Lyddiatt, *Trends Biotechnol.*, 9 (1991) 381.

ELSEVIER

Journal of Chromatography A, 668 (1994) 121–128

JOURNAL OF CHROMATOGRAPHY A

Polyethylene glycol–potassium phosphate aqueous two-phase systems
Insertion of short peptide units into a protein and its effects on partitioning

Cynthia Hassinen, Kristina Köhler[☆], Andres Veide*

Department of Biochemistry and Biotechnology, Royal Institute of Technology, S-100 44 Stockholm, Sweden

Abstract

Two different tetrapeptides, AlaTrpTrpPro and AlaIleIlePro, were inserted near the C-terminus of the protein ZZT0. The Trp-rich peptide unit strongly increased both the partitioning of ZZT0 into the polyethylene glycol (PEG)-rich phase in a PEG–potassium phosphate aqueous two-phase system and its retention on PEG and propyl hydrophobic interaction chromatographic columns with potassium phosphate as eluent. Both the partitioning and the retention increased with increasing number of Trp-rich peptide units inserted into ZZT0. Insertion of Ile-rich tetrapeptide units affected the partitioning and retention to a much lesser extent. Partition data also indicated a folding of inserted Trp tetrapeptides units, probably to minimize their water contact.

1. Introduction

Polyethylene glycol (PEG)–salt-based aqueous two-phase systems are used in protein purification processes. The distribution of a protein in such systems can be described with the partition coefficient, $K_p = C_t/C_b$, where C_t and C_b are the protein concentrations in the top and bottom phases, respectively. During process optimization one has to compromise between concentration and yield of the target protein, the compromise being dependent on K_p. K_p is governed by several factors, some of which can be related to the system parameters and others to the target protein [1]. It is well established that an increase in the molecular mass of a phase-forming polymer, in this instance PEG, generally leads to a decrease in K_p [2]. This can be attributed to the so-called excluded volume mechanism, where a large volume occupied by PEG molecules squeezes proteins out of solution into the salt-rich bottom phase [3,4]. Charge effects also seem to be involved and an increased negative net charge ($pI < pH$ of system) has been shown to favour the partitioning into the PEG-rich top phase [5]. In addition there are other system modifications that can be used for tuning the distribution of a protein, such as addition of other salts [6,7] or binding of affinity ligands to PEG [8].

* Corresponding author.

☆ Present address: BioScience Centre, Pharmacia AB, S-112 87 Stockholm, Sweden.

0021-9673/94/$07.00
SSDI 0021-9673(94)00024-4

The target protein behaviour is determined by the interaction of the surface exposed amino acid side-chains of the folded protein with solvent and solutes in the phase system. By changing or adding amino acids with charged, polar or non-polar residues to a protein, it should be possible to alter its partitioning.

Although a general picture of the features governing protein partitioning in PEG–salt systems can be given, the molecular mechanisms behind it are poorly understood. There is need for partition experiments performed with well characterized model peptides and proteins. We are using genetic engineering to modify a protein with respect to its content of short peptide units [9]. Several techniques will be used to probe the PEG–peptide and PEG–protein interactions. In this paper, we describe results obtained from partitioning in PEG–potassium phosphate aqueous two-phase systems. We also describe the interaction with two different solid surfaces, (i) PEG and (ii) propyl (C_3), measured as retention on packed-bed chromatographic columns.

2. Experimental

2.1. Chemicals

PEG 4000 (M_r 3500–4500) was obtained from Merck–Schuchardt, Germany. Yeast extract and casamino acids were obtained from Difco. IgG-Sepharose Fast Flow for affinity chromatography was purchased from Kabi Pharmacia. The tetrapeptide AlaTrpTrpPro was custom-made by the BM Unit, University of Lund. Indole-3-acrylic acid and dipeptide TrpTrp were purchased from Sigma. All other chemicals were of analytical-reagent grade.

2.2. Model proteins

The model proteins are shown in Fig. 1. Z is a hydrophilic synthetic IgG binding domain derived from the B domain of staphylococcal protein A (SpA) [10]. The three-dimensional solution structure of the recombinant B domain

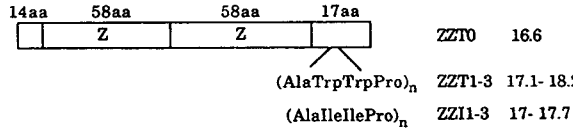

Fig. 1. Schematic structure of model proteins. ZZT0 is the control protein into which the two different tetrapeptide units, AlaTrpTrpPro and AlaIleIlePro, have been inserted. Proteins with up to three repeating peptide units inserted have been produced so far. Right-hand column: $M_r \times 10^{-3}$.

of SpA is composed of a bundle of three α-helices with most of the hydrophobic residues buried in the interior of the bundle [11]. The conformation of the C-terminal peptide stretch, into which the different peptide units are cloned, is not known. The design, cloning and cultivation of plasmid harbouring *Escherichia coli* RV308 and purification of ZZT0, ZZT1 and ZZT3 have been described previously [9]. ZZT2, ZZI1, ZZI2 and ZZI3 were produced following the same protocols. The IgG-binding property of Z was utilized for the purification of the different proteins and eluted fractions were freeze-dried and stored at −20°C until used. Relative amounts of full-length protein after the IgG step were in all instances except one ≥95% when determined by sodium dodecyl sulphate polyacrylamide gel electrophoresis. For ZZT2 it was *ca.* 60% (not shown).

2.3. Partition experiments

Aqueous two-phase partition experiments were performed with purified preparations of the proteins, the dipeptide TrpTrp and the tetrapeptide AlaTrpTrpPro. Two different protocols were used for the partition experiments. In both instances phase systems were prepared from 40% (w/w) stock solutions of PEG 4000 and potassium phosphate (dibasic/monobasic phosphate mole ratio = 1.42, corresponding to a pH of *ca.* 7). In the first instance phase systems were made up directly to their final total masses (5 or 10 g) in graduated centrifuge tubes by weighing in PEG and potassium phosphate from the stock

solutions and distilled water. Before the addition of the sample, which had been dissolved in distilled water to a desired concentration, the contents were thoroughly mixed. The phase systems were chosen as to obtain a top-to-bottom phase volume ratio of about 1:1, in order to provide more accurate sampling procedures. After a second mixing of the phases for 5 min, the phase systems were incubated at the desired temperature (indicated in the figure captions) for 5 min, centrifuged at 500 *g* for 4 min and incubated at the same temperature for a final 5 min. After reading the phase volume, samples from the top and bottom phases were carefully withdrawn with Pasteur pipettes for analysis. This procedure was followed in the partitioning of ZZT_n, ZZI_n and AlaTrpTrpPro.

In the second procedure, phase systems of the required compositions were made up in separation funnels (100–200 g total mass), mixed and left overnight for demixing of phases at a given temperature (indicated in the figure captions). Desired volumes (2–10 ml) of each of the equilibrated phases were removed and after addition of the solid sample and vortex mixing for 2 min the phase system was equilibrated overnight at the same temperature as previously. Finally, samples from the top and bottom phases were carefully withdrawn with Pasteur pipettes for analysis. This protocol was applied in the TrpTrp partition experiments.

Partition coefficients, K_p, were measured spectrophotometrically using absorbances at either 220 or 280 nm. Each top and bottom phase sample was referenced against an identical, but protein-free, top or bottom phase, respectively.

The phase system compositions (Fig. 2) used correspond to different tie-lines. Tie-lines describe the equilibrium in the phase system, *i.e.*, in this instance between PEG 4000-rich top phases and potassium phosphate-rich bottom phases, and with increasing length of the tie-line the difference in the composition of the phases increases. Although tie-lines have not yet been determined for the compositions in this phase system, the tie-line lengths for corresponding compositions can be assumed to increase in the order $TL_a \approx TL_b < TL_c < TL_d < TL_e < TL_f$.

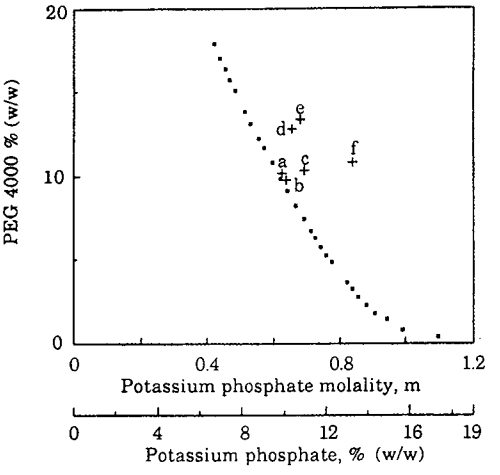

Fig. 2. The binodial (□) of a PEG 4000–potassium phosphate aqueous two-phase system (dibasic/monobasic phosphate mole ratio = 1.42) at 20°C [27]. Phase compositions indicated (+) are those referred to in this study used for partitioning of the dipeptide TrpTrp, the tetrapeptide AlaTrpTrpPro and ZZT_n and ZZI_n proteins. Phase compositions of PEG 4000 potassium phosphate are (a) 10.1:9.9, (b) 9.7:10.1, (c) 10.3:11.0, (d) 12.8:10.4, (e) 13.3:10.8 and (f) 10.8:13.3% (w/w).

2.4. Hydrophobic interaction chromatography

Hydrophobic interaction chromatography (HIC) was performed on two different column packings: (i) PEG HIC was run on a Hydropore-HIC Dynamax-TI bed, 5-μm packing, pore size 300 Å, 100 mm × 4.6 mm I.D., from Rainin Instrument; (ii) propyl (C_3) HIC was performed on a Bakerbond Wide-Pore HI-Propyl bed, 5 μm packing, pore size 300 Å, 50 mm × 4.4 mm I.D., from J.T. Baker. On both columns the ligands were covalently attached to a hydrophilic base matrix, which covers the wide-pore silica. Freeze-dried protein samples were dissolved in potassium phosphate (dibasic/monobasic phosphate mole ratio = 1.42) solutions of the same concentration as the elution buffer and spun on an Eppendorf centrifuge at 11 000 *g* for 5 min to remove solids. The injected sample volumes were 50 μl and the flow-rates were between 0.5 and 1.0 ml min^{-1}. Protein elution was followed at either 220 or 280 nm.

3. Results and discussion

The understanding of the partition behaviour of amino acids and short peptides is a starting point for understanding the partitioning of more complex structures such as peptides and proteins. Our concept based on genetic engineering of a model protein (*i.e.*, ZZT0, described under Experimental) allows us to study the interaction of PEG with short peptide units both as free molecules and as protein inserts. The reasons for selecting Trp as the first test amino acid were twofold. First, we know that *E. coli* β-galactosidase can be partitioned strongly into the PEG phase in a PEG 4000–potassium phosphate aqueous two-phase system [12,13], a property which has been utilized in process design [13]. What surface properties of β-galactosidase with a molecular mass of 460 000 prevent its exclusion from the PEG phase? Interestingly, β-galactosidase has an unusually high content of the amino acid Trp compared with the average *E. coli* protein, 3.8% in β-galactosidase [14] and 1% in average *E. coli* proteins [15]. Second, experiments with depeptides in PEG–phosphate aqueous two-phase systems (pH 7) have shown that Trp is the only amino acid to cause enhanced partitioning into the PEG-rich top phase [16]. Hence it may be that the partitioning of β-galactosidase reflects the fact that some of its 156 Trp residues are exposed at the protein surface.

3.1. Partitioning and HIC

Partition experiments with the ZZT_n proteins in PEG 4000–potassium phosphate systems (dibasic/monobasic phosphate mole ratio = 1.42) showed that with increasing number of Trp peptide units inserted the stronger was the distribution of the protein to the PEG-rich phase (Fig. 3) [9]. This was interpreted to be related to the exposure of Trp residues and their specific interaction with PEG. Thus, qualitatively, the importance of Trp as a partition enhancer was maintained when incorporated into a protein.

In another set of experiments, Ile, an aliphatic non-polar amino acid, was inserted into ZZT0 as

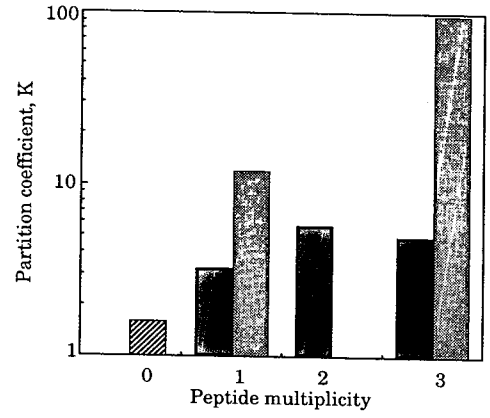

Fig. 3. Partition coefficients of (hatched box) ZZT0, (solid boxes) ZZI_n proteins and (screened boxes) ZZT_n proteins in a 13.3% (w/w) PEG 4000–10.8% (w/w) potassium phosphate (dibasic/monobasic phosphate mole ratio = 1.42) aqueous two-phase system (composition e, Fig. 2) at different tetrapeptide multiplicities, *n*. Partition experiments for ZZT_n and ZZI_n proteins were run at 20 and 22°C, respectively. Protein concentrations in the phase systems were approximately ZZT0 1, ZZT1 0.2, ZZT3 0.1, ZZI1 0.1, ZZI2 0.1 and ZZI3 0.1 mg ml^{-1}. Concentrations of ZZT_n and ZZI_n proteins in equilibrated phases were measured at 280 and 220 nm, respectively. Recoveries were about 100% for all proteins except ZZI2 and ZZI3, for which they were about 65% and 25%, respectively.

a tetrapeptide unit. It should be stressed that the solubility of ZZT0 in the phase system was lowered more significantly by the insertion of Ile-rich peptides compared with the Trp-rich peptides, as clearly demonstrated by the non-quantitative total recoveries of protein ZZI2 (*ca.* 65%) and ZZI3 (*ca.* 25%) (Fig. 3). Keeping the solubility reasoning in mind, it is still possible to conclude when comparing the partitioning of ZZI_n ($n = 1, 2, 3$) and ZZT_n ($n = 1, 3$) proteins that the insertion of Ile residues into ZZT0 had less impact on directing its partitioning into the PEG-rich top phase (Fig. 3). This is in agreement with the partition behaviour of Ile when part of a short peptide (see Fig. 5) [16].

Another way to characterize the interaction of peptides and proteins with PEG in aqueous solutions is to use systems where PEG has been immobilized on a solid surface. This gives the possibility of varying the potassium phosphate concentration much more freely than in the

phase system where one has to consider the phase formation. The potassium phosphate composition at the critical point gives the highest and the lowest potassium phosphate concentrations possible in the PEG-rich top phase and the potassium phosphate-rich bottom phase, respectively. In the particular system used here (20–23°C), compositions a and b are close to the critical point as judged by their phase volume ratios. Therefore, the potassium phosphate concentration of the critical point is concluded to be about 0.6 molal (*ca.* 9.5%, w/w) (Fig. 2). Retention of ZZT3 on the commercial PEG HIC column occurred in a pure aqueous solution, whereas for the other proteins one had to use molal potassium phosphate concentrations above 0.5 to obtain similar retentions (Fig. 4A). The results obtained on the HIC column with the model proteins correlated qualitatively with their behaviour in the PEG–potassium phosphate aqueous two-phase system. This was expected as the separations with both techniques are promoted by water-structuring salts (see below).

The application of the more hydrophobic propyl-based HIC column led to a stronger retention in general for all the model proteins in comparison with the PEG column (Fig. 4B). Interestingly, the greatest impact on the retention behaviour on ZZT0 was still caused by Trp, whereas Ile affected the retention to a much smaller extent. Thus, on both the PEG and C_3 columns available Trp residues seem to play a much more pronounced role than Ile in the retention behaviour of proteins. Whereas the aliphatic side-chain of Ile is chemically inert owing to its non-polar character and absence of functional chemical groups, the side-chain of Trp is much more chemically reactive. The indole side-chain of Trp is polar and is the only amino acid side-chain capable of entering into charge-transfer interaction with electrophilic structures. The pyrrole nitrogen of the indole ring can act as a hydrogen donor in hydrogen bond interactions [17].

According to HIC theory, (i) the limiting slope of the plot of ln k' against the salt molality is proportional to the contact surface area between the protein and the column and (ii) the intercept on the ordinate of the same plot seems to characterize the strength of the interaction between the protein and the column [18,19]. If this is considered for the ZZT_n and ZZI_n proteins (Fig. 4), one recognizes that there is a much more significant shift in the position of the curves than in their slopes which could imply that the insertions of the two different peptide units into ZZT0 affected the strength of the

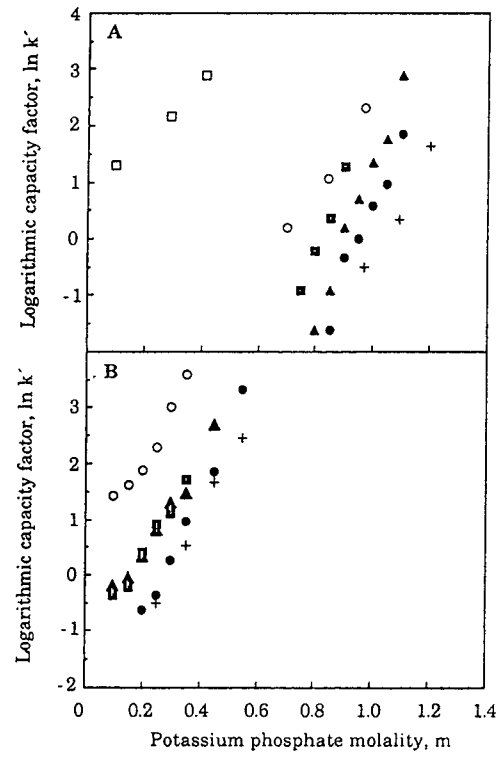

Fig. 4. Hydrophobic interaction chromatography of ZZT_n and ZZI_n proteins on (A) PEG- and (B) C_3 (propyl)-based columns. + = ZZT0; ○ = ZZT1; □ = ZZT3; ● = ZZI1; ▲ = ZZI2; ■ = ZZI3. The retention, expressed as the logarithmic capacity factor (ln k'), is plotted as a function of potassium phosphate concentration (dibasic/monobasic phosphate mole ratio = 1.42). The capacity factor is defined as $k' = (V_r/V_0) - 1$, where V_r and V_0 are the retention and void volumes, respectively. Approximate protein amounts loaded were: ZZT_n = 0.1–0.4 mg and ZZI_n = 0.05–0.1 mg for PEG HIC and ZZT_n = 0.05–0.1 mg and ZZI_n = 0.05 mg for C_3 HIC. Retention of ZZT_n proteins on the PEG column was detected at 280 nm. For all other runs 226 nm was used to follow protein elution. The void volumes were determined by measuring the retention of an injected aqueous pulse.

interactions more strongly than the contact surface area between the protein and either PEG or C_3. One exception to this could be protein ZZT3, where clearly both the limiting slope and the intercept are shifted.

3.2. Structural changes and interaction behaviour

An important issue, also when proteins are partitioned in PEG–potassium phosphate systems, is to understand the relationship between the conformation of a protein and its interaction with the surrounding environment. It is of importance for limiting target protein loss but also possibly as a tool for improving selectivity, *e.g.*, in the extraction. The structural effects of inserting various peptides into ZZT0 could be partly understood by comparing the partitioning of peptide units, the model protein ZZT0 and a protein in which a peptide unit has been inserted, ZZT1. A partition model for interacting molecules [20] can be applied:

$$K_{ab} = K_a K_b$$

where the individual partition coefficients for molecules a and b are used to predict the partition coefficient for the coupled/fused molecule ab. The equation is assumed to hold if the linking of molecules a and b does not change the structure of either of the two molecules involved. The model was tested on ZZT1 for different phase compositions by comparing measured K_{ZZT1} values with the calculated values, the latter obtained from K values for ZZT0 and TrpTrp. As TrpTrp, but so far, not AlaTrpTrpPro has been partitioned in exactly the same phase compositions as ZZT0 and ZZT1, this dipeptide was used for the comparison. That TrpTrp is a reasonable model for AlaTrpTrpPro is shown in Fig. 5. They have similar K values when partitioned in the PEG 4000–potassium phosphate systems and the K values of the two molecules follow a logical change with increasing tie-line length. Nevertheless, the model calculations revealed that $K_{ZZT1,\,measured} < K_{ZZT1,\,calculated}$ for all three compositions tested (Fig. 6). A reasonable explanation is that the tetrapeptide unit folds together with the C-terminal peptide region into which it was inserted in such a way that it thereby becomes less accessible to interaction with the solvent. An additional effect of the tetrapeptide insertion could be a disturbance of the closest Z domain structure, which in turn could have an impact on the partitioning. A possible increase in the Z domain flexibility was indicated by an increase in the susceptibility to *in vivo* proteolysis with increasing number of AlaTrpTrpPro units inserted into ZZT0 [21].

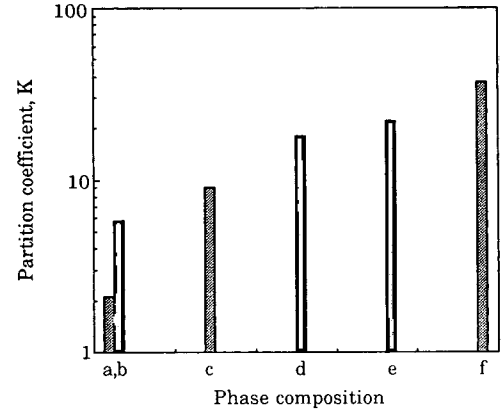

Fig. 5. Partitioning of the tetrapeptide AlaTrpTrpPro (screened boxes) in a PEG 4000–potassium phosphate (dibasic/monobasic phosphate mole ratio = 1.42) aqueous two-phase system at three different phase composition: a, c and f (indicated in Fig. 2). For comparison partition data for the dipeptide TrpTrp (solid boxes) at three different phase compositions, b, d and e, have been included (see Fig. 6) for TrpTrp details). The tie-lines (TL) corresponding to each phase composition increase in length in the order $TL_a \approx TL_b < TL_c < TL_d < TL_e < TL_f$. The partition temperature was 21°C. The total concentration of AlaTrpTrpPro in the phase systems was 0.4 mg ml^{-1} and the concentrations in equilibrated phases were measured at 280 nm. Recoveries were about 100%.

The possibility of Trp playing an active role in the partitioning will be determined by its surface accessibility in each particular protein. Clearly the Trp residues in the ZZT_n proteins are still available for interaction, as revealed by the partitioning and chromatographic behaviours. Although a Trp residue, owing to its hydrophobic character, could be expected to prefer the

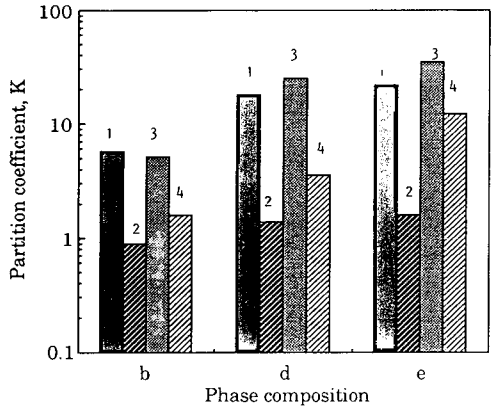

Fig. 6. Test of the model for interacting molecules, $K_{ZZT1} = K_{TrpTrp}K_{ZZT0}$, at three different phase compositions: b, d and e indicated in Fig. 2. The tie-lines (TL) corresponding to each phase composition increase in length in the order $TL_b < TL_d < TL_e$. Partition experiments for dipeptide and ZZT proteins were run at 22 and 20°C, respectively. Dipeptide and protein total concentrations in the phase systems were approximately TrpTrp 0.3, ZZT0 1 and ZZT1 0.2 mg ml^{-1}. Dipeptide and protein concentrations in equilibrated phases were measured at 280 nm. Recoveries were about 100% for all partitioned molecules. $1 = K_{TrpTrp}$; $2 = K_{ZZT0}$; $3 = K_{ZZT1}$ calculated; $4 = K_{ZZT1}$ measured.

interior of a protein, avoiding contact with the aqueous medium, it is also known that parts of it can be exposed on the surface of properly folded proteins [22]. Currently we are using an optical technique (total internal reflection fluorescence) to probe the accessibility of Trp residues in the C-terminal peptide stretch of ZZT0. The accessibility of the Ile residues in the C-terminal peptide stretch will be much more difficult to assess owing to a lack of suitable optical properties of Ile, although some information about the exposure of inserted Ile residues will be achieved when we apply the model for interacting molecules (see above) to AlaIleIlePro and ZZI_n proteins.

Finally, let us consider briefly the role that PEG and phosphate ions play as protein stabilizers [23]. Protein stabilizers seem to obey a general rule: co-solvents which, at high concentration, stabilize the native structure of proteins are preferentially excluded from the surface of a protein. On the one hand, phosphate ions (especially dibasic and tribasic), which are excluded from the protein surface through a mechanism referred to as the surface tension effect, stabilize folded protein structures under different types of physico-chemical conditions (*e.g.*, elevated temperatures, extreme pH). The stabilizing properties of salt ions (and salting-out effectiveness) increase with their effectiveness in increasing the surface tension of water. The formation of the PEG–phosphate system can be seen as salting-out of PEG by phosphate, which is related to the surface tension effect of phosphate on water. On the other hand, the interaction of PEG with proteins will depend to a great extent on the surrounding conditions. Under stabilizing conditions proteins are excluded from PEG through steric exclusion. However, under denaturing conditions, when a protein structure becomes more flexible or starts to unfold, PEG, owing to its hydrophobic character, can bind to unfolded proteins and folding intermediates. This property of PEG has been explored for the enhancement of protein refolding [24]. PEG is described as a strong hydrogen bond acceptor owing to the paired ether oxygen electrons, which provides for its water solubility [25]. It can form complexes with monomeric and polymeric electron acceptors (*e.g.*, hydrogen bond donors) [26]. A specific interaction between PEG and a protein UV 280-nm chromophore has been suggested to occur as an explanation for the large perturbations of the UV spectra of proteins in PEG solutions [22]. The chromophore could well be that of Trp.

4. Conclusion

Protein partitioning in a PEG–phosphate aqueous two-phase system could be described as a delicate balance between exclusion from the phosphate-rich phase by the surface tension effect, exclusion from the PEG-rich phase by the steric effect and/or a specific PEG–protein interaction, a limiting factor being the maximum solubility of the protein in the phase system.

A specific salt-promoted PEG–protein interaction via the Trp side-chain was indicated in this work. First, we have shown that Trp strongly

directed the partitioning of a model protein into the PEG-rich phase in a PEG 4000–potassium phosphate aqueous two-phase system and increased its retention on a PEG column with potassium phosphate as eluent. Both the partitioning and the retention increased with increasing number of Trp-rich peptide units inserted. Second, insertion of Ile-rich tetrapeptide units affected the partitioning and retention to a much smaller extent. The results also illustrated a relationship between PEG–phosphate partitioning and PEG HIC.

The model proteins showed a similar behaviour on C_3 and PEG columns, the only major difference being the stronger retention of each protein on the former.

Partition data also indicated a folding of inserted Trp tetrapeptides units, probably to minimize their contact with water. In future work to characterize PEG–salt interactions we would like to probe protein structure and structural changes more carefully and see how they are related to the interaction with PEG. In addition to methods described in this paper, we are now also using techniques such as ellipsometry, total internal reflection fluorescence spectrometry and microcalorimetry.

5. Acknowledgement

This investigation was supported by grants from Teknikvetenskapliga Forskningsrådet (Swedish Research Council for Engineering Sciences).

6. References

[1] J. Huddleston, A. Veide, K. Köhler, J. Flanagan, S.-O. Enfors and A. Lyddiatt, *Trends Biotechnol.*, 9 (1991) 381.
[2] P.-Å. Albertsson, *Partition of Cell Particles and Macromolecules*, Wiley-Interscience, New York, 3rd ed., 1986.
[3] K.C. Ingham, *Arch. Biochem. Biophys.*, 184 (1977) 59.
[4] T.F. Busby and K.C. Ingham, *Vox Sang.*, 39 (1980) 93.
[5] J.G. Huddleston, K.W. Ottomar, D.M. Ngonyani and A. Lyddiatt, *Enzyme Microb. Technol.*, 13 (1991) 24.
[6] H.L. Chiang and S.S. Wang, *Biotechnol. Techn.*, 2 (1988) 283.
[7] R.A. Hart and J.E. Bailey, *Enzyme Microb. Technol.*, 13, (1991) 788.
[8] S.D. Plunkett and F.H. Arnold, *Biotechnol. Techn.*, 4 (1990) 45.
[9] K. Köhler, C. Ljungquist, A. Kondo, A. Veide and B. Nilsson, *Bio/Technology* 9 (1991) 642.
[10] B. Nilsson and L. Abrahmsén, *Methods Enzymol.*, 185 (1990) 144.
[11] H. Gouda, H. Torigoe, A. Saito, M. Sato, Y. Arata and I. Shimada, *Biochemistry*, 31 (1992) 9665.
[12] L. von Bonsdorff-Lindeberg, *Licentiate Thesis*, Helsinki University of Technology, Esbo, 1989.
[13] A. Veide, T. Lindbäck and S.-O. Enfors, *Enzyme Microb. Technol.*, 6 (1984) 325.
[14] A. Kalnins, K. Otto, U. Rüther and B. Müller-Hill, *EMBO J.*, 2 (1983) 593.
[15] F.C. Neidhardt, in F.C. Neidhardt (Editor), Escherichia coli *and* Salmonella typhimurium. *Cellular and Molecular Biology*, Vol. 1, American Society of Microbiology, Washington, DC, 1987, p. 3.
[16] A.D. Diamond, K. Yu and J.T. Hsu, in M.R. Ladish, R.C. Wilson, C.C. Painton and S.E. Builder (Editors), *Protein Purification: from Molecular Mechanisms to Large-Scale Processes (American Chemical Society Symposium Series*, No. 427), American Chemical Society, Washington, DC, 1990, p. 52.
[17] T.E. Creighton, *Proteins, Structure and Molecular Properties*, Freeman, New York, 1984.
[18] J.L. Fausnaugh and F.E. Regnier, *J. Chromatogr.*, 359 (1986) 131.
[19] L. Szepesy and G. Rippel, *LC · GC Int.*, 5 (1992) 24.
[20] P.-Å. Albertsson, *Methods Biochem. Anal.*, 29 (1983) 1.
[21] S. Yang, A. Veide and S.-O. Enfors, *Eur. J. Biochem.*, submitted for publication.
[22] M. Laskowski, Jr., *Fed. Proc.*, 25 (1966) 20.
[23] S.N. Timasheff and T. Arakawa, in T.E. Creighton (Editor), *Protein Structure: a Practical Approach*, IRL Press, Oxford, 1990, Ch. 14, p. 331.
[24] J.L. Cleland, S.E. Builder, J.R. Swartz, M. Winkler, J.Y. Chang and D.I.C. Wang, *Bio/Technology*, 10 (1992) 1013.
[25] F.E. Bailey, Jr., and J.V. Koleske, *Poly(ethylene oxide)*, Academic Press, New York, 1976.
[26] F.W. Stone and J.J. Stratta, in H.F. Mark, G. Gaylord and N.M. Biales (Editors), *Encyclopedia of Polymer Science and Technology*, Vol. 6, Wiley-Interscience, New York, 1966, p. 103.
[27] K. Köhler, L. von Bonsdorff-Lindeberg and S.-O. Enfors, *Enzyme Microb. Technol.*, 11 (1989) 730.

ELSEVIER

Journal of Chromatography A, 668 (1994) 129–137

JOURNAL OF CHROMATOGRAPHY A

Separation and purification of recombinant proteins from *Escherichia coli* with aqueous two-phase systems

J.A. Asenjo*, R.E. Turner, S.L. Mistry, A. Kaul

Biochemical Engineering Laboratory, University of Reading, Reading RG6 2AP, UK

Abstract

The partition of the protein thaumatin in the presence of *Escherichia coli* contaminant proteins has been studied. Extraction of thaumatin was followed by back-extraction of the product into a new phosphate phase and also back extraction combined with recycle of the top polyethylene glycol (PEG) phase. When partitioned in the absence or presence of insoluble cell debris (whole cell homogenate) little effect on the partitioning of thaumatin or the soluble *E. coli* protein was observed. A back extraction step that allowed for dilution of the NaCl was successful in extracting thaumatin back into a heavy phosphate phase.

The PEG top phase was recycled to the first extraction stage. The stability ratio (tie-line length) had an effect on the average partition coefficient (K_{app}) of *E. coli* soluble proteins in PEG–phosphate systems but in PEG sulphate systems K_{app} was independent of this ratio. An increase in NaCl resulted in an increase in K_{app} but this was always below 1. A mathematical model that describes the continuous steady-state operation of extraction and back extraction has been developed; it is based on steady state mass balances of the main components and phase equilibrium data and was successfully used to simulate the extraction and back extraction processes.

1. Introduction

The production of protein products in *Escherichia coli* is still a cornerstone of the biotechnology industry and thus much attention has been focused on the recovery of intracellular recombinant proteins [1]. Aqueous two-phase technology offers an attractive step in the separation and purification of proteins from their major contaminants. The main advantages over traditional adsorption separation processes lies in their ability to handle particulate material and to process large volumes in a continuous mode. Separation can be achieved whereby the particulates and major contaminants partition to the bottom phase and the protein product to the top phase. Recovery of the product can be achieved in a second stage where conditions for the elution and partition of the target protein into the bottom phase is obtained [2–5].

Aqueous two-phase systems (ATPSs) can be composed of either two water-soluble polymers usually polyethylene glycol (PEG) and dextran or a polymer (PEG) and salt usually phosphate, sulphate or citrate. There are many factors which influence partition in ATPSs. These factors are inherent to the system itself (*e.g.* choice of the system components, distance of the system from the binodial, polymer molecular mass, concentration of polymers and salts, ionic composition and strength and pH) and to the protein to be partitioned (*e.g.* molecular mass, charge and hydrophobicity). Thus selectivity of separation is based on manipulating these variables.

* Corresponding author.

0021-9673/94/$07.00
SSDI 0021-9673(94)00126-T

An important drawback of ATPSs is the possible instability of the two phases being formed when compared to conventional chromatographic processes, where one of the phases is solid. To allow for the application and scale up of ATPSs this problem has to be overcome. Systems have to be robust so that variations in process streams will not destroy the system by causing the formation of one phase. By developing a model to describe and predict phase separation in the extraction and back extraction stages, based on experimental data, it can be possible to simulate and investigate regions of potential instability and thus allow for a robust process to be achieved. Such a process can be operated under steady state conditions which will also minimize batch to batch variations.

Thaumatin [2], a flavour enhancer, has been cloned into *E. coli* and yeast and has a molecular mass of 22 200 and an isoelectric point of around pH 10.5–11.0. In this study we have investigated the partition, in PEG phosphate systems, of pure thaumatin in the presence of *E. coli* contaminant proteins; extraction was followed by back extraction of the product into a new phosphate bottom phase and also back extraction combined with the recycle of the top PEG phase. The data for this has been used in a mathematical model to describe a continuous extraction process. We have also investigated the effect of the systems robustness (*i.e.* the stability ratio), on the partition of the *E. coli* soluble protein matrix.

2. Materials and methods

2.1. Materials

PEG with M_r 6000, dipotassium hydrogenphosphate and sodium dihydrogen phosphate were obtained from BDH, Leicester, UK. PEG with M_r 4000 and magnesium sulphate were obtained from Fluka, Buchs, Switzerland. Thaumatin was kindly donated by Four F Nutrition, North Yorkshire, UK. All other chemicals were analytical grade.

2.2. Growth and lysis of E. coli

A homogenate of *E. coli* K12 (in 50 m*M* Tris–HCl pH 7), was prepared by sonication. After centrifugation the supernatant (soluble fraction) was removed and the remaining cell debris (insoluble fraction) was washed and resuspended with 50 m*M* Tris–HCl at pH 7.

2.3. Preparation of phase systems

Systems had a final mass of 1.5 g and were prepared from stock solutions of PEG (50%, w/w), potassium phosphate (40%, w/w), magnesium sulphate (23%, w/w) and sodium chloride (25%, w/w). pH was set at 7 and stocks were stored in the cold and prior to use temperature equilibrated by standing at room temperature (20°C). For back extraction thaumatin, *E. coli* soluble fraction and cell debris were added to give a final concentration of 1 mg/ml. For the study on stability ratio (Fig. 1), systems had a final mass of 1.8 g and *E. coli* soluble fraction was added to give a final concentration of 0.5 mg/ml.

Systems were mixed thoroughly and centrifuged (3000 rpm, *ca.* 500 *g*, 3 min) to assist phase separation. Samples of 0.1 ml were removed from the top and bottom phases, diluted with deionised water and assayed for protein

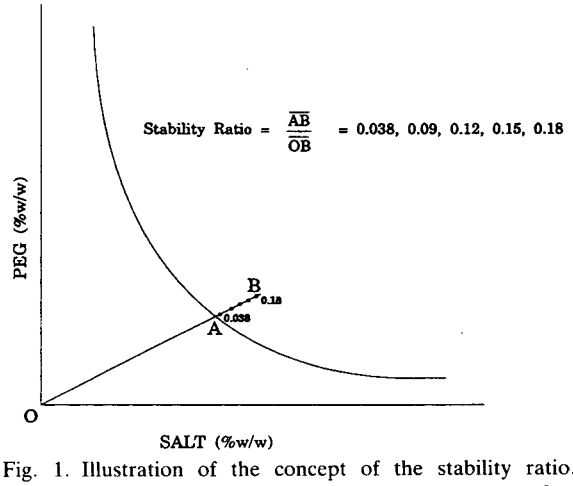

Fig. 1. Illustration of the concept of the stability ratio. B = System composition; A = point on the binodial; O = origin.

concentration. All experiments were carried out in duplicate.

2.4. Back extraction of thaumatin

A system with a phase composition of 12% (w/w) PEG, 13% (w/w) phosphate and 8.8% (w/w) NaCl and a phase volume ratio of 0.67 was used. Back extraction was achieved by the removal of the top phase and addition of a fresh bottom phase with no NaCl present. The back extraction was carried out three times into a fresh phosphate phase.

2.5. Back extraction and recycle of PEG

A system with a phase composition of 15.5% (w/w) PEG, 6% (w/w) phosphate and 8.8% (w/w) NaCl with a phase volume ratio of 0.2 was used. Recycling of PEG was achieved by removal of the top phase and addition of a fresh bottom phase with no NaCl present. The top phase was then removed and added to the original system where further NaCl and thaumatin, soluble fraction or insoluble fraction was added. This was repeated three times.

2.6. Protein determination

For the determination of protein concentration the modified Bradford assay (see ref. 6) was used. Standard curves of thaumatin and bovine serum albumin (BSA) were constructed which were linear within the range of protein concentration measured. Protein-free systems were used for control where the protein sample was replaced with 50 m*M* Tris–HCl at pH 7. The partition coefficient, K, corresponds to the ratio of protein concentration in the top and bottom phases.

3. Results and discussion

3.1. Partition of thaumatin and E. coli

When a particular ATPS has been selected for the separation and/or purification of a protein, the choice of the operating point in the phase diagram is important. If a chosen point is too far from the binodial, where concentrations of polymer and salt are high, the protein might precipitate out of solution. If the point is too near the binodial a small dilution of the system might cause a shift of the system composition to the left of the binodial and therefore the formation of a single phase where separation can not be achieved. The question of system robustness will depend to a large extent on the location of the operating point in relation to the binodial. This concept is reflected in the relative value of the tie-line length but, even simpler, in the value of the stability ratio as defined in Fig. 1. This ratio is conceptually similar to the tie-line length but is much easier to determine as it only requires a titration with water.

Cascone *et al.* [2] studied various systems for the separation of thaumatin from *E. coli* contaminant proteins. The results shown in Fig. 2 proved to have the best potential conditions to achieve a good separation. This particular system was therefore further analysed by reversed-phase chromatography to assess if the presence of *E. coli* proteins affects the partition of thaumatin. The K values obtained for thaumatin and *E. coli* proteins independently were maintained by the mixture of the proteins.

Fig. 2 shows the partitioning of pure

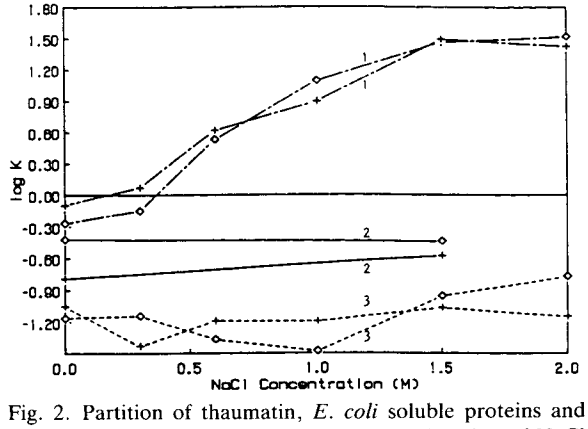

Fig. 2. Partition of thaumatin, *E. coli* soluble proteins and BSA in PEG 6000–phosphate systems as a function of NaCl concentration at (+) pH 7 and (◇) pH 9. 1 = Thaumatin; 2 = *E. coli*; 3 = BSA.

thaumatin, *E. coli* soluble proteins and BSA as a function of NaCl concentration at two pH values [2]. Log K for thaumatin increases dramatically as the NaCl concentration is increased to 1.5 M, while log K for *E. coli* soluble contaminants and BSA (a typical contaminant of mammalian cell culture), remains below 0. Exploiting this behaviour can allow for the selective separation of thaumatin at a high NaCl concentration where K for thaumatin is high ($K = 33$); further purification can be achieved by back extraction into a fresh phosphate bottom phase in the absence of NaCl thus decreasing the K value ($K = 0.53$). This can be achieved by diluting the NaCl from the top phase by using a large phosphate phase for back extraction. A similar but even more pronounced trend has recently been observed for the separation of α-amylase from its fermentation supernatant, where increasing the NaCl concentration increases K for α-amylase while K for the contaminants remains unaffected [7].

3.2. Partitioning of thaumatin and E. coli soluble and insoluble fractions

In order to assess the effect of processing a crude cell homogenate, without clarification of the cell debris, for the system described in Figs. 2 and 3 the protein partition coefficient at 8.8% NaCl (*ca.* 1.5 M) for the soluble, insoluble and combined fractions in the presence and absence of thaumatin (Table 1) was analysed. The partition coefficients for the *E. coli* fractions were all below 1 (log $K < 0$). In the presence of thaumatin, K for all fractions was somewhat lower than for thaumatin alone due to the presence of *E. coli* proteins, and in general little effect of the debris was observed.

3.3. Back extraction of thaumatin

To back extract thaumatin from the top PEG phase, dilution of NaCl present in this phase was necessary. A large phosphate bottom phase was used which lowered the concentration of NaCl in the new system and also allowed a large proportion of the thaumatin to be recovered (stage 2 in Fig. 3). Although K for thaumatin was relatively

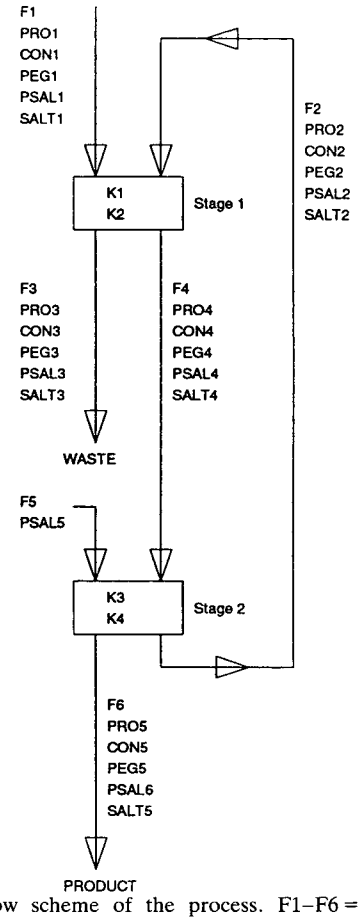

Fig. 3. Flow scheme of the process. F1–F6 = Flow-rates; PRO1–PRO5 = product protein concentrations; CON1–CON5 = contaminant protein concentrations; PEG1–PEG-5 = concentrations of PEG; PSAL1–PSAL6 = concentrations of phase forming salt (*e.g.* phosphate); SALT1–SALT5 = concentration of added salt (*e.g.* NaCl).

low, a proportion of thaumatin is still present in the top phase. Further purification was achieved in the following two back extraction steps (Table 2), where in the third back extraction step K for thaumatin was similar to that observed in Fig. 2 at 0% NaCl. This is evidently an effect of the decreasing concentration of NaCl in the second and third back extraction stages.

3.4. Recycle of PEG

The effect on the partition coefficients of pure thaumatin and protein measured in the presence of soluble and insoluble fractions when PEG was

Table 1
Partition of *E. coli* homogenate and thaumatin in a PEG 6000 (12%, w/w), potassium phosphate (13%, w/w) and NaCl (8.8%, w/w) system at pH 7

	Log *K*	
	+Thaumatin	−Thaumatin
Thaumatin only	1.5	–
Insoluble fraction	1.2	−0.4
Soluble fraction	1.3	−0.4
Combined fractions	1.3	−0.7

+Thaumatin = System with thaumatin; −Thaumatin = system without thaumatin.

recycled back to stage 1 (Fig. 3), is shown in Table 3. This was carried out batch-wise where three separations were performed. Manipulation of the phase volume ratio (0.2) enabled the dilution of NaCl from the system and a large proportion of the thaumatin to be recovered. It should be noted that the only loss of thaumatin is in the bottom phase at stage 1 as the thaumatin not recovered in stage 2, is recycled with the PEG phase. Table 3 shows that recycling of the PEG phase did not have a dramatic effect on the partition coefficients.

3.5. Partition of *E. coli* soluble proteins contaminants

To permit the selection of an ATPS for the separation of a protein cloned in *E. coli*, it was decided to characterise the behaviour of *E. coli* soluble proteins in polymer–salt ATPSs under different conditions; in particular the effect of

Table 2
Partition of thaumatin after back extraction in a PEG 6000 (12%, w/w), potassium phosphate (13%, w/w) and NaCl (8.8%, w/w) at pH 7

Log *K*			
Extraction, stage 1	B.E.1, stage 2	B.E.2, stage 3	B.E.3, stage 4
1.5	0.4	0.2	−0.3

B.E. = Back extraction.

Table 3
Partition of thaumatin and *E. coli* soluble and insoluble fractions after back extraction and recycle of the top PEG phase in a PEG 6000 (15.5%, w/w), potassium phosphate (6%, w/w) and NaCl (8.8%, w/w) system at pH 7

	Log *K*		
	Thaumatin	Soluble fraction	Insoluble fraction
Extraction	1.6	−0.3	0.2
B.E.1	−0.1	−0.1	0.0
Recycle	1.9	−0.2	−0.4
B.E.2	0.1	−0.1	−0.1
Recycle	1.7	−1.0	−0.2
B.E.3	0	0.1	0.1

NaCl and the stability ratio (Fig. 1). If known under which conditions the bulk of the *E. coli* matrix proteins partition into one phase (*e.g.* bottom phase), then a choice of systems will be available in which to test whether the target protein can be partitioned to the opposite phase (*e.g.* top phase).

Figs. 4 and 5 show the partition of *E. coli* soluble protein contaminants at different stability ratios as a function of NaCl concentration in PEG–phosphate and PEG–sulphate systems. In phosphate systems log K_{app} (K is "apparent" as it is an average K for *E. coli* soluble proteins) for the soluble proteins at 0% NaCl, increases as the stability ratio increases. At 4% and 8.8% NaCl,

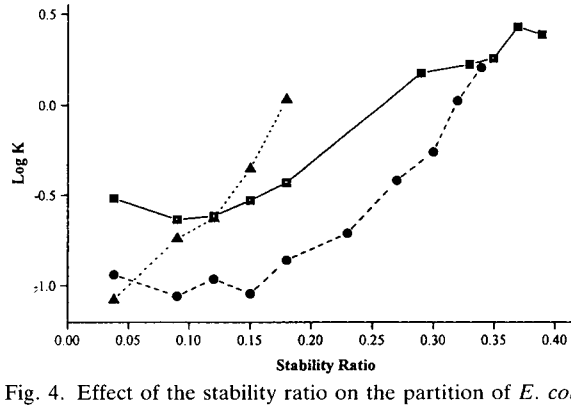

Fig. 4. Effect of the stability ratio on the partition of *E. coli* soluble proteins as a function of NaCl concentration in PEG 4000 phosphate systems at pH 7. ▲ = 0% NaCl; ● = 4% NaCl; ■ = 8.8% NaCl.

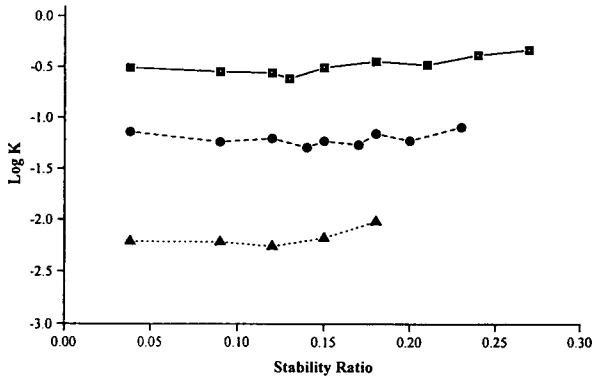

Fig. 5. Effect of the stability ratio on the partition of *E. coli* soluble proteins as a function of NaCl concentration in PEG 4000 sulphate systems at pH 7. Symbols as in Fig. 4.

log K_{app} remains low up to a stability ratio of 0.18 and then increases in both cases as the stability ratio increases. On the other hand, for sulphate systems (Fig. 5) log K_{app} for the soluble proteins at 0% NaCl remains relatively constant as the stability ratio is increased. The same trend is observed for 4 and 8.8% NaCl. In both cases NaCl causes an increase in K but in the sulphate systems the value of K is still well below 1 over the range of stability ratios studied. In these systems the stability ratio (tie-line length) seems to have little effect on K_{app} for *E. coli* soluble proteins. For both systems at 0, 4 and 8.8% NaCl the respective systems, at the same distance from the binodial, have approximately the same tie-line length. Log K_{app}, however, increases as a function of NaCl concentration suggesting that the presence of NaCl is changing the character of the phases and thus causing an increase in the value of K. In other systems this effect has been attributed to an increase in the hydrophobic character of the system [8]. These systems, with a partition coefficient lower than 1 ($\log K < 0$) are all suitable for partitioning target recombinant proteins into the top PEG phase.

4. Mathematical modelling and simulation for process robustness and optimisation

A mathematical model has been developed to describe the continuous, steady state operation of the flow sheet described in Fig. 3. The model is based on fundamental mass balances of the main components and phase equilibrium data in the form of equations of the binodial and tie-lines. SPEEDUP, a powerful equation based simulator, was used to solve the model [9], which has been fitted to two sets of data: (i) separation of *E. coli* homogenate proteins, and (ii) separation of α-amylase from *Bacillus subtilis* supernatant. Here we will describe the application of the model to the former data.

4.1. Process description

The process illustrated in Fig. 3 is a two-stage continuous separation system based on the results for thaumatin discussed above. The first stage is the main separation step where F1 is *E. coli* lysate with or without cell debris together with the protein product. As above, the protein product is partitioned to the top phase and then back extracted into a fresh bottom phase, the top phase is recycled and added to a fresh bottom phase. Recycle of the PEG phase minimises product loss, which in turn, increases process yield in comparison to a single stage batch extraction.

4.2. Phase equilibrium

To allow for a robust separation process, prediction of the phase diagram is essential. Although precise equations do not exist, an exponential empirical curve (Eq. 1) can be fitted to the experimental data, as shown in Fig. 6.

$$Y = A \exp(BX) \quad (1)$$

where Y is the PEG concentration, X is the phosphate concentration and A and B are system constants. For a binodial of PEG 4000–phosphate $A = 79\%$ (PEG) and $B = -0.26$ (1/% salt).

4.3. Phase separation

Phase separation was modelled by calculating the total amount of each component entering a stage divided by the sum of the flow-rates. This provided the point in the phase diagram corre-

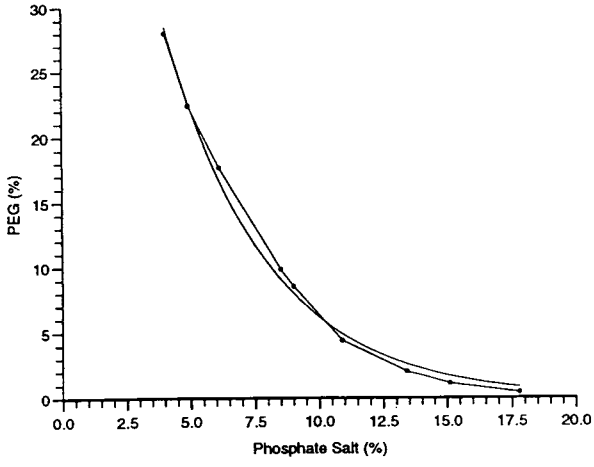

Fig. 6. Comparison graph of the binodial of the PEG 4000–phosphate system determined experimentally *versus* the exponential curve.

sponding to that stage. This point has an associated tie-line whose equation is calculated and then the intersections of the tie-line with the binodial curve are found, *i.e.* the composition of PEG in state 1 (Fig. 3), YM1 is:

$$YM1 = \frac{F1 \cdot \mathrm{PEG1} + F2 \cdot \mathrm{PEG2}}{F1 + F2} \quad (2)$$

where $F1$ and $F2$ are the flow-rates entering a stage and PEG1 and PEG2, the compositions of PEG in these streams.

From the point on the diagram, the associated tie-line is found which has the equation for a straight line:

$$Y = MX + C \quad (3)$$

where Y and X are the PEG and phase forming salt (*e.g.* phosphate) compositions, M is the slope and C is a constant [9].

4.4. Prediction of system performance

The model has been used to study the effects of input variables on system robustness, purity and yield over a range of conditions. The variables were increased/decreased until the model broke one of the following constraints: (1) the system entering the homogeneous region, left of the binodial curve; (2) the tie-line moving outside of the binodial curve (*i.e.* to the right). Examples of these simulations are shown in Fig. 7a and b.

4.5. System robustness

To study system stability and robustness (defined by operating at a predefined distance from the binodial), movements in the tie-line positions were studied for variations in PEG1, PSAL1, F5 and PSAL5 (see Fig. 3) over their working range. Fig. 8 represents a typical physico-chemi-

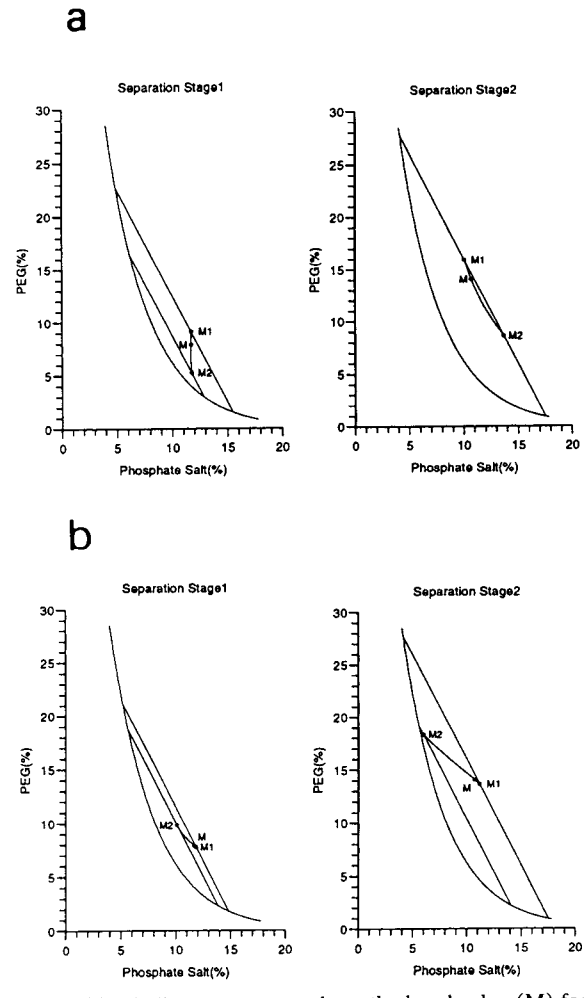

Fig. 7. (a) Tie-line movements about the basal value (M) for step change variations in the concentration of PEG into stage 1. (b) Tie-line movements about the basal value (M) for step change variations in the flow-rate of phosphate salt into stage 2.

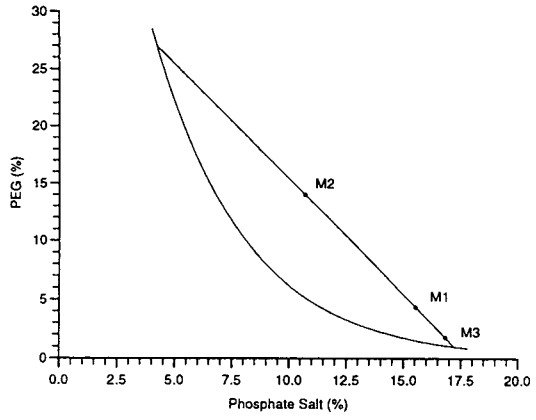

Fig. 8. Typical physico-chemical manipulation graph of the phase ratio.

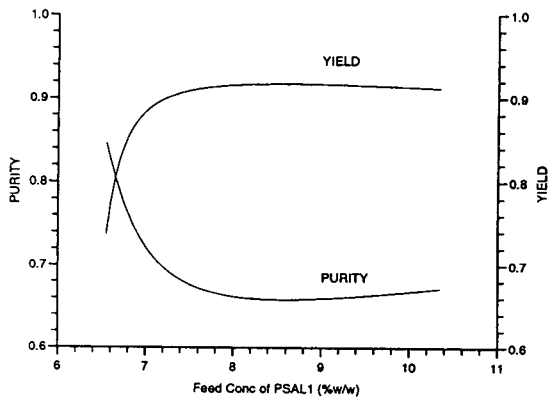

Fig. 9. The effect of varying the concentration of phosphate salt into stage 2 on the overall purity and yield of the process.

cal manipulation of the phase ratio within the same tie-line. This means equal composition of top and bottom phases but changing the phase ratio (equal value for $K_{\text{protein product}}$ and $K_{\text{contaminants}}$). The point M1, on Fig. 8 represents an "ideal" distance from the binodial. M2 is judged to be too far from the binodial; a high concentration of PEG and salt could lead to protein precipitation. Meanwhile M3 is "too close" to the binodial and the system is, therefore, not robust and small variations in system composition could lead to the system falling into the one phase region left of the binodial.

Fig. 7a illustrates the effect of varying the PEG1 concentration entering stage 1. Increasing the PEG 1 concentration (moving from M to M1) leads to a larger top phase and greater product separation in the first stage. This also leads to a smaller bottom phase in the second stage and lower product recovery. Moving from M to M2 represents decreasing the PEG1 concentration giving a smaller top phase in the separation. In the second stage the bottom phase becomes larger and product recovery is increased.

Illustrated in Fig. 7b is the effect of varying the F5 flow-rate (PO_4^{3-}) into stage 2. Increasing the flow-rate moves M to M1 representing a larger volume of PSAL in stage 2 and thus a greater bottom phase. The increased PSAL in stage 2 is recycled into stage 1 also giving a larger bottom phase. Decreasing the flow-rate F5 moves M to M2 which has a drastic effect in stage 2 leading to a very small bottom phase and hardly any product recovery. In stage 1 the bottom phase decreases due to lower PSAL recycle and aids product separation.

4.6. Purity and yield

The effect of varying the four variables, PEG1, PSAL1, F5 and PSAL5, on purity and yield in the overall process was studied. The effect of varying the concentration of phosphate salt into stage 2 is shown in Fig. 9. The purity and yield are fairly constant at high concentrations but there is a dramatic change at the lower range. The region below 7.5–8% PSAL1 concentration is very unstable and this can be attributed to the rapid decrease in tie-line length as we approach the binodial in stage 1. The high partition coefficient and minimal product loss (only in the bottom phase in stage 1) is the principal reason for the high yield observed (0.8–0.92). To improve product purity lowering the partition coefficient for the contaminants, has to be achieved experimentally.

5. Conclusions

The partition of the protein thaumatin in the presence of *E. coli* contaminant proteins has

been studied. Extraction of thaumatin was followed by back-extraction of the product into a new phosphate phase and also back extraction combined with recycle of the top PEG phase. When partitioned in the absence or presence of insoluble cell debris (whole cell homogenate) little effect on the partitioning of thaumatin or the soluble *E. coli* proteins was found. A back extraction step that allowed for dilution of the NaCl (necessary to obtain a high partition coefficient for thaumatin in the first extraction stage) was successful in extracting thaumatin back into a heavy phosphate phase. A second and third back extraction stage further increased this yield.

After back extraction the top PEG phase was successfully recycled to the first extraction. This minimised any loss of thaumatin as it is recycled together with the PEG. The stability ratio (tie-line length) had an effect on the average partition coefficient of *E. coli* soluble proteins in PEG/phosphate systems but in PEG sulphate systems K_{app} was independent of this ratio. An increase in NaCl resulted in an increase in K_{app} but this was always below 1 making these systems suitable for partitioning recombinant proteins into the top PEG phase. A mathematical model, that describes the continuous steady-state operation of extraction and back extraction has been developed: it proved to be an important tool to investigate regions of potential instability in the phase formation and to predict purity and yield after extraction and back extraction.

6. Acknowledgements

This work was partially supported by SERC and Smith, Kline Beecham to whom thanks are due.

7. References

[1] Y. Guan, X.-Y. Wu, T.E. Treffy and H. Lilley, *Biotechnol. Bioeng.*, 40 (1992) 517.
[2] O. Cascone, B.A. Andrews and J.A. Asenjo, *Enzyme Microb. Technol.*, 13 (1991) 629.
[3] J.A. Asenjo, T. Franco, A.T. Andrews and B.A. Andrews, in M.D. White, S. Reuveny and A. Shaffermanin (Editors), *Biologicals from Recombinant Microorganisms and Animal Cells: Production and Recovery*, VCH, Weinheim, 1991, p. 439.
[4] H. Hustedt, K.H. Kroner and N. Papamichael, *Process Biochem.*, 23 (1988) 129.
[5] M.R. Kula, in G. Durand (Editor), *Extraction Processes, Proceedings of the 8th International Biotechnology Symposium*, Vol. 1, Société Française de Microbiologie, Paris, 1988, p. 612.
[6] J.J. Sedmak and S.E. Grossberg, *Anal. Biochem.*, 79 (1977) 544.
[7] A.S. Schmidt, A.M. Ventom and J.A. Asenjo, *Enzyme Microb. Technol.*, 16 (1994) 131.
[8] J.A. Asenjo, A.S. Schmidt, F. Hachem and B.A. Andrews, *J. Chromatogr. A*, 668 (1994) 47.
[9] S.L. Mistry, J.A. Asenjo and C.A., Zaror, *Bioseparation*, 3 (1993) 343.

ELSEVIER

Journal of Chromatography A, 668 (1994) 139–144

JOURNAL OF CHROMATOGRAPHY A

Partitioning of recombinant *Fusarium solani pisi* cutinase in polyethylene glycol–aqueous salt solution two-phase systems

Maria José Sebastião, Joaquim M.S. Cabral, Maria Raquel Aires-Barros*

Laboratório de Engenharia Bioquímica, Instituto Superior Técnico, 1000 Lisbon, Portugal

Abstract

The partition behaviour of *Fursarium solani pisi* recombinant cutinase was studied in polyethylene glycol (PEG)–aqueous sodium or potassium phosphate solution biphasic systems. The partition coefficient of cutinase was enhanced with decreasing molecular mass of the PEG and increasing tie-line length and pH, and was also influenced by the type of cation (Na^+ or K^+) present in the system. Particular attention was paid to the influence of pH and the type of cation on the phase diagrams of PEG–phosphate systems.

1. Introduction

Liquid–liquid extraction using aqueous two-phase systems is a downstream processing technique that can be applied to the large-scale isolation of intracellular enzymes [1–3]. Besides being relatively easy to scale up, this purification technique offers mild conditions for the enzymes as both phases consist mainly of water and the interfacial tension between them is extremely low [4]. Further, aqueous biphasic systems show considerable versatility, allowing enzyme separations to be based on molecular mass, conformation, charge and/or hydrophobicity.

Lipases and other enzymes exhibiting lipolytic activity, such as cutinases [5], are particularly interesting catalysts for applications in the pharmaceutical, detergent and food industries [6]. The purification procedure for these enzymes could be improved by the introduction of liquid–liquid extraction in aqueous biphasic systems, which would avoid some drawbacks related to their hydrophobicity, namely non-specific adsorption on the surfaces of column supports and membranes [7]. A first approach to the optimization of PEG–sodium phosphate systems for the purification of some microbial extracellular lipases from fermentation broth was reported recently by Menge [7].

The aim of this work was to develop a polyethylene glycol (PEG)–sodium or potassium phosphate aqueous two-phase system for extraction of a cutinase from cell debris of a recombinant *Escherichia coli* strain. To define a successful purification system it is desirable to understand the main physico-chemical parameters that affect cutinase partitioning. Hence the influence of polymer molecular mass, polymer concentration, pH and type of cation on the enzyme partitioning properties was investigated using a purified cutinase preparation.

* Corresponding author.

0021-9673/94/$07.00
SSDI 0021-9673(93)E0002-C

2. Experimental

2.1. Chemicals

PEG 1000, 3350 and 8000 were supplied by Sigma. *Fusarium solani pisi* cutinase was produced and purified in our laboratory from an *Escherichia coli* recombinant strain [5], which was a kind gift from Corvas International (Ghent, Belgium).

2.2. Determination of binodials

Biphasic systems were prepared by the addition of appropriate amounts of NaH_2PO_4 or KH_2PO_4 and Na_2HPO_4 or K_2HPO_4 to PEG (50%, w/w) to obtain the required pH value. The systems were completed with water, leading to a total mass of 5.0 g. The mixtures were vortex mixed until complete solubilization of the salts. Fine adjustments of pH were made by adding small volumes of phosphoric acid.

The aqueous two-phase systems were diluted until they became clear after vortex mixing and the polymer and salt concentrations were calculated to determine the binodal. The assays were performed at 24 ± 1°C.

2.3. Preparation of aqueous two-phase systems for cutinase partition assays

The assays were carried out in 10-ml graduated centrifuge tubes with a conical tip. Stock aqueous solutions of PEG (50%, w/w) were measured by mass into the centrifuge tubes. Appropriate amounts of NaH_2PO_4 or KH_2PO_4 and Na_2HPO_4 or K_2HPO_4 were added to obtain the required pH. A 250-μl volume of an aqueous solution of purified cutinase (5 mg/ml) completed the system, which was made up to 5.0 g by addition of water. All phase systems were 10% (w/w) in phosphates. Biphasic systems at pH 5 and 6 were prepared with sodium salts while potassium phosphates were used for pH values ≥6, owing to the low solubility of Na_2HPO_4 and KH_2PO_4. The study of enzyme partitioning behaviour at different tie-lines was carried out by varying the PEG concentration as indicated in Table 1.

Table 1
Polyethylene glycol concentrations (%, w/w) in the phase systems studied

PEG M_r	Short tie-line	Long tie-line	Extra long tie-line
1000	20	25	30
3350	20	25	–
8000	6	12	–

The systems were vortex mixed until complete solubilization of the salts. The phases were separated by a 5-min centrifugation at 1000 *g* in a swing-out rotor. The volumes of the upper and lower phases were noted and a sample of each phase was taken with a pipette for the determination of cutinase activity. The assays were performed in triplicate.

2.4. Cutinase activity assay

The cutinase esterolytic activity was determined spectrophotometrically, following the hydrolysis of *p*-nitrophenyl acetate [8] or *p*-nitrophenyl palmitate [9]. For the former reaction, 5 μl of each phase, diluted 1:10 with distilled water, were added to 1 ml of a 0.5 m*M* *p*-nitrophenyl acetate solution in 50 m*M* potassium phosphate buffer (pH 8). The reaction was followed for 2–5 min at 400 nm. For the hydrolysis of *p*-nitrophenyl palmitate, 15 mg of this substrate were solubilized in 5 ml of 2-propanol and added to 45 ml of 50 m*M* potassium phosphate buffer (pH 8) containing 103.5 mg of sodium deoxycholate and 50 mg of gum arabic. A 40-μl volume of each phase diluted 1:10 with distilled water was added to 960 μl of the reaction buffer described above. The reaction was followed for 2–10 min at 410 nm. Both reactions were performed at 24 ± 1°C. A blank was prepared by the same procedure as described above, adding to the substrate solution a sample of top or bottom phase of a corresponding phase system that did not contain the enzyme. The total activity recovered in both

phases was compared with the initial preparation.

Preliminary studies in which the cutinase activity and stability were measured in the presence of high concentrations of PEG 1000, 3350, 8000 and phosphates were carried out. Under the conditions of the activity assays described above, no interference of these components of the phase systems on the enzyme activity was detected. Further, the cutinase maintained full activity for at least 3 h in the presence of polymer or salt.

3. Results and discussion

3.1. Effect of pH and type of cation on PEG–phosphate binodals

The influence of some physico-chemical parameters considered for the study of cutinase partitioning properties on the binodals of PEG–phosphate systems was analysed. Figs. 1 and 2 show the effect of pH and type of cation (Na^+ or K^+) on PEG 1000–phosphate and PEG 3350–phosphate binodals, respectively.

For both phase-forming polymers, decreasing pH values from 7.5 to 6.0 and from 6.0 to 4.5 increased the polymer and salt concentrations required for phase formation. This effect can be explained by the increase in the $H_2PO_4^-/HPO_4^{2-}$ ratio with decreasing pH. In fact, as the monovalent anion is less effective in salting out PEG [10], a higher salt and/or polymer concentration will be needed to obtain a biphasic system. At high pH values the displacement of binodals was almost negligible. The binodials obtained at pH 7.5 and 9.0 are almost coincident in systems formed by either PEG 1000 (Fig. 1) or PEG 3350 (Fig. 2).

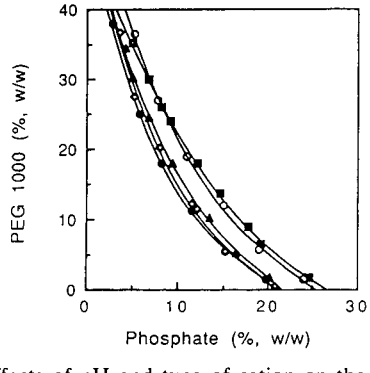

Fig. 1. Effects of pH and type of cation on the binodial of the PEG 1000–phosphate system at 24 ± 1°C. Sodium phosphate: ◘ = pH 4.5; ● = pH 6.0. Potassium phosphate: ○ = pH 6.0; ▲ = pH 7.5; ◇ = pH 9.0.

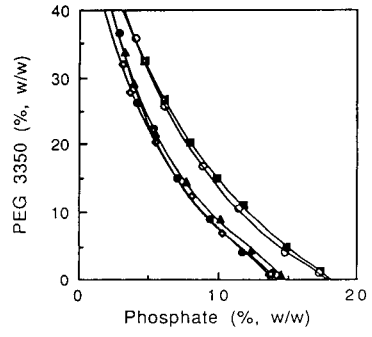

Fig. 2. Effects of pH and type of cation on the binodal of the PEG 3350–phosphate system at 24 ± 1°C. Symbols as in Fig. 1.

For the same pH (6), the replacement of sodium with potassium phosphates increased the polymer and/or salt concentrations required for phase formation (Figs. 1 and 2). The binodal obtained at pH 6 with sodium phosphates was almost coincident with that obtained at pH 9 with potassium phosphates and the binodals for the PEG 1000– or PEG 3350–potassium phosphate systems at pH 6 were almost coincident with those corresponding to PEG 1000– or PEG 3350–sodium phosphate systems at pH 4.5 (Figs. 1 and 2). These results suggest that Na^+ is more effective than K^+ in salting out PEG.

3.2. Effect of PEG molecular mass, pH and polymer concentration on cutinase partitioning

The influence of PEG molecular mass and concentration and pH on cutinase partitioning in PEG–sodium or potassium phosphate biphasic systems is shown in Tables 2–4. The partition coefficient, K, is defined as the ratio between cutinase activity per millilitre in the upper and lower phases. Each K value represents the average of three measurements. Eight independent

Table 2
Effects of pH and polymer concentration on the cutinase partition coefficient, K, and total enzyme yield from both upper and lower phases in PEG 1000–sodium or potassium phosphate (10%, w/w) biphasic systems at 24 ± 1°C

pH	PEG (%, w/w)	K	Yield (%)
5	–	–	–
	25	10	81
	30	48	97
6	20	6.8	97
	25	27	98
	30	91	100
8	20	20	100
	–	–	–
	30	141	100
9	20	41	100
	25	165	100
	30	303	100

measurements were carried out for one selected system to obtain the statistical significance of the results. The relative standard deviation of the partition coefficient was 11%. Results shown for pH 6 and 20% or 25% PEG are the average of the partition coefficients calculated for phase systems containing sodium and potassium phosphates.

In phase systems formed by PEG 1000, cutinase was mainly in the upper phase under all the experimental conditions tested (Table 2). When PEG 1000 was replaced with PEG 3350 (Table 3), pH and polymer concentration determined the predominance of the enzyme in either the upper or lower phase. Biphasic systems containing PEG 8000 led cutinase to accumulate preferentially in the lower phase under all the experimental conditions tested (Table 4). The decrease in protein partition coefficient with increasing PEG molecular mass in PEG–phosphate phase systems has been described previously and is probably a consequence of excluded volume effects [11].

Table 3
Effects of pH and polymer concentration on the cutinase partition coefficient, K, and total enzyme yield from both upper and lower phases in PEG 3350–sodium or potassium phosphate (10%, w/w) biphasic systems at 24 ± 1°C

pH	PEG (%, w/w)	K	Yield (%)
5	20	0.50	71
	25	0.75	63
6	20	0.36	81
	25	1.4	75
8	20	0.67	100
	25	3.9	98
9	20	2.8	100
	25	15	100

Table 4
Effects of pH and polymer concentration on the cutinase partition coefficient, K, and total enzyme yield from both upper and lower phases in PEG 8000–sodium or potassium phosphate (10%, w/w) biphasic systems at 24 ± 1°C

pH	PEG (%, w/w)	K	Yield (%)
6	–	–	–
	12	0.10	100
8	6	0.07	100
	12	0.06	100
9	6	0.11	100
	12	0.13	100

Polymer concentration and pH proved to be important factors for cutinase partitioning in biphasic systems formed by PEG 1000 and 3350 (Tables 2 and 3). The increase in enzyme partition coefficient with increase in PEG concentration may result from changes in the specific volume of the phases. As more PEG is added to the system the specific volume of the upper phase remains approximately constant while the specific volume of the lower phase decreases rapidly [12]. Hence the water molecules available for solute solvation in the lower phase decrease and cutinase reaches its solubility limit, being forced to partition to the upper phase.

The partition coefficient of cutinase increased strongly with increase in pH (Tables 2 and 3). These results may be partly explained by the displacement of the binodal towards lower polymer and salt concentrations with increasing pH (Figs. 1 and 2), which could be compared with the effect of increasing PEG concentration, as

described above. However, the binodals for phase systems at pH 7.5 and 9 (both containing potassium phosphates) are almost superimposable and the cutinase partition coefficients at these pH values are significantly different, particularly for the systems containing PEG 3350. In fact, the greatest increase in cutinase partition coefficient in these systems is observed when the pH is raised from 8 to 9.

In addition to changes in free volume, other physico-chemical factors seem to be involved in the enzyme partitioning behaviour with pH such as the charge variation of protein ionic groups and their interaction with polymer molecules [13].

3.3. Effect of type of cation on cutinase partitioning and yield

Table 5 shows the influence of the type of cation (Na^+ or K^+) on cutinase partitioning in phase systems formed by PEG 1000 or PEG 3350 and phosphates at the same pH (6). In biphasic systems containing PEG 1000 the enzyme partition coefficient appeared to decrease when Na^+ was replaced with K^+. The displacement of the binodal towards higher polymer and salt concentrations observed when potassium phosphates were used instead of sodium phosphates (Fig. 1) suggests that changes in the free volume of the phases are responsible for the effect of the type of cation on the cutinase partitioning pattern.

An opposite effect of the type of cation on the cutinase partitioning was observed for phase systems formed by PEG 3350, in which K increased when sodium phosphates were replaced with potassium phosphates. In these systems, sodium phosphates caused cutinase precipitation, only about 50% of the enzyme being recovered in both the upper and lower phases (Table 5). Protein precipitation did not occur when potassium salts were present or when PEG 1000 was the phase-forming polymer (Table 5). According to the influence of the type of cation on the binodial (Fig. 2), aqueous two-phase systems formed by PEG 3350 and sodium phosphates would possibly induce an increase in the cutinase partition coefficient, as happened for systems containing PEG 1000, if the enzyme did not reach its solubility limit in the upper phase.

Table 5
Effect of the type of cation on the cutinase partition coefficient, K, and total cutinase yield from both upper and lower phases in PEG (25%, w/w)–phosphate (10%, w/w) biphasic systems at 24 ± 1°C and pH 6

Cation	PEG M_r	K	Yield (%)
Na^+	1000	31	95
	3350	1.2	50
K^+	1000	22	100
	3350	1.6	100

4. Conclusions

The partition coefficient of cutinase was enhanced with decreasing PEG molecular mass, probably owing to PEG excluded volume effects. Increasing the polymer concentration promoted the salting out of cutinase, enhancing the partitioning of the enzyme to the upper phase. Increasing the pH also raised the cutinase partition coefficient, which may partly result from the displacement of the binodal towards lower polymer and/or salt concentrations. In fact, increasing the pH decreased the polymer and/or salt concentrations required for phase formation as the divalent anion HPO_4^{2-} is more effective in salting out PEG than the monovalent anion $H_2PO_4^-$.

For the same pH (6), the replacement of potassium with sodium phosphates displaced the binodal towards lower polymer and/or salt concentrations, suggesting that Na^+ is more effective than K^+ in salting out PEG. This shift of the binodal to lower compositions in the presence of Na^+ raised the tie-line length of PEG 1000 or PEG 3350 (25%)–phosphate (10%) phase systems, probably leading to an increase in the salting out of the enzyme. This effect resulted in the enhancement of the enzyme partition coefficient for the system formed by PEG 1000. In the PEG 3350–sodium phosphate phase system, cutinase apparently reached its solubility limit in

both phases, being subject to the excluded volume effects of PEG 3350, and was partially precipitated.

5. Acknowledgements

This work was partly financed by the BRIDGE Programme [contract BIOT-CT91-0274 (DTEE)]. M.J. Sebastião acknowledges a Ph.D. fellowship from Programa Ciência, Junta Nacional de Investigação Científica e Technológica, Portugal.

6. References

[1] H. Hustedt, K.H. Kroner, W. Stach and M.R. Kula, *Biotechnol. Bioeng.*, 20 (1978) 1989.
[2] K.H. Kroner, H. Schutte, W. Stach and M.R. Kula, *J. Chem. Technol. Biotechnol.*, 32 (1982) 130.
[3] A. Veide, A.L. Smeds and S.O. Enfors, *Biotechnol. Bioeng.*, 25 (1983) 1789.
[4] P.A. Albertsson, *Partition of Cell Particles and Macromolecules*, Wiley, New York, 1985.
[5] M. Lauwereys, P. De Geus, J. De Meutter, P. Stanssens and G. Matthyssens, in L. Algerghina, R.D. Schmid and R. Verger (Editors), *Lipases: Structure, Mechanism and Genetic Engineering (GBF Monographs*, Vol. 16), GBF Braunschweig, 1990, p. 243.
[6] K.D. Mukherjee, *Biocatalysis*, 3 (1990) 277.
[7] U. Menge, *J. Am. Chem. Soc.*, 2181 (1992) 331.
[8] M. Sugiura and M. Isobe, *Chem. Pharm. Bull.*, 24 (1976) 72.
[9] U.K. Winkler and M. Stuckmann, *J. Bacteriol.*, 138 (1979) 663.
[10] K.P. Ananthapadmanabhan and E.D. Goddard, *J. Colloid Interface Sci.*, 113 (1986) 294.
[11] D.H. Atha and K.C. Ingham, *J. Biol. Chem.*, 256 (1981) 12108.
[12] J.G. Huddleston, K.W. Ottomar, D.M. Ngonyani and A. Lyddiatt, *Enzyme Microb. Technol.*, 13 (1991) 24.
[13] J. Huddleston, A. Veide, K. Kohler, J. Flanagan, S.O. Enfors and A. Lyddiatt, *Trends Biotechnol.*, 9 (1991) 381.

ELSEVIER

Journal of Chromatography A, 668 (1994) 145–152

JOURNAL OF CHROMATOGRAPHY A

Integration of aqueous two-phase extraction and affinity precipitation for the purification of lactate dehydrogenase

Dong Guoqiang*, Rajni Kaul, Bo Mattiasson

Department of Biotechnology, Chemical Center, Lund University, Box 124, S-221 00 Lund, Sweden

Abstract

Integration of extraction in aqueous two-phase system and affinity precipitation was investigated as a technique for purification of lactate dehydrogenase (LDH) from porcine muscle extract. An enteric coating polymer, Eudragit S 100, which can be made reversibly soluble and insoluble by change in pH was used as the ligand carrier. The ligand used was Cibacron blue 3GA. The polymer is nearly totally partitioned to the top phase (>98%) in PEG–dextran aqueous two-phase system. The enzyme, lactate dehydrogenase, was first spontaneously partitioned to the bottom phase in a 6% (w/w) PEG 8000–8% (w/w) dextran T250 phase system. New PEG phase and Eudragit-dye were then added to the bottom phase, which helped in extraction of LDH to the top phase. After a washing step with a fresh bottom phase, Eudragit-dye–target protein affinity complex was precipitated out from the top phase by lowering the pH to 5.1. The enzyme was recovered by treatment of the complex with 0.5 *M* NaCl with a yield of 54% and a specific activity of 245 units/mg. The purification of LDH by this procedure was better than that obtained by a single step of affinity partitioning.

1. Introduction

Aqueous two-phase partitioning is an established technique for use during the initial stages of downstream processing of proteins [1]. The most attractive feature of these systems is the rapid removal of cell debris and particulate matter with minimal requirements of energy. The incorporation of affinity interactions in these systems has provided an element of specificity for purification of proteins. A number of studies have been carried out using this concept [2–4]. The most popular ligands for use in affinity partitioning have been reactive dyes, which are generally coupled to polyethylene glycol (PEG), the top phase polymer in the two-phase system.

Precipitation is another technique used often during large-scale protein purification. It is generally non-specific, the more specific form being termed affinity precipitation. One of the strategies of affinity precipitation involves the use of a reversibly soluble–insoluble polymer as a ligand carrier; the separation of the affinity complex being effected by the precipitation of the polymer [5]. The precipitation can be carried out by change in either pH, ionic strength, temperature, etc., depending on the nature of the polymer.

In an earlier report we described the integration of affinity precipitation with extraction in aqueous two-phase system for the purification of Protein A from recombinant *Escherichia coli* [6]. The affinity ligand, immunoglobulin G (IgG), was coupled to Eudragit, a polymer which precipitates under acidic conditions. Eudragit partitions to the PEG-rich phase, making it possible

* Corresponding author.

0021-9673/94/$07.00
SSDI 0021-9673(93)E0029-T

to design the affinity extraction on the same grounds as using PEG-bound ligands. This procedure combines the advantages of gentle and rapid separation obtained by aqueous two-phase extraction with the possibility of having a better control over the ligand and the easy recovery of the target protein from the phase polymers by affinity precipitation.

The present report deals with the use of the above concept for the purification of lactate dehydrogenase (EC 1.1.1.27) from porcine muscle extract using Eudragit-bound Cibacron blue.

2. Experimental

2.1. Materials

Eudragit S 100 was a gift from Röhm Pharma (Weiterstadt, Germany). Polyethylene glycol (PEG) 8000 was procured from Union Carbide Co. (New York, NY, USA). Dextran T250 (av. mol. mass 298 000), 1-ethyl-3-(3-dimethylaminopropyl) carbodiimide hydrochloride (EDC), Cibacron blue 3GA and β-nicotinamide adenine dinucleotide, reduced form (NADH), were purchased from Sigma (St. Louis, MO, USA). 1,4-Diaminobutane was from Merck (Darmstadt, Germany). All other chemicals were of analytical grade.

2.2. Methods

Preparation of muscle extract

100 g porcine muscle were homogenized with 250 ml of 100 m*M* ice-cold potassium phosphate buffer pH 7.9 in a standard household mixer for 5 min. The homogenate was centrifuged at 27 300 *g* for 20 min and the supernatant was collected. About 200 ml of ice-cold water were added to the settled debris, mixed well, homogenized and then centrifuged under the same conditions. The supernatants were pooled and filtered using filter paper to remove the floating fat. Muscle extract (280 ml) thus obtained was stored at −20°C until use.

Immobilization of Cibacron blue to Eudragit S 100

Eudragit S 100 (2.0 g) was suspended in 80 ml of 0.2 *M* K_2HPO_4 solution and pH adjusted to 8.0 with 1 *M* NaOH for dissolving the polymer. Initial use of phosphate buffer facilitated subsequent solubilization of Eudragit. However, to prevent the interference of phosphate ions during activation of carboxyl groups, the Eudragit was precipitated by reducing pH to 4.5 and centrifuged (10 400 *g* for 10 min). The precipitate was washed twice with distilled water and finally solubilized at a concentration of 4% in water at pH 6.2.

The above native Eudragit solution (25 ml) was stirred together with 0.3 g carbodiimide (EDC) at 22°C for 20 min. To this were then added 10 ml of 30% diaminobutane solution at final pH 9.2. The stirring was continued for 4 h at the same temperature, after which the Eudragit was precipitated by lowering the pH to 4.5, and centrifuged at 10 400 *g* for 10 min to get rid of unreacted diaminobutane. The precipitate was redissolved in water at pH 8.0 by adding 0.5 *M* NaOH.

To the modified Eudragit solution were added 1.0 g of Na_2CO_3 and 0.5 g of Cibacron blue, and the pH of the solution was adjusted to 10 with 1 *M* NaOH. After continuous shaking at 22°C for 20 h, the polymer-bound dye (Eudragit-dye) was precipitated by lowering pH of the solution to 4.8 and centrifuged at 3000 *g* for 10 min. The supernatant with the bulk of the free dye was discarded. The remaining unbound dye in the precipitate was later removed by adsorption to pretreated DEAE-cellulose [7].

The precipitate was dissolved in 100 ml of water at pH 6.8–7.0 and mixed with the pretreated ion exchanger (2.5 g dry weight). The suspension was filtered; the filtrate contained the bulk of the Eudragit-dye. The ion exchanger was then treated with 2 *M* KCl solution to elute the adsorbed Eudragit-dye. The Eudragit-dye in the filtrate and eluate were pooled and washed twice with water by alternating precipitation at pH 4.5 and resolubilization at pH 7.0. The Eudragit-dye was finally dissolved in water at pH 7.0 with a concentration of 0.38%.

Precipitation behavior of Eudragit-dye

To 0.5 ml of 0.38% Eudragit-dye solution in a test tube was added 0.5 ml of 0.1 *M* citrate buffer of a certain pH and 1 ml of water or 20% PEG 8000 solution. After proper mixing, the tube was allowed to stand for about 10 min at room temperature. As a control, the native Eudragit solution of the same concentration was treated in a similar manner. The precipitation of the native Eudragit at a particular pH was determined by measuring turbidity at 470 nm [6], and that of Eudragit-dye by measuring the absorbance of dye in the supernatant at 612 nm after centrifugation.

Two-phase system

Stock solutions of 30% PEG 8000, 30% dextran T250 and 0.5 *M* potassium phosphate buffer, pH 7.6 were prepared. The concentrations of the polymers are given as % (w/w). Unless specifically mentioned, the aqueous two-phase systems used were composed of 6% PEG and 8% dextran and the concentration of the phosphate buffer was 50 m*M*. The volume ratio of the top to bottom phase was 1.35. For affinity partitioning, Eudragit-dye was added to the above two-phase system.

Purification procedure

30% PEG solution, 30% dextran solution, the porcine muscle extract, 0.5 *M* phosphate buffer and water were mixed to form 13 g of aqueous two-phase system having a final concentration of 6% PEG, 8% dextran, 10% muscle extract and 0.05 *M* phosphate buffer. After mixing and centrifuging at 1625 *g* for 5 min, the top and bottom phase were separated. Fresh top phase with the same composition as above but containing 0.18% Eudragit-dye was added to the bottom phase. After mixing and subsequent separation by centrifugation, the bottom phase was discarded and replaced with a fresh bottom phase. Then the top phase was removed, the Eudragit-bound affinity complex was precipitated by reducing the pH of the top phase to 5.1 with 0.5 *M* citric acid and centrifuged at 3000 *g* for 10 min. After washing once with 5 ml of 20 m*M* citrate buffer, pH 5.1, the precipitate was solubilized in 4 ml of 0.5 *M* NaCl at pH 7.0. After 30 min incubation, Eudragit-dye was precipitated at pH 5.1 and centrifuged. The supernatant containing the enzyme was collected. The treatment of Eudragit-dye for desorption of the enzyme was repeated once more. The Eudragit-dye was washed once with water and re-used for the next cycle of purification.

Analytical methods

The partition coefficients (*K*: the ratio of concentration in the top phase to that in the bottom phase) of LDH, Eudragit-dye and protein in the two-phase system were determined by measuring their concentrations in the top and bottom phase, respectively.

Lactate dehydrogenase activity was determined according to Decken [8] by reduction of pyruvate to lactate. The consumption of NADH was followed by measuring the reduction in absorbance at 340 nm at room temperature. One unit of the LDH activity was defined as the amount of enzyme which catalyzes the consumption of 1 μmol of NADH per min under the standard assay conditions.

Total protein concentration was determined by the bicinchoninic acid method as described by Smith *et al.* [9]. Bovine serum albumin was used as a standard.

The amount of Cibacron blue immobilized on Eudragit was determined by measuring the absorbance of the dye in Eudragit-dye solution at 612 nm [10]. The weight of Eudragit-dye was estimated by precipitating it at pH 4.5, washing the precipitate with water at the same pH and drying overnight at 105°C and weighing.

Sodium dodecyl sulphate–polyacrylamide gel electrophoresis (SDS-PAGE) with 12% acrylamide was performed to check the purity of the samples [11]. The molecular mass markers consisted of rabbit muscle phosphorylase b (M_r 97 000), bovine serum albumin (M_r 66 000), ovalbumin (M_r 45 000), bovine carbonic anhydrase (M_r 31 000), soybean trypsin inhibitor (M_r 22 000) and hen egg white lysozyme (M_r 14 400), available as a standard kit (Bio-Rad Laboratories, Richmond, CA, USA).

3. Results and discussion

3.1. Binding of Cibacron blue to Eudragit

Eudragit is an anionic copolymer based on methacrylic acid and methylmethacrylate with an average molecular mass of 135 000. The carboxyl groups on the polymer have been utilized for the coupling of enzymes, proteins and other molecules via their amino groups [6,12,13]. As Cibacron blue does not possess the required amino group, its coupling to Eudragit could be performed in the presence of a spacer group like diaminobutane [14]. The reaction between this group and the dye is favored at high pH. At 22°C, the highest amount of immobilized dye was obtained at about pH 10.0.

Coupling of Cibacron blue to Eudragit at different temperatures showed that although the initial binding of the dye was greater at higher temperature, it was reduced after a period of 1.5–2 h (data not shown). In contrast, covalent coupling of the dye was favored at lower temperature and long reaction time. About 130 mg of Cibacron blue were bound per gram Eudragit preparation after coupling at pH 10, 22°C for 20 h. This temperature dependence was in full agreement with the result reported concerning coupling of Cibacron blue to PEG [7]. The separation of the free dye from the bound dye was facilitated due to the ability of Eudragit to precipitate under acidic conditions. Small amounts of the free dye left over could then be adsorbed to DEAE-cellulose as described earlier for removal of free dye from PEG-dye [7].

3.2. Eudragit-dye characteristics

Native Eudragit has a soluble–insoluble transitional region between pH 4.6 and 5.5. The region was shifted slightly upward on the pH scale after dye was immobilized on the Eudragit (Fig. 1). A similar shift was observed for the polymer in the presence of 10% PEG. These observations are in accordance with the results reported earlier for IgG–Eudragit [6]. This shift would mean that the separation of Eudragit bound affinity complex may be carried out at relatively favorable pH values, which in turn may lower the risk of enzyme denaturation.

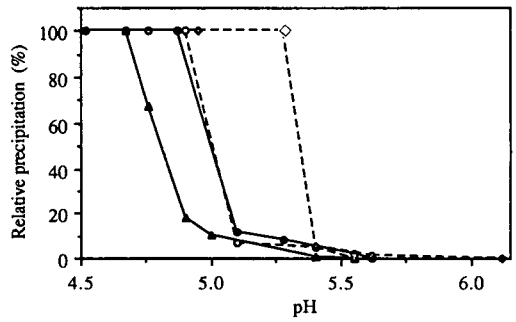

Fig. 1. Precipitation curve of Eudragit S 100 (solid lines) and Eudragit-dye (dashed lines) in response to variation of pH. Symbols: (▲) native Eudragit; (○) Eudragit-dye; (●) native Eudragit + 10% PEG and (◇) Eudragit-dye + 10% PEG.

The partitioning of Eudragit in aqueous two-phase systems is an important parameter to consider if the polymer is to be used as a ligand carrier. The earlier studies on partition of Eudragit in PEG–Reppal two phase system showed that at a concentration of 0.5%, more than 97% of the polymer partitioned into the top phase [6]. Eudragit-dye exhibited a similar partition behavior in PEG–dextran two-phase system. The effect of different salts on the partitioning was also studied (Fig. 2). Increase in potassium phosphate concentration strongly promoted the partitioning of Eudragit-dye to the top phase. Ammonium sulfate had a weaker effect while

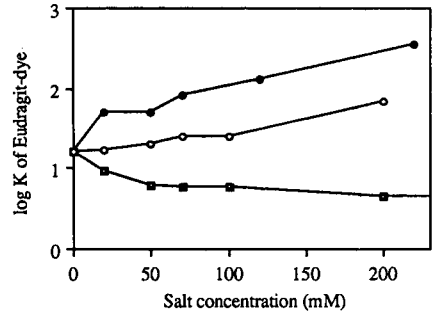

Fig. 2. Effect of salt on the partitioning of Eudragit-dye in 6% PEG 8000–8% dextran T250 system. The salts added were potassium phosphate (●), ammonium sulfate (○), and sodium chloride (■). The concentration of Eudragit-dye was 0.025%.

NaCl favored the partitioning to the bottom phase. This is also in agreement with the earlier observations [6].

3.3. Effect of Eudragit and Eudragit-dye on LDH partitioning in two-phase system

When the porcine muscle extract was added to a PEG–dextran two-phase system, most of the proteins including LDH (log $K = -1.0$) partitioned into the bottom phase. The presence of native Eudragit in the same two-phase system had little influence on protein and enzyme partitioning (Fig. 3). However, in the presence of increasing concentrations of Eudragit-dye, while most of the other proteins still remained in the bottom phase, the partitioning of LDH to the top phase was increased significantly. At an Eudragit-dye concentration of 0.05%, the increase of log K of LDH was 2.45, and more than 95% of the enzyme went into the top phase. While the partitioning of Eudragit-dye to the top phase continuously increased with the increase in phosphate concentration in the system (Fig. 2), the log K of LDH increased only up to a phosphate concentration of 70 mM (Fig. 4). With further increase in the salt concentration, the enzyme remained in the bottom phase because of the lowered affinity between the dye and the enzyme. Hence, 50 mM phosphate buffer (pH 7.6) was used during LDH purification in the two-phase system.

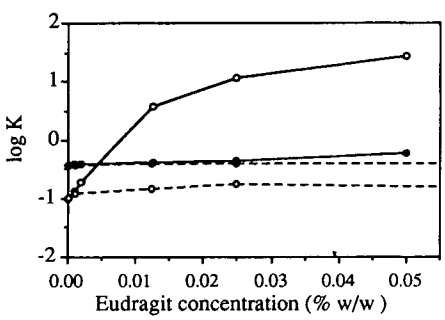

Fig. 3. Effect of native Eudragit (dashed lines) and Eudragit-dye (solid lines) concentration on the partition coefficient of the total protein (●) and LDH (○) in the 6% PEG 8000–8% dextran T 250 system at pH 7.6.

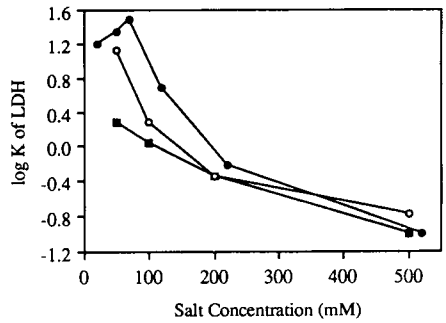

Fig. 4. Effect of salt on the partitioning of lactate dehydrogenase from porcine muscle extract in 6% PEG 8000–8% dextran T250 system containing 0.025% Eudragit-dye. The salts added were potassium phosphate (●), ammonium sulfate (○), and sodium chloride (□).

3.4. Effect of PEG and dextran concentration on LDH partitioning

Fig. 5 shows the effect of PEG and dextran concentration on the partition coefficient of LDH in a two-phase system without and with Eudragit-dye. In the absence of Eudragit-dye, enzyme partitioned predominantly into the bottom phase. The log K value of the enzyme decreased significantly with increase in PEG concentration, while a slight decrease was observed at higher dextran concentrations. The

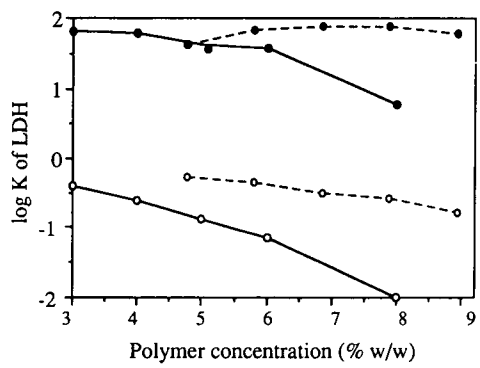

Fig. 5. Effect of PEG 8000 (solid lines) and dextran T 250 (dashed lines) concentration on partitioning of LDH from muscle extract in the two-phase system without Eudragit-dye (○) and with 0.025% Eudragit-dye (●). The dextran concentration was maintained at 7% as PEG concentration was varied, while the PEG concentration was 4% with change in dextran concentration.

extreme partitioning of proteins obtained by increasing the polymer concentrations has been documented earlier [15]. In the presence of Eudragit-dye, the enzyme partitioned efficiently into the top phase. There was a slight decrease in the partition coefficient with increase in PEG concentration, while it remained more or less constant with change in dextran concentration.

The pH of the two-phase system also influenced the enzyme partition in the presence of Eudragit-dye, the optimal pH being in the range of 7.4–8.7. This corresponds to the pH range in which LDH has maximal affinity for Cibacron blue.

3.5. Adsorption capacity of Eudragit-dye vs. enzyme concentration

The binding of LDH to Eudragit-dye in the aqueous two-phase system would be influenced by the components of the two-phase system, ion concentration, pH and protein load. Fig. 6 shows that at lower loading of the muscle extract in PEG–dextran system containing Eudragit-dye, more than 97% of LDH was taken into the top phase while the dye was still in excess with respect to LDH concentration. At the enzyme concentration of 54 U/g, the Eudragit-dye bound per mg 180 U of LDH corresponding to 89% of the total enzyme loaded in the two-phase system. Overloading of the extract in the system resulted in the excess enzyme remaining in the bottom phase. It is well known that Cibacron blue is a group-affinity ligand and that it has affinity for other dehydrogenases and kinases present in the muscle extract. Hence, the real capacity of the Eudragit-dye for pure LDH would be expected to be higher.

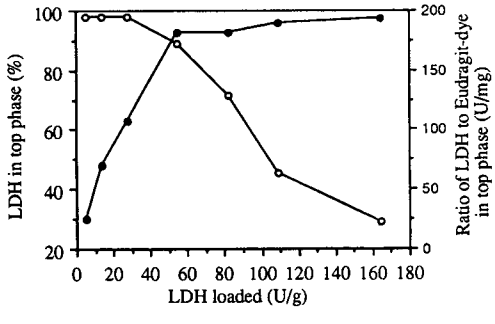

Fig. 6. Partitioning of LDH in 5% PEG 8000–7% dextran T 250 system containing 0.01% Eudragit-dye as a function of different amounts of muscle extract. Symbols: (○) % enzyme recovery in the top phase, and (●) ratio of L-LDH activity per mg Eudragit-dye.

3.6. Purification of lactate dehydrogenase from the muscle extract

Purification of LDH by affinity partitioning in aqueous two-phase systems using dye–PEG and sometimes even dye–dextran has been described earlier in several reports [2,16]. Normally 3 to 4 extraction steps are required to obtain LDH of high purity (around 300–500 U/mg protein) [4]. The effect of introducing additional "washing" steps besides that of affinity partitioning using Eudragit-dye was studied (Table 1). Affinity extraction of the enzyme directly from the crude extract resulted in only about 5-fold increase in purification. However, adding the "washing" steps before and after the affinity step resulted in almost 12 times increase in the enzyme specific activity. Fig. 7 shows the protein pattern obtained on electrophoresis of samples purified by different methods.

The number of steps required for purification would depend on the system under study. In the previous report, purification of Protein A by partitioning using IgG–Eudragit in PEG–Reppal system and subsequent elution of the protein after precipitation of the affinity complex yielded a nearly pure preparation in just one extraction step [6]. The present system is based on a ligand which is group-specific, it binds proteins present in the crude muscle extract with different affinities.

Based on the above experiments, a three-step purification protocol was adopted. Initially, the muscle extract was added to the PEG–dextran system and over 84% of LDH activity was recovered in the bottom phase (Table 2). The top phase with some of the contaminant proteins and the interface with cell debris were discarded. Fresh top phase containing Eudragit-dye (46 mg dye per gram Eudragit preparation) was equilibrated with the bottom phase, resulting in the

Table 1
Effect of different procedures on LDH purification from muscle extract

Method		Specific activity (U/mg protein)	Purification factor
1	Muscle extract and Eudragit-dye added into two-phase system. The Eudragit-dye–enzyme complex precipitated by reducing pH of PEG phase to 5.1. LDH eluted out with salt.	108.4	5.2
2	Method 1 + "washing" with fresh bottom phase before precipitation.	153.1	7.3
3	Muscle extract partitioned without Eudragit-dye before method 1.	181.0	8.6
4	Method 3 + "washing" with fresh bottom phase before precipitation.	247.7	11.8

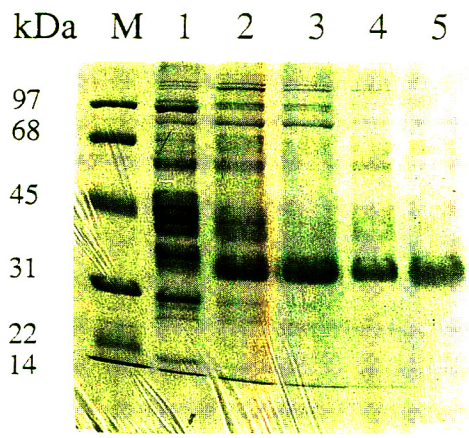

Fig. 7. SDS-PAGE pattern of LDH purification from muscle extract by different procedures. For details, see Table 1. Lane M, marker proteins; lane 1, crude muscle extract; lane 2, method 1; lane 3, method 2; lane 4; method 3; lane 5, method 4.

partitioning of LDH to the top phase. After washing, affinity precipitation and elution, the specific activity and the yield of eluted L-LDH were 245 U/mg and 54% respectively (Table 2). SDS-PAGE showed a single band having a molecular mass of 34 000 (Fig. 7). The reduced yield of LDH during the elution step may partly be due to the denaturation of the enzyme under conditions of low pH. After the whole procedure, the recovery of the Eudragit-dye was 91%. The 9% loss arose partly from the solution transfer during operation and partly from some Eudragit-dye sticking with the particulate matter from the muscle extract and partitioning into the interface. The possible dye leaching will also contribute to the loss.

As a comparison, dissociation of the enzyme from the affinity complex was performed by the addition of the salt phase (11% potassium phos-

Table 2
Purification of crude LDH by integration of two-phase extraction and affinity precipitation

Phase system no.	Stage	Total LDH (U)	Specific LDH (U/mg)	Purification factor	Yield (%)
	Muscle extract	427.1	21.0	1.0	100.0
1	Bottom phase	361.8	34.8	1.7	84.7
2	Top phase	306.9	125.0	6.0	71.9
3	Top phase	292.2	208.1	9.9	68.4
	Elution 1	196.0	245.0	11.7	45.9
	Elution 2	36.3	250.0	11.9	8.0

phate, pH 7.6) to the top phase such that the LDH was transferred to the salt rich phase. The yield of the enzyme was increased to 71%, however with a lowered specific activity of only 199 U/mg. Gel electrophoresis showed the presence of several faint protein bands along with the main band of LDH. To purify the enzyme further, the enzyme solution was dialysed against 10 m*M* phosphate buffer and then treated with DEAE-cellulose. After centrifugation at 3000 *g* for 10 min, 81% of LDH activity remained in the supernatant. The specific activity was 297 U/ml, showing a single band on the electrophoresis gel (Fig. 8).

These results show that using Eudragit as a ligand carrier in aqueous two-phase systems, one has the choice of either precipitating out the polymer bound affinity complex for subsequent enzyme desorption, or dissociating the affinity complex present in the top phase by addition of a salt phase. The former strategy avoids the introduction of salt into the PEG phase and also the removal of the phase polymers from the purified protein is simplified. This purification is also possible using the cheaper bottom phase polymer, Reppal PES, as evidenced from earlier studies [6]. Preliminary studies have also shown the possibility of reuse of Eudragit in two-phase systems.

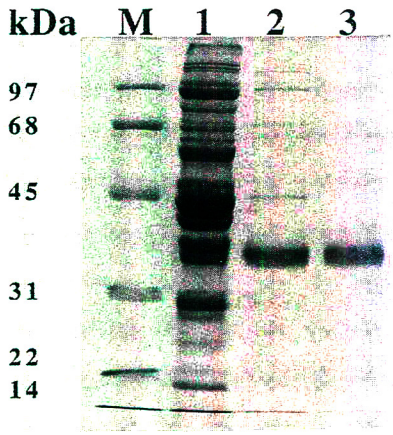

Fig. 8. SDS-PAGE pattern of muscle extract proteins at different stages of LDH purification. Lane M, marker proteins; lane 1, crude muscle extract; lane 2, the enzyme after purification by two-phase partitioning and lane 3, supernatant after DEAE-cellulose treatment.

This study has thus demonstrated that integration of aqueous two-phase extraction and affinity precipitation offers an interesting technology combining many of the strong features of the two sub-technologies.

4. Acknowledgements

This work was supported by a grant from the Swedish Agency for Research Cooperation with Developing Countries (SAREC) and the National Swedish Board for Technical and Industrial Development (NUTEK).

5. References

[1] H. Hustedt, K.H. Kroner and M-R. Kula, in H. Walter, D.E. Brooks and D. Fisher (Editors), *Partitioning in Aqueous Two-Phase Systems*, Academic Press, Orlando, FL, 1985, p. 529.
[2] G. Kopperschläger and G. Birkenmeier, *Bioseparation*, 1 (1990) 235.
[3] J. Kirchberger, G. Kopperschläger and M.A. Vijayalakshmi, *J. Chromatogr.*, 557 (1991) 325.
[4] F. Tjerneld, G. Johansson and M. Joelsson, *Biotechnol. Bioeng.*, 30 (1987) 809.
[5] R. Kaul and B. Mattiasson, *Bioseparation*, 3 (1992) 1.
[6] M. Kamihira, R. Kaul and B. Mattiasson, *Biotechnol. Bioeng.*, 40 (1992) 1381.
[7] G. Johansson and M. Joelsson, *Biotechnol. Bioeng.*, 27 (1985) 621.
[8] L.A. Decken, in *Worthington Enzyme Manual*, Worthington Biochemical Corporation, 1977, p. 19.
[9] P.K. Smith, R.I. Krohn and E.K. Hermanson, *Anal. Biochem.*, 150 (1985) 76.
[10] V. Bouriotis and P.D.G. Dean, *J. Chromatogr.*, 206 (1981) 521.
[11] U.K. Laemmli, *Nature*, 227 (1970) 680.
[12] M. Taniguchi, S. Tanahashi and M. Fujii, *Appl. Microbiol. Biotechnol.*, 33 (1990) 629.
[13] E. Linné-Larsson and B. Mattiasson, *Biotechnol. Tech.*, in press.
[14] C.R. Lowe, M. Glad, P.-O. Larsson, S. Ohlson, D.A.P. Small, T. Atkinson and K. Mosbach, *J. Chromatogr.*, 215 (1981) 303.
[15] G. Johansson and M. Andersson, *J. Chromatogr.*, 303 (1984) 39.
[16] G. Johansson and M. Joelsson, *Enzyme Microbiol. Technol.*, 7 (1985) 629.

ELSEVIER

Journal of Chromatography A, 668 (1994) 153–164

JOURNAL OF CHROMATOGRAPHY A

Studies of the interaction of NADH oxidase from *Thermus thermophilus* HB8 with triazine dyes

J. Kirchberger[a], H. Erdmann[b], H.-J. Hecht[b], G. Kopperschläger*,[a]

[a]*Institute of Biochemistry, University of Leipzig, Liebigstrasse 16, D-04103 Leipzig, Germany*

[b]*Gesellschaft für Biotechnologische Forschung mbH (GBF), Marscheroder Weg 1, D-38124 Braunschweig, Germany*

Abstract

NADH oxidase from *Thermus thermophilus* HB8 was selected to study the interaction of flavoproteins with structurally defined dye ligands. The fact that the enzyme binds NADH in addition to FAD favours the enzyme as a model for studying the interaction of enzymes with biomimetic ligands. In addition, the crystal structure of the holoenzyme is known. Applying affinity partitioning in aqueous two-phase systems, difference spectroscopy, affinity chromatography and kinetics, results about the chemistry of binding and the binding site(s) for various triazine dyes were obtained. The binding of the dyes to the enzyme is stabilized by hydrophobic and electrostatic forces. The binding behaviour is influenced by small differences in the structure of the dye ligands. In most instances the dye ligands occupy both FAD binding sites of the enzyme dimer; this is particularly shown for Procion Red H-8BN by kinetic and difference spectroscopic studies. An "optimum" structural model of a biomimetic ligand of NADH oxidase from *Thermus thermophilus* HB8 is proposed, requiring the presence of a disulphonated aminonaphthol ring combined with another aromatic negatively charged residue and a hydrophobic arm at a distance between 7 and 13 Å.

1. Introduction

The enzyme NADH oxidase from *Thermus thermophilus* HB8 catalyses the oxidation of NADH or NADPH with the formation of hydrogen peroxide in the presence of FAD, FMN or riboflavin as cofactor using oxygen as electron acceptor. In the absence of oxygen also other electron acceptors such as methylene blue, cytochrome *c* and 2,6-dichlorophenol are accepted [1]. The enzyme was found to be a dimeric flavoprotein with an apparent molecular mass of 43 600. Two molecules of FAD are bound per enzyme dimer [2].

For affinity chromatographic purification of the NADH oxidase from *Thermus thermophilus* HB8, Cibacron Blue F3G-A (CB F3G-A), a very common biomimetic dye ligand, has been used [1].

Although some data on the interaction between flavoproteins and dye ligands have already been published [3–5], the chemistry of binding and the binding site(s) are still unknown. For NADH- and ATP-dependent enzymes it has been reported that biomimetic dye ligands bind competitively to the nucleotide binding site [6]. As NADH oxidase from *Thermus thermophilus* HB8 binds NADH in addition to FAD, the latter, in contrast to many other flavoproteins, is not tightly bound, and this enzyme seems to be

* Corresponding author.

0021-9673/94/$07.00
SSDI 0021-9673(93)E1245-U

of particular interest for studying its interaction with biomimetic dye ligands. Further, a crystallographic analysis of the enzyme–dye complex appears to be feasible after the completion of the crystal structure analysis of the holoenzyme [7].

In this work, we applied the technique of affinity partitioning to study the interaction of a number of chemically defined reactive dyes with NADH oxidase. From the results of this screening procedure a set of dyes were selected to analyse the dye–enzyme interaction in more detail by application of difference spectroscopy, affinity chromatography and kinetic studies.

2. Experimental

2.1. Materials

Procion dyes were obtained from ICI Organics Division (Blackley, UK) and Cibacron dyes from Ciba Geigy (Basle, Switzerland). The dyes were deactivated and purified according to Lowe and Pearson [8] before use in difference spectroscopy and kinetics. The commercial names of the dyes are abbreviated as follows: P = Procion; C = Cibacron; B = blue; G = green; N = navy; O = orange; R = red; Y = yellow. NADH and FAD were purchased from Boehringer (Mannheim, Germany). Polyethylene glycol 6000 (PEG 6000), dextran 60 ($M_r \approx 75\,000$) and dextran 500 ($M_r \approx 450\,000$) were obtained from Serva (Heidelberg, Germany) and dextran T10 ($M_r \approx 9900$) from Pharmacia (Uppsala, Sweden). All other biochemicals were of analytical-reagent grade.

2.2. Preparation of the immobilised dye-derivatives

Dye–PEG

Triazine dyes were covalently coupled to PEG 6000 in aqueous alkaline solution and dye–PEG derivatives were purified by extraction with chloroform and followed by ion-exchange chromatography on DEAE-cellulose according to Johansson [9]. The purity of the conjugates was analysed by thin-layer chromatography on silica gel G 60 plates (Merck, Darmstadt, Germany) in 1-butanol–2-propanol–ethyl acetate–water (20:35:10:35, v/v). The cleavage of the azo linkages yielding H-E3B(M)–PEG and H-3B(M)–PEG, respectively was performed as described previously [10].

Dye–Sepharose

Procion and Cibacron dyes were coupled to Sepharose 4B as described by Hughes *et al.* [11].

2.3. Enzyme purification

NADH oxidase from *Thermus thermophilus* HB8 cloned and expressed in *Escherichia coli* has been purified by heat treatment, affinity chromatography on Blue-Sepharose and cation-exchange chromatography on S-Sepharose to homogeneity in the flavin-free form [12]. All experiments were performed with the flavin-free apoenzyme.

2.4. Enzyme assay

NADH oxidase was assayed by measuring the initial rate of oxidation of NADH at 340 nm in the presence of oxygen and FAD as described by Park *et al.* [1]. One unit of activity is defined as the amount of enzyme that converts 1 μmol of substrate per minute in 50 m*M* potassium phosphate buffer (pH 7.2) at 37°C. The protein concentration of the purified enzyme was determined spectrophotometrically at 280 nm based on $A^{1\%}_{1\,cm} = 14.88$.

2.5. Kinetics

The kinetic parameters and the inhibition constants were determined in 50 m*M* potassium phosphate buffer (pH 7.2) at 25°C by measuring the rate of oxidation of NADH at 340 nm. While varying the concentration of NADH the concentration of FAD was kept constant at 127 μM and while varying the concentration of FAD the concentration of NADH was fixed at 173 μM. The concentration of PR H-8BN–PEG was varied between 0 and 0.25 μM. The type of inhibi-

tion and the inhibition constants were calculated by non-linear regression analysis [13].

2.6. Aqueous two-phase partitioning

Two-phase systems were prepared from stock standard solutions of PEG 6000 (20%, w/w), dextran (30%, w/w) and 0.5 *M* potassium phosphate buffer (pH 7.2). The polymer concentrations are given as a percentage of the mass of the system. The amount of dye-liganded PEG given in per cent is refered to the total mass of PEG present in the system. The systems (2 g) containing about 5 units of NADH oxidase, equivalent to 58 μg of protein, were adjusted to 25°C and equilibrated by gently mixing for 30 s. After centrifugation at 1500 *g* for 5 min, samples were withdrawn from both phases for enzyme assay. Inhibition of the enzyme in the assay mixture by the dye–PEG was avoided by sufficient dilution of the samples with buffer. The partition coefficient, *K*, is defined as the ratio of the enzyme activity per unit volume in the top and bottom phases.

2.7. Affinity chromatography

Disposable columns (40 × 8 mm I.D.) (Bio-Rad Labs., Munich, Germany) containing a 1.0-ml bed volume of dye-liganded Sepharose 4B were equilibrated with 50 m*M* potassium phosphate buffer (pH 7.2) at 25°C. The dialysed enzyme was applied in excess to the column (*ca.* 35 units) and the unbound enzyme, *ca.* 2–5 units, was washed out with equilibration buffer at a flow-rate of 20 ml/h. The bound enzyme activity was eluted with equilibration buffer containing effectors as indicated in Table 6.

2.8. Difference spectroscopy

Difference spectroscopy was performed with a Specord M40 double-beam spectrophotometer (Carl Zeiss, Jena, Germany) using 50 m*M* potassium phosphate buffer (pH 7.2) at 25°C. The light path of the cuvettes was 10 mm and the spectra were recorded at a scan rate of 2 nm/s and a constant slit width of 0.5 nm. The difference spectra were recorded after adding the same amount of the dye to the reference and the sample cells, respectively, containing concentrations of the effectors and the enzyme as given in the legends of Fig. 4 and Table 3. The dye concentrations were determined spectrophotometrically by using the following molar absorption coefficients (l/mol · cm): Procion Red H-E3B (530 nm), 30 000; Procion Red H-8BN (546 nm), 21 300; Procion Red H-3B (530 nm), 18 100; Procion Red MX-8B (530 nm), 19 210; Procion Red MX-5B (523 nm), 23 690; Procion Green H-E4BD (628 nm), 45 610; Cibacron Blue F3G-A (610 nm), 13 600; and Cibacron Blue 3G-A (622 nm), 11 600.

3. Results

In order to optimize the conditions of the affinity partitioning, the distribution of the enzyme was studied in a first set of experiments as a function of the polymer concentration at a constant ratio of PEG and dextran and the relative molecular mass (M_r) of dextran (see Table 1). Systems of PEG–dextran T10 at ratios below 8:12 and systems of PEG–dextran 60 at ratios below 5:7.5 were completely miscible at 25°C. With increasing concentration of the two

Table 1
Partitioning of NADH oxidase depending on the polymer concentration and the relative molecular mass (M_r) of dextran

PEG 6000/dextran concentration ratio (w/w)	Log K^a		
	Dextran T10	Dextran 60	Dextran 500
4:6	c.m.	c.m.	−0.01
5:7.5	c.m.	−0.05	−0.12
6:9	c.m.	−0.16	−0.18
7:10.5	c.m.	−0.41	−0.20
8:12	−0.49	−0.49	−0.25
9:13.5	−0.70	−0.58	−0.29

The systems (2 g) contained 50 m*M* potassium phosphate buffer (pH 7.2), PEG 6000 (4–9%, w/w) and 5 units of purified apoenzyme. The systems were equilibrated at 25°C. The M_r values of dextrans are given under Experimental.
[a] c.m. = Complete miscibility.

polymers and by reducing the M_r of dextran, the partition coefficient of the enzyme decreased. In a system composed of 13.5% dextran T10, 9% PEG and 50 m*M* potassium phosphate buffer (pH 7.2), the partition coefficient of the enzyme was sufficiently low for the detection of changes in the partition behaviour of the enzyme caused by addition of the dye-liganded PEG to the system.

A series of 28 structurally different dyes, covalently coupled to PEG, were screened by determining the extent of the affinity partition effect (Δ log K). Δ log K was calculated from the difference in the logarithms of the partition coefficient of the enzyme in the presence and absence of the affinity ligand. In all instances 0.5% of the total PEG was replaced with dye-liganded polymer. Higher concentrations of dye–PEG led to increasing inhibition of the enzyme.

As shown in Fig. 1, the affinity partition effect of the dye ligands was heterogeneous. A number of dye ligands showed relatively low Δ log K values (PO MX-G, PO MX-2R, PY P-5GN, PY MX-R and CB BR-P), whereas others such as PN MX-RB, CR 3BA, PR H-8BN, PR H-E3B and PG H-E4BD generated a Δ log K higher than 1.5. Most of the screened dye ligands exhibited moderate Δ log K values between 0.5 and 1.5.

The strength of interaction was characterized by studying the affinity partitioning of the enzyme as a function of the concentration of selected dye ligands. With increasing concentration of dye–PEG, saturation curves were obtained as shown, for example, for CB F3G-A, PR H-8BN and PG H-E4BD in Fig. 2.

To determine the maximum extraction power (Δ log K_{max}) and the relative affinity (aff_R), defined as the ligand concentration that gener-

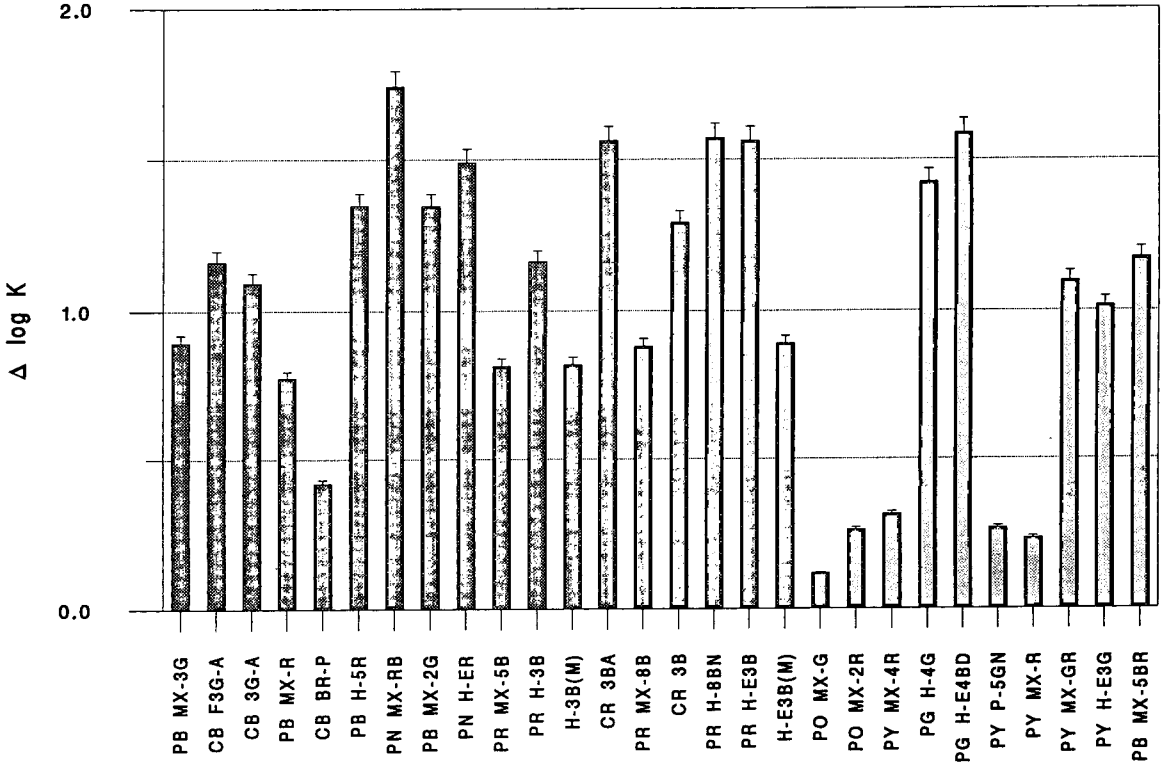

Fig. 1. Effect of diverse dye–PEG derivatives on the affinity partitioning of NADH oxidase. The systems (2 g) were composed of 13.5% (w/w) dextran T10 and 9% (w/w) PEG 6000 including 0.5% of the respective dye–PEG derivative, 50 m*M* potassium phosphate buffer (pH 7.2) and 5 units of enzyme. The systems were equilibrated at 25°C.

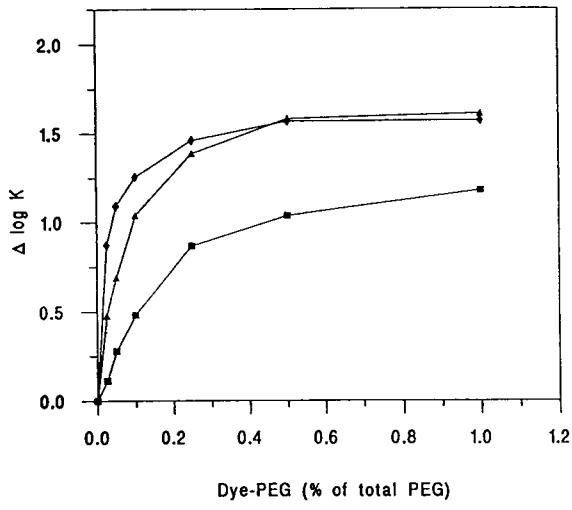

Fig. 2. Affinity partitioning of NADH oxidase as a function of the concentration of (□) CB F3G-A, (◆) PR H-8BN and (▲) PG H-E4BD covalently coupled to PEG 6000. The systems (2 g) contained 13.5% (w/w) dextran T10, 9% (w/w) PEG 6000, 50 m*M* potassium phosphate buffer (pH 7.2) and 5 units of enzyme. The partitioning was performed at 25°C.

ates 50% of Δ log K_{max}, a linear regression analysis of the double reciprocal plot was used. The highest Δ log K_{max} values were calculated for CB 3G-A, CB BR-P and PG H-E4BD (Table 2).

According to the mathematical approach of Flanagan and Barondes [14], which assumes different affinities of the dye ligand in the top and bottom phases, the dissociation constants (K_d) in both phases and the number of independent binding sites (n) were calculated by using a non-linear regression analysis [13]. The best curve fit for all dye ligands was achieved assuming two binding sites per enzyme dimer. The dissociation constants in the top phase (K_{d_T}) coincides with the values of the relative affinity (aff_R). The dissociation constant in the bottom phase (K_{d_B}) was found to be significantly lower than K_{d_T} for all dye ligands studied. Dye ligands exhibiting high affinity were PB MX-2G, PR H-E3B, PR H-8BN, PG H-E4BD and PR H-3B (azo dyes) and dyes with low affinity were CB B-RP, CB 3G-A, PB MX-3G (anthraquinone dyes) and PR MX-5B (azo dye).

By comparing the relationship between the structure of the ligand and the binding behaviour, it became obvious that small differences in the structure can cause drastic changes in the affinity to NADH oxidase. For example, a comparison of the affinities of PR H-8BN and PR MX-8B (Table 2) and the structures of these dyes (Fig. 3D) indicates that the removal of the methylanilino group gives rise to a significant decrease in the affinity of the ligand. Similar correlations were obtained after splitting off the sulphonated terminal ring(s) in PR H-E3B and PR H-3B by reducing the azo bridge with $Na_2S_2O_4$, yielding H-E3B(M) and H-3B(M), respectively, or by changing the position of the sulphonic acid group on the terminal aromatic ring from *meta/para-* (CB F3G-A) to *ortho-* (CB 3G-A) (for structures see Fig. 3C).

In order to correlate the strength of interaction with the structure of the dye ligand, difference spectroscopy was applied to the following pairs of free dyes; (A) PR H-E3B–PG H-E4BD; (B) PR H-3B–PR MX-5B; (C) CB F3G-A–CB 3G-A; and (D) PR H-8BN–PR MX-8B. The structures of these dyes are shown in Fig. 3. The results are summarized in Tables 3 and 4.

The kind of interaction was established according to Subramaniam [15] by comparing the shapes of the difference spectra of the dye–enzyme complex with that of the free dye in 0.5 *M* NaCl and 50% ethylene glycol, as shown for PR H-8BN in Fig. 4. In all instances a mixed type of hydrophobic and electrostatic interactions was found. All spectra showed one or two isosbestic points, indicating that only one class of binding sites is titrated.

Applying a non-linear regression analysis according to Barden *et al.* [16], the dissociation constants (K_d), the number of binding sites (n) and the absorption coefficients of the dye–enzyme complexes were calculated. A comparison of the dissociation constants obtained from affinity partitioning (Table 2) and difference spectroscopy is given in Table 4. The data from difference spectroscopy corroborate the existence of two binding sites for the dye per enzyme dimer. All dissociation constants are in the range of the K_m values for NADH and FAD. By

Table 2
Affinity partitioning of NADH oxidase

Dye–PEG	Double reciprocal plot (1/Δ log K *versus* 1/[Dye–PEG])		Constants calculated according to the model of Flanagan and Barondes [14]		
	Δ log K_{max}	aff_R (μM)	K_{d_T} (μM)	K_{d_B} (μM)	n
Cibacron Blue F3G-A	1.42	34.90	27.70	2.95	2
Procion Blue MX-R	1.24	26.81	23.32	2.00	2
Cibacron Blue 3G-A	2.09	91.28	55.72	19.58	2
Procion Blue B-RP	1.77	113.57	81.71	16.56	2
Procion Blue MX-3G	1.35	56.22	47.60	4.89	2
Procion Red H-E3B	1.51	4.55	3.17	0.38	2
H-E3B(M)[a]	1.02	30.29	29.50	2.02	2
Procion Blue MX-2G	1.52	3.28	2.33	0.29	2
Procion Green H-E4BD	1.77	8.61	5.45	0.84	2
Procion Red H-3B	1.43	10.47	8.14	0.85	2
H3B(M)[b]	1.60	58.10	43.99	6.58	2
Procion Red MX-5B	1.26	57.58	50.34	4.48	2
Cibacron Red 3BA	1.62	14.86	10.28	1.29	2
Procion Red MX-8B	1.24	39.76	34.79	3.00	2
Procion Red H-8BN	1.60	4.94	3.29	0.44	2
Procion Blue H-5R	1.50	15.88	11.77	1.43	2

The systems (2 g) containing 9% (w/w) PEG 6000 (0–1% dye-liganded PEG), 13.5% (w/w) dextran T10, 50 mM potassium phosphate buffer (pH 7.2) and 5 units of enzyme were equilibrated at 25°C.
[a] Procion Red H-E3B reduced with $Na_2S_2O_4$.
[b] Procion Red H-3B reduced with $Na_2S_2O_4$.

comparing the ratio of the k_{d_T}, K_{d_B} and K_d values within the four pairs of structurally related dyes a good correlation was found with both methods, with the exception of PR MX-8B–PR H-8BN.

In order to obtain information about the specificity of interactions, the influence of NADH and FAD on the affinity partitioning, the quenching effect in difference spectroscopy and the elution behaviour of the enzyme from affinity columns were studied. The affinity partitioning of the enzyme in the presence of 4 mM NADH and 2 mM FAD is shown in Table 5. To normalize the conditions of the competitive experiments, dye–PEG concentrations that were equivalent to $2K_{d_T}$ were applied. The partition coefficients of NADH and FAD were 0.88 and 1.11, respectively.

The addition of NADH caused a moderate decrease in the affinity partitioning effect (Δ log K) for all dyes studied. Only with PR MX5B a decrease in Δ log K of more than 40% was observed. The effect of FAD is more pronounced for these selected dyes. No influence could be detected with PR HE-3B and PR MX-5B. A stronger competition of the formation of the dye–enzyme complex by FAD was found with PG H-E4BD, PR MX-8B and PR H-8BN.

The influence of NADH and FAD on difference spectroscopy and on affinity chromatography is summarized in Table 6. NADH showed almost no quenching effect, with the exception of PR MX-5B. In affinity chromatography substantial amounts of enzyme were eluted with NADH when immobilized PR H-8BN, CB F3G-A and PR MX-5B were used. The stronger interfering effect of FAD was demonstrated by both methods. Minute quenching and no ability to elute the enzyme were found for PR H-E3B and PR MX-5B. However, the competition of

A

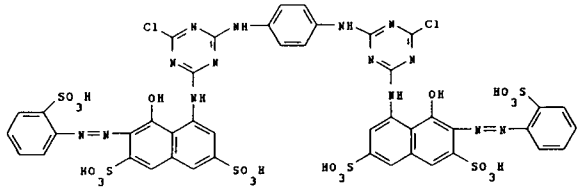

Procion Red H-E3B

B

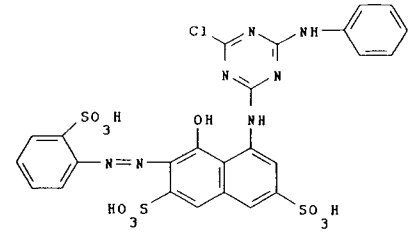

Procion Red H-3B

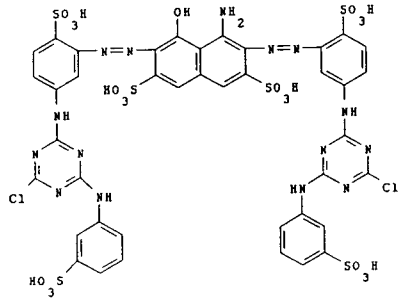

Procion Green H-4EBD

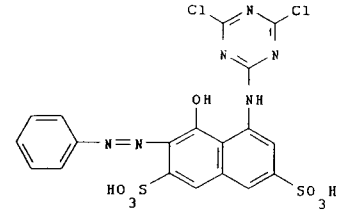

Procion Red MX-5B

C

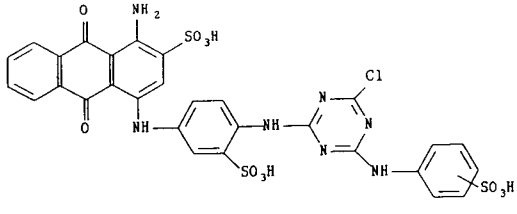

Cibacron Blue F3G-A

D

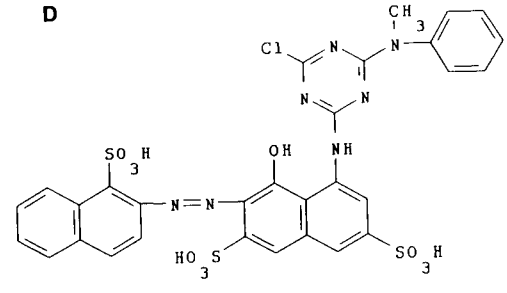

Procion Red H-8BN

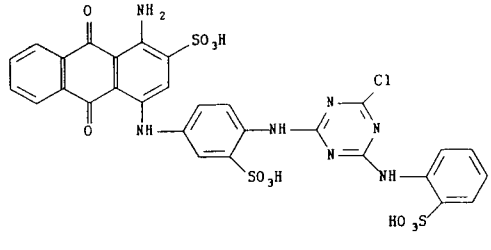

Cibacron Blue 3G-A

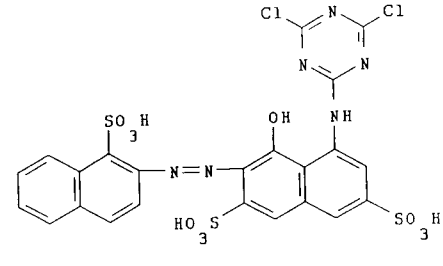

Procion Red MX-8B

Fig. 3. Structures of triazine dyes.

Table 3
Difference spectroscopy of NADH oxidase

Dye	Kind of interaction	λ_{max} (nm)	λ_{min} (nm)	Isosbestic point (nm)
Procion Red H-E3B	Mixed	555	496	510
Procion Green H-E4BD	Mixed	688	595	652
Procion Red H-3B	n.d.[a]	560	496	510
Procion Red MX-5B	Mixed	568	502	550
Procion Red MX-8B	Mixed	574	502	555
Procion Red H-8BN	Mixed	576	510	556
Cibacron Blue F3G-A	Mixed	688	586	645 and 512
Cibacron Blue 3G-A	Mixed	686	583	650 and 503

Both the sample and the reference cuvette contained 50 m*M* potassium phosphate buffer (pH 7.2). The initial enzyme concentration in the sample cuvette was 0.8–1.0 μM. The dye was added from a stock standard solution (1 m*M*) in small portions (1–5 μl) to both cuvettes. All measurements were made at 25°C.
[a] Not detectable.

FAD with the formation of the dye–enzyme complex is more pronounced with PR H-8BN, CB F3G-A, PR MX-8B and PG H-E4BD, as seen by the quenching effect and the elution recovery. The high recovery in the elution of the enzyme when using 50% ethylene glycol in buffer confirms the contribution of hydrophobic forces to the stabilization of the dye–enzyme complexes. The low recovery in the elution of the enzyme from dye-affinity columns containing PR H-8BN and CB F3G-A as immobilized ligands (Table 6) can be increased significantly without decreasing of the purification factor by addition of 25% (v/v) ethylene glycol to the NADH-containing elution buffer.

The kinetic analysis of the NADH oxidase in the presence of PR H-8BN covalently coupled to PEG 6000 revealed a competitive type of inhibition with respect to FAD. The type of inhibition

Table 4
Comparison of the dissociation constants obtained from affinity partitioning and difference spectroscopy

Dye	Affinity partitioning		*n*	Difference spectroscopy
	K_{d_T} (μM)	K_{d_B} (μM)		K_d (μM)
Procion Red H-E3B	3.17	0.38	2	1.72
Procion Green H-E4BD	5.45	0.84	2	2.37
Procion Red H-3B	8.14	0.85	2	2.24
Procion Red MX-5B	50.34	4.48	2	12.48
Procion Red MX-8B	34.79	3.00	2	0.14
Procion Red H-8BN	3.29	0.44	2	2.72
Cibacron Blue F3G-A	27.70	2.95	2	1.60
Cibacron Blue 3G-A	55.72	19.58	2	5.59

NADH, $k_m = 3\ \mu M$; FAD, $K_m = 72\ \mu M$.

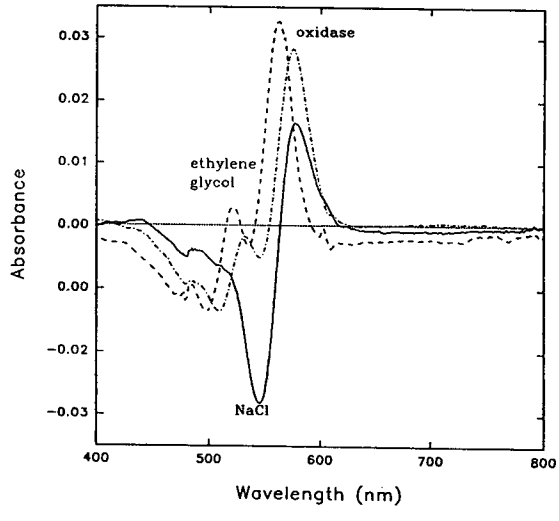

Fig. 4. Difference spectra of PR H-8BN. All spectra were recorded in 50 m*M* potassium phosphate buffer (pH 7.2) at 25°C in the presence of (——) 0.5 *M* NaCl at a dye concentration of 28.9 μM, (– – –) 50% (v/v) ethylene glycol at a dye concentration of 2.5 μM and (– · – · –) 0.9 μM NADH oxidase at a dye concentration of 2.7 μM.

Table 5
Influence of FAD and NADH on the affinity partitioning of NADH oxidase

Dye–PEG	Remaining Δ log K (%)[a]	
	2 m*M* FAD	4 m*M* NADH
Procion Red H-E3B	100	68
Procion Green H-E4BD	26	71
Procion Red H-3B	62	65
Procion Red MX-5B	100	52
Procion Red MX-8B	43	62
Procion Red H-8BN	48	74
Cibacron Blue F3G-A	59	71
Cibacron Blue 3G-A	67	73

The systems (2 g) contained 13.5% (w/w) dextran T10, 9% (w/w) PEG 6000, 50 m*M* potassium phosphate buffer (pH 7.2), 4 m*M* NADH or 2 m*M* FAD and 5 units of enzyme. The partitioning was performed at 25°C.
[a] Δ log K in the absence of NADH or FAD was taken as 100%.

with respect to NADH is not easy to distinguish. Both non- and uncompetitive effects are possible. The calculated kinetic constants are summarized in Table 7. All estimated inhibition constants (K_i; K_{ii}; K_{iii}) are significantly lower than the K_m for NADH and FAD, corroborating the finding of the high affinity of the dye ligand.

4. Discussion

This study has shown that affinity partitioning of NADH oxidase from *Thermus thermophilus* HB8 in aqueous two-phase systems is applicable to the study of the interaction of the enzyme with biomimetic dye ligands. The method seems to be sensitive enough to recognize even small differences in the affinity of the dye to the target enzyme which can be caused either by structural alterations of the dye ligand or by addition of competing effectors.

In comparison with difference spectroscopic studies applying the free dye and to kinetic analysis using dye-liganded PEG, the specific environment of a two-phase system [polymer concentrations up to 25% (w/w)] and the covalent attachment of the dye to PEG has to be taken into account. Therefore, dissociation constants obtained by difference spectroscopy, kinetics and affinity partitioning are not identical as free dyes bind with higher affinity than the polymer-coupled ligands and the affinity of the free dye ligand as well as the polymer-bound dye decreases with increasing concentration of PEG. This behaviour has been shown by inhibition studies with NADH oxidase and alkaline phosphatase from calf intestine in buffer–polymer mixtures (unpublished data) and from fluorescence spectroscopic measurements [17,18]. In conclusion, the study of dye–enzyme interaction using the free ligand cannot *per se* predict quantitatively the binding behaviour of the biomimetic dye in a conjugated form.

The present state of the knowledge about the chemistry of interaction of NADH oxidase from *Thermus thermophilus* HB8 and various triazine dyes can be summarized as follows:

(i) The binding of triazine dyes to NADH oxidase from *Thermus thermophilus* HB8 is realised by hydrophobic and electrostatic forces. This follows from the results of affinity chromatography (elution with ethylene glycol) and from the difference spectroscopic data. The low influence of ionic strength on affinity chromatography of the enzyme can be caused by the coupling of the dye to the matrix, which could decrease the accessibility of the negatively charged terminal ring of the dye ligand.

(ii) The binding of the dye ligands involves in most instances the FAD binding site of the enzyme. The extent to which the NADH-binding region is involved in the binding of the dye cannot be elucidated.

(iii) Small changes in the structure of the dye ligands can alter the binding properties drastically. PR H-E3B, which interacts with other flavoproteins [19,20], binds the NADH oxidase from *Thermus thermophilus* HB8 with high affinity but shows no change of interaction in the presence of FAD. PG H-E4BD seems to be a good biomimetic ligand for NADH oxidase, because a strong competition with FAD was found. Similarly, NADH oxidase from *Streptococcus faecalis* containing tightly bound FAD also possesses a high affinity to this dye ligand. However, the

Table 6
Influence of NADH and FAD on affinity chromatography and difference spectroscopy of NADH oxidase

Affinity chromatography							
Effector[a]	Dye-liganded Sepharose 4B						
	PR H-E3B	PG H-E4BD	PR H-3B	PR MX-5B	PR MX-8B	PR H-8BN	CB F3G-A
	Activity eluted (%)[b]						
NADH (4 m*M*)	0	3	0	19	3	27	28
FAD (2 m*M*)	0	52	14	0	25	35	26
NaCl (500 m*M*)	0	5	20	0	0	18	10
Ethylene glycol (50%, v/v)	0	95	99	92	95	99	92
Difference spectroscopy with free dyes							
Effector[a]	Quenching of the signal (%)[c]						
Effect of NADH (4 m*M*)	2	5	2	20	1	2	5
Effect of FAD (1 m*M*)	1	49	57	10	48	71	87
Type of interaction[d]	m	m	n.d.	m	m	m	m

All measurements were performed in 50 m*M* potassium phosphate buffer (pH 7.2) at 25°C.
[a] Dissolved in 50 m*M* potassium phosphate buffer (pH 7.2) at 25°C.
[b] Total bound activity was taken as 100%.
[c] Decrease of signal ($absorbance_{max} - absorbance_{min}$); the signal of the dye-saturated enzyme was taken as 100%.
[d] m = mixed; n.d. = not detectable.

Table 7
Inhibition of NADH oxidase by PR H-8BN covalently coupled to PEG 6000

Inhibition with respect to	Type of inhibition and kinetic constants (μM)					
	Competitive		Non-competitive		Uncompetitive	
	K_i	K_m	K_{ii}	K_m	K_{iii}	K_m
FAD (NADH constant at 173 μM)	0.07	72.2	–	–	–	–
NADH (FAD constant at 127 μM)	–	–	0.11	3.38	0.12	2.81

All measurements were made at 25°C in 50 m*M* potassium phosphate buffer (pH 7.2). Inhibition constants and K_m values were calculated at a constant concentration of NADH (173 μM) and varying the FAD concentration from 12 to 127 μM at dye–PEG concentrations between 0 and 0.12 μM and at a constant FAD concentration (127 μM) by varying the NADH concentration in the range 2–173 μM at dye–PEG concentrations between 0 and 0.25 μM, respectively.

dye–enzyme interaction can be diminished by both FAD and NADH [19]. CB F3G-A binds the NADH oxidase from *Thermus thermophilus* with only moderate affinity at its nucleotide binding site(s). However, the dye ligand has been successfully used in the affinity chromatography of this enzyme [1,12] and in the purification of other flavoproteins exhibiting tightly bound FAD [21–25].

(iv) The available data do not allow to predict all structural requirements of a dye acting as an optimum biomimetic ligand of NADH oxidase from *Thermus thermophilus* HB8. However, by summarizing all data, a structural model that fulfils basic requirements for binding can be proposed (Fig. 5).

The presence of a disulphonated aminonaphthol ring in combination with another aromatic negatively charged residue and a hydrophobic arm seems to be a good prerequisite to bind the enzyme with high affinity. A conformational analysis of the ligand structure by using molecular modelling (MOBY, Version 1.4; Springer, Berlin, Germany) gave distances between the negatively charged sulphonic acid group and the hydrophobic arm in the range 7–13 Å.

A comparison of all the dyes used revealed that the dye ligand PR H-8BN (for structure, see Fig. 3) fits best with the proposed model. It binds to the enzyme with high affinity and shows strong competition to the FAD binding site with an involvement of the NADH binding region.

As shown by X-ray diffraction analysis of the holoenzyme, there are two FAD binding sites per enzyme dimer with the fixation of the FAD molecules in the two clefts between both subunits stabilised by electrostatic forces between the phosphate group(s) of the cofactor and Arg_{17}, Arg_{21} and Arg_{195} and by hydrophobic interactions between Ala_{46} and Leu_{158} and the isoalloxazine ring of the flavin nucleotide [2]. A first preliminary X-ray diffraction analysis of an enzyme–PR H-8BN complex showed that the FAD cofactor is completely displaced by soaking the crystal with this dye ligand. The formation of the enzyme–dye complex seems to cause some smaller changes in the conformation in the FAD pocket, but the position of one phosphate group of the cofactor seems to be occupied by a sulphonic acid group of the dye with similar electrostatic interactions to arginine residues.

The preliminary crystallographic data are in accordance with the results of affinity partitioning, difference spectroscopy and kinetics, suggesting that PR H-8BN occupies both FAD binding sites of the enzyme.

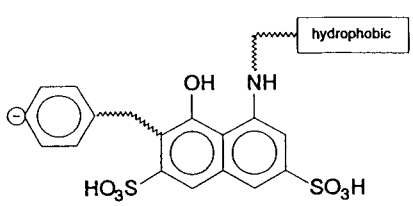

Fig. 5. Model for a biomimetic ligand of NADH oxidase from *Thermus thermophilus* HB8.

5. References

[1] H.-J. Park, C.O. Reiser, S. Kondruweit, H. Erdmann, R.D. Schmid and M. Sprinzl, *Eur. J. Biochem.*, 205 (1992) 881.
[2] H.-J. Hecht, H. Erdmann, H.-J. Park, M. Sprinzl, R.D. Schmid and D. Schomburg, presented at the *16th Congress of the International Union of Crystallography, Beijing, China, August 21–29, 1993.*
[3] D. Pompon and F. Lederer, *Eur. J. Biochem.*, 90 (1978) 563.
[4] T. Prestera, H.J. Prochaska and P. Talalay, *Biochemistry*, 31 (1992) 824.
[5] Y.C. Tsai, T.Y. Yang, S.W. Cheng, S.N. Li and Y.J. Wang, *Prep. Biochem.*, 21 (1991) 175.
[6] C.R. Lowe, S.J. Burton, N.P. Burton, W.K. Alderton, J.M. Pitts and J.A. Thomas, *Trends Biotechnol.*, 10 (1992) 442.
[7] H. Erdmann, H.-J. Hecht, H.-J. Park, M. Sprinzl, D. Schomburg and R.D. Schmid, *J. Mol. Biol.*, 230 (1993) 1086.
[8] C.R. Lowe and J.C. Pearson, *Methods Enzymol.*, 104C (1984) 97.
[9] G. Johansson, *Methods Enzymol.*, 104C (1984) 356.
[10] J. Kirchberger, F. Cadelis, G. Kopperschläger and M.A. Vijayalakshmi, *J. Chromatogr.*, 483 (1989) 289.
[11] P. Hughes, C.R. Lowe and R.F. Sherwood, *Biochim. Biophys. Acta*, 700 (1982) 90.
[12] H. Erdmann, H.-J. Hecht and R.D. Schmid, *Dechema Biotechnol. Conf.*, 5 (1992) 93.

[13] W.H. Press, B.P. Flannery, S.A. Teukolsky and W.T. Vetterling, *Numerical Recipes, the Art of Scientific Computing*, Cambrdige University Press, Cambridge, 1988.
[14] S.D. Flanagan and S.H. Barondes, *J. Biol. Chem.*, 250 (1975) 1484.
[15] S. Subramaniam, *Arch. Biochem. Biophys.*, 216 (1982) 116.
[16] R.E. Barden, P.L. Darke, R.A. Deems and E.A. Dennis, *Biochemistry*, 19 (1980) 1621.
[17] A. Cordes, J. Flossdorf and M.R. Kula, *Biotechnol. Bioeng.*, 30 (1987) 514.
[18] P.A. Alred, G. Johansson and F. Tjerneld, *Anal. Biochem.*, 205 (1992) 351.
[19] H.-L. Schmidt, W. Stöcklein, J. Danzer, P. Kirch and B. Limbach, *Eur. J. Biochem.*, 156 (1986) 149.
[20] V. Radjendirane, M.A. Bhat and C.S. Vaidyanathan, *Arch. Biochem. Biophys.*, 288 (1991) 169.
[21] J. Leonil, S. Langrene, S. Sicsic and F. Le Goffic, *J. Chromatogr.*, 347 (1985) 316.
[22] H.J. Prochaska, *Arch. Biochem. Biophys.*, 267 (1988) 529.
[23] D.H. Sharkis and R.P. Swenson, *Biochem. Biophys. Res. Commun.*, 161 (1989) 434.
[24] Q. Ma, R. Wang, C.S. Yang and A.Y. Lu, *Arch. Biochem. Biophys.*, 283 (1990) 311.
[25] C.M. Yea, A.R. Cross and O.T. Jones, *Biochem. J.*, 265 (1990) 95.

ELSEVIER

Journal of Chromatography A, 668 (1994) 165–171

JOURNAL OF CHROMATOGRAPHY A

Biochemical characterization of human erythrocytes fractionated by counter-current distribution in aqueous polymer two-phase systems

Montserrat Pinilla*, Jesus de la Fuente, Ana I. García-Pérez, Pilar Jimeno, Pilar Sancho, José Luque

Departamento de Bioquímica y Biología Molecular, Campus Universitario, Universidad de Alcalá, 28871-Alcala de Henares, Madrid, Spain

Abstract

The fractionation of normal human erythrocytes by counter-current distribution (CCD) in charge-sensitive dextran–polyethylene glycol two-phase systems was confirmed and extended to red blood cells from heterozygous β-thalassaemic patients. The differences between the distribution profiles of normal (homogeneous) and abnormal (heterogeneous) red blood cells reflect their different surface-charge properties. As suggested by the decline of membrane sialic acid released after neuraminidase treatment and the specific activities of two age-dependent enzymes (membrane acetylcholinesterase and intracellular pyruvate kinase) in the distribution profiles (from the left- to the right-hand side fractions), the fractionation seems to be according to red blood cell age. A constancy of the 2,3-bisphosphoglycerate level was observed in ageing red blood cells.

1. Introduction

Several approaches are used to study red blood cell (RBC) ageing. Bleeding and hypertransfusion or ageing of tagged cells are employed *in vivo* (in experimental animals). *In vitro*, the study of cellular ageing relies on the separation of circulating RBCs in subpopulations of various mean age on the basis of differences in physical properties (density, size, volume, surface area, shape, osmotic fragility or surface charge density). Most studies have consisted of comparisons of RBC properties in fractions obtained by centrifugation (or ultracentrifugation) or after centrifugation through phthalate esters or continuous and discontinuous density gradients (gum acacia, Stractan, albumin, dextran, Ficoll, Percoll, etc.) [1–8]. Density fractionation, the most widely used technique, is based on the relationship between increasing RBC age and density. Aged RBCs lose surface area and volume [9] and therefore become denser than young mature RBCs. A question still debatable, whether the two phenomena do in fact correlate throughout the RBC life-span, is in favour of a progressive increase of RBC density with age [8].

Multiple partitions in aqueous dextran–polyethylene glycol (Dx–PEG) two-phase systems, using a thin-layer counter-current distribution (CCD) apparatus [10], is an alternative method for fractionating erythrocytes on the basis of alterations of the negative surface charged properties that occur during ageing [11]. Rat RBC

* Corresponding author.

0021-9673/94/$07.00
SSDI 0021-9673(94)00038-B

^{59}Fe-labelling studies *in vivo* [11,12] and the decline in the CCD fractions of age-dependent enzymes [13–16] have shown in rats the positioning of maturing reticulocytes and ageing RBCs after fractionation in charge-sensitive two-phase systems. These studies were then extended to rat RBCs during animal development (*i.e.*, RBC switching) in order to distinguish between embryonic, foetal and adult RBCs [15]. Finally, this approach was applied comparatively to adult rat and human RBCs on the basis of the decline in specific activity of glycolytic enzymes (HK, PFK and PK) [16]. Our aim in this work was to compare the fractionation of normal and pathological RBCs and to document it as due to changes in cell age. Both β- (or A_2) and F- (or dβ) thalassaemia subgroups affect Mediterranean populations and are encountered in Spain [17]. Mutations in β-thalassaemia, which result in a deficit of β-chain synthesis, account for heterogeneity of these RBCs. The decreased β-chain production leads to an excess of unstable α-chains and intracellular inclusions that interact with the membrane, initiating oxidation reactions that contribute to heterogeneity and abnormality [18–20].

To demonstrate the fractionation according to age, three age-dependent parameters were measured in the fractions: membrane sialic acid released after neuraminidase treatment and specific activity of acetylcholinesterase (EC 3.1.1.7) (AChE) and pyruvate kinase (EC 2.7.1.40) (PK). A non-age-dependent enzyme, bisphosphoglycerate mutase (EC 5.4.2.4) (BPGM), was also measured in an attempt to relate it to 2,3-bisphosphoglycerate (2,3-BPG) levels in the fractions [13,15,16].

2. Experimental

2.1. Cell suspensions and haemolysates

Samples of blood from ten normal adults and five patients with anaemic heterozygous β-thalassaemia (University Hospital) were collected in heparin (10 units/ml). After centrifugation (400 *g* for 10 min) at 4°C, the cells were washed three times with cold 0.15 *M* NaCl, the supernatant and the top layer of packed cells being removed each time. Haemolysates were obtained by hypoosmotic shock with two volumes of stabilizing solution (2.7 m*M* EDTA-Na_2–0.7 m*M* mercaptoethanol), followed by freezing and thawing. RBC suspension and haemolysates were prepared on the day of assay.

2.2. Laboratory assessments

RBC count (cells/l), Hb content (g/dl), packed cell volume (PCV) (%), mean cell volume (MCV) (fl), mean cell haemoglobin (MCH) (pg) and mean cell haemoglobin concentration (MCHC) (g/dl) were measured in a Technicon H1 or a STKR Coulter Counter. Hb variants, were detected by standard cellulose acetate electrophoresis with an alkaline (pH 8.5) buffer system (Helena Labs.). An accurate determination of HbA_2 (%), for β-thalassaemia diagnosis, is given by the absorbance (415 nm) of fractions eluted with glycine–KCN developers after DEAE-cellulose anion-exchange microchromatography (Helena Labs.). HbF was determined as a total percentage using a commercialized immune diffusion radial (IDR) method (Helena Labs.).

2.3. Fractionation of RBCs

This was carried out as reported previously [16]. The affinity of phosphate for the Dx-rich bottom phase of charge-sensitive two-phase systems [5% (w/w) Dx–4% (w/w) PEG–0.03 *M* NaCl–isotonic 0.09 *M* sodium phosphate buffer (pH 6.8)] and the partitioning of chloride between both phases gives a relatively higher positive charge to the PEG-rich upper phase than to the bottom phase, thus allowing cell partitioning on the basis of surface charge properties [10,11]. The fractionation of cells differing closely in partition ratio values (total cells in top phase/cells adsorbed at interface), *e.g.*, ageing RBCs, need multiple partitionings to be fractionated. These are carried out in a CCD apparatus (Bioshef MK3; University of Sheffield, Sheffield, UK) with a circular thin-layer unit (60 concentric

cavities) formed by a bottom or stator plate and a top or rotor plate). The experimental conditions were as detailed for human RBCs [11,12,16]. Cell distribution profiles are given by the Hb absorbance values at 540 nm against cavity number. In order to obtain sufficient cells to study the enzyme activity and metabolite levels, some adjacent CCD cavities (with similar partition ratios) were joined in five pools (5–6 cavities) as indicated in Fig. 1.

2.4. Enzyme and metabolite assays

Sialic acid was measured (μg per 10^{10} cells) after neuraminidase (from 1 U/ml *Vibrio cholerae* solution) treatment of RBCs from pooled adjacent CCD fractions (Fig. 1) [21]. Haemolysates were prepared by hypo-osmotic shock of RBCs from pooled adjacent CCD fractions (Fig. 1). The specific enzyme activities (U/g Hb) in haemolysates were measured at 30°C for AChE [22]. PK and BPGM and Hb were determined as described previously [16]. 2,3-BPG was measured with a UV test (Boehringer). Reagents, substrates, cofactors and auxiliary enzymes were obtained, from Sigma and Boehringer.

3. Results and discussion

3.1. Erythrocytic indices

Standard hematological indices were used to study normal cells and to identify thalassaemic RBCs as microcytic hypochromic cells. The mean RBC count was higher in thalassaemic [$(5.7 \pm 1.0) \cdot 10^{12}$ cells/l] than in normal RBCs [$(5.1 \pm 0.4) \cdot 10^{12}$ cells/l]. A mild anaemia was observed, with lower mean Hb (12.2 ± 1.7 g/dl) and PCV ($39.5 \pm 3.1\%$) values in thalassaemic than in normal cells (15.3 ± 1.4 g/dl and $45.1 \pm 3.2\%$, respectively). As a consequence of a lower MCV value in thalassaemic (69.3 ± 6.1 fl) than in normal RBCs (89.3 ± 3.2 fl), the MCH and MCHC indices were characteristically lower in thalassaemic (21.6 ± 3.1 pg and 31.1 ± 0.6 g/dl) than in normal RBCs (30.4 ± 1.8 pg and 34.1 ± 1.5 g/dl). Abnormalities of thalassaemic RBCs, including anisocytosis, poikilocytosis, basophilic stippling and numerous target cells, were also observed by optical microscopy. The increase in the RDW index in thalassaemic cells ($16.1 \pm 1.8\%$) with respect to normal cells ($12.9 \pm 0.6\%$) is in agreement with the anisocytosis of thalassaemia. As a compensation for the defective synthesis of β-chains, the microcolumn chromatographic results show an increase in both Hb A_2 ($3.9 \pm 0.5\%$) and HbF ($5.1 \pm 0.8\%$) with respect to normal RBCs ($2.6 \pm 0.7\%$ and $0.6 \pm 0.2\%$, respectively).

3.2. Fractionation profiles

The reproducibility of the distribution profiles for normal RBCs was as shown previously under identical conditions [11,12,16]. An apparent homogeneous curve is usually observed. A representative profile is then shown (Fig. 1, Control). RBCs are located all along cavities 20–50. Cells with affinity for the top phase are found as fast-moving cells towards the right-hand side (pooled CCD fraction 5) whereas cells with affinity for the interface are found as slow-moving cells towards the left-hand side (pooled CCD fraction 1). This is due to the partition ratio of the ageing RBC subpopulation which, owing to the subtle differences in surface charge properties, are very close to each other. The relationship between RBC age and partition ratio (surface charge) seems to be similar to that between RBC age and density [8]: the RBC distribution is overall a normal curve, composed of the integral of a multitude of normal distribution curves of cells of progressively increasing age and density. Each cohort of cells ages and increases in density at a constant rate. The effect is exerted on the entire population, which become homogeneously distributed along the fractions with regard to density.

Such a progressive relationship between age and any other physical property does not exist for heterogeneous RBCs (*e.g.*, thalassaemic RBCs), which are then distributed as containing several populations. Representative profiles for two thalassaemic RBC samples are given in Fig. 1. The distribution curves are now generally

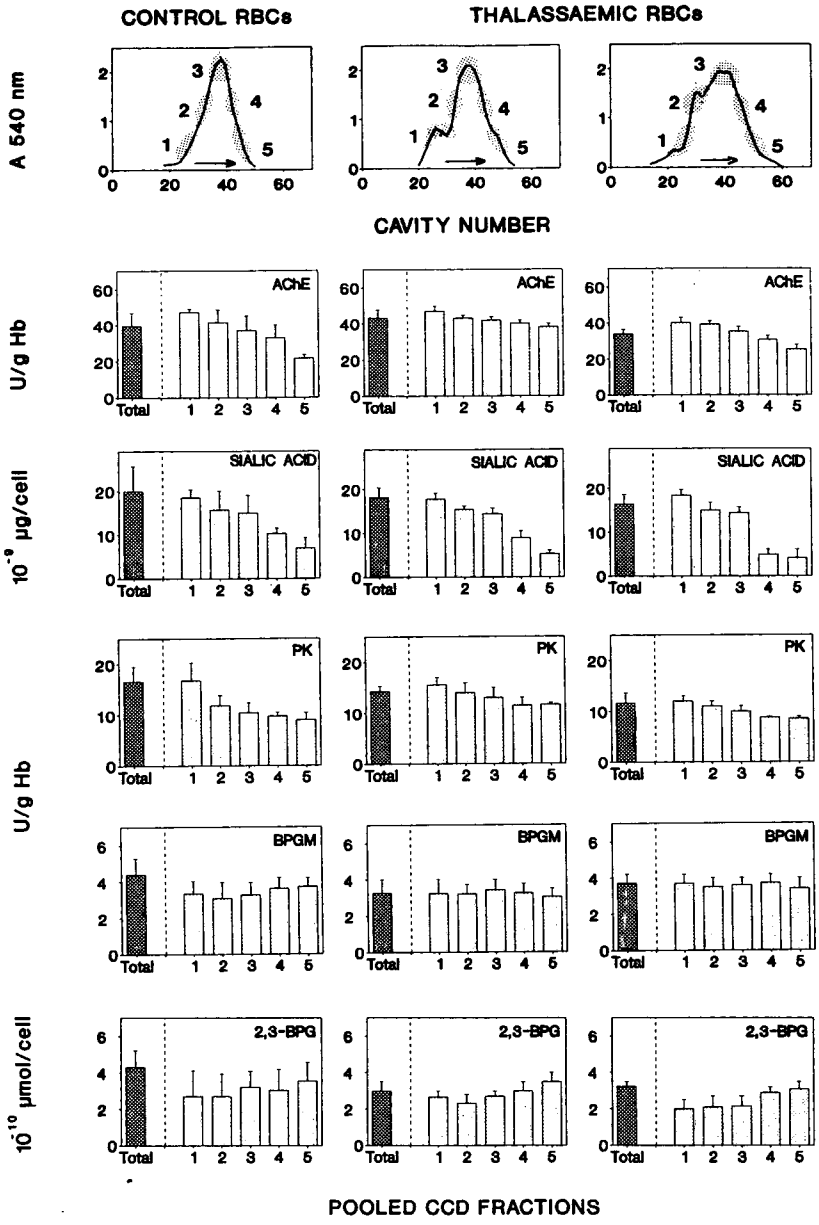

Fig. 1. Fractionation by counter-current distribution of human (normal and thalassaemic) RBCs. CCD profiles (top) show the Hb absorbance value (cell number) for each cell population. Acetylcholinesterase (AChE); sialic acid; pyruvate kinase (PK); bisphosphoglycerate mutase (BPGM); 2,3-bisphosphoglycerate (2,3-BPG). Whole RBC populations (total). Pooled CCD fractions (1–5) were prepared from adjacent cavities, as shown in the CCD profiles. Bars represent the mean ± S.D. for four separate CCD runs and quadruple measurements.

broader (between cavities 15 and 55) and clearly more heterogeneous. This is in agreement with a higher RDW index (see above) and a non-progressive relationship between RBC age and surface properties. Reproducibility was then not possible for RBCs from different patients.

3.3. Changes in age-dependent constituents

Although initial studies indicated that human RBCs of different age were not subfractionated by CCD, ^{51}Cr-labelling studies *in vitro* had shown that fractionation of human RBCs also reflects surface changes during ageing [11,12]: young human RBCs have a slightly lower partition value than the whole population and would be distributed towards the left-hand side of the CCD profile. Older RBCs, which have a higher partition value than the population as a whole, would be distributed towards the right of the CCD profile. Such a distribution was confirmed in rats and humans on the basis of the decline in the specific activity of three age-dependent glycolytic enzymes (HK, PFK and PK) [16]. However, in rats (*in vivo* ^{59}Fe-labelling plus enzyme changes), the fractions to the left contain older RBCs whereas the fractions to the right are progressively enriched in younger RBCs. This means that the positioning of ageing RBCs is reversed in humans and rats (is species specific). An additional important point is that reticulocytes (normally present as a minor subpopulation in the original RBC samples) are distributed in the cell fractions (from both species) located further to the left, as a consequence of their lower partition ratio [11,12,14]. The number of reticulocytes in the CCD fractions was not detected after staining with cresyl brilliant blue [16].

Specific acetylcholinesterase activity

The mean value for the specific activity of AChE (U/g Hb) in whole normal RBCs (total bars, Fig. 1) agrees with that given by others [22] and with the value found in whole thalassaemic RBCs. A decline in activity for normal RBCs is observed from pooled CCD fraction 1 (or fraction 2) to fraction 5, which means that the youngest RBCs (highest enzyme activity) are distributed towards the left-hand side fractions and older RBCs (with decreasing activity) towards the right-hand side of the profile. Although not always significant for different thalassaemic RBCs (Fig. 1), such a decline seems also to be observed from pooled CCD fraction 1 (or fraction 2) to fraction 5.

Sialic acid

Measurement of sialic acid is based on the hypothesis that desialylation during ageing is responsible for the recognition and subsequent phagocytic sequestration of senescent RBCs. Sialic acid, the final sugar residue in the carbohydrate chain of membrane RBC glycoproteins and glycolipids and the main factor responsible for negative charges, is released by neuraminidase from the receptor domain of the glycophorins on the outer surface of the membrane. A loss of surface charge density (decrease in partition ratio) and a loss of sialic acid are then a reflection of the RBC ageing process in peripheral blood [1,2,5–7,23].

In the whole normal RBC population (total bars, Fig. 1), the mean value for the concentration of sialic acid per cell is similar to that given by others [21], and similar to that measured in thalassaemic RBCs (Fig. 1). A marked decrease in the content of sialic acid is observed from pooled CCD fraction 1 (or fraction 2) to fraction 5, in both normal and abnormal RBCs. In general, such a decrease is more pronounced than the decrease in AChE activity. Using density fractionation, the decrease of sialic acid per normal RBC (from the least to the densest fractions) is around 10–15% in several mammalian species [1]. From our data, the sialic acid content in pooled CCD fractions is at least 20% higher in the left-hand side fractions, indicating a fractionation according to age.

To relate the decline of these (and other) membrane constituents to the membrane loss during cell ageing, the data must be expressed per unit membrane area as a loss of surface area (and volume) with RBC age was shown in density fractionation studies. Thus, the general conclusion is that sialic acid may not be decreasing during the ageing process [1,2,9]. The calculation of sialic acid per unit membrane area cannot be made here (surface area measurements in the pooled CCD fractions seems to be affected by the polymers). However, taking into account the basic differences between both tech-

niques (surface charge against density fractionation), the decrease in sialic acid per cell observed in the pooled CCD fractions (Fig. 1) is clearly in favour of the fractionation of RBCs according to age.

Specific activity of pyruvate kinase and bisphosphoglycerate mutase and 2,3-bisphosphoglycerate level

The incorrect assumption that certain enzymes (*e.g.*, PK) were not age-dependent enzymes came from a poor or imperfect relationship in gradient fractionation between RBC age and density, mainly owing to the presence of reticulocytes in the density fractions. While the light fractions represent a mixture of reticulocytes and young mature RBCs, the dense fractions represent predominantly old RBCs. As reticulocytes have higher enzyme activities than RBCs (*e.g.*, 300-fold for PK), the decline in enzyme level with increasing density appears to be more rapid in the uppermost fractions of the gradient and less rapid in the lowermost fractions. The biphasic disappearance sometimes observed, *e.g.*, for pyrimidine-5-nucleotidase activity, depends on both the RBC ageing and reticulocyte maturation processes [8]. The situation seems to be different in the CCD fractions mainly because RBCs seem not to be mixed with reticulocytes.

The specific activities of PK and BPGM (IU/g Hb) are apparently higher in normal than in thalassaemic whole RBCs (total bars, Fig. 1). The decline in PK activity is also higher in pooled CCD fraction 1 (or fraction 2) than in fraction 5, in both normal and thalassaemic RBCs. This decline was previously observed for both human [16] and rat [13–15] CCD fractions. In all instances, no significant variation was observed in BPGM activity. Both results have now been confirmed for human RBCs and extended to thalassaemic RBCs (Fig. 1). A non-significant variation in the level of 2,3-BPG is observed in any of the pooled CCD fractions. As 2,3-BPG synthesis is directly related to BPGM activity and indirectly related to PK activity, the PK/BPGM ratio was proposed as an index of 2,3-BPG formation. This was confirmed in reticulocyte populations from anaemic rats (and their CCD fractions) at different stages of reticulocyte maturation [13,14], and also in peripheral rat RBCs (and their CCD fractions) at different stages (RBC switching) of animal development [15]: the inverse relationship between 2,3-BPG and the PK/BPGM ratio was shown in all reticulocytes and switching RBCs. The slightly higher 2,3-BPG level in rat (1.15 ± 0.15 μmol/μmol Hb) than in human (0.96 ± 0.08 μmol/μmol Hb) whole RBCs [24] was also related to a lower PK/BPGM ratio in rats than in humans [16]. The higher PK/BPGM ratio observed in rat reticulocyte-rich populations also accounts for a lower 2,3-BPG level in reticulocytes than in circulating RBCs [13]. In all these situations, the lower PK/BPGM ratio is due to a decrease in PK and a simultaneous increase in BPGM.

However, a significant variation in the PK/BPGM ratio was not found in the CCD fractions from adult rat [13,15] and humans [16]. This is confirmed here (Fig. 1): a decline in PK activity without a parallel increase in BPGM activity is shown in the pooled CCD fractions from normal and thalassaemic RBCs. The reason for a non-significant variation in the PK/BPGM ratio, observed during rat or human RBC ageing [16] and thalassaemic RBCs (Fig. 1), is due to the standard deviations of the values for BPGM and PK in CCD fractions. When they are divided to give the PK/BPGM, the error bars for the ratio should be marked. As a consequence, the PK decrease is not enough by itself to explain the variations in 2,3-BPG. This is a different situation to those above described (reticulocyte maturation; RBC switching). Therefore, the maintenance of a constant 2,3-BPG level during the ageing process, necessary for the oxygenation of RBCs all along the life-span, can now be explained on the basis of a fairly constant BPGM activity, in addition to the non-variation of phosphoglycerate kinase [16]. The maintenance of the stability of these enzymes may be the mechanism the RBCs use to keep an appropriate level of 2,3-BPG. For this reason, these enzymes have to be kept away from the normal age-related decay suffered by most enzymes.

4. Acknowledgements

This work was supported by PGC-MEC and CICYT grants (Spain). We acknowledge the linguistic assistance of C.F. Warren of the ICE (University of Alcalá) and the collaboration of Dr. J.L. Merino and P. Ricard (Haematology Department, University Hospital).

5. References

[1] G. Bartosz, in J.R. Harris (Editor), *Blood Cell Biochemistry, 1, Erythroid Cells*, Plenum Press, New York, 1990, p. 45.
[2] G. Bartosz, *Gerontology*, 37 (1991) 33.
[3] E. Beutler, *Br. J. Haematol.*, 61 (1985a) 377.
[4] E. Beutler, *Blood Cells*, 14 (1988) 69.
[5] M.R. Clark, *Physiol. Rev.*, 68 (1988) 503.
[6] H.U. Lutz, in J.R. Harris (Editor), *Blood Cell Biochemistry, 1, Erythroid Cells*, Plenum Press, New York, 1990, p. 81.
[7] H.U. Lutz, P. Stammler, S. Fasler, M. Ingold and J. Fehr, *Biochim. Biophys. Acta*, 1116 (1992) 1.
[8] S. Piomelli and C. Seaman, *Am. J. Hematol.*, 42 (1993) 46.
[9] R.E. Waugh, N. Mohandas, C.W. Jackson, T.J. Mueller, T. Suzuki and G.L. Dale, *Blood*, 79 (1992) 1351.
[10] P.A. Albertsson, *Partition of Cell Particles and Macromolecules*, Wiley, New York, 3rd ed., 1986.
[11] H. Walter, in H. Walter, D.E. Brooks and D. Fisher (Editors), *Partitioning in Aqueous Two-Phase Systems: Theory, Methods, Uses and Applications to Biotechnology*, Academic Press, New York, 1985, p. 327.
[12] H. Walter and E.J. Krob, *Cell Biophys.*, 5 (1983) 205 and 301.
[13] J. Luque, M.D. Delgado, P. Rodriguez-Horche, M.T. Company and M. Pinilla, *Biosci. Rep.*, 7 (1987) 113.
[14] M. Pinilla, P. Rodriguez-Horche and J. Luque, *Cell Biochem. Funct.*, 5 (1987) 301.
[15] M. Pinilla, P. Jimeno, M. Moreno and J. Luque, *Mol. Cell Biochem.*, 94 (1990) 37.
[16] P. Jimeno, A.I. García-Pérez, J. Luque and M. Pinilla, *Biochem. J.*, 279 (1991) 237.
[17] A. Vayá, A. Carratala, C. Martinez and J. Aznar, *Nouv. Rev. Fr. Hématol.*, 25 (1983) 369.
[18] E.A. Rachmilewitz, E. Shinar, O. Shalev, U. Galili and S. Schrier, *Clin. Haematol.*, 14 (1985) 163.
[19] G. Athanasiou, N. Zoubos and Y. Missirlis, *Nouv. Rev. Fr. Hematol.*, 33 (1991) 15.
[20] S.L. Thein, *Br. J. Haematol.*, 80 (1992) 273.
[21] O.M. Smith and D. Fisher, in D. Fisher and I.A. Sutherland (Editors), *Separations Using Aqueous Two-Phase Systems: Applications in Cell Biology and Biotechnology*, Plenum Press, New York, 1989, p. 425.
[22] E. Beutler, *Red Cell Metabolism: a Manual of Biochemical Methods*, Grune & Stratton, Orlando, FL, 3rd ed., 1984.
[23] D. Aminoff, *Blood Cells*, 14 (1988) 229.
[24] P. Roncalés, C. Tejero, M. Pinilla and J. Luque, *Rev. Esp. Fisiol.*, 39 (1983) 91.

ELSEVIER

Journal of Chromatography A, 668 (1994) 173–178

JOURNAL OF CHROMATOGRAPHY A

Revealing surface changes associated with maturation of ram spermatozoa by centrifugal counter-current distribution in an aqueous two-phase system

M. Ollero, M.L. Pascual, T. Muiño-Blanco, J.A. Cebrián-Pérez, M.J. López-Pérez*

Departamento de Bioquímica y Biología Molecular y Celular, Facultad de Veterinaria, Miguel Servet 177, 50013 Zaragoza, Spain

Abstract

Centrifugal counter-current distribution (CCCD) in an aqueous two-phase system was used to detect changes associated with maturation of ejaculated ram spermatozao. Spermatozoa obtained form three successive ejaculates of rams maintained in abstinence for one, two and three days were fractionated by CCCD. The results show that these ejaculates are relatively enriched in a cell population which presents a very high enhanced affinity to the lower dextran-rich phase. This cell population is not associated with loss of acrosomal integrity. In addition, it tends to disappear with longer abstinence periods, or after successive ejaculations at the same abstinence period, strongly suggesting that it is composed of immature cells. Therefore, phase partitioning can detect surface changes accompanying sperm maturation and offers a new possibility for sperm quality analysis.

1. Introduction

Thin-layer counter-current distribution (TLCCD) in aqueous two-phase systems is a useful technique for the separation of sperm cell populations based on differences in their surface properties [1–4]. However, because long periods of time are necessary for phase separation at unit gravity, TLCCD may increase cell death during the separation process, thus progressively modifying the cell partition behaviour. This experimental drawback can be avoided if phase separation during counter-current distribution is centrifugally enhanced, thus greatly shortening the time required for the cell separation process. Thus, although speeding up phase separation may result in reduced efficiency of cell separation [5,6], shortening of the process can be very advantageous for fractionating cells, such as spermatozoa, sensitive to environmental aggression. In this respect, we have recently shown that sperm cell heterogeneity revealed by centrifugal counter-current distribution (CCCD) is at least associated with different viability states of the fractionated cells [7], if cell sedimentation during the separation process is managed by using a Percoll- or a Ficoll-containing dextran–poly(ethylene glycol) (PEG) two-phase system [7,8].

On the other hand, partitioning in aqueous two-phase systems is a powerful method for tracing subtle surface changes that accompany *in vivo* processes. Thus, changes in the surface properties taking place during maturation or ageing of red blood cells and some tissue cells

* Corresponding author.

0021-9673/94/$07.00
SSDI 0021-9673(93)E1079-F

have been detected by using this method (for a review, see ref. 9). In the case of spermatozoa, maturation is a relevant physiological process that enables these cells to maintain viability and to acquire fertilizing capacity. In this respect, it is well known that important changes in the surface properties take place during maturation of mammalian sperm cells (for a review, see ref. 10) involving, among other effects, acquisition of new surface proteins [11] and changes in the exposed saccharide residues [12]. These surface changes could account for the different partitioning behaviour of spermatozoa depending on the maturation state of the cells. Thus, it has been already shown that surface changes during the maturation of rat spermatozoa can be detected by using partitioning in dextran–PEG two-phase systems [2,13].

In order to characterize further the biological basis underlying the sperm cell heterogeneity revealed by CCCD, we undertook a study of the partitioning behaviour of immature spermatozoa in such a system. For this, we used ram ejaculates obtained after short periods of abstinence, a known approach for increasing the number of immature ejaculated cells. The results obtained show that these ejaculates are relatively enriched in a cell population which presents a very high enhanced affinity to the lower dextran-rich phase. This cell population is not associated with loss of acrosomal integrity. In addition, it tends to disappear with longer abstinence periods, or after successive ejaculations at the same abstinence period, strongly suggesting that it is composed of immature cells.

2. Experimental

2.1. Chemicals

Dextran T-500 (M_r 500 000) and Ficoll 400 (M_r 400 000) were obtained from Pharmacia (Uppsala, Sweden). PEG (M_r 6000) was purchased from Serva Feinbiochemica (New York, USA). Percoll and ionophore A23187 were obtained from Sigma (St. Louis, MO, USA). All other chemicals were of analytical-reagent grade.

2.2. Two-phase system

The system used consisted of 5.5% (w/w) Dextran T500, 2% (w/w) PEG 6000, 10.5% (w/w) Ficoll 400, 0.25 *M* sucrose, 0.1 m*M* EGTA, 7 m*M* sodium phosphate (pH 7.5) and 10% (v/v) of "10 × buffer stock Hepes" {50 m*M* glucose, 100 m*M* 4-(2-hydroxyethyl)-1-piperazine-ethanesulphonic acid (HEPES), 20 m*M* KOH}.

2.3. Preparation of cell samples

Semen from rams was collected using an artificial vagina and diluted to about $5 \cdot 10^8$ cells in a saline medium [14]. The pellet obtained after washing through 4 ml of 35% saline Percoll and 2 ml of 70% saline Percoll (5 min at 200 *g* and 15 min at 1200 *g*) was resuspended with 5 ml of saline medium and centrifuged for 5 min at 700 *g*. The pellet was resuspended with 5 ml of two-phase system medium [0.25 *M* sucrose, 0.1 m*M* EGTA, 7 m*M* sodium phosphate (pH 7.5) and 10% (v/v) of "10 × buffer stock Hepes") and centrifuged for 5 min at 700 *g*. The supernatant was removed and the pellet was resuspended with the two-phase system medium.

2.4. Centrifugal counter-current distribution

The counter-current distribution machine used and a detailed scheme of the process have already been described [7]. To carry out CCCD experiments, a two-phase system of the above composition was prepared and mixed. In each experiment, the volume ratio was calculated by batches of 5 ml. Then, the volume of the system loaded in chambers 1–59 (59 transfers) or 1–29 and 31–59 (29 transfers) was that estimated to maintain the desired volume of the bottom phase (0.7 ml). The cells were loaded in chamber 0 (59 transfers) or in chambers 0 and 30 (29 transfers). The shaking and centrifugation time was 60 s. After the run, the solutions were transformed into a one phase-system by addition of one volume of a dilution buffer (a polymer-free medium such as that used in the two-phase system). The fractions were then collected and the cells counted under a light microscope. All

operations were carried out at 20°C. For each CCCD run, results are expressed as the percentage of the value of cells counted in each fraction with respect to the value obtained in the chamber containing the maximum amount of cells. In some fractions assessment of viability was carried out by fluorescent staining with carboxyfluorescein diacetate and propidium iodide, according to Harrison and Vickers [14].

2.5. Acrosome reaction (AR)

The AR was induced by ionopore A23187. A stock solution of 1 m*M* in ethanol was prepared and added to a sperm suspension of $50 \cdot 10^6$ cells/ml in the calcium-enriched incubation medium described by Shams-Borhan and Harrison [15] to a final concentration of 1 μM. Spermatozoa were then incubated at 37°C for 30 min. Assessment of the acrosomal status was performed by the triple stain technique described by Garde *et al.* [16].

3. Results

We have previously shown that CCCD in a 10.5% (w/w) Ficoll 400-containing dextran–PEG two-phase system is a resolution technique for revealing ram spermatozoa heterogeneity [7]. In this system, assessment of viability by fluorescent probes showed a different enrichment of live cells in the different fractions tested, dead spermatozoa presenting enhanced affinity to the dextran-rich phase (*i.e.*, preferentially located in the left-hand fractions of the profile). Hence this two-phase system was also used in the experiments reported here undertaken to characterize the CCCD profiles of ram spermatozoa obtained after short periods of abstinence.

Washed spermatozoa obtained from three successive ejaculates of rams maintained in abstinence for one, two and three days were fractionated by 29-transfer CCCD. Representative profiles obtained (second ejaculates) are shown in Fig. 1. In agreement with previous results [7], the percentage of live cells increased in chambers further to the right. However, we had previously

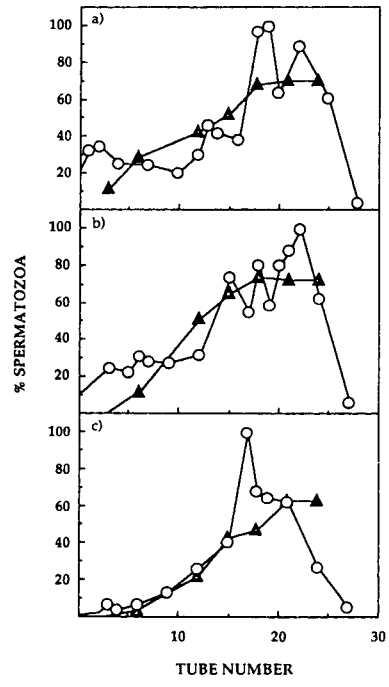

Fig. 1. Centrifugal counter-current distribution and viability of ram spermatozoa from second ejaculates after (a) 1, (b) 2 and (c) 3 days of abstinence. ○ = Percentage of the maximum of cells collected; ▲ = percentage of viable spermatozoa.

shown that loss of viability promoted by a prolonged (one month) period of abstinence accounted for a dramatic displacement to the left of CCCD profiles of ram spermatozoa [7]. In contrast, the appearance of an important number of cells fractionating in chambers 0–9 can be observed in Fig. 1. This dead cell-enriched population located in chambers 0–9 decreases as the time of abstinence increases, almost disappearing in ejaculated spermatozoa obtained after three days of abstinence (Fig. 1). This effect was large in the first and second ejaculates, whereas the percentage of cells found in these chambers was very similar in the third ejaculate obtained after any period of abstinence (Fig. 2). Thus, the number of cells found in the first nine chambers appeared to decrease as a consequence of two different effects: first, they decreased the longer the period of abstinence, and second, this cell population also tended to diminish as the cells were further submitted to maturation events

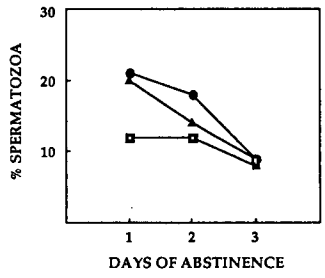

Fig. 2. Influence of the abstinence period on the percentage of cells found in chambers 0–9 with respect to the total number of cells counted in all the chambers (average of three experiments with different ejaculates) after centrifugal counter-current distribution of (●) first, (▲) second and (■) third ejaculates.

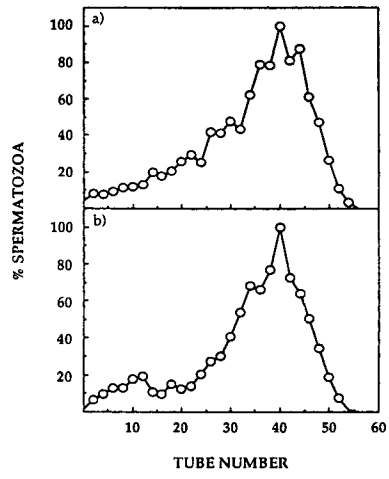

Fig. 3. Effect of the *in vitro* induction of acrosome reaction on the counter-current distribution of ram spermatozoa. Cells incubated in (a) the absence or (b) the presence of ionophore A23187. Data are expressed as a percentage of the maximum number of cells collected.

accomplished by successive ejaculations, as will be discussed later.

These results could suggest that surface changes promoted by death of hypermature (one month of abstinence) [7] or immature cells (one day of abstinence) (Figs. 1 and 2) could account for the very enhanced affinity to the dextran-rich phase. However, another possibility should be considered before drawing this conclusion. Cartwright *et al.* [2] recently described the low hydrophobicity of acrosome-reacted bovine spermatozoa located in left-hand fractions of a TLCCD in a dextran–PEG two-phase system. Further, we have also found that acrosome-reacted bovine spermatozoa show such low hydrophobicity when assayed by CCCD in the same two-phase system as used here (unpublished data). Therefore, the dead cell-enriched population that appears in chambers 0–9 after very short periods of abstinence (Figs. 1 and 2) could be composed of acrosome-reacted spermatozoa. This would imply that CCCD could be revealing the loss of acrosome by hypermature or immature cells rather than surface changes produced by loss of viability of these cells.

In order to find out whether the status of acrosome could significantly modify the CCCD behaviour of ram spermatozoa, acrosome reaction was induced *in vitro* by incubation in a calcium-rich medium in the presence of ionophore A23187 as described previously [15]. Incubation with the ionopore enhanced the number of acrosome-reacted cells (38%) with respect to controls (14%). However, the distribution profiles of treated and control ram spermatozoa did not show significant differences, even when assayed by 59-transfer CCCD (Fig. 3). These results strongly suggest that loss of acrosome does not appear to significantly affect the partitioning of ram spermatozoa, at least under the experimental conditions used here.

4. Discussion

Acquisition of adsorbed elements, such as proteins or lipids, by the sperm cell surface when spermatozoa pass through the epididymis and the vas deferens accounts for a masking effect of surface glycoproteins [17]. In addition, spermatozoa are stored in the cauda epididymis and vas deferens, when the last maturation events of sperm take place. Hence lately formed spermatozoa in short periods of abstinence could have lacked the masking effect of adsorbed elements, then presenting more saccharide residues exposed on the sperm cell surface. On the other hand, the low phosphate concentration used in the two-phase system used here could

result in a relatively charge-insensitive partitioning of cells. Therefore, the enhanced affinity to the dextran-rich phase shown by ram immature spermatozoa (chambers 0–9 in Figs. 1 and 2) could easily be interpreted as a low hydrophobicity of these immature cells which then would fractionate in the left-hand fractions of the CCCD.

These results agree with previous reports of Cartwright *et al.* [2] and Geada *et al.* [13], who found that rat spermatozoa obtained from the vas deferens (*i.e.*, more mature cells) presented a higher affinity to the PEG-rich upper phase than those obtained from the caput epididymis (*i.e.*, immature cells) when assayed either by batch experiments [13] or by TLCCD [2] in charge-insensitive or palmitate–PEG-containing two-phase systems.

On the other hand, adsorbed elements are responsible for maintaining the membrane cell stability against environmental aggression [18], thus somehow supporting viability of the cell. Consequently, immature cells could die more rapidly under experimental manipulations, further enhancing their affinity to the dextran-rich phase [7]. In addition, the dramatic enhancement of affinity to the dextran-rich phase observed in hypermature (dead) cells obtained after a very long period of abstinence (one month) [7] could be explained by the long exposure of the cells to proteolytic activity. Such proteolytic activity actually modifies sperm cell surface proteins during transit of the spermatozoa through the epididymis, as has already been described [19].

An interesting aspect of the results reported here was the observation that successive ejaculations diminish the percentage of cells fractionated in chambers 0–9. These results can be explained by cumulative maturation events undergone by preformed non-ejaculated spermatozoa (short times between ejaculations rule out the possibility of biogenesis of new cells). These cells, then kept at the cauda epididymus and/or vas deferens, would be further exposed to epididymal secretions and seminal plasma, enhancing maturation.

Experimental work in studies of the maturation of spermatozoa is usually performed by studying sperm cells isolated from different epididymal portions. However, to our knowledge, there are no methods available to discriminate populations enriched in ejaculated immature cells. The results presented here show that phase partitioning can be a useful technique for assessing such populations from ejaculates obtained after very short periods of abstinence.

In conclusion, these results emphasize the possibilities of using phase partitioning to detect surface changes accompanying cell maturation. Moreover, in the case of sperm cells, CCCD in an aqueous two-phase system can offer a new possibility for semen quality analysis, by which at least the integrity of the surface changes accounting for loss of viability [7] and maturity of cells (Figs. 1 and 2) can be assessed.

5. Acknowledgement

This work was supported by grant GAN 91-0950.

6. References

[1] E.J. Cartwright, A. Cowin and P.T. Sharpe, *Biosci. Rep.*, 11 (1991) 265.
[2] E.J. Cartwright, P. Harrington, L. Norbury, G. Leeming and P.T. Sharpe, *Biosci. Rep.*, 12 (1992) 57.
[3] E.J. Cartwright, P.M. Harrington, A. Cowin and P.T. Sharpe, *Mol. Reprod. Dev.*, 34 (1993) 323.
[4] R.A.P. Harrison, M.L. Jacques, M.L.P. Minguez and N.G.A. Miller, *J. Cell Sci.*, 102 (1992) 123.
[5] H. Walter and E.J. Krob, *Biochim. Biophys. Acta*, 966 (1988) 65.
[6] H. Walter, E.J. Krob and L. Wollenberger, *J. Chromatogr.*, 542 (1991) 397.
[7] M.L. Pascual, T. Muiño-Blanco, J.A. Cebrián-Pérez and M.J. López-Pérez, *J. Chromatogr.*, 617 (1993) 51.
[8] M.L. Pascual, T. Muiño-Blanco, J.A. Cebrián-Pérez and M.J. López-Pérez, *J. Biochem. Biophys. Methods*, 24 (1992) 275.
[9] H. Walter, G. Johanson and D.E. Brooks, *Anal. Biochem.*, 197 (1991) 1.
[10] C.R. Austin, in C.B. Metz and A. Monroy (Editors), *Biology of Fertilization*, Academic Press, New York, 1985, p. 121.

[11] R. Jones, C.R. Brown, K.I. von Glos and S.J. Gaunt, *Exp. Cell Res.*, 156 (1985) 31.
[12] S.F. Magargee, E. Kunze and R.H. Hammersted, *Biol. Reprod.*, 38 (1988) 667.
[13] A. Geada, G. Leeming and P.T. Sharpe, *Gamete Res.*, 24 (1989) 385.
[14] R.A.P. Harrison and S.E. Vickers, *J. Reprod. Fertil.*, 88 (1990) 343.
[15] G. Shams-Borhan and R.A. P. Harrison, *Gamete Res.*, 4 (1981) 407.
[16] J. Garde, C. Carcía Artiga, A. Gutiérrez and I. Vázquez, *Med. Vet.*, 9 (1992) 107.
[17] K.W. Metz, T. Berger and E.D. Clegg, *Theriogenology*, 34 (1990) 691.
[18] L.J.D. Zaneveld, C.J. Dejonge, R.A. Anderson and S.R. Mack, *Hum. Reprod.*, 6 (1991) 1265.
[19] E.M. Eddy, R.B. Vernon, C.H. Muller, A.C. Hahnel and B.A. Fenderson, *Am. J. Anat.*, 174 (1985) 225.

ELSEVIER

Journal of Chromatography A, 668 (1994) 179–183

JOURNAL OF CHROMATOGRAPHY A

Lactose hydrolysis in an aqueous two-phase system by whole-cell β-galactosidase of *Kluyveromyces marxianus*: partition and separation characteristics

Miroslav Stred'anský*[,a], Martin Tomáška[b], Adriana Tomašková[b], Ernest Šturdík[b]

[a]*Department of Chemical and Biochemical Engineering, Slovak Technical University, Radlinského 9, 812 37 Bratislava, Slovak Republic*

[b]*Department of Biochemical Technology, Slovak Technical University, Radlinského 9, 812 37 Bratislava, Slovak Republic*

Abstract

The selection of suitable aqueous two-phase system for lactose hydrolysis by whole-cell β-galactosidase is described. Partitioning of substrate, products, biocatalyst and viable, permeabilized and glutaraldehyde-treated cells of *Kluyveromyces marxianus* in various systems containing polyethylene glycol and dextran was studied. Some characteristics of the selected systems were also established.

1. Introduction

The utilization of sweet whey is an important economical and ecological problem in cheese manufacture [1]. This drawback can be solved by hydrolysis of lactose, which is the major component of whey. Various methods of lactose hydrolysis are used [1,2], and hydrolysis of lactose in an aqueous two-phase system (ATPS) has shown promising results [3,4].

Bionconversion in an ATPS is an interesting alternative to the use of immobilized biocatalysts or membrane bioreactors. This method offers several advantages, *e.g.*, efficient mass transfer, biocompatibility, stability of biocatalyst and simultaneous separation of product [5,6]. Biocatalysis in an ATPS can be easily realized in a semi-continuous or continuous mode and integrated with other purification techniques [7,8]. However, it is necessary to find a system that has favourable partitioning (biocatalyst, substrate, product) and separation characteristics for each individual bioconversion process.

In this paper, the partitioning behaviour of viable and treated cells of *Kluyveromyces marxianus*, β-galactosidase, lactose, glucose and galactose in various polyethylene glycol (PEG)–dextran (Dx) ATPSs and the separation characteristics of selected systems are described.

2. Experimental

2.1. Organisms

The yeasts used in this investigation were *Kluyveromyces marxianus* CCY eSY2 and *K. marxianus* CCY 51-1-1 obtained from the Czecho–Slovak Collection of Yeasts, Bratislava, Slovak Republic. Stock cultures were maintained

* Corresponding author.

0021-9673/94/$07.00
SSDI 0021-9673(93)E1178-3

on lactose-based agar at 5°C and subcultured monthly.

2.2. Materials

PEG 6000 was obtained from NCHZ (Nováky, Slovak Republic) and PEG 20 000 from LOBA Feinchemie (Austria).

Dextrans D 40, D 70, D 250, D 500 were a kind gift from Biotika (Slovenská Ľupča, Slovak Republic).

Boehringer Mannheim Biochemica tests for the determination of lactose, glucose, galactose were used.

o-Nitrophenyl-β-D-galactopyranoside (ONP-G), *o*-nitrophenol (ONP) and other chemicals of analytical-reagent grade were purchased from Lachema (Brno, Czech Republic).

2.3. Whole-cell yeast β-galactosidase preparation

The yeast biomass was prepared by aerobic cultivation in lactose-based medium [60 g l^{-1} lactose, 5 g l^{-1} yeast extract, 5 g l^{-1} $(NH_4)_2SO_4$ and 2 g l^{-1} $(NH_4)_2HPO_4$]. After the cultivation the cells were centrifuged (3000 *g*, 10 min), washed three times with cold tap water and suspended in 0.05 *M* potassium phosphate buffer (pH 6.5) to a concentration of 100 g l^{-1} (dry mass). The cells were permeabilized by the addition of 15% (v/v) of chloroform–ethanol (1:9) at 25°C for 15 min [9]. The solvents were removed by centrifugation and the cell ghosts were washed with buffer. Finally, this suspension was treated with 0.4% (w/v) glutaraldehyde at 5°C for 10 min and washed with cold buffer [10].

2.4. Partitioning experiments

The cells (viable, permeabilized and glutaraldehyde treated) were added to the tubes with various ATPS at a concentration of 10 g l^{-1}. The tubes were vigorously shaken for 2 min to allow the phases to homogenize. After sufficient separation (2 h), the numbers of cells in both phases were determined microscopically.

The partitioning of free β-galactosidase, lactose, glucose and galactose was measured after centrifugal separation of the phases (1500 *g*, 4 min). The partition coefficient was defined as the ratio of the concentrations (cells, saccharides) or activity (β-galactosidase) in the top and bottom phases.

All partitioning experiments were carried out at pH 6.5 and 25°C. The samples were measured in triplicate.

2.5. Characteristics of phase systems

The phase systems were prepared in 0.05 *M* phosphate buffer (pH 6.5) from a stock solution of the phase polymers. The systems were mixed intensively with a magnetic stirrer and allowed to settle in a test-tube at 25°C. The percentage of dextran-rich bottom phase dispersed in the PEG-rich top phase was determined turbidimetrically and by centrifugation of the top phase [6,8]. After phase separation, top-to-bottom volume ratio was also measured. The effect of the yeast cells on the phase separation rate and the volume ratio was investigated in the concentration range 1–40 g l^{-1}.

2.6. Analytical methods

β-Galactosidase activity was measured with the chromogenic substrate ONPG [9] at 25°C. A 0.05-ml volume of the sample was added to 0.45 ml of 4 m*M* ONPG solution in 0.05 *M* potassium phosphate buffer (pH 6.5) with 0.1 m*M* $MnCl_2$. The reaction was stopped by adding 1 ml of 0.2 *M* Na_2CO_3 after 4 min and the absorbance at 416 nm was measured. The molar absorbtivity for ONP of 4600 l mol^{-1} cm^{-1} was determined under the same conditions. One unit of β-galactosidase activity was defined as the amount of enzyme required to release 1 μmol of ONP per minute.

Glucose, galactose and lactose concentrations were determined by using kits prepared by Boehringer Mannheim Biochemicals.

3. Results and discussion

3.1. Partition of viable and treated cells

For semi-continuous or continuous extractive bioconversion, minimizing the removal of biocatalyst with the product-containing phase is crucial. Hence extremely one-sided partitioning of the biocatalyst is required. This is easy to accomplish for cells, but much more difficult for soluble enzymes [5,6]. Some workers [9,10] have described the use of whole-cell β-galactosidase preparations, which could be more advantageous than using free enzymes for lactose hydrolysis in ATPSs. Moreover, the whole-cell biocatalysts often exhibit higher operational stability and their preparation is easier and cheaper.

First the partitioning behaviour of intact cells of two strains of lactose utilizing the yeast *K. marxianus* in various PEG–dextran systems was investigated. Some partition coefficients are given in Table 1. As expected, the cells preferred the dextran-rich bottom phase. The cell partitioning was more extreme with increasing polymer molecular mass and concentration. Only the partition coefficients of *K. marxianus* CCY 51-1-1 increased with increase in the dextran molecular mass. Such behaviour of the yeast cells in an ATPS can be explained by the strong affinity of cell walls containing polysaccharides (glucans, mannans) to the more hydrophilic dextran phase. Although there are not many data about partitioning of yeast cells or cell walls, similar results have been reported for baker's yeasts, *Saccharomyces cerevisiae* and *Candida boidinii* [6,11].

As the best results were obtained in ATPSs containing PEG 20 000, these systems were used in the following experiments. In addition, separation of products from high-molecular-mass PEG with ultrafiltration, which is a potential method for product separation from the polymer, is easier.

Permeabilization of the cells with solvents (described under Experimental) did not affect the distribution (Table 2). Probably the surface properties of the cells, which determine their partitioning, were not changed by this operation. Under the experimental conditions the solvent

Table 2
Partitioning of the permeabilized cells of *K. marxianus* CCY eSY2 in PEG 20 000–dextran (6:4, w/w) systems

Dextran	Partition coefficient
D 40	$<10^{-6}$
D 70	$<10^{-6}$
D 250	$<10^{-6}$
D 500	$<10^{-6}$

Table 1
Partitioning of the viable cells of *K. marxianus* CCY eSY2 and CCY 51-1-1 in various PEG–dextran systems

PEG (%, w/w)	Dextran (4%, w/w)	Partition coefficient	
		K. marxianus CCY eSY2	*K. marxianus* CCY 51-1-1
6% PEG 20 000	D 40	$<10^{-6}$	$<10^{-6}$
	D 70	$<10^{-6}$	$<10^{-6}$
	D 250	$<10^{-6}$	$<10^{-6}$
	D 500	$<10^{-6}$	$<10^{-6}$
6% PEG 6000	D 70	$1.5 \cdot 10^{-2}$	$2.0 \cdot 10^{-4}$
	D 250	$5.4 \cdot 10^{-4}$	$5.0 \cdot 10^{-3}$
	D 500	$8.9 \cdot 10^{-4}$	$6.1 \cdot 10^{-3}$
4% PEG 20 000	D 250	$7.9 \cdot 10^{-4}$	$3.1 \cdot 10^{-4}$
	D 500	$4.9 \cdot 10^{-4}$	$7.6 \cdot 10^{-4}$

only modified the membrane composition, which resulted in the removal of diffusion barriers for small molecules, such as lactose, glucose and galactose [9,12]. Stabilization of β-galactosidase inside the cells with glutaraldehyde cross-linking also did not have any effect on the partitioning behaviour of the cells (Table 3).

3.2. Partitioning of free enzyme and saccharides

As partial release of β-galactosidase from treated cells during the long-term hydrolysis process could occur [9,10], it is important to establish the partitioning behaviour of the free enzyme. The partitioning of soluble β-galactosidase from *K. marxianus* CCY eSY2 was interesting (Table 4). This enzyme preferred the dextran-rich phase directly with increase in PEG concentration. A similar behaviour of yeast β-galactosidase in the PEG–pullulan system and mould β-galactosidase in PEG–salt systems has been described [3,4]. In contrast, β-galactosidase from *Escherichia coli* exhibited affinity to the PEG phase in PEG–salt systems [4,13]. The structure and properties of β-galactosidases differ according to their producing microorganisms and therefore it is difficult to predict the partitioning behaviour of the enzyme in ATPSs [4].

The partitioning of the saccharides (lactose, glucose and galactose) is shown in Table 5. As expected [7], partition coefficients of about 1 were found. Hence a shift of the reaction equilibrium in these systems is improbable.

3.3. Phase separation characteristics

In addition to partitioning of the biocatalyst, substrate, product, some properties of the ATPS used, such as the volume ratio of the phases and the separation time of the system, play important roles in extractive bioconversion.

The volume ratios of the phases of the systems considered are given in Table 3. Generally, a high volume ratio of the top to the bottom phase is suitable when the biocatalyst prefers the bottom phase, because a higher yield of product is obtained in the opposite phase.

The separation characteristics of the selected systems are shown in Fig. 1. The system PEG 20 000–dextran 40 (8:4, w/w), which exhibits a high volume ratio and slow phase separation, was selected for semi-continuous lactose hydrolysis because a high product yield is the most important factor in this instance. In contrast, rapid phase separation is needed for the continu-

Table 4
Partitioning of β-galactosidase from *K. marxianus* CCY eSY2 in PEG 20 000–dextran D 40 systems

PEG 20 000–dextran D 40 (w/w)	Partition coefficient
4:8	$5.9 \cdot 10^{-3}$
6:6	$1.7 \cdot 10^{-3}$
8:4	$1.2 \cdot 10^{-4}$

Table 5
Partitioning of saccharides in PEG 20 000–dextran D 40 two-phase systems

PEG 20 000–dextran (w/w)	Partition coefficient		
	Glucose	Galactose	Lactose
4:8	0.99	0.88	0.91
6:6	0.94	0.91	0.91
8:4	1.06	0.97	0.88

Table 3
Partitioning of the stabilized cells of *K. marxianus* CCY eSY2 in PEG 20 000 systems

PEG 20 000–dextran D 40 (w/w)	Partition coefficient	Volume ratio (top/bottom phase, ml/ml)
4:8	$<10^{-6}$	10.1/9.9
6:6	$<10^{-6}$	13.0/7.0
8:4	$<10^{-6}$	16.1/3.9

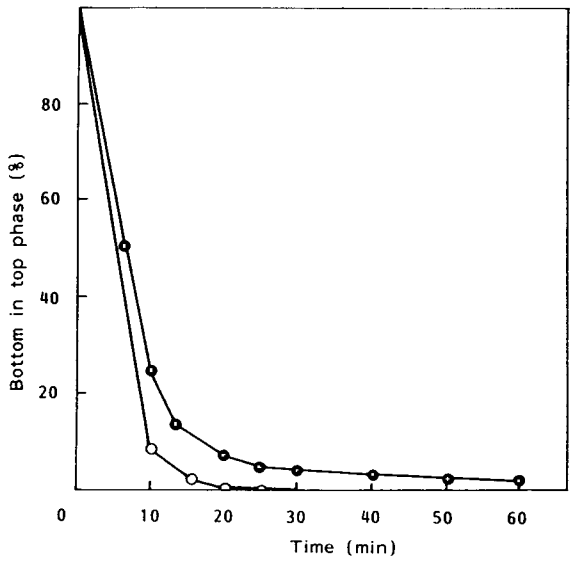

Fig. 1. Phase separation characteristics at 25°C and pH 6.5 of PEG 20 000–dextran D 40 (●) 8:4 (w/w); (○) 4:8 (w/w).

ous process. Slow phase separation lowers the volume productivity and requires a large volume

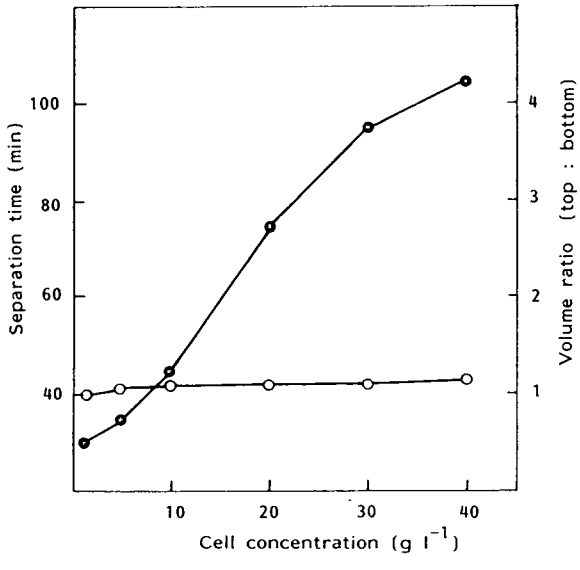

Fig. 2. Effect of treated cells of *K. marxianus* on (●) the separation time and (○) the phase volume ratio of the system PEG 20 000–dextran D 40 (4:8, w/w) at 25°C and pH 6.5.

of a settler. Therefore, the system PEG 20 000–dextran D 40 (4:8, w/w) is more suitable for the continuous process.

The presence of cells is known to influence both the volume ratio of the phases and the separation time [6]. The effect of the whole cell concentration is illustrated in Fig. 2. The volume ratio was affected negligibly in the concentration range considered, but the separation time was affected significantly. Hence some limitation of lactose hydrolysis in the ATPS occurs at high biocatalyst concentrations.

In conclusion, the selection of suitable ATPSs for lactose hydrolysis with whole-cell yeast β-galactosidase and some its characteristics have been reported We are now investigating the semi-continuous and continuous processes of lactose hydrolysis in the selected ATPSs.

4. References

[1] V. Gekas and M. López-Leiva, *Process Biochem.*, 20 (1985) 2.
[2] V.H. Holsinger and A.E. Kigerman., *Food Technol.*, 45 (1991) 92.
[3] A.-L. Nguyen, S. Grothe and J.H.T. Luong, *Appl. Microbil. Biotechnol.*, 27 (1988) 241.
[4] J.-P. Chen and C.H. Wang, *J. Ferment. Bioeng.*, 71 (1991) 168.
[5] E. Andersson and B. Hahn-Hägerdahl, *Enzyme Microb. Technol.*, 12 (1990) 242.
[6] H. Hustedt, K.H. Kroner and M.-R. Kula, in H. Walter, D.E. Brooks and D. Fisher (Editors), *Partitioning in Aqueous Two-Phase Systems*, Academic Press, Orlando, 1985, p. 529.
[7] M. Larsson, V. Arasatnam and B. Mattiasson, *Biotechnol. Bioeng.*, 33 (1989) 758.
[8] M. Stred'anský, Ľ. Kremnický, E. Šturdík and A. Fecková, *Appl. Biochem. Biotechnol.*, 38 (1993) 269.
[9] B. Champluvier, B. Kamp and P.G. Rouxhet, *Enzyme Microb. Technol.*, 10 (1988) 611.
[10] M.S. Joshi, N. Bachhawat and S.G. Bhat, *Biotechnol. Lett.*, 11 (1989) 349.
[11] J. Kühn, *Biotechnol. Bioeng.*, 22 (1980) 2393.
[12] J.A. Brodsky and J.W.D. Grootwassink, *J. Food Sci.*, 51 (1986) 897.
[13] A. Veide, A.-L. Smeds and S.O. Enfors, *Biotechnol. Bioeng.*, 25 (1983) 1789.

ELSEVIER

Journal of Chromatography A, 668 (1994) 185–190

JOURNAL OF CHROMATOGRAPHY A

Cell partitioning in two-polymer aqueous phase systems and cell electrophoresis in aqueous polymer solutions Red blood cells from different species

Harry Walter*, Kim E. Widen

Laboratory of Chemical Biology-151, Veterans Affairs Medical Center, Long Beach, CA 90822-5201, USA

Abstract

A correlation, with some exceptions, between the partitioning behavior of red blood cells (RBCs) from different species in charge-sensitive dextran–poly(ethylene glycol) (PEG) aqueous phase systems and their relative electrophoretic mobilities (EPMs) in phosphate-buffered saline (PBS) has previously been reported. This relationship has now been further probed by carrying out RBC electrophoresis in media (*i.e.*, dextran-rich bottom or PEG-rich top phases) more closely approximating the environment in which RBC partitioning takes place to see whether a better correlation would ensue.

The ratios of viscosity-corrected EPMs of different species' RBCs in (diluted) dextran-rich *or* PEG-rich phases/EPMs of the respective species' RBCs in PBS differ for a number of species, and from each other, reflecting thereby differences in kind (*i.e.*, dextran or PEG) and nature of polymer interaction with these RBCs. There is a general tendency for EPMs in any of the tested media to correlate with both the cells' relative partition ratios as well as with their relative EPMs in one of the other media. However, examination of the behavior of different species' RBCs taken two species at a time indicates that their relative EPMs in any two suspending media or in one suspending medium and partitioning often differ.

Thus, both the cell partition ratio and the cell EPMs obtained in polymer media must, at least in some cases, reflect surface properties other than or in addition to the charge reflected by EPM measurements in PBS or saline. Cell electrophoresis in polymer solutions thereby provides an additional parameter for discriminating between surface properties of certain closely related cell populations.

1. Introduction

Partitioning in dextran–poly(ethylene glycol) (PEG) aqueous phase systems is an established method for the separation and characterization of biomaterials including cells [1–3]. The separation of cell populations and their fractionation into subpopulations by partitioning depends on the interaction of the cells' surface properties with the physical properties of the phase system. Certain salts (*e.g.*, alkali phosphates) give rise to a Donnan potential between the phases thus rendering the system "charge-sensitive". Surface charge-related properties can then, under appropriate conditions [4,5], be a major determinant of the cells' partitioning behavior.

The current investigation on cell electrophoretic mobilities (EPMs) in aqueous polymer solutions (*i.e.*, dextran-rich bottom or PEG-rich top phases) was initiated to determine whether the previously reported correlation between the partition ratios of red blood cells (RBCs) from

* Corresponding author.

0021-9673/94/$07.00
SSDI 0021-9673(94)00129-W

different species and their relative EPMs in isotonic salt solution [6] would be improved by carrying out measurements in an environment more closely approximating that in which RBC partitioning takes place. Such a result could be envisaged because cell–polymer interactions affect both the cell partition ratio [7] and the cell EPM in polymer solutions [8,9]. Cell electrophoresis in polymer solutions was found, however, to provide an additional parameter, and one distinct not only from partitioning but also from EPM measurements in phosphate-buffered saline (PBS) [8,9], for discriminating between surface properties of cells.

2. Experimental

2.1. Reagents

Dextran T500 (lot No. 01 06905) was obtained from Pharmacia LKB (Piscataway, NJ, USA). PEG 8000 (Carbowax 8000) was from Union Carbide (Long Beach, CA, USA). All salts used were of analytical-reagent grade.

2.2. Preparation of two-polymer aqueous phase systems and other standard solutions

Aqueous two-phase systems having the dextran and PEG concentrations and salt compositions and concentrations indicated in the text below and in Table 1 were prepared as previously described [4,5]. PBS contained 0.15 *M* NaCl + 0.01 *M* sodium phosphate buffer, pH 6.8.

2.3. Collection of blood from different species

Blood from nine different species was collected in either acid–citrate–dextrose (ACD) anticoagulant solution or in citrate vacutainers. With ACD the ratio used was 10 ml of blood to 3 ml of ACD. Human blood was obtained by venipuncture from presumably hematologically normal individuals; rhesus monkey blood came from the Oregon Regional Primate Research Center (Beaverton, OR, USA); dog blood was from the femoral vein; and rat and mouse blood were obtained by heart puncture. Beef blood came from Shamrock Meats (Vernon, CA, USA); while horse, pig and sheep blood were from the Animal Resource Facility, University of California, Irvine, CA, USA. Erythrocytes were used within one week of collection.

2.4. Viscosity determinations of suspending media used in EPM measurements

The viscosities of the various suspending media were estimated by means of an Ostwald

Table 1
Viscosity-corrected electrophoretic mobilities of red blood cells from different species in three different suspending media

Species	PBS[a]	Top phase[b]	Bottom phase[b]
Beef	−0.89 ± 0.03 (8)	−1.32 ± 0.05 (8)	−2.90 ± 0.14 (8)
Dog	−1.26 ± 0.02 (4)	−2.14 ± 0.03 (4)	−5.48 ± 0.03 (4)
Horse	−1.24 ± 0.01 (4)	−2.17 ± 0.01 (4)	−5.75 ± 0.04 (4)
Human	−1.08 ± 0.01 (26)	−1.82 ± 0.03 (13)	−4.55 ± 0.07 (26)
Rhesus monkey	−1.03 ± 0.01 (3)	−1.71 ± 0.00 (3)	−4.35 ± 0.01 (3)
Mouse	−1.19 ± 0.01 (4)	−2.14 ± 0.04 (4)	−5.26 ± 0.07 (4)
Pig	−0.81 ± 0.02 (4)	−1.32 ± 0.02 (4)	−3.41 ± 0.05 (4)
Rat	−1.25 ± 0.01 (4)	−1.97 ± 0.01 (4)	−5.00 ± 0.02 (4)
Sheep	−1.15 ± 0.01 (4)	−1.84 ± 0.02 (4)	−4.64 ± 0.04 (4)

Data present the mean electrophoretic mobilities ($\mu m\ s^{-1}\ V^{-1}\ cm$) ± S.D. with the number of experiments in parentheses.
[a] PBS was composed of 0.15 *M* NaCl + 0.01 *M* sodium phosphate buffer, pH 6.8.
[b] Top and bottom phases were from a system containing 5% (w/w) dextran T500, 3.5% (w/w) PEG 8000, 0.15 *M* NaCl and 0.01 *M* sodium phosphate buffer, pH 6.8. Top phase is PEG-rich and bottom phase is dextran-rich. Top and bottom phases were diluted 1:1 with the indicated RBC suspension in PBS followed by measuring cell EPMs.

viscometer immersed in a tank thermostated at 25 ± 0.2°C.

2.5. EPM measurements on erythrocytes in various suspending media

RBCs were washed three times with PBS and a suitable cell aliquot was, finally, suspended in PBS.

Phase systems, at 21–24°C, were mixed and permitted to settle in a separatory funnel overnight. Top and bottom phases were then separated with the material at the interface being discarded. The PEG-rich top and the dextran-rich bottom phases were centrifuged at 12 000 *g* for 15 min to ensure that phase separation was complete. Top phase was removed leaving all remaining bottom phase and some top phase behind in the centrifuge tube. Bottom phase was pipetted out of the latter from the middle of the bottom phase being careful to keep residual top phase from entering the pipette.

Aliquots of the cell suspensions in PBS (see above) were diluted 1:1 (w/w) with top or bottom phase of the phase system (for phase composition see Table 1).

Cell microelectrophoresis was carried out in a cylindrical chamber (Rank Brothers, Cambridge, UK) at 25 ± 0.2°C with transillumination [10]. Measurements were made using an applied voltage of 50.0 resulting in a field strength ranging from 2.28 to 2.58 V/cm depending on the suspension medium used. In each sample the rates of migration of ten RBCs were obtained at the stationary level for the calculation of EPMs in $\mu m\ s^{-1}\ V^{-1}$ cm [10]. The rates of migration were observed in alternate directions.

2.6. Partitioning of erythrocytes in aqueous two-phase systems

The procedure used for partitioning cells has previously been described [7]. The partitioning data in Figs. 1 and 2 were taken from ref. 11 except for rhesus monkey RBCs. The partition ratio for the latter was determined (together with those of a couple of other species' RBCs as reference) and interpolated. The phase system was composed of 5% (w/w) dextran, 4% (w/w)

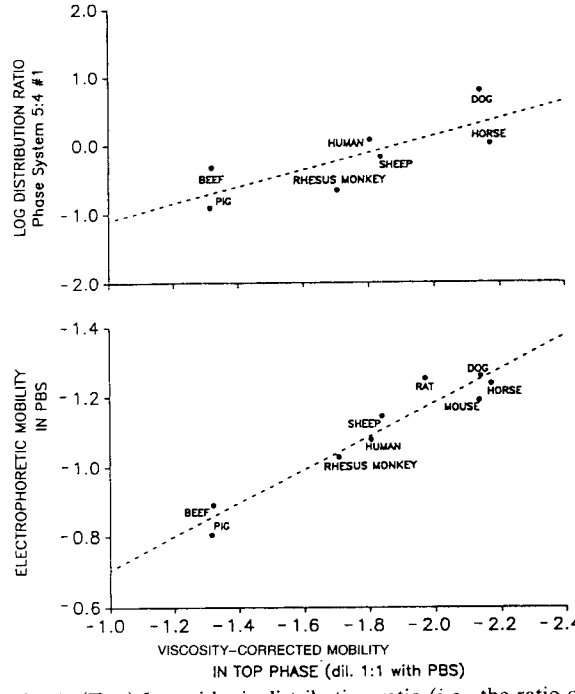

Fig. 1. (Top) Logarithmic distribution ratio (*i.e.*, the ratio of the number of cells in top phase divided by the number of cells at the interface plus bottom phase, taken from ref. 11) in a charge-sensitive dextran–PEG phase system plotted against the viscosity-corrected, relative electrophoretic mobility (EPM) in a top phase (diluted 1:1 with PBS) of erythrocytes (RBCs) from a number of different species. (Bottom) EPMs in PBS of RBCs from different species plotted against their viscosity-corrected EPMs in diluted top phase. For composition of phase systems see text and Table 1. Mobilities in $\mu m\ s^{-1}\ V^{-1}$ cm.

PEG and 0.11 *M* sodium phosphate buffer, pH 6.8, shorthand "5:4 #1" [4,5]. It was selected (for detailed procedure and discussion see ref. 5) so that the polymer concentrations were the lowest at which, in the absence of a Donnan potential, RBCs from the species, shown in the top parts of Figs. 1 and 2, would not partition but would remain at the interface. In this manner partitioning in the presence of a Donnan potential can be considered to be predominantly charge-related [5].

The partitioning data for beef RBCs plotted are those belonging to partition class 1 (deemed the most suitable comparison because (see ref. 12) these cells have the lowest partition ratio but

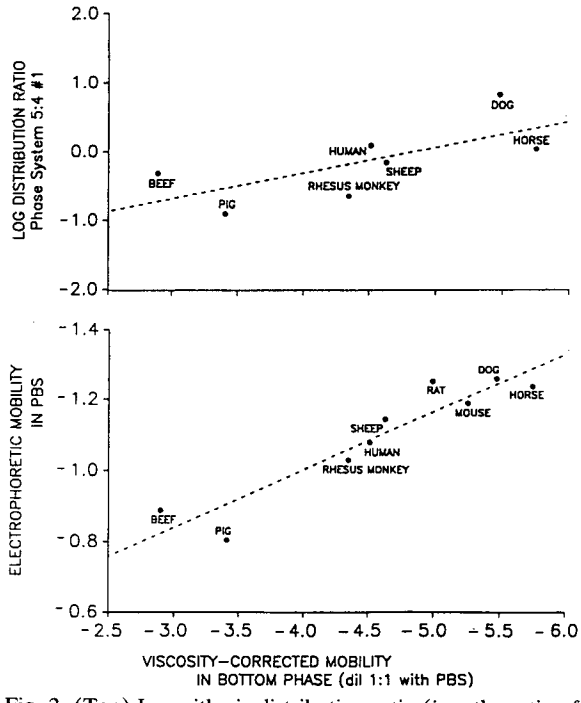

Fig. 2. (Top) Logarithmic distribution ratio (*i.e.*, the ratio of the number of cells in top phase divided by the number of cells at the interface plus bottom phase, taken from ref. 11) in a charge-sensitive dextran–PEG phase system plotted against the viscosity-corrected, relative electrophoretic mobility (EPM) in a bottom phase (diluted 1:1 with PBS) of erythrocytes (RBCs) from a number of different species. (Bottom) EPMs in PBS of RBCs from different species plotted against their viscosity-corrected EPMs in diluted bottom phase. For composition of phase systems see text and Table 1. Mobilities in $\mu m\ s^{-1}\ V^{-1}\ cm$.

the same EPM in saline as the other two beef RBC partition classes).

2.7. Presentation of data

The EPMs of the RBCs in the different media were corrected to the viscosity of water. The EPMs obtained in the different suspending media are presented, in Table 1, as the mean ± S.D. with the number of individuals or animals in parentheses. p values (Table 2) were obtained by one-way analysis of variance (ANOVA).

Partitions are expressed in terms of log distribution ratios (*i.e.*, the ratio of number of cells in top phase/number of cells in bottom phase + interface).

3. Results and discussion

3.1. Electrophoresis of RBCs from different species in PBS and in selected polymer solutions

In Table 1 we present the viscosity-corrected EPMs of RBCs from a number of species in three different suspending media (PBS, diluted PEG-rich top phase and diluted dextran-rich bottom phase of the system indicated). The cell mobilities, in top and bottom phase, are plotted (in lower parts of Figs. 1 and 2, respectively) against their respective EPMs in PBS. It is apparent that the EPMs of some species' RBCs differ in PBS but not in top phase (*e.g.*, beef, pig) and that the relative mobilities of RBCs from some species' reverse depending on whether PBS or top phase is the suspending medium used (*e.g.*, rat and mouse) (Fig. 1, bottom). Comparison of Figs. 1 and 2 further indicates that the relative EPMs of some of the different species' RBCs are differentially affected by the top and bottom phases (*e.g.*, beef and pig RBCs which have the same EPM in top but differ in mobility in bottom phase).

The significance, in terms of p, of the difference between the ratios of one species' RBCs EPM in top phase/EPM in PBS *or* EPM in bottom phase/EPM in PBS to those of another species' ratios is indicated in the top and bottom parts, respectively, of Table 2. Note that there is a significant difference in most cases but that a difference in one phase for a given comparison of two species' RBCs does not necessarily mean that a difference will be found in the other (*e.g.*, dog and mouse).

It thus appears that the EPMs of cells in polymer solutions depend on the interaction of the particular polymer used with the particular cell examined. Since the EPMs of different cell populations can be differentially affected by the same polymer, and that of some cell populations can be differentially affected by different polymers, the nature of the surface properties re-

Table 2
Significance (p values) of difference between ratios of electrophoretic mobilities of red blood cells from different species compared in top phase/phosphate-buffered saline (top) *or* bottom phase/phosphate-buffered saline (bottom)

	Beef	Dog	Horse	Human	Rhesus monkey	Mouse	Pig	Rat	Sheep
Beef		$p<0.01$	$p<0.01$	$p<0.01$	$p<0.01$	$p<0.01$	$p<0.01$	$p<0.01$	$p<0.01$
Dog	$p<0.01$		$p<0.01$	N.S.	$p<0.01$	$p<0.01$	$p<0.02$	$p<0.01$	$p<0.01$
Horse	$p<0.01$	$p<0.01$		$p<0.01$	$p<0.01$	N.S.	$p<0.01$	$p<0.01$	$p<0.01$
Human	$p<0.01$	$p<0.01$	$p<0.01$		N.S.	$p<0.01$	N.S.	$p<0.01$	$p<0.01$
Rhesus monkey	$p<0.01$	$p<0.05$	$p<0.01$	N.S.		$p<0.01$	N.S.	$p<0.01$	$p<0.01$
Mouse	$p<0.01$	N.S.	$p<0.01$	$p<0.01$	$p<0.01$		$p<0.01$	$p<0.01$	$p<0.01$
Pig	$p<0.01$	N.S.	$p<0.01$	N.S.	N.S.	$p<0.05$		$p<0.05$	N.S.
Rat	$p<0.01$	$p<0.01$	$p<0.01$	$p<0.01$	$p<0.01$	$p<0.01$	$p<0.01$		$p<0.01$
Sheep	$p<0.01$	$p<0.01$	$p<0.01$	N.S.	$p<0.01$	$p<0.01$	$p<0.05$	N.S.	

N.S. = Not significant.

flected, though unknown, need not be related directly to the cell surface charge estimated by cell electrophoresis in PBS or saline.

3.2. Relationship between the EPMs of RBCs from different species in polymer solutions and the cells' relative partition ratios in a charge-sensitive dextran–PEG phase system

The mobilities in top and bottom phase are plotted (in upper parts of Figs. 1 and 2, respectively) against the partition ratios of the cells obtained in charge-sensitive phase system 5:4 #1 [4,11]. It is apparent that some species' RBCs differ in partition ratios but have the same EPM in top phase (*e.g.*, beef and pig) while others show the reverse behavior (*e.g.*, beef and sheep, human and horse) (Fig. 1, top).

The partitions of RBCs from different species in a charge-sensitive dextran–PEG aqueous phase system tend to display an overall correlation with the cells' relative EPMs in top or bottom phase (as has previously been found for EPMs measured in saline [4–6]). However, while such a tendency exists, examination of the behavior of RBCs from two species at a time reveals that these may have the same mobility and differ in partition ratio or the reverse. Thus, just as in the cases of EPM measurements in PBS and in top or bottom phases (see above), partitioning in a charge-sensitive phase system can reflect yet other surface properties than those indicated not only by the cell EPM in PBS but also those discriminated by cell EPM in top or bottom phases.

3.3. Relationship between the EPMs of beef RBCs from different animals in polymer solutions and the cells' relative partition ratios in a charge-sensitive dextran–PEG phase system

It is known from previous work that cell partitioning in charge-sensitive dextran–PEG phase systems and cell electrophoresis in saline (or PBS) do not necessarily reflect the same surface charge [12]. This can be illustrated by the fact that beef RBCs from different animals have the same EPM but fall into three partition classes: classes comprised of cells having low (class 1), intermediate (class 2) or high (class 3) partition ratios [12]. The classes reflect, to some extent, the quantity of charge-bearing groups on the respective cells' surfaces [12]. EPM in saline measures charge at the shear plane while partitioning may be able to gauge charge also deeper into the membrane.

The EPMs of beef RBCs presented in Table 1 were obtained from eight animals of which three belonged to partition class 1, four to class 2 and one to class 3. The EPMs in dextran-rich bottom

and PEG-rich top phases of these RBCs did not discriminate among the partition classes to which the cells belonged. This result reinforces the conclusion that partitioning in charge-sensitive phase systems and EPM measurements even in top and bottom phases can reflect different cell surface properties.

4. Conclusions

While both the (red blood) cell partition ratio obtained in a charge-sensitive dextran–PEG phase system and the (red blood) cell EPMs measured in polymer media are surface charge-related they must, at least in some cases, also reflect surface properties other than or in addition to the charge determined by EPM measurements in PBS or saline. Thus, the possibility that polymer solutions serve to amplify cell EPM differences too small to detect in PBS (see ref. 9) seems unlikely since EPM differences in polymer solutions can also be qualitatively unlike those measured in PBS.

Cell electrophoresis in polymer solutions provides a useful and distinct parameter with which to test for differences in surface properties between closely related cell populations. This is borne out by the EPM differences found between Alzheimer and normal RBCs [9] and between human young and old RBCs [8] in appropriately selected polymer solutions, differences which cannot be observed in PBS.

5. Acknowledgements

We thank Geoffrey V.F. Seaman for instructing us in the use of the cell microelectrophoresis apparatus. This work was supported by the Medical Research Service of the Department of Veterans Affairs.

6. References

[1] H. Walter, D.E. Brooks and D. Fisher (Editors), *Partitioning in Aqueous Two-Phase Systems —Theory, Methods, Uses, and Applications to Biotechnology*, Academic Press, Orlando, FL, 1985.

[2] P.-Å. Albertsson, *Partition of Cell Particles and Macromolecules*, Wiley-Interscience, New York, NY, 1986.

[3] H. Walter and G. Johansson (Editors), *Methods in Enzymology*, Vol. 228, Academic Press, San Diego, CA, 1994.

[4] H. Walter, in H. Walter, D.E. Brooks and D. Fisher (Editors), *Partitioning in Aqueous Two-Phase Systems —Theory, Methods, Uses, and Applications to Biotechnology*, Academic Press, Orlando, FL, 1985, pp. 327–376.

[5] H. Walter and C. Larsson, *Methods Enzymol.*, 228 (1994) 42–63.

[6] H. Walter, F.W. Selby and R. Garza, *Biochim. Biophys. Acta*, 136 (1967) 148.

[7] H. Walter, T.J. Webber and E.J. Krob, *Biochim. Biophys. Acta*, 1105 (1992) 221.

[8] G.B. Nash, R.B. Wenby, S.O. Sowemimo-Coker and H.J. Meiselman, *Clin. Hemorheology*, 7 (1987) 93.

[9] H. Walter, K.E. Widen and S.L. Read, *Biochem. Biophys. Res. Commun.*, 194 (1993) 23.

[10] G.V.F. Seaman, in M.D. Surgenor (Editor), *The Red Blood Cell*, Vol. II, Academic Press, New York, 1975, pp. 1135–1229.

[11] H. Walter, E.J. Krob and D.E. Brooks, *Biochemistry*, 15 (1976) 2959.

[12] H. Walter, R. Tung, L.J. Jackson and G.V.F. Seaman, *Biochem. Biophys. Res. Commun.*, 48 (1972) 565.

ELSEVIER

Journal of Chromatography A, 668 (1994) 191–200

JOURNAL OF CHROMATOGRAPHY A

Fragmentation and separation of the thylakoid membrane Effect of light-induced protein phosphorylation on domain composition

Hreinn Stefánsson, Louie Wollenberger, Per-Åke Albertsson*

Department of Biochemistry, Chemical Centre, University of Lund, P.O. Box 124, S-221 00 Lund, Sweden

Abstract

The thylakoid membrane consists of three main compartments, the stroma lamellae, the central appressed region of grana and the peripheral grana margins. These three domains can be separated from each other by fragmentation and aqueous two-phase partitioning. Upon phosphorylation the light-harvesting chlorophyll *a*/*b* binding complex II (LHC II) dissociates away from photosystem II in grana and migrates into the stroma lamellae. Dynamic processes, such as lateral migration of LHC II, can be examined by analysing corresponding fragments from phosphorylated and non-phosphorylated thylakoids. Our results show that we can detect not only the well studied lateral migration of phosphorylated LHC II from grana to stroma lamellae, but also migration within the grana disc, from the core of grana to the margins of grana. Furthermore, we show that the grana margin vesicles and the stroma lamellae vesicles are heterogeneous populations that can be fractionated further by counter-current distribution.

1. Introduction

The photosynthetic membrane in higher-plant chloroplasts is thought to be a single-membrane continuum, organized into grana stacks and intergranal connections of stroma-exposed membranes, the so called stroma lamellae. The membrane consists of several domains that have probably evolved in order to carry out specialized functions. The main function of the thylakoid membrane is to capture light quanta and to convert the light energy into chemical energy. The light energy is used to drive a series of redox reactions whereby water is oxidized to protons and oxygen while ferrodoxin is reduced concomitantly with the synthesis of ATP.

Protein complexes involved in the light reactions of photosynthesis, such as α and β forms of photosystems I and II, are segregated laterally in the membrane continuum. The thylakoid membrane can be fragmented by mechanical means such as press treatments or sonication. The fragments so obtained are in the form of membrane vesicles which can be separated by a combination of centrifugation and aqueous two-phase partitioning. Thus, sonication of thylakoid membranes followed by centrifugation and partitioning by aqueous two-phase systems gives rise to many membrane fragments of differing properties. Based on earlier work [1–4] we have shown that the thylakoid membrane consists of

* Corresponding author.

0021-9673/94/$07.00
SSDI 0021-9673(93)E0030-X

at least three domains, the stroma lamellae, the central appressed region of grana and the peripheral grana margins. Fragments derived from domains of the thylakoid membrane can yield valuable information for a better understanding of the light reaction of photosynthesis.

Proteins are known to migrate between domains within the thylakoid membrane due to changes in environmental conditions such as light intensity. Regulation of the light-harvesting antenna of photosystem (PS) II by phosphorylation of the light-harvesting chlorophyll *a*/*b* binding complex (LHC II) causes detachment of LHC II from PS II. Phosphorylated LHC II is then believed to migrate away from PS II into PS I-enriched domains [5–7] but whether or not the redirected excitation energy can be trapped by PS I has not been unequivocally established. Migration of phosphorylated LHC II from grana into PS I-rich domains has been explained by different mechanisms such as protein–protein electrostatic forces [7,8] or by thermal diffusion once LHC II is detached from PS II [9].

In this study we use a rapid procedure to fractionate the thylakoid membrane into vesicle populations deriving from grana and stroma lamellae. By fractionating the grana-derived vesicles further by sonication and partitioning by means of an aqueous two-phase system we obtain vesicles representing grana core and grana margins. By comparing these vesicle populations from phosphorylated and control thylakoids we are able to investigate lateral migration of proteins within the grana stacks, that is from the core of granum to the margins of granum.

2. Materials and methods

2.1. Chemicals

Dextran T500 was obtained from Pharmacia (Uppsala, Sweden). Poly(ethylene glycol) (PEG) 4000 (Carbovax PEG 3350) was supplied by Union Carbide (New York, NY, USA). [γ-^{32}P]ATP was prepared as described [10].

2.2. Chloroplast isolation

Spinach chloroplasts were isolated from dark adapted leaves, osmotically broken and washed as described in ref. 2 except the final wash which was carried out in medium comprising 10 m*M* sodium phosphate buffer (pH 7.4)/5 m*M* NaCl/10 m*M* $MgCl_2$/5 m*M* NaF/100 m*M* sucrose. The thylakoids were resuspended in the same medium to give a concentration of about 1 mg chlorophyll/ml prior to illumination.

2.3. Light-induced protein phosphorylation

Phosphorylation took place in the above mentioned medium by illuminating thylakoids in the presence of 0.1 m*M* ATP for 15 min at 18°C under continuous stirring. Incubation took place under red light (630–680 nm, 200 μE m^{-2} s^{-1}). Control thylakoids were illuminated in absence of ATP. When samples for phosphorimaging were prepared phosphorylation was performed as described above except that 50 μCi/ml [γ-^{32}P] ATP was also added. After the illumination, samples were washed twice in the illumination medium and resuspended in the same medium to a chlorophyll concentration of about 4 mg/ml.

2.4. Fragmentation of the thylakoid membrane

Thylakoid suspension (2 g) was added to 9.66 g of a polymer mixture to give 5.8% (w/w) Dextran T500/5.8% (w/w) PEG 4000/10 m*M* sodium phosphate buffer (pH 7.4)/5 m*M* NaF/2 m*M* $MgCl_2$/20 m*M* sucrose. After 45 min incubation on ice the thylakoids were sonicated in a Vibra-cell ultrasonic processor, Model VC 500 (Sonics and Materials, Danbury, CT, USA) equipped with a 1/2-in. (1 in. = 2.54 cm) horn. Thylakoids were sonicated six times for 30 s with resting intervals of 1 min in a cylindrical aluminium tube immersed in ice. The ultrasonic exposure had an intensity output setting of 7, with 20% duty pulses. After sonication 6.43 g lower phase and 5 g top phase (composition of lower and top phase as described below) were

added to the sonicate. This then constituted the "sample system".

2.5. Separation of membrane fragments by phase partitioning

Vesicles derived from grana and stroma lamellae were separated by a batch procedure in three steps [2] or in a quantitative way by counter-current distribution at 4°C. In both procedures the composition of the phase system used for the separation of grana vesicles from the stroma lamellae vesicles, and the grana core vesicles from the grana margin vesicles was always 5.8% (w/w) Dextran T500/5.8% PEG 4000/10 m*M* sodium phosphate buffer (pH 7.4)/20 m*M* sucrose/10 m*M* NaF. For counter-current distribution an apparatus where the phase separation is speeded up by centrifugation was used [11]. The apparatus contains 60 cavities, cavities 0–2 were loaded with 1.8 ml "sample system" and cavities 3–59 by 1.8 ml phase system (0.9 ml top phase and 0.9 ml lower phase). One operation cycle comprised 30 s mixing followed by 90 s centrifugation and one transfer. Normally a total of 55 cycles were carried out. When phosphorylated and control vesicles were compared the respective samples were loaded in three cavities on opposite halves of the plate and only 25 operation cycles carried out.

Preparation of grana core and grana margins vesicles was carried out by sonicating the grana vesicles further. The lower phase from the batch procedure containing the grana derived vesicles was sonicated sixteen times for 30 s, under the same conditions and using the same settings as described above for the sonication of whole thylakoids, then fractionated by counter-current distribution.

Further fractionation of the grana margin vesicles and the stroma lamellae vesicles was carried out without sonication in phase systems of higher polymer concentrations. The phase systems contained 6.0% (w/w) of both polymers (Dextran T500 and PEG 4000) for fractionation of the grana margin vesicles but 6.2% (w/w) of both polymers (Dextran T500 and PEG 4000) for separation of the stroma lamellae-derived vesicles, otherwise the phase systems had the same composition as the phase system previously described.

After fractionation the vesicles were released from the polymers by two-fold dilution in a medium comprised of 100 m*M* sucrose/10 m*M* sodium phosphate buffer/10 m*M* NaF and absorbance at 680 and 650 nm recorded for each cavity. Fractions were then pooled in order to collect peaks of interest and pelleted by centrifugation at 100 000 *g* for 90 min. Pellets were then resuspended in the dilution medium and dimethyl sulphoxide added to yield 5% (w/v) when vesicles were to be stored in liquid nitrogen.

2.6. Analysis

Measurements of chlorophyll concentration and the determination of chlorophyll *a*/*b* ratio of the various samples was carried out according to Arnon [12].

Absorbance difference measurements for the quantification of P_{700} (reaction centre of PS I) were performed according to ref. 13 using a DW-2 Aminco spectrophotometer operating in a split-beam mode. The concentration of P_{700} was determined from the amplitude of the light–dark absorbance change at 700 nm, using an extinction coefficient of 64 mM^{-1} cm^{-1}.

Kinetic measurements of P_{700} photooxidation were carried out according to ref. 14, and the potassium cyanide treatment of isolated membrane vesicles according to ref. 15 using 150 m*M* KCN for 2 h. A DW-2 Aminco spectrophotometer, working in dual-wavelength mode with 700 nm as measuring wavelength and 730 nm as reference, was used for the kinetic measurements. The optical path-length of the cuvette was 10 mm. The actinic beam was transmitted by a 380–600-nm broad band filter, a 566.9-nm interference filter HBW 80, and attenuated by a neutral filter to give an uniform light between 500 and 600 nm and an intensity of 25 $\mu E\ m^{-2}\ s^{-1}$. Nicolet NIC Model 527 was used for signal averaging.

Cytochrome *f* content was determined immu-

nologically by rocket immunoelectrophoresis [16] at pH 8.6. The concentration of cytochrome *f* standard (Sigma) was determined spectroscopically.

Sodium dodecyl sulphate (SDS)–polyacrylamide gel electrophoresis was performed according to the method of Laemmli [17], using a 12–22.5% polyacrylamide gradient slab gel containing 4 *M* urea.

Measurements of ^{32}P-labeled polypeptides in SDS gels were performed by phosphorimaging with a Fuji BAS 2000 Bio-Imaging Analyzer.

3. Results

The schematic model of the thylakoid membrane shown in Fig. 1a represents a structure thought to be a single-membrane continuum with different domains. Fig. 1b illustrates the proposed domain organization within the grana stacks with PS IIα in the central core of the granum and PS Iα at the margins of granum. It is assumed that upon light-induced phosphorylation, LCH II is detached from PS IIα and migrates into PS I-rich domains.

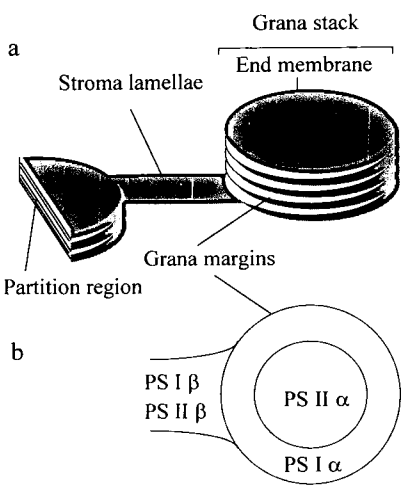

Fig. 1. Model for organization of the thylakoid membrane. (a) Different domains of the membrane. (b) Proposed domain organization within the grana stack with PS IIα in the core of granum and PS Iα in the margins of the granum. PS Iβ and PS IIβ with their smaller antennae are located in stroma lamellae.

3.1. Fractionation strategy

Fig. 2 illustrates the fractionation strategy. Thylakoids are first fragmented by sonication and separated into grana (α) and stroma lamellae (β) vesicles (Fig. 2a). By further sonication of the grana vesicles their margins can be peeled off resulting in two, occasionally three, well separated peaks in the counter-current distribution diagram (Fig. 2b). The peak labeled α3 represents the margin fraction while the vesicles

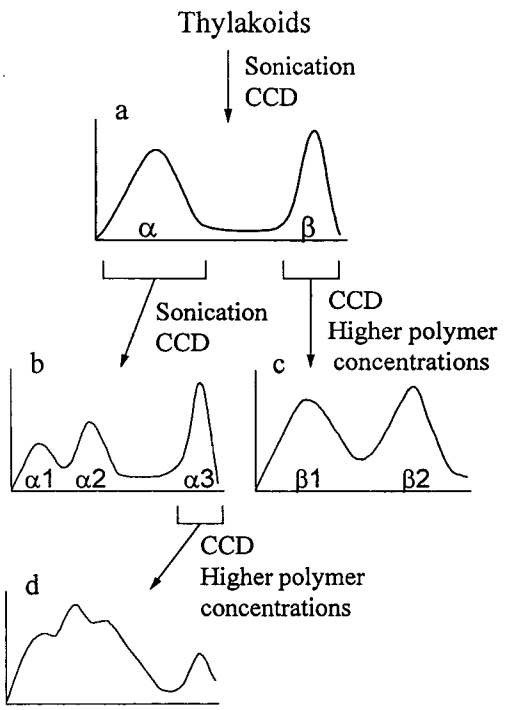

Fig. 2. Fractionation strategy demonstrating: (a) Separation of grana (α) and stroma lamellae vesicles (β) by counter-current distribution (CCD). (b) Sub-fractionation of the grana vesicles, margins of grana labeled α3 and the core of grana, fractions labeled α1 and α2. (c) Separation of stroma lamellae vesicles and (d) separation of grana margin vesicles in phase systems of higher polymer concentrations. Ordinates represent absorbance at 680 nm and abscissas fractions 1–60 from the counter-current distribution plate.

of the $\alpha 1$ and $\alpha 2$ peaks originate from the central core of the grana [3,18]. The margin vesicle population ($\alpha 3$) can be further separated without additional sonication in a phase system of higher polymer concentration (Fig. 2d) giving rise to three or four peaks. Likewise the stroma lamella vesicles (b) can be separated into two sub-populations $\beta 1$ and $\beta 2$ (Fig. 2c).

3.2. Fractionation of thylakoids

Counter-current distribution of sonicated thylakoids is shown in Fig. 3a. Individual cavities were pooled to obtain nine fractions for further analysis (see bar at the top of Fig. 3a). Chlorophyll a/b ratios, P_{700} content and polypeptide pattern (not shown) confirm that stroma lamellae vesicles are in the peak to the right. The grana peak is quite heterogeneous, chlorophyll a/b ratios range from 2.2 to 2.7 (see bar at the top of Fig. 3a).

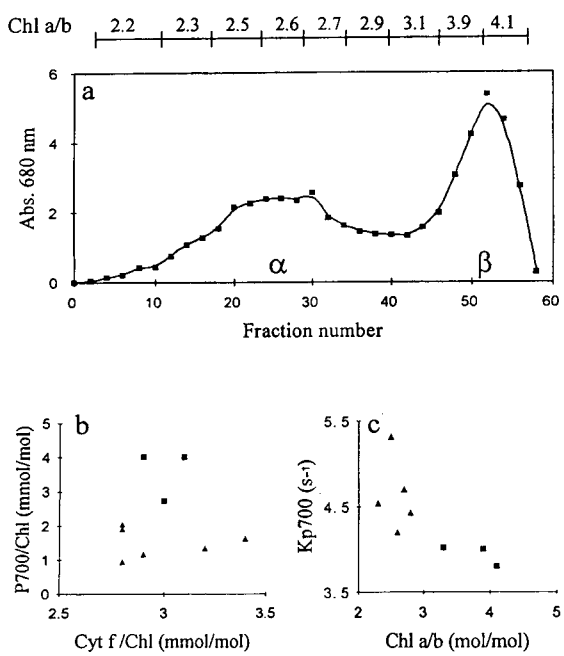

Fig. 3. Heterogeneity within the grana and stroma lamellae populations. (a) Counter-current distribution of sonicated thylakoids. For each of the nine pooled fractions (see bar at the top) the content of cytochrome (Cyt) f and P_{700} was determinated as also the kinetics of P_{700} photooxidation. Chlorophyll (Chl) a/b ratios for nine pooled fractions shown at the top. (b) P_{700}/Chl as a function of Cyt f/Chl for the pooled fractions. (c) The rate constant, KP_{700}, for photooxidation of P_{700} as a function of chlorophyll a/b ratio for the pooled fractions. Triangles in b and c represent fractions from the grana peak (α) and squares stand for fractions from the stroma peak (β) in Fig. 3a.

Fig. 3b is a plot of P_{700} *vs.* cytochrome f from the pooled fractions. The P_{700} content varies from 0.9 to 4.2 (mmol/mol chlorophyll) while the content of cytochrome f varies from 2.8 to 3.5 (mmol/mol chlorophyll). The non-linear relationship amongst these data indicate the existence of at least three different pools of cytochrome f as demonstrated in ref. 19.

The value for the kinetic constant for P_{700} photooxidation and thereby also the antenna size of PS I in the different fractions is decreasing with higher chlorophyll a/b ratio (Fig. 3c). It shows that the PS I of the two peaks differ in antenna size. A 20 to 30% larger antenna size is found in the population originating from grana as compared to the population originating from the stroma lamellae. Others [20] have reported an even larger antenna size difference (40%) between these PS I populations of the grana and stroma lamellae vesicles.

3.3. Subfractionation of grana lamellae

When the grana vesicles (α) are collected, sonicated and then fractionated by counter-current distribution a diagram as seen in Fig. 4a is obtained; $\alpha 1$ and $\alpha 2$ represent the grana core with low chlorophyll a/b ratio (2.2–2.3) and large PS II antennae size; $\alpha 3$ represents the grana margins with higher chlorophyll a/b ratio (2.6), and more PS I as compared to the core fractions. Further fractionation of the grana margin fraction ($\alpha 3$) in a phase system of higher polymer concentration containing 6.0% (w/w) of the polymers Dextran T500 and PEG 4000 gives rise to three or four new peaks (Fig. 4b). These populations derived from the grana margin region have slightly different chlorophyll and polypeptide compositions (see bar at the top of Fig. 4b for the chlorophyll a/b ratios).

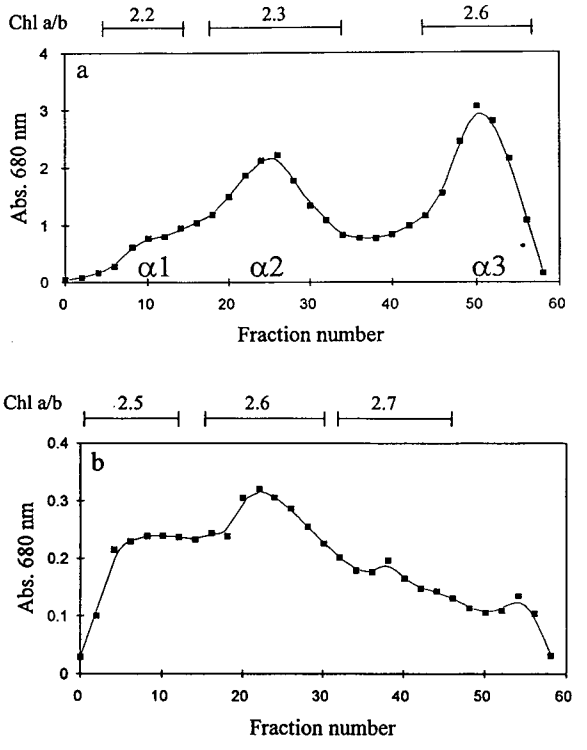

Fig. 4. (a) Counter-current distribution of sonicated grana (α) vesicles. The peak to the right (α3) consists of grana margin vesicles and the peaks to the left consist of grana core vesicles (α1 and α2). (b) Counter-current distribution of grana margin vesicles (α3) in a phase system of higher polymer concentrations.

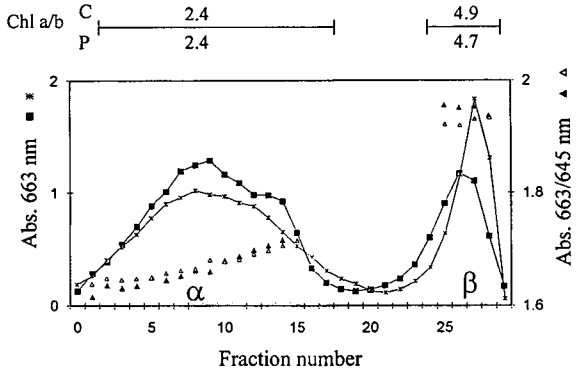

Fig. 5. Counter-current distribution of phosphorylated and non-phosphorylated sonicated thylakoids. Absorption at 663 nm for (□) non-phosphorylated thylakoids and (*) phosphorylated thylakoids. Absorption ratio 663/645 nm for (▲) non-phosphorylated thylakoids and (△) phosphorylated thylakoids.

3.4. Fractionation of phosphorylated thylakoids

In the counter-current distribution diagram for sonicated phosphorylated thylakoids (Fig. 5) more material is obtained on a chlorophyll basis in the stroma lamellae fraction (β) compared to the non-phosphorylated stroma fraction. Furthermore, the chlorophyll *a*/*b* ratio of the phosphorylated stroma lamellae fraction is lower. In contrast, the control (non-phosphorylated) and the phosphorylated grana fractions have very similar chlorophyll *a*/*b* ratios. A closer examination of all the tubes under the α peak (grana) shows, however, a significant variation in the chlorophyll *a*/*b* ratio as revealed by the ratio between the light absorption at 663 and 645 nm.

The lower chlorophyll *a*/*b* ratio for the phosphorylated stroma lamellae fraction can be explained by lateral movements of phosphorylated LHC II, with low chlorophyll *a*/*b* ratio (about 1.0), from the grana lamellae to stroma lamellae or by partial destacking of grana stacks resulting in the formation of more non-appressed membrane vesicles during sonication. Concomitant increase in the chlorophyll *a*/*b* ratio for the grana fractions is not seen which can be explained by the fact that the chlorophyll *a*/*b* ratio of LHC II (about 1.0) is closer to that of the grana fraction (2.4) compared to the chlorophyll *a*/*b* ratio for the stroma lamellae fraction (4.9) and also that the loss of membrane material from the α peak is relatively less than the concomitant gain in the β peak (Fig. 5). The loss of phosphorylated LHC II does therefore not contribute significantly to an increase in the chlorophyll *a*/*b* ratio of the phosphorylated grana fraction.

The α peaks of both the phosphorylated and non-phosphorylated samples are heterogeneous with respect to the chlorophyll *a*/*b* ratios (ranging from 2.2 to 2.7 for different pooled fractions as seen in Fig. 3a.) This heterogeneity might be explained by assuming that vesicles containing relatively more grana margins are present in the right-hand part of the α peak whereas vesicles in the left-hand part consist of vesicles more rich in the partition region from which most of the margins have been peeled off by sonication.

The two plots 663/645 nm for control and phosphorylated thylakoids cross at fraction 8 under the α peak in Fig. 5. In fractions 1–7 the phosphorylated fractions have a higher chlorophyll a/b ratio than their controls while the opposite holds for fractions 9–14. This can be explained by lateral migrations of phosphorylated LHC II from the centre into the margins of grana due to its phosphorylation (see Discussion below). The experiment of Fig. 5 has been repeated two times and the 663/645 plots cross under the α peak in both cases. It should be stressed that a counter-current distribution with 25 transfers (Fig. 5) involves 25 separate partitions and therefore errors of individual partitions are cancelled to a great extent. The difference between the two 663/645 plots of Fig. 5 is therefore significant even though it is small.

When the stroma lamellae vesicles from phosphorylated and control thylakoids are fractionated by counter-current distribution in a phase system of higher polymer concentration, without further sonication, two peaks are obtained (Fig. 6). For the control β vesicles the peak to the left has higher chlorophyll a/b ratio than the peak to the right in the counter-current distribution diagram. In the case of phosphorylated vesicles the peaks have similar chlorophyll a/b ratio but more material is found in the peak to the right as compared to control β vesicles. Both peaks from the phosphorylated membrane have lower chlorophyll a/b ratios than their corresponding control fractions. This shows that more LHC II is found in both stroma lamellae populations $\beta 1$ and $\beta 2$ after phosphorylation.

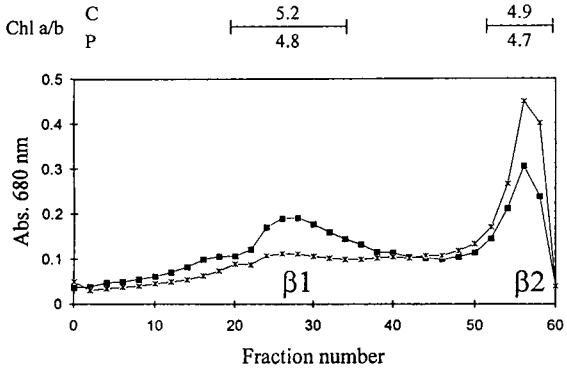

Fig. 6. Counter-current distribution of stroma lamellae (β) vesicles. (□) = Non-phosphorylated (β) vesicles; (*) = phosphorylated (β) vesicles.

3.5. Imaging and analysis of phosphoprotein heterogeneity

The phosphorimage (Fig. 7) shows that ^{32}P-labeled PS II polypeptides [CP 43, D1,D2 and 9 kDa (*i.e.* M_r 9000)] are predominantly found in the grana derived fractions, grana core and grana margins. Two additional polypeptides of apparent molecular mass 62 000 and 64 000 are found most labeled in the grana fractions, where slightly more labeling is found in the grana margin fraction compared to the grana core fraction. These polypeptides may represent the M_r 64 000 protein kinase associated with the cytochrome b/f complex [21,22] which is in agreement with previous results where the M_r 64 000 protein kinase is found to be enriched in the grana margins [21–23]. ^{32}P-Labeled LHC II polypeptides are found rather evenly distributed throughout the membrane.

Analyses of ^{32}P-labeled PS II polypeptides and LHC II polypeptides quantified from SDS gels (Fig. 7) are shown in Fig. 8 a, c and d. In Fig. 8a photo-stimulated luminescence (PSL) for CP 43

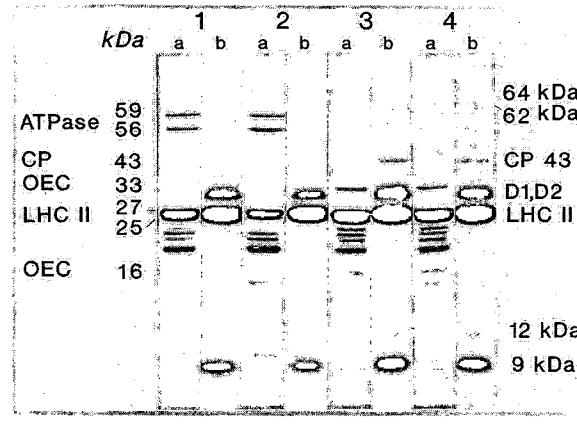

Fig. 7. SDS–polyacrylamide gel electrophoresis analysis (lanes a) and subsequent phosphorimages (lanes b) of fragments from phosphorylated thylakoid membrane: 1 = thylakoids, 2 = stroma lamellae, 3 = grana core and 4 = grana margins. The same amount of chlorophyll (17 mg) was loaded in each lane. kDa = kilodalton.

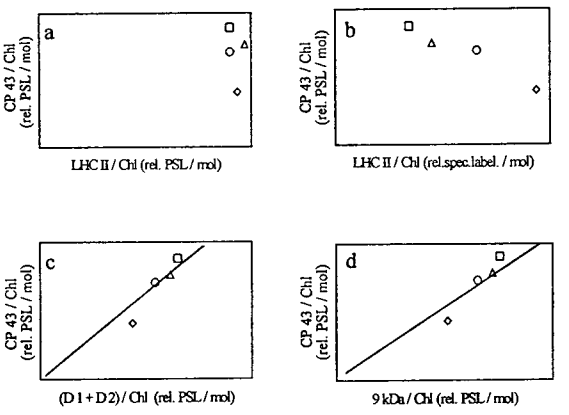

Fig. 8. Relation between ^{32}P-labeled thylakoid proteins for the different fractions estimated from SDS gels (Fig. 7). □ = Grana core; △ = grana margins; ○ = thylakoids; ◇ = stroma lamellae. Photostimulated luminescence (PSL) obtained for CP 43 as a function of: (a) PSL obtained from LHC II polypeptides, (b) specific labeling of LHC II polypeptides, (c) PSL obtained from D1 and D2 polypeptides and (d) PSL obtained from the M_r 9000 (9 kDa) phosphoprotein of PS II.

is plotted against PSL obtained for LHC II which gives a straight vertical line showing that almost the same amount of ^{32}P-labeled LHC II is found in all the fractions. In Fig. 8b PSL for CP 43 is plotted against specific labeling of LHC II (the relative amount of LHC II was estimated from the peak area after scanning of the Coomassie brilliant blue-stained gels). The plot shows linear relationship with a negative slope, *i.e.* the specific labeling of LHC II decreases with increased labeling of CP 43. This means that phosphorylated light-harvesting complexes II migrate from grana to stroma lamellae whereas phosphorylated CP 43 polypeptides remain in the grana. Another explanation might be that phosphorylation causes partial destacking at the edges of the grana which contain phosphorylated LHC II and PS Iα and that these areas are removed from the grana by sonication and end up in the stroma lamellae fraction. Fig. 8c and d show that there is a linear stochiometric relationship between the labeled PS II polypeptides CP 43, D1 + D2 and M_r 9000 phosphoprotein in the different membrane domains. This shows that under our conditions no detectable movement of any one individual PS II polypeptide away from the PS II complex into other domains is observed.

4. Discussion

The thylakoid membrane consists of three main compartments, the stroma lamellae, the central appressed region of grana and the peripheral grana margins. These three domains can be separated from each other by fragmentation and aqueous two-phase partitioning [24]. It has been shown that those photosystem II units with large antennae, PS IIα, are localized in the grana partitions while those PS II centres with smaller antennae, PS IIβ, are localized in the stroma lamellae and grana margins [3]. The PS I units with large antennae, PS Iα, are localized in the grana margins while PS Iβ having smaller antennae are localized in the stroma lamellae [2,3]. The cytochrome *b/f* complex is found to be uniformly distributed within the thylakoid membrane but in varying concentrations, highest in the grana partitions and lowest in the grana margins [19]. The ratio between PS IIα and cytochrome *b/f* in the partition region is about 2 to 1 and these two complexes may form a super complex in the membrane [25]. The ATP synthase is found only in the unappressed regions, *i.e.* in the stroma lamellae and the grana margins.

This work shows that these three main domains of the thylakoid membrane consist of subdomains. The reason for this conclusion is that upon further fragmentation and separation, or by only further separation by counter-current distribution in a new phase system, the vesicle populations are found to be heterogeneous, giving rise to distinct peaks in the counter-current distribution diagram. For example, the margin vesicle fraction designated α3 in Fig. 4a is separated into three, probably four different sub-populations having different chlorophyll *a/b* ratios, and the stroma lamellae fraction (β in Figs. 2a or 3a) splits up into two separate peaks (Fig. 6) also having different chlorophyll *a/b* ratios.

It has been shown that the grana vesicles (α) are inside-out while the stroma lamellae vesicles (β) are right side out [26]. It is probably this

difference in sideness which contributes to the efficient separation of these two types of vesicles. The grana margin vesicles ($\alpha 3$), which are peeled off from grana core by sonication, have a right side out conformation [3] and are separated efficiently from the remaining inside-out vesicles originating from the centre of the grana. The mechanism behind the separation of the different stroma lamellae vesicles (Fig. 6) or margin vesicles (Fig. 4b) which are all right side out is however not known to us. It may reflect the number of ATP synthase or LHC II complexes, exposed on the surface of the vesicles.

Light-induced protein phosphorylation results in a significant effect on the counter-current distribution patterns. The peak representing grana vesicles (α peak in Fig. 5) becomes smaller and the peak representing the stroma lamellae vesicles (β peak in Fig. 5) becomes larger than the control peak. This may be due to partial unstacking of the grana stacks whereby some of the grana margins, which are enriched in PS Iα, (*i.e.* more LHC II is bound to PS I in grana margins compared to PS I in stroma lamella) are peeled off and turned right-side out and collected in the β peak. Alternatively some LHC II may have migrated from the grana to the stroma lamellae as has been suggested to occur upon phosphorylation [5–7]. Both explanations are supported by the lower chlorophyll *a*/*b* ratio of the β peak after phosphorylation.

Of particular interest is the shift in the chlorophyll *a*/*b* ratio in the various fractions under the α peak of Fig. 5 (fractions 1–15). This shows that in fractions 1–8 the chlorophyll *a*/*b* ratio goes up upon phosphorylation while the opposite change occurs in fractions 9–14. It is reasonable to assume that the fractions 9–14, because of their higher chlorophyll *a*/*b* ratios, contain vesicles relatively rich in grana margins. Margin vesicles have a chlorophyll *a*/*b* ratio of 2.6–3 compared to a ratio of 2.0–2.2 for the vesicles originating from the partion region [3]. Hence the reason for the decrease in the chlorophyll *a*/*b* ratio of fractions 9–14 and corresponding increase for fractions 1–8 upon phosphorylation may be due to migration of LHC II, with its low chlorophyll *a*/*b* ratio, from the central core of the grana disc to the peripheral margins. If this interpretation is correct then this is the first time a migration of LHC II from the centre of the grana to the margins has been demonstrated. Since it has been suggested [1,20] that the linear electron transport occurs in the grana, between PS IIα and PS Iα, it is reasonable to suggest that a migration of LHC II within the grana is important for the regulation of non-cyclic electron transport.

Also in the case of stroma lamellae the phosphorylation has a significant effect on the counter-current distribution pattern (Fig. 6). Here the relative size of the two peaks change after phosphorylation. The largest shift in the chlorophyll *a*/*b* ratio occurs in the peak to the left of Fig. 6. This might mean that the left peak represents vesicles which originate from a special domain of the stroma lamellae which receives selectively more LHC II from the grana.

Taken together our results indicate that there is, after phosphorylation of the thylakoid membrane proteins, a movement of LHC II from the centre of the grana into both the margins of grana and into the stroma lamellae. This may be relevant for the regulation of the photosynthetic electron transport, both non-cyclic in the grana and cyclic in the stroma lamellae.

This work demonstrates the usefulness of fragmentation in combination with aqueous two-phase partitioning for analysis of both the domain organization of the thylakoid membrane and dynamic processes within this membrane. The same approach described here should, with slight modifications, also be applicable to other biological membranes. [27]

5. Acknowledgements

We thank Ms. Agneta Persson for skillful technical assistance. This work was supported by the Swedish Natural Science Research Council.

6. References

[1] P.-Å. Albertsson, E. Andreasson and P. Svensson, *FEBS Lett.*, 273 (1990) 36.

[2] E. Andreasson, P. Svensson, C. Weibull and P.-Å. Albertsson, *Biochim. Biophys. Acta*, 936 (1988) 339.
[3] L. Wollenberger, H. Stefánsson, S.-G. Yu and P.-Å. Albertsson, *Biochim. Biophys. Acta*, in press.
[4] P.-Å Albertsson, *Partition of Cell Particles and Macromolecules*, Wiley, New York, 3rd ed., 1986.
[5] L.A. Staehelin and C.J. Arntzen, *J. Cell Biol.*, 97 (1983) 1327–1337.
[6] D.J. Kyle, T.-Y. Kuang, J.L. Watson and C.J. Arntzen, *Biochim. Biophys. Acta*, 725 (1984) 113–120.
[7] J. Barber, *Annu. Rev. Plant Physiol.*, 33 (1982) 261–295.
[8] J.F. Allen and N.G. Holmes, *FEBS Lett.*, 202 (1986) 175–181.
[9] J.F. Allen, *Biochim. Biophys. Acta*, 1098 (1992) 275.
[10] K.J. Chang, N.A. Marcus and P. Cuatrecasas, *J. Biol. Chem.*, 249 (1974) 6854.
[11] H.-E. Åkerlund, *J. Biochem. Biophys. Methods*, 9 (1984) 133.
[12] D.I. Arnon, *Plant Physiol.*, 24 (1949) 1.
[13] A. Melis and J.S. Brown, *Proc. Natl. Acad. Sci. U.S.A.*, 77 (1980) 4712.
[14] A. Melis, *Arch. Biochem. Biophys.*, 217 (1982) 536.
[15] R. Ouitrakul, and S. Izawa, *Biochim. Biophys. Acta*, 305 (1973) 105.
[16] B. Andersson, C. Larsson, C. Jansson, U. Ljungberg and H.-E. Åkerlund, *Biochim. Biophys. Acta*, 766 (1984) 21.
[17] U.K. Laemmli, *Nature*, 227 (1970) 680.
[18] P.-Å. Albertsson, *Physiol. Veg.*, 23 (1985) 731.
[19] P.-Å. Albertsson, E. Andreasson, P. Svensson and S.-G. Yu., *Biochim. Biophys. Acta*, 1098 (1991) 90.
[20] P. Svensson, E. Andreasson and P.-Å. Albertsson, *Biochim. Biophys. Acta*, 1060 (1991) 45
[21] S.J. Coughlan and G. Hind, *Biochemistry*, 26 (1987) 6515.
[22] A. Gal, G. Hauska, R. Herrmann and I. Ohad, *J. Biol. Chem.*, 265 (1990) 19742.
[23] S.-G. Yu, H. Stefánsson and P.-Å. Albertsson, in N. Murata (Editor), *Res. Phot. —Proceedings of the IXth International Congress on Photosynthesis, Nagoya, August 30–September 4, 1992*, Vol. I, Kluwer, 1992, p. 283.
[24] P.-Å. Albertsson, E. Andreasson, H. Stefánsson and L. Wollenberger, *Methods Enzymol.*, 228 (1994) 469–482.
[25] S.-G. Yu and P.-Å. Albertsson, *Photosynth. Res.*, 37 (1993) 227.
[26] B. Andersson, H.-E. Åkerlund and P.-Å. Albertsson, *FEBS Lett.*, 77 (1977) 141.
[27] P.-Å. Albertsson, *Quart. Rev. Biophys.*, 21 (1988) 61.

ELSEVIER

Journal of Chromatography A, 668 (1994) 201–213

JOURNAL OF CHROMATOGRAPHY A

Experimental basis for separation of membrane vesicles by preparative free-flow electrophoresis

D. James Morré*,[a], James Lawrence[a], Keri Safranski[a], Timothy Hammond[b], Dorothy M. Morré[c]

[a]*Department of Medicinal Chemistry, Purdue University, West Lafayette, IN 47907, USA*
[b]*Department of Medicine, University of Wisconsin Medical School, Madison, WI 53792, USA*
[c]*Department of Foods and Nutrition, Purdue University, West Lafayette, IN 47907, USA*

Abstract

In practice it has been possible to separate membrane particles of different origins but of similar chemical composition by preparative free-flow electrophoresis. Examples include the vacuolar (tonoplast) and plasma membranes of plants and membranes derived from the *cis* and *trans* regions of the rat liver Golgi apparatus. Yet, when analyzed for intrinsic molecules that might contribute to significant differences in surface charge, the separated membranes were surprisingly similar. As more information was generated, it became apparent that the membranes with greatest electrophoretic mobility (*i.e.* lysosomes, rightside-out tonoplast vesicles and membranes from the trans region of the Golgi apparatus), where those membranes with an inherent ability to acidify their interiors. By so doing, the vesicles generate a membrane potential, negative outside, which might serve as a basis for enhanced electrophoretic mobility. To test the hypothesis, tonoplast membranes were incubated with ATP to drive proton import or with monensin to dissipate the ATP-supported proton gradient. With ATP, mobility was enhanced. Also, when ATP-treated vesicles were analyzed in the presence of monensin, the ATP effect on mobility was reversed. Similarly with Golgi apparatus, mobility of the most electrophoretically mobile portions of the separation was enhanced by ATP and the ATP effect was reversed with monensin. A *trans* origin of the vesicles was verified by assay of the *trans* Golgi apparatus marker, thiamine pyrophosphatase. Finally, incubation with ATP (and reversal by monensin) was employed as an aid to the free-flow electrophoretic separation of kidney endosomes from complex mixtures. These lysosomal derivatives also are capable of acidification of their interiors in an ATP-dependent process and of generating, at the same time, a negative (outside) membrane potential. The findings provide both an experimental basis to enhance membrane separations by preparative free-flow electrophoresis and, at the same time, a theoretical basis to help explain why certain membranes of very similar overall chemical composition may be separated by electrophoretic methods.

1. Introduction

The techniques of preparative free-flow electrophoresis have been employed to separate a variety of cell types, membrane vesicles and macromolecules based on differential electrophoretic mobility in buffered solutions [1,2]. In this technique, the material to be separated is injected as a fine stream into a solution which is flowing perpendicular to the lines of force of an electric field (Fig. 1). Electrically charged particles are deflected from the direction of flow at an angle determined by a combination of flow

* Corresponding author.

0021-9673/94/$07.00
SSDI 0021-9673(94)00020-A

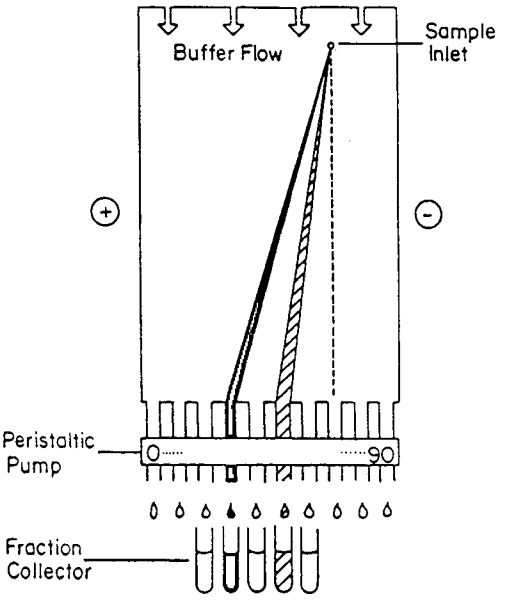

Fig. 1. Principles of preparative free-flow electrophoresis. From Morré *et al.* [16].

velocity and the electrophoretic mobility of the particles. Components with different electrophoretic mobilities move to different extents and are collected separately in a fraction collector after leaving the separation chamber.

Aqueous two-phase partition also has been successfully employed to fractionate membranes [3,4]. However, for the most part, these applications have been primarily to isolate highly purified plasma membranes [5–8], to subfractionate purified plasma membrane into rightside-out and inside-out vesicles [9], or to remove plasma membrane contaminants during the purification of internal membranes [10, 11]. However, with important exceptions using countercurrent distribution [12,13], there has been little progress in the separation of internal membranes by aqueous two-phase partition.

In contrast, preparative free-flow electrophoresis does provide for additional separations. Especially successful have been applications to the separation of vacuole (tonoplast) and plasma membranes of plants [14,15], Golgi apparatus subfractionations [16,17], isolation of endosomes [18,19] and isolation of transport vesicles induced with ATP to bud from transitional endoplasmic reticulum of rat liver [20]. Despite much success in effecting membrane separations, the molecular basis of free-flow electrophoretic separations of the type described above remain unclear.

Normally, intrinsic electrophoretic mobility of cells or membrane vesicles is a function of charged molecules exposed at the cell or vesicle surface. However, it has not been possible to relate electrophoretic separations of internal membranes to the content of charged surface molecules. Lysosomes, which are the most electrophoretically mobile of all internal membranes [21], are much less richly endowed with charged surface molecules than rightside-out plasma membrane vesicles regarded to be extensively coated with sialic acid-rich, anionic glycoprotein chains. Also the Golgi apparatus, which is a polarized structure consisting of *cis* and *trans* elements, can be unstacked and the component cisternae resolved into *cis*-derived fractions of low electrophoretic mobility, *trans*-derived fractions of greatest electrophoretic mobility and a medial fraction of intermediate electrophoretic mobility. However, a chemical gradient of externally exposed charged molecules to explain the differences in electrophoretic mobility has not been detected. There is a *cis*-to-*trans* gradient of sialic acid [16] but this sialic acid should be present at the inside surface of the sealed membrane vesicles and unavailable to influence electrophoretic mobility.

Even more difficult to understand is the basis for the tonoplast-plasma membrane separation of higher plant homogenates. Neither membrane appears to have an abundance of uniquely charged macromolecules at its surface. Sialic acid is absent and even their phospholipid compositions are similar [22]. Yet tonoplast membranes and plasma membranes from plants are readily separated by preparative free-flow electrophoresis.

The relationships described above for free-flow electrophoretic separation of membrane

vesicles are summarized in Fig. 2. What became evident was a correlation between electrophoretic mobility and the ability to accumulate protons. Those electrophoretic components endowed with the greatest electrophoretic mobility were membrane vesicles characterized by ATP-driven proton pumps capable of acidification of their interiors. Such vesicles may develop internal pH values approaching 5.0. These include lysosomes [23], tonoplast vesicles [24–26] and *trans* Golgi apparatus cisternae [27–29]. In parallel to acidification, the vesicles will develop an outside negative diffusion potential. In this report, we provide evidence for a pH-gradient-induced diffusion potential as a major contributing factor to membrane separation by preparative free-flow electrophoresis not based on intrinsic ionizable groups at the cell surface.

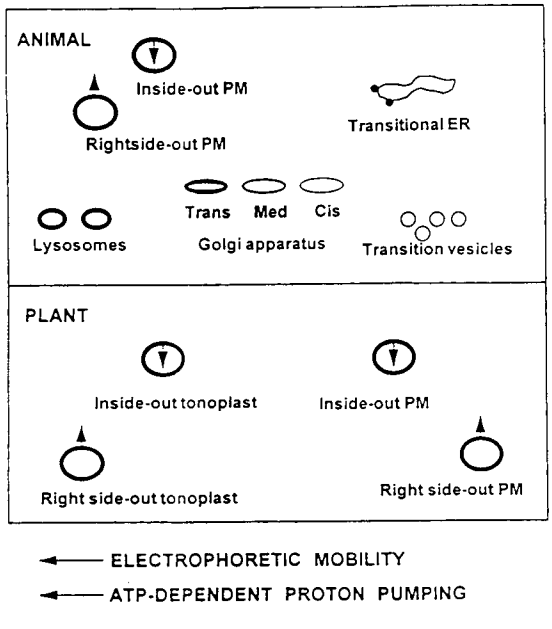

Fig. 2. Summary of particles separated by preparative free-flow electrophoresis showing relative mobility on the ordinate. The correlation is between electrophoretic mobility and the capacity for ATP-dependent inward proton pumping (acidification of vesicle interiors) with a concomitant generation of a membrane potential, negative outside, is indicated.

2. Materials and methods

2.1. Isolation of plant membranes

Seeds of soybean (*Glycine max* L. Merr. var. Williams) were soaked in tap water 4 to 6 h, planted in moist vermiculite, and grown 4 to 5 days in darkness. Segments of 2 cm long, cut from the hypocotyl 5 mm below the cotyledons, were harvested under normal laboratory conditions and used for isolation of membranes. The hypocotyl segments (25 g) were homogenized in 100 ml of a medium containing 25 m*M* Tris–2-(N-morpholino)ethanesulphonic acid (MES) (pH 7.5), 300 m*M* sucrose, 10 m*M* KCl and 1 m*M* $MgCl_2$ using a blender. After filtration through one layer of Miracloth (Chicopee Mills, NY), the filtrate was centrifuged for 10 min at 6000 g_{max} (6000 rpm, Sorvall, HB-4 rotor), and the pellet was discarded. The resulting supernatant was centrifuged for 30 min at 40 000 *g* (Beckman, SW-28 rotor), and the supernatant was discarded. The 40 000-*g* pellets were resuspended in electrophoresis chamber buffer (see below) and centrifuged for 30 min at 40 000 *g*. The final pellets again were resuspended in electrophoresis chamber buffer using about 1 ml per 10 g starting fresh mass of hypocotyl segments. For plant membranes, 10 μM $CaCl_2$ was added to the electrophoresis medium and the pH was 7.5.

2.2. Preparative free-flow electrophoresis

Preparative free-flow electrophoresis was performed on a VAP-22 free-flow electrophoresis device (Bender & Hobein, Munich, Germany). The electrophoresis medium contained 10 m*M* triethanolamine, 10 m*M* acetic acid, 5 m*M* glucose, 0.25 *M* sucrose and 0.5 m*M* $MgCl_2$, final pH 6.5 (1 *M* sodium hydroxide), osmolality 270 mosm, conductivity $5.9 \cdot 10^2$ μS. The conditions for the electrophoresis were: 167 mA, 131 ± 10% V/cm, buffer flow 2.75 ml/h per fraction, sample injection 3.5 ml/h, temperature 6°C. Absorption at 280 nm was determined on collected fractions. Each fraction was pelleted

for 20 min at 20 000 g, and resuspended in 30 m*M* mannitol, 12 m*M* 4-(2-hydroxyethyl)-1-piperazineethanesulphonic acid (HEPES), pH 7.4 (1 *M* Tris). Aliquots were kept for flow cytometry analysis and electron microscopy.

2.3. Assay of thiamine pyrophosphatase

The assays contained 50 m*M* Tris–HCl (pH 8.0), 15 m*M* $CaCl_2$, 3 m*M* thiamine pyrophosphate and 50 to 100 μg protein, in a total volume of 1 ml [30]. Incubations were at 37°C for 30 min and the reaction was terminated with cold 10% trichloroacetic acid. Inorganic phosphate was determined by the method of Harris [31].

2.4. Flow cytometry analysis

Flow cytometry analysis was performed on a Becton Dickinson FACStar Plus flow cytometer interfaced to a VAX 40 computer [32]. Flow cytometry conditions optimized to single molecule detection [33] were utilized as described for small particle resolutions [34,35]. All flow cytometry was in the presence of antifluorescein antibodies to quench fluorescence from extravesicular fluorescein.

2.5. Preparation of renal cortical endosomes

Renal cortical endosomes were prepared by differential Percoll gradient centrifugation [32,36,37]. Prior to harvesting kidneys the endosomal pathway was labeled by administering 100 mg of either non-fluorescent or fluorescein-conjugated dextran (10 000S; Sigma, St. Louis, MO, USA) intravenously. The dextran was small enough to be rapidly filtered through the renal glomeruli and taken up by endocytosis in the renal proximal tubule [38].

2.6. Enrichment of endosomes prior to free-flow electrophoresis by aqueous two-phase partition

A single 5.8% (w/w) aqueous two-phase partition of the endosomal fraction was performed [7,32]. The basic procedure was as described below for incremental aqueous two-phase partition.

2.7. Incremental aqueous two-phase partition fractionation of rat kidney endosomes

For incremental aqueous two-phase partitioning, stock solutions of 20% (w/w) dextran T-500 (Pharmacia) and 40% (w/w) poly(ethylene glycol) PEG 3350 (Union Carbide) were prepared in double-distilled water. For example, the 6.0% (w/w) two-phase system contained 4.80 g of 20% dextran and 2.40 g of 40% PEG in 30-ml Pyrex tubes on ice, after which were added 0.32 ml of 0.2 *M* potassium phosphate at pH 7.2. The total mass of the contents then was adjusted to 14 g with distilled water. Other mass ratios were prepared by varying the amounts of dextran and PEG added to the system, as described [7]. Membranes to be separated were resuspended in buffer, (total volume <2 ml), added to the two-phase system, and the final mass of the contents was adjusted to 16 g with buffer. The Pyrex tube was covered with Parafilm, and then inverted vigorously 40 times in the cold (9°C). The resultant mixture was centrifuged at 1000 *g* for 5 min at 4°C to separate the phases. The upper phase was removed using a Pasteur pipette and diluted 10-fold with buffer. Membranes were collected from the upper phase by centrifugation (20 000 *g* for 30 min).

2.8. Incubations with ATP and ionophore

To induce negative diffusion potentials, preparations were incubated for 15 min at room temperature in the presence of 1 m*M* ATP contained in 2.5 m*M* Tris–MES (pH 7.0), 50 m*M* chloride (KCl or NaCl), 3 m*M* $MgCl_2$, 0.5 m*M* dithiothreitol (DTT), and 75 to 100 μg protein in a total volume of 1.5 ml, combined with preparative free-flow electrophoresis chamber buffer [10 m*M* triethanolamine–acetic acid (pH 6.5) and 0.25 *M* sucrose]. For their dissipation, 1 μM monensin (final concentration) was added to the chamber buffer during free-flow electrophoresis.

2.9. Electron microscopy

Samples were fixed for electron microscopy with 2% glutaraldehyde in phosphate buffered saline. The samples were then transferred to 1% osmium tetroxide in 0.05 *M* sodium phosphate (pH 7.2) for several hours, the samples were dehydrated in an acetone series followed by embedding in Epon [6,7]. Lead-stained thin sections were examined and photographed using a Philips EM/200 electron microscope.

3. Results

When plant homogenates were incubated with ATP, the mobility of the tonoplast fractions was greatly enhanced (Fig. 3). Plant tonoplast vesicles isolated by preparative free-flow electrophoresis were active in acidification of their interiors and this acidification was ATP-dependent [39]. A shift also was noted in the plasma membrane portion of the separation (fractions 45–50).

Purified tonoplast fractions were analyzed under conditions similar to those of Fig. 3 where the vesicles carried a negative diffusion potential outward. Two distinct populations of vesicles were observed (Fig. 4). The tonoplast fraction having the greatest electrophoretic mobility (T_A) was identified as cytoplasmic side-out (rightside-out) based on the orientation of the stalked ATPase particles at the vesicle surface. To determine ATPase orientation, the freshly-isolated membrane vesicles were contrasted directly on electron microscope grids with phosphotungstic acid (negative staining) [39]. With T_A fractions, the stalked ATPase particles were on the external surface of the vesicles. The vesicles of the tonoplast fractions having the lower electrophoretic mobilities (T_B) also contained stalked ATPase particles on their surfaces but with the

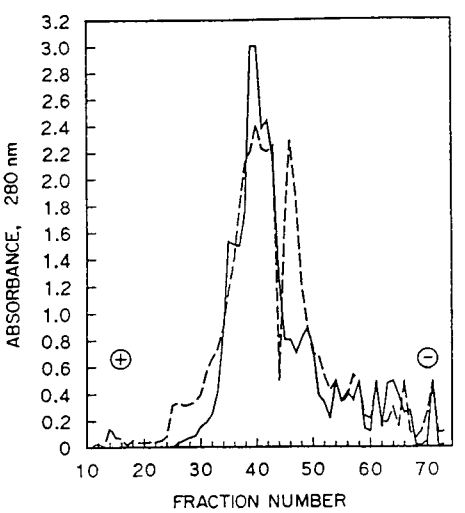

Fig. 3. Free flow electrophoresis separation of a homogenate of plant stems (dark-grown soybean) incubated (---) or not incubated (——) in the presence of ATP. After incubation with ATP, the mobility of the anodel fractions (fractions 22–32) representing tonoplast is increased. Also altered in mobility are fractions 45–50, probably representing plasma membranes. Addition of 1 μM monensin to the electrophoresis chamber buffer after ATP incubation resulted in a loss of the increased mobility of the anodal fractions (not shown).

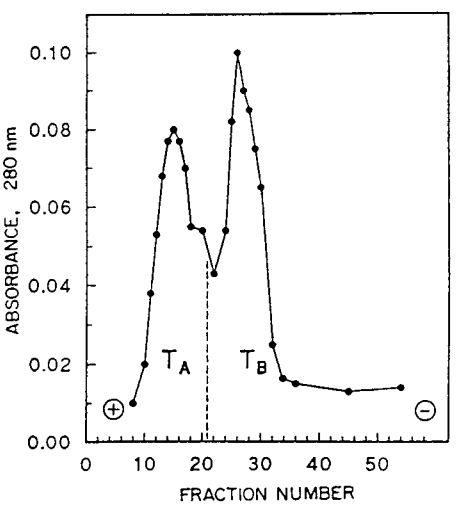

Fig. 4. Electrophoretic separation of purified tonoplast fractions as in Fig. 3 except that the tonoplast was first separated from other membranes of the homogenate as described [39]. The identity of the fraction as tonoplast was verified from analysis of marker enzymes. Two populations of vesicles were resolved. Tonoplast fraction A (T_A) was characterized by stalked ATPase particles on the outside of the vesicle and therefore rightside- (cytoplasmic side-)out [39]. Tonoplast fraction B (T_B) also contained vesicles with stalked ATPase particles but the particles were now on the inside of the vesicle [39]. This population of tonoplast vesicles therefore was inside-out or cytoplasmic side-in.

T_B vesicles the stalked ATPase particles were on the vesicle interiors [39]. This arrangement of ATPase particles identified the tonoplast vesicles of the T_B fraction as being inside-out or cytoplasmic side-in.

A response to ATP was seen as well with Golgi apparatus subfractions. The Golgi apparatus normally distributed over about 10 electrophoretic fractions (Fig. 5). Also correlated with the *cis*-to-*trans* gradient of rat liver Golgi apparatus membranes was the ability to acidify the vesicle interiors [29] in an ATP-dependent manner.

If rat liver Golgi apparatus fractions were incubated with ATP prior to and during electrophoresis (Fig. 6), the separation based on A_{280} was increased from 10 to about 15 fractions. This increase was due to an increased electrophoretic mobility of *trans*-derived Golgi apparatus as shown by measurements of the *trans* Golgi apparatus marker, thiamine pyrophosphatase (Fig. 7). With both A_{280} measurements (Fig. 6) and measurement of thiamine pyrophosphatase (Fig. 8), the mobility shift induced by ATP was reversed by treatment with the ionophore monensin.

The utility of the ATP-induced shift in electro-

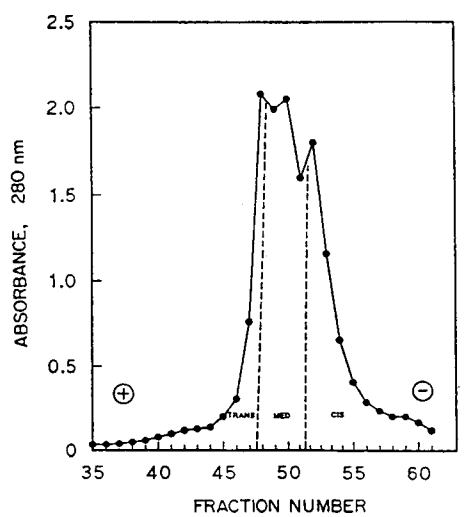

Fig. 5. Preparative free-flow electrophoretic profile depicting a typical Golgi apparatus separation. Values are based on $A_{280\,nm}$. The separations are normally divided for analysis into three regions representing membranes of derivation from the *cis*, medial (MED) and *trans* regions of the Golgi apparatus as indicated.

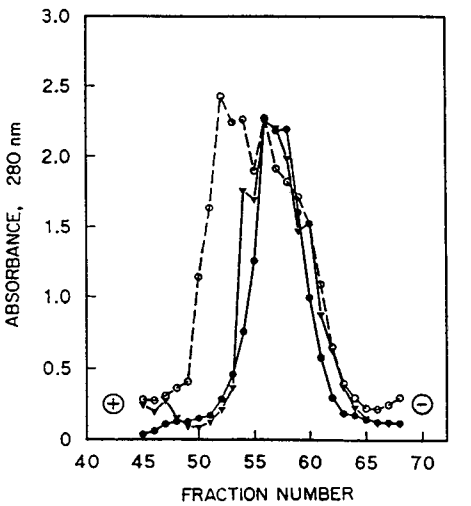

Fig. 6. Preparative free-flow electrophoresis separation of rat liver Golgi apparatus without (●) and with (○) ATP. Total material was correlated with A_{280} as verified by determination of total protein for each fraction (not shown). The effects on material in the electrophoretic fractions of high mobility induced by ATP were reversed by the addition of monensin (▼).

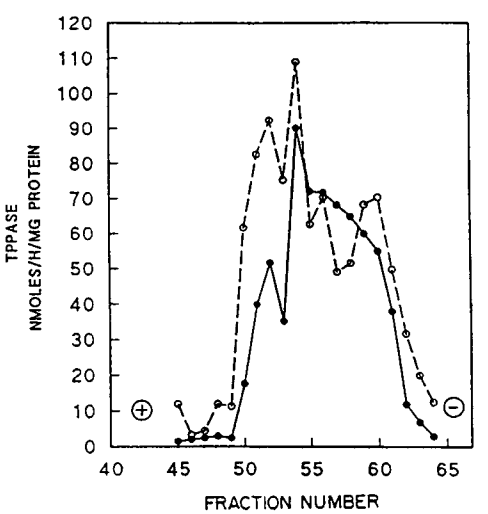

Fig. 7. As in Fig. 6 except a comparison of the specific activity of the trans Golgi apparatus marker thiamine pyrophosphate without (●) and with (○) ATP.

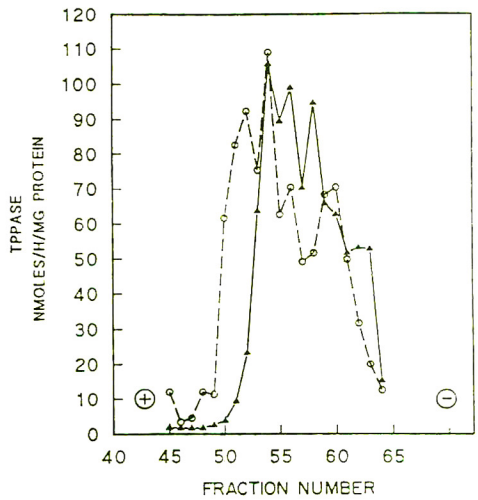

Fig. 8. As in Fig. 7 except a comparison of the electrophoretic mobility with ATP (○) and after the addition of 1 μM monensin during electrophoresis (▲).

phoretic mobility in organelle isolation was illustrated by an additional example involving rat kidney endosomes. For these studies, the starting material was a crude endosome preparation obtained by percoll gradient centrifugation as described [34,36,37]. When analyzed by preparative free-flow electrophoresis, these fractions were shown to be mixtures only partially resolved by the electrophoretic method (not shown). The relative distribution of membranes in these studies was determined by electron microscope morphometry.

To remove brush border membranes, the percoll gradient-purified endosomes were first partitioned using a 6.4% dextran–PEG phase system followed by incremental aqueous two-phase partition as described in section 2. The results are summarized diagramatically in Fig. 9 and representative electron micrographs are shown in Fig. 10.

Brush border membranes were concentrated in the upper phase of the initial 6.4% dextran–PEG phase separation (Fig. 10A). The lower phase still contained basolateral plasma membranes, endosomes, mitochondria and endoplasmic reticulum (ER) (Fig. 9). An upper phase equilibrated from a 6.0% dextran–PEG phase

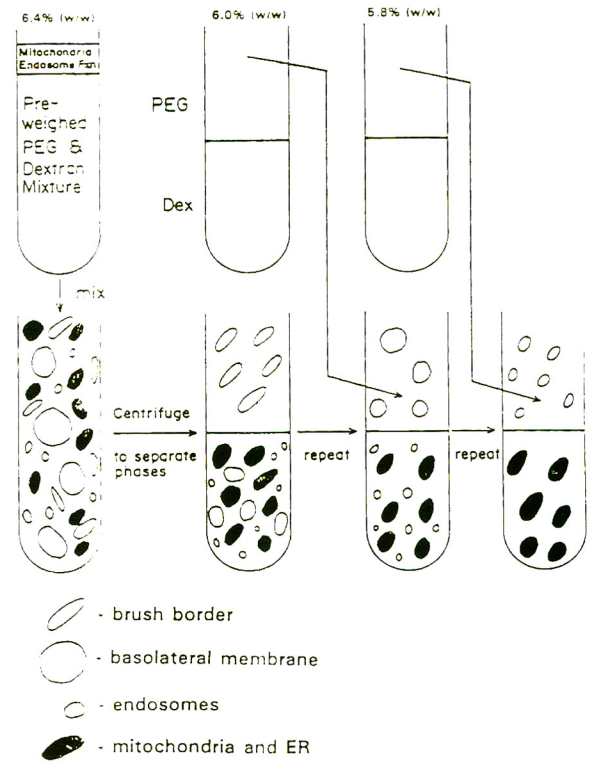

Fig. 9. Results of the incremental two-phase partition for the resolution of different plasma membrane domains and a partially purified endosome fraction from a rat kidney particulate fraction. The initial partition used a 6.4% PEG–dextran phase system. Brush border membranes partitioned into the upper phase. A 6.0% phase system was equilibrated in parallel and the upper phase of this phase system replaced the brush border-containing upper phase of the 6.4% system. After mixing and resolution of the two new phases, the upper phase now contained the remainder of the plasma membrane including basolateral-derived vesicles. A 5.8% phase system also was equilibrated in parallel and the upper phase replaced the plasma membrane-containing upper phase of the second partition. After mixing and resolution into two phases, a third upper phase enriched in endosomes and depleted in plasma membrane was obtained. The fraction, however, was still contaminated by mitochondrial fragments (Fig. 10C). The bulk of the mitochondria, endoplasmic reticulum and nuclei remained in the lower phase after the last partitioning step. Fxn = Fraction.

system extracted the basolateral plasma membranes (Fig. 9, Fig. 10B). An upper phase equilibrated from a 5.8% dextran–PEG phase system extracted the endosomes in a third partitioning step (Fig. 9, Fig. 10C). The bulk of the

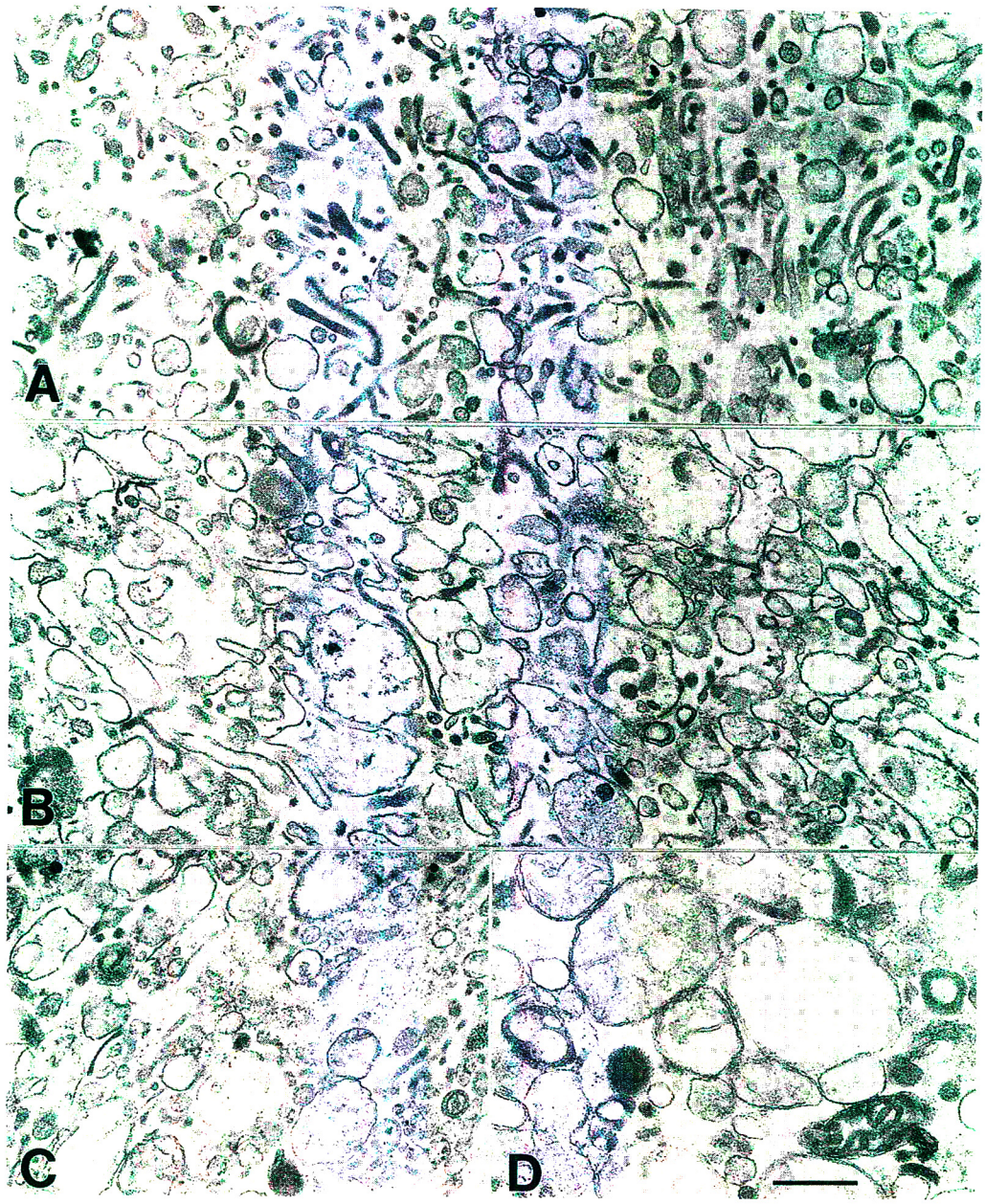

Fig. 10. Electron micrographs of rat kidney membrane fractions obtained by incremental aqueous two-phase separation diagrammed in Fig. 9. (A) Brush border-enriched fraction. (B) Basolateral plasma membrane-enriched fraction. (C) Endosome-enriched fraction. (D) Final lower phase containing mitochondria, nuclear envelope, endoplasmic reticulum and other membrane fragments. Scale bar = 0.5 μm.

mitochondria, endoplasmic reticulum, nuclei and other internal membranes were retained in the lower phase (Fig. 9, Fig. 10D).

The endosome fractions prepared by aqueous two-phase partition, while enriched in endosomes, were still heavily contaminated by mitochondria and/or mitochondrial fragments (Fig. 10C). To further purify endosomes, the pH shift technique was employed (Fig. 11). As shown in Fig. 12A, the particles concentrated in the region of highest electrophoretic mobility induced by ATP treatment, were primarily a population of endosomes or endosome-like vesicles. This region of high electrophoretic mobility was collapsed by the ionophore monensin (Fig. 11) to confirm that the ATP-induced mobility shift was related to proton uptake and concomitant endosome acidification.

The trailing portion of the separation unaffected by ATP or monensin consisted primarily of mitochondria and mitochondrial fragments (Fig. 12B). Also present were other vesicles, some of which might represent early endosomes still incapable of generating a significant proton gradient in response to ATP.

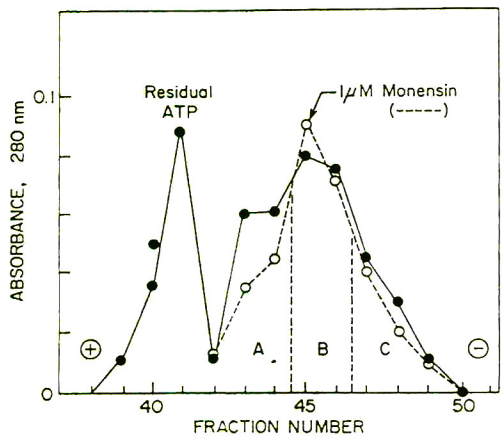

Fig. 11. Free-flow electrophoretic purification of endosomes prepared by aqueous two-phase partition using the ATP shift technique. In the absence of ATP, the distribution of components was symmetrical and mitochondria and endosomes were incompletely resolved (not shown). When equal portions of the preparations were incubated with ATP in the absence or presence of 1 μM monensin an ATP-induced region of particles with increased electrophoretic mobility was observed.

To demonstrate that the pH shift was exhibited by authentic endosomes in the preparations rather than endosome-like vesicles of some other origin, kidney endosomes loaded with FITC (fluorescein isothiocyanate)–dextran were purified by flow cytometry based solely on the criterion of having participated in an endocytic event [40]. When subjected to electrophoretic analysis, these highly purified endosomes also exhibited an enhanced electrophoretic mobility when incubated with ATP (Fig. 13).

4. Discussion

In order to improve free-flow electrophoretic separations of membranes and to provide some basis for the rational design of buffering systems, it would be helpful to know the theoretical basis for particle migration in solution in response to a particular electric field strength.

From our experience and that of others [2], the electrophoretic mobility is largely independent of size and shape of membrane particles within the range of sedimentable particles found in cell or tissue homogenates. Nor does the electrophoretic mobility of a particle in buffered solution correlate exactly with the content of negatively charged surface molecules [14]. A case in point is the widely different electrophoretic mobilities of vesicles derived from vacuoles (tonoplast vesicles) and from the plasma membrane of plants. The two types of membranes are compositionally very similar [22] and have similar surface charges [42]. Yet, they are readily separated by preparative free-flow electrophoresis with tonoplast vesicles having the greater electrophoretic mobility. A difference in mobility is given by vesicles having both inside-out and rightside-out orientations.

In ongoing studies, we have determined that the common parameter among free-flow electrophoretic separations may not be due entirely to charged molecules at the vesicle surface but to the ability of the vesicles to create an (outside) negative diffusion potential as well. This is probably why we are able to separate such markedly similar membranes such as tonoplast

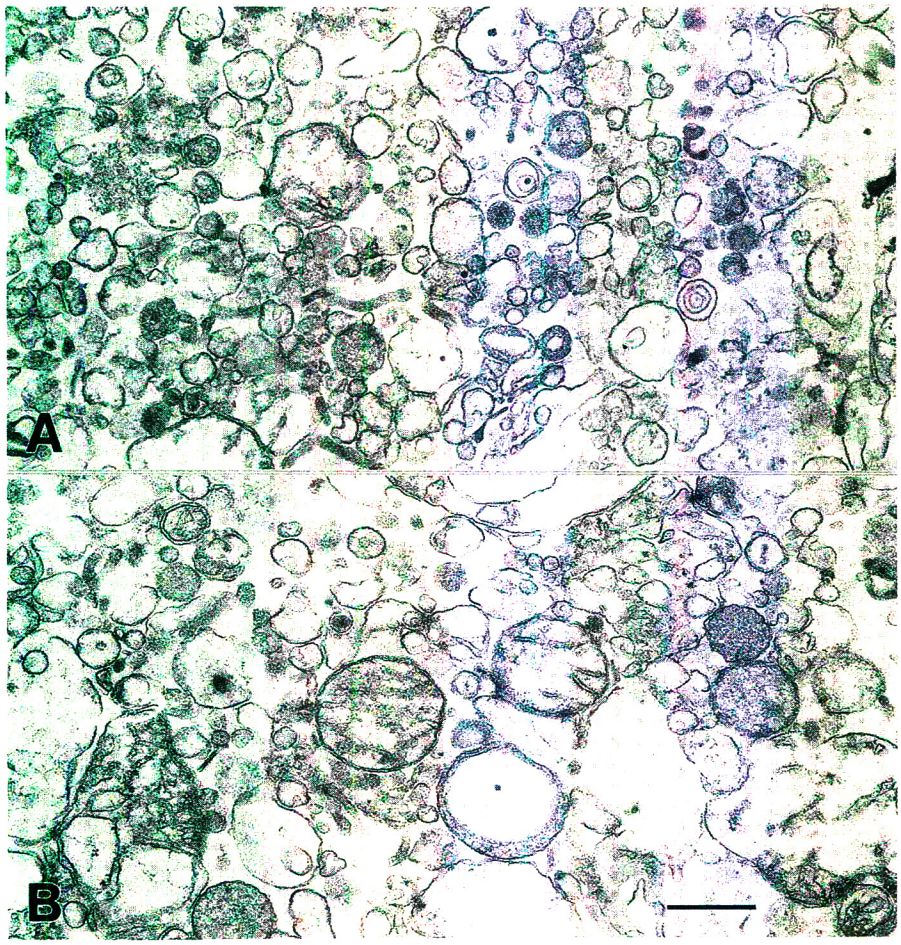

Fig. 12. Electron micrographs of endosomes purified by the ATP-shift technique shown in Fig. 11. (A) Fractions 43 and 44, responsive to ATP and monensin were highly enriched in endosomes. Renal tubules were labeled for 6 h with FITC–dextran to label the endosomes. Only a few mitochondrial fragments remained. (B) Fractions 45–48, unresponsive to ATP and monensin, contained the bulk of the mitochondria and proportionally fewer and smaller endosomes. Scale bar = 0.5 μm.

and plasma membrane of plants and why inside-out plant plasma membrane vesicles migrate more rapidly than rightside-out plasma membrane vesicles under certain conditions but not others. It will also explain why we are able to subfractionate Golgi apparatus membranes so effectively by preparative free-flow electrophoresis and why the monensin treatment is able to shift the electrophoretic mobility of endosomes. Also explained is the lack of direct correlation between membrane composition and electrophoretic mobility. Charged surface molecules, while a primary determinant of electrophoretic mobility may be augmented by diffusion potential.

However, a diffusion potential, negative outside, will not of itself alter the electrophoretic mobility of a particle in buffered solution. Electrophoretic mobility is universally considered to be determined by a mobile ion cloud around the particle, the so-called Debye–Hückel layer [1,43] (Fig. 14). The Debye–Hückel layer is the outer region of an electric double-layer of ions surrounding bioparticles in an electric field. Its distribution around the particle is determined by

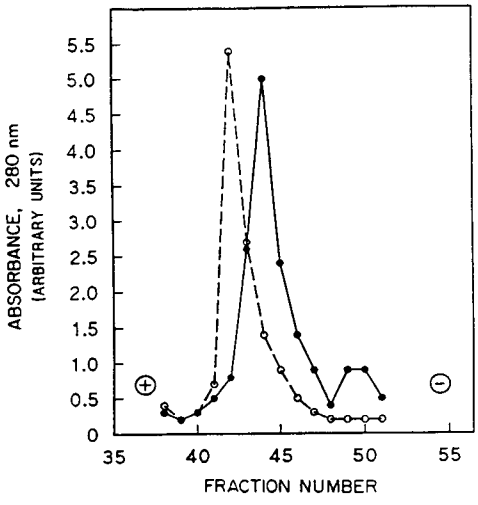

Fig. 13. Endosomes purified by flow cytometry (enrichment of particles containing FITC–dextran) showed the shift in electrophoretic mobility induced by incubation with ATP. From T.G. Hammond and D.J. Morré [40]. ○ = +ATP; ● = no ATP.

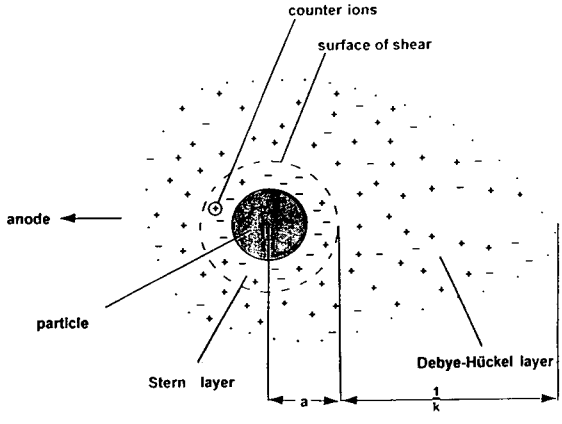

Fig. 14. Theoretical basis for free-flow electrophoretic separations based on diffusion potential. The figure illustrates how the electric double layer of a particle in a solution of electrolytes is thought to be influenced by an electric field [1]. The inner region includes absorbed ions and a diffuse region in which ions redistribute according to the electrical force exerted on the particle. The ζ potential, the so-called actual electrical charge arises from a "surface of shear" at the border with the inner hydrate = Stern layer to then influence electrophoretic mobility. It is the electrical charge at this surface of sheer that we suggest is modified by diffusion potential. Modified from Hannig and Heidrich [1].

both electrical forces and random thermal motion. When subjected to an electric field, the layer is deformed such that the outer ion cloud is shifted in a direction opposite to that of particle movement to expose underlying charged groups and allow their contribution to electrophoretic mobility.

The inner region of the double-layer includes absorbed ions. The ζ potential of the particle, its actual electrical charge, is determined at the surface of shear between the two layers during electrophoresis (Fig. 14). The hydrate or Stern layer at the particle surface includes many absorbed cations which tend to reduce the overall negative charge of the surface. What is missing from our information is a practical theoretical basis for how the composition and arrangement of charged groups underlying the Stern layer may be translated into a given ζ potential of that portion of the ion cloud that influences electrophoretic mobility. That separations by free-flow electrophoresis should be governed by a ζ potential of a region determined of itself by the conditions of electrophoresis (Fig. 14) is the principle theoretical argument advanced here. We argue that, as a result, organelle separations are possible by free-flow electrophoresis that are not accomplished readily by other separation techniques currently employed, including aqueous two-phase partition. The tonoplast and plasma membrane vesicle separation provides one example. It is difficult to completely resolve inside-out plasma membrane vesicles from right-side-out tonoplast vesicles by aqueous two-phase partition. Yet these two types of vesicles are readily resolved by free-flow electrophoresis.

How specific deformations of the Stern layer may relate to ζ potential and how such deformations may be induced and experimentally confirmed is a subject of continuing investigation. We can now alter electrophoretic mobility of tonoplast vesicles, *trans* Golgi apparatus cisternae and certain classes of endosomes by modifying diffusion potential through addition of ATP to induce proton entry or addition of ionophores such as monensin to induce proton release. This provides the primary experimental basis for

suggesting that electrophoretic mobility (ζ potential) can be modified during particle separation and related to a known experimentally determined property (diffusion potential) of the membrane (Fig. 14).

An initial important application of an ATP-induced diffusion potential is in the isolation and subfractionation of endosomes. Endosomes are defined as a heterogeneous population of prelysosomal, acidic organelles which play pivotal roles in the sorting and targeting of internalized membrane and content and that direct their specific transport to appropriate intracellular destinations [44]. A first major compartment is the aggregate of incoming vesicles, some clathrin coated, some without coats, derived by budding from the plasma membrane and rapidly modified by fusion among compartments. These are referred to variously as primary or secondary pinosomes or simply as early pinosomes or as early endosomes. These components have a very short life time and either recycle back to the plasma membrane or fuse with other endosomal compartments [45]. Eventually, pinosome contents are delivered into endosomes. The third major player in endocytic membrane traffic is the lysosome. Primary lysosomes deliver newly synthesized digestive enzymes to the endosomes with the formation, after fusion, of a secondary lysosome or digestive vacuole. These can participate in repeated rounds of digestion, for example, with the resultant formation of residual bodies, the content of which can be discharged from the cell.

Because of the anticipated heterogeneity of endosomal populations and the rather small differences in membrane and content properties that may distinguish different endosomal classes, new separation methods clearly are needed. Of those thus far applied to this difficult study area, preparative free-flow electrophoresis has been among the most effective. Marsh et al. [18] reported that functionally and structurally distinct subpopulations of endosomes could be resolved by preparative free-flow electrophoresis. Since cell fractionation by free-flow electrophoresis was rapid, large amounts of highly enriched early and late endosomes and endosomal subpopulations could, in principle, be prepared for biochemical and functional analyses and/or for antibody production.

Marsh *et al.* [18] reported that the anodal migration of endosomes and lysosomes during free-flow electrophoresis was dependent upon mild trypsinization of the membranes. The reasons for the trypsin requirement was unclear but there was apparently very little or no separations of endosomes or lysosomes from the bulk of the input membranes in the absence of the trypsinization step [18,19,46]. Control experiments [47], suggested little or no detectable alteration in the protein composition or in the functional integrity of either endosomes or lysosomes as a result of trypsinization. Nevertheless, a procedure in which the trypsin treatment could be eliminated would be advantageous for many applications.

It is clear that the electrophoretic mobility of endosomes and lysosomes was greater than that of most of the other membranes with the possible exception of plasma membrane vesicles. This was in contrast, for example, to their buoyant density which may be very similar to that of other membrane systems. The fact that endosomes, together with lysosomes, were separated from most other organelles by free-flow electrophoresis, indicates that differences in the net charge can be exploited for fractionation. Ionizable groups responsible for conferring these charge differences are not known. Acidic sialoglycoproteins are present but associated with the luminal aspects of the lysosomal membrane [48] and are unlikely to contribute. These considerations, taken together with the mobility shift experiments, suggest potentially important roles for diffusion potential as an exploitable parameter to effect endosome and other types of membrane separations involving vesicles with an inherent capacity to develop diffusion potentials, negative outside.

5. References

[1] K. Hannig and H.G. Heidrich, *Free-flow Electrophoresis*, GIT Verlag, Darmstadt, 1990, p. 119.

[2] K. Hannig and H.G. Heidrich, in Bloemendal (Editor), *Cell Separation*. North-Holland, Amsterdam, 1977, p. 95.
[3] P. Albertsson, A.B. Andersson, C.K. Larsson and H.-E. Akerlund, *Methods Biochem. Anal.*, 28 (1982) 115.
[4] H. Walter, D.E. Brooks and D. Fisher (Editors), *Partitioning in Aqueous Two-Phase Systems*, Academic Press, New York, 1985, p. 704.
[5] P. Gierow, M. Sommarin, C. Larsson and B. Jergil, *Biochem. J.*, 249 (1986) 685.
[6] P. Navas, D.D. Nowack and D.J. Morré, *Cancer Res.*, 49 (1989) 2147.
[7] D.J. Morré and D.M. Morré, *BioTechniques*, 7 (1989) 946.
[8] A.S. Sandelius and D.J. Morré, in C. Larsson and I.M. Møller (Editors), *The Plant Plasma Membrane —Structure, Function and Molecular Biology*, Springer, Heidelberg, New York, 1990, p. 44.
[9] C. Larsson, S. Widell and M. Sommarin, *FEBS Lett.*, 229 (1988) 289.
[10] D.J. Morré, C. Penel, D.M. Morré, A.S. Sandelius, P. Moreau and B. Andersson, *Protoplasma*, 160 (1991) 49.
[11] D.J. Morré and B. Andersson, *Methods Enzymol.*, in press.
[12] Y. Hino, A. Asano and R. Sato, *J. Biochem. (Japan)*, 83 (1978) 925.
[13] Y. Hino, A. Asano and R. Sato, *J. Biochem. (Japan)*, 83 (1978) 935.
[14] A.S. Sandelius, C. Penel, G. Auderset, A. Brightman, M. Millard and D.J. Morré, *Plant Physiol.*, 81 (1986) 177.
[15] G. Auderset, A.S. Sandelius, C. Penel, A. Brightman, H. Greppin and D.J. Morré, *Physiol. Plantarum*, 68 (1986) 1.
[16] D.J. Mooré, D.M. Morré and H.-G. Heidrich, *Eur. J. Cell Biol.*, 31 (1983) 263.
[17] D.J. Morré, K.E. Creek, G.R. Matyas, N. Minnifield, I. Sun, P. Baudoin, D.M. Morré and F.L. Crane, *BioTechniques*, 2 (Sept./Oct.) (1984) 224.
[18] M. Marsh, S. Schmid, H. Kern, E. Harms, P. Male, I. Mellman and A. Helenius, *J. Cell Biol.*, 104 (1987) 875.
[19] S.L. Schmidt, R. Fuchs, P. Male and I. Mellman, *Cell*, 52 (1988) 73.
[20] M. Paulik, D.D. Nowack and D.J. Morré, *J. Biol. Chem.*, 263 (1988) 17738.
[21] E. Harms, J. Kartenbeck, G. Darai and J. Schneider, *Exp. Cell Res.*, 131 (1981) 251.
[22] C. Penel, G. Auderset, N. Bernardini, F.J. Castillo, H. Greppin and D.J. Morré, *Physiol. Plant.*, 73 (1988) 134.
[23] F.R. Maxfield, in I. Pastan and M.C. Willingham (Editors), *Endocytosis*, Plenum Press, New York, 1985, p. 235.
[24] A.B. Bennett and R.M. Spanswick, *J. Membr. Biol.*, 71 (1983) 95.
[25] H. Sze, *Annu. Rev. Plant Physiol.*, 36 (1985) 175.
[26] D.P. Briskin, in I. Møller and K. Larsson (Editors), *The Plant Plasma Membrane —Structure, Function and Molecular Biology*, Springer, Heidelberg, 1990, pp. 154.
[27] J. Glickman, K. Croen, S. Kelly and Q. Al-Awqati, *J. Cell Biol.*, 97 (1983) 1303–1308.
[28] R. Barr, K. Safranski, I.L. Sun, F.L. Crane and D.J. Morré, *J. Biol. Chem.*, 259 (1984) 14064.
[29] A.O. Brightman, P. Navas, N.M. Minnifield and D.J. Morré, *Biochim. Biophys. Acta*, 1104 (1992) 188.
[30] R.D. Cheetham, D.J. Morré, C. Panneck and D.S. Friend, *J. Cell Biol.*, 49 (1971) 899.
[31] W.D. Harris, *J. Am. Oil Chem. Soc.*, 31 (1954) 124.
[32] T.G. Hammond, R.R. Majewski, J.J. Onorato, P.C. Brazy and D.J. Morré, *Biochem. J.*, 238 (1993b).
[33] J.H. Jett, R.A. Keller, J.C. Martin, B.L. Marrone, R.K. Moyzis, R.L. Ratliff, N.K. Seitzinger, E.B. Shera and C.C. Stewart, *J. Biomol. Struct. Dyn.*, 7 (1989) 301.
[34] T.G. Hammond, R.R. Majewski, D.J. Morré, K. Schell and L.W. Morrisey, *Cytometry*, 14 (1993a) 411.
[35] T.G. Hammond, P. Verroust, K.E. Muse and T.D. Oberley, unpublished results.
[36] I. Sabolic and G. Burkhardt, *Methods Enzymol.*, 191 (1990) 505.
[37] I. Sabolic, W. Haase and M.G. Burckhardt, *Am. J. Physiol.*, 248 (1985) F835.
[38] W.I. Lencer, P. Weyer, A.S. Verkman, D.A. Ausiello and D. Brown, *Am. J. Physiol.*, 258 (1990) C309.
[39] D.J. Morré, C. Liedtke, A.O. Brightman and G.F.E. Scherer, *Planta*, 184 (1991) 343.
[40] T.G. Hammond and D.J. Morré, unpublished results.
[41] P. Navas, N. Minnifield, I. Sun and D.J. Morré, *Biochim Biophys. Acta*, 881 (1986) 1.
[42] A. Bérezi, I.M. Mollar, T. Lundborg and A. Kylin, *Physiol. Plant*, 61 (1984) 535.
[43] M. Bier, *Electrophoresis*, Academic Press, New York, 1967, p. 3.
[44] I. Mellman, R. Fuch and A. Helenius, *Ann. Rev. Biochem.*, 55 (1986) 663.
[45] L. Thilo, in D.J. Morré, K.E. Howell, G.M.W. Cook (Editors), *Cell Free Analysis of Membrane Transport*, Alan R. Liss, New York, 1988, p. 377.
[46] W.H. Evans and N. Flint, *Biochem. J.*, 232 (1985) 25.
[47] S.L. Schmid and I.R. Mellman, in D.J. Morré, K.E. Howell, G.M.W. Cook (Editors), *Cell Free Analysis of Membrane Transport*, Alan R. Liss, New York, 1988, p. 35.
[48] V. Lewis, S.A. Green, M. Marsh, P. Vikho, A. Helenius and I. Mellman, *J. Cell Biol.*, 100 (1985) 1839.

ELSEVIER

Journal of Chromatography A, 668 (1994) 215–228

JOURNAL OF CHROMATOGRAPHY A

Partitioning of proteins and thylakoid membrane vesicles in aqueous two-phase systems with hydrophobically modified dextran

Min Lu, Per-Åke Albertsson, Göte Johansson, Folke Tjerneld *

Department of Biochemistry, Chemical Center, University of Lund, P.O. Box 124, S-221 00 Lund, Sweden

Abstract

Dextrans were modified with hydrophobic groups, *i.e.* benzoyl and valeryl groups. Benzoyl dextran and valeryl dextran form aqueous two-phase systems with poly(ethylene glycol) (PEG) as well as with dextran. Two-phase systems are also formed between two valeryl dextrans with different degrees of substitution as well as between benzoyl dextran and valeryl dextran. Phase diagrams for aqueous two-phase systems composed of PEG–valeryl dextran, dextran–valeryl dextran, valeryl dextran–valeryl dextran and valeryl dextran–benzoyl dextran have been determined. The effects of these hydrophobic groups on the partitioning of amino acids, proteins and membrane vesicles in aqueous two-phase systems have been studied. In a PEG 8000–dextran T500 aqueous two-phase system containing only phosphate buffer β-galactosidase was partitioned mostly to the top phase. However, by introducing a small amount of benzoyl groups (degree of substitution 0.054) or valeryl groups (degree of substitution 0.12) in the lower phase, the partition coefficient of this enzyme could be decreased by more than 100 times. A similar, but weaker, effect on partitioning was observed for bovine serum albumin, lysozyme, lipase and β-lactoglobulin. The partitioning of thylakoid membrane vesicles was strongly affected by the hydrophobic groups on dextran. The membrane vesicles were partitioned toward the phase containing the hydrophobic groups.

1. Introduction

Aqueous polymer two-phase systems formed of poly(ethylene glycol) (PEG) and dextran are widely used for separation and purification of macromolecules, membranes, cell organelles and cells [1]. In some applications of aqueous two-phase systems, the basic phase forming polymers (PEG and dextran) have been substituted by other polymers, *e.g.* poly(vinyl alcohol), hydroxypropyl starch or ethylhydroxyethyl cellulose [2–4]. In other cases, the basic phase forming polymers have been modified with different groups for special applications. PEG has been used to carry different ligands for affinity partitioning [nicotinamide–adenine dinucleotide (NADH), fatty acids, textile dyes, charged groups] [5–8]. Dextran derivatives have also been used in aqueous two-phase systems (hydroxypropyl-dextran, diethylaminoethyl-dextran, textile dye-dextran) [1,8,9]. In a previous study benzoyl dextran was synthesized and its use in aqueous two-phase systems was investigated [10]. In the present work, dextran has been modified with valeryl groups. The valeryl group was chosen in order to make comparisons with benzoyl dextran, *i.e.* to compare the effects of

* Corresponding author.

0021-9673/94/$07.00
SSDI 0021-9673(93)E1295-B

aromatic and aliphatic substitutions. The degree of substitution of valeryl dextran was changed by varying the reaction conditions. Phase diagrams for aqueous two-phase systems composed of PEG–valeryl dextran, dextran–valeryl dextran, valeryl dextran–valeryl dextran and valeryl dextran–benzoyl dextran have been determined.

Aqueous two-phase systems containing hydrophobically modified dextran have new and different properties for partitioning of biological materials compared to the mostly used PEG–dextran systems. The present study is devoted to a systematic investigation into the properties of aqueous two-phase systems containing dextran with covalently bound benzoyl or valeryl groups. The partitioning of amino acids, dipeptides, proteins and thylakoid membrane vesicles was studied in systems with hydrophobically modified dextrans. A series of proteins with differing surface hydrophobicities was studied in order to observe the effect of hydrophobic interactions on protein partitioning. Viscosity measurements were made in order to study the interactions between hydrophobic groups on the dextran backbone.

2. Materials and methods

2.1. Chemicals

Dextran T500 with a mass-average molecular mass of 500 000, was obtained from Pharmacia (Uppsala, Sweden), and PEG 8000 with a number-average molecular mass of 8000, from BP Chemicals (Hythe, UK). Valeryl chloride and triethylamine were obtained from Aldrich-Chemie (Steinheim, Germany). Benzoyl dextrans were synthesized according to our previous work [10]. All other chemicals were of analytical grade.

2.2. Biological materials

Amino acids (L-tryptophan, L-phenylalanine) were obtained from E. Merck (Darmstadt, Germany); L-tyrosine from Becton Dickinson (Orangeburg, NY, USA) and the dipeptides tyrosine–tyrosine and glycine–tryptophan from Sigma (St. Louis, MO, USA). Bovine serum albumin (BSA) was purchased from Boehringer (Mannheim, Germany). The following proteins were obtained from Sigma: β-galactosidase (EC 3.2.1.23), from *Escherichia coli;* lysozyme (EC 3.2.1.17), from chicken egg white; lipase type 1 (EC 3.1.1.3), from wheat germ; β-lactoglobulin A, from bovine milk ; myoglobin, from horse skeletal muscle and cytochrome *c*, from horse heart. Thylakoid membranes, membrane vesicles from grana stack (B3) and membrane vesicles from stroma lamellae (T3) were isolated from spinach leaves according to Albertsson and Yu [11] and Andreasson *et al.* [12].

2.3. Synthesis of valeryl dextran

Valeryl dextrans were obtained by reacting dextran T500 with valeryl chloride in presence of triethylamine. The reactions were carried out in an ice bath. The reaction and purification procedures are the same as described in our earlier paper [10]. The concentration of dextran was determined by polarimetry [1]. The content of valeryl groups on dextran was determined by NMR measurements using ^2H_2O as solvent. The degree of substitution (DS) is defined as the number of valeryl groups per glucose unit.

2.4. Two-phase systems

The two-phase systems were prepared from stock solutions of 40% PEG 8000 [all compositions are given in % (w/w) throughout this paper], 20% dextran T500, 11–12% valeryl dextran and 12–15% benzoyl dextran. The stock solutions were weighed out and mixed together with buffer, salt, biomaterials and water. The systems were equilibrated at room temperature and centrifuged 2 min at 1200 *g* for partitioning of amino acids, dipeptides and proteins. For partitioning of thylakoid membranes, B3 and T3 vesicles, the systems were just mixed and left standing for 20 min at room temperature. Suitable amounts of each phase were withdrawn, diluted 5–20 times and analysed. The partition coefficients (K) of the substances are defined as

the ratio of their respective concentrations in top and bottom phase. All partition coefficients are mean values from two or three repeated experiments.

2.5. Assays of amino acids, dipeptides, proteins and thylakoid membrane vesicles

Amino acids (L-tryptophan, L-tyrosine and L-phenylalanine) and dipeptides (tyrosine–tyrosine and glycine–tryptophan) were determined by high-performance liquid chromatographic (HPLC) measurements. A gel filtration column was used to separate the amino acids and dipeptides from polymers. The tryptophan and glycine–tryptophan were detected at 279 nm, tyrosine–tyrosine at 223 nm, phenylalanine at 259 nm and tyrosine at 278 nm. Proteins (BSA, lipase and β-lactoglobulin) were assayed by using Coomassie Brilliant Blue G and measured at 595 nm with BSA as standard [13]. Myoglobin and cytochrome *c* were determined by absorbance at 409 and 408 nm. Phases of the same two-phase systems but without proteins were used as references. β-Galactosidase activity was measured according to Veide *et al.* [14]. Lysozyme activity was measured according to the Worthington Manual [15]. Thylakoid membranes, B3 and T3 vesicles were determined at 680 nm.

2.6. Phase diagrams

Phase diagrams were determined by combining titration and analysis of the composition of top and bottom phases [1]. In the systems composed of PEG and valeryl dextran, the concentration of valeryl dextran was determined by polarimetry and PEG by refractive index. The introduction of valeryl and benzoyl groups had no noticeable effect on the specific rotation of dextran, $[\alpha]_D^{25} = +199°$ ml g^{-1} dm^{-1}. The concentration of valeryl dextran in each phase was determined separately and its contribution was subtracted from the refractive index values. In the system valeryl dextran–benzoyl dextran, the total dextran concentration was measured with polarimetry and the benzoyl dextran was measured by absorbance at 273 nm. The valeryl dextran concentration was obtained by subtracting the benzoyl dextran from the total dextran concentration [10]. In the systems composed of dextran–valeryl dextran and valeryl dextran–valeryl dextran, the binodal curves were determined by titration. The compositions of the phases were not determined in this case.

2.7. Measurement of viscosity

The viscosity of benzoyl dextran and valeryl dextran solutions were measured in both dilute and concentrated systems. In the dilute system the viscosity was determined by the time spent for a certain volume (7.0 ml) of polymer solution to pass through a Ostwald capillary viscometer at constant temperature (25°C). In the concentrated systems the viscosity was measured in a similar way but the viscometer was replaced by a Pasteur capillary pipette. The solution volume was 1.65 ml and temperature 22°C.

3. Results

3.1. Stability of hydrophobically modified dextrans

Dextran T500 modified with benzoyl and valeryl groups have been stored in the cold room (4°C) for long periods. The stability of the hydrophobically modified dextrans was determined by HPLC measurement. For a 13.8% solution of benzoyl dextran (DS = 0.137) stored for one year and a 11.1% valeryl dextran solution (DS = 0.20) stored for four months at 4°C, no low-molecular-mass components were found.

3.2. Viscosities

The viscosities of benzoyl dextran solutions were measured in both dilute systems with a polymer concentration of 0.00225 g/ml at 25°C and in concentrated systems with polymer concentrations of 2–15%. In a dilute dextran solution system, no significant viscosity change was observed when the DS of benzoyl dextran was

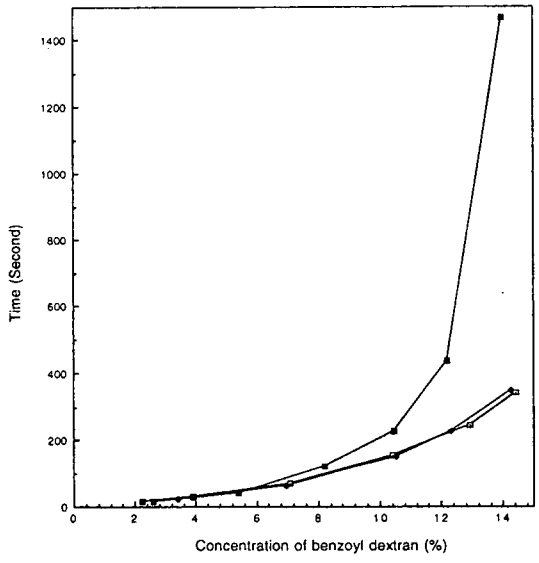

Fig. 1. The influence of polymer concentration on the viscosity of benzoyl dextran. Aqueous solutions (1.65 ml) of dextran T500 (□) and benzoyl dextran with DS of 0.087 (◆) and 0.137 (■) were passed through a Pasteur capillary pipette at room temperature (22°C).

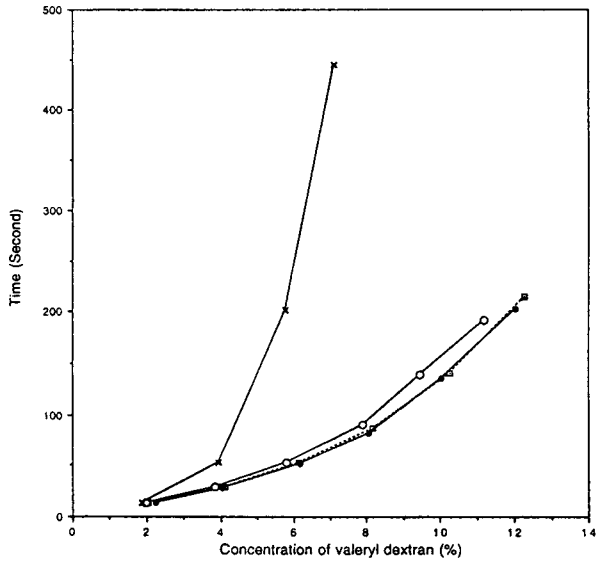

Fig. 2. The influence of polymer concentration on the viscosity of valeryl dextran. Aqueous solutions (1.65 ml) of dextran T500 (□, broken line) and valeryl dextran with DS of 0.025 (●), 0.12 (○) and 0.20 (×) were passed through a Pasteur capillary pipette at room temperature (22°C).

varied between 0 and 0.137. The viscosities of concentrated solutions of benzoyl dextran at room temperature are shown in Fig. 1. The viscosities of valeryl dextran solutions were measured in solutions with polymer concentrations of 1.8–13% at room temperature (22°C). The results are shown in Fig. 2. For benzoyl and valeryl dextran with DS of 0.14 and 0.20, respectively, a sharp increase in solution viscosity is observed when the polymer concentration is increased.

3.3. Phase diagrams

In PEG–valeryl dextran systems, the valeryl dextrans are enriched in the bottom phase and PEG in the top phase. The phase diagrams for systems composed of PEG 8000 and valeryl dextran with DS values of 0.025, 0.12 and 0.20 at room temperature (22°C) are shown in Figs. 3. For comparison the binodal curve of the PEG 8000–dextran T500 system is also shown in Fig. 3 [1]. Valeryl dextran with a high degree of substitution (DS = 0.20) also forms two-phase systems with dextran, valeryl dextran and benzoyl dextran with low degree of substitution. Valeryl dextran with lower degree of substitution (DS = 0.025) forms two-phase systems with benzoyl dextran with higher degree of substitution (DS = 0.137). The phase diagrams of valeryl dextran (DS = 0.025)–benzoyl dextran (DS = 0.137) and benzoyl dextran (DS = 0.054)–valeryl dextran (DS = 0.20) are shown in Fig. 4. The phase diagrams of dextran–valeryl dextran (DS = 0.20) and valeryl dextran (DS = 0.025)–valeryl dextran (DS = 0.20) are shown in Fig. 5. In these systems the dextran with the highest degree of substitution is always enriched in the bottom phase.

3.4. Partition of amino acids and dipeptides

Amino acids and dipeptides with aromatic groups (L-tyrosine, L-tryptophan, L-phenylalanine, tyrosine–tyrosine and glycine–tryptophan) were partitioned in PEG–valeryl dextran and PEG–benzoyl dextran aqueous two-phase systems. The valeryl dextrans with DS = 0.025, 0.12 and 0.20 were used in PEG–valeryl dextran

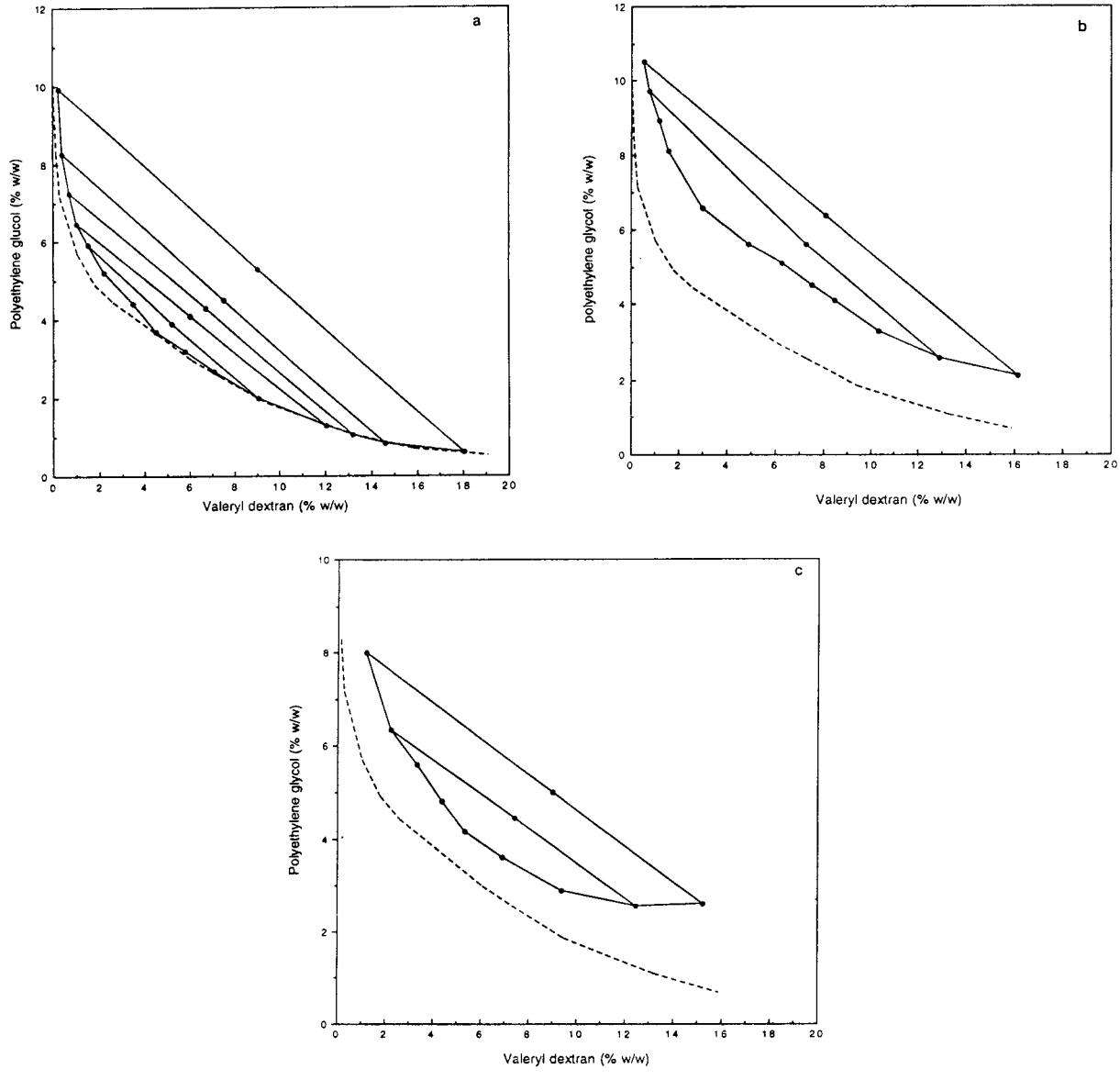

Fig. 3. Phase diagrams for the system PEG 8000–valeryl dextran at room temperature (22°C). The DS of valeryl dextran was (a) 0.025; (b) 0.12 and (c) 0.20. The dashed line shows the binodial curve for the system PEG 8000–dextran T500 at 20°C, the data are from Albertsson [1].

systems and benzoyl dextrans with DS = 0.054, 0.087 and 0.137 were used in PEG–benzoyl dextran systems. In both PEG–valeryl dextran and PEG–benzoyl dextran systems, the system compositions were: 6% PEG 8000, 6% valeryl dextran (or benzoyl dextran) without addition of buffer or salts. The partitionings were carried out at room temperature. The partition coefficients are all close to 1 which shows that the amino acids and dipeptides partition evenly between the top and bottom phases in these systems.

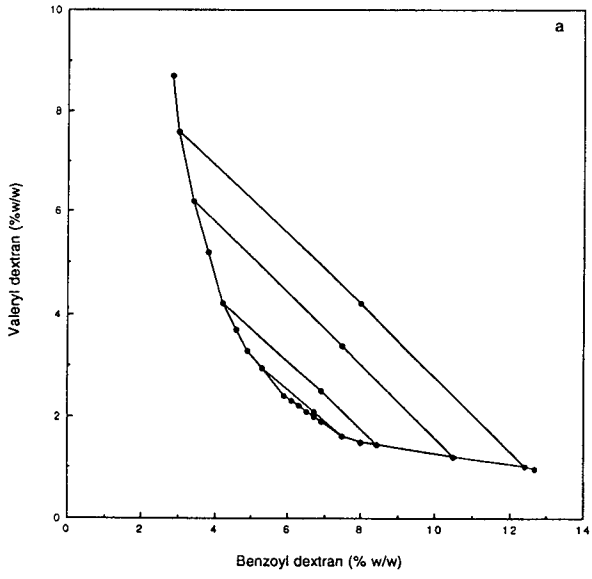

Fig. 4. Phase diagrams for the system benzoyl dextran–valeryl dextran. (a) Valeryl dextran DS = 0.025–benzoyl dextran DS = 0.137. (b) Benzoyl dextran DS = 0.054–valeryl dextran DS = 0.20. The temperature was 22°C.

3.5. Partition of proteins

The proteins β-galactosidase, BSA, lysozyme, lipase-1, β-lactoglobulin A, cytochrome *c* and myoglobin were partitioned in aqueous two-phase systems containing benzoyl dextrans and

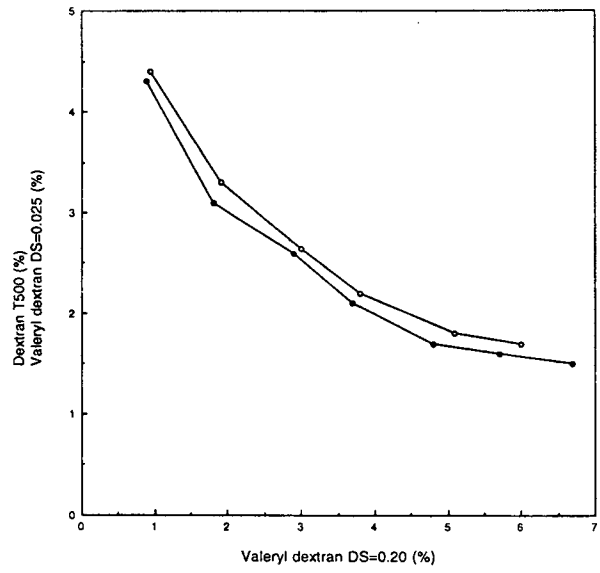

Fig. 5. Phase diagrams for the system dextran T500–valeryl dextran DS = 0.2 (●) and the system valeryl dextran DS = 0.025–valeryl dextran DS = 0.20 (○). The temperature was 22°C.

valeryl dextrans. Tables 1–7 show the partition coefficients of the proteins in PEG–benzoyl dextran, PEG–valeryl dextran systems and in the same systems containing 100 m*M* sodium chloride. All systems contained 10 m*M* sodium phosphate buffer, pH 7.4 for β-galactosidase and

Table 1
Partition coefficient of β-galactosidase in PEG–benzoyl dextran and PEG–valeryl dextran aqueous two-phase system

	K	*K* (with 100 m*M* NaCl)
DS of benzoyl dextran		
0	72	0.095
0.054	0.12	0.0096
0.087	0.026	0.012
0.137	0.022	0.013
DS of valeryl dextran		
0.025	59	0.030
0.12	0.47	0.0079
0.20	0.63	0.0059

The system composition was: 6.0% PEG 8000, 6.0% benzoyl dextran (or valeryl dextran), 10 m*M* sodium phosphate buffer, pH 7.4, without or with 100 m*M* NaCl. Room temperature (22°C).

Table 2
Partition coefficient of bovine serum albumin in PEG–valeryl dextran aqueous two-phase system

DS of valeryl dextran	K	K (with 100 mM NaCl)
0	0.35	0.10
0.025	0.26	0.082
0.12	0.16	0.072
0.20	0.59	0.12

The system composition was: 6% PEG 8000, 6% valeryl dextran, 10 mM sodium phosphate buffer, pH 7.0, without or with 100 mM NaCl. Room temperature (22°C).

pH 7.0 for rest of proteins. For β-galactosidase (Table 1) a strong decrease in the partition coefficient is observed when the DS of benzoyl and valeryl dextran is increased.

Table 2 shows the partition coefficient of BSA in systems composed of PEG and valeryl dextran. The partitioning properties of this protein in PEG–benzoyl dextran systems were shown in an earlier work [10]. The partition coefficients of lipase-1, lysozyme and β-lactoglobulin A are shown in Tables 3, 4 and 5. For these four proteins the same tendency is observed. The K value is first decreased with increasing DS but at high DS the K value is again increased.

Table 3
Partition coefficient of lipase-1 in PEG–benzoyl dextran and PEG–valeryl dextran aqueous two-phase system

	K	K (with 100 mM NaCl)
DS of benzoyl dextran		
0	0.51	0.39
0.054	0.28	0.30
0.087	0.23	0.23
0.137	0.92	0.55
DS of valeryl dextran		
0.025	0.51	0.37
0.12	0.31	0.28
0.20	1.13	1.22

The system composition was: 6% PEG 8000, 6% benzoyl dextran (or valeryl dextran), 10 mM sodium phosphate buffer, pH 7.0, without or with 100 mM NaCl. Room temprature (22°C).

Table 4
Partition coefficient of lysozyme in PEG–benzoyl dextran and PEG–valeryl dextran aqueous two-phase system

	K	K (with 100 mM NaCl)
DS of benzoyl dextran		
0	0.29	2.06
0.054	0.087	0.052
0.087	0.18	0.50
0.137	0.16	0.45
DS of valeryl dextran		
0.025	0.41	1.81
0.12	0.25	0.71
0.20	0.38	1.11

The system composition was: 6% PEG 8000, 6% benzoyl dextran (or valeryl dextran), 10 mM sodium phosphate buffer, pH 7.0, without or with 100 mM NaCl. Room temperature (22°C).

Table 6 shows the partition coefficient of cytochrome c and Table 7 shows the partition coefficient of myoglobin. The partition coefficient of these two proteins is increased when the degree of substitution of hydrophobic groups is increased.

For all proteins a change in the K value is observed when comparing partitioning in equiva-

Table 5
Partition coefficient of β-lactoglobulin A in PEG–benzoyl dextran and PEG–valeryl dextran aqueous two-phase system

	K	K (with 100 mM NaCl)
DS of benzoyl dextran		
0	1.11	0.29
0.054	0.36	0.075
0.087	0.36	0.12
0.137	0.58	0.044
DS of valeryl dextran		
0.025	0.96	0.22
0.12	0.39	0.16
0.20	2.67	0.039

The system composition was: 6% PEG 8000, 6% benzoyl dextran (or valeryl dextran), 10 mM sodium phosphate buffer, pH 7.0, without or with 100 mM NaCl. Room temperature (22°C).

Table 6
Partition coefficient of cytochrome *c* in PEG–benzoyl dextran and PEG–valeryl dextran aqueous two-phase system

	K	*K* (with 100 m*M* NaCl)
DS of benzoyl dextran		
0	0.19	0.42
0.054	0.16	0.36
0.087	0.34	0.54
0.137	0.48	0.67
DS of valeryl dextran		
0.025	0.20	0.43
0.12	0.35	0.54
0.20	0.52	0.70

The system composition was: 6.0% PEG 8000, 6.0% benzoyl dextran (or valeryl dextran), 10 m*M* sodium phosphate buffer, pH 7.0, without or with 100 m*M* NaCl. Room temperature (22°C).

lent systems containing only a 10 m*M* sodium phosphate buffer and a buffer plus 100 m*M* sodium chloride. This is due to the electrical potential difference generated between the phases by the salts [16].

Table 8 shows the molecular masses, isoelectric points and surface hydrophobicities of the proteins studied. The table also shows the maximum difference in log *K* between the systems

Table 7
Partition coefficient of myoglobin in PEG–benzoyl dextran and PEG–valeryl dextran aqueous two-phase system

	K	*K* (with 100 m*M* NaCl)
DS of benzoyl dextran		
0	0.34	0.36
0.054	0.32	0.29
0.087	0.35	0.35
0.137	0.48	0.49
DS of valeryl dextran		
0.025	0.30	0.33
0.12	0.39	0.38
0.20	0.54	0.47

The system composition was: 6.0% PEG 8000, 6.0% benzoyl dextran (or valeryl dextran), 10 m*M* sodium phosphate buffer, pH 7.0, without or with 100 m*M* NaCl. Room temperature (22°C).

PEG–dextran (Dx) and PEG–benzoyl dextran (BzDx) [or PEG–valeryl dextran (VaDx)] (Eqs. 1 and 2), either without or with 100 mM NaCl.

$$\Delta \log K_{(BzDx)} = \log K_{(PEG-Dx)} - \log K_{(PEG-BzDx)} \quad (1)$$

$$\Delta \log K_{(VaDx)} = \log K_{(PEG-Dx)} - \log K_{(PEG-VaDx)} \quad (2)$$

3.6. Partition of thylakoid membrane vesicles

Whole thylakoid membranes, grana (B3) and stroma lamellae (T3) vesicles were partitioned in aqueous two-phase systems composed of 5% PEG 8000, 5% (dextran T500 + valeryl dextran), 40 m*M* boric acid–tris(hydroxymethyl)aminomethane buffer (H_3BO_3-Tris), pH 7.83. Whole thylakoid membranes as well as B3 and T3 vesicles were almost exclusively partitioned to the top phase in systems without valeryl groups (100% for whole thylakoid membranes, 90% for B3 and 85% for T3 vesicles). By introducing a

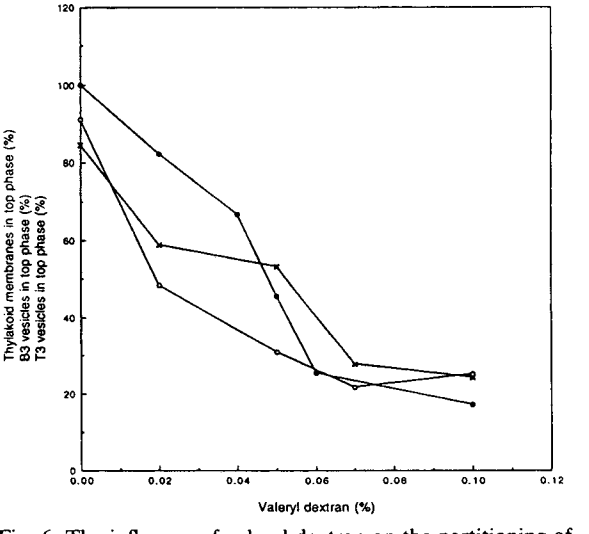

Fig. 6. The influence of valeryl dextran on the partitioning of thylakoid membranes (●), grana (B3) (○) and stroma lamellae (T3) (×) vesicles between the top phase and the interface. The system composition was: 5% PEG 8000, 5% (dextran T500 + valeryl dextran DS = 0.12), 40 m*M* H_3BO_3-Tris, pH 7.83, room temperature (22°C). The percentage of valeryl dextran is the amount of dextran replaced by valeryl dextran.

Table 8
Molecular masses, isoelectric points, surface hydrophobicities and Δlog K of proteins

Protein	M_r	pI	Surface hydrophobicity	ΔLog K^a (no salt)	ΔLog K^b (100 mM NaCl)
β-Galactosidase	465 400 [17,18]	4.6 [19]	–	3.51 2.18	0.86 (BzDx) 1.21 (VaDx)
BSA	69 000 [20]	5.0 [20]	10.33[c]	0.40[d] 0.34	0.19[d] (BzDx) 0.14 (VaDx)
Lipase-1	66 000 [20][e]	5.1 [20][e]	–	0.35 0.22	0.23 (BzDx) 0.14 (VaDx)
Lysozyme	13 900 [22]	11 [23]	7.49[c]	0.25 0.06	0.66 (BzDx) 0.46 (VaDx)
β-Lactoglobulin	35 000 [20]	5.1 [20]	4.41[c]	0.49 0.45	0.82 (BzDx) 0.87 (VaDx)
Myoglobin	17 500 [20]	7.1 [20]	2.99[c]	−0.15 −0.20	−0.13 (BzDx) −0.12 (VaDx)
Cytochrome c	13 000 [22]	9.4 [20]	0[f]	−0.40 −0.44	−0.20 (BzDx) −0.22 (VaDx)

[a] ΔLog K is the maximum log K difference between the systems PEG–Dx and PEG–BzDx or PEG–VaDx without salt.
[b] ΔLog K is the maximum log K difference between the systems PEG–Dx and PEG–BzDx or PEG–VaDx with 100 mM NaCl.
[c] Retention coefficient in hydrophobic interaction chromatogrophy on butylepoxy-Sepharose [24].
[d] Data from ref. 10.
[e] Value for enzyme from guinea pig pancreas.
[f] Determined by hydrophobic partition using fatty acids bound to PEG [25].

small amount of valeryl groups, *e.g.* when 0.1% of dextran was replaced by valeryl dextran (DS = 0.12) the three types of membranes were transferred from the top phase to the interface. The results are shown in Fig. 6. The systems composed of 5% PEG 8000, 5% (dextran + benzoyl dextran) and 15 mM H_3BO_3-Tris, pH 7.83 were also used for partitioning of these thylakoid membranes, B3 and T3 vesicles. The results were qualitatively similar to what was obtained with valeryl dextran (Fig. 7).

The aqueous two-phase systems composed of 6% PEG 8000, 6% (dextran T500 + valeryl dextran) and 10 mM sodium phosphate buffer, pH 7.4, were used to partition the thylakoid membranes, B3 and T3 vesicles from the interface to the bottom phase with increased polymer concentration (Fig. 8). In this system the thylakoid membranes, B3 and T3 vesicles were partitioned to the interface in the absence of valeryl groups on dextran (> 80% for all of them). When 20% of dextran was replaced by valeryl dextran (DS = 0.12), the material was partitioned to the bottom phase (> 80%) (Fig. 8).

4. Discussion

4.1. Hydrophobic association of benzoyl dextran and valeryl dextran

Dextran is a relatively hydrophilic polymer. But benzoyl dextran and valeryl dextran are more hydrophobic compared with dextran and show hydrophobic association in aqueous solutions. The hydrophobicity depends on the degree of substitution. The determination of polymer solution viscosity, phase diagrams, and partition

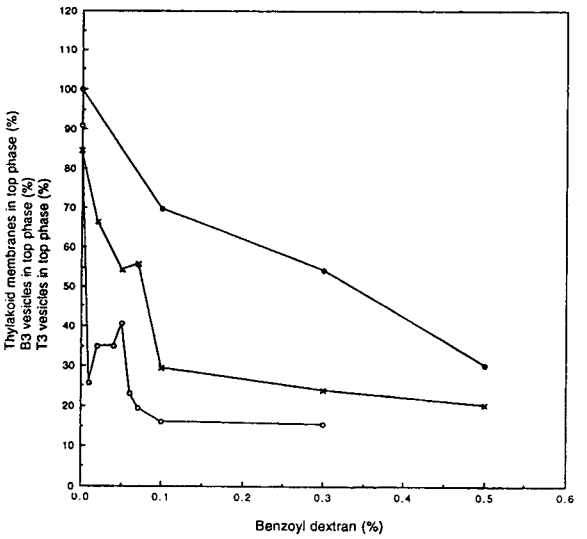

Fig. 7. The influence of benzoyl dextran on the partitioning of thylakoid membranes (●), grana (B3) (○) and stroma lamellae (T3) (×) vesicles between the top phase and the interface. The system composition was: 5% PEG 8000, 5% (dextran T500 + benzoyl dextran DS = 0.087), 15 m*M* H_3BO_3-Tris, pH 7.83, room temperature (22°C). The percentage of benzoyl dextran is the amount of dextran replaced by benzoyl dextran.

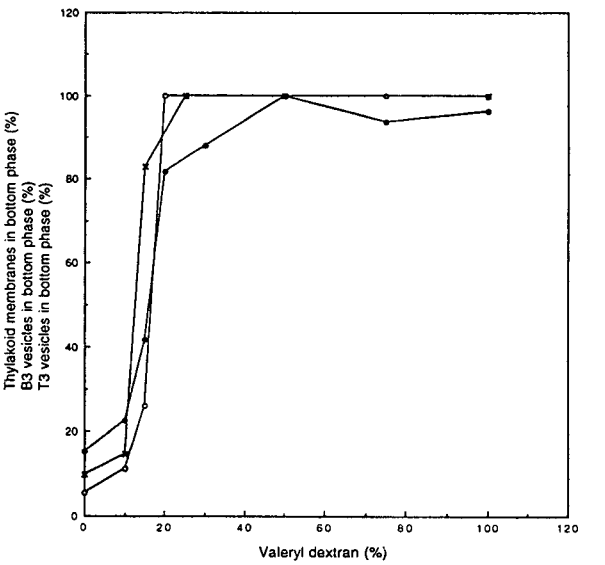

Fig. 8. The influence of valeryl dextran on the partitioning of thylakoid membranes (●), grana (B3) (○) and stroma lamellae (T3) (×) vesicles between the interface and bottom phase. The system composition was: 6% PEG 8000, 6% (dextran T500 + valeryl dextran DS = 0.12), 10 m*M* sodium phosphate buffer, pH 7.4, room temperature (22°C). The percentage of valeryl dextran is the amount of dextran replaced by valeryl dextran.

coefficients of proteins show that the hydrophobic association is increased with increasing of degree of substitution.

The viscosity measurements of benzoyl dextrans with DS of 0.053, 0.087 and 0.137 at low concentrations (0.00225 g/ml and less) show that this concentration is low enough to eliminate interactions between polymer molecules. The viscosities of the benzoyl dextrans are very close to normal dextran.

The viscosities of benzoyl and valeryl dextrans in concentrated systems show association between the polymers at high degrees of substitution. The viscosity of benzoyl dextran with DS = 0.137 is increased at concentrations above 6% compared with dextran and benzoyl dextran with lower DS (0.087). This phenomenon shows the hydrophobic interactions between benzoyl dextran molecules and the interactions are increased with increasing polymer concentrations. The hydrophobic association of several dextran molecules makes them behave like a larger molecule.

At lower DS or lower polymer concentrations the hydrophobic interactions are too weak to affect the viscosity. The hydrophobic interactions between valeryl dextran polymers with DS = 0.2 are stronger than the interactions for benzoyl dextran with DS = 0.137 as judged from the strong increase in viscosity at 6% concentration for valeryl dextran compared to 12% for benzoyl dextran.

4.2. Phase diagrams

The binodal curve of PEG–valeryl dextran (DS = 0.025) is very close to the binodal curve of PEG–dextran T500 but at slightly higher polymer concentrations. When valeryl dextran with DS 0.12 is used, the binodal curve is moved to higher concentrations. This reflects the increased compatability between PEG and valeryl dextrans. When the DS of valeryl dextran is increased to 0.20 the binodal curve is moved to

lower concentrations compared with valeryl dextran with DS = 0.12 (see Fig. 3b and c). This could be due to the higher DS of the valeryl dextran which gives stronger hydrophobic interactions between the valeryl groups on the dextran backbones. This interaction makes the valeryl dextran like a pseudo-higher-molecular-mass polymer. Generally, the higher the molecular mass is, the lower polymer concentration is needed to achieve phase separation [1].

Valeryl dextran with a high degree of substitution (DS = 0.20) can form a two-phase system with benzoyl dextran having a low degree of substitution (DS = 0.054). Conversely, benzoyl dextran with a high DS (0.137) can form a two-phase system with a valeryl dextran which has a low DS (0.025) (see Fig. 4). In these two systems the valeryl dextran and benzoyl dextran with low degree of substitution phase separate in the same way as normal dextran. The valeryl dextran with a high DS (0.20) cannot phase separate with benzoyl dextran which has a high DS (0.137). To form a two-phase system the difference in the degree of substitution of hydrophobic groups between the two phase forming polymers has to be large enough.

4.3. Partitioning of amino acids, dipeptides and proteins

Amino acids and dipeptides with aromatic groups (L-tryptophan, L-tyrosine, L-phenylalanine, tyrosine–tyrosine and glycine–tryptophan) were partitioned in aqueous two-phase systems containing benzoyl dextrans and valeryl dextrans. The partition coefficients of these hydrophobic amino acids and dipeptides are close to 1 which indicates that the amino acids and dipeptides are too small to be affected by the hydrophobic groups on dextran.

The partitioning of proteins is affected by many factors, mainly the composition of the two-phase system and the protein properties [1,3]. In this work, seven proteins (β-galactosidase, BSA, lipase, lysozyme, β-lactoglobulin, cytochrome *c* and myoglobin) were partitioned in PEG–benzoyl dextran and PEG–valeryl dextran systems. The protein properties are collected in Table 8. The Δlog *K* values in Table 8 show the maximum effect of the hydrophobic groups on protein partitioning.

When proteins are partitioned in PEG–benzoyl dextran and PEG–valeryl dextran systems two opposite effects are observed. For β-galactosidase, BSA, lipase, lysozyme and β-lactoglobulin a decrease in the *K* value is observed when the DS is increased. For cytochrome *c* and myoglobin the *K* value is increased with increasing DS. The partitioning behaviour of the first group of proteins can be explained by hydrophobic interactions with the benzoyl or valeryl groups.

The *K* value for all proteins is affected when the salt composition is changed from 10 m*M* sodium phosphate by addition of 100 m*M* NaCl to the phase system. This effect has been thoroughly studied in PEG–dextran systems [1,16,26] and can be explained by the electrical potential difference generated by the salts. Phosphate ions have a tendency to partition to the dextran phase [26]. Electroneutrality forces the counterions to partition in the same direction, but the net effect is the generation of an electrical potential difference across the interface with a net negative charge in the bottom phase. The partitioning of proteins will then depend on the protein net charge. A protein with a high negative charge (*e.g.* β-galactosidase at pH 7.4) will partition towards the top (PEG) phase in a system containing 10 m*M* sodium phosphate. For NaCl there is a weak tendency for Na^+ to partition to the dextran phase and a weak tendency for Cl^- to partition to the PEG phase [16]. When 100 m*M* NaCl is added to the system containing 10 m*M* sodium phosphate the NaCl salt will be dominating in the system, and the electrical potential difference will be of opposite sign relative to the potential generated by sodium phosphate. In accordance, β-galactosidase (at pH 7.4) will partition towards the bottom (dextran) phase when NaCl is the dominating salt.

The partition coefficient for β-galactosidase (M_r 465 400, p*I* 4.6) [17–19] was decreased more than 100 times by introducing benzoyl groups (*K* from 72 to 0.022) or valeryl groups (*K* from 72 to

0.63). The addition of sodium chloride also decreased the partition coefficient. In the system PEG–valeryl dextran (DS = 0.2) and 1.0 *M* NaCl, no enzyme activity was found in the top phase. Therefore, this enzyme could be completely transferred from top phase to bottom phase by adjusting the polymer hydrophobicity, the salt composition and concentration. This strong change of the partition coefficient may be due to the hydrophobic interactions between hydrophobic groups (benzoyl and valeryl) on the dextran backbone and hydrophobic groups on the protein surface [27,28]. In 1.0 *M* NaCl the hydrophobic interactions are increased. For β-galactosidase from *E. coli* the ratio of tryptophan to all amino acids is unusually high, 3%, compared to 1% for an average *E. coli* protein [17,18,29]. There are 39 tryptophans in each subunit giving a total of 156 tryptophans in *E. coli* β-galactosidase [17]. Tryptophan is a very hydrophobic amino acid. Exposed tryptophans on protein surfaces have been shown to direct the partitioning of proteins to the PEG phase in PEG–salt systems [30]. The much stronger effect on β-galactosidase partitioning observed with benzoyl dextran compared with valeryl dextran (Table 1, systems without salt), could be due to aromatic "stacking" interactions with exposed tryptophans. The Δlog *K* values (Table 8) show that the effect of the hydrophobic groups on the partitioning are much stronger for β-galactosidase than for the rest of the proteins studied.

For BSA the partition coefficient was decreased from 0.35 to 0.16 by increasing the DS of valeryl dextran from 0 to 0.12. A similar effect was observed with benzoyl dextran [10]. The partition coefficients of lipase, lysozyme and β-lactoglobulin in the systems of PEG–benzoyl dextran and PEG–valeryl dextran show the same tendency as for BSA. This can be explained by interactions between benzoyl and valeryl groups on dextran and hydrophobic sites or surfaces on the proteins. The proteins BSA and β-lactoglobulin are known to bind hydrophobic compounds. This has been demonstrated by affinity partitioning using PEG esterified with fatty acids [25]. From Table 8 can be seen that BSA, lysozyme and β-lactoglobulin are relatively hydrophobic proteins as determined by hydrophobic interaction chromatography [24]. Lipase has hydrophobic sites for binding of lipids [21]. The Δlog *K* values in Table 8 are relatively similar for the four proteins in this group. The values are significantly smaller than the corresponding values for β-galactosidase. This can be due to the much larger molecular mass of β-galactosidase or that specific interactions (*e.g.* with tryptophans) are involved with this protein.

The partitioning of cytochrome *c* and myoglobin is affected in a different way by the hydrophobic groups on the dextran. Both proteins are relatively less hydrophobic compared with the proteins in the previous group (Table 8). In both PEG–benzoyl dextran and PEG–valeryl dextran systems the partition coefficient of cytochrome *c* and myoglobin is increased with increasing DS. As an effect of increased hydrophilicity the proteins may experience a repulsive force from the hydrophobic groups.

The increased hydrophobic interactions between the benzoyl or valeryl dextrans with increased DS will also lead to increased *K* values for proteins. The increased interactions lead to association of the dextran polymers as observed in the viscosity measurements (Figs. 1 and 2). This association will result in an exclusion of the protein molecules from the bottom phase, *i.e.* the *K* value will increase much in the same way as when the molecular mass of dextran is increased [1,31]. Increased *K* values are also observed at high DS of hydrophobic groups for BSA, lipase, lysozyme and β-lactoglobulin.

For cytochrome *c* the addition of 100 m*M* NaCl leads to increasing *K* values in all systems studied, but this salt has a very small effect on the partition coefficient of myoglobin (Tables 6 and 7). Cytochrome *c* has a p*I* of 9.4 and myoglobin 7.1 [20]. At pH 7 cytochrome *c* is positively charged and will be partitioned to the bottom phase in a system with sodium phosphate due to the electrical potential difference. The *K* value for cytochrome *c* is increased with addition of NaCl which is in accordance with the reversal of the potential by this salt. The partitioning of myoglobin is affected very little by the change in salt composition which agrees with that the

partitioning is performed close to the p*I* of the protein (7.1). The change of salt composition has an even stronger effect on lysozyme compared with cytochrome *c*. This is in accordance with the higher positive charge of lysozyme due to its higher p*I*.

4.4. Partitioning of thylakoid membrane vesicles

The effect of hydrophobic groups bound to dextran on the partitioning of thylakoid membranes, grana (B3) and stroma lamellae (T3) vesicles is very strong (Fig. 6). In the absence of valeryl groups the three types of membranes are partitioned mostly to the top phase. More than 70% of these materials are transferred to the interface by replacing only 0.1% of the total dextran with valeryl dextran, DS = 0.12. Benzoyl groups show a similar strong effect on these materials (Fig. 7). By replacing 0.01–0.02% of dextran with benzoyl dextran significant separation between grana (B3) and stroma lamellae (T3) vesicles was achieved. This is not surprising since they are of opposite sidedness [32]. At 0.1% there is a considerable separation between whole thylakoid membranes and stroma lamellae vesicles. It is of interest that the two latter are separated although both are right-side out. However, the stroma lamellae vesicles are much smaller in size and their membranes are more curved than the flat membranes of the whole thylakoids, which may explain the difference in affinity for the benzoyl dextran phase. It is also possible with the hydrophobic groups to change the partitioning of thylakoid membranes, grana and stroma lamellae vesicles from the interface to the bottom phase (Fig. 8). The fact that thylakoid membrane vesicles are always partitioned to the phase containing the hydrophobic groups reflects the interactions between hydrophobic groups in the membrane fractions and the benzoyl (or valeryl) groups. The strong effect of dextran bound hydrophobic groups may be used to increase the specificity of PEG–dextran systems in the area of membrane separations, *e.g.* the separation of thylakoid membranes and plasma membranes (see ref. 10).

5. Conclusions

Dextran can be modified with aromatic and aliphatic groups. The hydrophobically modified dextran (benzoyl dextran and valeryl dextran) can offer a relatively more hydrophobic bottom phase compared to dextran in two-phase systems with PEG. These systems provide a special environment to study the hydrophobic interactions between proteins, membranes and hydrophobic groups on the dextrans. These hydrophobic groups show strong interaction with some proteins, like β-galactosidase, and thylakoid membrane vesicles. By changing the degree of substitution of benzoyl or valeryl dextrans, salt composition and concentration, the partitioning of proteins with hydrophobic sites can be influenced. Thylakoid membrane vesicles could be almost totally collected in the hydrophobic phase or at the interface.

6. Acknowledgement

We thank Mr. Krister Thuresson for NMR measurements. This work was supported by the Swedish Natural Science Research Council, the Swedish Research Council for Engineering Sciences and the Swedish National Board for Industrial and Technical Development (NUTEK).

7. References

[1] P.-Å. Albertsson, *Partition of Cell Particles and Macromolecules*, Wiley, New York, 3rd ed., 1986.
[2] F. Tjerneld, in D. Fisher and I.A. Sutherland (Editors), *Separations Using Aqueous Phase Systems*, Plenum Press, New York, 1989, pp. 429–438.
[3] F. Tjerneld, in J.M. Harris (Editor), *Poly(ethylene glycol) Chemistry: Biotechnical and Biomedical Applications*, Plenum Press, New York, (1992) 85–102.
[4] S. Sturesson, F. Tjerneld and G. Johansson, *Appl. Biochem. Biotechnol.*, 26 (1990) 281–295.
[5] H. Walter, G. Johansson and D. Brooks, *Anal. Biochem.*, 197 (1991) 1–18.
[6] G. Johansson, *J. Chromator.*, 284 (1984) 63–72.
[7] G. Johansson, A. Hartman and P.-Å. Albertsson, *Eur. J. Biochem.*, 33 (1973) 379–386.
[8] G. Johansson and M. Joelsson, *J. Chromatogr.*, 393 (1987) 195–208.

[9] F. Tjerneld and G. Johansson, *Bioseparation*, 1 (1990) 255–263.
[10] M. Lu, F. Tjerneld, G. Johansson and P.-Å. Albertsson, *Bioseparation*, 2 (1991) 247–255.
[11] P.-Å. Albertsson and S.G. Yu, *Biochim. Biophys. Acta*, 936 (1988) 215–221.
[12] E. Andreasson, P. Svensson, C. Weibull and P.-Å. Albertsson, *Biochim. Biophys. Acta*, 936 (1988) 339–350.
[13] M.M. Bradford, *Anal. Biochem.*, 72 (1976) 248–254.
[14] A. Veide, A.-L. Smdes and S.-O. Enfors, *Biotechnol. Bioeng.*, 25 (1983) 1789–1800.
[15] L.A. Decker (Editor), *Enzyme Manual*, Worthington, Freehold, NJ, 1977.
[16] G. Johansson, *Acta Chem. Scand. B*, 28 (1974) 873–882.
[17] A. Kalnins, K. Otto, U. Rüther and B. Müller-Hill, *EMBO J.*, 2 (1983) 593–597.
[18] A.V. Fowler and I. Zabin, *J. Biol. Chem.*, 253 (1978) 5521–5525.
[19] K. Wallenfels and R. Weil, in P.D. Boyer (Editor), *The Enzymes*, Vol. VII, Academic Press, New York, 3rd ed., 1972, p. 627.
[20] P.G. Righetti and T. Caravaggio, *J. Chromatogr.*, 127 (1976) 1–28.
[21] C. Ehnholm and T. Kuusi, *Methods Enzymol.*, 129 (1986) 718–727.
[22] G. Zubay, *Biochemistry*, Macmillan, New York, 2nd ed., 1988, p. 88.
[23] M. Wahlgren, *Ph.D. Thesis*, University of Lund, Lund 1992.
[24] E. Keshavarz and S. Nakai, *Biochim. Biophys. Acta*, 576 (1979) 269–279.
[25] V.P. Shanbhag and C.-G. Axelsson, *Eur. J. Biochem.*, 60 (1975) 17–22.
[26] G. Johansson, *Biochim. Biophys. Acta.*, 221 (1970) 387–390.
[27] C.T. Chang, B.J. McCoy, and R.G. Carbonell, *Biotechnol. Bioeng.*, 22 (1980) 377–399.
[28] A. Veide, *Ph.D. Thesis*, The Royal Institute of Technology, Stockholm, 1987.
[29] K. Köhler, A. Veide and S.-O. Enfors, *Enzyme Microb. Technol.*, 13 (1991) 204–209.
[30] K. Köhler, C. Ljungquist, A. Kondo, A. Veide and B. Nilsson, *Bio/Technol.*, 9 (1991) 642–646.
[31] P.-Å. Albertsson, A. Cajarville, D.E. Brooks and F. Tjerneld, *Biochim. Biophys. Acta*, 926 (1987) 87–93.
[32] P.-Å. Albertsson, E. Andreasson, H. Stefansson and L. Wollenberger, *Methods Enzymol.*, 228 (1994) 469–482.

ELSEVIER

Journal of Chromatography A, 668 (1994) 229–236

JOURNAL OF CHROMATOGRAPHY A

Utilization of temperature-induced phase separation for the purification of ecdysone and 20-hydroxyecdysone from spinach

Richard F. Modlin*[,a], Patricia A. Alred[b], Folke Tjerneld[b]

[a] *Department of Biological Sciences, The University of Alabama in Huntsville, Huntsville, AL 35899, USA*

[b] *Department of Biochemistry, Chemical Center, University of Lund, S-221 00 Lund, Sweden*

Abstract

An aqueous solution of the ethylene oxide–propylene oxide random copolymer UCON 50-HB-5100 was successfully used to extract ecdysone and 20-hydroxyecdysone from the common spinach plant, *Spinacia oleracea*. The UCON spinach extract was mixed with a hydroxypropyl starch Reppal PES 200 solution and allowed to form an aqueous two-phase system. After the polymers separated cell debris, proteins and other comtaminants partitioned to the lower Reppal phase and ecdysone and 20-hydroxyecdysone partitioned to the upper UCON phase. The UCON phase was isolated and subjected to a temperature increase to 56°C which induced phase separation between UCON and water. Ecdysone and 20-hydroxyecdysone partitioned between the UCON phase and the water phase at concentrations determined by their degree of hydrophobicity. The less hydrophobic 20-hydroxyecdysone had a greater affinity for the water-rich phase than did ecdysone. Due to the larger volume of the water phase both ecdysteroids were obtained in this phase at 56°C with yields higher than 80%. With 20% ethanol in the primary system recovery was 88.7% for ecdysone and 91.2% for 20-hydroxyecdysone. Results indicate that aqueous two-phase partitioning coupled with temperature-induced phase separation is a quick, easy and inexpensive bench-top technique for extracting and purifying ecdysteroids from raw material. This technique can also be readily up-scaled for commercial use.

1. Introduction

Ecdysone and 20-hydroxyecdysone, hormones that regulate molting cycles of arthropods, are also found in some plants [1,2]. Both are of commercial interest as insecticides [3–6] and indicators of helminth and nematod parasitism and other medical disorders in humans [7–10]. Both molecules are steroids [1,11], but soluble in water. Their structures differ only in the substitution of a hydroxyl group in 20-hydroxyecdysone for a hydrogen (in ecdysone) on the C-20 position. This substitution changes the hydrophobicity of the two molecules, with ecdysone being the more hydrophobic.

Extraction and recovery of ecdysone, 20-hydroxyecdysone and other ecdysteroids from raw material, *e.g.*, insects and plants, follow classic protocols originally developed by Karlson and Shaaya [12]. Generally, one or several non-polar solvents (*e.g.*, methanol, butanol, light petroleum, etc.) and/or hot water (80–90°C) are used to extract the desired molecules. The molecules are recovered in a residue obtained after the evaporation of the solvent in the final extraction step. Quantification is determined from the mass of this residue and verification is obtained in a bioassay that determines the ability of ecdysone

* Corresponding author.

0021-9673/94/$07.00
SSDI 0021-9673(93)E1293-9

and 20-hydroxyecdysone to induce molting of dipteran fly, *Calliphora erythrocephala*, pupae [12]. Although the original extraction procedures have received little or no improvements and methanol remains the solvent of choice [13–16], detection and quantification of ecdysteroids have become more sophisticated [16–23]. Presently, extraction, detection, quantification and recovery procedures for the ecdysteroids are time consuming and require costly, sophisticated chromatographic equipment. Nevertheless, without additional purification steps, desired compounds are contaminated with solvent residues which can have lethal and/or sublethal effects on animals.

Aqueous two-phase partitioning systems, widely used to separate and purify biomolecules, are usually composed of aqueous solutions of two biologically inert and immiscible polymers, *e.g.*, polyethylene glycol (PEG) (upper phase) and dextran or hydroxypropyl starch (lower phase) [24–27]. These systems have gained widespread use for separation of biomolecules, cell particles and cells. In the recent development of temperature-induced phase separation the ethylene oxide–propylene oxide random copolymer of UCON 50-HB-5100 (UCON) had been used instead of PEG in phase systems with dextran or hydroxypropyl starch. The upper UCON-rich phase is removed and isolated in a separate container which is then subjected to increased temperature above the cloud point of UCON. The temperature-induced phase separation results in the formation of a UCON-rich and a water-rich phase. The phase separation can be made to occur at biologically favorable temperatures (37–56°C) which allows purification of biomolecules to a water-rich phase free of polymers [28,29]. The partition behavior of authentic ecdysone and 20-hydroxyecdysone in aqueous two-phase systems (UCON–dextran primary system) combined with temperature-induced phase separation was successfully determined [30]. Ecdysone and 20-hydroxyecdysone, because of their hydrophobicity, partitioned mainly to the upper UCON-rich phase in the primary systems. When temperature was increased on the isolated UCON-rich phase, above the cloud point of UCON (50°C), the two ecdysteroids partitioned between the water-rich phase and the UCON phase at concentrations determined by their degree of hydrophobicity [30].

An aqueous two-phase system composed of the random copolymer UCON 50-HB-5100 (upper phase) and Reppal PES 200 (Reppal; hydroxypropyl starch) (lower phase) was tested in an attempt to obtain ecdysone and 20-hydroxyecdysone from raw material. The use of Reppal in the lower phase, rather than dextran, appeared more desirable because of its lower affinity for hydrophobic molecules and lower cost. In this project we attempted to (1) extract ecdysteroids from raw material using a UCON solution rather than non-polar solvents described in classic protocols [12], (2) develop an UCON–Reppal aqueous two-phase system that would specifically partition ecdysone and 20-hydroxyecdysone to the upper hydrophobic phase, and (3) allow us, after the primary partitioning step, to isolate the ecdysteroids in a non-polymer water-rich solution by subjecting the UCON-rich phase to temperature-induced phase separation.

Although best known as hormones that mediate the molting cycle in insects and other arthropods, concentrations of ecdysone and 20-hydroxyecdysone in plants are more predictable and far exceed that found in insects by several orders of magnitude [1,11]. Consequently, because of its availability and ease of culturing, our choice of raw material was the common spinach plant, *Spinacia oleracea* [31].

2. Experimental

2.1. Chemicals

UCON 50-HB-5100 [ethylene oxide (EO)–propylene oxide (PO) random copolymer, EO–PO ratio 1:1, M_r 4000] was a kind gift from Union Carbide (New York, NY, USA). Prior to use, UCON was purified by extraction into methylene chloride. Reppal PES 200 [hydroxypropyl starch, M_r 200 000] was a kind gift from Reppe (Växjö, Sweden). Ecdysone (M_r 464.6, EC 3604-87-3) was dissolved in methanol–water

(20:80) and 20-hydroxyecdysone (M_r 480.6, EC 5289-74-7) was dissolved in water prior to use. Both ecdysteroids were purchased in crystalline form (>95% purity) from Sigma (St. Louis, MO, USA). All other chemicals were of analytical-reagent grade.

2.2. UCON Spinach extract

Spinach plants were grown from seed in a greenhouse at ambient temperature, light intensity and photoperiod for 46 days before leaves were removed (194 g fresh mass), homogenized (Waring Blender) and sonicated (Branson Cell Disrupter) for 15 min in a solution comprised of 100 g UCON and 294 g phosphate buffer (P.B.) (0.1 *M*, pH 7.0). Ecdysteroid concentrations in spinach leaves is fairly constant at 65 μg/g fresh mass in 44–76-day-old plants [31]. Extraction was allowed to proceed for 72 h at 4.0°C. The extract was then centrifuged at 17 000 *g* for 20 min at 4.0°C to remove plant particulates. Based on fluid volume of the extract after centrifugation (394 ml), UCON concentration was 25.4%.

2.3. Primary aqueous two-phase partition system (primary system)

The phase diagram for the system UCON–Reppal–water (Fig. 1) was determined as described previously [28]. All polymer concentrations were calculated as mass percentages. The UCON spinach extract was mixed with an aqueous stock solution of Reppal (21%, w/w) to a final concentration of 11.0% UCON and 7.5% Reppal. Two duplicate experimental primary phase systems were tested, one with 20% ethanol added and the other without ethanol. The primary phase systems were kept at room temperature (22°C). Phase systems were separated by centrifugation at 125 *g* for 10 min after which the UCON-rich upper phase was removed and isolated in a separate container. The lower, Reppal-rich phase, was treated with methanol–water (45:55) to precipitate the Reppal and concentrate any ecdysones in the supernatant. These tubes were centrifuged at 200 *g* for 15 min before the supernatant was analyzed.

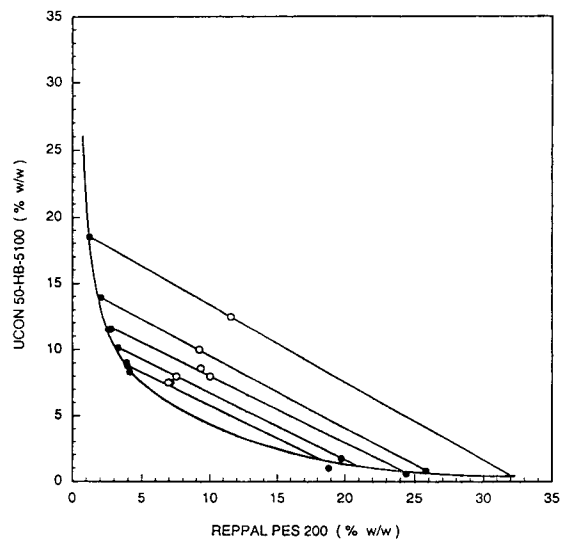

Fig. 1. Phase diagram for UCON 50-HB-5100 (M_r 4000), Reppal PES 200 (hydroxypropyl starch, M_r 200 000) and water at 22°C. ● = points obtained by tritration [28,31] or analysis of separate phases; ○ = points obtained by mixing of polymers.

2.4. Temperature-induced phase separation

Containers with upper UCON-rich phase were placed in a water bath at 56°C for 20 min to allow temperature-induced phase separation to occur. The upper water–buffer phase was removed and isolated prior to analysis. Because of increased viscosity, the UCON phase was diluted by a factor of 10 prior to analysis.

2.5. Detection and analysis

Reversed-phase high performance liquid chromatography (RP-HPLC) coupled with UV spectrophotometry was used to determine presence and concentrations of ecdysone and 20-hydroxyecdysone in all samples. A Waters Delta Pak C_{18} 100-Å, 150 mm × 3.9 mm I.D. column (Waters Chromatography Division, Tokyo, Japan) was coupled to a Bio-Rad HPLC pump attached to a Perkin-Elmer LC75 UV-absorbance detector (wavelength preset at 254 nm) connected to a potentiometric recorder. The column was equilibrated before use with methanol–water (40:60). Flow-rate of the methanol–water (40:60)

medium was 0.7 ml min^{-1} and pressures ranged from 95–114 kg $(cm^2)^{-1}$. The injection volume was 0.1 ml. Samples were filtered through a 0.2-μm Gelman syringe filter before injection.

Elution time and absorption for ecdysteroids was determined by injecting known amounts of authentic ecdysone (0.042 mg ml^{-1}) and 20-hydroxyecdysone (0.05 mg ml^{-1}) separately and in mixed samples. Elution times were 11.0 min for 20-hydroxyecdysone and 23 min for ecdysone. Peak heights were used to calibrate dose–response curves because of the narrowness of the traces and to allow comparison with previous work [30]. Peak heights for 20-hydroxyecdysone and ecdysone standards were, respectively, at 3.6 cm and 1.7 cm with sensitivity set at 0.2 absorption units.

Blank injections with no ecdysteroids were made with UCON polymer, methanol supernatant of the Reppal lower phase, the upper water phase after separation at 56°C and the lower UCON phase after separation at 56°C.

2.6. Quantification

Degree of partitioning of ecdysteroids between the various phases was determined by removing known quantities from the methanol supernatant after Reppal precipitation, the upper water phase at 56°C and UCON phase at 56°C and subjecting them to RP-HPLC analysis. Concentration in the upper UCON phase from the primary partition step was calculated to be the sum of the ecdysteroids obtained in the upper and lower phases produced by an increase in temperature. Blank systems were made for all partitioning experiments and samples were removed and injected to determine any interference. Results are defined by the partition coefficient, $K = C_t/C_b$, where C_t and C_b are the concentrations of partitioned substances in the upper and lower phases, respectively, under equilibrium conditions [25] and by the distribution ratio, $G = K(V_t/V_b)$, where V_t and V_b are the volumes of the upper and lower phases, respectively. G gives the ratio between the total amounts of ecdysteroid in each phase [25].

3. Results and discussion

A 25% aqueous solution of UCON was effective in extracting ecdysone and 20-hydroxyecdysone from plant material. Results compare favorably with those obtained by utilizing classic extracting techniques [13,31]. An average of 73.4 μg/g fresh mass (f.m.) (68.8–83.3 μg/g f.m.) of 20-hydroxyecdysone was obtained from 46-day-old spinach leaves using UCON solution. Concentrations of ecdysone in the UCON spinach extract were an order of magnitude less, 2.4–5.0 μg/g f.m. Total ecdysteroid concentration obtained using UCON extraction is slightly more than that realized by Grebenok *et al.* [31] with standard methanol extraction. However, quantitative comparisons are dubious without considering the biological and environmental conditions that influence ecdysteroid amounts in spinach plants.

A phase diagram for the system UCON–Reppal–water at 22°C was constructed (Fig. 1). This was done in order to select suitable polymer concentrations for the primary aqueous two-phase system. The phase diagram is relatively similar to the phase diagram for the system UCON–Dextran T500–water [28]. Phase separation is obtained at slightly higher polymer concentrations because of the lower molecular mass (200 000) of Reppal compared with Dextran T500 (500 000) [26].

Once extraction was completed and the suspension was centrifuged, the primary phase system was easily constructed by mixing an aqueous solution of Reppal into the supernatant to obtain the desired polymer concentrations. The purification scheme is shown in Fig. 2. Phase separation occurs within 10–20 min, or more rapidly if the systems are centrifuged. Cell debris, proteins and other contaminants partitioned to the lower Reppal-rich phase. Chlorophylls were, for the most part, removed during the initial centrifugation. Those that remained partitioned to the lower Reppal-rich phase. Based on the tint of the upper UCON-rich phase, which was extremely pale, chlorophylls appeared to remain attached to membranes and/or chloroplast (cell debris). Coloration in the Reppal-rich

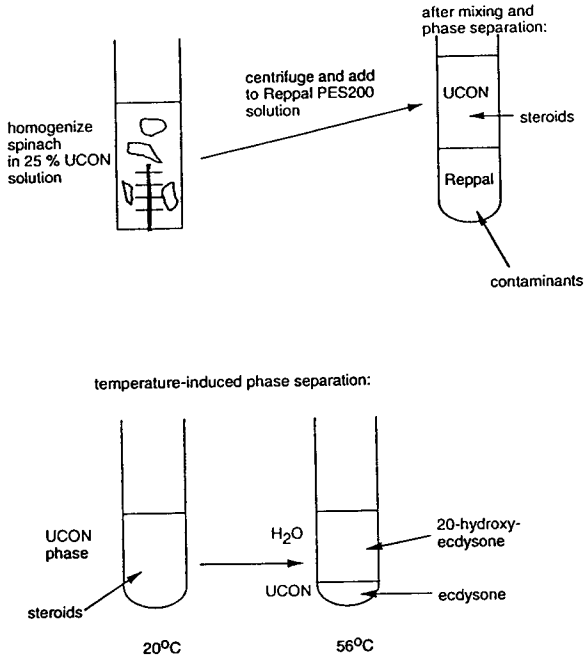

Fig. 2. Scheme for the purification of ecdysteroids from spinach leaves using aqueous two-phase partitioning and temperature-induced phase separation.

phase was noticeable. The ecdysteroids partitioned very strongly to the upper UCON-rich phase with partition coefficients of 50.3 for ecdysone and 30.6 for 20-hydroxyecdysone (Table 1).

After phase separation in the primary aqueous two-phase system the upper UCON-rich phase is removed and isolated in a separate container (Fig. 2). This is then subjected to increased temperature above the cloud point of UCON (50°C). The temperature-induced phase separation results in the formation of a UCON-rich and a water-rich phase. The phase separation was induced at 56°C (Fig. 2). The greater hydrophobicity of ecdysone caused it to partition more to the UCON-rich phase ($K = 0.51$) in systems not containing ethanol, while 20-hydroxyecdysone partitioned to the water-rich phase ($K = 2.16$, Table 1). Ecdysone and 20-hydroxyecdysone could both be recovered in the water-rich phase at yields of 80.5 and 93.8%, respectively, calculated for the original amounts in the spinach extract. The high recovery of the hydrophobic ecdysone (80.5%) in the water phase, in spite of the unfavorable partition coefficient, is due to the larger volume of the water phase relative to the UCON phase. The volume ratio water phase–UCON phase was 8.4 and the G value, which determines the yield, was 4.28 for ecdysone and 18.1 for 20-hydroxyecdysone (Table 1).

Manipulation of the hydrophobicity of aqueous two-phase systems with salts and/or solvents improves their specificity [24–30]. Addition of 20% ethanol to the primary systems containing authentic compounds yielded 73.6% ecdysone and 85.6% 20-hydroxyecdysone of the original amount in the water-rich phase after temperature-induced phase separation [30]. The extraction and recovery of these ecdysteroids from spinach substantiates these results (Table

Table 1
Partitioning of ecdysone and 20-hydroxyecdysone from spinach

Compound	System	K (22°C)	G (22°C)	K (56°C)	G (56°)	Y
Ecdysone	1	50.3	159	0.51	4.28	80.5
	2	>100	>100	1.74	7.0	88.7
20-Hydroxyecdysone	1	30.6	94.5	2.16	18.1	93.8
	2	>100	>100	1.94	11.7	91.2

Primary phase systems: 11% UCON 50-HB-5100 spinach extract, 7.5% Reppal PES 200 and 0.1 M sodium phosphate buffer, pH 7.0. System 1 did not contain ethanol and system 2 contained 20% ethanol. K and G values at 56°C are for partitioning between the water and UCON phases formed by increasing the temperature. Volume ratios (V_t/V_b) at 22°C and 56°C, respectively: system 1, 3.0 and 8.4 and system 2, 3.8 and 5.0. Y = percentage yield of ecdysteroids in the water phase. All values given are mean values from duplicate experiments.

1). Addition of 20% ethanol to the primary phase systems increased the hydrophobicity of the upper UCON-rich phase and forced both ecdysteroids to completely partition into the upper phase ($K > 100$, Table 1). The ethanol affected also the partitioning of the hydrophobic ecdysteroid, ecdysone, between the water and UCON phases formed by raising the temperature. Ecdysone was partitioned to the water-phase in systems containing ethanol. The K value was 1.74 compared with 0.51 obtained in systems without ethanol (Table 1). This can be explained by the increased solubility of ecdysone in the water phase due to the presence of ethanol. The addition of ethanol had little effect on the partitioning of the less hydrophobic 20-hydroxyecdysone. K values for the partitioning between water and UCON phases in systems with ethanol and without were 1.94 and 2.16, respectively. For systems containing ethanol the yields of ecdysone and 20-hydroxyecdysone in the final water phase were 88.7 and 91.2%, respectively (Table 1). Thus, the addition of ethanol increased the recovery of ecdysone in the water phase from 80 to 89%, while the recovery of 20-hydroxyecdysone was kept at more than 90%.

The purification scheme using phase systems without ethanol is shown in Fig. 2. In the last step ecdysone is partitioned to the UCON phase and 20-hydroxyecdysone to the water phase after temperature increase. This is in agreement with results from a recent study on the partitioning of carboxylic acids in UCON–water phase systems [32]. It was found that carboxylic acids of increasing hydrophobicity were, to an increasing degree, partitioned to the UCON-rich phase. Thus, the different partitioning of the two ecdysteroids in the UCON–water system can be explained by the difference in hydrophobicity between the two compounds. It should be pointed out that the system is very sensitive and can detect very small differences in hydrophobicity. In this case only one hydrogen atom in ecdysone has been substituted for one hydroxyl group in 20-hydroxyecdysone. In the UCON–water system it should be possible to utilize the separation based on hydrophobicity for a further purification of the ecdysteroids. After the temperature-induced phase separation both ecdysteroids could be obtained in a water phase virtually free of polymer (Table 1). For the hydrophobic ecdysone this was made possible by having a large volume ratio so that more than 80% of the ecdysteroid was obtained in the water phase in spite of an unfavorable partition coefficient. Alternatively, by adding 20% ethanol in the primary system the partition coefficient of ecdysone was changed in the second phase system, and this ecdysteroid was partitioned to the final water phase with a yield of 89%. However, the ethanol addition removed the difference in the partitioning for the two ecdysteroids and both were partitioned to the same extent to the water phase. Thus, ethanol addition has the advantage that both ecdysteroids are obtained in the water phase with high yield and the drawback that it is not possible to exploit a difference in ecdysteroid partitioning for further purification.

Ecdysone has not previously been reported in spinach. Its presence was verified with RP-HPLC co-chromatography with authentic compound. Additionally, heights of elution peaks generated by presence of ecdysone and 20-hydroxyecdysone were increased when the UCON spinach extract was spiked with authentic compounds. No further verification of ecdysone was preformed.

Polypodine B (5β,20-dihydroxyecdysone) is also an ecdysteroid commonly found in spinach, but in concentrations approximately 25% lower than that of 20-hydroxyecdysone [11,31]. Polypodine B is less hydrophobic, and usually elutes slightly earlier, than 20-hydroxyecdysone [11]. We did not test for its presence. However, a small peak at 10.3 min elution time occurred on RP-HPLC traces obtained during the analysis of the temperature-induced upper and lower phases. This peak suggests the presence of polypodine B in our samples because it appeared only in the experimental samples and not the blanks. The peak was not verified with authentic compound.

4. Conclusions

Ecdysteroids could be extracted from spinach leaves with a solution of the copolymer UCON in water. UCON–Reppal–aqueous two-phase systems were successfully used to partition ecdysone and 20-hydroxyecdysone from the spinach plant. Additionally, purification of these ecdysteroids was made possible using temperature-induced phase separation. This ability supports previous research with authentic compounds of these ecdysteroids [30]. The technique is a relatively simple, rapid, inexpensive bench-top procedure that can be performed in a laboratory not equipped with sophisticated equipment and instrumentation (Fig. 2). An attractive advantage of temperature-induced phase separation is that slight chemical and/or physical manipulation increases selectivity and forces desired biocompounds into either water-rich or polymer-rich phases [32]. Ability to obtain ecdysteroids, destined for experimentation, in non-toxic media is desirable. However, phase-forming polymers are themselves non-toxic. An added benefit of this procedure is that it can easily be scaled-up for commercial use.

5. Acknowledgements

We would like to thank Dr. J. Milton Harris for providing laboratory space and instrumentation for this project. Support was provided by the Swedish Research Council for Engineering Sciences (TFR), the Swedish National Board for Industrial and Technical Development (NUTEK), the University of Alabama in Huntsville Mini-Grant Program, and Reppe AB, Växjö, Sweden.

6. References

[1] J. Koolman, *Zool. Sci.*, 7 (1990) 563.
[2] P. Karlson, *Naturwissenschaften*, 53 (1966) 445.
[3] I. Kubo, J.A. Klocke and S. Asano, *Agric. Biol. Chem.*, 45 (1981) 1925.
[4] I. Kubo, J.A. Klocke and S. Asano, *J. Insect Physiol.*, 29 (1983) 307.
[5] M.N. Galbraith and D.H.S. Horn, *Chem. Commun.*, (1966) 905.
[6] P. Singh and G.B. Russel, *J. Insect Physiol.*, 26 (1980) 139.
[7] P. Nirde, M. de Reggi, G. Tsoupras, G. Torpier, P. Fessancort and A. Capron, *FEBS Lett.*, 168 (1984) 235.
[8] J. Koolman and H. Moeller, *Insect Biochem.*, 16 (1968) 287.
[9] B. Gharib, S. Baswaid, M. Quilici and M. de Reggi, *Clin. Chim. Acta*, 199 (1991) 159.
[10] F. Guo, in J. Koolman (Editor), *Ecdysone: From Chemistry to Mode of Action*, Thieme Medical Publishers, New York, 1989, p. 442.
[11] R. Lafont and D.H.S. Horn, in J. Koolman (Editor), *Ecdysone: From Chemistry to Mode of Action*, Thieme Medical Publishers, New York, 1989, p. 39.
[12] P. Karlson and E. Shaaya, *J. Insect Physiol.*, 10 (1964) 797.
[13] H.H. Rees and R.E. Isaac, *Methods Enzymol.*, 111 (1985) 377.
[14] I.D. Wilson, E.D. Morgan and S.J. Murphy, *Anal. Chim. Acta*, 236 (1990) 145.
[15] J.E. Wright and B.R. Thomas, *J. Liq. Chromatogr.*, 6 (1983) 2055.
[16] I. Kubo and S. Komatsu, *Agric. Biol. Chem.*, 51 (1987) 1305.
[17] I.D. Wilson, C.R. Bielby, E.D. Morgan and A.E.M. McLean, *J. Chromatogr.*, 194 (1980) 343.
[18] I.D. Wilson, S. Scalia and E.D. Morgan, *J. Chromatogr.*, 212 (1980) 211.
[19] I. Kubo and S. Komatsu, *J. Chromatogr.*, 362 (1986) 61.
[20] M. Zhang, M.J. Stout and I. Kubo, *Phytochemistry*, 31 (1992) 247.
[21] R. Lafont, J.-L. Pennetier, M. Andrianjafintrimo, J. Claret, J.F. Modde and C. Blais, *J. Chromatogr.*, 236 (1982) 137.
[22] R.E. Isaac, N.P. Milner and H.W. Rees, *J. Chromatogr.*, 246 (1982) 317.
[23] S. Scalia and E.D. Morgan, *J. Chromatogr.*, 346 (1985) 301.
[24] H. Hustedt, K.H. Kroner and M.R. Kula, in H. Walter, D.E. Brooks and D. Fisher (Editors), *Partitioning in Aqueous Two- Phase Systems*, Academic Press, New York, 1985, p. 529.
[25] P.-Å. Albertsson, *Partition of Cell Particles and Macromolecules*, Wiley, New York, 3rd ed., 1986.
[26] F. Tjerneld, in J.M. Harris (Editor), *Poly(ethylene glycol) Chemistry*, Plenum Press, New York, 1992, p. 85.
[27] H. Walter and G. Johansson, *Encycl. Human Biol.*, 1 (1991) 355.
[28] P. Harris, G. Karlström and F. Tjerneld, *Bioseparation*, 2 (1992) 237.

[29] P.A. Alred, F. Tjerneld, A. Kozlowski and J.M. Harris, *Bioseparation*, 2 (1992) 363.
[30] P.A. Alred, F. Tjerneld and R.F. Modlin, *J. Chromatogr.*, 628 (1993) 205.
[31] R.J. Grebenok, P.V. Ripa and J.H. Adler, *Lipids*, 26 (1991) 666.
[32] H.-O. Johansson, G. Karlshön and F. Tjerneld, *Macromolecules*, 26 (1993) 4478.

ELSEVIER

Journal of Chromatography A, 668 (1994) 237–240

JOURNAL OF CHROMATOGRAPHY A

Liquid–liquid extraction of clavulanic acid using an aqueous two-phase system of polyethylene glycol and potassium phosphate

Mafalda Videira, Maria Raquel Aires-Barros*

Laboratório de Engenharia Bioquímica, Instituto Superior Técnico, 1000 Lisbon, Portugal

Abstract

An aqueous two-phase system of polyethylene glycol (PEG) and potassium phosphate was developed for *in situ* extraction of clavulanic acid from fermentation broth. Preliminary studies to identify the relevant parameters that determine the partitioning of clavulanic acid in the two-phase system were carried out using potassium clavulanate. The effect of pH, polymer molecular mass and tie-line length were investigated. For all conditions tested potassium clavulanate showed a high affinity to the PEG-rich top phase ($K = 1.5–114$), and high recoveries (90–99%) were obtained.

1. Introduction

Clavulanic acid is a naturally occurring compound isolated from *Streptomyces clavuligerus* [1], and it consists of a β-lactam ring fused to an oxozilidine ring [2]. It shows weak antibacterial activity against most bacteria, but is a potent inhibitor of a wide range of β-lactamase and is able to potentiate the antibacterial activity of penicillins and cephalosporins against many β-lactamase-producing resistant bacteria [3]. It is currently used in combination with amoxicillin for the treatment of infections caused by β-lactamase-producing bacteria.

Clavulanic acid is produced industrially by fermentation and is isolated and purified from the fermentation medium in several steps. The first step involves clarification of the medium by filtration or centrifugation followed by either adsorption or liquid–liquid extraction with an organic solvent, normally butanol. Further purification is achieved by anion-exchange chromatography. Owing to the unstable nature of the free acid, clavulanic acid is isolated as the lithium, potassium or sodium salt.

In this work, an aqueous two-phase system of polyethylene glycol (PEG) and potassium phosphate was developed as an alternative process to be used as the first step in the isolation and purification of clavulanic acid, in order to decrease the number of downstream processing steps. Potassium clavulanate was used as a model system for the partitioning studies in PEG–potassium phosphate two-phase systems. Some relevant parameters, such as pH, polymer molecular mass and polymer and potassium salt concentrations, which affect the partitioning behaviour of potassium clavulanate in PEG–salt phases were investigated.

* Corresponding author.

0021-9673/94/$07.00
SSDI 0021-9673(94)00031-4

2. Experimental

2.1. Chemicals

PEG 400, 1000, 4000 and 6000 were supplied by Sigma. Potassium phosphates (analytical-reagent grade) and imidazole (99% purity) were obtained from Merck (Darmstadt, Germany). Potassium clavulanate (70% purity) was a kind gift from CIPAN (Lisbon, Portugal).

2.2. Preparation of aqueous two-phase systems

Phase systems of 5 g each were prepared in 10-ml graduated centrifuge tubes by weighing the PEG (100%, w/w) and by addition of appropriate amounts of KH_2PO_4–K_2HPO_4 solutions at pH 7.0 (22.9%, w/v) and pH 8.0 (32.7%, w/v). This mixture was vortex mixed for 5–30 min until a two-phase system was obtained. The system was completed by addition of 50 μl of potassium clavulanate stock solution (5 mg/ml) with agitation. The phases were separated by centrifugation at 1000 *g* for 5 min. After phase separation the phase volumes were noted and potassium clavulanate was determined, in both phases, by the imidazole assay method, as described below. The assays were performed in triplicate.

The study of potassium clavulanate partitioning in PEG–KH_2PO_4–K_2HPO_4 systems was carried out at pH 7.0 and 8.0 with PEG 400, 1000, 4000 and 6000 and for different tie-line lengths by varying the PEG and salt concentrations. The tie-line lengths were measured directly from the phase diagram.

2.3. Potassium clavulanate assay

Potassium clavulanate in PEG and phosphate phases was determined spectrophotometrically at 312 nm by analysis of the reaction product with imidazole reagent [4].

Imidazole reagent was prepared by dissolving 8.25 g of imidazole in 100 ml of distilled water, and the pH was adjusted to 6.8 ± 0.05 with 5 *M* hydrochloric acid. A 1-ml volume of top/bottom phase was added to a tube containing 5 ml of imidazole reagent (tube A). This mixture was incubated in a water-bath at 30°C for 12 min and then cooled rapidly to 20°C. To a second tube (tube B), 1 ml of top/bottom phase was mixed with 5 ml of distilled water. The absorbances at 312 nm of the solutions in tubes A and B were measured using as a reference a mixture of 1 ml of top/bottom phase and 5 ml of imidazole reagent heated at 30°C for 12 min. The absorbance difference between solutions A and B was calculated and the clavulanate concentration of the samples was determined from a calibration graph obtained from a sample of known purity reacted under the same conditions for the same time. Interferences from PEG molecular mass and high PEG and salt concentrations in the potassium clavulanate assay method were checked; none were observed.

3. Results and discussion

The effect of PEG molecular mass, tie-line length and pH on potassium clavulanate partitioning in the PEG–phosphate potassium two-phase system is shown in Figs. 1 and 2. *K* is the partition coefficient of potassium clavulanate, defined as the ratio between potassium clavula-

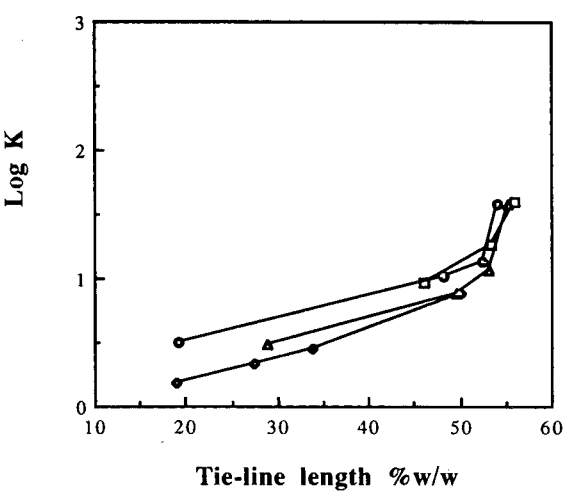

Fig. 1. Variation of the partitioning of potassium clavulanate with tie-line length at pH 7.0 for different PEG molecular masses: ◆ = PEG 6000; △ = PEG 4000; O = PEG 1000; □ = PEG 400.

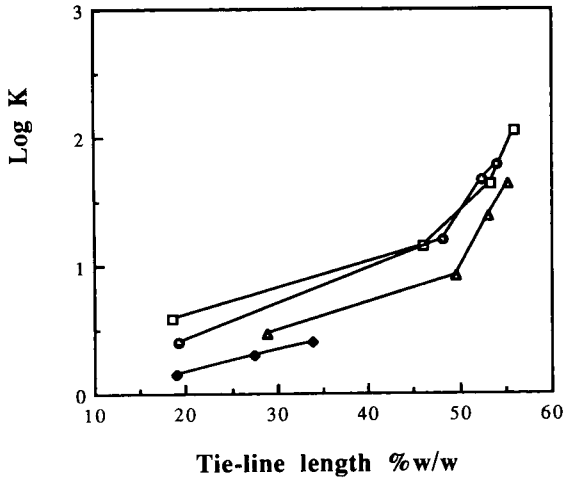

Fig. 2. Variation of the partitioning of potassium clavulanate with tie-line length at pH 8.0 for different PEG molecular masses: ◆ = PEG 6000; △ = PEG 4000; ○ = PEG 1000; □ = PEG 400.

nate concentrations in the top and bottom phases. The reported values are the average of three measurements.

The results in Figs. 1 and 2 show that potassium clavulanate has a higher affinity for the PEG phase, as partition coefficients varying from 1.5 to 114 were obtained for the different PEG molecular masses, with short and long tie-lines, and at pH 7.0 and 8.0. High recoveries from 60 to 99% were also observed. The potassium clavulanate recovery, Y, was calculated as the fraction of potassium clavulanate recovered in the PEG phase.

The partition coefficients observed are higher than theoretically expected for small molecules such as clavulanic acid [5]. However, partitioning of penicillin G in PEG–potassium salt systems also showed high partition coefficients (above 10) [6]. Degradation of cholesterol by *Micobacterium* sp. in aqueous two-phase systems has been reported [7] and the substrate partitioned to the upper phase or the interface, while the products had partition coefficients of *ca.* 2. Deacylation of benzylpenicillin (BP) to 6-aminopenicillanic acid (6-APA) using penicillin acylase in a PEG–potassium phosphate system showed partition coefficients of $K_{BP} = 8.3$, for the substrate and $K_{6\text{-APA}} = 1.35$ and $K_{\text{phenylacetic acid}} = 1.7$ for the products [8].

Potassium clavulanate has a great affinity for the PEG-rich phase, leading to high partition coefficients. However, at pH 7.0 and 8.0, clavulanic acid ($pK_a = 2.3$–2.7) is mostly present in the ionic form but is extracted into the more hydrophobic top phase.

The partitioning of potassium clavulanate in the PEG–potassium phosphate system is not greatly influenced by variations in the molecular mass of PEG, for low polymer molecular masses. Similar partition coefficients and recoveries were obtained for PEG 1000 and 400, for a fixed tie-line, at pH 7.0 and 8.0. For higher polymer molecular masses (PEG 6000 and 4000), a decrease in the partition coefficients with increasing polymer molecular mass was observed.

The effect of polymer molecular mass can be attributed to the increasing number of hydrophilic end-groups on shorter PEG chains, which decreases the overall hydrophobicity [9], and to the excluded volume effects which increase with increasing polymer molecular mass [10]. As clavulanic acid is a small molecule it probably is less influenced by the excluded volume effects.

Increasing the tie-line length raised the clavulanic acid salt partition coefficients from 1.5 (lower value) to 114 (highest value) and high recoveries (97–99%) were obtained (Figs. 1 and 2). This was noted for all the PEGs tested. An increase in tie-line length promotes an increase in phosphate concentration in the lower phase whereas in the upper phase it remains relatively constant [11]. This probably leads to salting-out of the potassium clavulanate from the phosphate-rich phase to the PEG-rich phase as its solubility limit is reached. Partitioning of the potassium clavulanate to the top phase increases until its solubility limit in that phase is not exceeded or is molecular excluded.

The pH also influences potassium clavulanate partitioning in the PEG–phosphate potassium two-phase system as higher partition coefficients are obtained with increasing pH for PEG 1000 and 400 (Figs. 1 and 2). For PEG 6000 and 4000 this behaviour was not observed.

The effect of pH on the PEG–salt phase

diagram was studied and it was found that decreasing pH leads to an increase of the polymer and salt concentrations required for phase formation [9]. When the pH is lowered from 8 to 7 the $H_2PO_4^-/HPO_4^{2-}$ ratio increases and owing to the rejection of multivalent anions by PEG [12,13] a higher salt and/or polymer concentration will be needed to obtain a two-phase system. The displacement of the phase diagram towards higher salt concentrations, which can be compared with the effect of shortening the tie-line length, probably accounts for the decrease in K with decrease in pH.

4. Conclusions

Potassium clavulanate showed a high affinity for the PEG-rich phase with partition coefficients ranging from 1.5 to 114 and high recoveries (75–99%).

The partition coefficient of potassium clavulanate is independent of PEG molecular mass for PEG 1000 and 4000, but increases with increasing polymer molecular mass for higher PEG molecular masses.

Increasing the tie-line length and pH raised the potassium clavulanate partition coefficient and 99% of the clavulanate was recovered in the PEG phase.

5. Acknowledgement

Mafalda Videira acknowledges an M.Sc. fellowship from Programa Ciência, Junta Nacional de Investigação Científica e Tecnológica, Portugal.

6. References

[1] A.G. Brown, D. Butterworth, M. Cole, G. Hanscomb, J.D. Hood, C. Reading and G.N. Rolinson, *J. Antibiot.*, 29 (1976) 668.
[2] T.T. Howarth, A.G. Brown and T.J. King, *J. Chem. Soc., Chem. Commun.*, (1976) 226.
[3] E.J. Vandamme, *Clavulanic Acid: Properties, Biosynthesis and Fermentation* (*Biotechnology of Industrial Antibiotics*, Vol. 22), Marcel Dekker, New York, 1984, p. 225.
[4] A.E. Bird, J.M. Bellis and B.C. Gasson, *Analyst*, 107 (1982) 1241.
[5] P.A. Albertsson, *Partition of Cell Particles and Macromolecules*, Wiley, New York, 1986.
[6] I.-M. Chu, S.-L. Chang, S.-H. Wang and W.-Y. Yang, *Biotechnol. Tech.*, 4 (1990) 143.
[7] S. Flygare and P.-O. Larsson, *Enzyme Microb. Technol.*, 11 (1989) 752.
[8] E. Andersson, B. Mattiasson and B. Hahn-Hagerdal, *Enzyme Microb. Technol.*, 6 (1984) 301.
[9] M.-R. Kula, in C.L. Cooney and A.E. Humphrey (Editors), *Comprehensive Biotechnology*, Vol. 2, Pergamon Press, New York, 1985, pp. 451–467.
[10] C.W. Kim, *Ph.D. Thesis*, Massachusetts Institute of Technology, Cambridge, MA, 1986.
[11] J.G. Huddleston, K.W. Ottomar, D.M. Ngonyani and A. Lyddiatt, *Enzyme Microb. Technol.*, 13 (1991) 24.
[12] G. Johanasson, *Biochim. Biophys. Acta*, 221 (1970) 387.
[13] B. Yu. Zaslavsky, L. Miheeva, Yu. P. Aleschko-Ozhevskii, A.U. Mahmudov and T.O. Bagirov, *J. Chromatogr.*, 439 (1988) 267.

ELSEVIER

Journal of Chromatography A, 668 (1994) 241–247

JOURNAL OF CHROMATOGRAPHY A

Interactions between fluoroquinolones, Mg^{2+}, DNA and DNA gyrase, studied by phase partitioning in an aqueous two-phase system and by affinity chromatography

Sandrine Bazile-Pham Khac, Nicole J. Moreau*

Centre National de la Recherche Scientifique, CERCOA, B.P. 28, 94320 Thiais, France

Abstract

The primary target of fluroquinolones has been identified as the enzyme DNA gyrase, but the mechanism of action of these antibacterial agents is still a matter of controversy. Using partitioning in aqueous polyethylene glycol (PEG)–dextran systems, the affinities of several fluoroquinolones for DNA were determined with accuracy and at equilibrium. It was proved that the binding was strongly dependent on the ability of the drugs to bind Mg^{2+}, with K_A values of about 40 000 l mol^{-1}, but was poorly related to the antibacterial activity [minimal inhibitory concentration (MIC) and gyrase inhibition]. Using affinity chromatography on immobilized fluoroquinolone, it was shown that DNA gyrase was unable to bind fluoroquinolones in the absence of DNA, but that a DNA–quinolone–gyrase complex was formed in the presence of Mg^{2+}.

1. Introduction

Fluoroquinolones (FQ) are antimicrobial agents widely used against various infections. Their primary target has been identified as the enzyme DNA gyrase (EC 5.99.1.3) [1,2], as fluoroquinolones are able to inhibit isolated gyrase [3] and as gyrases isolated from resistant organisms are resistant to fluoroquinolones [4]. DNA gyrase consists of two A and two B subunits (the products of the *gyrA* and *gyrB* genes, respectively). Since the first model proposed by Shen and Pernet [5] for the mechanism by which quinolones inhibit gyrase, this group have refined their model [6], which implies binding of the quinolone to DNA. Palù *et al.* [7] pinpointed the role played by Mg^{2+} ion in the DNA–quinolone interaction, and recently the role of DNA gyrase in the interaction was examined [8,9]. The important role played in antimicrobial activity of quinolones by Mg^{2+}, which impairs both oral absorption [10,11] and uptake by bacterial cell [12], prompted us to measure the affinity of Mg^{2+} for several fluoroquinolones. Having the K_D values of the Mg^{2+}–FQ complexes at hand, and having proved that Mg^{2+} was situated between the ketone and the carboxylate of quinolones [13], we decided to examine the effects of magnesium on the FQ–DNA interaction. We investigated whether the affinity of a quinolone for magnesium was determinant in the FQ–DNA interaction, and whether the affinity of a fluoroquinolone for DNA in the presence of magnesium was related to its inhibitory activity against DNA gyrase-catalysed supercoiling. The way in which DNA gyrase modified these interactions was also investigated.

* Corresponding author.

0021-9673/94/$07.00
SSDI 0021-9673(94)00058-H

Most studies on interactions between an enzyme and its substrates or inhibitors have been carried out using equilibrium dialysis. In the present instance, the major limitation of this technique would be undesirable interactions between DNA and the dialysis membrane. Moreover, the size of both enzyme and substrate precluded the use of membranes. This problem could be overcome by using chromatography, but such experiments would not be performed under equilibrium conditions. Therefore, we decided to use aqueous two-phase partitioning [14,15], where the interface between the two phases plays the role of the separating membrane [16,17]. Some assays were performed using affinity chromatography on a resin coated with immobilized quinolone.

2. Experimental

2.1. Chemicals

Pefloxacin, sparfloxacin and RP 65279 were gifts from Rhône-Poulenc Rorer (Vitry sur Seine, France). [^{14}C]Pefloxacin and [^{14}C]sparfloxacin, from Rhône-Poulenc Rorer, were used at a specific activity of 40 μCi/mol. Compounds named BMY were donated by Bristol–Myers Squibb France (Marne la Vallée, France). These compounds have been described in refs. 18 and 19: BMY 33315, 42230, 43261 and 40062 are compounds 32, 33, 35 and 36, respectively, in ref. 18 and BMY 180820 and 180821 are compounds 39 and 43, respectively, in ref. 19. Ciprofloxacin was provided by Bayer France (Paris la Défense, France). Pefloxacin ethyl ester and norfloxacin methyl ester were synthesized in our laboratory using ethanol or methanol and thionyl chloride [20].

Dextran T500 and epoxy-activated Sepharose were obtained from Pharmacia France (Saint Quentin en Yvelines, France), polyethylene glycol (PEG) 6000 from Touzart et Matignon (Vitry sur Seine, France), Indubiose A37 was from IBF (Villeneuve la Garenne, France), covalently closed supercoiled plasmid pBR322 from Boehringer (Meylan, France) and DNA "highly polymerized" from calf thymus and DNA from *Escherichia coli* from Sigma (Saint-Quentin-Fallavier, France).

2.2. Minimal inhibitory concentrations (MICs)

Bacteria were routinely grown in trypticase soy broth (TSB) from Biomérieux (Marcy l'Etoile, France). MICs were determined by using twofold dilutions of antibiotic in TSB, to which 10^6 colony-forming units of bacteria were added. Cultures were incubated for 18 h at 37°C.

2.3. DNA gyrase purification and supercoiling assays

Purification of gyrase from *E. coli* K12 J53 and assays for inhibition of supercoiling using plasmid pBR322 were performed as described earlier [21]. The inhibition was expressed as MED (minimal effective dose, the minimal fluoroquinolone concentration able to affect supercoiling), as described previously [21].

2.4. Phase system and partitioning experiments

A 6% (w/w) dextran–4% (w/w) PEG mixture was made in buffer consisting of 4-(2-hydroxyethyl)-1-piperazineethanesulphonic acid (HEPES)–50 m*M* KOH (pH 7.5)–20 m*M* KCl–0 or 5 m*M* $MgCl_2$ as specified. The mixture was left overnight at 4°C, where separation occurred, and the phases were separated and kept at 4°C.

Partitioning experiments were carried out in glass test-tubes. Fluoroquinolone was added to 1.1 ml of the dextran phase up to 4 μM, then DNA was added and its concentration was varied from 16.4 to 1640 μM of base. In another series of experiments, the concentration of DNA was fixed at 57 μM of base, and the fluoroquinolone concentration varied from 0.9 to 120 μM (final concentration). Incubation was carried out for 10 min at 20°C, then 1.1 ml of PEG phase was added and the phases were mixed by inversion and separated by centrifugation for 10 min at 2000 *g*. The volume of added reagents was constant (total volume 200 μl for a 2.2 ml total reaction volume). The dosage of DNA in

the phases was carried out either by measuring the absorbance at 260 nm ($\epsilon_{260\,nm} = 6600$ mol base l^{-1} cm^{-1}) or using ethidium bromide [22]; fluoroquinolones were assayed using radio-labelled molecules when available, or by fluorescence (Hitachi F-2000 Spectrofluorimeter, supplied by Braun, Les Ulis, France). Standard dosage curves were established at the maximum wavelength of each compound in the PEG phase. When DNA was present, dosage cannot be performed in the dextran phase because of modification of the fluorescence of the quinolone on binding to DNA. The partition coefficient was the ratio of the concentration of material in the top phase to that in the bottom phase.

2.5. Affinity chromatography

Norfloxacin (the desmethyl analogue of pefloxacin, with an NH instead of an NCH_3 group on the piperazine) was immobilized on epoxy-activated Sepharose following the supplier's recommendations (see Fig. 1). Briefly, 2 g of epoxy-activated Sepharose were reacted with 200 mg of norfloxacin in 6 ml of 0.3 *M* carbonate buffer (pH 9.5) for 17 h at 37°C. Ethanolamine (0.55 ml) was then added and reacted for 4 h at 37°C. After thorough washings [carbonate buffer (pH 9.5), water, acetate buffer (pH 4), water, 5 *M* urea, water], a 1-ml column was packed and equilibrated with buffer E [Tris–50 m*M* HCl (pH 7.5)–20 m*M* KCl–2 m*M* $MgCl_2$].

DNA (100 μl of a 4 mg ml^{-1} solution, calf thymus or *E. coli*), gyrase (500 μl of a 40 μg ml^{-1} solution) or mixtures of both were added to the column, and after 1 h of contact at 4°C under gentle rocking, to ensure good contact of the reagents, washing was performed with buffer E until there was no more absorbance at 260 nm (DNA) or no more fluorescence (protein, excitation at 280 nm, emission at 340 nm). Elution was then carried out as described in the figure captions, followed by a washing with 4 *M* NaCl to regenerate the column before re-equilibration.

3. Results

3.1. Affinity of fluoroquinolones for DNA

Under the experimental conditions used, high-molecular-mass DNA totally partitioned into the dextran-rich phase, whereas the fluoroquinolones have partition coefficients between 0.9 and 1.3. Table 1 presents the MICs for *E. coli*, MEDs for *E. coli* gyrase and the affinity (expressed as nK_A for calf thymus DNA of the assayed fluoroquinolones, for the experiments carried out with fixed fluoroquinolone concentration, or as the K_A for calf thymus DNA of the quinolones assayed with fixed DNA concentrations). Some experiments were carried out using *E. coli* double-stranded DNA. As the results were the same as with calf thymus DNA, the

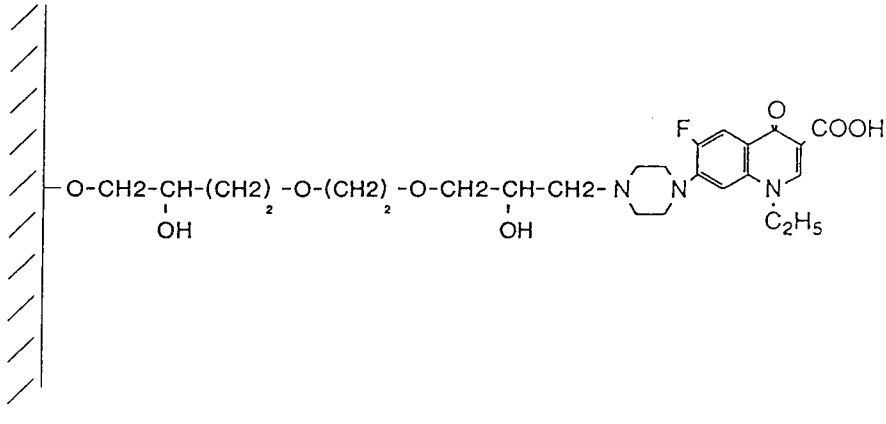

Fig. 1. Structure of norfloxacin immobilized on epoxy-activated Sepharose.

Table 1
Antibacterial activity of fluoroquinolones, their inhibitory activity against DNA gyrase and their affinity for DNA

Quinolone	MIC (mg l^{-1})	MED (mg l^{-1})	K_A ($\times 10^3$ l mol^{-1})[a]		nK_A ($\times 10^3$ l mol^{-1})[b]	
			Without Mg^{2+}	With Mg^{2+}	Without Mg^{2+}	With Mg^{2+}
Sparfloxacin	0.05	0.2	2.6	41	–	–
Pefloxacin	0.2	1	2.6	54	0.7	3.0
Ciprofloxacin	0.05	0.1	2.4	31	0.5	6.7
RP 65 279	>64	50	2.7	10	–	–
Pefloxacin ethyl ester	>128	>35	2.8	3.5	0.9	0.6
BMY 33315	0.1	1	–	–	0.4	3.5
BMY 42230	0.2	10	–	–	0.4	3.1
BMY 43261	3.5	40	–	–	0.1	2.6
BMY 40062	0.03	0.6	–	–	2.4	6.2
BMY 180820	3.5	10	–	–	1.0	3.2
BMY 180821	0.15	0.12	–	–	1.1	3.4

Antibacterial activity was expressed as MICs, the lowest concentration of the antibiotic that inhibited the growth of the culture. The inhibitory activity of a quinolone against DNA gyrase-catalysed supercoiling is expressed as minimal effective dose (MED; the minimum amount of drug required to cause any inhibition of activity).

[a] Experiments were carried out using a fixed concentration of DNA (57 μM of base) and various concentrations of fluoroquinolones, using partitioning in a 6% (w/w) dextran–4% (w/w) PEG system as described under Experimental. Affinity is given by K_A, where K_A is the intrinsic association constant.

[b] As above, but experiments were carried out using a fixed concentration of quinolone (4 μM) and various concentrations of DNA. Affinity is given as nK_A, where n is the number of sites.

latter was always used, because it was cheaper. The representation of Pearlman and Crepy [23] for the binding of ciprofloxacin with and without Mg^{2+} is given in Fig. 2 as an example of the method with fixed fluoroquinolone concentration, and the Scatchard representation for the binding of sparfloxacin is given in Fig. 3 as an example of the "fixed DNA method". In the absence of Mg^{2+}, for the series with fixed quinolone concentration, all the assayed compounds have roughly the same affinity, with nK_A varying from 400 to 1000 l mol^{-1}, with the exception of BMY 43261 ($nK_A = 100$ l mol^{-1}) and BMY 40062 ($nK_A = 2400$ l mol^{-1}). For the series with fixed DNA concentrations, the K_A values varied from 2400 l mol^{-1} for ciprofloxacin up to 2800 l mol^{-1} for sparfloxacin. In the presence of 5 mM Mg^{2+}, the values of nK_A increased by factors of 3–26 for the compounds of the "fixed quinolone" series. For the compounds assayed with fixed DNA concentration, the binding of sparfloxacin, pefloxacin and ciprofloxacin increased, and a second class of sites appeared, with K_A values of $41 \cdot 10^{-3}$, $54 \cdot 10^{-3}$, $31 \cdot 10^{-3}$ l mol^{-1}, respectively. The affinity constant of RP 65279 increased by a factor of 4. For both series, the binding of norfloxacin methyl ester (not shown) and pefloxacin ethyl ester remained unchanged.

3.2. *Affinity chromatographic results*

The chromatographic behaviour of DNA, gyrase and a mixture of both is shown in Fig. 4. In the presence of magnesium, DNA gyrase had no affinity for the column of immobilized norfloxacin. Under the same conditions, DNA was retained and was eluted by the addition of 0.1 M NaCl in buffer E (Fig. 4A). If the mixture of DNA and gyrase was introduced onto the column, the complex was retained and eluted with 0.2 M NaCl (Fig. 4B). The small peak eluted with 0.1 M NaCl in Fig. 4B is probably due to some DNA bound without gyrase on the column. A control experiment carried out using Sepharose without immobilized norfloxacin showed that DNA and gyrase do not bind the resin alone.

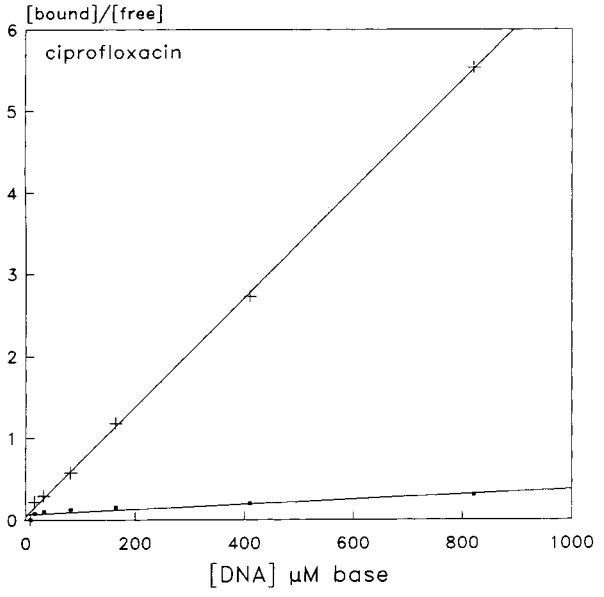

Fig. 2. Binding of ciprofloxacin determined by partitioning, using a fixed concentration of quinolone (4 μM). The ratio of the concentration of bound quinolone to the concentration of free quinolone is plotted against the concentration of DNA, in moles of base per litre. The slope of the curve (regression line) gives nK_A, defined in Table 1. + = Buffer with 5 mM Mg^{2+}; O = buffer without Mg^{2+}.

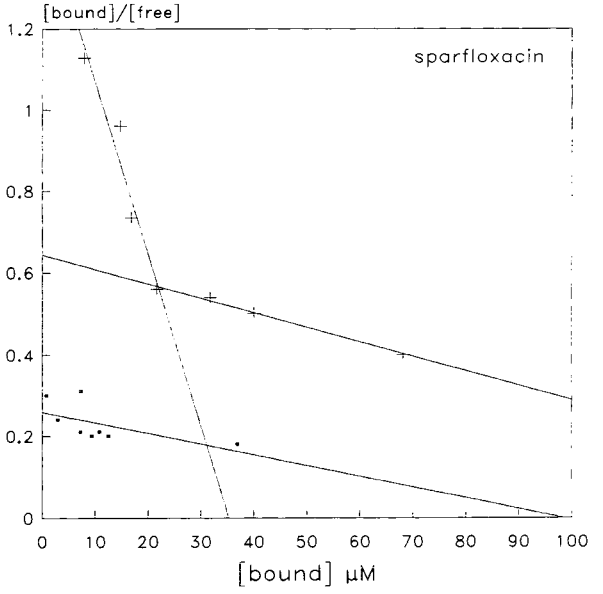

Fig. 3. Determination of K_A, the equilibrium constant of association of sparfloxacin, with calf thymus DNA. The ratio of bound to unbound quinolone is plotted against the molar concentration of bound quinolone. The DNA concentration (57 μmol of base per litre) was kept constant and various amounts of [^{14}C]sparfloxacin were added. Partitioning in the dextran–PEG system was used as described under Experimental. + = Buffer with 5 mM Mg^{2+}; O = buffer without Mg^{2+}.

4. Discussion

Using partitioning in a PEG–dextran aqueous phase system, it is easily possible to find conditions where DNA totally partitions into the dextra-rich lower phase. Hence it was possible to use such systems to study the interactions between quinolones and DNA. The two-phase partitioning experiments clearly indicated that the binding of quinolone to DNA is mediated by magnesium. In the absence of this ion, the assayed compounds had roughly the same binding parameters, with a mean value of nK_A of 800 l mol^{-1} for the experiments carried out at fixed quinolone concentration, and a mean affinity constant K_A of 2600 l mol^{-1} for the experiments carried out at fixed DNA concentration. We could assume that this binding is totally non-specific, mediated by various factors, such as hydrophobicity, charge and stacking properties of the quinolone. In the presence of Mg^{2+}, the affinity increased for all compounds, except for pefloxacin ethyl ester and norfloxacin methyl ester, the binding constants of which remained unchanged. These latter compounds were unable to bind Mg^{2+} in the same manner as the corresponding acids [13], as this binding needs the presence of both the ketone and the carboxylate. On the other hand, the affinity constant in the presence of Mg^{2+} was not strongly dependent on the activity of the quinolone, because RP 65279, although devoid of activity on both bacteria and gyrase (but able to bind Mg^{2+}), had an affinity constant of 10 000 l mol^{-1} in the presence of magnesium. We conclude that the binding in the presence of Mg^{2+} implies a ternary complex between quinolone, Mg^{2+} and DNA; its formation depends mainly on the ability of the drug to bind Mg^{2+}.

Our results, obtained under equilibrium con-

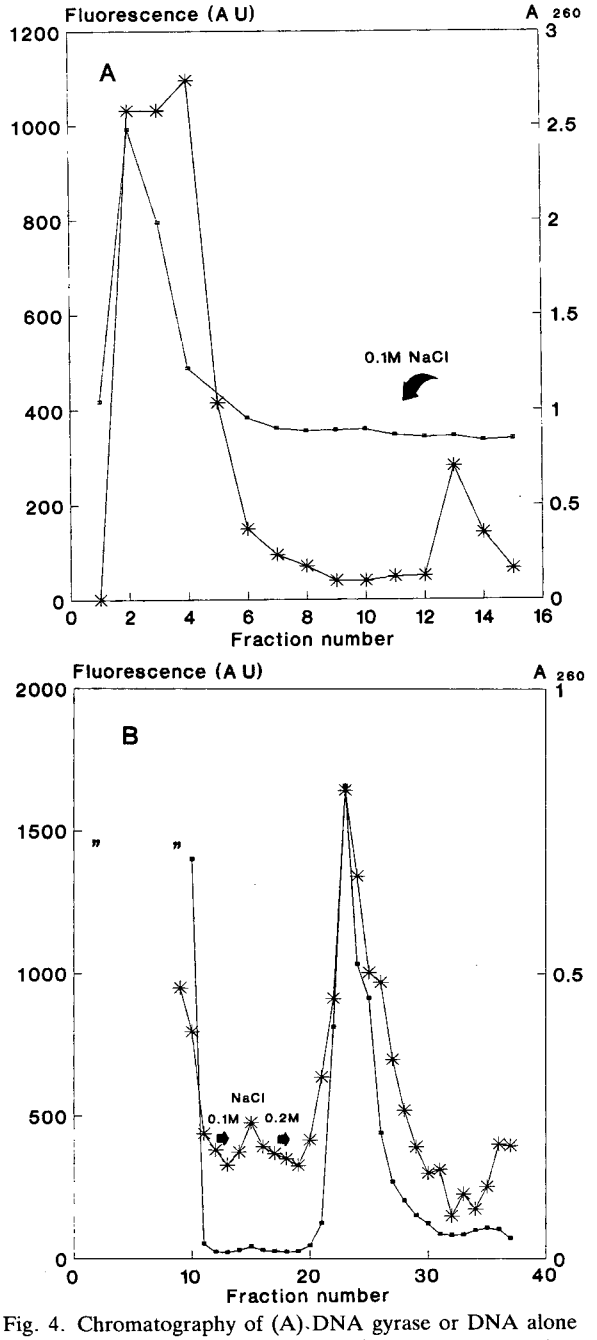

Fig. 4. Chromatography of (A) DNA gyrase or DNA alone and (B) a mixture of both on immobilized norfloxacin (for fraction numbers 0–10, " " indicates that the fluorescence is higher than 2000). The column was equilibrated with the buffer Tris–50 m*M* HCl (pH 7.5)–20 m*M* KCl–2 m*M* $MgCl_2$. Elution was carried out with the same buffer containing 0.1 or 0.2 *M* NaCl as indicated by the arrows. ● = Protein concentration; * = DNA concentration, measured as indicated in Section 2.5. A.U. = arbitrary units.

ditions, can be compared with those of Palù *et al.* [7], who determined the binding constants of [^{14}C]norfloxacin to DNA in the presence of Mg^{2+}, using DNA affinity chromatography and fluorescence experiments. They found a K_A between 1900 and 42 000 l mol^{-1} depending on whether they considered the binding of the quinolone to the DNA–Mg^{2+} complex or of the quinolone–Mg^{2+} complex to the DNA. These values fit with our mean value of 31 000 l mol^{-1}.

The experiments carried out using affinity chromatography on a column of norfloxacin confirmed the results from phase partitioning experiments. Norfloxacin was used as an affinity ligand, because it contained on the piperazine ring an NH function able to react with the epoxide of epoxy-activated Sepharose, and is the desmethyl analogue of pefloxacin. The latter, having an NCH_3 group on the piperazine, could not be immobilized on the resin. The NH function of norfloxacin was the only one able to react with the epoxide, so that the immobilized drug presents the sequence N–CH_2–spacer arm–resin on the piperazine moiety, resembling the N–CH_3 group of pefloxacin (Fig. 1). Therefore, this affinity column should be a good model for pefloxacin. Its use suggested interactions between quinolone, Mg^{2+} and DNA. A relatively low ionic strength (0.1 *M* NaCl) is sufficient to elute the DNA from the column, and this is in good agreement with the low affinity of DNA for fluroquinolone found using two-phase partitioning (K_A = 54 000 l mol^{-1} for pefloxacin). These results completed those of Palù *et al.* [7], who used a DNA cellulose column (*i.e.*, immobilized DNA), and observed binding of norfloxacin on their column only in the presence of Mg^{2+}.

When DNA gyrase was loaded on the column, no appreciable binding was observed, but when the mixture of gyrase plus DNA was loaded on immobilized quinolone, the complex was bound. Moreover, the affinity of the complex was higher than that of DNA alone, as the ionic strength required for elution is slightly higher for the former. This suggests that the quaternary system (DNA–Mg^{2+}–quinolone–gyrase) is more stable than the ternary complex without gyrase.

A possible explanation for the results presented here is that pharmacologically meaningful

recognition between a quinolone and the elements of DNA supercoiling occurs only when DNA, gyrase and Mg^{2+} are simultaneously present. A first step of non-biologically relevant (but Mg^{2+}-dependent) binding would take place between quinolone and DNA, without great differences between various quinolones, provided that they are able to bind Mg^{2+}, as shown here using eleven fluoroquinolones. When gyrase binds to DNA, the presence of the quinolone would then lead the enzyme to adopt slightly different conformations depending on the structure of the quinolone, and this would lead to various impairments of the catalytic activity of the enzyme. This step would then be the pharmacologically relevant one. The proposals made here are in good agreement with the model suggested by Palù *et al.* [7]. Further experiments would be necessary to understand fully the mechanism of inhibition of DNA gyrase by quinolones, and the use of partitioning in dextran–PEG aqueous phase systems offers the great advantage of performing experiments under equilibrium conditions.

5. Acknowledgements

We are indebted to Miss Maryline Masson for skilful technical assistance. S.B.-P.K. was supported by a grant from Roussel-Uclaf.

6. References

[1] R.J. Reece and A. Maxwell, *CRC Crit. Rev. Biochem. Mol. Biol.*, 26 (1991) 335.
[2] J.C. Wang, *Annu. Rev. Biochem.*, 54 (1985) 665.
[3] C.L. Peebles, N.P. Higgins, K.N. Kreuzer, A. Morrison, P.O. Brown, A. Sugino and N.R. Cozzarelli, *Cold Spring Harbor Symp. Quant. Biol.*, 43 (1979) 41.
[4] P. Heisig, H. Schedletzky and H. Falkenstein-Paul, *Antimicrob. Agents Chemother.*, 37 (1993) 696.
[5] L.L. Shen and A.G. Pernet, *Proc. Natl. Acad. Sci. U.S.A.*, 82 (1985) 307.
[6] L.L. Shen, L.A. Mitsher, P.N. Sharma, T.J. O'Donnell, D.W.T. Chu, C.S. Cooper, T. Rosen and A.G. Pernet, *Biochemistry*, 28 (1989) 3886.
[7] G. Palù, S. Valisena, G. Ciarrochi, B. Gatto and M. Palumbo, *Proc. Natl. Acad. Sci. U.S.A.*, 89 (1992) 9671.
[8] C.J.R. Willmott and A. Maxwell, *Antimicrob. Agents Chemother.*, 37 (1993) 126.
[9] H. Yoshida, M. Nakamura, M. Bogaki, H. Ito, T. Kojima, H. Hattori and S. Nakamura, *Antimicrob. Agents Chemother.*, 37 (1993) 839.
[10] C. Perez-Giraldo, C. Hurtado, F. Moran and M. Blanco, *J. Antimicrob. Chemother.*, 25 (1990) 1021.
[11] J.R.B.J. Brouwers, H.J. Van Der Kam, J. Sijtsma and J.H. Proost, *Drug Invest.*, 2 (1990) 197.
[12] J.S. Chapman and N.H. Georgopapadakou, *Antimicrob. Agents Chemother.*, 32 (1988) 438.
[13] S. Lecomte, C. Coupry, M.T. Chenon and N.J. Moreau, in *Abstracts of the 32nd Interscience Conference on Antimicrobial Agents and Chemotherapy, Anaheim, October 1992*, American Society for Microbiology, Washington, DC, 1992, p. 241, abstract No. 785.
[14] H. Walter, D.E. Brooks and D. Fisher (Editors), *Partitioning in Aqueous Two-Phase Systems—Theory, Methods, Uses, and Applications to Biotechnology*, Academic Press, Orlando, FL, 1985.
[15] H. Walter, G. Johansson and D. Brooks, *Anal. Biochem.*, 197 (1991) 1.
[16] F. Le Goffic, N. Moreau, S. Langrené and A. Pasquier, *Anal. Biochem.*, 107 (1980) 417.
[17] B. Nordén, F. Tjerneld and E. Palm, *Biophys. Chem.*, 8 (1978) 1.
[18] P. Remuzon, D. Bouzard, P. Di Cesare, M. Essiz, J.P. Jacquet, J.R. Kiechel, B. Ledoussal, R.E. Kessler and J. Fung-Tomc, *J. Med. Chem.*, 34 (1991) 29.
[19] P. Remuzon, D. Bouzard, C. Guiol and J.P. Jacquet, *J. Med. Chem.*, 35 (1992) 2898.
[20] H. Koga, A. Itoh, S. Murayama, S. Suzue and T. Irikura, *J. Med. Chem.*, 23 (1980) 1358.
[21] S. Bazile, N. Moreau, D. Bouzard and M. Essiz, *Antimicrob. Agents Chemother.*, 36 (1992) 2622.
[22] E. Andrea, K. Adachi and A.R. Morgan, *Mol. Pharmacol.*, 40 (1991) 495.
[23] W.H. Pearlman and O. Crepy, *J. Biol. Chem.*, 242 (1967) 182.

PUBLICATION SCHEDULE FOR THE 1994 SUBSCRIPTION

Journal of Chromatography A and *Journal of Chromatography B: Biomedical Applications*

MONTH	O 1993	N 1993	D 1993	J	F	M	A	
Journal of Chromatography A	652/1 652/2 653/1	653/2 654/1 654/2 655/1	655/2 656/1 + 2 657/1 657/2	658/1 658/2 659/1 659/2	660/1 + 2 661/1 + 2 662/1 662/2	663/1 663/2 664/1	664/2 665/1 665/2 666/1 + 2 667/1	The publication schedule for further issues will be published later.
Bibliography Section						681/1		
Journal of Chromatography B: Biomedical Applications				652/1	652/2 653/1	653/2 654/1	654/2 655/1	

INFORMATION FOR AUTHORS

(Detailed *Instructions to Authors* were published in *J. Chromatogr. A*, Vol. 657, pp. 463–469. A free reprint can be obtained by application to the publisher, Elsevier Science B.V., P.O. Box 330, 1000 AH Amsterdam, Netherlands.)

Types of Contributions. The following types of papers are published: Regular research papers (full-length papers), Review articles, Short Communications and Discussions. Short Communications are usually descriptions of short investigations, or they can report minor technical improvements of previously published procedures; they reflect the same quality of research as full-length papers, but should preferably not exceed five printed pages. Discussions (one or two pages) should explain, amplify, correct or otherwise comment substantively upon an article recently published in the journal. For Review articles, see inside front cover under Submission of Papers.

Submission. Every paper must be accompanied by a letter from the senior author, stating that he/she is submitting the paper for publication in the *Journal of Chromatography A* or *B*.

Manuscripts. Manuscripts should be typed in **double spacing** on consecutively numbered pages of uniform size. The manuscript should be preceded by a sheet of manuscript paper carrying the title of the paper and the name and full postal address of the person to whom the proofs are to be sent. As a rule, papers should be divided into sections, headed by a caption (*e.g.*, Abstract, Introduction, Experimental, Results, Discussion, etc.) All illustrations, photographs, tables, etc., should be on separate sheets.

Abstract. All articles should have an abstract of 50–100 words which clearly and briefly indicates what is new, different and significant. No references should be given.

Introduction. Every paper must have a concise introduction mentioning what has been done before on the topic described, and stating clearly what is new in the paper now submitted.

Experimental conditions should preferably be given on a *separate* sheet, headed "Conditions". These conditions will, if appropriate, be printed in a block, directly following the heading "Experimental".

Illustrations. The figures should be submitted in a form suitable for reproduction, drawn in Indian ink on drawing or tracing paper. Each illustration should have a caption, all the *captions* being typed (with double spacing) together on a *separate sheet*. If structures are given in the text, the original drawings should be provided. Coloured illustrations are reproduced at the author's expense, the cost being determined by the number of pages and by the number of colours needed. The written permission of the author and publisher must be obtained for the use of any figure already published. Its source must be indicated in the legend.

References. References should be numbered in the order in which they are cited in the text, and listed in numerical sequence on a separate sheet at the end of the article. Please check a recent issue for the layout of the reference list. Abbreviations for the titles of journals should follow the system used by *Chemical Abstracts*. Articles not yet published should be given as "in press" (journal should be specified), "submitted for publication" (journal should be specified), "in preparation" or "personal communication".

Vols. 1–651 of the *Journal of Chromatography*; *Journal of Chromatography, Biomedical Applications* and *Journal of Chromatography, Symposium Volumes* should be cited as *J. Chromatogr.* From Vol. 652 on, *Journal of Chromatography A* (incl. Symposium Volumes) should be cited as *J. Chromatogr. A* and *Journal of Chromatography B: Biomedical Applications* as *J. Chromatogr. B.*

Dispatch. Before sending the manuscript to the Editor please check that the envelope contains four copies of the paper complete with references, captions and figures. One of the sets of figures must be the originals suitable for direct reproduction. Please also ensure that permission to publish has been obtained from your institute.

Proofs. One set of proofs will be sent to the author to be carefully checked for printer's errors. Corrections must be restricted to instances in which the proof is at variance with the manuscript.

Reprints. Fifty reprints will be supplied free of charge. Additional reprints can be ordered by the authors. An order form containing price quotations will be sent to the authors together with the proofs of their article.

Announcing...

International Ion Chromatography Symposium 1994

19-22 September , 1994
Turin, Italy

Program Chairman:
Corrado Sarzanini
Analytical Chemistry
University of Turin
Via Giuria 5
I - 10125 Turin, Italy
Telephone: +39-11-670-7628
Fax: +39-11-670-7615

Session Topics

- Separation Selectivity and Column Technology
- Developments in Separation Methodology
- Advances in Detection
- Special Sample Treatment Procedures
- Novel Applications
- Process Monitoring and Control
- Separation of Metal Ions
- Pharmaceutical Applications
- Environmental Applications
- Ion analysis in the Electrical Generating Industry
- Standard Methods and Data Processing

For more information, contact:

Century International, Inc.
P.O.Box 493 • 25 Lee Road
Medfield, MA 02052-0493 USA
508/359-8777 • 508/359-8778 (FAX)

0021-9673(19940506)668:1;1-Q